Facultad de Ciencias

Departamento de Química Orgánica

Highly efficient Ni- and Fe-catalyzed borylative cyclizations of enynes

TESIS DOCTORAL

Natalia Cabrera Lobera

Madrid, octubre 2019

Facultad de Ciencias
Departamento de Química Orgánica

Memoria presentada por

Natalia Cabrera Lobera

para optar al grado de

DOCTORA EN QUÍMICA

Directores de la presente Tesis Doctoral

Dr. Diego J. Cárdenas Morales

Dra. M. Elena Buñuel Magdalena

Madrid, octubre 2019

A mi familia y a Miguel,
por su apoyo y cariño incondicionales

y a Lena,
por ser una más de la familia

“No hay nada más maravilloso que ser un científico, en ninguna parte preferiría estar más que en mi laboratorio, manchando mi ropa y cobrando por jugar.”

(Marie Curie)

PRÓLOGO

PRÓLOGO

La presente memoria recoge el trabajo realizado y los resultados obtenidos durante la Tesis Doctoral. Dicho manuscrito comienza con una **Introducción**, estructurada en tres apartados principales: (i) el primero de ellos describe las propiedades y características más relevantes de los *ácidos borónicos y sus derivados*, más en concreto, de los ésteres borónicos; (ii) en un segundo apartado, se abordan los aspectos generales de las *reacciones de cicloisomerización*, describiendo en mayor profundidad las diferentes reacciones de ciclación de eninos catalizadas por metales de transición de la primera serie; (iii) el tercer y último apartado detalla las reacciones de *ciclación borilativa* que emplean eninos como sustratos de partida, tanto en presencia como en ausencia de metales de transición. A continuación, se plantean y justifican los diferentes **Objetivos** propuestos para el desarrollo de la presente Tesis Doctoral.

El apartado de **Resultados y Discusión**, redactado en inglés, consta de cinco capítulos que, a su vez, se dividen en: (i) *objetivo* principal del capítulo, (ii) *antecedentes* más directamente relacionados con el tema desarrollado; (iii) *resultados* obtenidos y (iv) *parte experimental,* donde se describen los procedimientos y la caracterización de los compuestos recogidos en la presente memoria. El material suplementario, compuesto por espectros de RMN, estructuras de rayos X y datos computacionales, se recoge en formato electrónico en el USB adjunto.

El **Capítulo 1** describe la síntesis de los diversos eninos empleados como sustratos de partida en los diferentes capítulos.

El **Capítulo 2** incluye las reacciones más relevantes de hidroboración de especies insaturadas catalizadas por Fe. Dicho capítulo aborda también la reacción de ciclación hidroborilativa de eninos catalizada por Fe, explicando tanto el desarrollo y aplicación sintética de la misma como el estudio mecanístico a partir de pruebas experimentales, cálculos computacionales y el empleo de diferentes técnicas espectroscópicas.

El **Capítulo 3** expone las reacciones de hidroboración de especies insaturadas catalizadas por Ni. Así mismo, se describe la reacción de ciclación hidroborilativa de eninos catalizada por Ni llevada a cabo. Además, se incluye una propuesta del mecanismo de reacción, apoyado por diferentes pruebas mecanísticas y un exhaustivo estudio computacional.

En el **Capítulo 4**, se describen las reacciones de diboración catalizadas por metales de transición de la primera serie. Los resultados detallan el desarrollo sintético de la reacción de ciclación diborilativa de eninos catalizada por Ni y la utilidad sintética de los productos obtenidos. Diferentes pruebas mecanísticas, aislamiento de complejos metálicos y cálculos teóricos permiten realizar una propuesta del mecanismo de reacción.

Finalmente, el **Capítulo 5** trata las reacciones de carboboración catalizadas por metales de transición de la primera fila. Seguidamente, se muestran los inesperados resultados obtenidos en el desarrollo de la ciclación carboborilativa de eninos empleando un catalizador de Ni. Así mismo, se incluye una propuesta del camino de reacción consistente con las diferentes pruebas mecanísticas realizadas.

Al final de la presente memoria se recogen las principales **Conclusiones** del trabajo desarrollado en los diferentes capítulos.

El alcance estructural desarrollado en el **Capítulo 2** se realizó en colaboración con Juan Carlos Nieto Carmona. Los estudios mecanísticos del **Capítulo 2** y **4**, que emplean espectroscopia Mössbauer, EPR y difracción de rayos X de complejos metálicos de Fe y Ni,

fueron llevados a cabo en colaboración con el grupo del Dr. Michael L. Neidig durante mi estancia breve en Rochester. Los cálculos computacionales incluidos en los **Capítulos 2**–**5** han sido realizados por el Dr. Diego J. Cárdenas y la Dra. M. Teresa Quirós.

Hasta el momento de redactar esta memoria, el trabajo realizado a lo largo de la presente Tesis Doctoral ha conducido a las siguientes publicaciones:

- "*Iron-Catalyzed Hydroborylative Cyclization of 1,6-Enynes*"

  N. Cabrera-Lobera, P. Rodríguez-Salamanca, J. C. Nieto-Carmona, E. Buñuel, D. J. Cárdenas, *Chem. Eur. J.* **2018**, *24*, 784–788. (*HOT PAPER*)

- "*Atom-economical regioselective Ni-catalyzed hydroborylative cyclization of enynes: development and mechanism*"

  N. Cabrera-Lobera, M. T. Quirós, E. Buñuel, D. J. Cárdenas, *Catal. Sci. Technol.* **2019**, *9*, 1021–1029.

- "*Atom-economical Ni-catalyzed diborylative cyclization of enynes: preparation of unsymmetrical diboronates*"

  N. Cabrera-Lobera, M. T. Quirós, W. W. Brennessel, M. L. Neidig, E. Buñuel, D. J. Cárdenas, *Org. Lett.* **2019**, 21, 6552–6556.

- "*Ni-catalyzed Carboborylative Cyclization of Enynes: Atom-economical Synthesis of Boryl-1,4-dienes*"

  N. Cabrera-Lobera, E. Buñuel, D. J. Cárdenas, *Angew. Chem. Int. Ed.* **2019**, *enviado*.

RESUMEN – ABSTRACT

RESUMEN

Una de las principales preocupaciones de la química orgánica moderna es el desarrollo de métodos sintéticos sencillos y eficientes. Actualmente, existe un creciente interés por la mejora de las metodologías convencionales existentes, con el objetivo de desarrollar procedimientos sintéticos útiles, económicos y más respetuosos desde el punto de vista medioambiental. Esta es una de las principales razones por las que el empleo de los metales de transición de la primera serie ha crecido exponencialmente en los últimos años. Las reacciones catalíticas basadas en estos metales han abierto nuevas perspectivas para la química sintética, mediante mecanismos de reacción novedosos y extraordinarios.

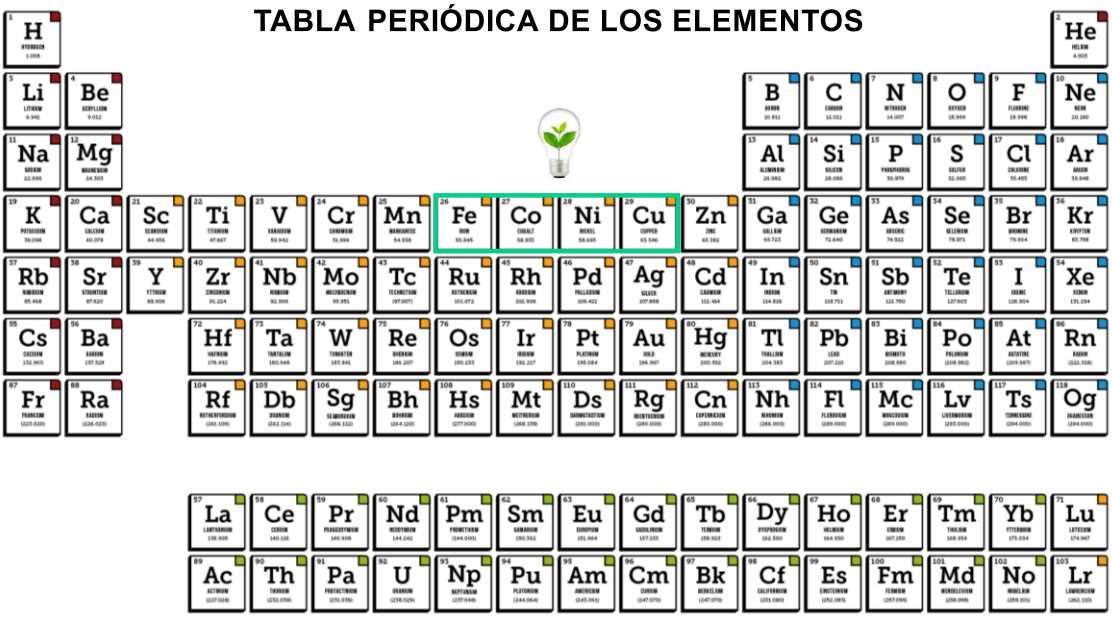

El desarrollo de métodos sintéticos baratos, versátiles y comprometidos con el medioambiente también requiere el empleo de sustratos fácilmente accesibles que toleren la presencia de grupos funcionales en la estructura y que puedan ser preparados en condiciones suaves de reacción, evitando el uso de nucleófilos muy básicos (como los reactivos de organomagnesio y organolitio). En este contexto, los boronatos son reactivos especialmente relevantes debido a su estabilidad frente al oxígeno y a la humedad, alta compatibilidad con grupos funcionales, baja toxicidad, versatilidad y amplia aplicabilidad. Los compuestos de organoboro (en concreto, ácidos borónicos y boronatos) han sido ampliamente empleados como atractivos intermedios sintéticos tanto en síntesis orgánica como en química médica.

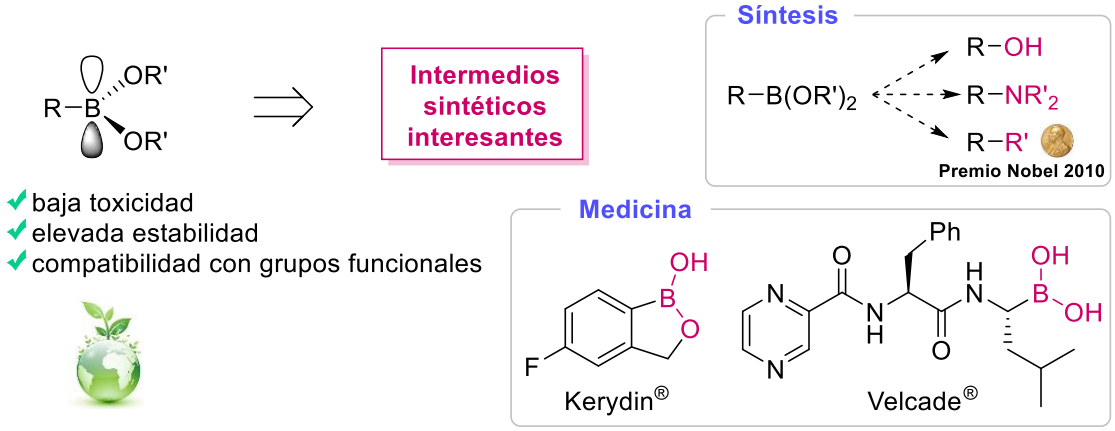

Las reacciones catalizadas por metales de transición que emplean sustratos poliinsaturados permiten la preparación de compuestos cíclicos, estructuras clave en síntesis orgánica. En esta área, los eninos han demostrado ser materiales de partida muy versátiles para la construcción de una gran variedad de carbociclos y heterociclos.

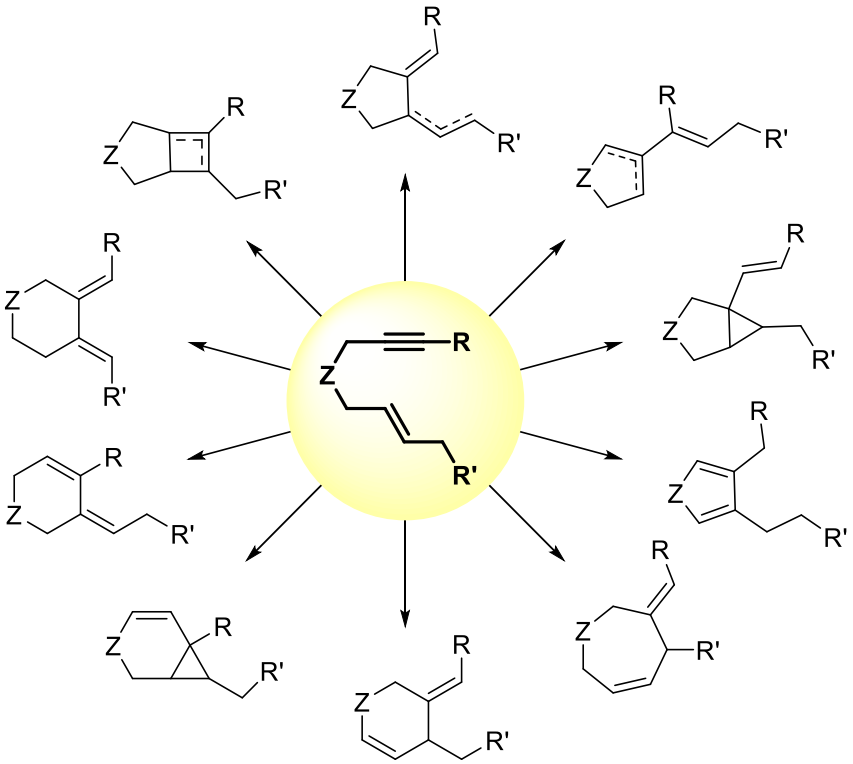

Más en concreto, las reacciones de ciclación borilativa de sustratos poliinsaturados constituyen una poderosa herramienta para la formación de carbo- y heterociclos complejos con sustituyentes de boro en su estructura, mediante la formación en cascada de enlaces C–C y C–B. En los últimos años, nuestro grupo de investigación ha centrado su trabajo en el desarrollo de novedosas reacciones de ciclación borilativa de especies di- y poliinsaturadas (como por ejemplo, eninos, enalenos, aleninos, endiinos) empleando un catalizador de Pd y reactivos de diboro, permitiendo así la síntesis de alil- y homoalilboronatos con la consecuente formación de 1 o 2 anillos, y evitando además el empleo de haluros y de nucleófilos de Li o Mg. Sin embargo, esta metodología presenta algunos inconvenientes, como es el uso de derivados de diboro B_2pin_2 (que conlleva la pérdida de una unidad de Bpin) y la imposibilidad de modificar las propiedades catalíticas del sistema, dado que la reacción transcurre en ausencia de ligandos auxiliares.

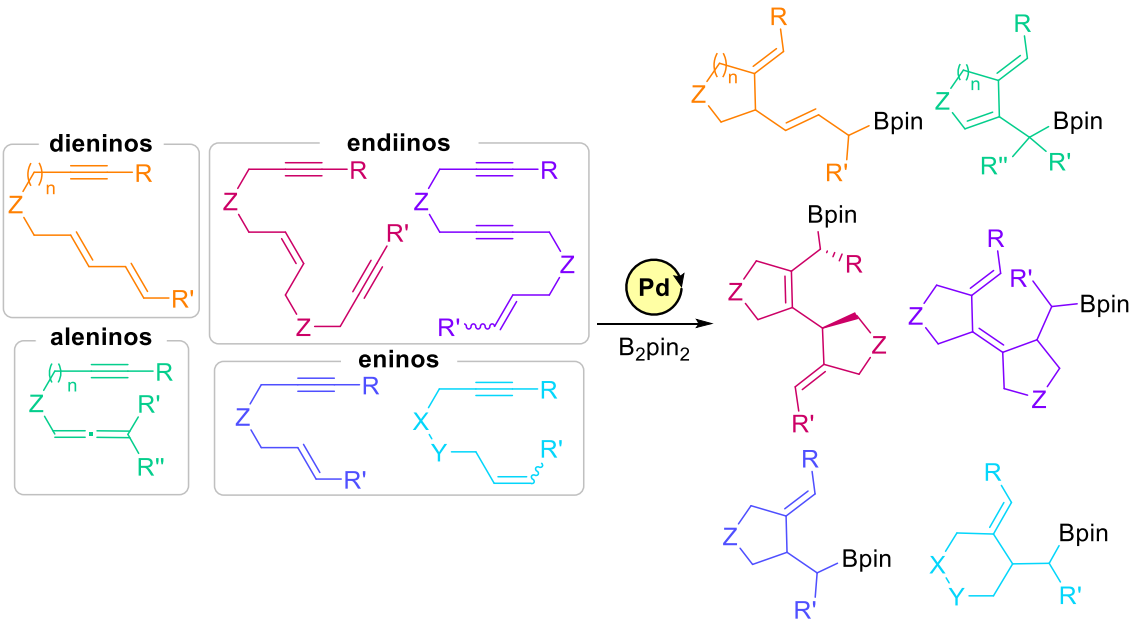

Teniendo en cuenta los antecedentes anteriormente mencionados, se planteó buscar catalizadores más convenientes para la formación de enlaces C–C y C–B. Por ello, en la presente Tesis Doctoral se han desarrollado diversas reacciones de ciclación borilativa de eninos catalizadas por metales de la primera serie de transición, con el objetivo de establecer nuevas metodologías para la síntesis de organoboronatos cíclicos y respetando la economía atómica de la reacción.

En el primer capítulo de resultados de la Tesis, se describe el alcance estructural y el mecanismo de la primera reacción de ciclación hidroborilativa de 1,6-eninos catalizada por Fe. Dicha reacción emplea una sal de hierro y un ligando sencillos y de coste económico reducido, y HBpin como fuente de boro, siendo, por tanto, completamente átomo-económica. Además, la reacción muestra un amplio alcance estructural, proporcionando alquilboronatos con buenos rendimientos, los cuales no son tan fácilmente accesibles como los alquenil- o arilboronatos correspondientes.

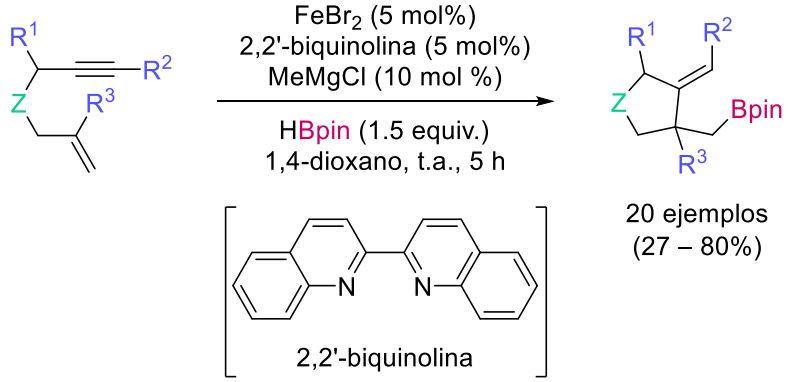

El mecanismo de la reacción propuesto implica la formación de un intermedio clave de dialquil-Fe, que rápidamente reacciona con el pinacolborano presente en el medio para generar un hidruro de hierro altamente reactivo frente al alquino presente en el enino. Los siguientes pasos transcurren rápidamente y permiten la regeneración de la especie activa de hierro de forma fácil. Además, el mecanismo de reacción propuesto presenta una energía de activación baja en todas las etapas, lo que lo hace factible y altamente probable. Cabe

destacar que los estudios experimentales llevados a cabo sugieren que el Fe no se reduce durante el proceso, implicando un ciclo catalítico de Fe(II).

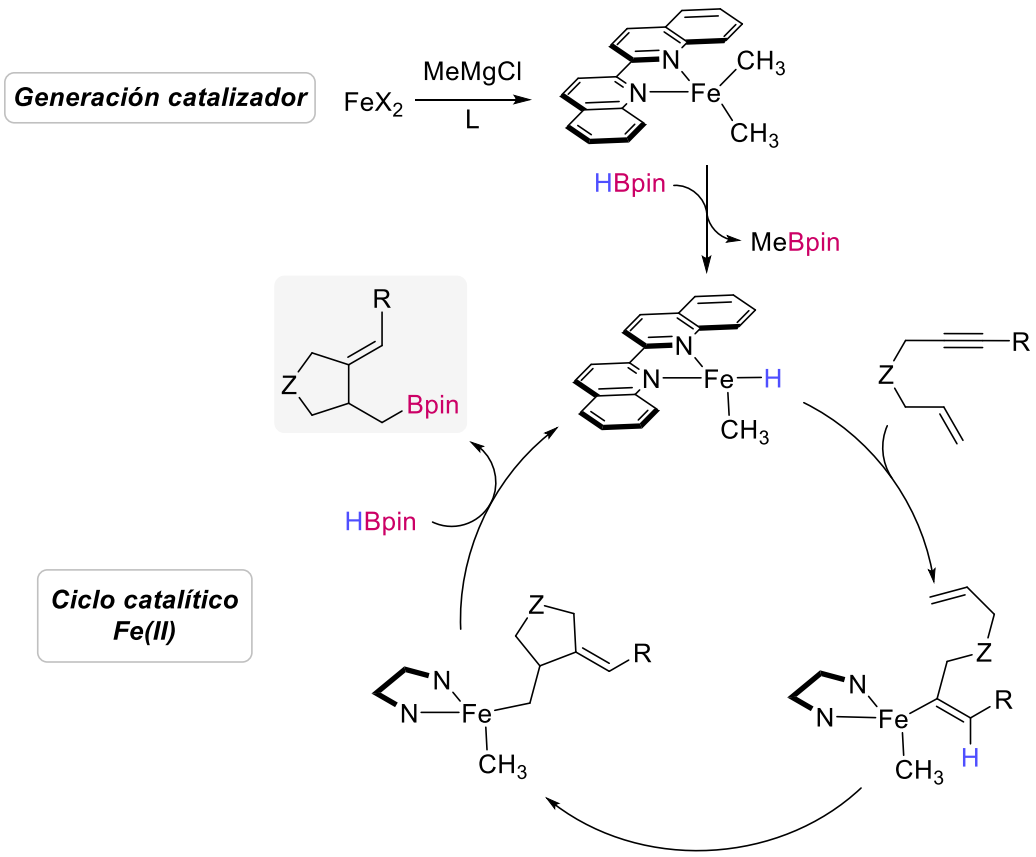

En segundo lugar, se describe la ciclación hidroborilativa de eninos catalizada por Ni, sintetizando homoalil- y alquenilboronatos en función de la sustitución del alquino. La reacción tiene un amplio alcance estructural y permite la formación de carbo- y heterociclos en una sola etapa sintética, en condiciones suaves de reacción y empleando un sistema catalítico barato y altamente átomo-económico.

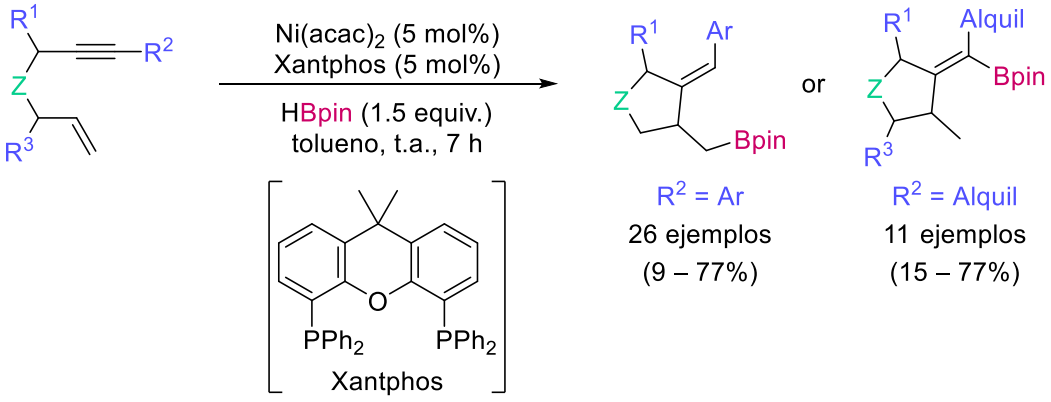

El estudio mecanístico llevado a cabo, tanto a nivel experimental como computacional, nos ha permitido establecer un ciclo catalítico Ni(0)–Ni(II) detallado, comenzando con una ciclometalación oxidante del enino, seguido de una metátesis σ con el reactivo de boro y una última etapa de eliminación reductora. El mecanismo de reacción propuesto para cada uno de los regioisómeros obtenidos presenta en común la formación de un hidruro de Ni intermedio en la etapa clave de metátesis σ.

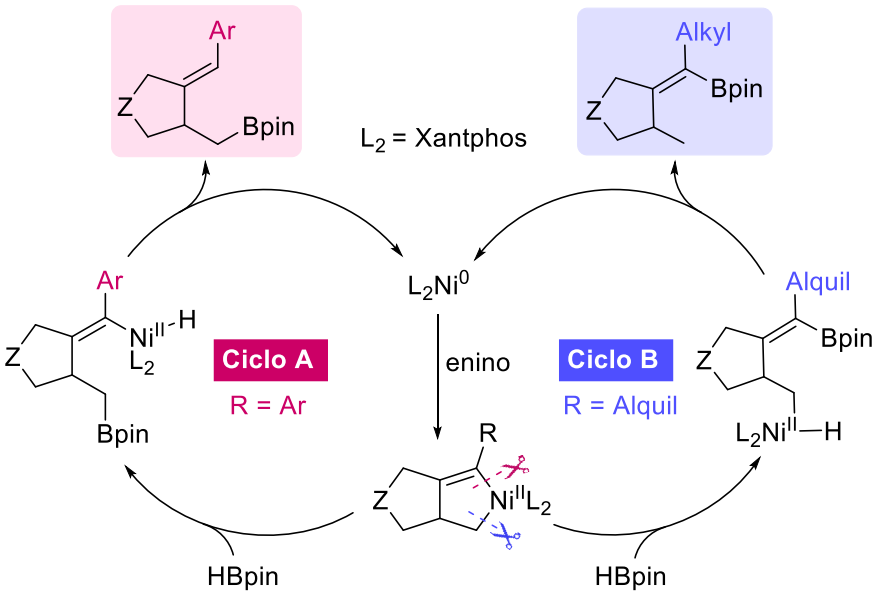

El tercer proceso desarrollado en la presente Tesis describe un método sintético completamente átomo-económico, versátil y de gran aplicabilidad para la preparación de compuesto cíclicos que contienen dos restos de boro en su estructura, a partir de una gran variedad de eninos sencillos. Esta reacción de ciclación diborilativa ofrece un gran alcance estructural con una compatibilidad de grupos funcionales elevada.

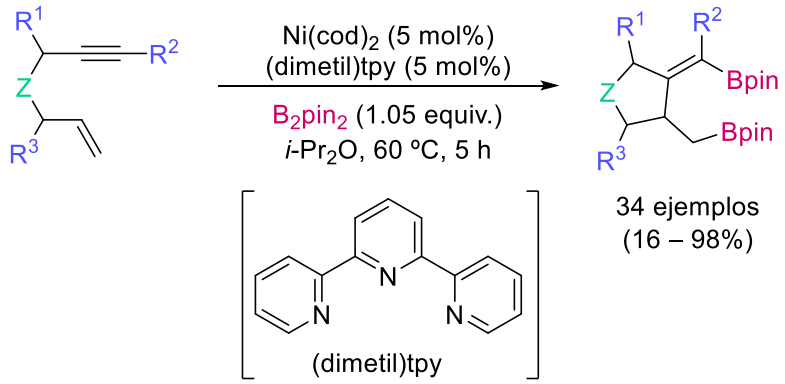

Los estudios mecanísticos sugieren que la reacción podría tener lugar a través tanto de una catálisis cooperativa homometálica como de una catálisis monometálica de complejos de Ni, donde la activación del sustrato orgánico ocurre anteriormente a la reacción con el reactivo de boro. Además, se describe la estructura del primer complejo de bis[organoníquel(I)] con dos enlaces Ni–C de diferente naturaleza.

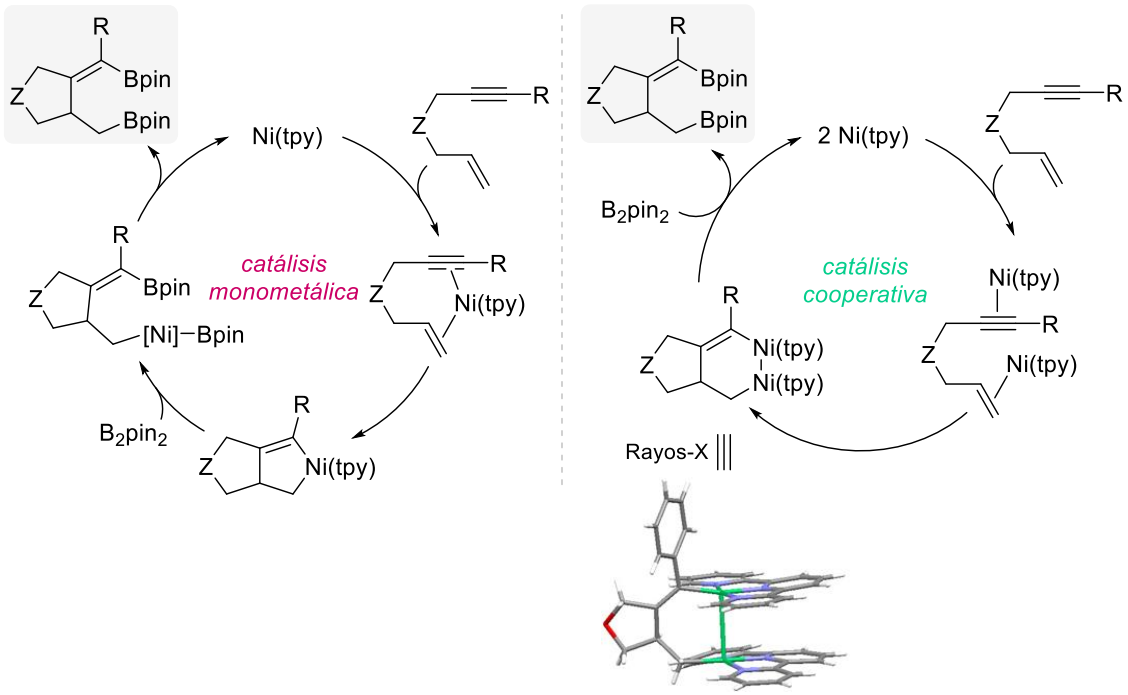

Finalmente, la primera ciclación carboborilativa de eninos catalizada por Ni, que emplea alquinilboronatos fácilmente manejable y accesibles, se describe en el cuarto capítulo de la Tesis. La reacción necesita un sistema catalítico de Ni simple y económico, y procede con completa economía atómica, generando 1,4-ciclohexadienos como productos finales de reacción con altos rendimientos y en tiempos cortos de reacción. Así mismo, se obtienen estructuras bicíclicas fusionadas complejas a partir de estructuras sencillas, como son los eninos y los alquinilboronatos.

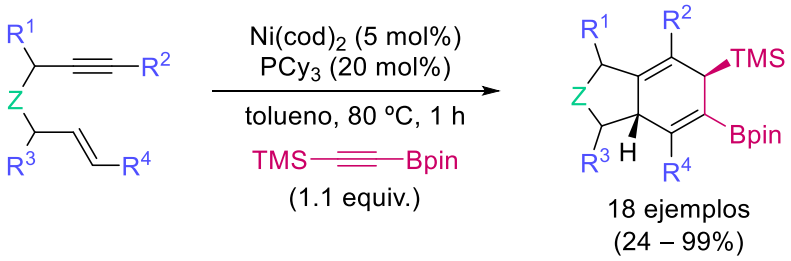

Los estudios mecanísticos llevados a cabo descartan tanto la adición oxidante del enlace C–B al Ni como la formación de un niquelaciclopentadieno intermedio a partir de la ciclometalación oxidante del enino. Por el contrario, se propone una ciclometalación oxidante inicial entre los restos alquino presentes en el enino y en el alquinilboronato. El correspondiente niquelaciclo obtenido da lugar a una carbometalación del alqueno, seguida de una eliminación reductora para formar 1,3-dienos y regenerar la especie activa de Ni(0). Adicionalmente, una isomerización externa al ciclo catalítico daría lugar a una migración 1,3 de hidrógeno que explicaría la formación de los boronatos obtenidos en la reacción.

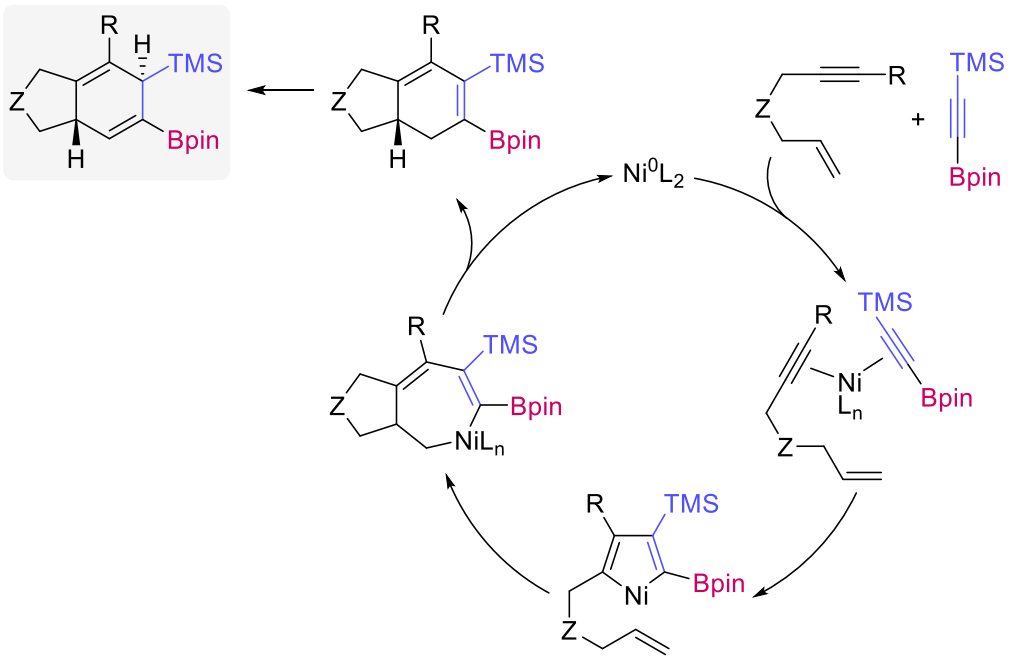

También, se ha demostrado la utilidad y el potencial de los boronatos finales obtenidos como interesantes intermedios sintéticos. Para ello, se llevaron a cabo diversas funcionalizaciones de los grupos Bpin, como oxidación, transformación en las sales de trifluoroborato correspondientes y reacciones de acoplamiento cruzado de tipo Suzuki.

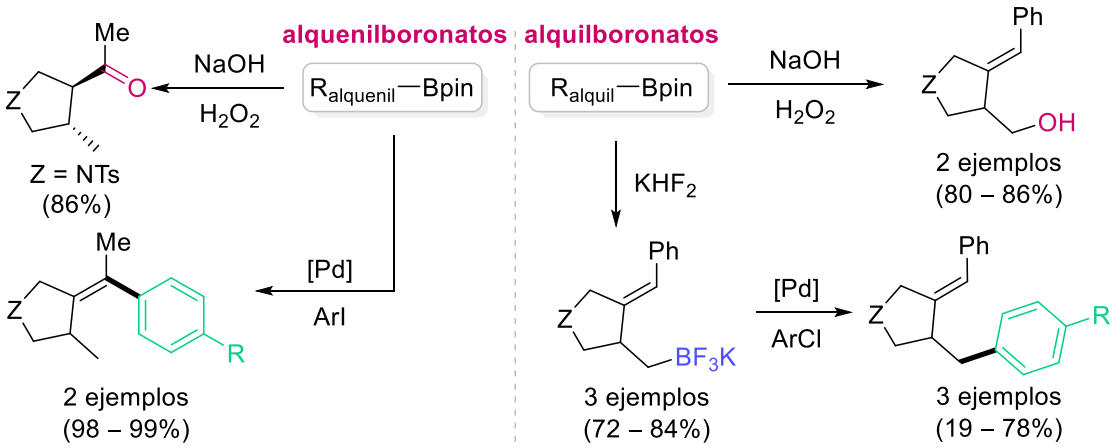

Además, se ha descrito la funcionalización ortogonal de los diboronatos sintetizados, aprovechando la reactividad dispar de los grupos boronatos presentes debido a su diferente naturaleza.

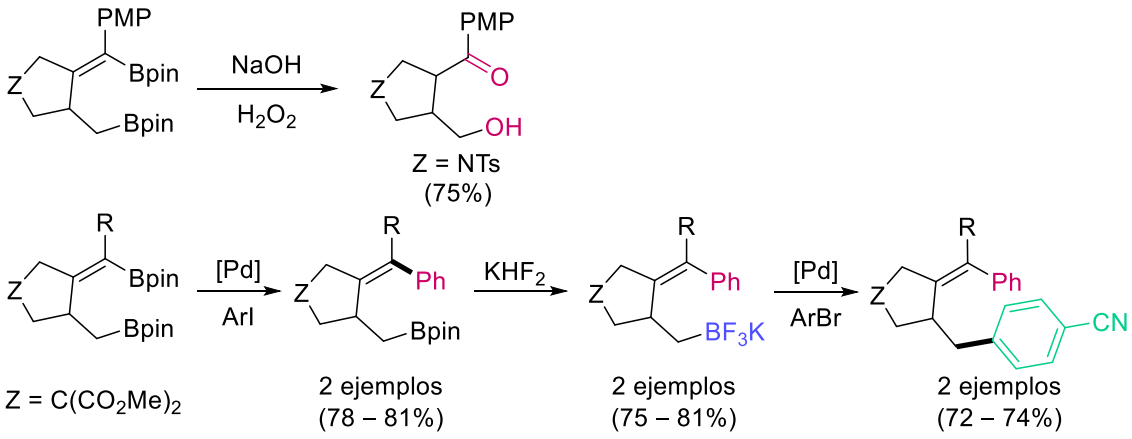

ABSTRACT

The development of practical, simple and highly efficient synthetic methods is one of the priorities of novel organic chemistry. We are witnessing a necessary and increasing interest in the improvement of conventional methodologies in order to describe useful and more respectful synthetic procedures, since economic and environmental aspects cannot be ignored nowadays. This is one of the reasons why the use of the first-row transition metals has increased during the last decades. Catalytic reactions based on these metals have opened up new perspectives since they provide novel activation pathways and astonishing reaction mechanisms, accessing to a unique chemical space.

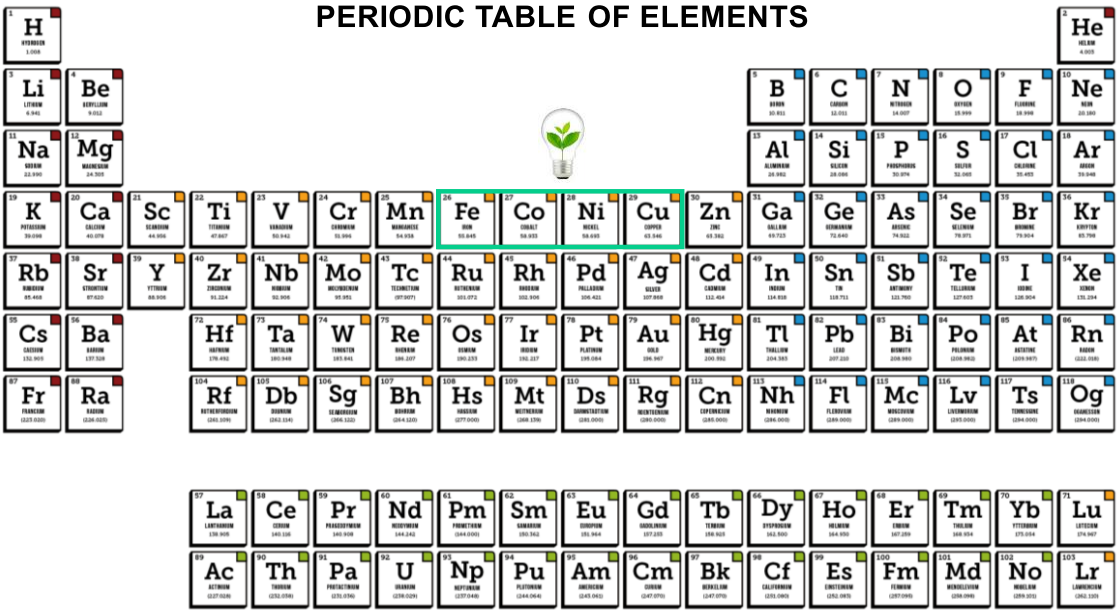

The development of eco-friendly, inexpensive and versatile synthetic methods requires the use of readily available substrates that allow the presence of functional groups and that can be prepared and reacted under smooth conditions, avoiding the use of highly basic reagents (such as organomagnesium or organolithium reagents). In this regard, boronates are especially relevant intermediates due to their oxygen and moisture stability, high functional group tolerance, low toxicity, versatility and wide applicability. Organoboron compounds (especially boronic acids and boronates) have been widely employed as powerful building blocks in both synthetic organic chemistry and medicinal chemistry.

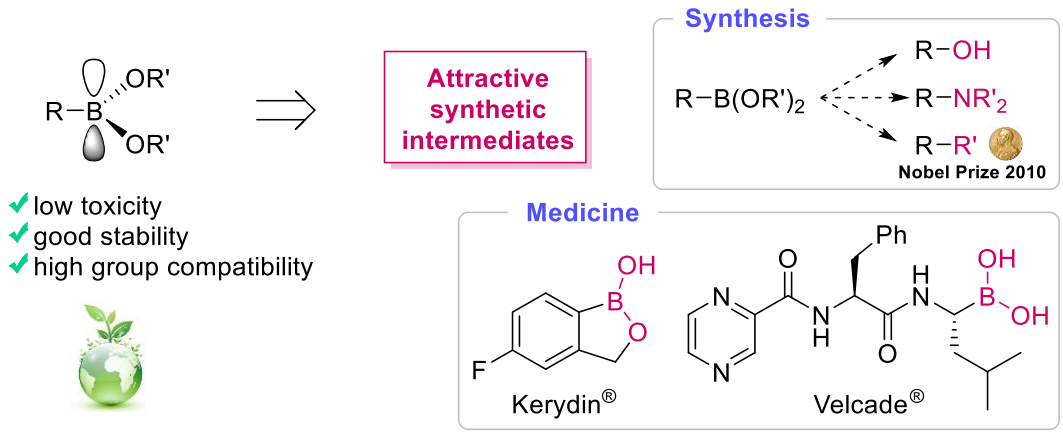

Transition metal-catalyzed reactions of polyunsaturated structures allow the preparation of cyclic compounds, which are important scaffolds in synthetic organic chemistry. In this context, enynes are versatile starting materials for the construction of a wide range of carbo- and heterocycles.

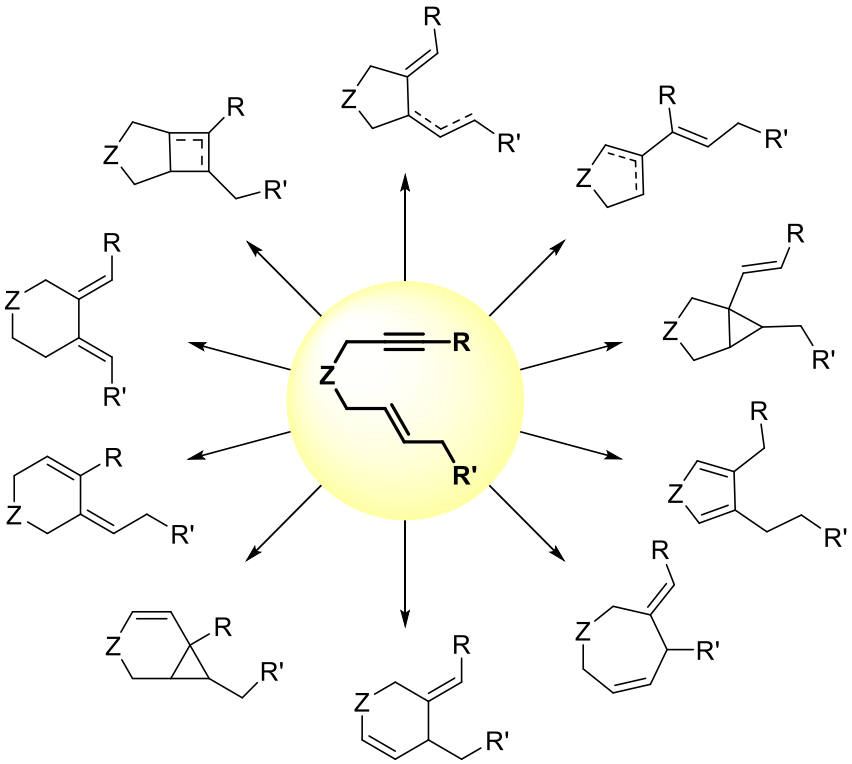

Specifically, borylative cyclization reactions of polyunsaturated compounds constitute powerful methods for the formation of complex boron-containing carbo- and heterocycles by formation of C–C and C–B bonds through cascade reactions. During the last years, our group has focused its efforts on developing novel borylative cyclization reactions of di- and polyunsaturated species (e.g., enynes, enallenes, allenynes, enediynes) using Pd catalysis and diboron reagents, which have allowed to access allylic, homoallylic and alkenylic boronates with concomitant formation of 1 or 2 rings, avoiding the use of organohalides and Li and Mg nucleophiles. However, this methodology shows some drawbacks, as the use of diboron derivatives B_2pin_2 (that leads to the loss of one B unit) and the impossibility to tune the catalyst properties since it takes place in the absence of added ligands.

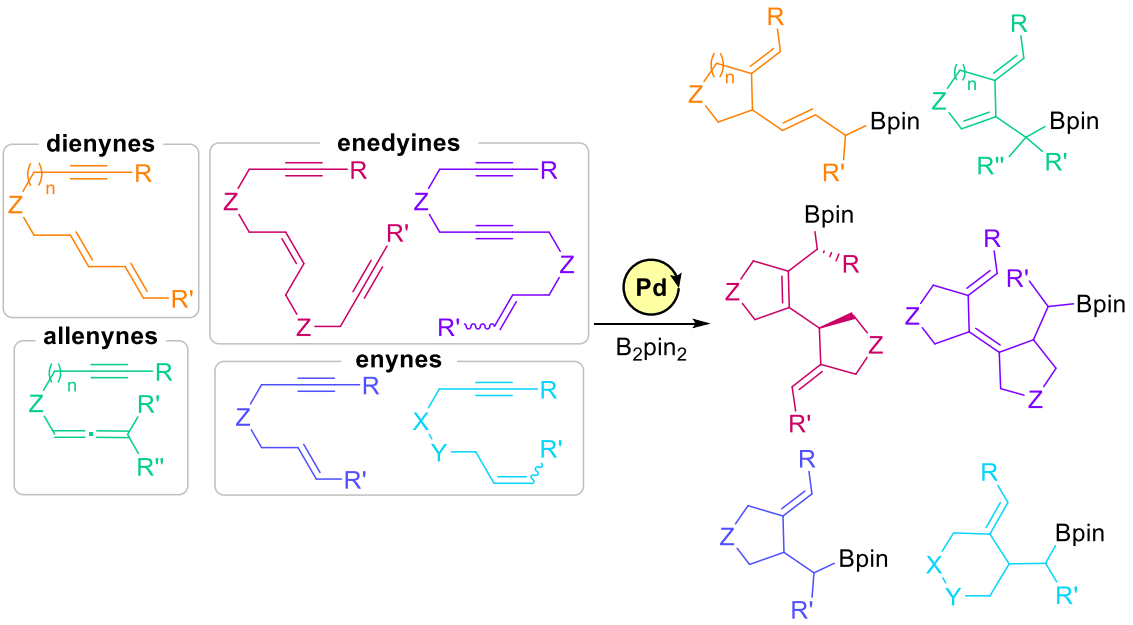

Taking into account the aforementioned precedents, we sought to find more convenient catalysts for the formation of C–C and C–B bonds. Thus, we developed useful, atom-economical first-row transition metal-catalyzed borylative cyclization reactions of enynes, with the aim of stablishing novel synthetic methodologies for the synthesis of cyclic organoboron derivatives.

In the first chapter of the Thesis, our results on the scope and mechanism of the first Fe-catalyzed hydroborylative cyclization reaction of 1,6-enynes are reported. This reaction uses an inexpensive Fe salt, simple 2,2'-biquinoline ligand and HBpin as the boryl source, being therefore atom-economical. It shows a wide scope, providing alkylboronates, which are usually not as readily accessible as alkenyl- or arylboron derivatives, in good yields.

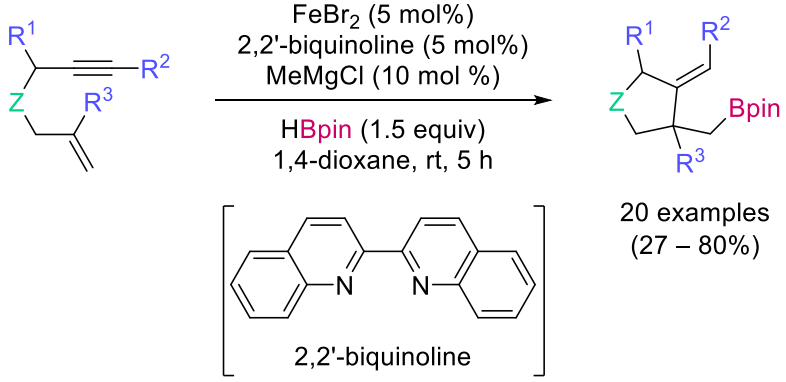

The proposed reaction mechanism implies the formation of a key dialkyl-Fe intermediate, which readily reacts with HBpin to afford a hydride complex highly reactive towards the alkyne moiety. The subsequent steps are very fast and allow a facile regeneration of the active species. The proposed reaction pathway shows extremely low activation energies for all steps, what makes it feasible and highly likely. Noticeably, experimental studies suggested that Fe is not reduced during the process, meaning a Fe(II) catalytic cycle.

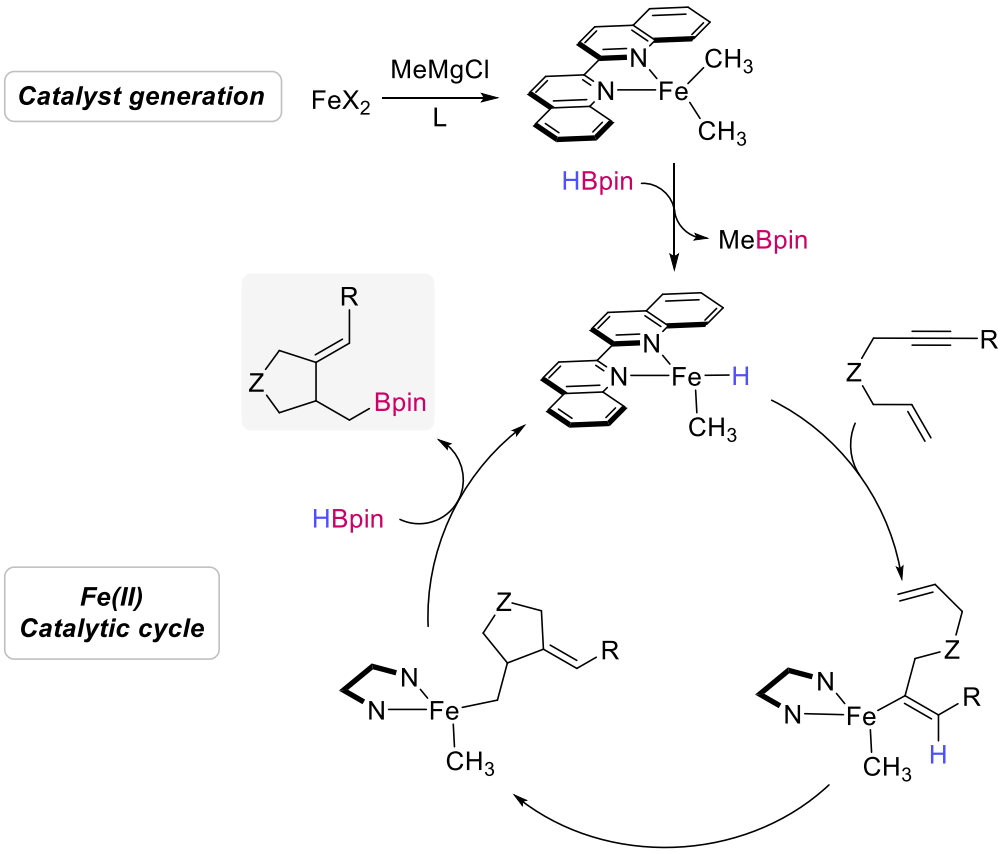

Secondly, a novel Ni-catalyzed hydroborylative cyclization reaction that provides either homoallyl- or alkenylboronates, depending on the substitution of the alkyne is described. The reaction shows a broad scope and allows the formation of carbo- and heterocycles in a single step, under smooth conditions, with an inexpensive catalytic system and full atom economy.

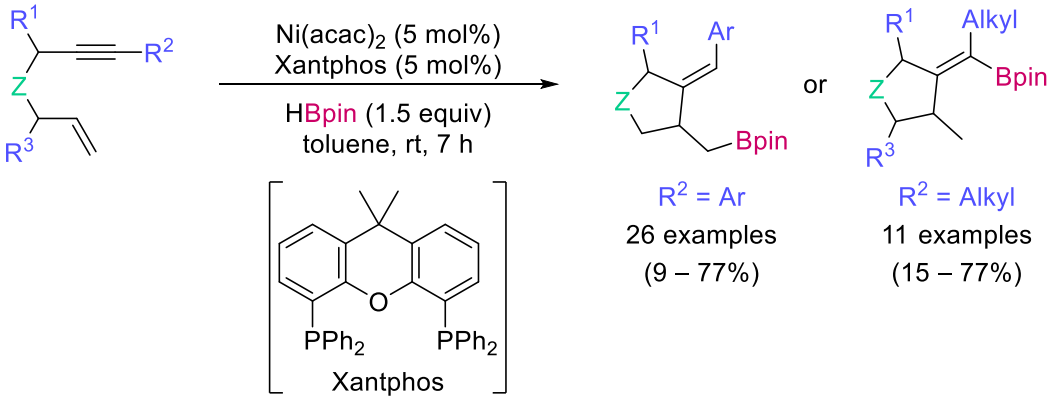

A mechanistic study performed both experimentally and computationally has led to propose a detailed Ni(0)–Ni(II) catalytic cycle, implying initial oxidative cyclometalation on the enyne, a subsequent feasible σ-metathesis reaction with pinacolborane and a final reductive elimination. The proposed reaction pathways, which account for the observed regioselectivity, have in common the formation of nickel hydrides as key intermediates in the σ-metathesis step.

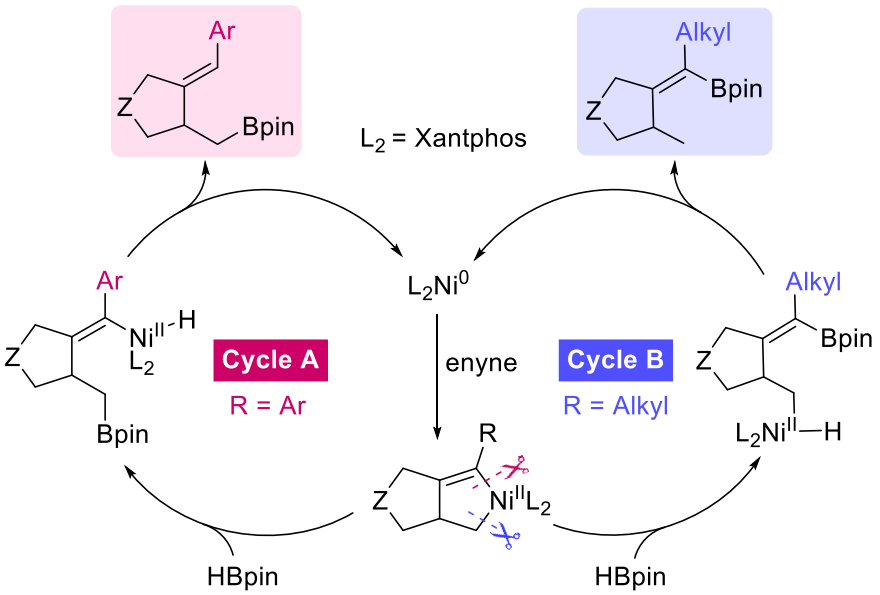

The third objective of the Thesis describes a full atom-economical, versatile, widely applicable synthetic method for the preparation of cyclic compounds containing two different kinds of boronate units, starting from an ample variety of simple enynes. This diborylative cyclization reaction shows a broad scope with high functional group compatibility.

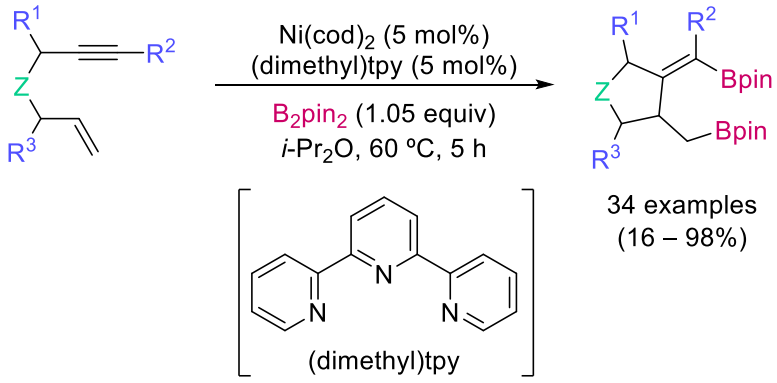

Mechanistic studies suggest that the reaction pathway could involve either a cooperative homometallic or a monometallic catalysis with Ni complexes, where activation of the organic substrate takes place prior to reaction with the borylation reagent. We report the structure of the first bis[organonickel(I)] complex showing two different Ni–C bonds.

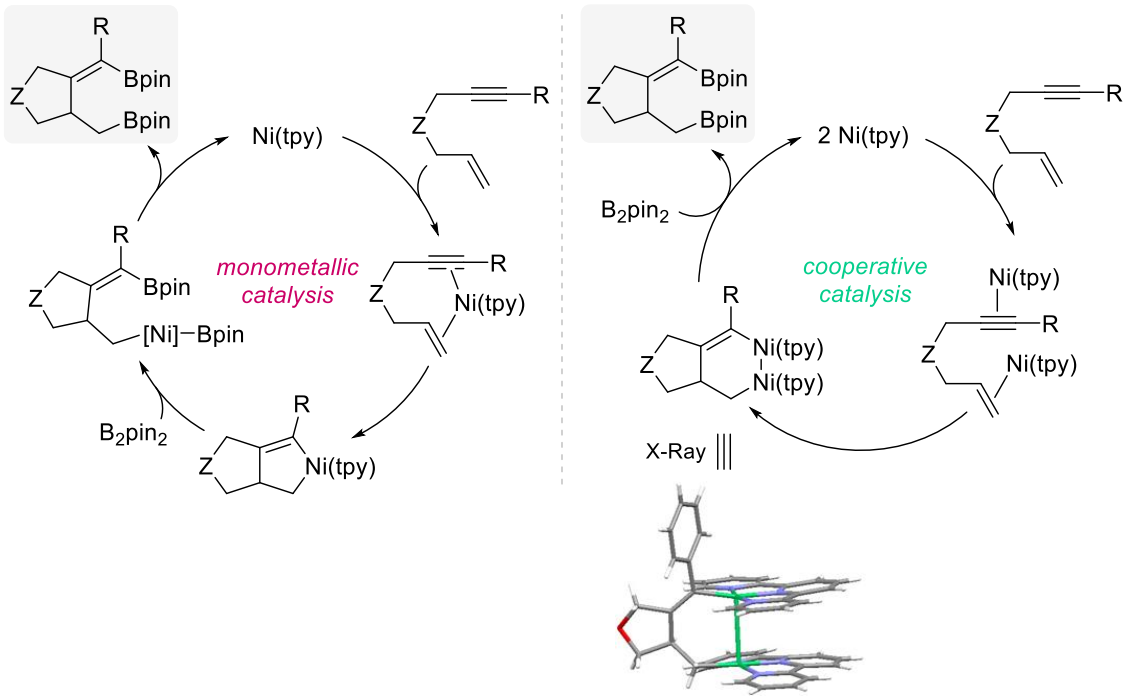

Finally, the first Ni-catalyzed carboborylative cyclization of enynes using easy-handling and readily accessible alkynylboronates has been described in the fourth chapter of this Thesis. The reaction requires simple and inexpensive Ni-based catalytic system and proceeds with complete atom economy in a short reaction time, furnishing unexpected 1,4-cyclohexadienes in high yields. Furthermore, we are able to obtain complex fused-bicyclic structures from simple structures, such as enynes and alkynylboronates.

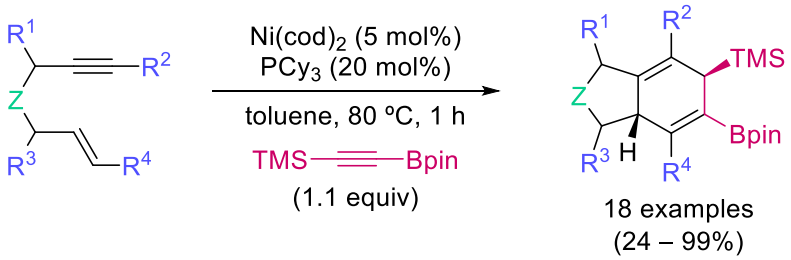

Mechanistic experiments lead to disregard both the oxidative addition of C–B bond to Ni and the formation of a nickelacyclopentadiene by oxidative cyclometalation of the coordinated enyne. Instead, we propose an initial oxidative cyclometalation involving the alkyne groups present in the alkynylboronate and the enyne. The resulting nickelacyclopentadiene would evolve by carbometalation of the alkene and subsequent reductive elimination to afford a 1,3-diene and regenerating the Ni(0) species. An off-cycle isomerization involving a 1,3-hydrogen migration would lead to the observed products.

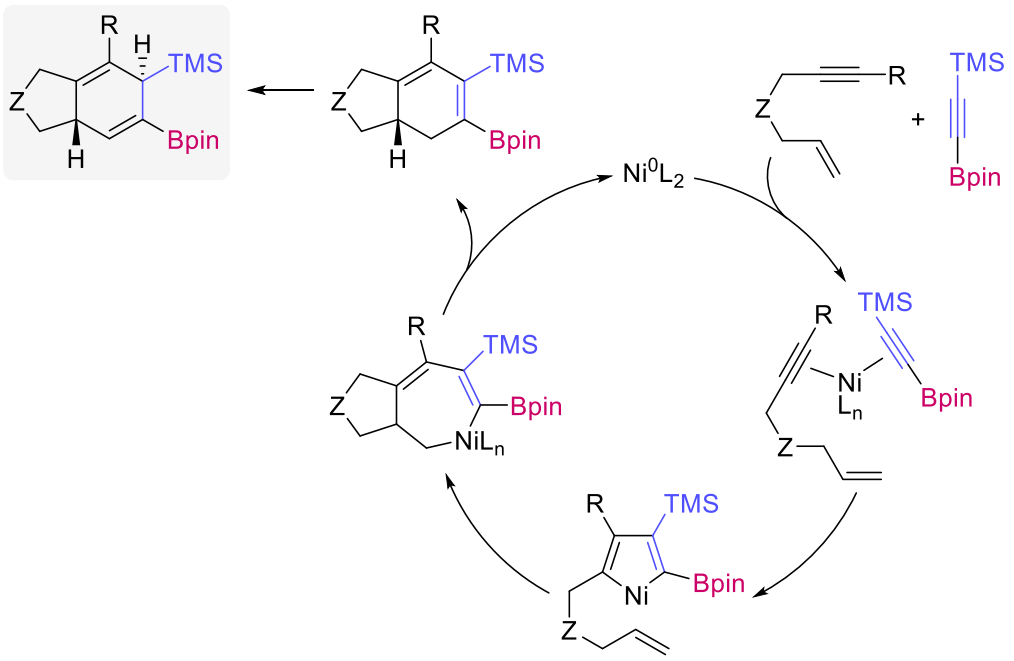

The reactivity and potential applicability of these boron derivatives for synthetic purposes have also been illustrated. Thus, some transformations on the synthetized boronates, such as oxidation, transformation into the synthetically useful trifluoroborate salts and Suzuki cross-coupling reaction were performed.

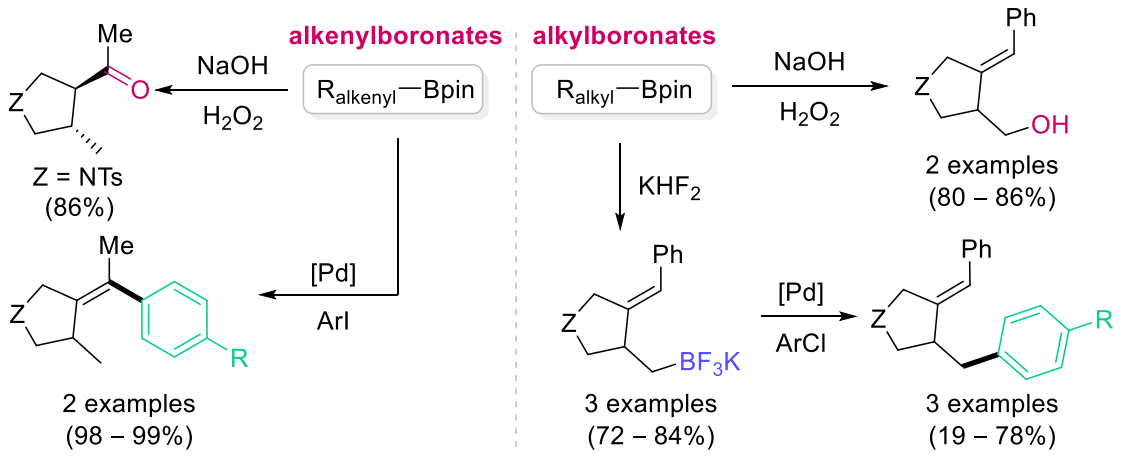

Moreover, the orthogonal derivatization of the obtained bis(boronates) was successfully accomplished by taking advanced on the different nature of the two boryl units.

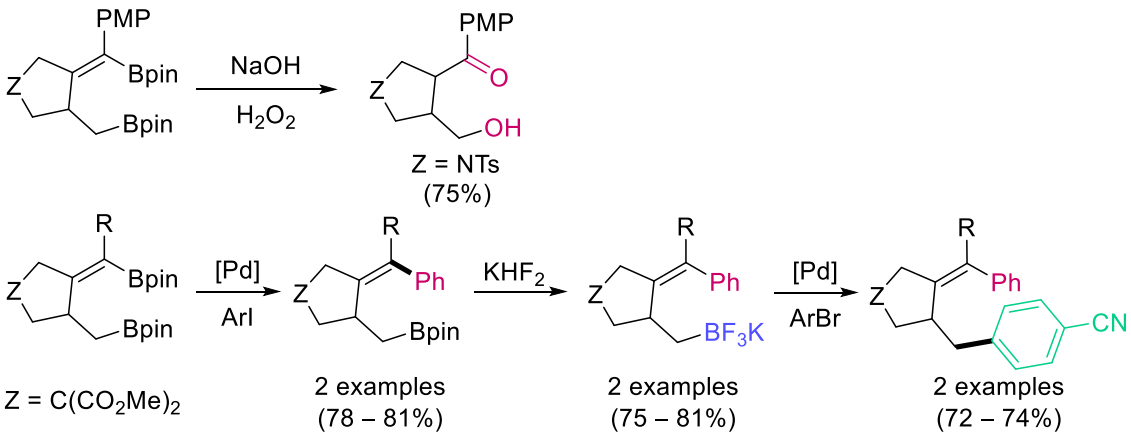

ABBREVIATIONS AND ACRONYMS

ABBREVIATIONS AND ACRONYMS

In this Thesis, the abbreviations and acronyms recommended by Guidelines for Authors (*J. Org. Chem.* **2017**) have been used. Herein, some of them are disclosed:

(+)-DIOP	(+)-2,3-*O*-isopropylidene-2,3-dihydroxy-1,4-bis(diphenylphosphino)butane
9-BBN	9-borabicyclo[3.3.1]nonane
Ac	acetyl
acac	acetilacetonate
AIBN	2,2-azobisisobutyronitrile
Ar	aryl
atm	atmosphere
B_2cat_2	bis(catecolato)diboron
B_2pin_2	bis(pinacolato)diboron
BINAP	(±)-2,2′-bis(diphenylphosphino)-1,1′-binaphthalene
BIP	bis(imino)piridine
Bn	benzyl
Boc	*tert*-butoxycarbonyl
Box	bis(oxazoline)
Bpin	pinacolboryl
bpy	bipyridine
br	broad
Bu	butyl
Bz	benzoyl
ca.	*circa,* about
Calc.	calculated
cat	catecol
cat.	catalytic/catalítico
Cbz	benzyloxycarbonyl
Co.	company
cod	cyclooctadiene
conv.	conversion
COSY	correlation spectroscopy
Cp	cyclopentadienyl
CPME	cyclopentylmethyl ether
Cy	cyclohexyl
Cyp	cyclopentyl
δ	chemical shift
d	doublet
d.r./dr	relación diastereomérica/diastereomeric ratio
dan	1,8-diaminonaphthalene
dba	dibenzylideneacetone
DCC	*N,N″*-dicyclohexylcarbodiimide
DCE	1,2-dichloroethane
dcpe	1,2-bis(dicyclohexylphosphino)ethane
DEPT	Distortionless Enhancement by Polarization Transfer
DFT	Density Functional Theory
diast	diastereoisomer
DIBAL-H	diisobutylaluminium hydride
DIPEA	*N,N*-diisopropylethylamine
DMA	*N*,*N*-dimethylacetamide

DMAP	4-(dimethylamino)pyridine
DMBQ	2,6-dimethoxybenzoquinone
DME	dimethoxyethane
DMF	*N*,*N*-dimethylformamide
DMPU	1,3-dimethyl-3,4,5,6-tetrahydro-2(1*H*)-pirimidinone
DMSO	dimethyl sulfoxide
DPEPhos	bis[(2-diphenylphosphino)phenyl] ether
dppb	1,3-bis(diphenylphosphino)butane
dppbz	1,2-bis(diphenylphosphino)benzene
dppe	1,2-bis(diphenylphosphino)ethane
dppf	1,1'-bis(diphenylphosphino)ferrocene
dppmbz	1,3-bis(diphenylphosphinomethyl)benzene
dppp	1,3-bis(diphenylphosphino)propane
DuanPhos	2,2′-di-*tert*-butyl-2,3,2′,3′-tetrahydro-1*H*,1′*H*-(1,1′)biisophosphindolyl
E	electrófilo/electrophile
e.e./ee	exceso enantiomérico/enantiomeric excess
e.g.	*exempli gratia*, for example
E_a	activation energy
EI	electronic impact
EPR	Electron Paramagnetic Resonance
equiv./equiv	equivalente/equivalent
er	enantiomeric ratio
ESI	electrospray ionization
Et	ethyl
et al.	*et alii*, and others
etc.	etcétera/etcetera
etpo	4-ethyl-2,6,7-trioxa-1-phosphabicyclo[2.2.2]octane
G	Gibbs free energy
GC/MS	Gas Chromatography – Mass Spectrometry
GD/DG	grupo director/directing group
glyme/DME	1,2-dimetoxyethane
h	hour
HAT	Hydrogen Atom Transfer
HB	hydroboration product
Hex	hexyl
HMPT	hexamethyltriaminophosphine
HOMO	Highest Occupied Molecular Orbital
HRMS	High-Resolution Mass Spectrometry
i	*iso*
IAd·HCl	1,3-bis(1-adamantyl)imidazolium chloride
ICy	1,3-dicyclohexylimidazolium
IMes·HCl	1,3-bis(2,4,6-trimethylphenyl)imidazolium chloride
IP	iminopiridine
IPr	2,6-diisopropylphenyl
IPr·HCl	1,3-bis(2,6-diisopropylphenyl)imidazol-2-ylidene
J	coupling constant (in NMR)
LUMO	Lowest Unoccupied Molecular Orbital
m	multiplet
M	molarity
m	*meta*

M.p.	melting point
Me	methyl
Mes	2,4,6-trimethylphenyl (mesityl)
MIDA	*N*-methyliminodiacetic acid
min	minute
MOM	methoxymethyl
MS	mass spectrometry
nba	norbornane
nbe	norbornene
nep	neopentyl glycol
NEt_2-Xantphos	*P*,*P′*-(9,9-dimethyl-9*H*-xanthene-4,5-diyl)bis[*N*,*N*,*N′*,*N′*-tetraethyl-phosphonous diamide]
NHC	*N*-heterocyclic carbene
nOe	nuclear Overhauser effect
np	nanoparticles
NR	no reaction
N-Xantphos	4,6-bis(diphenylphosphino)-10*H*-phenoxazine
o	*ortho*
ºC	Celsius
OIP	oxazoline(imino)piridine
OP	(oxazoline)pyridine
OPPA	oxazolinylphenyl picolinamide
OTf	triflate
p	*para*
PEPPSI-IPr	[1,3-bis(2,6-diisopropylphenyl)imidazol-2-ylidene](3-chloropyridyl)
Ph	phenyl
pin	pinacol
Piv	pivaloyl
PMDTA	*N*,*N*,*N′*,*N″*,*N″*-pentamethyldiethylenetriamine
PMHS	polymethylhydrosiloxane
PMP	*para*-methoxyphenyl
Pnd	pinanodiol
ppm	part(s) per million
Pr	propyl
PTSA	*para*-toluenesulfonic acid
Py	pyridine
PyBox	pyridine bis(oxazoline)
q	quartet
QuinoxP*	2,3-bis(*tert*-butylmethylphosphino)quinoxaline
quint	quintuplet
RCM	Ring-Closing Methatesis
Rdto.	rendimiento/yield
RMN / NMR	resonancia magnética nuclear/nuclear magnetic resonance
RuPhos	2-dicyclohexylphosphino-2′,6′-diisopropoxybiphenyl
s	singlet
SET	single electron transfer
sia	siamyl
SIMes	1,3-bis(2,4,6-trimethylphenyl)-2-imidazolidinylidene
SPhos	2-dicyclohexylphosphino-2′,6′-dimethoxybiphenyl
t	triplet

t	*tert*
t.a./rt	temperatura ambiente/room temperature
Taniaphos	(S_P)-1-[(S)-α-(dimethylamino)-2-(diphenylphosphino)benzyl]-2-diphenylphosphinoferrocene
TBP	2,4,6-tri-*tert*-butylpyridine
TBS/TBDMS	*tert*-butyldimethylsilyl
Tf	triflyl
TFA	trifluoroacetic acid
THF	tetrahydrofuran
ThiXantphos	(2,8-dimethylphenoxathiine-4,6-diyl)bis(diphenylphosphane)
THP	tetrahydropyranyl
TIPS	triisopropylsilyl
TLC	Thin Layer Chromatography
TMEDA	*N*,*N*,*N′*,*N′*-tetramethylethylenediamine
TMS	trimethylsilyl
TOF	time-of-flight
Tol	tolyl
tpy	2,2′:6′,2″-terpyridine
Triphos	bis(2-diphenylphosphinoethyl)phenylphosphine
Ts	*para*-toluenesulfonyl (tosyl)
TS	transition state
vs	versus
w/o	without
Xanpthos	4,5-bis(diphenylphosphino)-9,9-dimethylxanthene
Xphos	2-dicyclohexylphosphino-2′,4′,6′-triisopropylbiphenyl

ÍNDICE

ÍNDICE

PRÓLOGO XIII

RESUMEN / ABSTRACT XIX

ABBREVIATIONS AND ACRONYMS XXXVII

1. INTRODUCCIÓN 1

1.1. ÁCIDOS BORÓNICOS Y SUS DERIVADOS 3

1.1.1. Estructura y propiedades 4

1.1.2. Derivados de ácidos borónicos 5

1.1.3. Métodos de síntesis de ácidos y ésteres borónicos 9

1.1.4. Transformaciones de los compuestos de organoboro 14

1.2. REACCIONES DE CICLACIÓN DE ENINOS 15

1.2.1. Aspectos generales de las cicloisomerizaciones 15

1.2.2. Cicloisomerizaciones catalizadas por metales de transición de la primera serie. 19

1.3. CICLACIONES BORILATIVAS DE ENINOS 33

1.3.1. Ciclaciones borilsililativas de eninos 34

1.3.2. Ciclaciones borilestannilativas de eninos 37

1.3.3. Ciclaciones hidroborilativas de eninos 38

2. OBJETIVOS 53

3. RESULTS AND DISCUSSION 59

3.1. CHAPTER 1. *Synthesis of starting enynes* 61

3.1.1. Synthesis of starting enynes 63

3.1.2. Experimental section 69

3.2. CHAPTER 2. *Fe-catalyzed hydroborylative cyclization of enynes* 91

3.2.1. Goal 93

3.2.2. Precedents 93

3.2.3. Results 105

3.2.4. Experimental section 122

3.3. CHAPTER 3. *Ni-catalyzed hydroborylative cyclization of enynes* 137

3.3.1. Goal 139

3.3.2. Precedents 139

3.3.3. Results 147

3.3.4. Experimental section 167

3.4. CHAPTER 4. *Ni-catalyzed diborylative cyclization of enynes* 185

3.4.1. Goal 187

3.4.2. Precedents 187

3.4.3. Results 202

3.4.4. Experimental section 215

3.5. CHAPTER 5. *Ni-catalyzed carboborylative cyclization of enynes* 235

3.5.1. Goal 237

3.5.2. Precedents 237

3.5.3. Results 251

3.5.4. Experimental section 264

4. CONCLUSIONES / CONCLUSIONS 279

APPENDICES 287

APPENDIX I: Crystallographic data 289

APPENDIX II: Publications USB

APPENDIX III: NMR spectra USB

APPENDIX IV: Computational studies USB

INTRODUCCIÓN

1. INTRODUCCIÓN

1.1. ÁCIDOS BORÓNICOS Y SUS DERIVADOS

A lo largo de la historia, los ácidos borónicos han sido ampliamente estudiados y utilizados tanto en síntesis orgánica como en numerosas aplicaciones biológicas.

El primer aislamiento de un ácido borónico fue llevado a cabo por Frankland en 1860.[1] En 1979, Suzuki y Miyaura describieron las primeras reacciones de acoplamiento cruzado entre haluros de carbono y ácidos borónicos catalizadas por Pd.[2] Desde ambos descubrimientos hasta el día de hoy, el número de publicaciones y aplicaciones de los ácidos borónicos ha crecido exponencialmente (**Figura I.1**).[3]

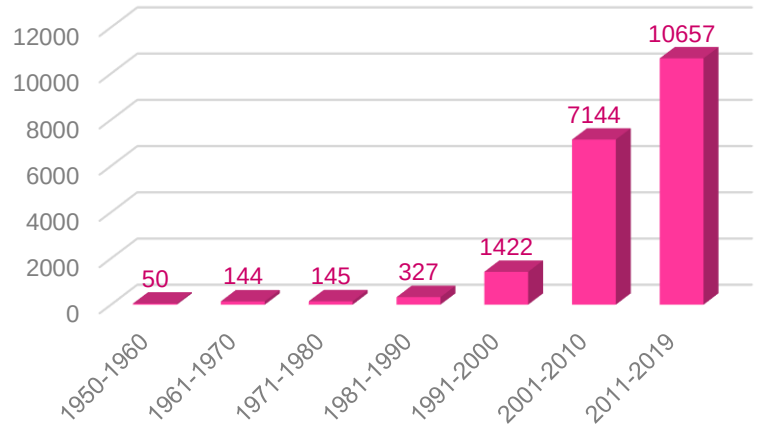

Figura I.1. Publicaciones de ácidos borónicos en los últimos años.

Este hecho refleja la importancia y la gran utilidad de estos compuestos como intermedios sintéticos en química orgánica,[4] destacando su principal aplicación en la formación de enlaces C–C. Tanto es así, que el Premio Nobel de Química de 2010 fue otorgado al Prof. Akira Suzuki, junto con los profesores Richard F. Heck y Ei-ichi Negishi, por sus pioneros trabajos en acoplamientos cruzados catalizados por Pd.

Los ácidos borónicos también han sido evaluados en el campo de la Medicina, concretamente, en el desarrollo de fármacos.[5] Debido a que el boro es similar, aunque diferente al carbono, posee la habilidad de mimetizarse como tal. El empleo de boro como análogo al carbono es una herramienta muy recurrida en química médica. La sustitución de determinados grupos carbonados por ácidos borónicos en productos naturales ha permitido el desarrollo de nuevos medicamentos con actividad biológica antiviral, antibacteriana y

[1] E. Frankland, B. F. Duppa, *Justus Liebigs Ann. Chem.* **1860**, *115*, 319–322.
[2] (a) N. Miyaura, K. Yamada, A. Suzuki, *Tetrahedron Lett.* **1979**, 20, 3437–3444. (b) N. Miyaura, A. Suzuki, *J. Chem. Soc., Chem. Commun.* **1979**, 866–867.
[3] Búsqueda realizada a través de SciFinder®. Sólo se incluyen aquellas publicaciones que contienen el concepto *boronic acid* en su interior.
[4] (a) N. Miyaura, *Bull. Chem. Soc. Jpn.* **2008**, *81*, 1535–1553. (b) L. Xu, S.Zhang, P. Li, *Chem. Soc. Rev.* **2015**, *44*, 8848–8858. (c) J. Carreras, A. Caballero, P. J. Pérez, *Chem. Asian J.* **2019**, *14*, 329–343.
[5] (a) W. Yang, X. Gao, B. Wang, *Med. Res. Rev.* **2003**, *23*, 346–368. (b) H. M. H. G. Albers, L. J. D. Hendrickx, R. J. P. van Tol, J. Hausmann, A. Perrakis, H. Ovaa, *J. Med. Chem.* **2011**, *54*, 4619–4626. (c) Z. J. Leśnikowski, *Expert. Opin. Drug. Dis.* **2016**, *11*, 569–578.

antitumoral.[6] El primer ácido borónico comercializado como fármaco fue el bortezomib, conocido como Velcade®, empleado como agente antitumoral (**Figura I.2**).[7]

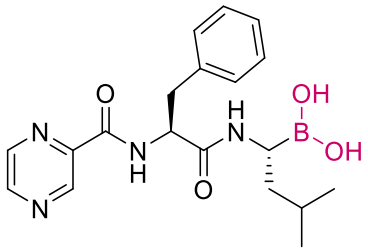

Figura I.2. Estructura del Velcade®.

1.1.1. Estructura y propiedades

La estructura de los ácidos borónicos consiste en un boro trivalente con un sustituyente carbonado y dos grupos hidroxilo. Dicho átomo de boro es deficiente en electrones, ya que solo tiene seis electrones de valencia en sus orbitales con hibridación sp^2. Además, cuenta con un orbital *p* vacío de baja energía ortogonal a los sustituyentes, que se encuentran en disposición de geometría plano trigonal (**Figura I.3,** izquierda).

Los ácidos borónicos no existen como tal en la naturaleza, a diferencia de sus análogos de carbono, los ácidos carboxílicos. Estos compuestos abióticos se sintetizan a partir de fuentes primarias de boro, como el ácido bórico, el cual se obtiene por acidificación del bórax (borato de sodio) con CO_2. Según el nivel de oxidación del borano, encontramos diferentes estructuras (**Figura I.3**): los ácidos borínicos resultan de la primera oxidación del borano, los ácidos borónicos, de la segunda y el ácido bórico, de la tercera oxidación.

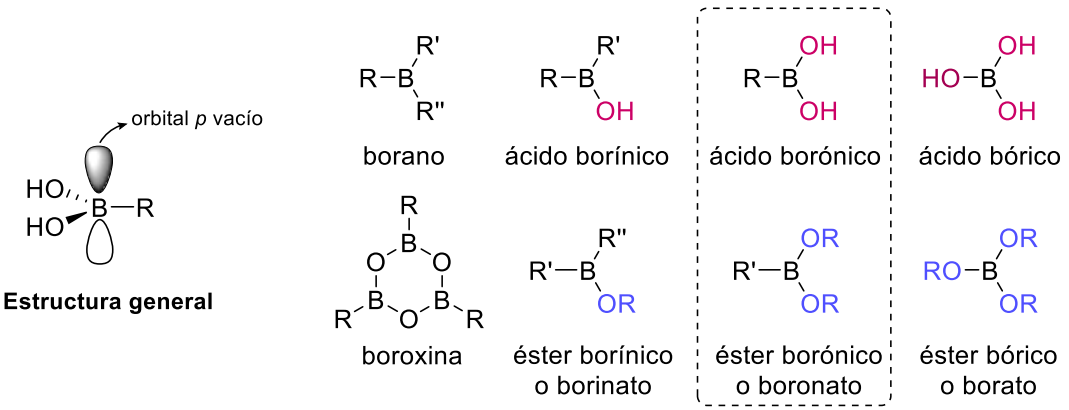

Figura I.3. Estructuras de diferentes compuestos de boro según el grado de oxidación.

Debido a la singular reactividad que ofrecen los ácidos borónicos como ácidos suaves de Lewis, así como su fácil manipulación y alta estabilidad, son considerados una clase de intermedios sintéticos muy atractivos en numerosos procesos. Del mismo modo, los ácidos borónicos se pueden encuadrar dentro de los denominados “compuestos verdes”, ya que

[6] P. C. Trippier, C. McGuigan, *Med. Chem. Commun.* **2010**, *1*, 183–198.
[7] (a) J. A. Adams, M. Behnke, S. Chen, A. A. Cruickshank, L. R. Dick, L. Grenier, J. M. Klunder, Y.-T. Ma, L. Plamondon, R. L. Stein, *Bioorg. Med. Chem. Lett.* **1998**, *8*, 333–338. (b) A. Paramore, S. Frantz, *Nat. Rev.* **2003**, *2*, 611–612 (Drug Discovery).

presentan una baja toxicidad y su degradación final conduce al ácido bórico, que es un compuesto relativamente benigno para el ser humano y respetuoso con el medio ambiente. A pesar de la presencia de los dos grupos hidroxilo en su estructura, los ácidos borónicos se comportan como ácidos de Lewis (ecuación 1, **Esquema I.1**) en lugar de ácidos de Brønsted (ecuación 2, **Esquema I.1**).

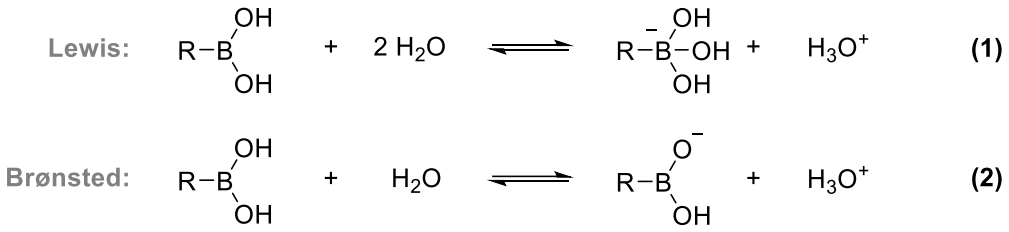

Esquema I.1. Carácter ácido de los ácidos borónicos en agua.

Los ácidos borónicos son sólidos cristalinos químicamente estables que no muestran degradación con el tiempo, incluso a altas temperaturas. Son estables en el agua en un amplio rango de pH y no requieren de medidas específicas para su manejo. Sin embargo, es recomendable almacenarlos en atmósfera inerte para minimizar la posible oxidación. Tienden a existir como mezclas de anhídridos oligoméricos, más concretamente, como boroxinas cíclicas de seis miembros. Generalmente, la presencia de estas boroxinas no provoca problemas en los procesos sintéticos, pero pueden ocasionar inconvenientes a la hora de la caracterización y el análisis. Para evitar la formación de estos anhídridos, los ácidos borónicos se suelen almacenar y comercializar ligeramente húmedos.[8] Además, muchos ácidos borónicos presentan una solubilidad parcial tanto en agua (pH neutro) como en los disolventes orgánicos, dificultando su aislamiento y purificación.

1.1.2. Derivados de ácidos borónicos

Debido a los inconvenientes anteriormente mencionados que presenta el empleo de ácidos borónicos, los ésteres borónicos son extensamente utilizados en su lugar como intermedios sintéticos, donde ambos grupos hidroxilos se encuentran protegidos. Por otro lado, la transformación de los grupos hidroxilo en otros sustituyentes, como por ejemplo fluoruros, permite incrementar la reactividad de estos compuestos y extender su aplicación a otros procesos. A continuación, se describen algunos de los derivados más representativos.

1.1.2.1. Ésteres borónicos

La sustitución de los grupos hidroxilo presentes en los ácidos borónicos por grupos alcoxi o ariloxi conduce a la obtención de ésteres borónicos. Como consecuencia, se pierde la posibilidad de formación de enlaces de hidrógeno entre grupos hidroxilo, siendo los ésteres borónicos menos polares y más fácilmente manejables que los correspondientes ácidos. Existe una gran diversidad estructural de ésteres borónicos empleados en procesos sintéticos (**Figura I.4**).

Desde un punto de vista termodinámico, la estabilidad de los enlaces B–O en los ésteres borónicos es comparable con la de los ácidos borónicos. Por lo tanto, se debe tener en

[8] Presumiblemente, la coordinación de agua o de iones hidróxido al boro ayuda a proteger a los ácidos borónicos de la acción del oxígeno. (a) J. R. Johnson, M. G. Van Campen, O. Grummitt, *J. Am. Chem. Soc.* **1938**, *60*, 111–115. (b) J. R. Johnson, M. G. Van Campen, *J. Am. Chem. Soc.* **1938**, *60*, 121–124.

cuenta la posible hidrólisis de los mismos durante su manipulación. Concretamente, la hidrólisis tiene lugar de forma muy rápida en los ésteres acíclicos (**A**) y de poco impedimento estérico como los derivados del etilen- y propilenglicol (**B1** y **B2**) y los derivados del tartrato (**C1**). Los ésteres de catecol (**H**) poseen mayor carácter de ácido de Lewis debido a la conjugación opuesta entre los oxígenos y el anillo de benceno, siendo más susceptibles de sufrir la hidrólisis y, generalmente, son inestables a la cromatografía en gel de sílice. Por el contrario, la hidrólisis puede verse drásticamente reducida en el caso de ésteres cíclicos impedidos (**D** y **J**), derivados del pinacol (**I**), del pinanodiol (**K**) y del alcanfor (**L1** y **L2**). Estos tipos de ésteres presentan una mayor estabilidad ante tratamientos acuosos y ante la purificación mediante cromatografía en gel de sílice.

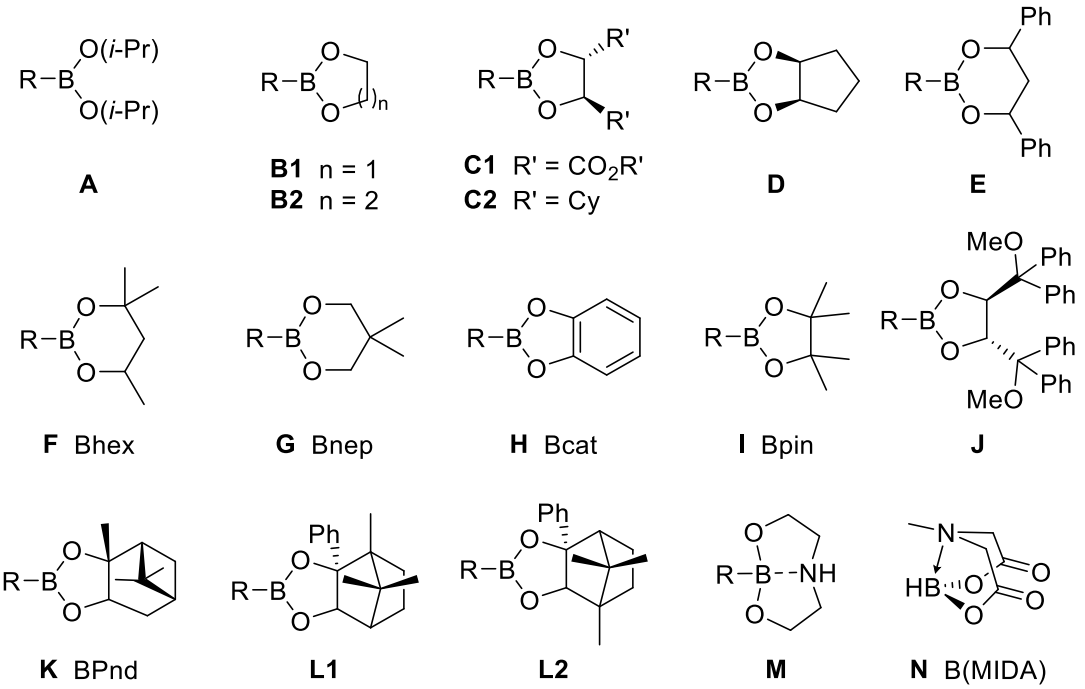

Figura I.4. Ésteres borónicos comúnmente empleados.

Determinados compuestos son tan resistentes a la hidrólisis que son empleados como grupos protectores de los ácidos borónicos (**J**, **K**, **L1** y **L2**), requiriendo transformaciones previas a la hidrólisis como, por ejemplo, su derivatización a sales de difluoro- o trifluoroborato, para recuperar de nuevo el correspondiente ácido borónico. Los ésteres borónicos de aminas (**M** y **N**) representan una clase muy útil de derivados, ya que la coordinación interna entre el par de electrones desapareado del nitrógeno y el orbital vacante del boro confiere unas características únicas a este tipo de compuestos. En particular, esa coordinación dificulta tanto la hidrólisis como la oxidación del átomo de boro, confiriéndoles una gran estabilidad.

1.1.2.2. Ésteres diborínicos

Los ésteres diborínicos presentan dos ésteres borónicos en su estructura unidos mediante un enlace B–B. Estos derivados pueden ser preparados por condensación del correspondiente diol con tetrakis(dimetilamino)diboro (ecuación 1, **Esquema I.2**).[9] En 2003, Hartwig describió un proceso más sencillo para su síntesis basado en el homoacoplamiento

[9] T. Ishiyama, M. Murata, T.-a. Ahiko, N. Miyaura, *Org. Synth.* **2000**, *77*, 176–182.

de diferentes derivados de clorocatecolborano mediante el empleo de una amalgama de Na/Hg (ecuación 2, **Esquema I.2**).[10]

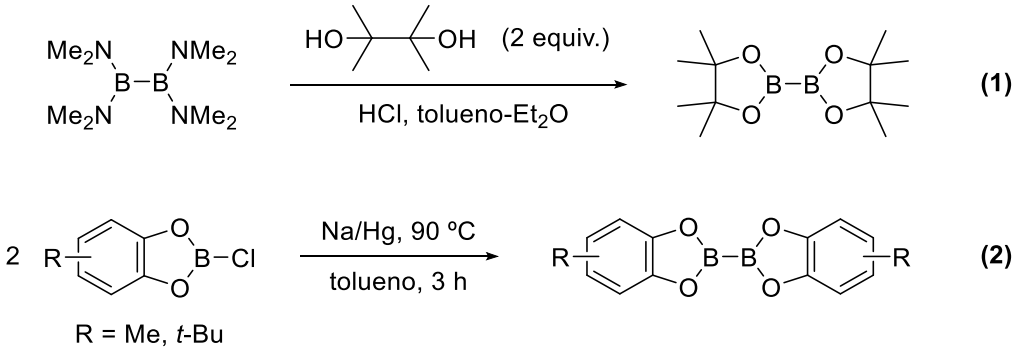

Esquema I.2. Síntesis de ésteres diborínicos.

Los ésteres diborínicos se emplean en numerosas reacciones de diboración de especies insaturadas,[11] siendo los más frecuentes los derivados del pinacol (B_2pin_2), del catecol (B_2cat_2) y del neopentilglicol (B_2nep_2), existiendo también reactivos mixtos (pinB-Bdan) donde uno de los ácidos borónicos se encuentra protegido mediante una diamina (**Figura I.5**). Estos últimos, permiten llevar a cabo diboraciones de forma regioselectiva.[12]

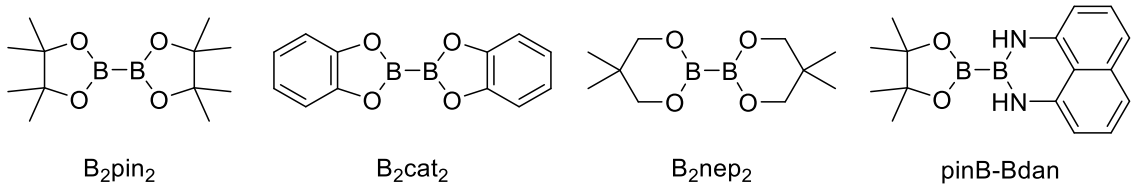

Figura I.5. Ésteres diborínicos más frecuentes.

1.1.2.3. Dialcoxiboranos

Los dialcoxiboranos son fácilmente sintetizados mediante la reacción estequiométrica entre borano y el correspondiente diol. Los derivados del pinacol (HBpin) y del catecol (HBcat) son utilizados con mayor frecuencia (**Figura I.6**). Su aplicación fundamental se centra en reacciones de hidroboración,[13] pero también son ampliamente empleados como agentes borilantes en reacciones de acoplamiento cruzado.

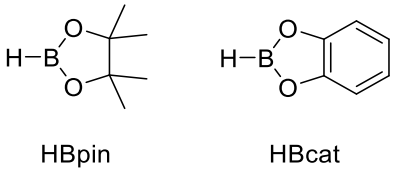

Figura I.6. Dialcoxiboranos más comunes.

[10] N. R. Anastasi, K. M. Waltz, W. L. Weerakoon, J. F. Hartwig, *Organometallics* **2003**, *22*, 365–369.
[11] Ver apartado *1.1.3.6. Bismetalación.*
[12] (a) N. Iwadate, M. Suginome, *J. Am. Chem. Soc.* **2010**, *132*, 2548–2549. (b) N. Miralles, J. Cid, A. B. Cuenca, J. J. Carbó, E. Fernández, *Chem. Commun.* **2015**, *51*, 1693–1696. (c) X. Guo, A. K. Nelson, C. Slebodnick, W. L. Santos, *ACS Catal.* **2015**, *5*, 2172–2176. (d) A. B. Cuenca, J. Cid, D. García-López, J. J. Carbó, E. Fernández, *Org. Biomol. Chem.* **2015**, *13*, 9659–9664. (e) S. Krautwald, M. J. Bezdek, P. J. Chirik, *J. Am. Chem. Soc.* **2017**, *139*, 3868–3875. (f) A. Verma, R. F. Snead, Y. Dai, C. Slebodnick, Y. Yang, H. Yu, F. Yao, W. L. Santos, *Angew. Chem. Int. Ed.* **2017**, *56*, 5111–5115. (g) S. Peng, G. Liu, Z. Huang, *Org. Lett.* **2018**, *20*, 7363–7366.
[13] Ver apartado *1.1.3.5. Hidroboración*.

1.1.2.4. Sales de trifluoroborato

Las sales de organotrifluoroborato son derivados cristalinos, estables y fáciles de manejar. La ausencia del orbital vacío sobre el B tiene como consecuencia que el enlace C–B se pueda mantener intacto mientras se llevan a cabo otras transformaciones en la estructura, como por ejemplo la epoxidación de un doble enlace (ecuación 1, **Esquema I.3**).[14]

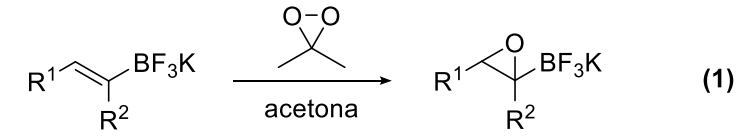

(1)

R^1 = H, $R_{Alquilo}$, Ph
R^2 = H, Me

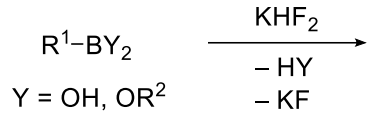

(2)

Esquema I.3. Reacciones con sales de organotrifluoroborato.

Estos compuestos pueden ser preparados mediante el método descrito por Vedejs, a partir tanto de ácidos borónicos[15] como de ésteres borónicos[16] (ecuación 2, **Esquema I.3**). Las sales de trifluoroborato han sido ampliamente utilizadas a lo largo de los últimos años.[17] Cabe destacar el trabajo realizado por el grupo de Molander, donde describen numerosas reacciones de acoplamiento cruzado de Suzuki-Miyaura de alquiltrifluoroboratos.[18]

1.1.2.5. Boroxinas

Las boroxinas son los anhídridos ciclotriméricos de los ácidos borónicos. Se caracterizan por ser isoelectrónicas con el benceno, pudiendo tener un ligero carácter aromático en función del orbital *p* vacante del átomo de boro. Se obtienen fácilmente a partir de la deshidratación de los ácidos borónicos mediante destilación azeotrópica del agua o bien secado exhaustivo con H_2SO_4 o pentóxido de fósforo.[19]

Las boroxinas se pueden emplear en diversos procesos sintéticos similares a los que emplean ácidos borónicos. Sin embargo, su aplicación más inmediata se destina a la fabricación de materiales ignífugos y funcionales.[20]

---

[14] G. A. Molander, M. Ribagorda, *J. Am. Chem. Soc.* **2003**, *125*, 11148–11149.
[15] (a) E. Vedejs, R. W. Chapman, S. C. Fields, S. Lin, M. R. Schrimpf, *J. Org. Chem.* **1995**, *60*, 3020–3027. (b) E. Vedejs, S. C. Fields, R. Hayashi, S. R. Hitchcock, D. R. Powell, M. R. Schrimpf, *J. Am. Chem. Soc.* **1999**, *121*, 2460–2470.
[16] D. S. Matteson, G. Y. Kim, *Org. Lett.* **2002**, *4*, 2153–2155.
[17] (a) S. Darses, J.-P. Genet, *Eur. J. Org. Chem.* **2003**, 4313–4327. (b) S. Darses, J.-P. Genet, *Chem. Rev.* **2008**, *108*, 288–325. (c) H. Doucer, *Eur. J. Org. Chem.* **2008**, 2013–2030.
[18] (a) G. A. Molander, D. Pfeiffer, *Org. Lett.* **2001**, *3*, 361–363. (b) G. A. Molander, Y. Yokoyama, *J. Org. Chem.* **2006**, *71*, 2493–2498 (c) G. A. Molander, J. Hama, D. G. Seapy, *Tetrahedron* **2007**, *63,* 768–775. (d) G. A. Molander, N. Ellis, *Acc. Chem. Res.* **2007**, *40*, 275–286. (e) S. D. Dreher, S.-E. Lim, D. L. Sandrock, G. A. Molander, *J. Org. Chem.* **2009**, *74*, 3626–3631. (f) G. A. Molander, L. Jean-Gérard. *J. Org. Chem.* **2009**, *74*, 5446–5450. (g) G. A. Molander, B. Canturk, *Angew. Chem. Int. Ed.* **2009**, *48*, 9240–9261.
[19] H. R. Snyder, J. A. Kuck, J. R. Johnson, *J. Am. Chem. Soc.* **1938**, *60*, 105–111.
[20] A. L. Korich, P. M. Iovine, *Dalton Trans.* **2010**, *39*, 1423–1431.

1.1.2.6. Alquinilboronatos

Los alquinilboronatos son otro tipo de derivados de los ácidos borónicos extensamente utilizados en síntesis orgánica.[21] Su síntesis más general consiste en hacer reaccionar reactivos de alquinillitio con B(*i*-PrO)$_3$, seguido de una etapa final de hidrólisis con HCl (**Esquema I.4**). Estos derivados de boro se emplean frecuentemente en cicloadiciones.[22]

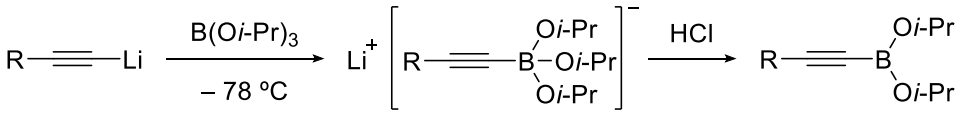

Esquema I.4. Procedimiento común de síntesis de alquinilboronatos.

1.1.3. Métodos de síntesis de ácidos y ésteres borónicos

En la bibliografía, existen numerosos ejemplos descritos para la síntesis de ácidos y ésteres borónicos, debido a su creciente importancia como intermedios sintéticos.[23] A continuación, se describen algunos de los más relevantes y actuales.

1.1.3.1. Captura de intermedios organometálicos con boratos

Este método implica la reacción entre un intermedio organometálico fuertemente nucleófilo, generalmente derivados de Li o Mg, y un éster bórico (ecuación 1, **Esquema I.5**). Este procedimiento puede ser extendido a numerosos sustratos, destacando su aplicación en la formación de aril-[24] y alquenilboronatos[25] a partir tanto de bromuros como de yoduros. Además, se pueden obtener los correspondientes ácidos borónicos mediante una hidrólisis ácida como etapa final. A pesar de su utilidad, este método presenta el inconveniente de una baja compatibilidad de grupos funcionales debido a la nucleofilia y basicidad de los organometálicos empleados, requiriendo también el empleo de bajas temperaturas y condiciones estrictamente anhidras. Otro proceso similar para la síntesis de los derivados aromáticos es la orto-metalación,[26] en la cual se requiere la presencia de un grupo director coordinante en la estructura, tales como aminas, amidas, ésteres, etc. (ecuación 2, **Esquema I.5**).

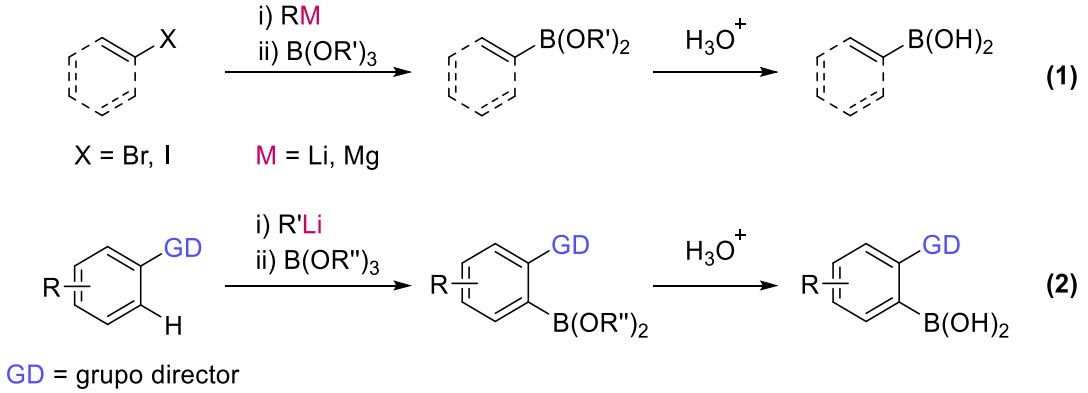

Esquema I.5. Esquema general de captura de intermedios organometálicos con boratos.

---

[21] (a) G. M. L. Cragg, K. R. Koch, *Chem. Soc. Rev.* **1977**, *6*, 393–412. (b) A. Suzuki, *Acc. Chem. Res.* **1982**, *15*, 178–184. (c) Jiao J, Y. Nishihara, *J. Organomet. Chem.* **2012**, *721–722*, 3–16.
[22] G. Hilt, P. Bolze, *Synthesis* **2005**, 2091–2115.
[23] D. G. Hall, *Boronic Acids: Preparation and Applications in Organic Synthesis, Medicine and Materials*, (Ed. D. G. Hall), Wiley-VCH, Weinheim, **2011**.
[24] S. Das, V. L. Alexeev, A. C. Sharma, S. J. Geib, S. A. Asher, *Tetrahedron Lett.* **2003**, *44,* 7719–7722.
[25] J. Uenishi, K.Matsui, A. Wada, *Tetrahedron Lett.* **2003**, *44,* 3093–3096.
[26] M. Lauer, G. Wulff, *J. Organomet. Chem.* **1983**, *256*, 1–9.

1.1.3.2. Transmetalación de arilsilanos

Uno de los primeros métodos empleados para la síntesis de ácidos arilborónicos es la transmetalación directa entre trialquilarilsilanos y haluros de boro fuertes, como el BBr_3 (**Esquema I.6**).[27] El carácter espontáneo de esta reacción se basa en la mayor estabilidad de los enlaces C–B y Si–Br formados frente a los correspondientes enlaces C–Si y B–Br de los sustratos de partida. Los arildibromuros de boro obtenidos pueden hidrolizarse para obtener los ácidos arilborónicos correspondientes o emplearse *in situ* en acoplamientos de tipo Suzuki catalizados por Pd.

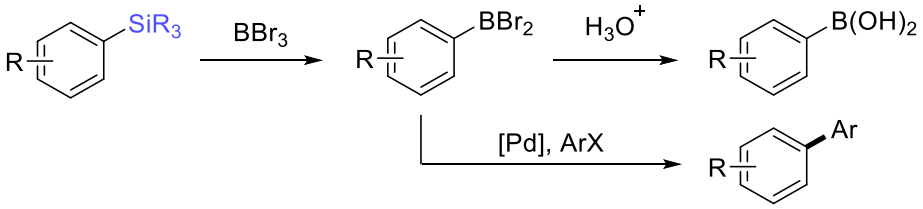

Esquema I.6. Esquema general de transmetalación.

1.1.3.3. Reacción de Miyaura

En 1995, Miyaura describió la reacción de acoplamiento de haloarenos y ésteres diborínicos catalizada por Pd (**Esquema I.7**).[28] Este método requiere unas condiciones de reacción más suaves que el procedimiento anterior, permitiendo la síntesis de nuevos ésteres borónicos con diversos grupos funcionales en su estructura. Con el tiempo, este procedimiento ha sido extendido a derivados de alquenilo, pudiendo acoplar tanto bromuros y yoduros como triflatos.[29]

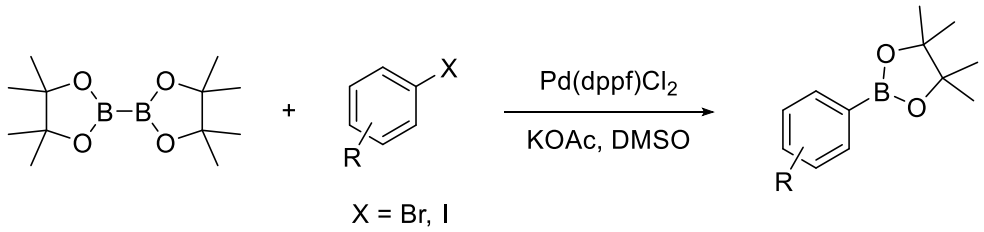

Esquema I.7. Condiciones generales de la reacción de Miyaura.

Esta reacción procede por un mecanismo con las etapas tradicionales de las reacciones de acoplamiento (**Figura I.7**). En primer lugar, se propone la adición oxidante del haloareno a la especie catalíticamente activa de Pd(0), generando una especie de Pd(II). Sobre esta especie, y mediante la acción de la base, se produce un intercambio X/OAc. La especie de acetoxipaladio (II) obtenida da lugar a una transmetalación con el reactivo de bis(pinacolato)diboro, para liberar el producto de acoplamiento deseado tras sufrir una eliminación reductora que regenera la especie inicial de Pd(0).

[27] (a) M.J. Sharp, W. Cheng, V. Snieckus, *Tetrahedron Lett.* **1987**, *28*, 5093–5096. (b) K.Itami, T.Kamei, J.-i. Yoshida, *J. Am. Chem. Soc.* **2003**, *125*, 14670–14671. (c) Z. Zhao, V. Snieckus, *Org. Lett.* **2005**, *7*, 2523–2526.
[28] T. Ishiyama, M. Murata, N. Miyaura, *J. Org. Chem.* **1995**, *60*, 7508–7510.
[29] (a) J.Takagi, K. Takahashi, T. Ishiyama, N. Miyaura, *J. Am. Chem. Soc.* **2002**, *124*, 8001–8006. (b) T. Ishiyama, J. Takagi, A. Kamon, N. Miyaura, *J. Organomet. Chem.* **2003**, *687*, 284–290.

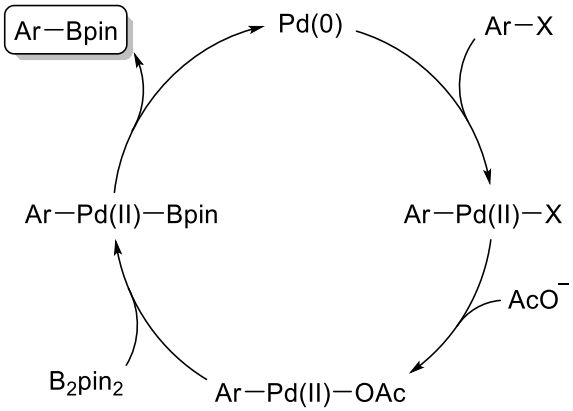

Figura I.7. Ciclo catalítico de la reacción de Miyaura.

1.1.3.4. Activación C–H

Una estrategia más atractiva para la síntesis de organoboranos es la funcionalización de enlaces C–H catalizadas por metales de transición (**Esquema I.8**). Esta aproximación da lugar a reacciones átomo-económicas, eficientes, versátiles y respetuosas con el medio ambiente. Los catalizadores empleados se basan, mayoritariamente, en complejos de Rh, Ru, Pd e Ir, utilizando HBpin o B_2pin_2 como agentes borilantes.[30] Este tipo de funcionalización se ha conseguido llevar a cabo sobre una gran variedad de sustratos aromáticos, bencílicos, alifáticos y olefínicos.

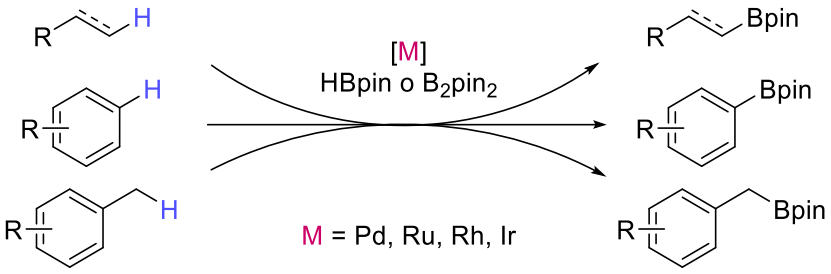

Esquema I.8. Resumen de borilaciones mediante activación C–H.

1.1.3.5. Hidroboración

Desde 1956, cuando Herbert C. Brown describió por primera vez la hidroboración de alquenos,[31] gracias a la cual recibió el premio Nobel de Química de 1979, hasta la actualidad, la hidroboración de especies insaturadas se ha convertido en uno de los métodos más empleados para la síntesis de compuestos de organoboro. Los métodos más primitivos se caracterizan por ser procesos no catalizados. No obstante, durante las últimas décadas se ha descrito una amplia gama de procesos de hidroboración de especies insaturadas catalizados[32] y/o mediados por metales.[33]

---

[30] (a) I. A. I. Mkhalid, J. H. Barnard, T. B. Marder, J. M. Murphy, J. F. Hartwig, *Chem. Rev.* **2010**, *110,* 890–931. (b) J. F. Hartwig, *Chem. Soc. Rev.* **2011**, *40*, 1992–2002.
[31] H. C. Brown, B. C. Subba Rao, *J. Am. Chem. Soc.* **1956**, *78*, 5694–5695.
[32] (a) I. Beletskaya, A. Pelter, *Tetrahedron* **1997**, *53*, 4957–5026. (b) C. M. Vogels, S. A. Westcott, *Curr. Org. Chem.* **2005**, *9*, 687–699.
[33] K. Burgess, M. J. Ohlmeyer, *Chem. Rev.* **1991**, *91*, 1179–1191.

En los procesos no catalizados, la fuente de boro más empleada es el borano (en la naturaleza existe como B_2H_6, siendo formalmente "BH_3"). Este reactivo suele dar lugar a hidroboraciones con regioquímica *anti*-Markovnikov y estereoquímica *sin*, pudiendo reaccionar hasta tres veces en el mismo proceso según el impedimento estérico de la molécula (**Esquema I.9**). El empleo de reactivos de boro disustituidos impedidos (9-BBN, $HB(sia)_2$) permite una mejor regio- y diastereoselectividad en las hidroboraciones. Los procesos de hidroboración se pueden aplicar a alquenos y alquinos, obteniendo alquil- y alquenilboronatos, respectivamente. En síntesis, se emplea comúnmente combinado con una etapa posterior de oxidación.

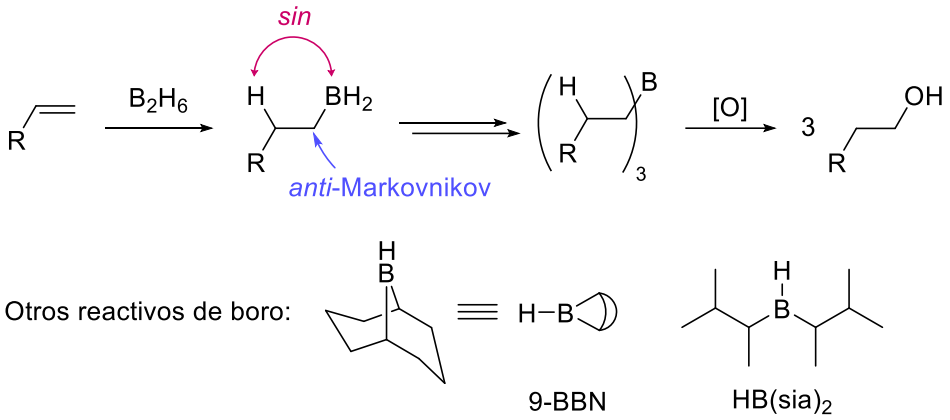

Esquema I.9. Hidroboraciones de alquenos no catalizadas.

El empleo de metales de transición en las hidroboraciones acelera la adición del enlace H–B a las especies insaturadas, permitiendo además modular la regio- y estereoselectividad de la reacción. En este ámbito, el empleo de complejos de Rh juega un papel fundamental, permitiendo obtener selectivamente productos Markovnikov o *anti*-Markovnikov,[34] y desarrollando versiones enantioselectivas en muchas hidroboraciones.[35] Sin embargo, debido a la necesidad de una química más verde y comprometida con el medioambiente, el empleo de estos metales genera un gran inconveniente a nivel económico y de toxicidad. Es por ello que el empleo de los metales de la primera serie de transición para la catálisis de estas reacciones ha crecido exponencialmente en los últimos años.[36] A lo largo de la presente Tesis Doctoral, se describirán de forma más específica estos procesos.

1.1.3.6. Bismetalación

A lo largo de este apartado nos referiremos con el término "metal" al boro. Aunque en rigor este término no es correcto, se viene empleando así debido a la menor electronegatividad del B en relación al C. De modo análogo, también se habla de "metales" en este contexto en el caso de otros elementos de grupos principales como el Si.

De un modo similar a la hidroboración, el empleo de especies bimetálicas de boro ha permitido el desarrollo de útiles procesos sintéticos para la obtención de ésteres borónicos.[37] Según el reactivo utilizado, se pueden clasificar en reacciones de diboración (B–B),

[34] G. Fu, *Transition Metals for Organic Synthesis*, Vol. 2, (Ed. M. Beller, C. Bolm), Weinheim, **2004**, 193–198.
[35] (a) C. M. Crudden, D. Edwards, *Eur. J. Org. Chem.* **2003**, 4695–4712. (b) A.-M. Carroll, T. P. O'Sullivan, P. J. Guiry, *Adv. Synth. Catal.* **2005**, *347*, 609–631.
[36] J. Chen, J. Guo, Z. Lu, *Chin. J. Chem.* **2018**, *36*, 1075–1109.
[37] (a) I. Beletskaya, C. Moberg, *Chem. Rev.* **1999**, *99*, 3435−3461. (b) I. Beletskaya, C. Moberg, *Chem. Rev.* **2006**, *106*, 2320–2354. (c) H. Y. Cho, J. P. Morken, *Chem. Soc. Rev.* **2014**, *43*, 4368–4380.

borilsililación (B–Si) y borilestannilación (B–Sn) (**Esquema I.10**). Este tipo de reacciones presentan la gran ventaja de realizar una doble funcionalización en la estructura, pudiendo transformar estos grupos funcionales de forma selectiva y secuencial. En la mayoría de los casos, se propone la adición oxidante del enlace B–(B,Si,Sn) como etapa inicial del proceso.

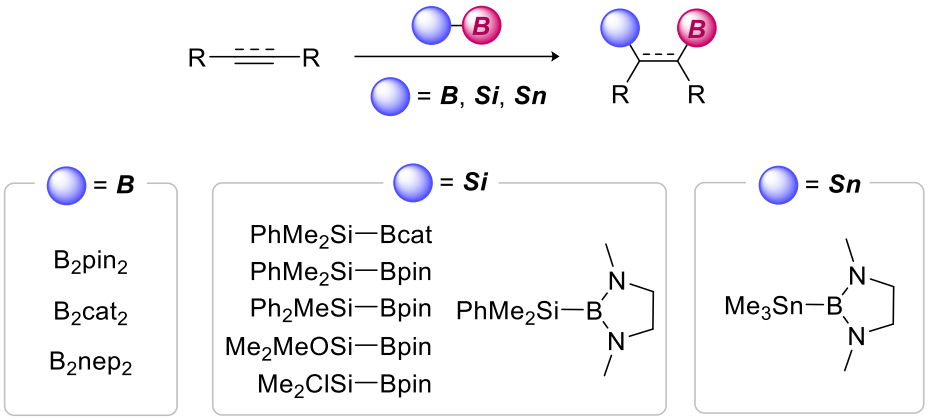

Esquema I.10. Esquema general de bismetalaciones.

Dentro de las diboraciones, se conocen una gran variedad de ejemplos catalizados por metales de transición (Pd, Pt, Rh, Ag, Au, Ir, Cu) sobre sustratos de tipo alqueno, alquino, dieno y aleno.[38] La versión asimétrica de algunas de estas diboraciones también ha sido estudiada.[39] Del mismo modo, se conocen ejemplos de diboraciones no catalizadas.[40] Las 1,2-diboraciones de especies monoinsaturadas son las más comunes, pero también se han descritos algunos ejemplos de diboraciones geminales catalizas por Co, Pd, Pt, Ir y Rh, y no catalizadas.[41]

Las reacciones con reactivos bimetálicos de B–Sn[42] han sido menos desarrolladas en comparación con las de B–Si, de las que se conocen ejemplos catalizados por Pd y Pt,[43] así como procesos de ciclación borilsililativa sobre 1,6-eninos y 1,7-diinos.[44] En este tipo de reacciones, la catálisis con complejos de Ni también ha sido evaluada,[45] llevando a cabo la borilsililación de alquenos, alquinos y dienos, incluyendo un ejemplo de ciclación con diinos.

[38] (a) T. B. Marder, N. C. Norman, *Top. Catal.* **1998**, *5*, 63–73. (b) T. Ishiyama, N. Miyaura, *J. Organomet. Chem.* **2000**, *611*, 392–402. (c) J. Takaya, N. Iwasawa, *ACS Catal.* **2012**, *2*, 1993–2006.
[39] (a) J. Ramírez, V. Lillo, A. M. Segarra, E. Fernández, *C. R. Chimie* **2007**, *10*, 138–151. (b) J. M. Brown. B. N. Nguyen, *Science of Synthesis, 1: Stereoselective Synthesis 1* (Ed. J. G. de Vries), **2011**, 295–324.
[40] F. Zhao, X. Jia, P. Li, J. Zhao, Y. Zhou, J. Wang, H. Liu, *Org. Chem. Front.* **2017**, *4*, 2235–2255.
[41] J. Royes, A. B. Cuenca, E. Fernández, *Eur. J. Org. Chem.* **2018**, 2728–2739.
[42] (a) S.-y. Onozawa, Y. Hatanaka, T. Sakakura, S. Shimada, M. Tanaka, *Organometallics* **1996**, *15,* 5450–5452. (b) S.-y. Onozawa, Y. Hatanaka, M. Tanaka, *Chem. Commun.* **1999**, 1863–1864. (c) R. R. Singidi, T. V. RajanBabu, *Org. Lett.* **2010**, *12*, 2622–2625.
[43] T. Ohmura, M. Suginome, *Bull. Chem. Soc. Jpn.* **2009**, *82*, 29–49.
[44] (a) M. Gerdin, S. K. Nadakudity, C. Worch, C. Moberg, *Adv. Synth. Catal.* **2010**, *352*, 2559–2570. (b) Y.-C. Xiao, C. Moberg, *Org. Lett.* **2016**, *18*, 308−311. (c) Q. Zhang, Q.-J. Liang, J.-L. Xu, Y.-H. Xu, T.-P. Loh, *Chem. Commun.* **2018**, *54*, 2357–2360.
[45] (a) M.Suginome, T. Matsuda, Y. Ito, *Organometallics* **1998**, *17,* 5233–5235. (b) M. Suginome, T. Matsuda, T. Yoshimoto, Y. Ito, *Org. Lett.* **1999**, *1*, 1567–1569. (c) M. Suginome, T. Matsuda, T. Yoshimoto, Y. Ito, *Organometallics* **2002**, *21,* 1537–1539.

1.1.4. Transformaciones de los compuestos de organoboro

La mayoría de los derivados borilados descritos anteriormente pueden emplearse como punto de partida para diversas derivatizaciones, siendo los ácidos y los ésteres borónicos junto con las sales de trifluoroborato los que aportan los mejores resultados.[46] En el **Esquema I.11**, se muestran algunas de las transformaciones más comunes. De todas ellas, y sin lugar a dudas, la reacción de acoplamiento cruzado de tipo Suzuki es la más extensamente empleada en el ámbito de la síntesis orgánica.[47] El abanico de posibilidades tan amplio que ofrece esta reacción, para la formación de enlaces C(sp^2)–C(sp^2), C(sp^2)–C(sp^3) y C(sp^3)–C(sp^3), ha provocado que los derivados de organoboro se utilicen reiteradamente como intermedios sintéticos en procesos de síntesis total.[48]

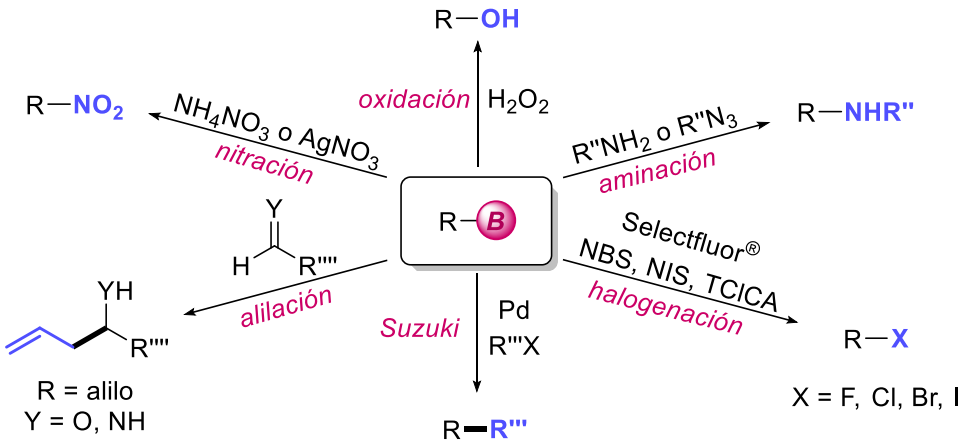

Esquema I.11. Transformaciones comunes de los compuestos de organoboro.

La sinergia entre procesos borilativos y posteriores transformaciones permite obtener moléculas complejas con diferentes funcionalidades en su estructura en pocos pasos de reacción. Este hecho reitera una vez más la transcendencia que tiene el desarrollo de nuevos procesos sintéticos de compuestos de organoboro para la química moderna.

[46] (a) C. Zhu, J. R. Falck, *Adv. Synth. Catal.* **2014**, *356*, 2395–2410. (b) J. W. B. Fyfe, A. J. B. Watson, *Chem.* **2017**, *3*, 31–55.
[47] (a) A. Suzuki, *Heterocycles* **2010**, *80*, 15–43. (b) C. M. Crudden, B. W. Glasspoole, C. J. Lata, *Chem. Commun.* **2009**, 6704–6716. (c) A. J. J. Lennox, G. C. Lloyd-Jones, *Chem. Soc. Rev.* **2014**, *43*, 412–443.
[48] F. Meng, K. P. McGrath, A. H. Hoveyda, *Nature* **2014**, *513*, 367–374.

1.2. REACCIONES DE CICLACIÓN DE ENINOS

Las reacciones de ciclación de especies poliinsaturadas ha sido una herramienta sintética muy empleada a lo largo de la historia de la química. Su empleo ha permitido sintetizar una gran variedad de carbo- y heterociclos, siendo los ciclos de 5 y 6 miembros los más frecuentemente obtenidos. No obstante, estas ciclaciones también han sido utilizadas para la síntesis de macrociclos de hasta 19 unidades. Esta metodología permite, a partir de sencillos precursores acíclicos, obtener moléculas cíclicas de una elevada complejidad estructural en una sola etapa sintética, pudiendo llevarse a cabo a gran escala en la mayoría de los casos. A diferencia de las ciclaciones que emplean haloderivados, la elección de especies poliinsaturadas como sustratos de partida evita la formación de subproductos no deseados, manteniendo así la economía atómica de la reacción.

1.2.1. Aspectos generales de las cicloisomerizaciones

Dentro de las reacciones de ciclación, el proceso conocido como cicloisomerización ha sido uno de los más estudiados. Una cicloisomerización se define como aquella reacción en la que una insaturación C–C o C–heteroátomo se isomeriza, generando uno o más sistemas cíclicos, con la consecuente pérdida de una o más insaturaciones y sin observar ganancia o pérdida formal de átomos.[49] En este ámbito, los eninos juegan un papel fundamental, ofreciendo una reactividad muy variada (**Esquema I.12**).

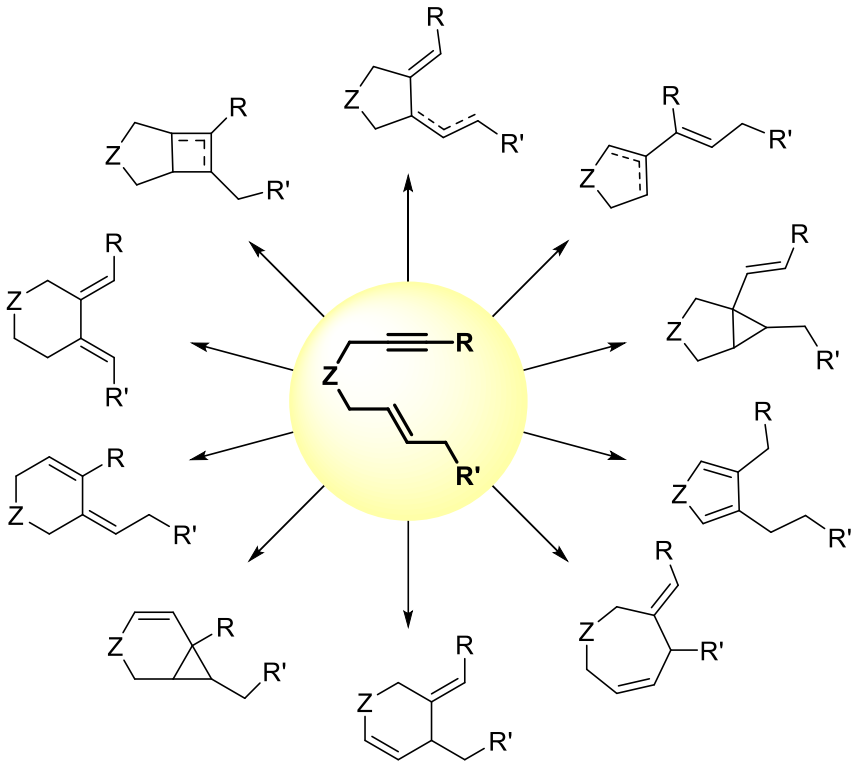

Esquema I.12. Estructuras que ofrece la cicloisomerización de 1,6-eninos.

Estas cicloisomerizaciones pueden ser incluidas dentro de las ciclaciones de tipo Alder-eno, descubiertas por Trost en 1984.[50] Este tipo de transformación consiste en la migración 1,5 del hidrógeno alílico de un alqueno a un enlace múltiple, conduciendo a la formación de un

[49] G. C. Lloyd-Jones, *Org. Biomol. Chem.* **2003**, *1*, 215–236.
[50] B. M. Trost, M. Lautens, M.-H. Hung, C. S. Carmichael, *J. Am. Chem. Soc.* **1984**, *106*, 7641–7643.

enlace σ y la migración de un enlace π con subsecuente formación de una estructura cíclica (**Esquema I.13**).

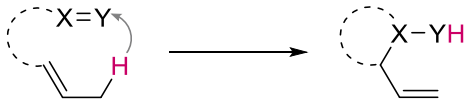

Esquema I.13. Reacción de tipo Alder-eno.

El empleo de metales de transición como catalizadores de cicloisomerizaciones ha sido esencial para el desarrollo de métodos sintéticos eficientes, lográndose la formación selectiva de enlaces C–C muy difíciles o imposibles de conseguir con reactivos convencionales. De entre todos los metales de transición, los más utilizados han sido Pd, Pt, Ru, Rh, Ir, Ga, In, Au, y Ag, debido a la versatilidad y la diferente reactividad que muestran.[51] Además, el empleo de auxiliares quirales ha permitido desarrollar versiones enantioselectivas de estas reacciones,[52] encontrando su aplicación principal en la síntesis total de productos naturales.[53]

Las reacciones de cicloisomerización se pueden clasificar según el mecanismo que tiene lugar, dependiendo principalmente del tipo de catalizador empleado. Se pueden distinguir hasta cinco vías de activación, donde una o las dos insaturaciones presentes pueden ser activadas desde el principio o en diferentes etapas del ciclo. Así mismo, estas cicloisomerizaciones se pueden dividir en dos grandes grupos: las que dan lugar a una reorganización del esqueleto de la molécula y las que no.

1.2.1.1. Cicloisomerizaciones sin transposición del esqueleto

Dentro del primer grupo, encontramos tres tipos de mecanismos de activación (**Esquema I.14**). La ciclometalación oxidante (*ruta a*) supone la activación de ambas insaturaciones por acción del metal, el cual aumenta su estado de oxidación en dos unidades al generar el metalaciclo correspondiente. El mecanismo denominado metal π-alilo (*ruta b*) es menos común, requiriendo la activación inicial del enlace C–H del alilo. En muchos de los casos, se requiere una sustitución adecuada del alilo con un grupo saliente para que este proceso tenga lugar. Por último, la hidrometalación (*ruta c*) tiene lugar cuando se genera un hidruro metálico que inicia el mecanismo por la insaturación del alquino, generando el correspondiente vinil metal. A parte de la etapa final de eliminación del metal, los complejos metálicos pueden sufrir otro tipo de transformaciones como eliminación reductora, ruptura con una especie electrófila o acoplamientos con una especie organometálica.

[51] (a) C. Aubert, O. Buisine, M. Malacria, *Chem. Rev.* **2002**, *102,* 813–834. (b) V. Michelet, P. Y. Toullec, J.-P. Genêt, *Angew. Chem. Int. Ed.* **2008**, *47*, 4268–4315. (c) M. T. Quirós, M. P. Muñoz, *Top. Heterocycl. Chem.* **2016**, *46*, 117–174.
[52] (a) A. Marinetti, H. Jullien, A. Voituriez, *Chem. Soc. Rev.* **2012**, *41*, 4884–4908. (b) I. D. G. Watson, F. D. Toste, *Chem. Sci.* **2012**, *3*, 2899–2919.
[53] (a) K. C. Nicolaou, P. G. Bulger, D. Sarlah, *Angew. Chem. Int. Ed.* **2005**, *44*, 4490–4527. (b) C. I. Stathakis, P. L. Gkizisa, A. L. Zografos, *Nat. Prod. Rep.* **2016**, *33*, 1093–1117. (c) Y. Hu, M. Bai, Y. Yang, Q. Zhou, *Org. Chem. Front.* **2017**, *4*, 2256–2275.

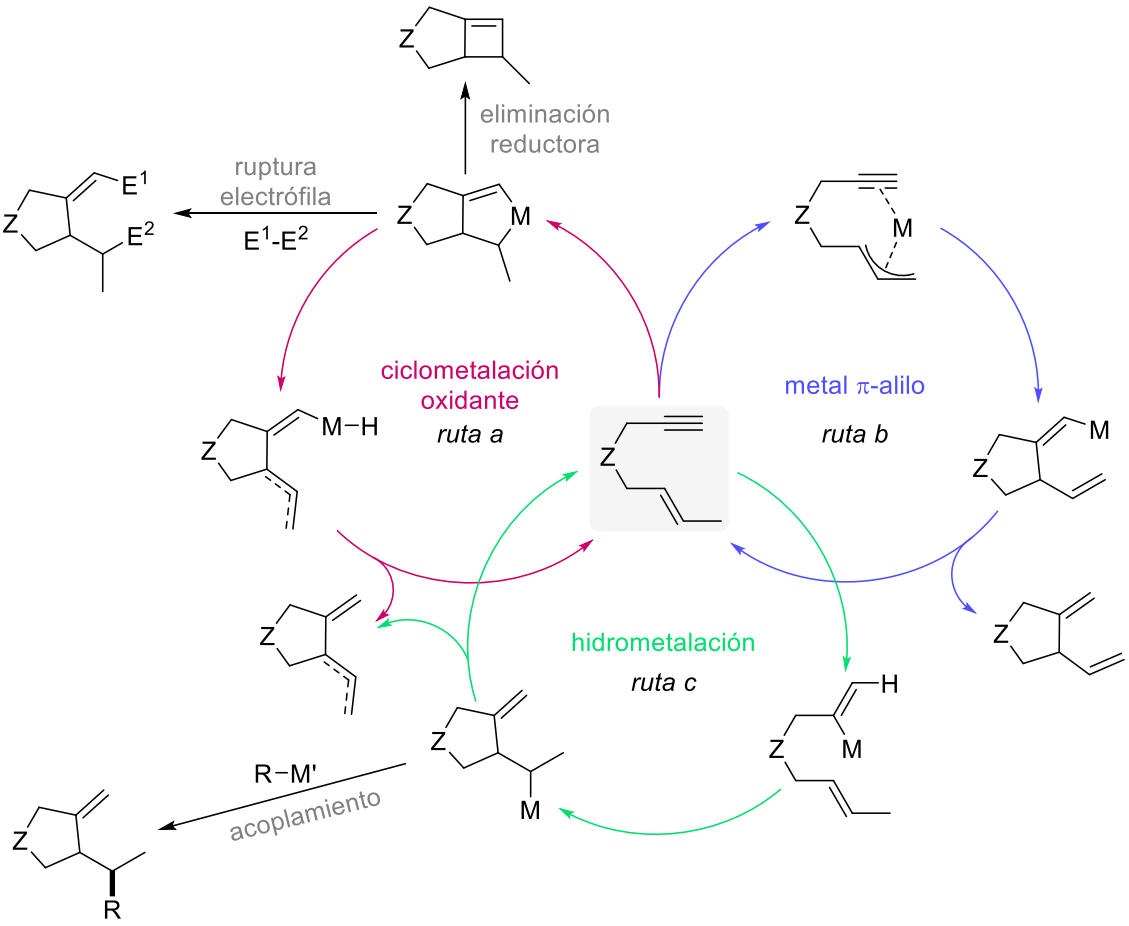

Esquema I.14. Mecanismos de activación sin transposición del esqueleto.

1.2.1.2. Cicloisomerizaciones con transposición del esqueleto

Dentro del segundo grupo, encontramos las otras dos vías de activación restantes (**Esquema I.15**). La primera de ellas, la metátesis (*ruta d*), implica la formación de carbenos metálicos. Esta reacción, también denominada metátesis con cierre de anillo (*Ring-Closing Metathesis*, RCM de sus siglas en inglés) ha sido una reacción extensamente estudiada, conduciendo a estructuras del tipo I.[54] La quinta vía de activación (*ruta e*) también se caracteriza por involucrar carbenos metálicos en su mecanismo, pudiendo conducir a transposiciones en el esquema de la molécula de tipo I y II.

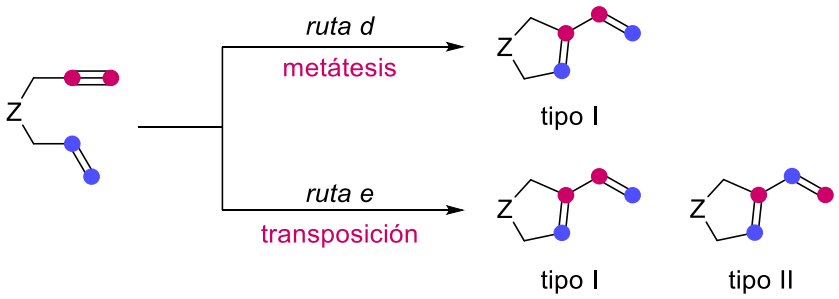

Esquema I.15. Mecanismos de activación con transposición del esqueleto.

[54] (a) *Handbook of Metathesis* (Ed.: R. H. Grubbs), Wiley-VCH, Weinheim, **2003**. (b) S. T. Diver, A. J. Giessert, *Chem. Rev.* **2004**, *104,* 1317–1382.

Estos dos procesos se caracterizan por dar lugar al mismo tipo de productos, 1-vinilciclopentenos. Sin embargo, el mecanismo y la conectividad de los productos no son los mismos en ambos procesos. En el caso de la metátesis, el mecanismo que tiene lugar está bien establecido, involucrando la formación de un metalaciclobutano intermedio entre el carbeno metálico y la insaturación (**Esquema I.16**).

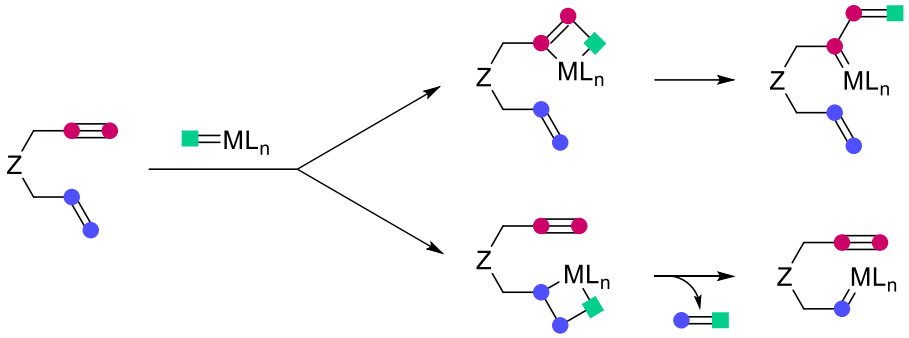

Esquema I.16. Mecanismo general de la metátesis de eninos.

En el caso del proceso de transposición, el mecanismo es más complejo, existiendo diversas vías de reacción (**Esquema I.17**). El primer paso consiste en la complejación tipo π del metal con el alquino. A continuación, la ciclación puede ser de tipo *exo* o *endo*, obteniendo anillos de 5 y 6 miembros, respectivamente.

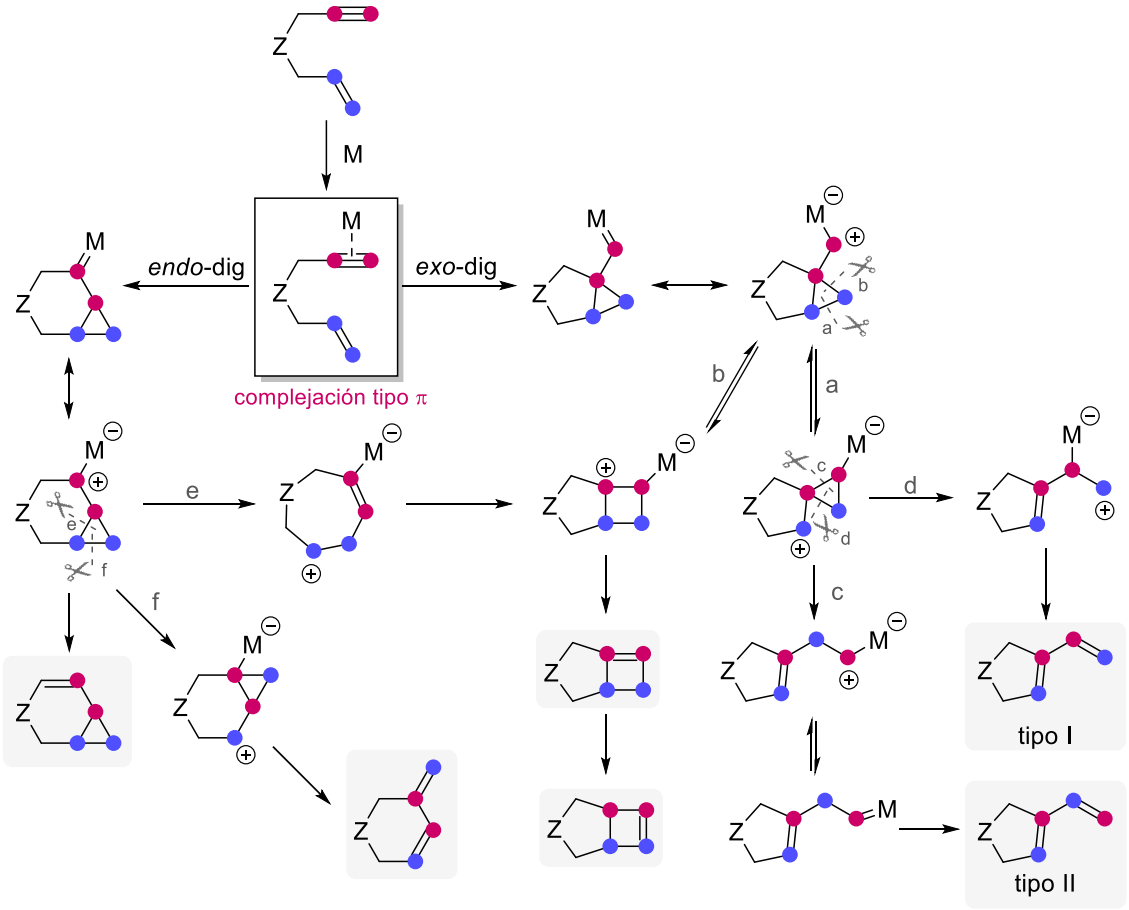

Esquema I.17. Mecanismos posibles en el proceso de transposición.

1.2.1.3. Reacciones tándem con cicloisomerizaciones

Los intermedios metálicos formados durante las reacciones de ciclación anteriormente descritas pueden emplearse como intermedios sintéticos para otras reacciones, antes de sufrir la etapa final de eliminación. En consecuencia, se consigue la formación secuencial de varios enlaces en una sola etapa mediante la combinación de procesos (**Esquema I.18**). Dependiendo del tipo de reacción que se combine con la ciclación podemos clasificarlas en ciclación reductora (a), policiclaciones (b), ciclación/adición nucleófila (c), cicloisomerización oxidante (d), ciclación-acoplamiento (e) y ciclación-metalación (f).

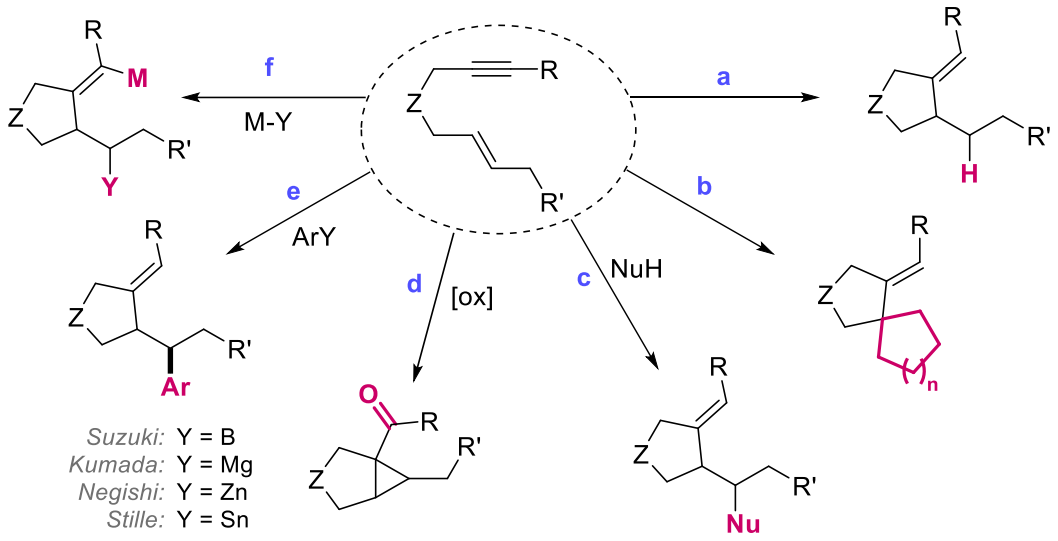

Esquema I.18. Tipos de reacciones tándem con cicloisomerizaciones.

Cabe destacar la importancia y el impacto que los procesos de ciclación-acoplamiento, así como los de ciclación-metalación, han tenido en la química orgánica. Estos métodos se emplean como potente herramienta sintética para la obtención selectiva de estructuras cíclicas complejas funcionalizadas, implicando la formación de más de un enlace en una sola etapa sintética y respetando la economía atómica de la reacción. En particular, la presente Tesis Doctoral se centra en el desarrollo de nuevos procesos átomo-económicos de ciclaciones borilativas de eninos (ruta f, empleando reactivos de boro).

1.2.2. Cicloisomerizaciones catalizadas por metales de transición de la primera serie

Teniendo en cuenta la creciente necesidad de la química moderna de desarrollar métodos eficientes, económicos y respetuosos con el medio ambiente,[55] el empleo de los metales de transición anteriormente mencionados supone un gran inconveniente a nivel económico y de toxicidad. El empleo de metales del primer periodo de transición, tales como Fe, Co, Ni y Cu, ha sido una inteligente solución a este problema. Estos metales ofrecen sistemas catalíticos menos costosos y poco tóxicos para las reacciones, abriendo la puerta a nuevas reactividades e insólitos mecanismos. Entre ellos, cabe destacar el empleo de Fe[56] y Ni,[57]

[55] (a) R. A. Sheldon, I. W. C. E. Arends, U. Hanefeld, *Green Chemistry and Catalysis*, Wiley-VCH, Weinheim, **2007**. (b) M. S. Holzwarth, B. Plietker, *ChemCatChem* **2013**, *5*, 1650–1679. (c) K. S. Egorova, V. P. Ananikov, *Angew. Chem. Int. Ed.* **2016**, *55*, 12150–12162.
[56] J. Teske, B. Plietker, *Isr. J. Chem.* **2017**, *57*, 1082–1089.
[57] (a) J. Montgomery, *Acc. Chem. Res.* **2000**, *33*, 467–473. (b) J. Montgomery, *Angew. Chem. Int. Ed.* **2004**, *43*, 3890–3908.

siendo de los más abundantes disponibles en la Tierra (Fe, 5.05%; Ni, 0.02%). A continuación, se describen las reacciones de cicloisomerización de eninos que emplean estos metales como catalizadores.

1.2.2.1. Ciclaciones catalizadas por Fe

1.2.2.1.1. Cicloisomerizaciones

El primer ejemplo descrito en la bibliografía fue desarrollado por Fürstner, quién llevó a cabo la cicloisomerización de eninos lineales y cíclicos empleando complejos ato de Fe(0) (**Esquema I.19**).[58] En general, se observa buena diastereoselectividad en la reacción, obteniendo en la mayoría de los casos la fusión *trans* de los anillos. En un trabajo posterior realizado por el mismo grupo, estas especies de Fe de baja valencia se evaluaron en reacciones de cicloisomerización y cicloadiciones donde se amplió el alcance de la reacción y se propuso que el mecanismo que tiene lugar comienza con una ciclometalación oxidante.[59]

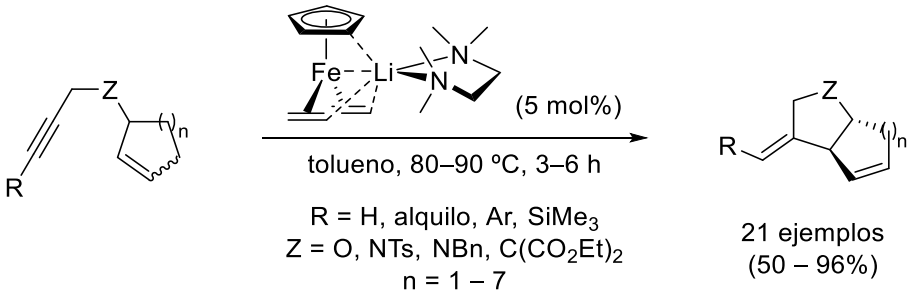

Esquema I.19. Cicloisomerización de eninos catalizadas por complejos ato de Fe(0).

En 2006, el grupo de Echavarren describió la cicloisomerización de eninos catalizada por Au.[60] Así mismo, observaron que el empleo de sales de hierro sencillas como el $FeCl_3$ también conducía a la obtención de los mismos productos, pero el alcance de esta reacción es más limitado en comparación con el sistema de Au (**Esquema I.20**).

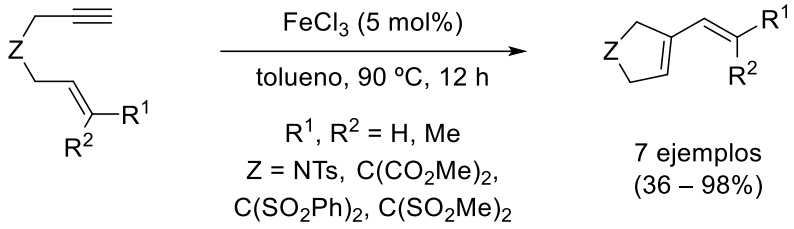

Esquema I.20. Cicloisomerización de eninos catalizadas por $FeCl_3$.

La cicloisomerización de 1,5-eninos catalizada por Fe ha permitido la síntesis de derivados de tipo indol gracias al trabajo realizado por el grupo de Jana.[61] Las condiciones de reacción implican el empleo de $Fe(OTf)_3$ como catalizador, 1,2-dicloroetano como disolvente y temperaturas de 75–80 ºC (**Esquema I.21**). El alcance la reacción muestra buena

[58] A. Fürstner, R. Martin, K. Majima, *J. Am. Chem. Soc.* **2005**, *127*, 12236–12237.
[59] A. Fürstner, K. Majima, R. Martín, H. Krause, E. Kattnig, R. Goddard, C. W. Lehmann, *J. Am. Chem. Soc.* **2008**, *130*, 1992–2004.
[60] C. Nieto-Oberhuber, M. P. Muñoz, S. López, E. Jiménez-Núñez, C. Nevado, E. Herrero-Gómez, M. Raducan, A. M. Echavarren, *Chem. Eur. J.* **2006**, *12*, 1677–1693.
[61] S. Jalal, K. Paul, U. Jana, *Org. Lett.* **2016**, *18*, 6512–6515.

compatibilidad con grupos funcionales en diversas posiciones de la estructura, obteniendo los correspondientes derivados de indol con muy buenos rendimientos.

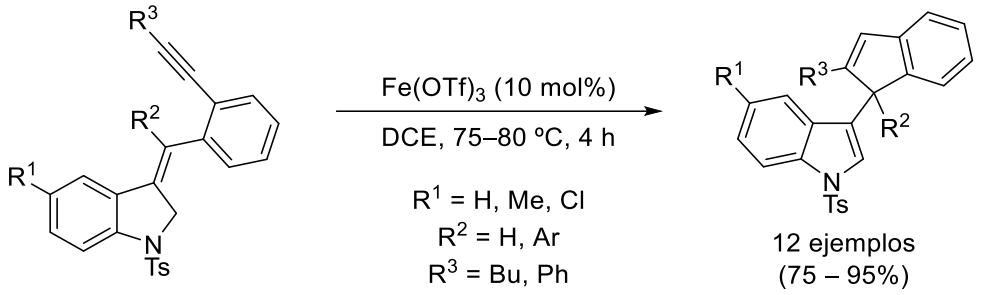

Esquema I.21. Síntesis de derivados de indol mediante cicloisomerización catalizada por Fe.

El grupo de Plietker ha aplicado las cicloisomerizaciones sobre 1,6-eninos con un grupo acetato en su estructura, obteniendo heterociclos con rendimientos moderados en condiciones suaves de reacción.[62] El catalizador empleado consiste en un complejo catiónico de Fe inspirado en el catalizador empleado inicialmente por Fürstner (**Esquema I.22**).

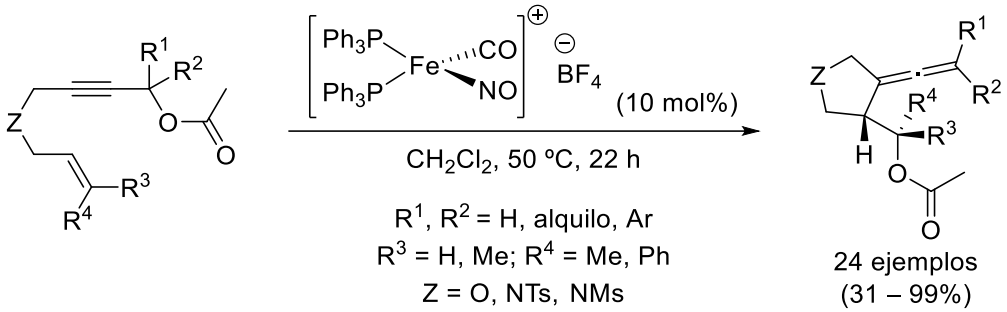

Esquema I.22. Cicloisomerización de acetato-eninos catalizada por Fe.

A pesar de que la diastereoselectividad de la reacción es completa, el alcance de la reacción queda restringido al empleo de alquenos internos y a conectores de tipo sulfonamidas y éteres. Incentivados por esa limitación de la reacción, el mismo grupo de investigación llevó a cabo la reacción de cicloisomerización de acetato-eninos con el resto alílico sin sustituir, empleando el mismo catalizador de Fe.[63] Sin embargo, no obtuvieron el aleno esperado, sino un biciclo [3.2.0], lo que implicaba una migración 1,3 del grupo acetato que transcurría de manera completamente diastereoselectiva (**Esquema I.23**).

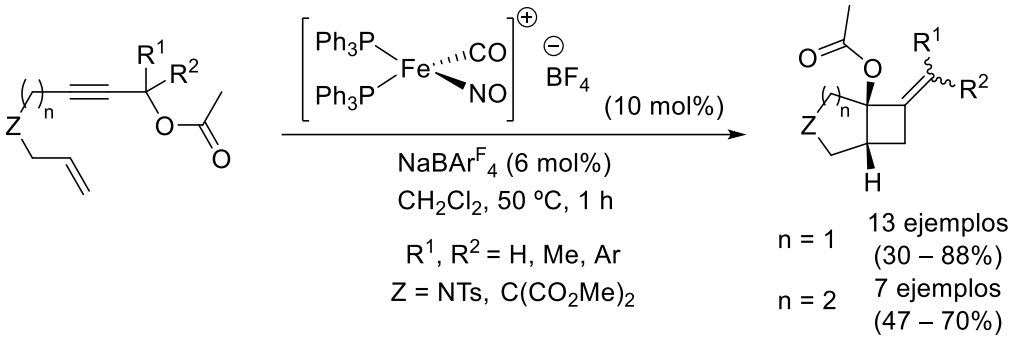

Esquema I.23. Síntesis de ciclobutanos bicíclicos catalizada por Fe.

[62] J. Teske, B. Plietker, *ACS Catal.* **2016**, *6*, 7148−7151.
[63] F. Kramm, J. Teske, F. Ullwer, W. Frey, B. Plietker, *Angew. Chem. Int. Ed.* **2018**, *57*, 13335–3338.

En este caso, el alcance de la reacción se limita al empleo de eninos con conectores de tipo sulfonamida y malonato. No obstante, fueron capaces de aplicar este procedimiento tanto a 1,6- como a 1,7-eninos. Del mismo modo, llevaron a cabo experimentos mecanísticos para proponer un posible mecanismo de reacción, en el cuál proponen una etapa de oxiferración con asistencia del grupo acetato presente como primer paso del ciclo.

1.2.2.1.2. Ciclaciones reductoras

El empleo de complejos de Fe también ha permitido el desarrollo de reacciones de ciclación reductora de 1,6- y 1,7-eninos eficientes y económicas. El grupo de Chirik llevó a cabo dicha reacción tanto en versión estequiométrica como en catalítica,[64] empleando un complejo de Fe con un ligando tridentado de nitrógeno de tipo bis(imino)piridina (BIP), requiriendo de una atmósfera de H_2 para que la reducción tuviera lugar e incluso logrando la obtención de estructuras completamente saturadas (**Esquema I.24**).

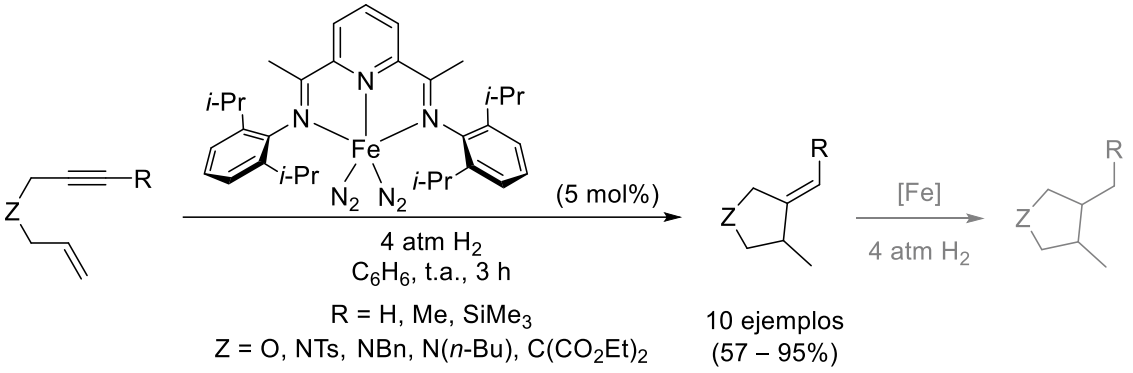

Esquema I.24. Ciclación-reducción de 1,6-eninos descrita por el grupo de Chirik.

Inspirado por el tipo de ligando empleado por Chirik, el grupo de Lu diseñó un ligando tridentado de nitrógeno que combina en su estructura una oxazolina con un grupo iminopiridina (OIP). Dicho ligando fue efectivo para la ciclación reductora de 1,6-eninos junto con $FeCl_2$ y Et_2Zn como reductor (**Esquema I.25**), mostrando buenos rendimientos y alta compatibilidad con varios grupos funcionales como alcohol, cetona, éster, nitrilo, haluro, amina, etc.[65] El mecanismo propuesto comienza con la reducción del precatalizador de Fe(II) y posterior formación de un ferraciclo mediante ciclometalación oxidante de ambas insaturaciones del enino. Este mecanismo está apoyado por experimentos de deuteración, observándose ciclación e incorporación de D en ambas posiciones del enino.

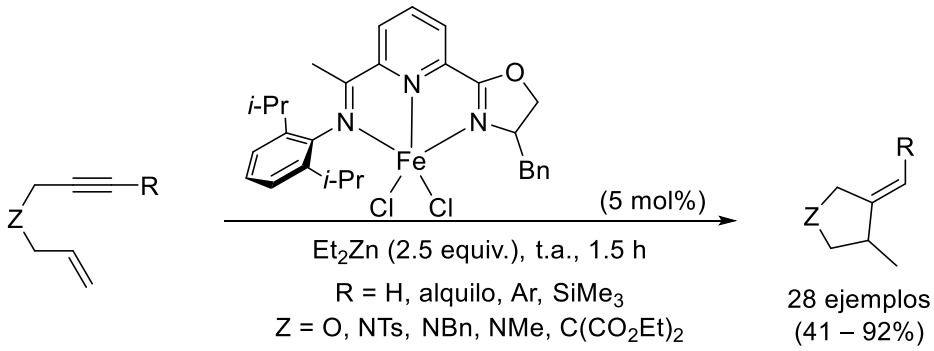

Esquema I.25. Ciclación reductora de 1,6-eninos catalizada por Fe con ligando tipo OIP.

[64] (a) K. T. Sylvester, P. J. Chirik, *J. Am. Chem. Soc.* **2009**, *131*, 8772–8774. (b) J. M. Hoyt, K, T. Sylvester, S. P. Semproni, P. J. Chirik, *J. Am. Chem. Soc.* **2013**, *135*, 4862–4877.
[65] T. Xi, X. Chen, H. Zhang, Z. Lu, *Synthesis* **2016**, *48*, 2837–2844.

Urabe y colaboradores desarrollaron un proceso sintético para la ciclación reductora de eninos con grupos funcionales en su estructura difícilmente tolerables en presencia de organomagnesianos.[66] A pesar de las dificultades, dicho método proporciona altos rendimientos a partir de eninos sustituidos con grupos éster, amida y ciano, en versión estequiométrica y catalítica (**Esquema I.26**).

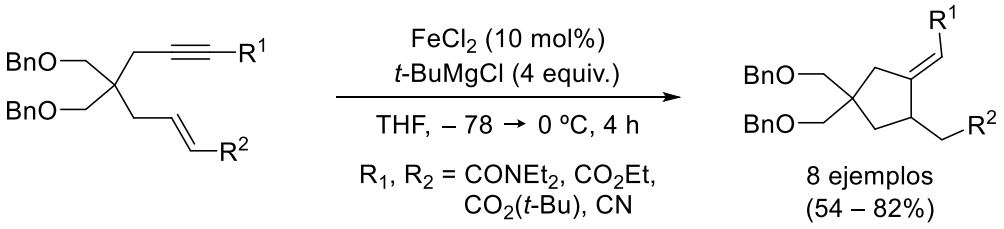

Esquema I.26. Ciclación-reducción de eninos con grupos funcionales en su estructura.

Además, esas mismas condiciones de reacción se pudieron emplear en 1,6-dienos y alquinos con un epóxido en la estructura, obteniendo reactividades algo diferentes. El mecanismo propuesto consiste en la ciclometalación oxidante como primera etapa, apoyado también por experimentos de deuteración.

El grupo de Yang ha descrito este tipo de reacción sobre 1,6-eninos empleando $FeCl_2$ y un ligando iminopiridina (IP) en presencia de Et_2Zn como reductor y $MgBr_2{\cdot}Et_2O$ como aditivo, proponiendo una vez más la cicloferración oxidante como primera etapa del ciclo catalítico (**Esquema I.27**).[67]

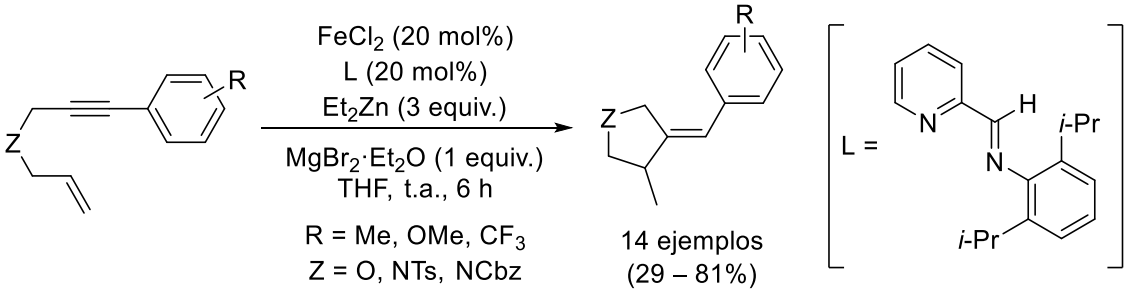

Esquema I.27. Ciclación reductora descrita por Yang.

Recientemente, el grupo de investigación de Xia ha descrito la ciclación reductora de 1,6-eninos mediante la formación de radicales.[68] En dicho estudio, combinan los procesos de ciclación, transferencia de un átomo de hidrógeno (*Hydrogen Atom Transfer*, HAT de sus siglas en inglés) e inserción de oxígeno empleando $FeCl_2$ como catalizador (**Esquema I.28**). El alcance de la reacción es bastante general, siendo compatible con grupos funcionales como nitrilo, cetona, éster y nitro, pero mostrando rendimientos entre bajos y moderados. Los productos finales obtenidos son 3-acilobenzofuranos y tiofenos, compuestos interesantes por su involucración en productos naturales.

[66] (a) T. Hata, N. Hirone, S. Sujaku, K. Nakano, H. Urabe, *Org. Lett.* **2008**, *10*, 5031–5033. (b) T. Hata, S. Sujaku, N. Hirone, K. Nakano, J. Imoto, H. Imade, H. Urabe, *Chem. Eur. J.* **2011**, *17*, 14593–14602.

[67] A. Lin, Z.-W. Zhang, J. Yang, *Org. Lett.* **2014**, *16*, 386–389.

[68] X.-F. Xia, W. He, G.-W. Zhang, D. Wang, *Org. Chem. Front.* **2019**, *6*, 342–346.

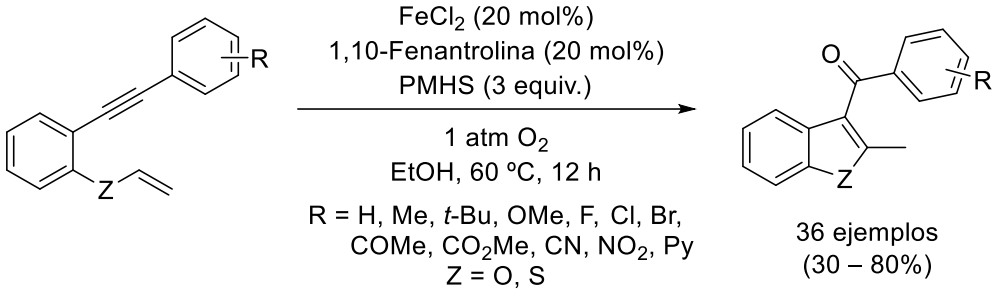

Esquema I.28. Ciclación-HAT-inserción oxígeno catalizado por Fe sobre 1,6-eninos.

1.2.2.1.3. Ciclación con apertura del ciclo

Una metodología que se aleja de la cicloisomerización tradicional es la desarrollada recientemente por el grupo de Fürstner, en la que combinan la ciclación de 1,6-eninos catalizada por Fe con posterior ruptura del enlace C–Z y acoplamiento con un reactivo de Grignard (**Esquema I.29**).[69]

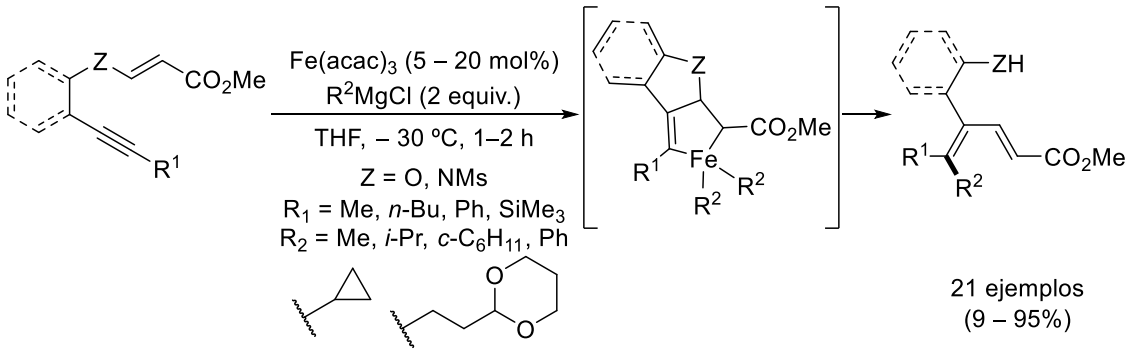

Esquema I.29. Ciclación-apertura-acoplamiento de eninos con organomagnesianos.

Este grupo planteó que la presencia de un buen grupo saliente en posición α al alqueno del enino podría dar lugar a una β-eliminación con apertura de la estructura, generando formalmente la pérdida del conector Z por extrusión de la estructura. El mecanismo propuesto transcurre por la formación del ferraciclo como etapa inicial, conduciendo a 1,3-dienos de forma completamente regio- y estereoselectiva. La variedad estructural tolerada por la reacción es bastante amplia, mostrando buenos rendimientos. Además, esta metodología ha sido aplicada también con acoplamientos de tipo Suzuki empleando Pd como catalizador.

1.2.2.2. Ciclaciones catalizadas por Ni

1.2.2.2.1. Cicloisomerizaciones

En 1987, Trost describió el primer ejemplo de cicloisomerización de eninos catalizado por una mezcla de Ni-Cr.[70] El sistema catalítico consiste en la combinación de $Ni(PPh_3)_2Cl_2$, $CrCl_2$ (30 mol%) y PPh_3 adicional (20 mol%), todo ello soportado sobre un 10 mol% de un

[69] (a) P.-G. Echeverria, A. Fürstner, *Angew. Chem. Int. Ed.* **2016**, *55*, 11188–11192. (b) F. Gomes, P.-G. Echeverria, A. Fürstner, *Chem. Eur. J.* **2018**, *24*, 16814–16822.
[70] B. M. Trost, J. M. Tour, *J. Am. Chem. Soc.* **1987**, *109*, 5268–5270.

polímero de poliestireno fosforilado cruzado al 2% (**Esquema I.30**). Dicho sistema permite la obtención de 1,3-dienos con buena selectividad hacia la ciclación 5-*exo* de 1,6- y 1,7-eninos.

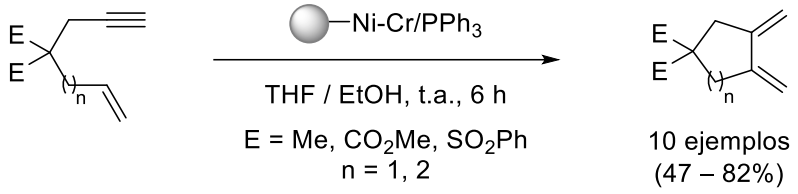

Esquema I.30. Cicloisomerización de eninos catalizada por Ni-Cr.

Varios años más tarde, el grupo de Ikeda y colaboradores desarrollaron este tipo de reacciones empleando un sistema de Ni-Zn.[71] Las condiciones óptimas de reacción se lograron con dos sistemas similares basados en el uso de $Ni(cod)_2$, polvo de Zn (2 equiv.) y un 20 mol% de CH_3CO_2H o de $ZnCl_2$, obteniendo la mezcla de 1,3- y 1,4-dienos con rendimientos elevados (**Esquema I.31**). Este sistema se extiende sobre algunos dieninos para obtener la policiclación de la estructura. Los autores proponen que una especie protonada de Ni(II)-PPh_3, previamente generada en el medio, es reducida por acción del Zn presente, dando lugar a la formación de la especie catalíticamente activa de hidruro de Ni(I), la cual inicia la activación del enino mediante una hidroniquelación del alquino.

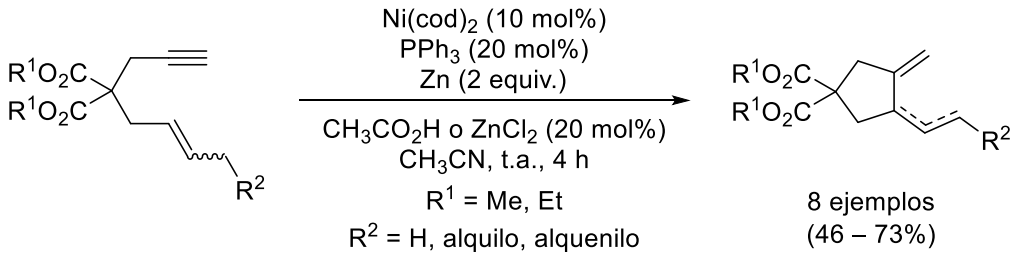

Esquema I.31. Cicloisomerización de eninos catalizada por un sistema Ni-Zn.

El empleo de complejos de Ni(0) con ligandos de tipo carbeno *N*-heterocíclico (NHC) ha permitido la cicloisomerización de 1,7-eninos para la obtención de anillos de 6 miembros (**Esquema I.32**).[72] Los autores del estudio proponen la formación de una especie de hidruro de Ni durante el ciclo catalítico mediante la activación C–H del ligando presente. Los experimentos de deuteración que realizan apoyan dicha propuesta.

[71] S.-i. Ikeda, N. Daimon, R. Sanuki, K. Odashima, *Chem. Eur. J.* **2006**, *12*, 1797–1806.
[72] T. N. Tekavec, J. Louie, *Tetrahedron* **2008**, *64*, 6870–6875.

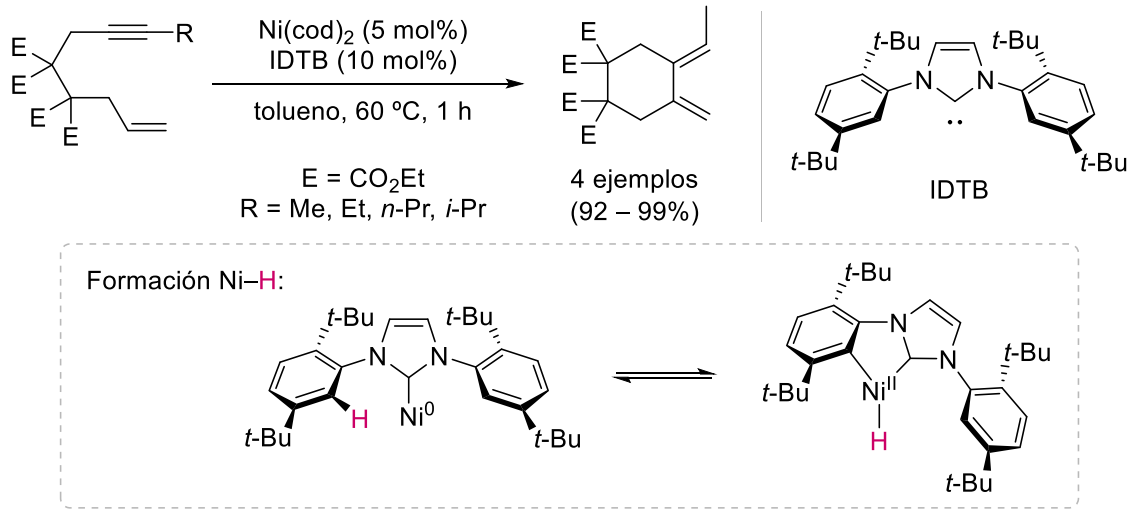

Esquema I.32. Sistema catalítico de Ni-NHC para la cicloisomerización de 1,7-eninos.

1.2.2.2.2. Ciclaciones reductoras

En la bibliografía, también se encuentran ciclaciones reductoras de eninos catalizadas por complejos de Ni. El grupo de Lei observó fortuitamente este tipo de reacción en un intento de estudiar la conocida reacción de Pauson-Khand empleando un catalizador de Ni en lugar de Co.[73] En su lugar, obtuvo el correspondiente producto de ciclación-reducción del enino (**Esquema I.33**). Tras una optimización de las condiciones de reacción, logró llevar a cabo dicha reacción con rendimientos excelentes hacia la formación selectiva de alquenos de configuración *Z*, a partir del empleo de $Ni(acac)_2$ con un reactivo de organozinc.

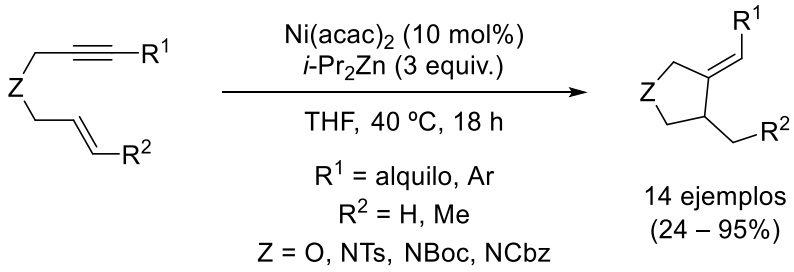

Esquema I.33. Ciclación reductora de 1,6-eninos catalizada por Ni.

El alcance de la reacción muestra una variedad limitada de sustituyentes y conectores, pero ofrece buenos rendimientos en la mayoría de los casos. El mecanismo propuesto comienza con la ciclometalación oxidante del enino, obteniendo un niquelaciclo que evoluciona por dos vías diferentes mediante transmetalación con el organozinc, activando el enlace alquenil-Ni o alquil-Ni, respectivamente (**Figura I.8**). Los experimentos de deuteración realizados apoyan la propuesta mecanística, observando la incorporación de deuterio en ambas posiciones.

[73] M. Chen, Y. Weng, M. Guo, H. Zhang, A. Lei, *Angew. Chem. Int. Ed.* **2008**, *47*, 2279–2282.

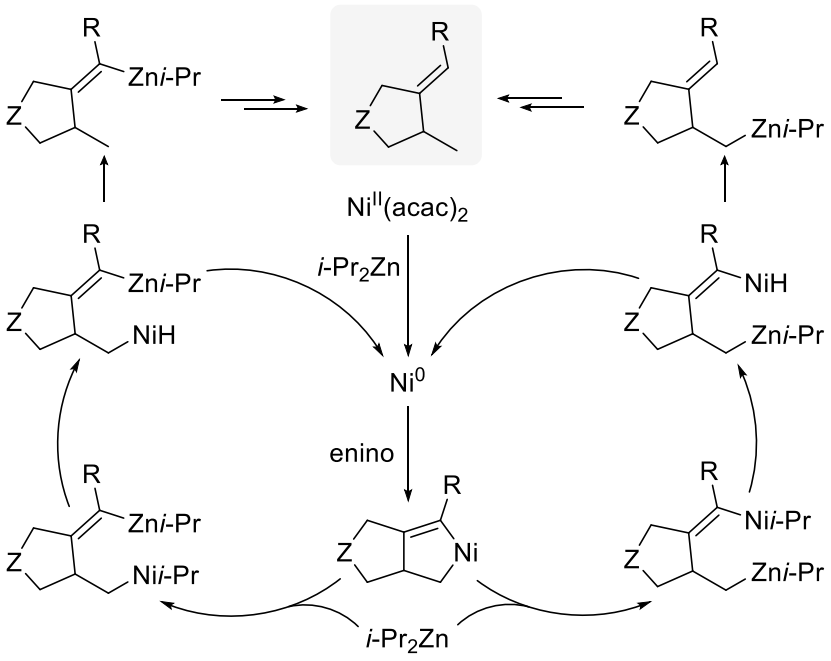

Figura I.8. Propuesta mecanística realizada por el grupo de Lei.

El grupo de Zhao llevó a cabo el estudio de reacciones de ciclación de eninos catalizada por Ni en presencia de reactivos de dialquilzinc.[74] Curiosamente, observaron que el tipo de dialquilzinc condicionaba el tipo de reacción que tenía lugar. Por un lado, el empleo de Me_2Zn condujo a la formación de productos de dimerización-cicloadición [2+2+2+2] y [2+2+2]. Por el contrario, observaron el correspondiente producto de ciclación-reducción al emplear Et_2Zn (**Esquema I.34**). Esta diferencia de reactividad se justifica por la posibilidad que tiene el dietilzinc frente al dimetilzinc para generar un hidruro de Ni a partir de los grupos etilo que posee.

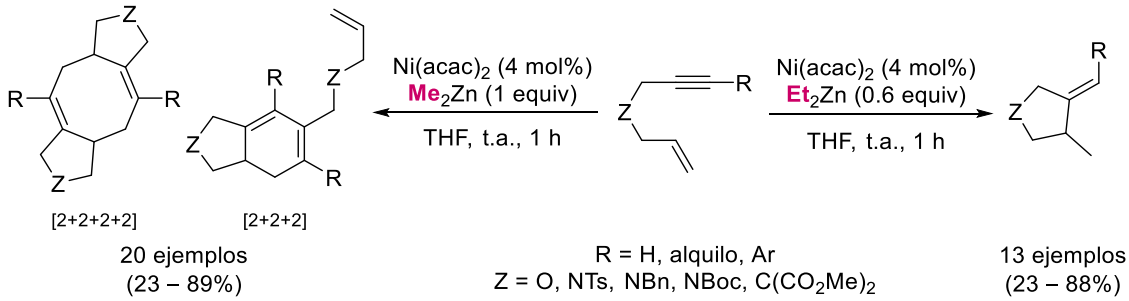

Esquema I.34. Reacciones de ciclación descritas por Zhao.

1.2.2.2.3. Ciclación-acoplamiento

Otro tipo de procedimiento que emplea complejos de Ni como catalizadores son las reacciones de ciclación-acoplamiento. En ellas, a parte de la obtención de estructuras cíclicas con la formación subsiguiente de enlaces C–C, se produce la inserción de un nuevo grupo en la estructura mediante el proceso conocido como acoplamiento.

Dentro de este tipo de ciclaciones, cabe destacar la brillante contribución realizada por el grupo de Montgomery. Inicialmente, su grupo llevó a cabo la ciclación de enonas en

[74] Z. Chai, H.-F. Wang, G. Zhao, *Synlett* **2009**, 1785–1790.

presencia de reactivos de organozinc (sintetizados a partir de $ZnCl_2$ y organolíticos u organomagnesianos) y una fuente de Ni(0).[75] La reactividad de dicha reacción puede ser modulada con la adición de PPh_3 a la mezcla de reacción. En ausencia de PPh_3, se obtiene el correspondiente producto de ciclación-acoplamiento con buenos rendimientos. Por el contrario, la adición de PPh_3 a la reacción conduce al proceso de ciclación-reducción del enino (**Esquema I.35**). La presencia de otros alquenos deficientes en electrones sustituidos con uno o dos grupos éster o nitro, en lugar de un grupo cetona, también condujo a buenos rendimientos en la ciclación.

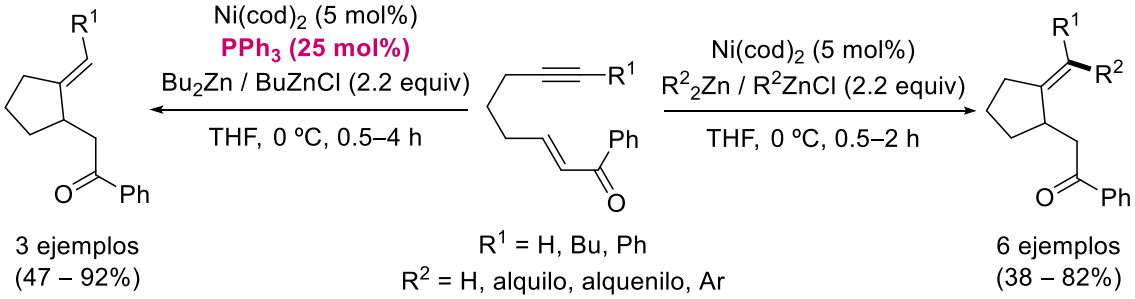

Esquema I.35. Ciclación-reducción *vs* ciclación-acoplamiento de enonas.

El alcance de esta reacción fue extendido a otros eninos más complejos, con la intención de obtener estructuras interesantes por su presencia en diversos productos naturales.[76] Se lograron sintetizar varios heterociclos con buenos rendimientos y de forma estereoselectiva (**Figura I.9**).

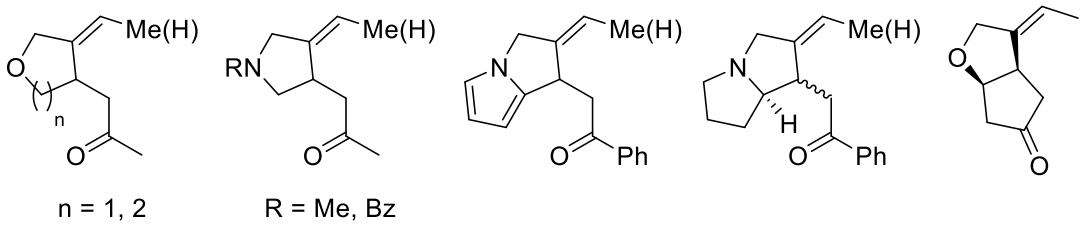

Figura I.9. Heterociclos sintetizados por el grupo de Montgomery.

Más adelante, el grupo llevó a cabo un estudio más exhaustivo de dicha reacción, atendiendo a los aspectos mecanísticos de la misma.[77] Entre los mecanismos posibles, consideraron cuatro posibles vías de reacción (**Figura I.10**): (a) carbozincación del alquino, (b) ciclometalación oxidante, (c) formación de un complejo π-Ni y (d) una transferencia electrónica del Ni a la enona con la consecuente generación de radicales. A partir de diversos ensayos experimentales, llegaron a la conclusión de que el mecanismo más probable implicaba la formación de un metalaciclo como paso inicial.

[75] (a) J. Montgomery, A. V. Savchenko, *J. Am. Chem. Soc.* **1996**, *118*, 2099–2100. (b) J. Montgomery, J. Seo, H. M. P. Chui, *Tetrahedron Lett.* **1996**, *37*, 6839–6842.

[76] J. Montgomery, M. V. Chevliakov, H. L. Brielmann, *Tetrahedron* **1997**, *53*, 16449–16462.

[77] J. Montgomery, J. Seo, *Tetrahedron* **1998**, *54*, 1131–1144.

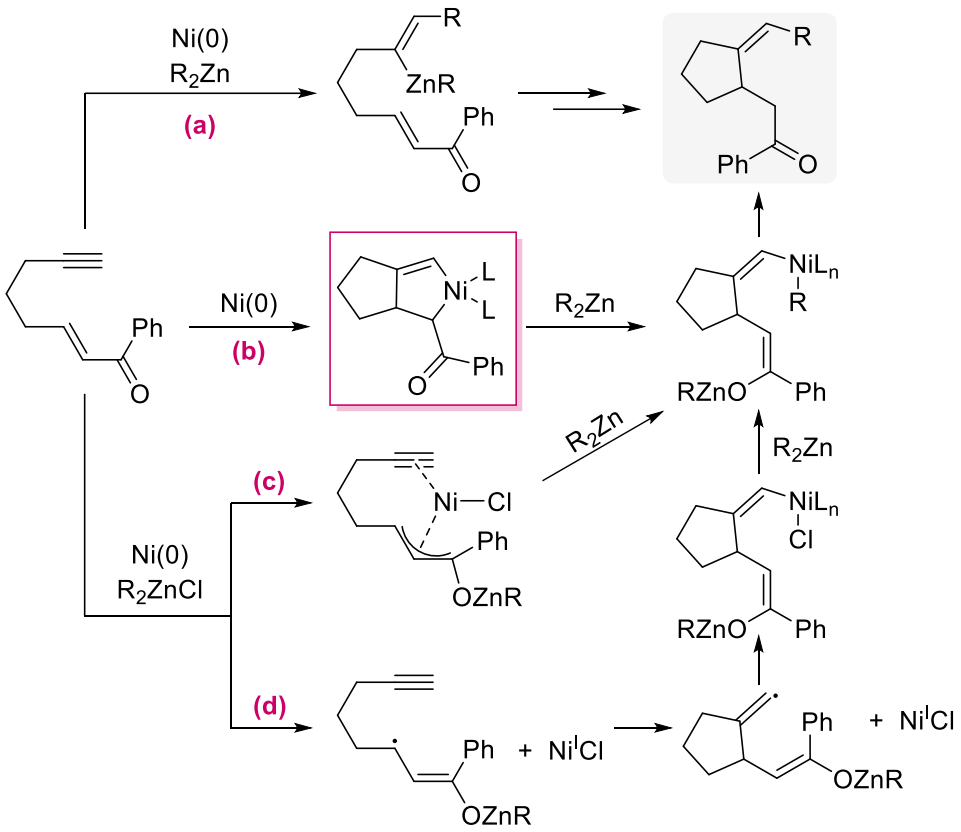

Figura I.10. Posibles mecanismos de reacción para la ciclación-acoplamiento de enonas.

Sin embargo, no llegaron a obtener evidencias claras de este proceso. No fue hasta años más tarde, cuando el mismo grupo de investigación aisló y caracterizó de forma exitosa las primeras estructuras conocidas por el momento de niquelaciclos formados a partir de una enona (**Figura I.11**), confirmando así el mecanismo propuesto para dicha reacción.[78]

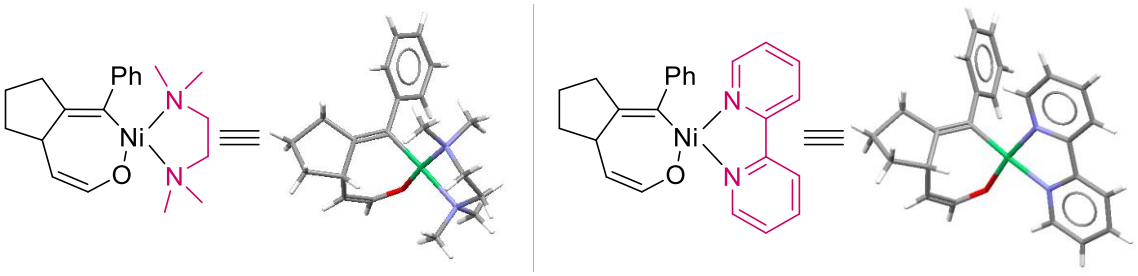

Figura I.11. Estructura de rayos X de los metalaciclos de Ni aislados.

La reacción descrita por el grupo de Ikeda emplea cloruro de alilo como agente de acoplamiento, obteniendo los correspondientes productos de ciclación-alilación 5-*exo* con isomerización del doble enlace del alqueno.[79] El sistema catalítico empleado es idéntico al utilizado por este mismo grupo para llevar a cabo la cicloisomerización de eninos, requiriendo del uso de $Ni(cod)_2$, PPh_3 y Zn (**Esquema I.36**). La principal limitación de la reacción se encuentra en que el alquino del enino debe ser necesariamente terminal.

[78] K. K. D. Amarasinghe, S. K. Chowdhury, M. J. Heeg, J. Montgomery, *Organometallics* **2001**, *20*, 370–372.
[79] S.-i. Ikeda, K. Suzuki, K. Odashima, *Chem. Commun.* **2006**, 457–459.

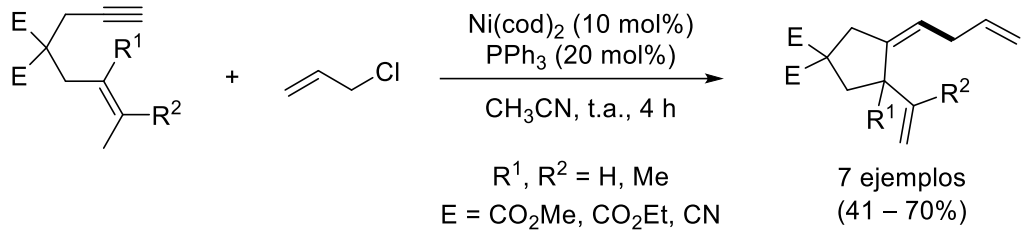

Esquema I.36. Cicloisomerización-acoplamiento de cloruros de alilo y eninos.

Los ácidos borónicos han sido igualmente empleados en este tipo de reacciones en combinación con una fuente de Ni(0), ofreciendo una buena alternativa al empleo de cloruros y otros agentes organometálicos más agresivos. Concretamente, el grupo de Cheng estudió la ciclación-acoplamiento de ácidos alquenilborónicos con 1,6-eninos,[80] observando una buena selectividad hacia la inserción del resto alquenilo en la posición terminal del alqueno del enino con elevados rendimientos (**Esquema I.37**). Así mismo, el alcance estructural de la reacción es muy extenso tanto en la sustitución y conectores del enino como en el agente de acoplamiento. A partir de experimentos de deuteración, los autores del trabajo demuestran que el metanol actúa como fuente de protones y proponen la ciclometalación oxidante como primera etapa del ciclo catalítico.

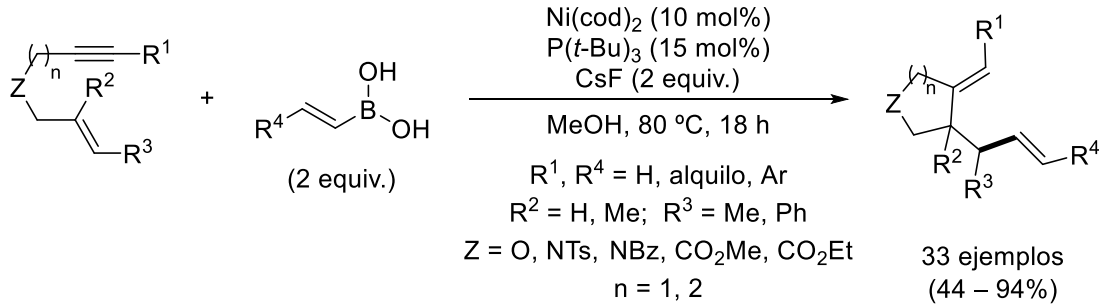

Esquema I.37. Ciclación-acoplamiento de eninos y ácidos borónicos catalizada por Ni.

Recientemente, Lam y colaboradores han descrito la versión enantioselectiva de esta reacción, a partir de eninos sustituidos en el alilo con un grupo fosfato y ácidos arilborónicos (**Esquema I.38**).[81] El empleo de un ligando quiral bidentado de nitrógeno y fósforo junto con una sal de Ni(II), en cantidades catalíticas, permite la formación selectiva de anillos de seis miembros con un dieno no conjugado, produciéndose el acoplamiento en la posición interna del alquino y mostrando excesos enantioméricos muy elevados.

[80] C.-M. Yang, S. Mannathan, C.-H. Cheng, *Chem. Eur. J.* **2013**, *19*, 12212–12216.
[81] C. Yap, G. M. J. Lenagh-Snow, S. N. Karad, W. Lewis, L. J. Diorazio, H. W. Lam, *Angew. Chem. Int. Ed.* **2017**, *56*, 8216–8220.

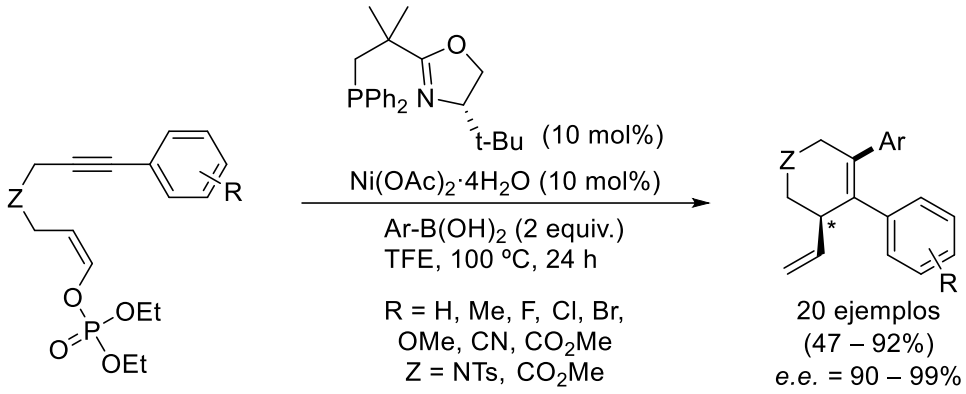

Esquema I.38. Reacción de ciclación-acoplamiento descrita por el grupo de Lam.

El mecanismo propuesto comienza con la transmetalación de un complejo de Ni(II) con el ácido borónico para, posteriormente, dar lugar a una inserción 1,2 en el alquino. A continuación, el intermedio de alquenil-Ni reaccionaría con el resto alilo para dar lugar a la ciclación con consecuente eliminación del grupo fosfato. No obstante, los autores del trabajo no realizan ningún experimento mecanístico que apoye esta propuesta.

1.2.2.2.4. Ciclación hidrocarboxilativa

El interés en la incorporación de un ácido carboxílico a la estructura ha crecido notablemente en los últimos años, provocando el desarrollo de novedosos métodos para la síntesis de derivados de ácidos carboxílicos. Recientemente, el grupo de Ma ha descrito la ciclación de eninos catalizada por especies de Ni(0) en presencia de CO_2, dando lugar a la incorporación del grupo funcional CO_2H en la estructura (**Esquema I.39**).[82]

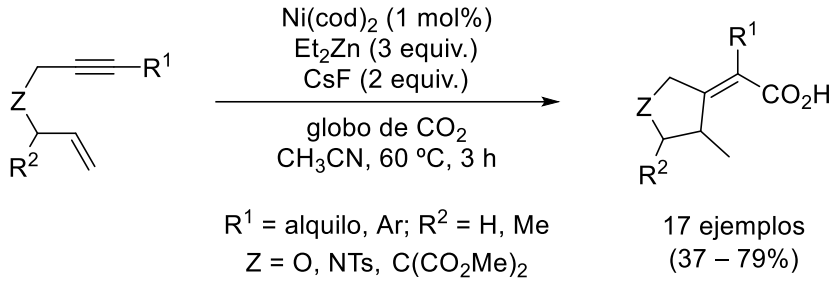

Esquema I.39. Ciclación hidrocarboxilativa descrita por el grupo de Ma.

La adición de dietilzinc a la mezcla de reacción es necesaria para que el proceso tenga lugar. A partir de los experimentos de deuteración realizados, es difícil proponer la ciclometalación oxidante como vía de reacción. Como alternativa, los autores proponen la coordinación de una especie de Ni(0) con el alquino del enino. Ese intermedio (**I**, **Figura I.12**) daría lugar a una transmetalación con el organozínquico e inserción 1,2 del alqueno, generando un alquil-Ni intermedio (**II**) que puede continuar reaccionando por dos vías: una transmetalación adicional con el dietilzinc (**III**) o sufrir una ***β***-eliminación y posterior eliminación reductora (**IV**). Finalmente, la reacción con CO_2 y posterior hidrólisis de ambos intermedios conduciría al producto final de reacción.

[82] T. Cao, Z. Yang, S. Ma, *ACS Catal.* **2017**, *7*, 4504−4508.

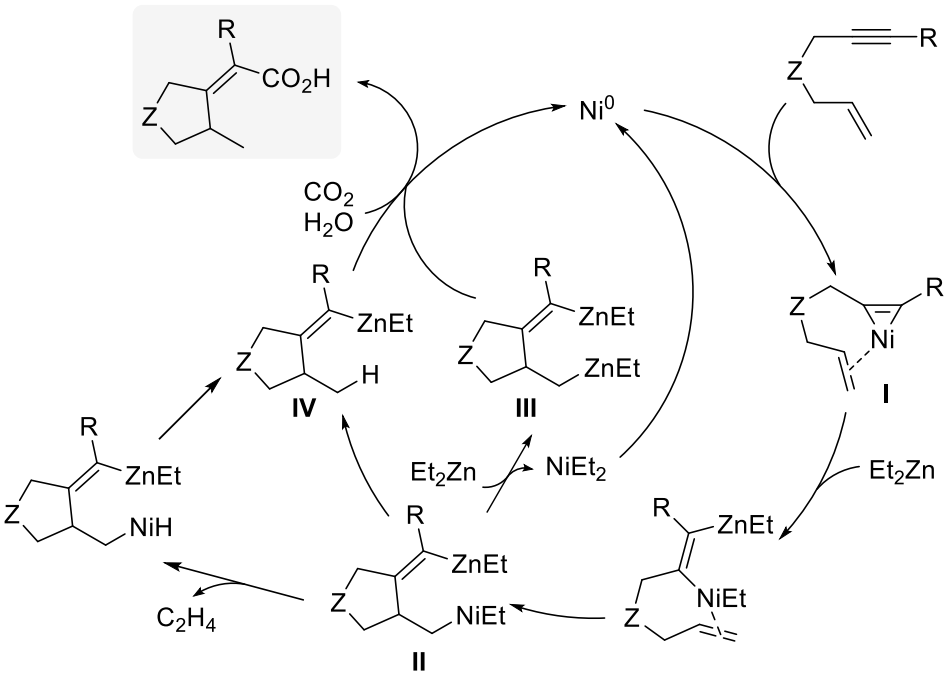

Figura I.12. Propuesta mecanística de la reacción desarrollada por Ma.

De forma prácticamente simultánea, el grupo de Diao llevó a cabo la ciclación hidrocarboxilativa de 1,6- y 1,7-eninos empleando complejos de Ni(0) con ligandos NHC.[83] La reacción muestra un buen alcance y unos buenos rendimientos (**Esquema I.40**). Los autores llevaron a cabo diversos experimentos mecanísticos, determinando que el camino de reacción más probable consiste en la formación de una especie catalíticamente activa de hidruro de Ni(II) mediante la activación del precatalizador de Ni(0) con CO_2 y Et_2Zn. Dicha especie inicia la reacción mediante la hidrometalación del resto alqueno presente en el enino.

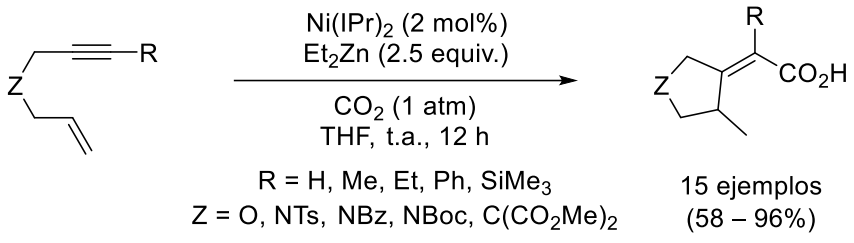

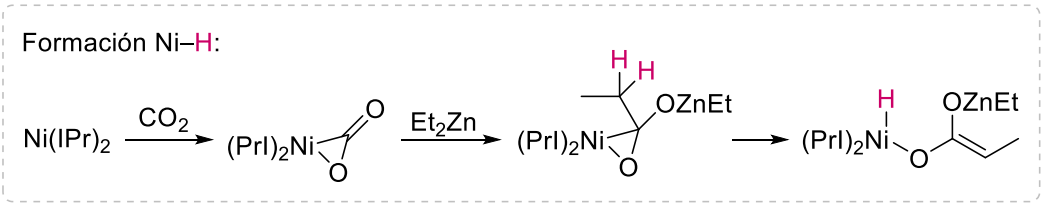

Esquema I.40. Reacción descrita por el grupo de Diao.

[83] J. B. Diccianni, T. Heitmann, T. Diao, *J. Org. Chem.* **2017**, *82*, 6895–6903.

1.3. CICLACIONES BORILATIVAS DE ENINOS

Como ya se ha mencionado anteriormente, los compuestos de organoboro se emplean constantemente como intermedios sintéticos de reacción debido a las propiedades únicas que poseen, en términos de estabilidad, reactividad y toxicidad. En consecuencia, existe un creciente interés en el desarrollo de novedosos y eficaces procedimientos para la síntesis de estos derivados borilados, siendo clave el empleo de los metales de transición como catalizadores. La sinergia entre esta metodología y los procesos de ciclación sobre especies poliinsaturadas ofrece una vía interesante y eficiente, obteniendo moléculas cíclicas funcionalizadas con un alto nivel de complejidad estructural a partir de sencillos precursores lineales y en un solo paso de reacción. Este tipo de reacciones recibe el nombre de ciclaciones borilativas. Dentro de ellas, se puede realizar una clasificación en función del tipo de funcionalización obtenida en el producto final (**Figura I.13**).

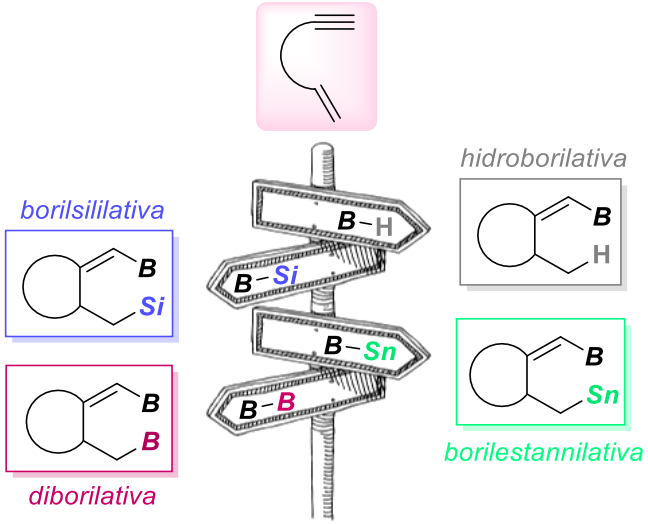

Figura I.13. Tipos de ciclaciones borilativas sobre eninos.

Cuando la incorporación del grupo borilo va acompañada por la inserción de un átomo de hidrógeno se obtienen ciclaciones hidroborilativas. El empleo de reactivos de boro-silicio y boro-estaño da lugar, respectivamente, a ciclaciones borilsililativas y borilestannilativas. Por último, el empleo de compuestos bimetálicos de boro permite llevar a cabo ciclaciones diborilativas.

En la bibliografía, se describen numerosos estudios de este tipo de reacciones sobre sustratos poliinsaturados, tales como dienos, diinos, eninos, aleninos, enalenos, alquinilisocianatos y alquenilcetonas, así como alquenos y alquinos con buenos grupos salientes en su estructura.[84] En la presente Tesis, se describen aquellos ejemplos que emplean eninos como punto de partida. Cabe destacar que, hasta la realización de este trabajo, no existía ningún precedente de ciclación diborilativa sobre eninos.

[84] (a) E. Buñuel, D. J. Cárdenas, *Eur. J. Org. Chem.* **2016**, 5446–5464. (b) E. Buñuel, D. J. Cárdenas, *Chem. Eur. J.* **2018**, *24*, 11239–11244.

1.3.1. Ciclaciones borilsililativas de eninos

El primer ejemplo de ciclación borilsililativa de eninos fue descrita por el grupo de Tanaka. Los autores del trabajo desarrollaron, de forma simultánea al grupo de Ito,[85] la borilsililación de alquinos catalizada por Pd. Así mismo, sometieron a esas condiciones de reacción un diino y un enino, observando la ciclación de la estructura con inserción *cis* regioselectiva de ambos restos de boro y silicio (**Esquema I.41**).[86]

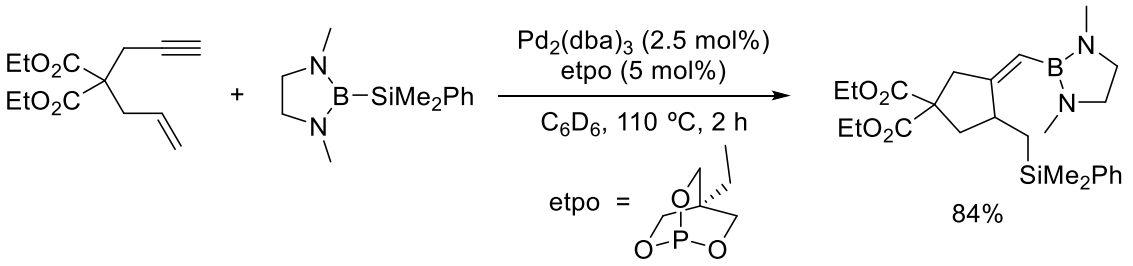

Esquema I.41. Primera reacción de ciclación borilsililativa de eninos.

Incentivado por el resultado observado por Tanaka, el grupo de Moberg decidió evaluar dichas ciclaciones borilsililativas de 1,6-eninos empleando un catalizador de Pd con un ligando tipo NHC.[44a] Inicialmente, el precatalizador comercial de Pd(II) es reducido a una especie catalíticamente activa de Pd(0) por reacción con MeMgCl. La reacción procede con rendimientos excelentes para eninos terminales, pero la sustitución de la posición terminal del alqueno o alquino provoca bajos rendimientos o incluso que la reacción no tenga lugar (**Esquema I.42**). Así mismo, el estudio incluye la posterior derivatización de los restos borilo y sililo introducidos en la estructura por procesos de acoplamiento de tipo Suzuki y oxidación, respectivamente.

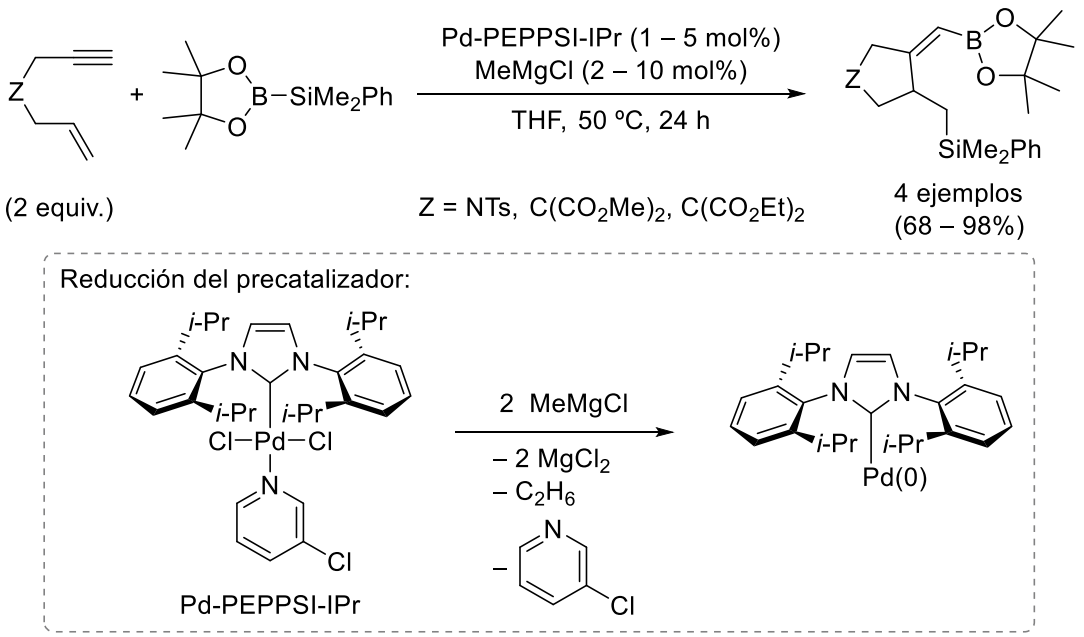

Esquema I.42. Ciclación borilsililativa de eninos catalizada por Pd-PEPPSI-IPr.

[85] M. Suginome, H. Nakamura, Y. Ito, *Chem. Commun.* **1996**, 2777–2778.
[44] (a) M. Gerdin, S. K. Nadakudity, C. Worch, C. Moberg, *Adv. Synth. Catal.* **2010**, *352*, 2559–2570. (b) Y.-C. Xiao, C. Moberg, *Org. Lett.* **2016**, *18*, 308−311.
[86] S.-y. Onozawa, Y. Hatanaka, M. Tanaka, *Chem. Commun.* **1997**, 1229–1230.

Posteriormente, el mismo grupo de investigación extendió esa metodología sobre 1,7-eninos, obteniendo anillos de 6 miembros.[44b] Bajo las mismas condiciones de reacción, se obtienen derivados de cromeno como productos finales de reacción con mejores rendimientos (**Esquema I.43**). El alcance de la reacción es más amplio, pero vuelve a estar limitado al empleo de alquenos y alquinos terminales. Además, el empleo de eninos cíclicos permite la síntesis diastereoselectiva de biciclos fusionados.

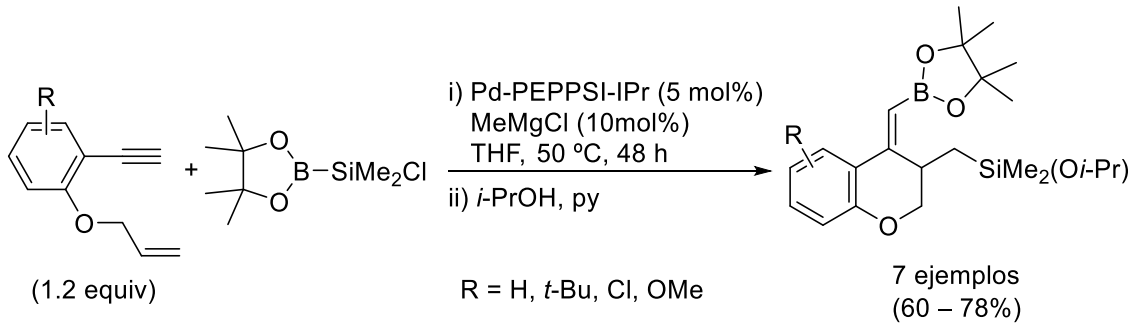

Esquema I.43. Ciclación borilsililativa de 1,7-eninos catalizada por Pd.

En 2010, Suginome y Ohmura lograron modular la regioselectividad de la borilsililación de alquinos terminales mediante el empleo de diferentes ligandos fosfina y complejos de Pd.[87] El empleo de PPh_3, da lugar a la inserción *cis* común, donde el resto borilado se incorpora en la posición menos sustituida. Por el contrario, el empleo de un ligando fosfina más voluminoso conduce a la obtención de la regioselectividad contraria (**Esquema I.44**). Los autores proponen un mecanismo tradicional basado en la adición oxidante del enlace B–Si al Pd y posterior inserción del alquino en el enlace Pd–B, con diferente regioselectividad en función del ligando empleado.

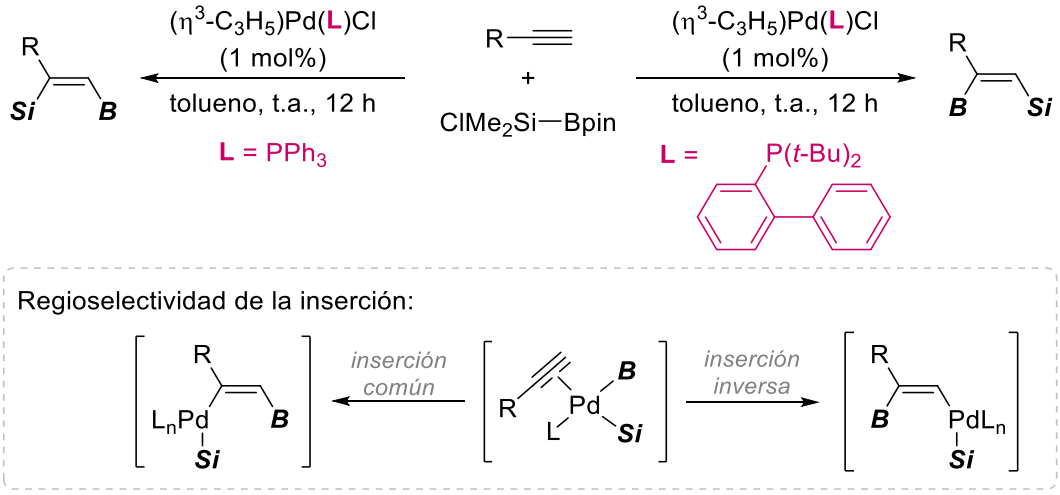

Esquema I.44. Modulación de la regioselectividad en la inserción B–Si en alquinos.

Para obtener información adicional acerca del mecanismo, aplicaron estas mismas condiciones de reacción sobre un 1,6-enino, obteniendo inserción B–Si en el alquino y ciclación borilsililativa en distintas proporciones, según el ligando empleado (**Esquema I.45**).

[87] T.i Ohmura, K. Oshima, H. Taniguchi, M. Suginome, *J. Am. Chem. Soc.* **2010**, *132*, 12194–12196.

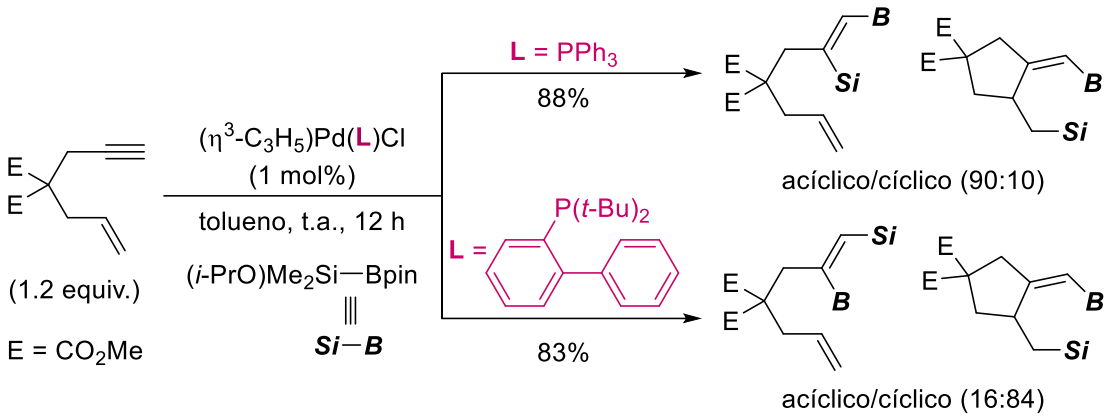

Esquema I.45. Condiciones descritas por Suginome y Ohmura sobre un 1,6-enino.

Sin embargo, este resultado no puede ser explicado simplemente por la diferente regioselectividad en la inserción del enlace Pd–B, ya que la inserción inversa no podría dar lugar a la ciclación de la estructura para formar un anillo de 5 miembros. A partir de experimentos mecanísticos, proponen que la inserción común e inversa del enlace Pd–B están en equilibrio por la posibilidad de sufrir una *β*-eliminación del resto de B y posterior reinserción, favoreciéndose finalmente la regioselectividad observada para cada tipo de ligando.

De forma genérica, el ciclo catalítico que tiene lugar en estas reacciones se muestra en la **Figura I.14**. Inicialmente, se produce una adición oxidante del enlace B–Si al complejo de Pd(0) inicial, generando una nueva especie de Pd(II). A continuación, se produce la inserción *cis* del alquino en el enlace Pd–B, seguido de otra inserción 1,2 del alqueno del enino en el enlace Pd–C(sp^2). Finalmente, la eliminación reductora libera el producto de ciclación borilsililativa y cierra el ciclo regenerando la especie activa de Pd(0).

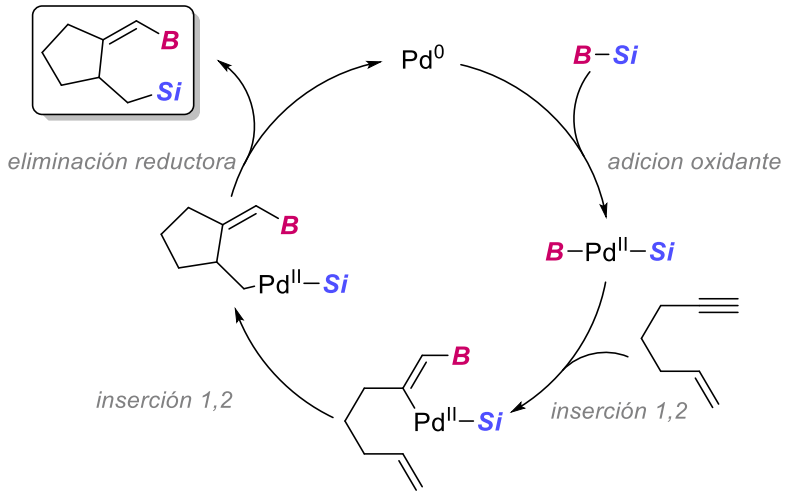

Figura I.14. Ciclo catalítico simplificado de la ciclación borilsililativa de eninos.

1.3.2. Ciclaciones borilestannilativas de eninos

En 1997, el grupo de Tanaka describió la primera reacción de ciclación borilestannilativa de eninos.[88] Dicho trabajo estudia este tipo de ciclaciones sobre 1,5-, 1,6- y 1,7-diinos, extendiendo el alcance de la reacción a un 1,6-enino, obteniendo la inserción completamente regioselectiva del resto de boro en la posición terminal del alquino (**Esquema I.46).**

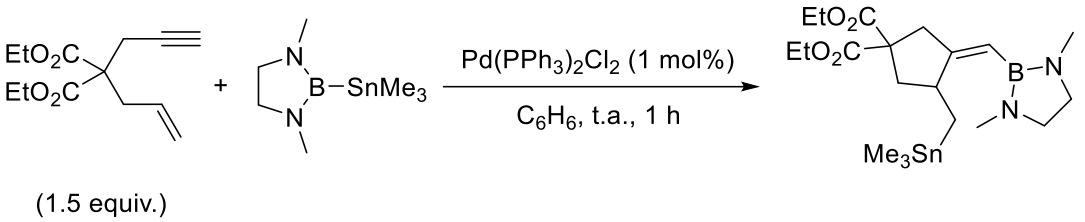

Esquema I.46. Primer ejemplo descrito de ciclación borilsililativa de eninos.

La metodología descrita por el grupo de RajanBabu para la ciclación borilestannilativa de diinos también puede ser aplicada sobre sustratos de tipo enino y alenino.[89] Bajo las mismas condiciones de reacción descritas por Tanaka, junto con una etapa final de tratamiento con pinacol en medio ácido, consiguen aislar los correspondientes vinilboronatos con buenos rendimientos (**Esquema I.47**).

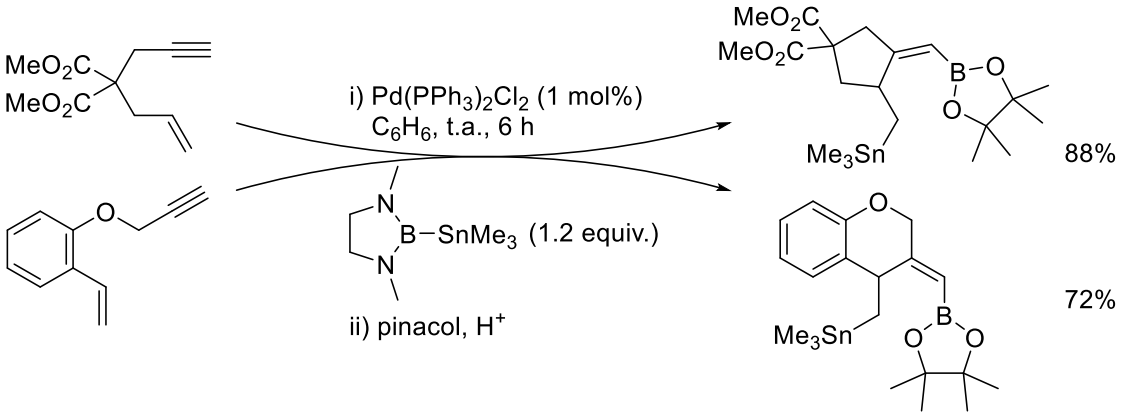

Esquema I.47. Ciclación borilsililativa de eninos descrita por RajanBabu.

El mecanismo propuesto para este tipo de reacciones es idéntico al propuesto para las ciclaciones borilsililativas (**Figura I.15**): adición oxidante del enlace B–Sn, inserción del alquino en el enlace Pd–B seguido de inserción del alqueno en el complejo de alquenil-Pd intermedio. Finalmente, la eliminación reductora forma el enlace C–Sn y regenera la especie activa inicial de Pd(0).

[88] S.-y. Onozawa, Y. Hatanaka, N. Choi, M. Tanaka, *Organometallics* **1997**, *16*, 5389–5391.
[89] R. R. Singidi, A. M. Kutney, J. C. Gallucci, T. V. RajanBabu, *J. Am. Chem. Soc.* **2010**, *132*, 13078–13087.

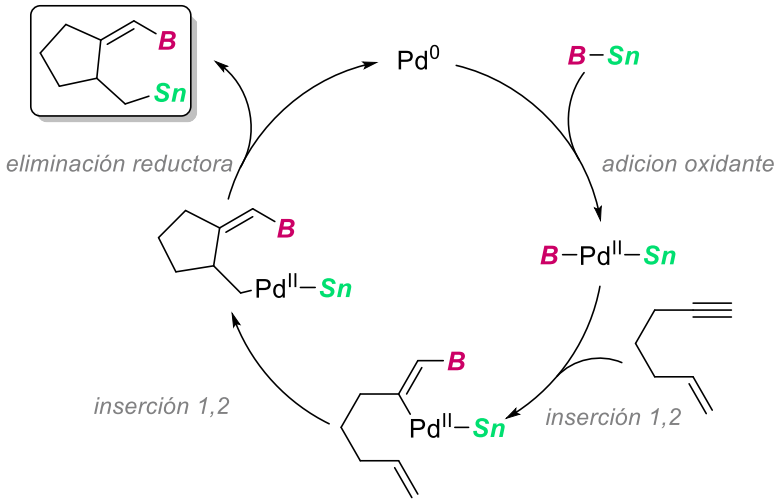

Figura I.15. Ciclo catalítico general para la ciclación borilestannilativa de eninos.

1.3.3. Ciclaciones hidroborilativas de eninos

1.3.3.1. Reacciones catalizadas por Pd

Nuestro grupo de investigación ha sido pionero en el desarrollo de novedosas ciclaciones hidroborilativas de diversas estructuras poliinsaturadas catalizadas por Pd. En 2007, desarrolló el primer ejemplo combinando $Pd(OAc)_2$ con B_2pin_2, en presencia de MeOH y en ausencia de ligandos, observando la ciclación de 1,6-eninos con la inserción de un resto Bpin en la posición externa del alqueno (**Esquema I.48**).[90]

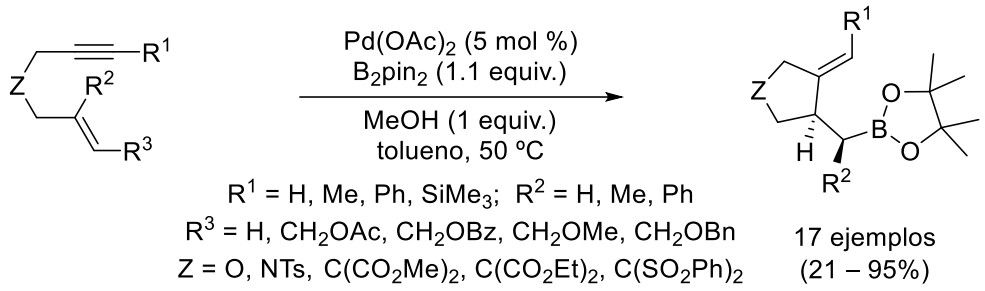

Esquema I.48. Ciclación hidroborilativa de 1,6-eninos catalizada por Pd.

Esta reacción ofrece una gran variedad estructural en los eninos de partida, permitiendo la síntesis de diversos alquilboronatos con rendimientos entre moderados y muy buenos. Cabe destacar que la reacción transcurre de forma estereoespecífica, obteniendo un único diastereoisómero en función de la configuración inicial del alqueno del enino. No obstante, a pesar de utilizar un compuesto bimetálico de boro, solamente se observa la incorporación de uno de los restos borilo.

El mecanismo propuesto para dicha reacción comienza con la reducción del complejo de Pd(II) a Pd(0), siendo éste el catalizador real de la reacción (**Figura I.16**). A continuación, se forma un hidruro de Pd por protonación a partir del alcohol (**I**), seguido de una inserción del alquino en el enlace Pd–H. Sobre el alquenil-Pd formado (**II**), tendría lugar la inserción del

[90] J. Marco-Martínez, V. López-Carrillo, E. Buñuel, R. Simancas, D. J. Cárdenas, *J. Am. Chem. Soc.* **2007**, *129*, 1874–1875.

alqueno para generar un complejo de alquil-Pd (**III**), el cual sufriría una transmetalación con el reactivo de diboro ayudada por el alcóxido (**IV**) para, tras una eliminación reductora, liberar el producto observado y regenerar la especie inicial de Pd(0). Otra posible vía de actuación podría ser la formación de un paladaciclo (**V**) por ciclometalación oxidante del enino, seguido de una protonólisis del enlace C(sp^2)–Pd, llegando al mismo intermedio **III**. No obstante, estudios computacionales previos conducen a energías de activación elevadas para la ciclometalación de eninos con Pd en ausencia de ligandos dadores.

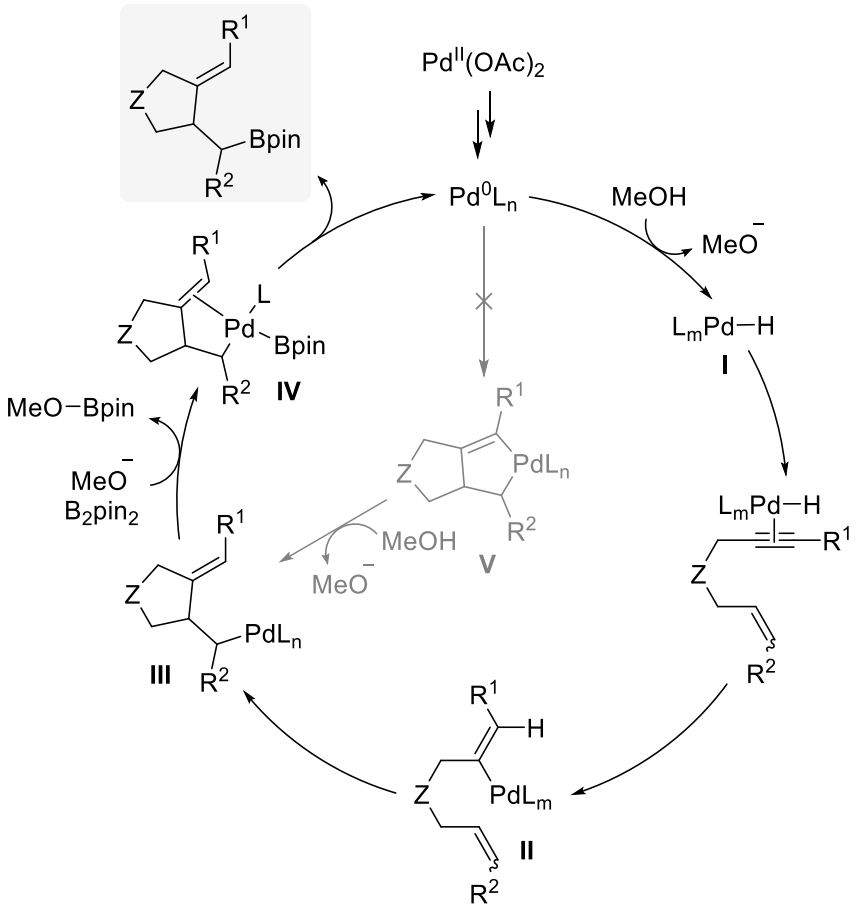

Figura I.16. Propuesta mecanística para la ciclación hidroborilativa descrita por Cárdenas.

Esta nueva metodología pudo ser aplicada igualmente a 1,7-eninos, conduciendo a la obtención de homoalilboronatos con buenos rendimientos y a la formación de anillos de 6 miembros.[91] En este caso, el complejo de Pd empleado fue Pd(TFA)$_2$ en lugar de Pd(OAc)$_2$ por ofrecer mejores resultados (**Esquema I.49**).

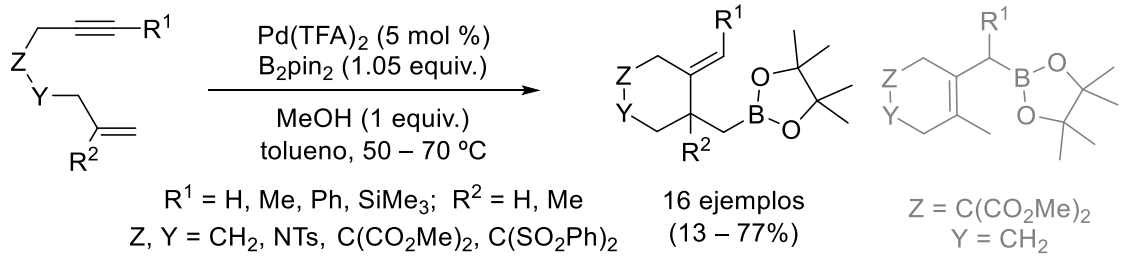

Esquema I.49. Ciclación hidroborilativa de 1,7-eninos.

[91] V. Pardo-Rodríguez, E. Buñuel, D. Collado-Sanz, D. J. Cárdenas, *Chem. Commun.* **2012**, *48*, 10517–10519.

El mecanismo propuesto por nuestro grupo se basa en la formación de un hidruro de Pd inicial, como propone en el primer trabajo descrito. Es interesante destacar que la naturaleza del conector presente en el enino condiciona parcialmente la reactividad, ya que con algunos eninos se obtiene mezcla del alquilboronato con el resto Bpin en el alqueno junto con el alquilboronato que tiene el Bpin en el alquino (*marcado en gris en el* ***Esquema I.49***). Esta observación parece justificarse porque los grupos malonato podrían coordinarse más fácilmente al Pd durante el proceso, una vez que el alqueno se ha descoordinado (**Figura I.17**). Durante ese proceso, se genera una vacante de coordinación en el Pd, compitiendo el proceso de *β*-eliminación.

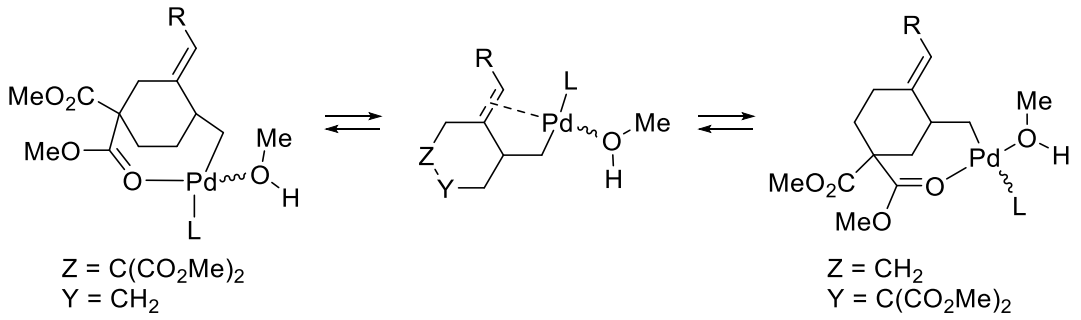

Figura I.17. Coordinación del grupo malonato al Pd.

A continuación, nuestro grupo decidió estudiar la diferente reactividad de 1,6-eninos frente a las ciclaciones hidroborilativas catalizadas por Pd.[92] La sustitución del alqueno con un grupo carbonato junto con la selección adecuada del ligando, permitió modular la reactividad observada (**Esquema I.50**). En este caso, la mayor facilidad del carbonato para actuar como grupo saliente provoca que la reacción comience por la adición oxidante del enlace C–O a un complejo de Pd(0) para dar lugar un complejo de alil-Pd(II).

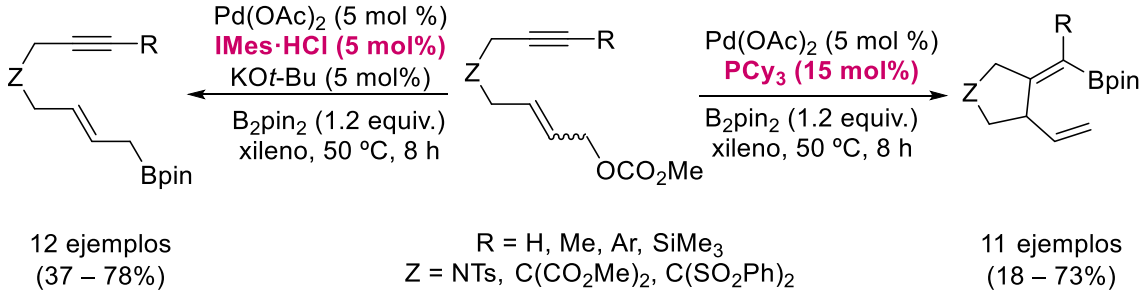

Esquema I.50. Reactividad de 1,6-eninos en función del ligando empleado.

En presencia de PCy_3 como ligando, se logra llevar a cabo la ciclación de la estructura con incorporación del resto Bpin en la posición del alquino, permitiendo la síntesis de alquenilboronatos con elevados rendimientos, independientemente de la configuración inicial del alqueno. Por el contrario, el empleo de un ligando tipo NHC conduce a la obtención de alilboronatos lineales. Este hecho se debe a la facilidad de coordinación al Pd que posee el alquino, requiriendo de la disociación previa del ligando para generar una vacante de coordinación en el metal. A diferencia del ligando de fosfina, el IMes es un ligando fuertemente coordinante, ralentizando su disociación y favoreciendo que el proceso de transmetalación y eliminación reductora tenga lugar más rápidamente que la ciclación.

[92] A. Martos-Redruejo, R. López-Durán, E. Buñuel, D. J. Cárdenas, *Chem. Commun.* **2014**, *50*, 10094–10097.

Con el objetivo de aprovechar la reactividad del intermedio de alquil-Pd formado (complejo **III** en **Figura I.16**), el grupo de Cárdenas sometió compuestos poliinsaturados a estas condiciones de reacción, observando policiclaciones en la estructura (**Esquema I.51**). En el caso de endiinos, la fuente de Pd óptima es $Pd(OAc)_2$, obteniendo alquil-[93] y alilboronatos[94] en función de la posición relativa de las insaturaciones. En el caso de dieninos,[95] el empleo de $Pd(TFA)_2$ conduce a la obtención regioselectiva de alilboronatos con rendimientos moderados.

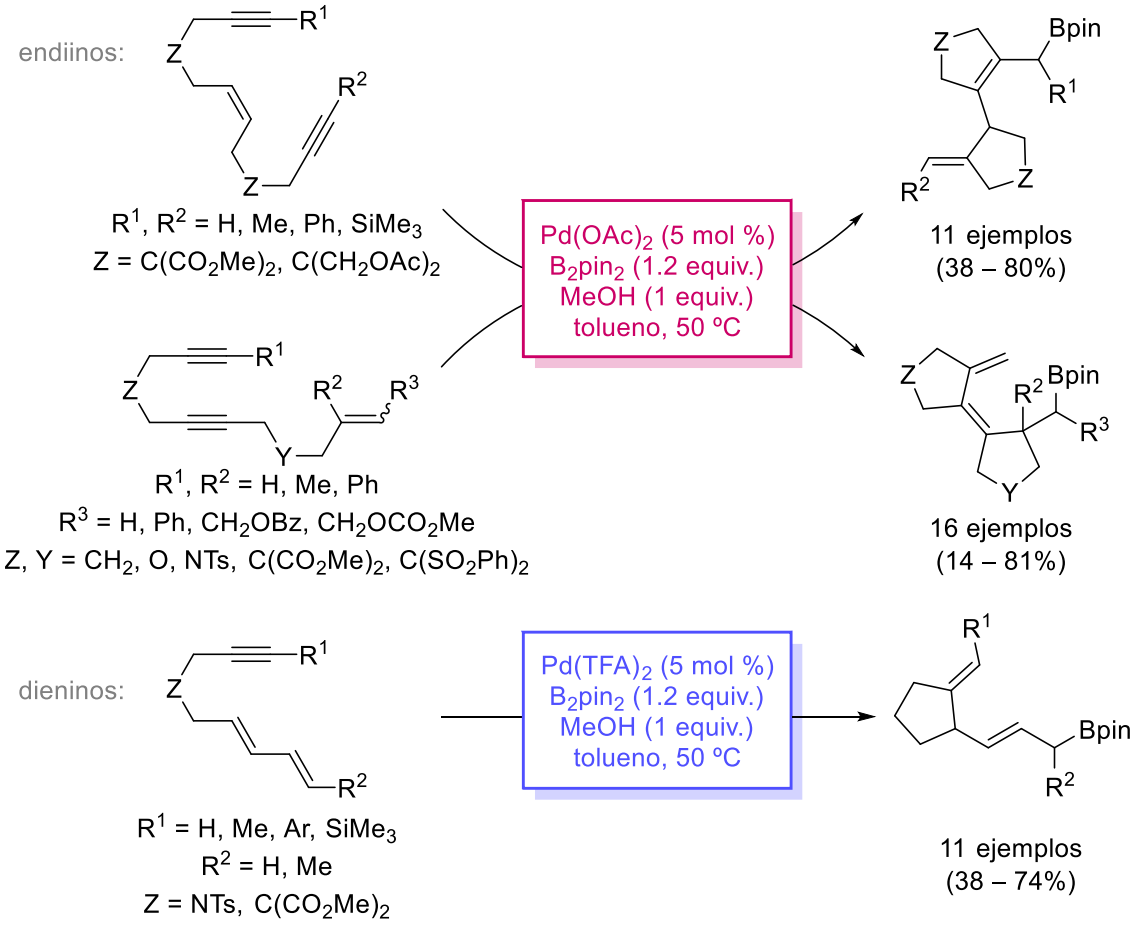

Esquema I.51. Policiclaciones hidroborilativas catalizadas por Pd.

Cabe destacar que todas las reacciones transcurren de forma estereoespecífica. Los boronatos obtenidos se emplearon para posteriores funcionalizaciones de la estructura a partir de reacciones de oxidación y de acoplamiento de tipo Suzuki, requiriendo de la transformación previa de los boronatos C(sp^3)–Bpin a las correspondientes sales de trifluoroborato. Así mismo, también se llevó a cabo esta reacción sobre enalenos y aleninos.[96]

El mecanismo de estas reacciones se asemeja al propuesto para la reacción pionera, transcurriendo a través de la formación de un hidruro de Pd . Sin embargo, en el caso de los 6-en-1,11-diinos la disposición relativa de los dobles enlaces en los productos finales no era

[93] J. Marco-Martínez, E. Buñuel, R. López-Durán, D. J. Cárdenas, *Chem. Eur. J.* **2011**, *17*, 2734–2741.
[94] J. Marco-Martínez, E. Buñuel, R. Muñoz-Rodríguez, D. J. Cárdenas, *Org. Lett.* **2008**, *10*, 3619–3621.
[95] R. López-Durán, A. Martos-Redruejo, E. Buñuel, V. Pardo-Rodríguez, D. J. Cárdenas, *Chem. Commun.* **2013**, *49*, 10691–10693.
[96] V. Pardo-Rodríguez, J. Marco-Martínez, E. Buñuel, D. J. Cárdenas, *Org. Lett.* **2009**, *11*, 4548–4551.

la esperada, lo que implicaba la intervención de un proceso de *β*-eliminación de hidrógeno y posterior inserción (**Figura I.18**). Cabe destacar que la reacción es estereoespecífica: la información esteroquímica contenida en el doble enlace del enino de partida se transmite a lo largo del ciclo catalítico, y la configuración relativa de los dos carbonos estereogénicos en diposición 1,4 del producto final de reacción depende de la configuración del doble enlace en el enino.

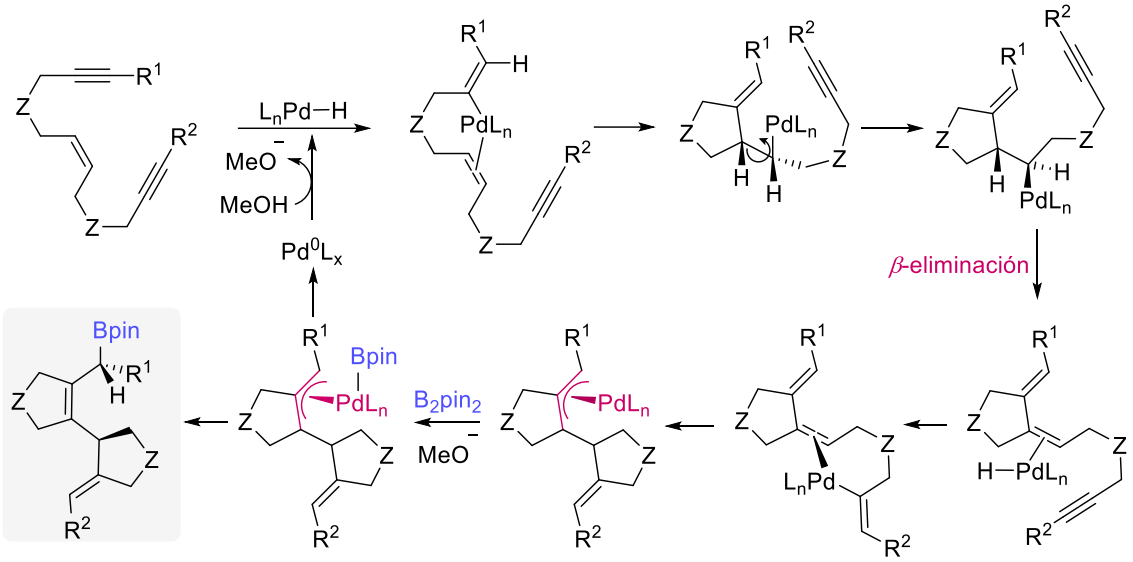

Figura I.18. Mecanismo de ciclación hidroborilativa de endiinos catalizada por Pd.

El grupo de Siegel empleó la metodología desarrollada por nuestro grupo de investigación para la ciclación de 1,6-eninos sustituidos con un grupo hidroxilo, con el objetivo de evaluar el efecto director que ejerce dicho sustituyente en el proceso.[97] La etapa de ciclación hidroborilativa se combina con una etapa final de oxidación, obteniendo los correspondientes alcoholes. Mientras que el empleo de alcoholes propargílicos conduce a los productos esperados con pobre selectividad y rendimientos variados, el empleo de alcoholes homopropargílicos permite la síntesis diastereoselectiva de los productos *cis* con rendimientos de buenos a moderados (**Esquema I.52**).

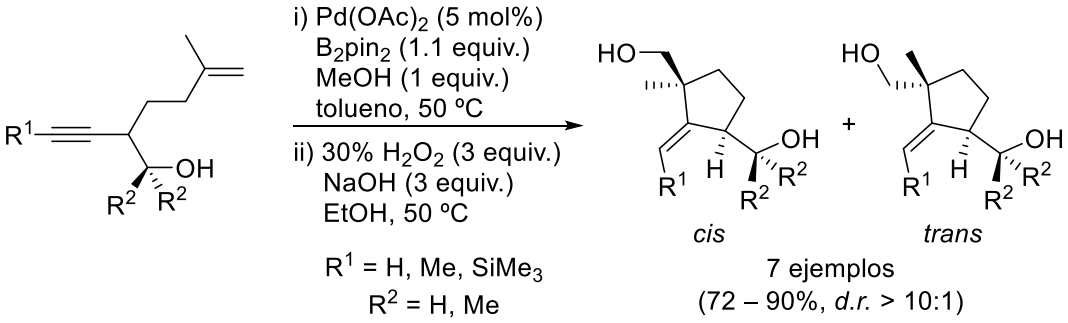

Esquema I.52. Aplicación de las ciclaciones hidroborilativas descritas por Cárdenas.

Recientemente, el grupo de Wang ha descrito la ciclación hidroborilativa de eninonas en presencia de B_2pin_2 y un complejo de Pd, permitiendo la síntesis de alquenilboronatos sustituidos con un anillo de furano (**Esquema I.53**).[98]

[97] A. M. Camelio, T. Barton, F. Guo, T. Shaw, D. Siegel, *Org. Lett.* **2011**, *13*, 1517–1519.
[98] Y. Ping, T. Chang, K. Wang, J. Huo, J. Wang, *Chem. Commun.* **2019**, *55*, 59–62.

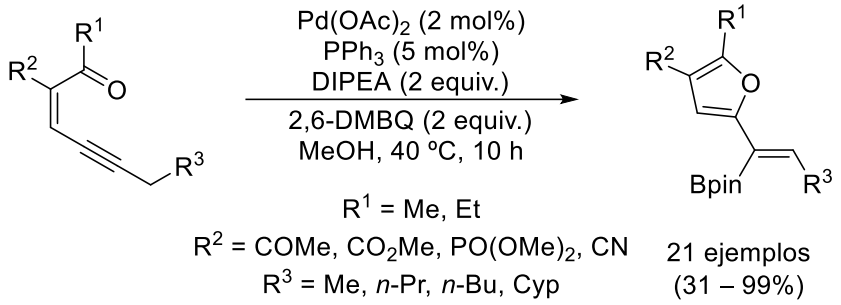

Esquema I.53. Condiciones descritas por el grupo de Wang.

El mecanismo propuesto por los autores se inicia con la formación de un complejo de boril-Pd que reacciona con la eninona de partida, generando un carbeno de Pd intermedio. A continuación, el resto Bpin da lugar a una inserción 1,1 del carbeno en el enlace Pd–B que permite al complejo de alquil-Pd obtenido sufrir una *β*-eliminación de hidrógeno para liberar el producto de reacción. El hidruro de Pd generado es reducido a Pd(0) por la base para, posteriormente, oxidarse a Pd(II) por acción de la benzoquinona. Finalmente, el complejo de boril-Pd catalíticamente activo se regenera por transmetalación con el B_2pin_2 (**Figura I.19**).

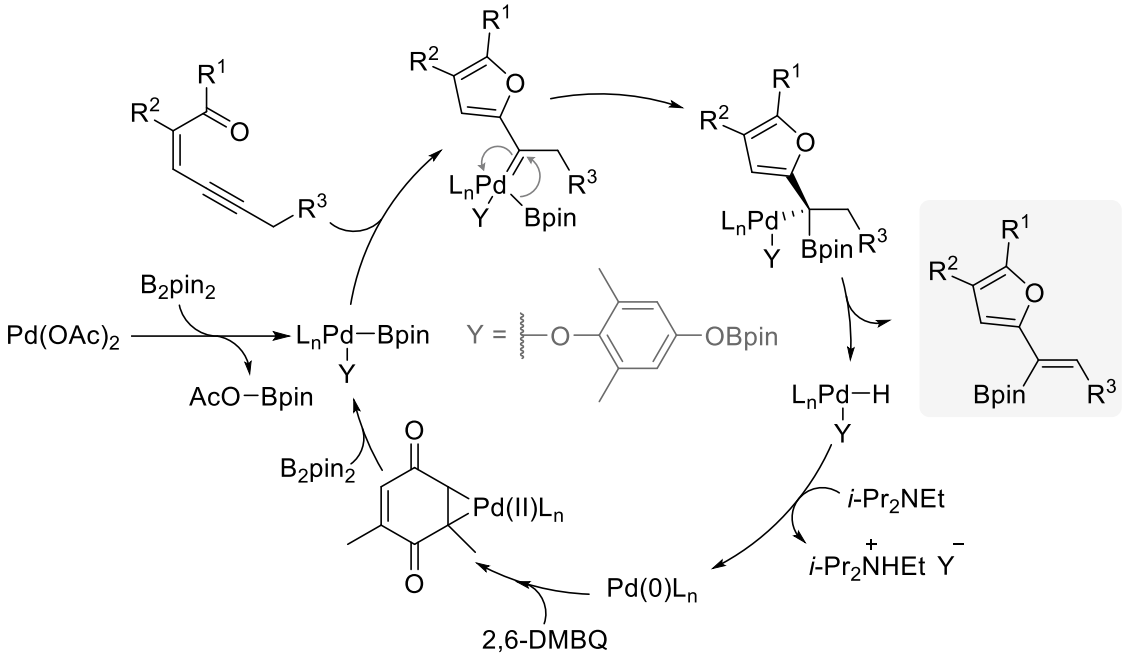

Figura I.19. Propuesta mecanística de la reacción del grupo de Wang.

1.3.3.2. Reacciones catalizadas por Rh

En 2006, Widenhoefer y colaboradores describieron la ciclación hidroborilativa asimétrica de 1,6-eninos empleando un complejo de Rh como catalizador.[99] El empleo de catecolborano, en vez de pinacolborano, permite la síntesis de alquenilboronatos con mejores rendimientos. Debido a la inestabilidad de los boronatos obtenidos, los autores realizan *in situ* una segunda etapa de oxidación o acoplamiento de tipo Suzuki, obteniendo productos más estables y más fácilmente aislables (**Esquema I.54**).

[99] R. E. Kinder, R. A. Widenhoefer, *Org. Lett.* **2006**, *8*, 1967–1969.

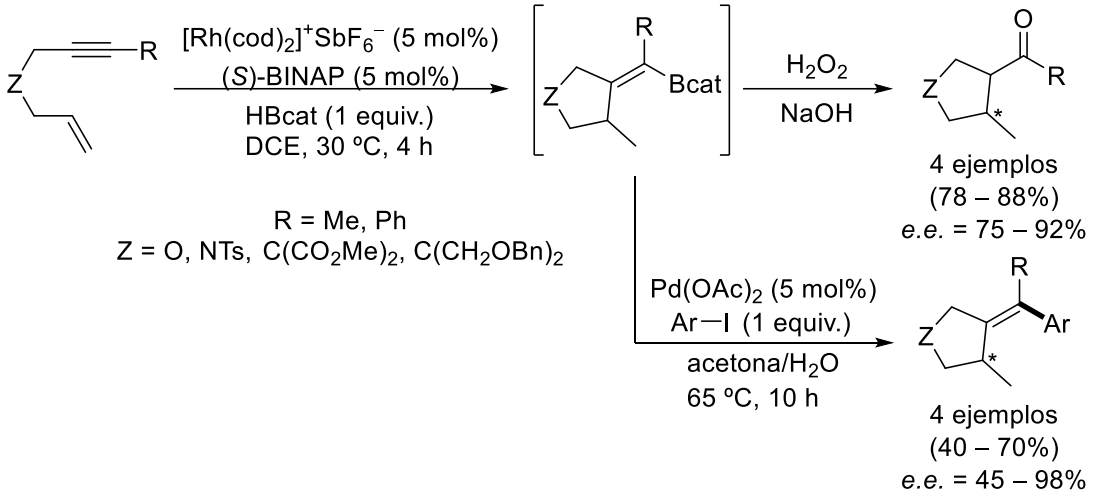

Esquema I.54. Ciclación hidroborilativa asimétrica catalizada por Rh.

En el estudio, no se realizan ensayos mecanísticos, pero los autores proponen que el camino de reacción comienza con la adición oxidante del enlace B–H al Rh.

1.3.3.3. Reacciones catalizadas por Co

La catálisis con Co de ciclaciones hidroborilativas de eninos ha sido estudiado por primera vez en el grupo de Lu.[100] Las condiciones de reacción requieren del empleo de un complejo de Co junto con $NaBHEt_3$, utilizando pinacolborano como fuente de boro. La regioselectividad de la reacción se puede controlar en función del ligando empleado, obteniendo alquilboronatos al usar un ligando tridentado de nitrógeno (OIP), o alquenilboronatos a partir de un ligando bidentado (IP), respectivamente (**Esquema I.55**). En el caso de los alquilboronatos, los autores realizan una etapa adicional de oxidación para aislar los correspondientes alcoholes y minimizar una pérdida de rendimiento por descomposición de los boronatos. A pesar de los buenos rendimientos y la economía atómica de la reacción, el alcance queda restringido al empleo de alquenos terminales.

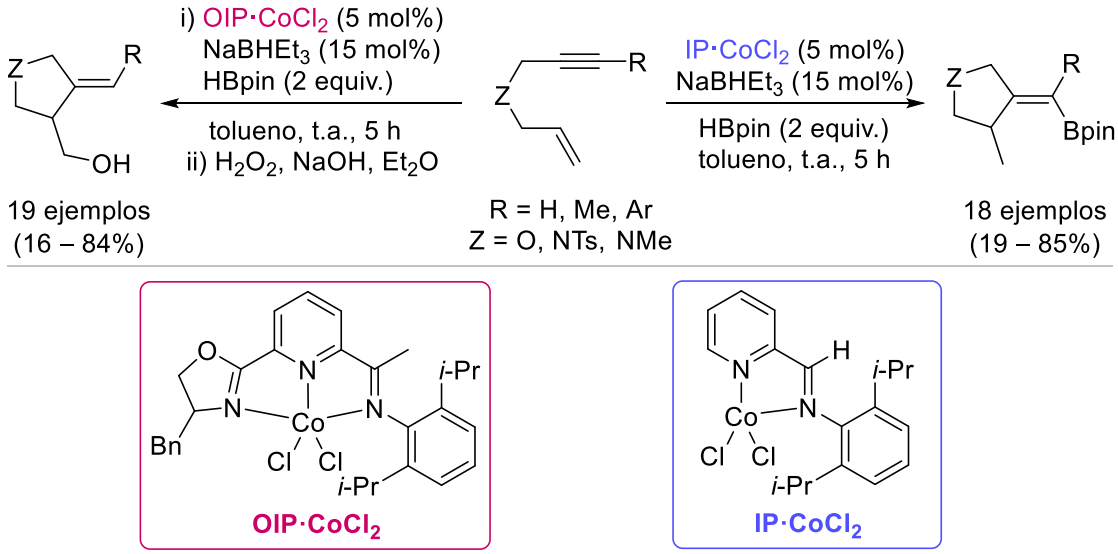

Esquema I.55. Primer ejemplo de ciclación hidroborilativa de eninos catalizada por Co.

[100] T. Xi, Z. Lu, *ACS Catal.* **2017**, *7*, 1181–1185.

El mecanismo de reacción propuesto comienza con la formación de un hidruro de Co por reacción con el $NaBHEt_3$, el cual sufre la inserción del alqueno o alquino, dependiendo del ligando presente en la reacción. Por último, la inserción de la insaturación restante, y posterior metátesis σ con el pinacolborano, libera el boronato correspondiente y regenera el hidruro de Co catalíticamente activo (**Figura I.20**).

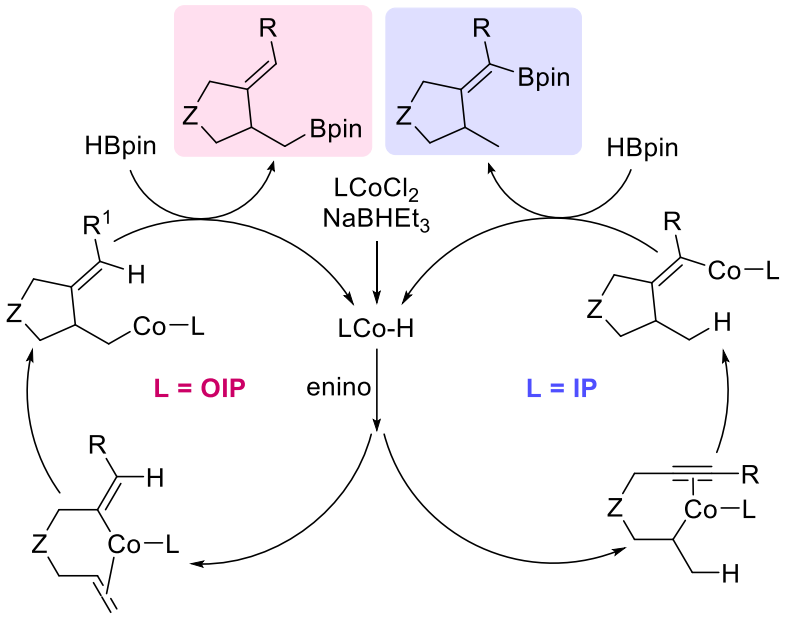

Figura I.20. Mecanismo propuesto por el grupo de Lu.

Poco tiempo después, el grupo de Ge desarrolló la versión enantioselectiva de dicha reacción, sintetizando una gran variedad de alquil- y alquenilboronatos con buenos rendimientos y excelentes excesos enantioméricos en la mayoría de los casos (**Esquema I.56**).[101]

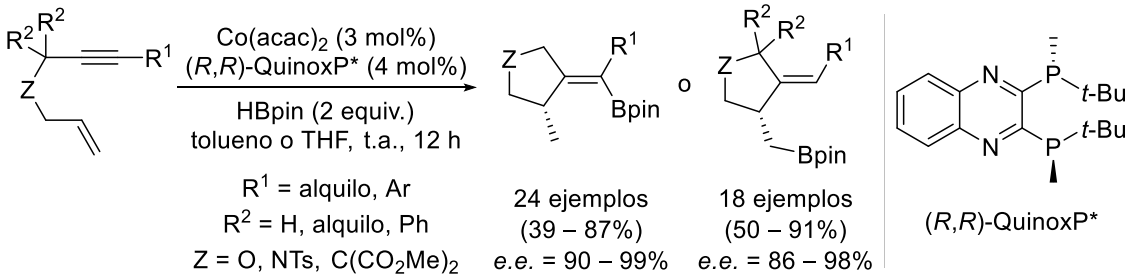

Esquema I.56. Ciclación hidroborilativa enantioselectiva de eninos catalizada por Co.

Los boronatos obtenidos son eficazmente empleados en transformaciones como oxidación y acoplamiento de tipo Suzuki-Miyaura. El interés de esta metodología se ilustró mediante su empleo en la etapa final para la síntesis de un producto natural, la (−)-Magnofargesina.

Además, el mismo grupo de investigación empleó complejos de Co para la síntesis enantioselectiva de alquilboronatos con la consecuente formación de un centro estereogénico sustituido con grupos carbonados.[102] La reacción muestra una gran variedad estructural en los eninos de partida y buena compatibilidad de grupos funcionales,

[101] S. Yu, C. Wu, S. Ge, *J. Am. Chem. Soc.* **2017**, *139*, 6526–6529.
[102] C. Wang, S. Ge, *J. Am. Chem. Soc.* **2018**, *140*, 10687–10690.

conduciendo a alquilboronatos con buenos rendimientos y elevados excesos enantioméricos (**Esquema I.57**). Una vez más, los alquilboronatos obtenidos se emplean en diversas transformaciones, destacando la importancia y utilidad sintética de estos productos.

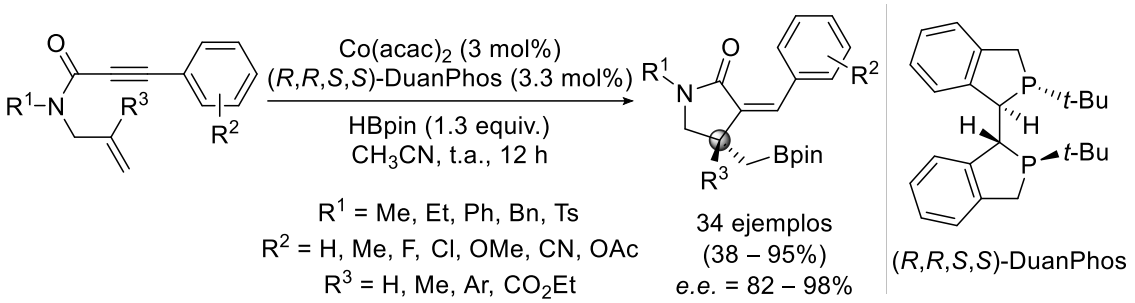

Esquema I.57. Sintesis de alquilboronatos con un centro estereogénico carbonado.

El mecanismo propuesto por el grupo de Ge para ambas metodologías consiste en la formación inicial de un hidruro de Co por reacción con pinacolborano, seguido de la inserción del alquino o alqueno para conducir a la obtención de alquil- o alquenilboronatos, respectivamente. A partir de reacciones estequiométricas en ausencia del enino, el grupo de Ge fue capaz de aislar y caracterizar el hidruro de Co mostrado en el **Esquema I.58**.

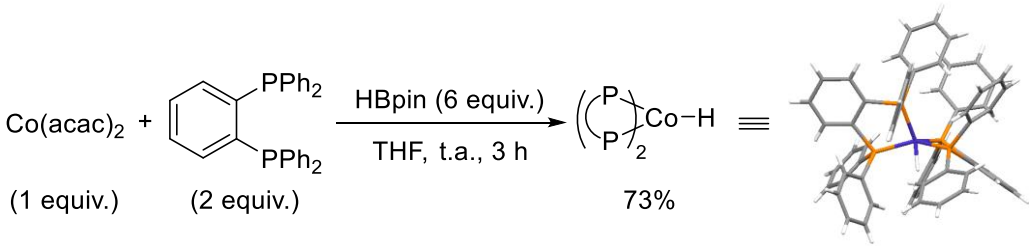

Esquema I.58. Aislamiento y caracterización de Co–H.

Recientemente, el grupo de Ge ha aplicado también esta metodología sobre 1,7-eninos para la síntesis asimétrica de quinolinas, debido a su presencia en abundantes moléculas con actividad biológica.[103] El alcance de la reacción es bastante amplio, ofreciendo elevados rendimientos y excelentes excesos enantioméricos (**Esquema I.59**).

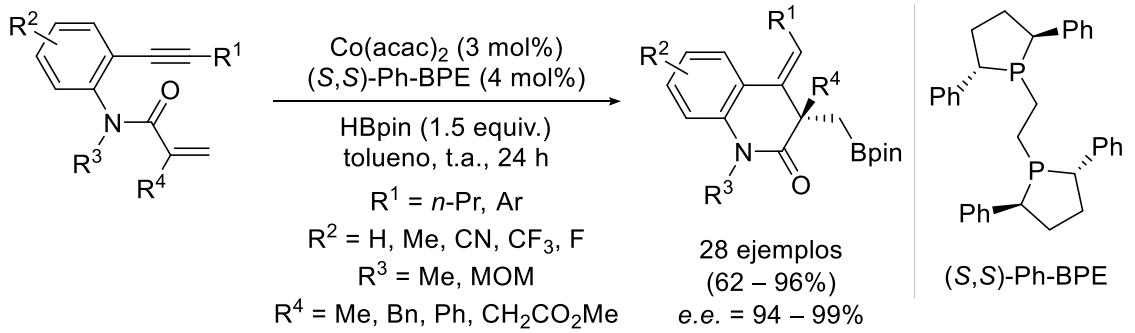

Esquema I.59. Síntesis enantioselectiva de quinolinas por ciclación hidroborilativa de eninos.

El mecanismo propuesto por los autores comienza con la formación de un hidruro de Co por reacción con pinacolborano, teniendo lugar a continuación la inserción del alquino.

[103] C. Wu, J. Liao, S. Ge, *Angew. Chem. Int. Ed.* **2019**, 58, 8882–8886.

1.3.3.4. Reacciones catalizadas por Ni

El grupo de Cheng junto con el grupo de Hsieh han descrito el único ejemplo, conocido hasta el momento, de ciclación hidroborilativa de eninos catalizada por Ni.[104] La regioselectividad de la reacción varía en función de la sustitución del alqueno presente en el enino, pudiendo obtener alquilboronatos a partir de alquenos terminales y alquenilboronatos a partir de alquenos deficientes en electrones (**Esquema I.60**).

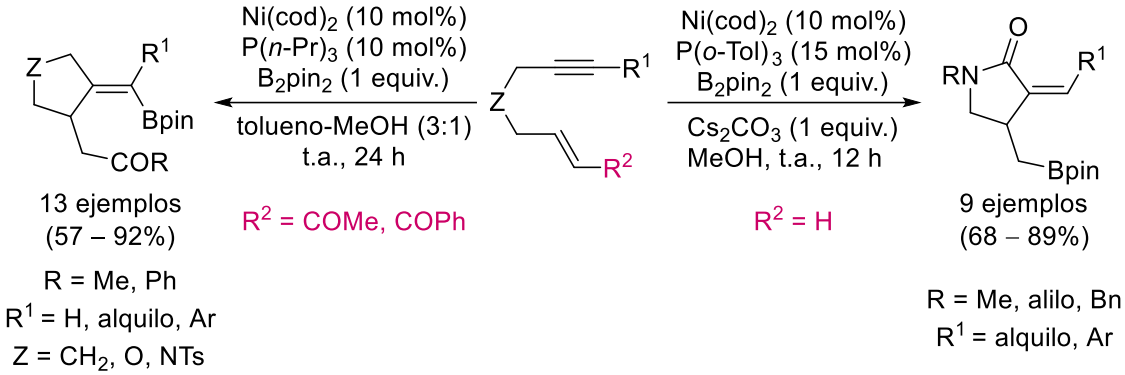

Esquema I.60. Ciclación hidroborilativa de eninos catalizada por Ni.

El mecanismo propuesto por los autores comienza con la ciclometalación oxidante del Ni con el enino. El niquelaciclo obtenido sufre una protonación con el MeOH por dos vías diferentes en función del tipo de alqueno, insertándose el hidrógeno en el alqueno o en el alquino, respectivamente. La transmetalación con el reactivo de boro, asistida por el alcóxido liberado anteriormente, y posterior eliminación reductora conduce regioselectivamente a la obtención de los alquil- y alquenilboronatos (**Figura I.21**).

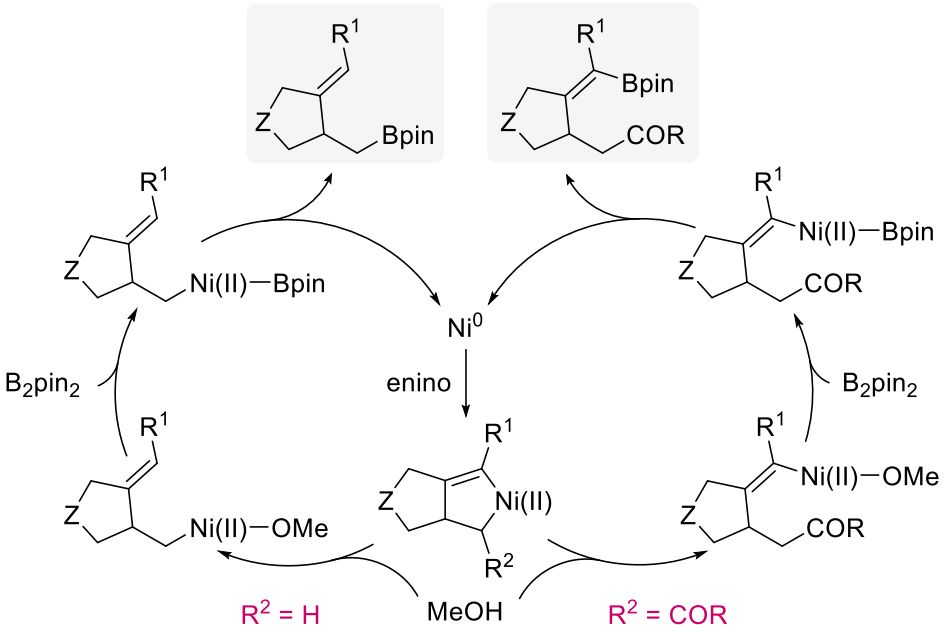

Figura I.21. Ciclo catalítico propuesto para la reacción descrita por Cheng y Hsieh.

La reacción transcurre de forma regio- y estereoselectiva, proporcionando elevados rendimientos. Sin embargo, el alcance estructural está limitado a un tipo concreto de

[104] J.-C. Hsieh, Y.-C. Hong, C.-M. Yang, S. Mannathan, C.-H. Cheng, *Org. Chem. Front.* **2017**, *4*, 1615–1619.

sustratos para que la reacción tenga lugar de forma eficaz, y la economía atómica de la reacción se pierde al producirse únicamente la inserción de uno de los restos Bpin.

1.3.3.5. Reacciones catalizadas por Cu

En 2013, Tian y Lin llevaron a cabo la ciclación hidroborilativa enantioselectiva de 1,6-eninos empleando B_2pin_2 y un catalizador de Cu.[105] Este procedimiento conduce a buenos rendimientos y altos excesos enantioméricos, obteniendo únicamente la fusión *cis* de los anillos (**Esquema I.61**). Los boronatos obtenidos se emplean en transformaciones adicionales conduciendo a estructuras complejas y funcionalizadas.

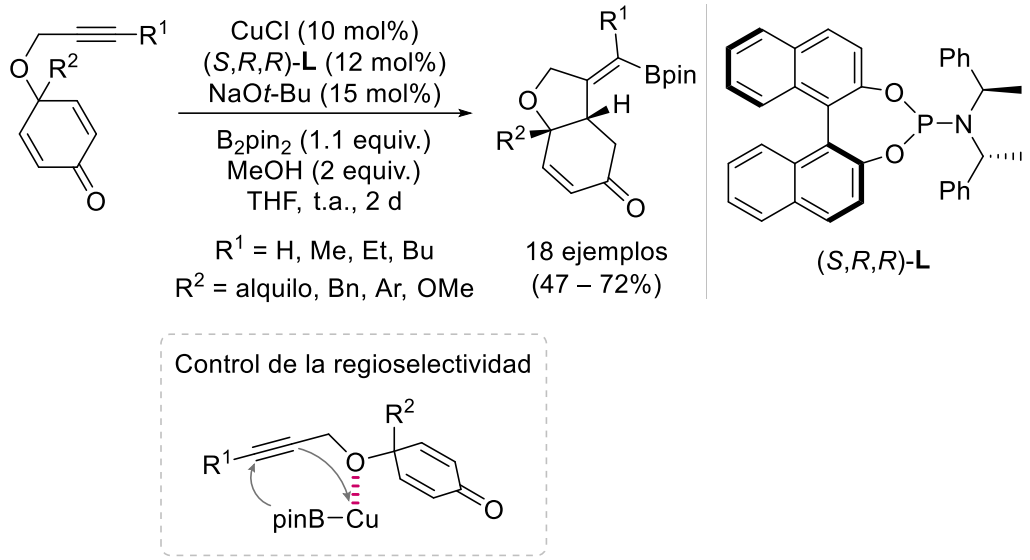

Esquema I.61. Ciclación hidroborilativa de 1,6-eninos catalizada por Cu.

Esta reacción parece tener lugar a partir de un proceso tándem de β-borilación del éter propargílico y posterior adición conjugada enantioselectiva a la ciclohexadienona. La presencia del conector de oxígeno en dicha posición es crucial para que la reacción tenga lugar, debido a la posible coordinación entre complejo de Cu–Bpin y el O que orienta la reactividad de la reacción.

Más tarde, el grupo de Bai y Zhu describió un tipo parecido de reacciones empleando un sistema catalítico sencillo de $CuCl/PPh_3$ (**Esquema I.62**).[106] El alcance de la reacción es muy amplio, siendo compatible con diversos conectores del enino y sustituyentes en el alquino, llegando a obtener anillos de entre 5 y 8 miembros. Sin embargo, este sistema requiere la sustitución del alqueno con un grupo fosfato para que el proceso tenga lugar.

[105] P. Liu, Y. Fukui, P. Tian, Z.-T. He, C.-Y. Sun, N.-Y. Wu, G.-Q. Lin, *J. Am. Chem. Soc.* **2013**, *135*, 11700–11703.
[106] F. Zhang, S. Wang, Z. Liu, Y. Bai, G. Zhu, *Tetrahedron Lett.* **2017**, *58*, 1448−1452.

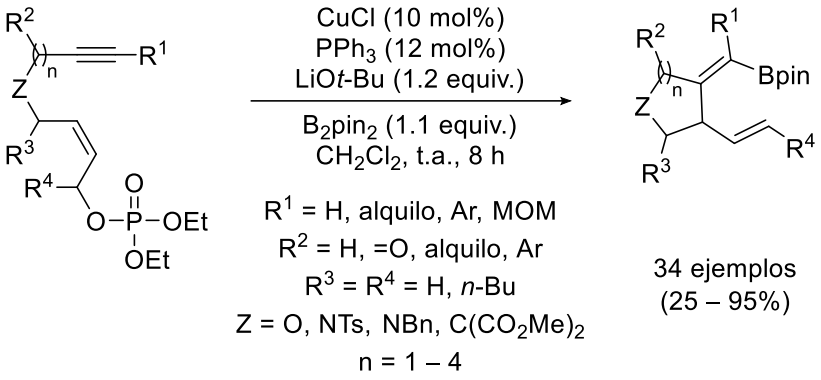

Esquema I.62. Ciclación hidroborilativa de eninos descrita por Bai y Zhu.

El mecanismo de la reacción propuesto por los autores comenzaría con la formación de un complejo Cu–Bpin inicial que sufriría la inserción del alquino, a diferencia de otros estudios en los que se plantea la formación de un complejo alil–Cu por adición oxidante del fosfato alílico.

El grupo de Carretero y colaboradores ha llevado a cabo un exhaustivo estudio mecanístico de estas reacciones catalizadas por Cu, centrándose en la etapa de carboboración del alquino.[107] Más en concreto, determinan que la presencia de una base en cantidad estequiométrica o catalítica no es un hecho trivial, condicionando la reactividad de la reacción. En el caso de los epóxidos, el alcóxido se une preferentemente al resto borilado en lugar de al Cu, generando un "complejo vinilborato" que orienta el ataque para dar lugar a la ciclación, requiriéndose cantidades estequiométricas de alcóxido para que el proceso tenga lugar. Por el contrario, en el caso de los eninos, la coordinación del alqueno al alquenil-Cu formado da lugar a la ciclación sin necesitar de la activación previa entre el alcóxido y el boro. Por lo tanto, la presencia de cantidades catalíticas de base es suficiente para que el proceso tenga lugar (**Esquema I.63**).

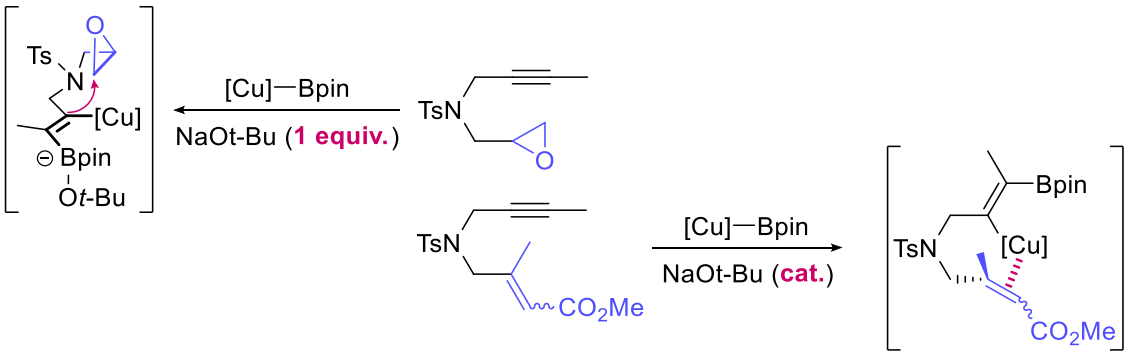

Esquema I.63. Efecto del alcóxido en el mecanismo de la reacción.

Además, evalúan la generalidad de la reacción para diversos 1,6-eninos, conduciendo a estructuras cicladas con un centro estereogénico con los cuatro sustituyentes carbonados con rendimientos de moderados a excelentes (**Esquema I.64**).

[107] S.-H. Kim-Lee, I. Alonso, P. Mauleón, R. Gómez Arrayás, J. C. Carretero, *ACS Catal.* **2018**, *8*, 8993−9005.

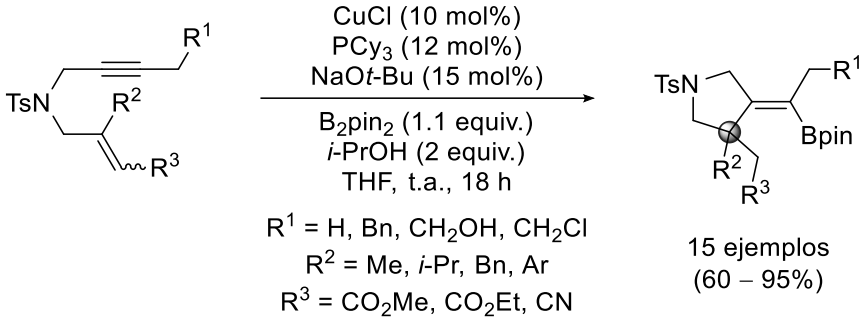

Esquema I.64. Alcance de la reacción catalizada por Cu.

1.3.3.6. Reacciones sin metales de transición

El continuo interés por desarrollar métodos eficientes y concienciados con el medio ambiente, así como por explorar diferentes y novedosas aproximaciones para la síntesis de compuestos de organoboro, ha permitido el desarrollo de ciclaciones borilativas en ausencia de catalizadores metálicos.

Concretamente, en la bibliografía encontramos algunos ejemplos. Aunque los sustratos de partida no son eninos, merece una mención el trabajo descrito por Ingleson, donde se describe la ciclación hidroborilativa de alquinos con BCl_3 como fuente de boro.[108] La ciclación tiene lugar a partir de la activación C–H del grupo aromático presente en la estructura, mostrando una buena compatibilidad de grupos funcionales y obteniendo derivados de 1,2-dihidronaftalenos con muy buenos rendimientos (**Esquema I.65**). El camino de reacción más probable comienza con la activación del alquino con el BCl_3, viéndose desfavorecida la reacción de haloboración por el empleo de alquinos internos.

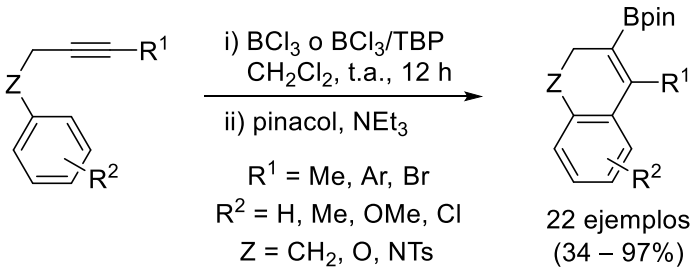

Esquema I.65. Ciclación hidroborilativa descrita por Ingleson.

Hashmi y colaboradores han descrito un proceso de ciclopropanación/carboboración de 1,6-eninos empleando $B(C_6F_5)_3$ en condiciones suaves de reacción.[109] Estudios mecanísticos proponen que la reacción comienza con la activación del alquino hacia la formación del ciclopropano correspondiente, seguido de la migración de un resto C_6F_5. Dependiendo de la sustitución del grupo alqueno presente en el enino, se observa la apertura del ciclopropano hacia la formación de derivados de ciclopentano o ciclohexano (**Esquema I.66**).

[108] A. J. Warner, J. R. Lawson, V. Fasano, M. J. Ingleson, *Angew. Chem. Int. Ed.* **2015**, *54*, 11245–11249.
[109] M. M. Hansmann, R. L. Melen, M. Rudolph, F. Rominger, H. Wadepohl, D. W. Stephan, A. S. K. Hashmi, *J. Am. Chem. Soc.* **2015**, *137*, 15469−15477.

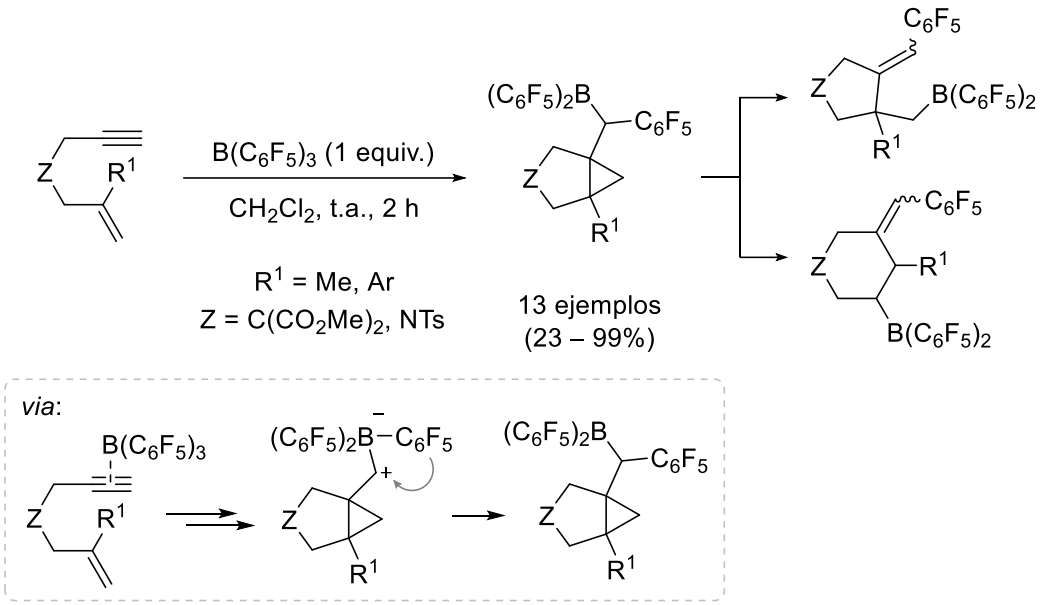

Esquema I.66. Ciclopropanación/carboboración de eninos.

Recientemente, el grupo de Wang ha llevado a cabo la ciclación borilativa radicalaria de 1,6-eninos en presencia de un radical NHC-borilo (**Esquema I.67**).[110] La generación de dicho radical se produce entre un borano y un iniciador (AIBN). Este procedimiento permite la síntesis selectiva de alquenil- y alquilboranos a partir de alquinos terminales o alquinos internos sustituidos con un grupo aromático, respectivamente.

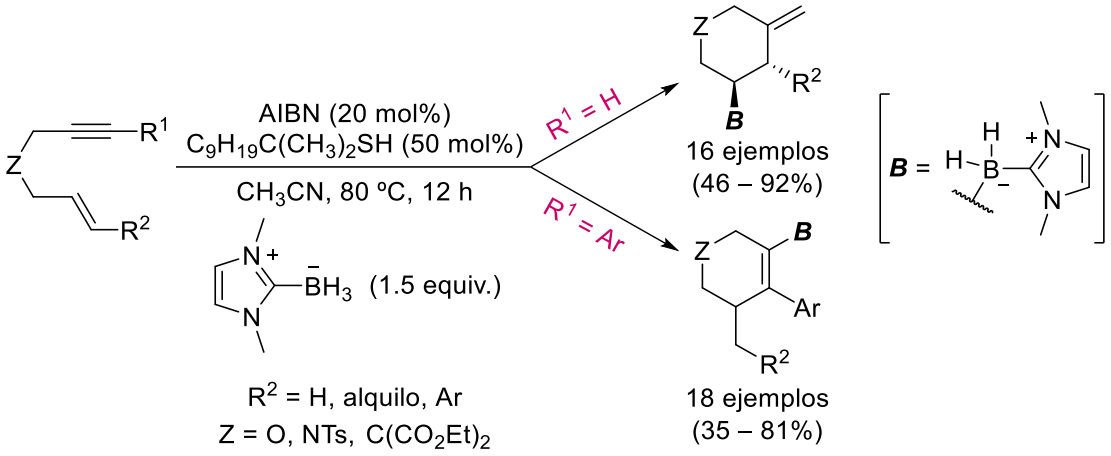

Esquema I.67. Ciclación borilativa radicalaria de 1,6-eninos.

A partir de experimentos mecanísticos, demuestran la formación de radicales en el transcurso de la reacción. Así mismo, los autores realizan diversas transformaciones de los boranos finales obtenidos para recalcar la utilidad sintética de estos productos.

[110] S.-C. Ren, F.-L. Zhang, J. Qi, Y.-S.i Huang, A.-Q. Xu, H.-Y. Yan, Y.-F. Wang, *J. Am. Chem. Soc.* **2017**, *139*, 6050−6053.

OBJETIVOS

2. OBJETIVOS

Como se ha podido ver en los antecedentes descritos, el desarrollo de procesos eficaces para la síntesis de compuestos de organoboro es uno de los principales intereses de la química orgánica sintética. Debido a la creciente preocupación por el desarrollo de metodologías concienciadas con el medio ambiente, el estudio de nuevos procesos sintéticos debe tener en cuenta factores de toxicidad, economía atómica y eficacia de la reacción, siendo importante también la síntesis de moléculas con elevada complejidad estructural en pocos pasos de reacción.

Por un lado, el empleo de metales de la primera fila de transición ofrece condiciones de reacción muy diferentes para llevar a cabo estos procesos, siguiendo insólitos mecanismos y disminuyendo los inconvenientes derivados del uso de metales preciosos. Además, estos metales permiten alcanzar reactividades muy difíciles de conseguir hasta el momento. Por otro lado, la ciclación borilativa de especies poliinsaturadas permite la síntesis de moléculas cíclicas funcionalizadas en una sola etapa sintética, permitiendo transformaciones posteriores que aumenten la complejidad estructural.

Con todo ello, la presente Tesis Doctoral se focaliza en el estudio y desarrollo de nuevas reacciones átomo-económicas de ciclación borilativa de estructuras poliinsaturadas catalizadas por metales de la primera serie de transición. Concretamente, esta se centra en el empleo de eninos, debido a su gran versatilidad como materiales de partida y a que permiten la introducción de grupos funcionales de diferente naturaleza en función de la distinta reactividad de sus insaturaciones. Respecto a los metales de transición de la primera fila, hemos escogido Fe y Ni como posibles catalizadores para estas reacciones (**Figura O.1**).

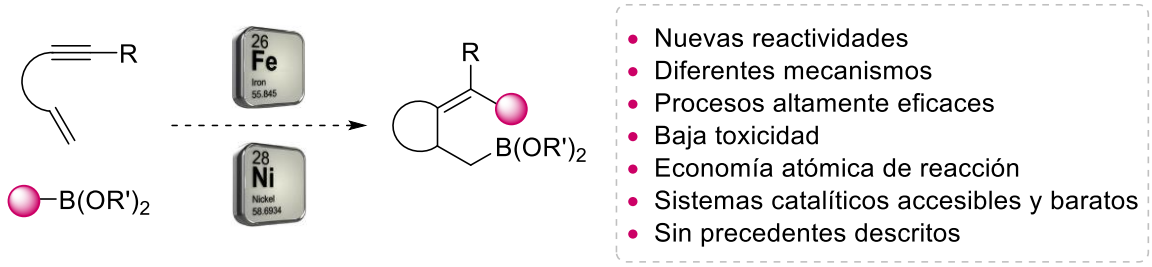

Figura O.1. Objetivos generales de la Tesis.

El primer objetivo de la Tesis consiste en extender la reacción hidroborilativa de eninos con pinacolborano empleando un catalizador de Fe. Hasta el momento, no existe ningún precedente en la bibliografía que describa la catálisis con Fe de este tipo de reacciones, siendo un ámbito inexplorado que puede permitir el descubrimiento de reactividad y mecanismos nuevos (**Esquema O.1**).

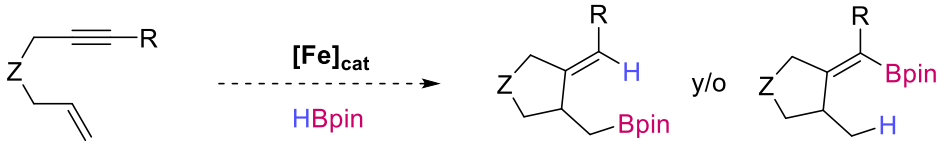

Esquema O.1. Ciclación hidroborilativa de eninos catalizada por Fe.

Del mismo modo, se consideró que el empleo de catalizadores de Ni junto con HBpin sobre sustratos de tipo enino conduciría a procesos sintéticos eficaces y completamente átomo-

económicos para la obtención de derivados borilados (**Esquema O.2**), siendo un interesante objetivo a desarrollar en esta Tesis.

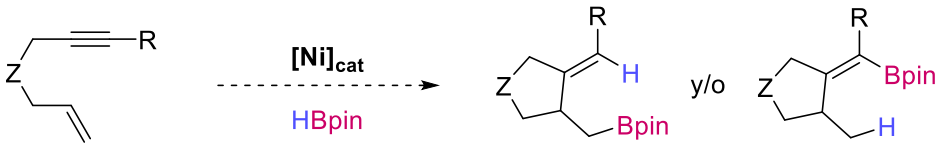

Esquema O.2. Ciclación hidroborilativa de eninos catalizada por Ni.

Considerando los antecedentes, se observó que no se describía ningún ejemplo de ciclación diborilativa de eninos en la bibliografía. Por ello, el tercer objetivo se centra en el estudio de este tipo de reacción empleando un catalizador de Ni y un complejo bimetálico de boro, pudiendo introducir simultáneamente dos sustituyentes de boro en la estructura (**Esquema O.3**). No obstante, la naturaleza resultante en ambos restos será diferente según el carácter de alquenilo o alquilo que posea, permitiendo una posterior transformación selectiva de cada uno de ellos.

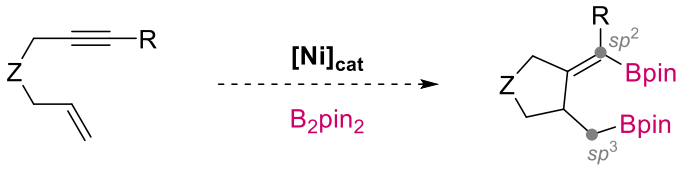

Esquema O.3. Ciclación diborilativa de eninos catalizada por Ni.

Finalmente, se consideró que el empleo de reactivos de organoboro, en lugar de los reactivos más comúnmente empleados como HBpin y B_2pin_2, podría ser una vía interesante de estudio dentro de las ciclaciones borilativas. Debido a ello, el cuarto objetivo de la Tesis consiste en el desarrollo de la ciclación carboborilativa átomo-económica de eninos catalizada por Ni, a través de la activación del enlace C–B (**Esquema O.4**). Una vez más, en la bibliografía no se encuentran precedentes de este tipo de reacciones.

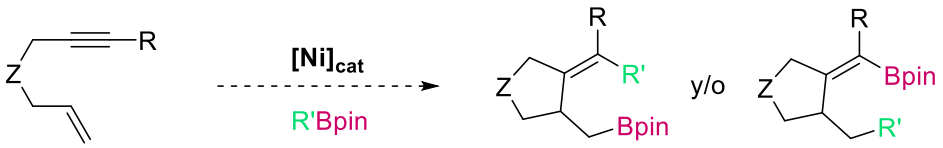

Esquema O.4. Ciclación carboborilativa de eninos catalizada por Ni.

Otro objetivo intrínseco de la presente Tesis consiste en demostrar la utilidad sintética de los productos obtenidos a partir de posteriores transformaciones descritas en la bibliografía, como oxidaciones y acoplamientos de tipo Suzuki, entre otras. Del mismo modo, a parte del desarrollo experimental de estas nuevas metodologías, se llevarán a cabo diferentes ensayos mecanísticos y estudios computacionales para proponer un mecanismo de reacción razonable para todas estas reacciones.

RESULTS AND DISCUSSION

CHAPTER 1:

Synthesis of starting enynes

3. RESULTS AND DISCUSSION

3.1. CHAPTER 1

3.1.1. Synthesis of the starting enynes

In order to develop the objectives of this Thesis, the synthesis of several enynes was carried out. These enynes contain different substituents in the alkyne, alkene, propargylic and allylic positions. Besides, a variety of atom-tethered enynes was evaluated. The yields shown below for the final product correspond to overall isolated yields after two or three reaction steps.

Firstly, *O*-tethered enynes (**1a**) were synthesized in good to excellent yields by a Sonogashira-type reaction from propargylic alcohols with iodoarenes, followed by the nucleophilic substitution with allyl bromide (**Scheme 1.1**) or allylic bromide derivatives (**Scheme 1.2**).

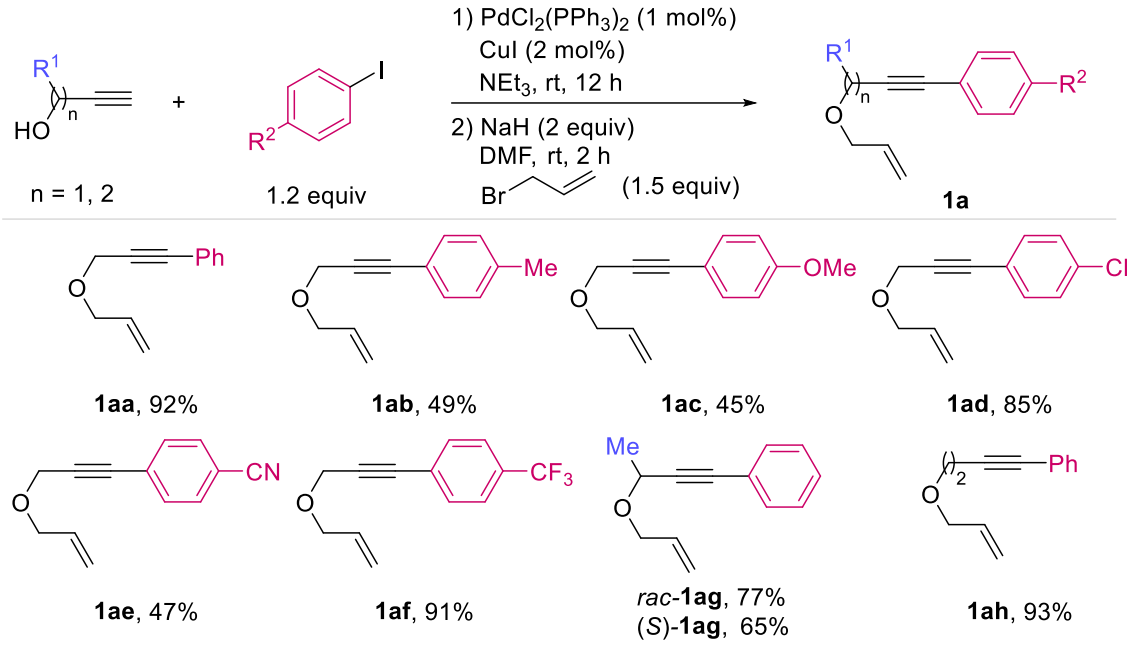

Scheme 1.1. Synthesis of enynes **1aa-ah** (Z = O) with aromatic moiety in the alkyne.

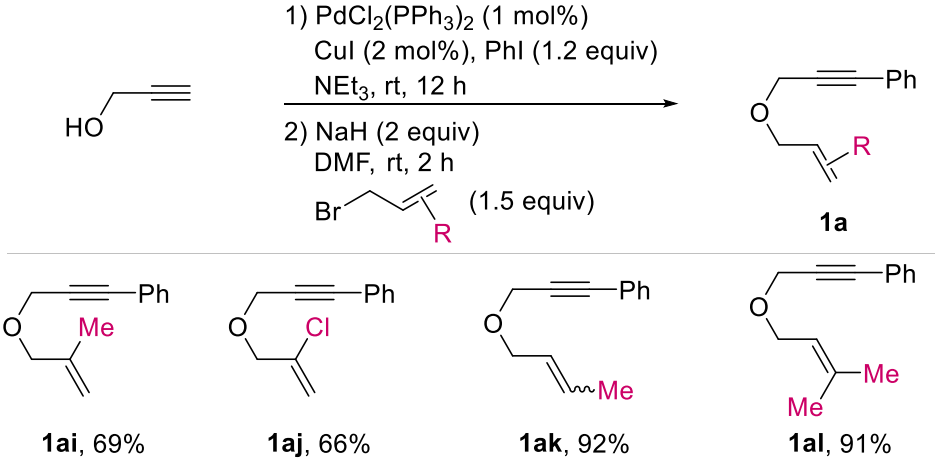

Scheme 1.2. Synthesis of enynes **1ai-al** (Z = O) with substituents in the alkene.

Starting with commercially available allylic alcohols, other enynes were synthetized by reaction with propargylic bromides (**Scheme 1.3**).

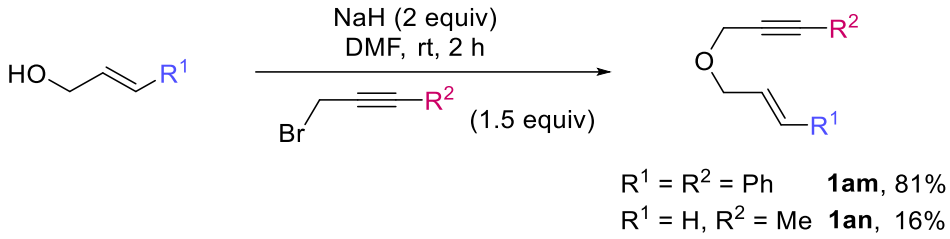

Scheme 1.3. Synthesis of enynes **1am-an** (Z = O) with other substituents.

Internal substituted alkene **1ao** was prepared by Sonogashira reaction and methylation of the hydroxyl group of 2-methylenepropane-1,3-diol (**Scheme 1.4**).

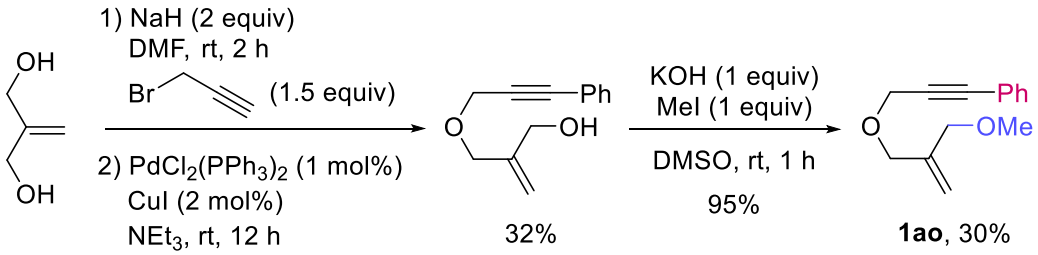

Scheme 1.4. Synthesis of enyne **1ao** (Z = O).

Following the literature, enyne **1ap** was obtained in low yield by a double nucleophilic substitution at both hydroxyl groups of but-2-yne-1,4-diol (**Scheme 1.5**).

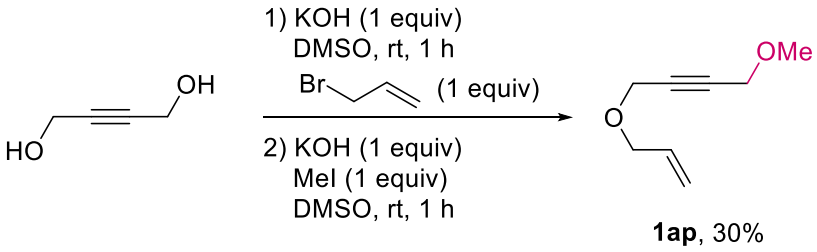

Scheme 1.5. Synthesis of enyne **1ap** (Z = O) with alkyl moiety in the alkyne.

N-tethered enynes (**1b**) were synthetized by a three-step procedure. First, the tosylation reaction of the amine group and subsequent nucleophilic substitution with allyl bromide were performed in order to obtain the core-structure of most enynes (**1ba**). Then, Sonogashira-type reaction or one-pot reaction with *n*-BuLi, paraformaldehyde and iodomethane led to the formation of several enynes in high yields (**Scheme 1.6**).

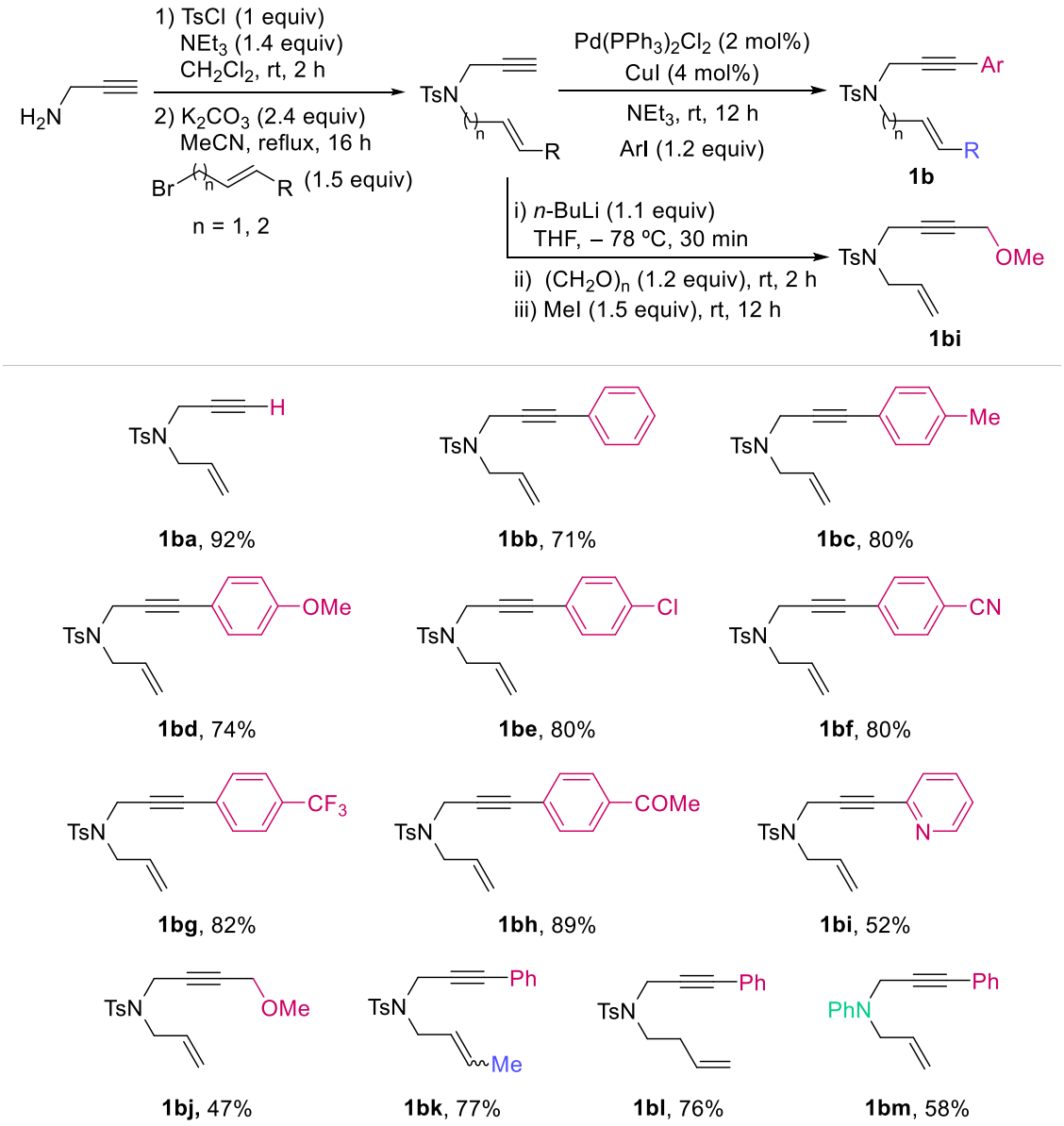

Scheme 1.6. Synthesis of enynes **1ba-bm** (Z = NTs) with aromatic moiety in the alkyne.

To explore the reactivity of differently substituted alkynes, an array of enynes were synthetized by reaction of allyl amine with tosyl chloride and propargylic bromide derivatives bearing alkyl moieties in the alkyne (**Scheme 1.7**). In addition, enynes with different *N*-connectors were obtained from the corresponding commercial allyl amine derivatives (**1bw** and **1bx**).

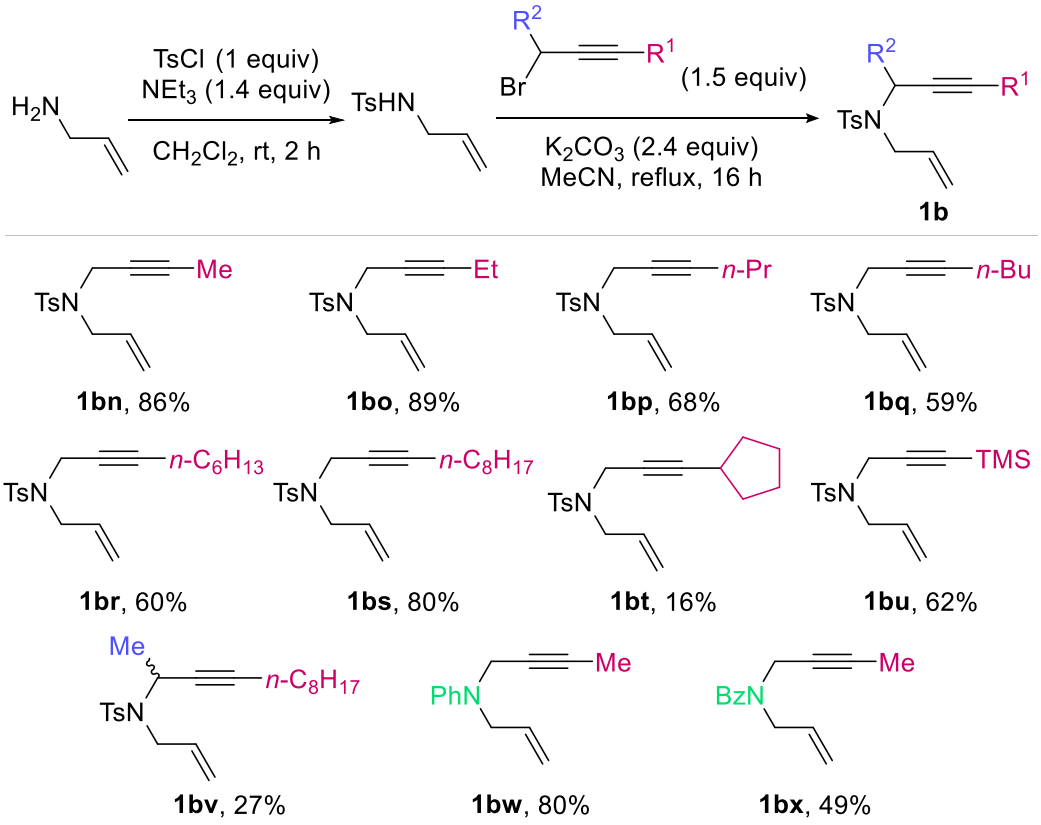

Scheme 1.7. Synthesis of enynes **1bn-bx** (Z = NR) with alkyl substitution on the alkyne.

The required propargylic bromides were previously synthetized by reaction of simple alkynes with *n*-BuLi and paraformaldehyde (or acetone in the case of **1bv**), followed by the nucleophilic substitution of the hydroxy group by an Appel-type reaction (**Scheme 1.8**). These bromides were used as starting materials without further purification.

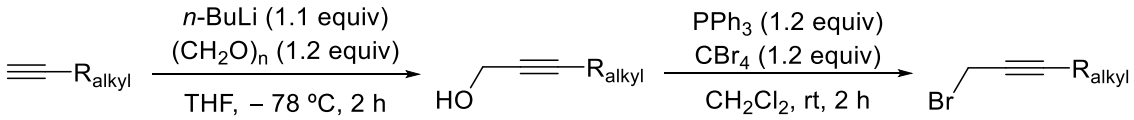

Scheme 1.8. Synthesis of propargylic bromide derivatives.

Substrates showing substitution at the propargylic or allylic positions of the enyne were prepared by Mitsunobu-type reaction of suitable amines and alcohols (**Scheme 1.9**).

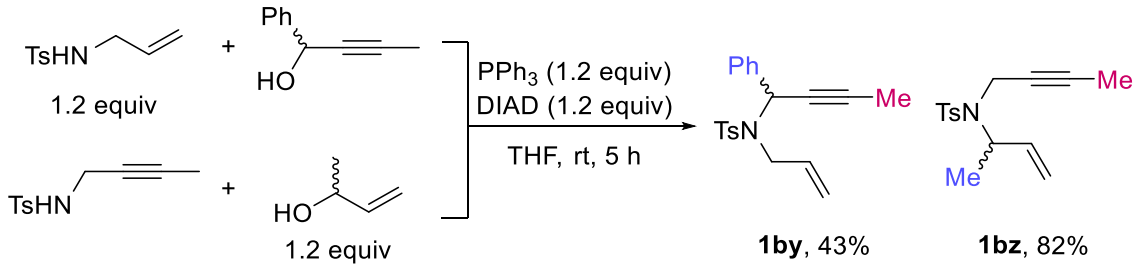

Scheme 1.9. Synthesis of enynes **1by-bz** (Z = NTs) bearing allylic or propargylic substituents.

The synthesis of several enynes bearing a quaternary center was carried out as well (**1c**–**d**). These structures could experience Thorpe-Ingold effect,[111] facilitating the cyclization process. On one hand, dimethyl malonate derivatives (**1c**) were obtained in high yields by reaction of dimethyl allylmalonate with propargyl bromide followed by Sonogashira-type reaction (**Scheme 1.10**).

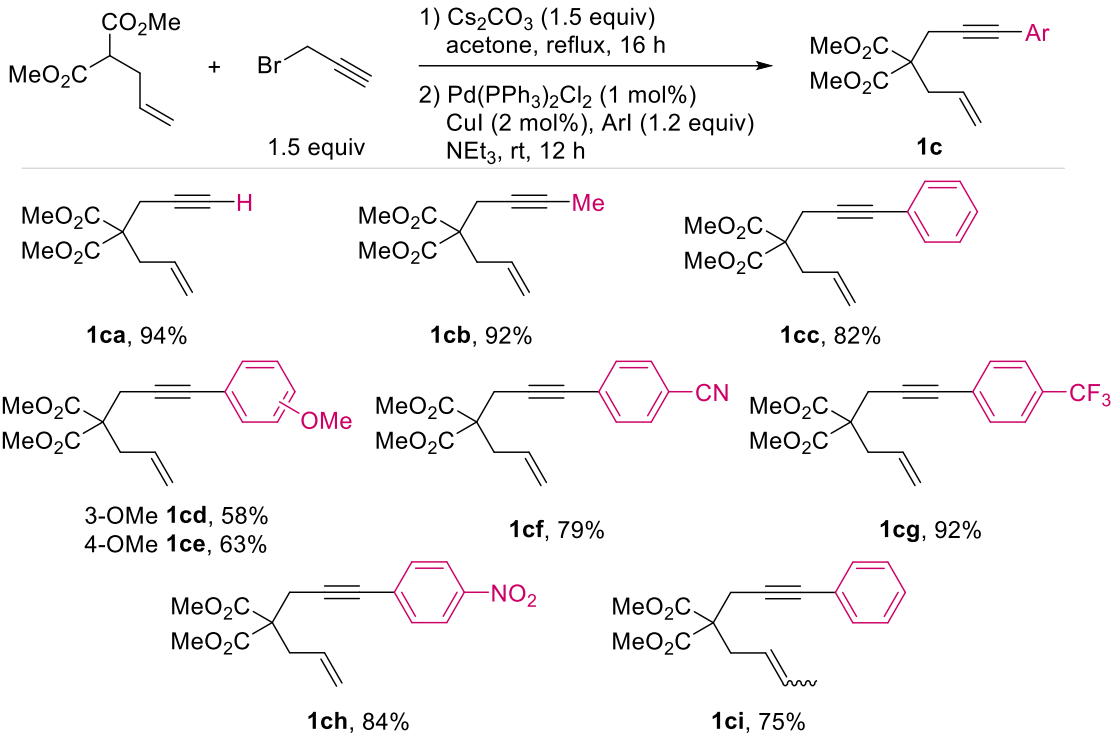

Scheme 1.10. Synthesis of enynes **1c** (Z = $C(CO_2Me)_2$).

On the other hand, the transformation of the dimethyl malonate group was performed in order to evaluate different substrates (**Scheme 1.11**). Reduction of ester groups of enyne **1ca** with $LiAlH_4$ followed by a Sonogashira reaction led to the diol derivative in high yield, whose alcohol moieties were protected as a ketal (**1da**) and dibenzyl diether (**1db**), respectively.

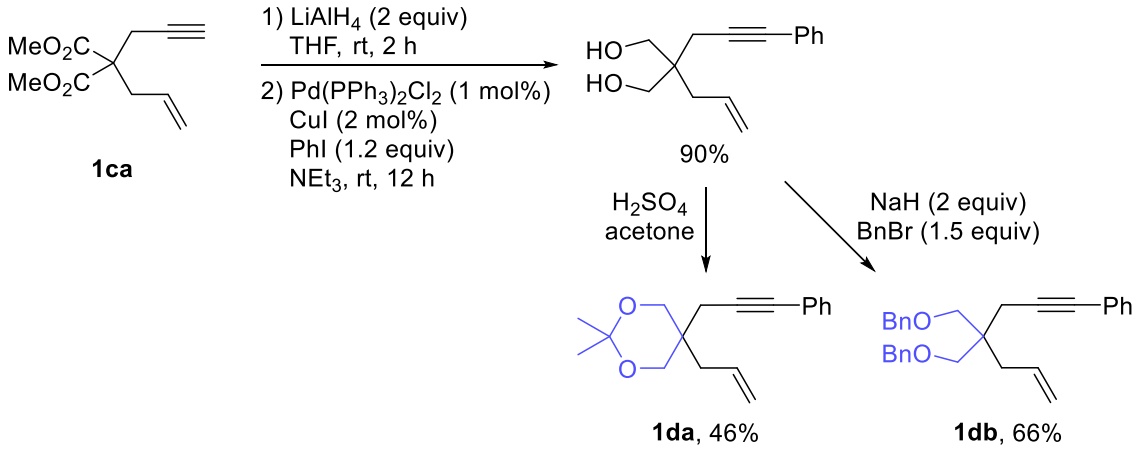

Scheme 1.11. Synthesis of enynes **1d** (Z = $C(CH_2OR)_2$).

[111] (a) R. M. Beesley, C. K. Ingold, J. F. Thorpe, *J. Chem. Soc.* **1915**, *107*, 1080–1106. (b) C.K. Ingold, *J. Chem. Soc.* **1921**, *119*, 305–329. (c) C. K. Ingold, S. Sako,J. F. Thorpe, *J. Chem. Soc.* **1922**, *121*, 1177–1198.

Enynes without a heteroatom as connector in the structure (**1e**) were synthetized by simple deprotonation of terminal alkynes with *n*-BuLi followed by reaction with 5-bromopent-1-ene (**Scheme 1.12**).

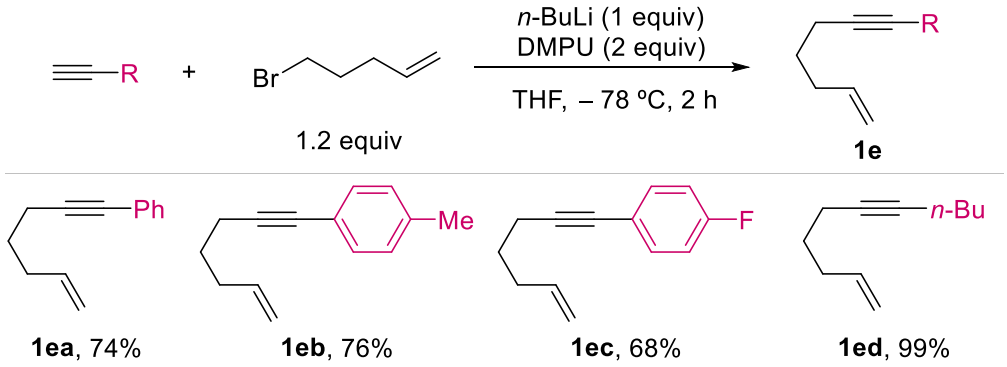

Scheme 1.12. Synthesis of enynes **1e** (Z = CH_2).

In addition, enynes of very different nature (**1f**) were synthetized by nucleophilic substitution at unsaturated carbon such as carboxylic acid (**Scheme 1.13**).

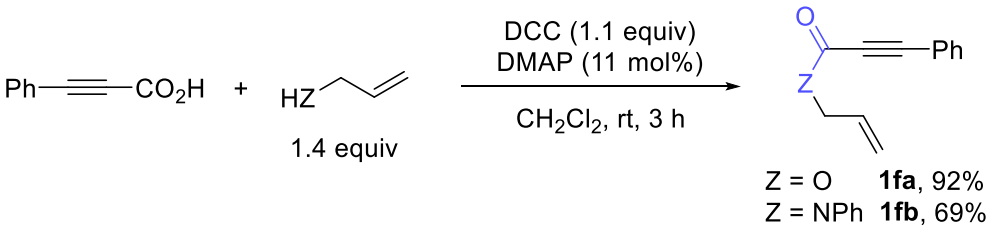

Scheme 1.13. Synthesis of enynes **1f**.

Finally, a set of enynes with the alkene conjugated to a ketone group (**1g**) were synthetized by oxidation of the corresponding alcohol to aldehyde followed by Wittig reaction (**Scheme 1.14**).

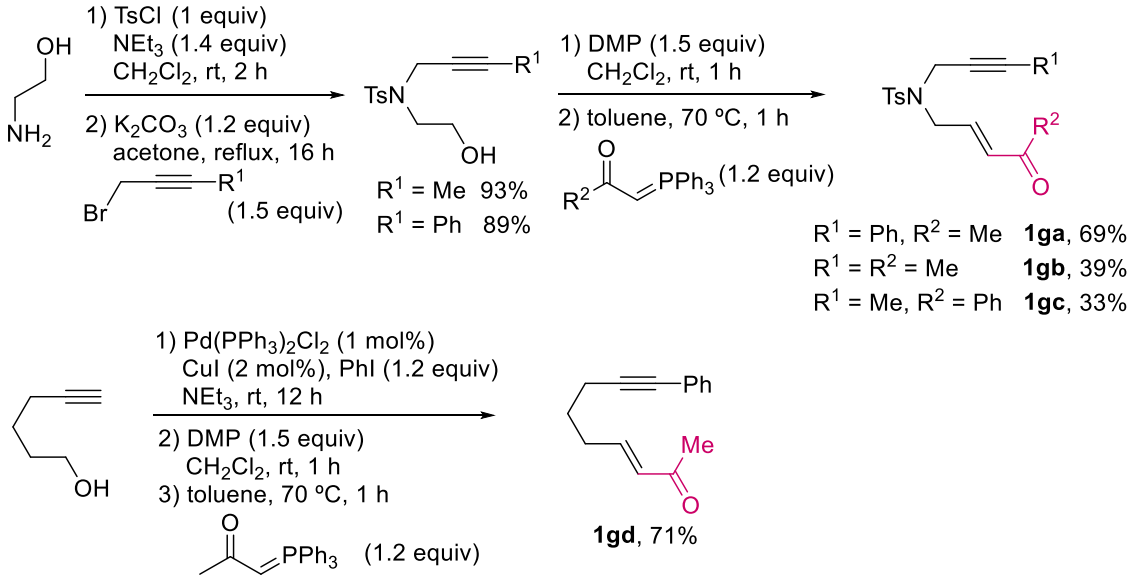

Scheme 1.14. Syntesis of enones **1g**.

3.1.2. Experimental section

3.1.2.1. Materials and methods

Triethylamine, acetone and acetonitrile (VWR) were used as purchased. Commercially available chemicals were purchased and used as received without further purifications. Thin layer chromatography was carried out using pre-coated TLC-aluminum sheets with 0.20 mm of silica gel and fluorescent indicator UV_{254} (ALUGRAM® Xtra SIL G/UV_{254}) and visualized under UV light and/or using phosphomolybdic acid, cerium (IV) sulfate, potassium permanganate or vanillin/conc. H_2SO_4 solutions in ethanol. Column chromatography was carried out using 60 Å pore size silica gel, 40 – 63 µm particle size (230 – 400 mesh particle size), from Sigma-Aldrich Co. NMR spectra were recorded at 23 °C on a Bruker AV-300. The ^1H and the ^{13}C NMR chemical shifts were given in parts per million (ppm) relative to the residual signals of the deuterated solvents.[112] Carbon types were determined from DEPT135-^{13}C NMR. The following abbreviations were used to indicate the multiplicity: br, broad; s, singlet; d, doublet; t, triplet; q, quartet; quin, quintuplet; hept, heptuplet; m, multiplet. Mass spectra were recorded on a Waters VG AutoSpec and GC-MS experiments on a Bruker SCION TQ.

3.1.2.2. General procedure for the synthesis of propargylic alcohols

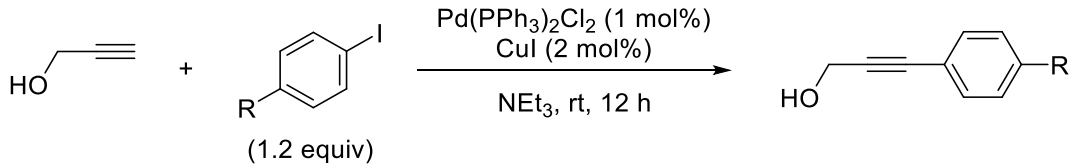

To a solution of iodoarene (1.2 equiv, 9.8 mmol) in triethylamine (0.34 M, 26 mL), $Pd(PPh_3)_2Cl_2$ (1 mol%, 0.89 mmol) and CuI (2 mol%, 0.18 mmol) were added. The reaction was stirred for 5 min before the addition of propargyl alcohol (1.0 equiv, 8.9 mmol). The resulting mixture was stirred for 12 h. Then, the reaction was treated with a saturated $NaHCO_3$ solution and was extracted with EtOAc (3 × 20 mL). The combined organic phases were washed with brine and dried over anhydrous $MgSO_4$.The solvent was removed under vacuum and the product was purified by column chromatography (cyclohexane/EtOAc, 9:1 – 7:3).[113]

3-Phenylprop-2-yn-1-ol:[114] The product was obtained as a brown oil in 98% yield (1.15 g).

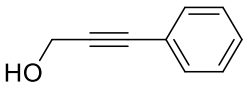

^1H NMR (300 MHz, $CDCl_3$) δ 7.39 (m, 2H), 7.26 (m, 3H), 4.45 (d, J = 6.2 Hz, 2H), 1.63 (t, J = 6.2 Hz, 1H).

3-(*p*-Tolyl)prop-2-yn-1-ol:[115] The product was obtained as a yellow oil in 63% yield (820 mg).

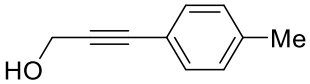

^1H NMR (300 MHz, $CDCl_3$) δ 7.28 (d, J = 7.8 Hz, 2H), 7.06 (d, J = 7.8 Hz, 2H), 4.43 (d, J = 6.1 Hz, 2H), 2.29 (s, 3H), 1.58 (t, J = 6.1 Hz, 1H).

[112] H. E. Gottlieb, V. Kotlyar, A. Nudelman, *J. Org. Chem.* **1997**, *62,* 7512–7515.
[113] G.-Y. Lin, C.-Y. Yang, R.-S. Liu, *J. Org. Chem.* **2007***, 72*, 6753–6757.
[114] S. Bong, H. Alper, *Chem. Commun*. **2004**, 1306–1307.
[115] F. M. Irudayanathan, J. Kim, K. Ho Song, S. Lee, *Asian J. Org. Chem.* **2016**, *5*, 1148–1154.

3-(4-Methoxyphenyl)prop-2-yn-1-ol:[116] The product was obtained as a yellow oil in 61% yield (882 mg). ^{1}H NMR (300 MHz, $CDCl_3$) δ 7.38 (d, J = 8.9 Hz, 2H), 6.84 (d, J = 8.9 Hz, 2H), 4.48 (d, J = 6.1 Hz, 2H), 3.81 (s, 3H), 1.64 (t, J = 6.1 Hz, 2H).

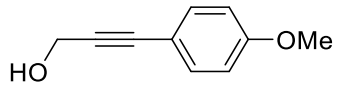

3-(4-Chlorophenyl)prop-2-yn-1-ol:[115] The product was obtained as a pale brown solid in 98% yield (1.45 g). ^{1}H NMR (300 MHz, $CDCl_3$) δ 7.36 (d, J = 8.6 Hz, 2H), 7.28 (d, J = 8.6 Hz, 2H), 4.49 (d, J = 6.1 Hz, 2H), 1.83 – 1.73 (t, J = 6.1 Hz, 1H).

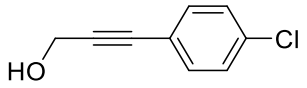

4-(3-Hydroxyprop-1-yn-1-yl)benzonitrile:[117] The product was obtained as a brown oil in 99% yield (698 mg). ^{1}H NMR (300 MHz, $CDCl_3$) δ 7.64 (d, J = 8.2 Hz, 2H), 7.54 (d, J = 8.2 Hz, 2H), 4.55 (d, J = 6.2 Hz, 2H), 1.68 (t, J = 6.2 Hz, 1H).

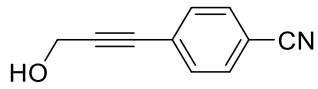

3-(4-(Trifluoromethyl)phenyl)prop-2-yn-1-ol:[115] The product was obtained as a red oil in 99% yield (1.77 g). ^{1}H NMR (300 MHz, $CDCl_3$) δ 7.52 (d, J = 8.7 Hz, 2H), 7.48 (d, J = 8.7 Hz, 2H), 4.47 (d, J = 6.2 Hz, 2H), 1.62 (t, J = 6.2 Hz, 1H).

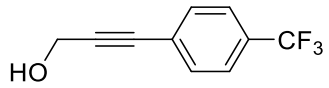

(*S*)-4-Phenylbut-3-yn-2-ol:[118] The product was obtained as a pale yellow oil in 96% yield (1.0 g). ^{1}H NMR (300 MHz, $CDCl_3$) δ 7.40 – 7.35 (m, 2H), 7.28 – 7.23 (m, 3H), 4.70 (dt, J = 6.6, 5.2 Hz, 1H), 1.86 (d, J = 5.2 Hz, 1H), 1.50 (d, J = 6.6 Hz, 3H).

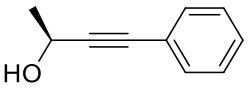

4-Phenylbut-3-yn-2-ol:[119] The product was obtained as a pale yellow oil in 95% yield (987 mg). The spectral data are identical to (*S*)-4-phenylbut-3-yn-2-ol.

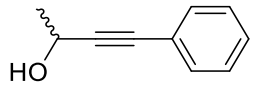

4-Phenylbut-3-yn-1-ol:[120] The product was obtained as a brown oil in 99% yield (1.1 g). ^{1}H NMR (300 MHz, $CDCl_3$) δ 7.46 – 7.38 (m, 2H), 7.33 – 7.28 (m, 3H), 3.82 (q, J = 6.3 Hz, 2H), 2.70 (t, J = 6.3 Hz, 2H), 1.81 (t, J = 6.3 Hz, 1H).

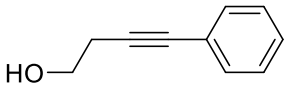

3.1.2.3. General procedures for the synthesis of 4-methylbenzenesulfonamide derivatives

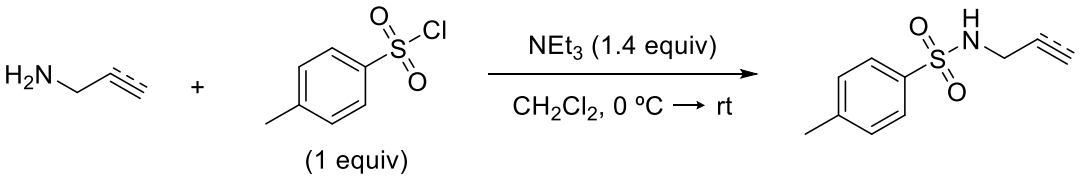

To a solution of allylamine (1.2 equiv, 8.1 mmol) or propargylamine (1.2 equiv, 54.5 mmol) in dichloromethane (1 M), triethylamine (1.4 equiv) was added. The reaction was cooled to 0 °C and *p*-toluenesulfonyl chloride (1 equiv) was added in portionwise. The mixture was stirred

---

[115] F. M. Irudayanathan, J. Kim, K. H. Song, S. Lee, *Asian J. Org. Chem.* **2016**, *5*, 1148–1154.
[116] F. Y. Kwong, H. W. Lee, W. H. Lam, L. Qiu, A. S. C. Chan, *Tetrahedron: Asymmetry* **2006**, *17*, 1238–1252.
[117] A. Nowak-Król, B. Koszarna, S. Y. Yoo, J. Chromiński, M. K. Węcławski, C.-H. Lee, D. T. Gryko, *J. Org. Chem.* **2011**, *76*, 2627–2634.
[118] X. Zhang, Z. Lu, C. Fu, S. Ma, *Org. Biomol. Chem.* **2009**, *7*, 3258–3263.
[119] M. R. Crittall, N. W. G. Fairhurst, D. R. Carbery, *Chem. Commun*. **2012**, *48*, 11181–11183.
[120] J. Tummatorn, S. Ruchirawat, P. Ploypradith, *Chem. Eur. J.* **2010**, *16*, 1445–1448.

at room temperature for 5 h. Then, water was added to the reaction and the mixture was extracted with dichloromethane. The combined organic phases were washed with brine and dried over anhydrous $MgSO_4$. Solvent was removed under vacuum and the residue was purified by column chromatography in silica gel using cyclohexane/EtOAc 7:3 as an eluent.[121]

***N*-Allyl-4-methylbenzenesulfonamide**:[122] The product was obtained as a white solid in 95% yield (1.5 g). ^{1}H NMR (300 MHz, $CDCl_3$) δ 7.75 (d, J = 8.2 Hz, 2H), 7.32 (d, J = 8.2 Hz, 2H), 5.73 (ddt, J = 16.5, 10.3, 5.9 Hz, 1H), 5.17 (dd, J = 16.5, 1.0 Hz, 1H), 5.10 (dd, J = 10.3, 1.0 Hz, 1H), 4.39 (s, 1H), 3.59 (t, J = 5.9 Hz, 2H), 2.43 (s, 3H).

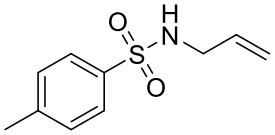

4-Methyl-*N*-(prop-2-yn-1-yl)benzenesulfonamide:[123] The product was obtained as a white solid in 96% yield (9.2 g). ^{1}H NMR (300 MHz, $CDCl_3$) δ 7.82 (d, J = 8.1 Hz, 2H), 7.36 (d, J = 8.1 Hz, 2H), 4.68 (t, J = 6.0 Hz, 1H), 3.82 (dd, J = 6.0, 2.6 Hz, 2H), 2.48 (s, 3H), 2.15 (t, J = 2.6 Hz, 1H).

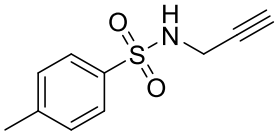

3.1.2.4. Synthesis of enynes 1a (Z = O)

3.1.2.4.1. General procedure A for the synthesis of enynes

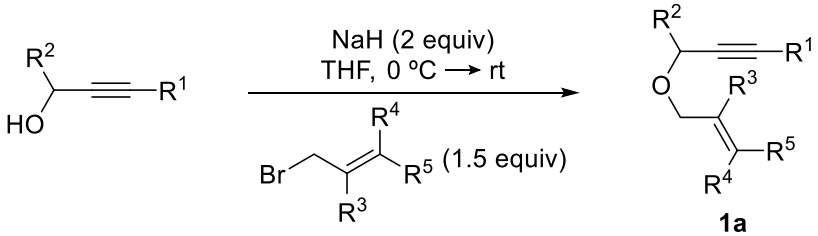

1a

Under an argon atmosphere, NaH (2 equiv, 60% dispersion mineral oil) and THF (0.4 M) were added to a round bottom flask. The resulting suspension was cooled to 0 °C, and the corresponding propargyl alcohol (1 equiv, 8.9 mmol) was added dropwise. The mixture was stirred for 1 h at rt. Then, the mixture was cooled to 0 °C and was kept at this temperature during the addition of the allyl bromide (1.5 equiv). Next, it was stirred for 2 additional hours at room temperature. When the starting propargyl alcohol had been consumed, water was added dropwise at 0 °C. The mixture was extracted with EtOAc, the combined organic layers were washed with brine and dried over anhydrous $MgSO_4$. The solvent was removed under vacuum and the product was purified by column chromatography (cyclohexane/EtOAc, 95:5).[124]

[121] A. R. O. Venning, M. R. Kwiatkowski, J. E. Roque Peña, B. C. Lainhart, A. A. Guruparan, E. J. Alexanian, *J. Am. Chem. Soc.* **2017**, *139*, 11595–11600.
[122] S. E. Gibson, K. A. C. Kaufmann, P. R. Haycock, A. J. P. White, D. J. Hardick, M. J. Tozer, *Organometallics* **2007**, *26*, 1578–1580.
[123] N. Dieltiens, K. Moonen, C. V. Stevens, *Chem. Eur. J.* **2007**, *13*, 203–214.
[124] Y. Xie, M. Yu, Y. Zhang, *Synthesis* **2011**, 2803–2809.

3.1.2.4.2. General procedure B for the synthesis of enynes

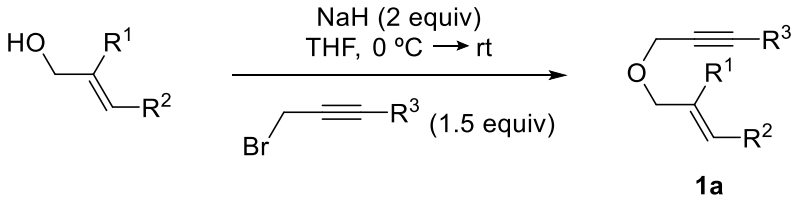

1a

Under an argon atmosphere, NaH (2 equiv, 60% dispersion mineral oil) and THF (0.4 M) were added to a round bottom flask. The reaction was cooled to 0 °C, and the corresponding allyl alcohol (1 equiv, 23 mmol) was added dropwise. The mixture was stirred for 1 h at rt. Then, the mixture was cooled to 0 °C and was kept at this temperature during the addition of the allyl bromide derivate (1.5 equiv). Next, it was stirred for 2 additional hours at room temperature. When the starting propargyl alcohol had been consumed, water was added dropwise at 0 °C. The mixture was extracted with EtOAc, the combined organic layers were washed with brine and dried over anhydrous $MgSO_4$. The solvent was removed under vacuum and the product was purified by column chromatography (cyclohexane/EtOAc, 95:5).[124]

(3-(Allyloxy)prop-1-yn-1-yl)benzene (1aa):[125] The product was obtained following the *General procedure A* as a yellow oil in 94% yield (1.4 g). ^{1}H NMR (300 MHz, $CDCl_3$) δ 7.47 – 7.44 (m, 2H), 7.33 – 7.30 (m, 3H), 5.96 (ddt, J = 16.6, 10.4, 5.8 Hz, 1H), 5.35 (ddd, J = 16.6, 3.2, 1.6 Hz, 1H), 5.24 (dd, J = 10.4, 1.6 Hz, 1H), 4.39 (s, 2H), 4.14 (dt, J = 5.8, 1.6 Hz, 2H).

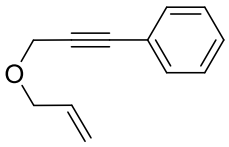

1-(3-(Allyloxy)prop-1-yn-1-yl)-4-methylbenzene (1ab):[125] The product was obtained following the *General procedure A* as a yellow oil in 77% yield (805 mg). ^{1}H NMR (300 MHz, $CDCl_3$) δ 7.29 (d, J = 8.0 Hz, 2H), 7.06 (d, J = 8.0 Hz, 2H), 5.90 (ddt, J = 16.1, 10.4, 5.8 Hz, 1H), 5.29 (dq, J = 16.1, 1.4 Hz, 1H), 5.18 (dd, J = 10.4, 1.4 Hz, 1H), 4.32 (s, 2H), 4.08 (dt, J = 5.8, 1.4 Hz, 2H), 2.29 (s, 3H).

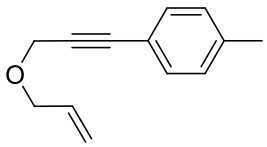

1-(3-(Allyloxy)prop-1-yn-1-yl)-4-methoxybenzene (1ac):[125] The product was obtained following the *General procedure A* as a colorless oil in 93% yield (1.0 g). ^{1}H NMR (300 MHz, $CDCl_3$) δ 7.39 (d, J = 8.9 Hz, 2H), 6.84 (d, J = 8.9 Hz, 2H), 5.95 (ddt, J = 17.2, 10.4, 5.8 Hz, 1H), 5.34 (ddd, J = 17.2, 3.0, 1.4 Hz, 1H), 5.23 (ddd, J = 10.3, 3.0, 1.4 Hz, 1H), 4.37 (s, 2H), 4.13 (dt, J = 5.8, 1.4 Hz, 2H), 3.81 (s, 3H).

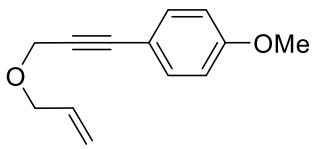

1-(3-(Allyloxy)prop-1-yn-1-yl)-4-chlorobenzene (1ad):[125] The product was obtained following the *General procedure A* as an orange liquid in 87% yield (1.6 g). ^{1}H NMR (300 MHz, $CDCl_3$) δ 7.37 (dt, J = 8.7, 2.1 Hz, 2H), 7.28 (J = 8.7, 2.1 Hz, 2H), 5.95 (ddt, J = 17.2, 10.4, 5.8 Hz, 1H),

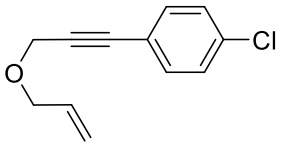

[124] Y. Xie, M. Yu, Y. Zhang, *Synthesis* **2011**, 2803–2809.

[125] F. Y. Kwong, Y. M. Li, W. H. Lam, L. Qiu, H. W. lee, C. H. Yeung, K. S. Chan, A. S. C. Chan, *Chem. Eur. J.* **2005**, *11*, 3872–3880.

5.34 (ddd, *J* = 17.2, 3.0, 1.4 Hz, 1H), 5.25 (ddd, *J* = 10.4, 3.0, 1.4 Hz, 1H), 4.37 (s, 2H), 4.13 (dt, *J* = 5.8, 1.4 Hz, 2H).

4-(3-(Allyloxy)prop-1-yn-1-yl)benzonitrile (1ae):[101] The product was obtained following the *General procedure A* as an orange oil in 47% yield (405 mg). ^{1}H NMR (300 MHz, $CDCl_3$) *δ* 7.55 (d, *J* = 8.4 Hz, 2H), 7.47 (d, *J* = 8.4 Hz, 2H), 5.89 (ddd, *J* = 17.3, 10.5, 5.8 Hz, 1H), 5.29 (dd, *J* = 17.3, 1.5 Hz, 1H), 5.20 (d, *J* = 10.5 Hz, 1H), 4.34 (s, 2H), 4.07 (d, *J* = 5.8 Hz, 2H).

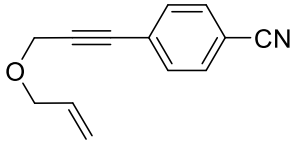

1-(3-(Allyloxy)prop-1-yn-1-yl)-4-(trifluoromethyl)benzene (1af):[116] The product was obtained following the *General procedure A* as a yellow liquid in 91% yield (1.9 g). ^{1}H NMR (300 MHz, $CDCl_3$) *δ* 7.58 (d, *J* = 9.0 Hz, 2H), 7.54 (d, *J* = 9.0 Hz, 2H), 5.95 (ddd, *J* = 17.2, 10.4, 5.7 Hz, 1H), 5.35 (dd, *J* = 17.2, 1.3 Hz, 1H), 5.26 (dd, *J* = 10.4, 1.3 Hz, 1H), 4.39 (s, 2H), 4.14 (dt, *J* = 5.7, 1.3 Hz, 2H).

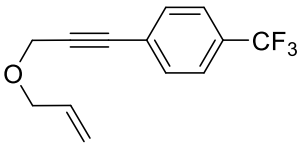

(*S*)-(3-(Allyloxy)but-1-yn-1-yl)benzene ((*S*)-1ag):[126] The product was obtained following the *General procedure A* as a yellow oil in 68% yield (862 mg). ^{1}H NMR (300 MHz, $CDCl_3$) *δ* 7.37 – 7.31 (m, 2H), 7.22 (dd, *J* = 4.1, 2.4 Hz, 3H), 5.97 – 5.77 (m, 1H), 5.25 (dd, *J* = 17.2, 1.3 Hz, 1H), 5.12 (dd, *J* = 10.4, 1.3 Hz, 1H), 4.35 (q, *J* = 6.6 Hz, 1H), 4.26 – 4.18 (ddt, *J* = 12.5, 6.3, 1.2 Hz, 1H), 3.95 (ddt, *J* = 12.5, 6.3, 1.2 Hz, 1H), 1.45 (d, *J* = 6.6 Hz, 3H).

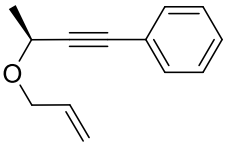

(3-(Allyloxy)but-1-yn-1-yl)benzene (*rac*-1ag):[126] The product was obtained following the *General procedure A* as a yellow oil in 78% yield (1.0 g). The spectral data are identical to (*S*)-(3-(allyloxy)but-1-yn-1-yl)benzene ((S)-**1ag**).

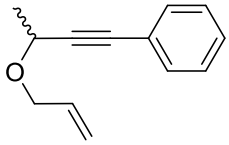

(4-(Allyloxy)but-1-yn-1-yl)benzene (1ah):[127] The product was obtained following the *General procedure A* as a yellow oil in 95% yield (1.3 g). ^{1}H NMR (300 MHz, $CDCl_3$) *δ* 7.46 – 7.33 (m, 2H), 7.30 – 7.27 (m, 3H), 5.94 (ddt, *J* = 17.2, 10.4, 5.6 Hz, 1H), 5.32 (ddd, *J* = 17.2, 3.2, 1.4 Hz, 1H), 5.21 (ddd, *J* = 10.4, 2.9, 1.4 Hz, 1H), 4.06 (dt, *J* = 5.6, 1.4 Hz, 2H), 3.66 (t, *J* = 7.1 Hz, 2H), 2.71 (t, *J* = 7.1 Hz, 2H).

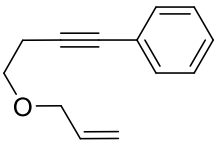

(3-((2-Methylallyl)oxy)prop-1-yn-1-yl)benzene (1ai):[125] The product was obtained following the *General procedure A* as a yellow liquid in 70% yield (1.5 g). ^{1}H NMR (300 MHz, $CDCl_3$) *δ* 7.45 (dd, *J* = 6.7, 3.1 Hz, 2H), 7.34 – 7.28 (m, 2H), 5.03 (s, 1H), 4.95 (s, 1H), 4.36 (s, 2H), 4.05 (s, 2H), 1.78 (s, 3H).

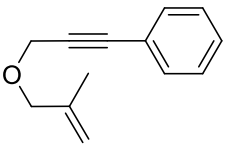

[101] S. Yu, C. Wu, S. Ge, *J. Am. Chem. Soc.* **2017**, *139*, 6526–6529.
[116] F. Y. Kwong, H. W. Lee, W. H. Lam, L. Qiu, A. S. C. Chan, *Tetrahedron: Asymmetry* **2006**, *17*, 1238–1252.
[125] F. Y. Kwong, Y. M. Li, W. H. Lam, L. Qiu, H. W. lee, C. H. Yeung, K. S. Chan, A. S. C. Chan, *Chem. Eur. J.* **2005**, *11*, 3872–3880.
[126] S. C. Berk, R. B. Grossman, S. L. Buchwald, *J. Am. Chem. Soc.* **1994**, *116*, 8593–8601.
[127] Z. Zhao, Y. Ding, G. Zhao, *J. Org. Chem.* **1998**, *63*, 9285–9291.

(3-((2-Chloroallyl)oxy)prop-1-yn-1-yl)benzene (1aj): The product was obtained following the *General procedure A* as an orange oil in 68% yield (1.1 g). ^{1}H NMR (300 MHz, $CDCl_3$) δ 7.49 – 7.43 (m, 2H), 7.33 (dt, J = 4.9, 1.6 Hz, 3H), 5.55 (quin, J = 1.4 Hz, 1H), 5.43 (quin, J = 1.4 Hz, 1H), 4.44 (d, J = 1.6 Hz, 2H), 4.27 – 4.18 (m, 2H). ^{13}C NMR (75 MHz, $CDCl_3$) δ 137.7 (C), 131.9 (2 × CH), 128.7 (CH), 128.4 (2 × CH), 122.5 (C), 114.4 (CH_2), 87.0 (C), 84.4 (C), 71.9 (CH_2), 58.1 (CH_2). HRMS (ESI, MeOH) calcd. for $C_{12}H_{11}ClO$ [M + Na]$^+$: 229.6690; Found: 229.0391.

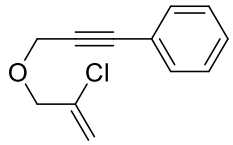

(3-(But-2-en-1-yloxy)prop-1-yn-1-yl)benzene (1ak):[128] An isomeric mixture (*E*/*Z*, 1:4) was obtained following the *General procedure A* as a yellow oil in 95% yield (641 mg). ^{1}H NMR (300 MHz, $CDCl_3$) δ 7.44 – 7.32 (m, 2H), 7.26 (m, 3H), 5.83 – 5.63 (m, 1H), 5.63 – 5.47 (m, 1H), 4.31 (d, J = 6.8 Hz, 2H), 4.16 (d, J = 6.8 Hz, 0.4H, *cis*-), 4.05 – 3.95 (m, 1.6H, *trans*-), 1.77 – 1.63 (m, 3H).

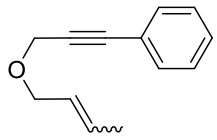

(3-((3-Methylbut-2-en-1-yl)oxy)prop-1-yn-1-yl)benzene (1al):[129] The product was obtained following the *General procedure A* as an orange liquid in 93% yield (1.5 g). ^{1}H NMR (300 MHz, $CDCl_3$) δ 7.45 (dd, J = 6.6, 3.0 Hz, 2H), 7.35 – 7.28 (m, 3H), 5.39 (t, J = 7.1 Hz, 1H), 4.35 (s, 2H), 4.13 (d, J = 7.1 Hz, 2H), 1.75 (d, J = 12.4 Hz, 6H).

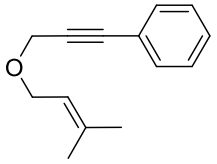

(3-(Cinnamyloxy)prop-1-yn-1-yl)benzene (1am):[130] The product was obtained following the *General procedure B* as a yellow oil in 81% yield (626 mg). ^{1}H NMR (300 MHz, $CDCl_3$) δ 7.50 – 7.39 (m, 4H), 7.35 – 7.35 (m, 5H), 7.27 – 7.25 (m, J = 6.9 Hz, 1H), 6.68 (d, J = 15.9 Hz, 1H), 6.33 (dt, J = 15.9, 6.2 Hz, 1H), 4.43 (s, 2H), 4.31 (dd, J = 6.2, 1.3 Hz, 2H).

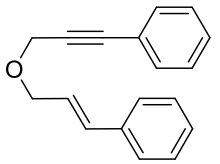

1-(Allyloxy)but-2-yne (1an):[125] The product was obtained following the *General procedure B* as a yellow oil in 16% yield (130 mg). ^{1}H NMR (300 MHz, $CDCl_3$) δ 5.91 (ddd, J = 17.0, 10.4, 5.8 Hz, 1H), 5.30 (dd, J = 17.0, 1.4 Hz, 1H), 5.20 (dd, J = 10.4, 1.4 Hz, 1H), 4.11 (q, J = 2.3 Hz, 2H), 4.04 (d, J = 5.7 Hz, 2H), 1.86 (t, J = 2.3 Hz, 3H).

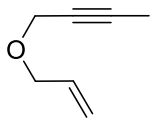

(3-((2-(Methoxymethyl)allyl)oxy)prop-1-yn-1-yl)benzene (1ao): The product was obtained following the *General procedure B* in two steps, using first (3-bromoprop-1-yn-1-yl)benzene and the 2-methylenepropane-1,3-diol as starting materials and then, using the enyne resulting in previous step and iodomethane, as a pale yellow liquid in 90% yield (603 mg). ^{1}H NMR (300 MHz, $CDCl_3$) δ 7.45 (dd, J = 6.7, 3.0 Hz, 2H), 7.34 – 7.29 (m, 3H), 5.25 (d, J = 8.1 Hz, 2H), 4.38 (s, 2H), 4.15 (s, 2H), 3.97 (s, 2H), 3.35 (s, 3H). ^{13}C NMR (75 MHz, $CDCl_3$) δ 142.0 (C), 131.6 (2 × CH), 128.3 (CH), 128.2 (2 × CH), 122.6 (C), 114.5 (CH_2), 86.2 (C), 85.1 (C), 73.1 (CH_2), 70.2 (CH_2), 57.9 (CH_2), 57.9 (CH_3). HRMS (ESI, MeOH) calcd. for $C_{14}H_{16}O_2$ [M + Na]$^+$: 239.2800; Found: 239.1052.

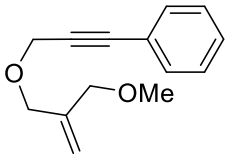

---

[125] F. Y. Kwong, Y. M. Li, W. H. Lam, L. Qiu, H. W. lee, C. H. Yeung, K. S. Chan, A. S. C. Chan, *Chem. Eur. J.* **2005**, *11*, 3872–3880.
[128] T. Morimoto, K. Fuji, K. Tsutsumi, K. Kakiuchi, *J. Am. Chem. Soc.* **2002**, 124, 3806–3807.
[129] C. Nieto-Oberhuber, P. Pérez-Galán, E. Herrero-Gómez, T. Lauterbach, C. Rodríguez, S. López, C. Bour, A. Rosellón, D. J. Cárdenas, A. M. Echavarren, *J. Am. Chem. Soc.* **2008**, *130*, 269–279.
[130] H. Teller, M. Corbet, L. Mantilli, G. Gopakumar, R. Goddard, W. Thiel, A. Fürstner, *J. Am. Chem. Soc.* **2012**, *134*, 15331–15342.

1-(Allyloxy)-4-methoxybut-2-yne (1ap):[131] To a suspension of KOH (1 equiv, 1.3 g) in DMSO (2 M) were added propargyl bromide (1 equiv, 2 mL) and but-2-yne-1,4-diol (1 equiv, 2 g). The mixture was stirred for 1 h, diluted with water and extracted with dichloromethane. Then, the aqueous layer was acidified with aqueous HCl (4 N) and extracted with dichloromethane. The combined organic layers were dried over anhydrous $MgSO_4$ and concentrated in vacuo. The crude was purified by column chromatography using dichloromethane as an eluent, affording 4-(allyloxy)but-2-yn-1-ol as an colorless oil in 80% yield. To another suspension of KOH (1 equiv, 1.3 g) in DMSO (2 M) were added iodomethane (1 equiv, 1.4 mL) and 4-(allyloxy)but-2-yn-1-ol (1 equiv, 2.3 g). The mixture was stirred for 1 h, diluted with water and extracted with dichloromethane. The combined organic layers were dried over anhydrous $MgSO_4$ and concentrated in vacuo. The residue was purified by column chromatography using cyclohexane as an eluent. The product was obtained as a colorless oil in 30% yield (903 mg). ^{1}H NMR (300 MHz, $CDCl_3$) δ 5.91 (ddt, J = 17.2, 10.4, 5.7 Hz, 1H), 5.34 (dq, J = 17.2, 1.3 Hz, 1H), 5.22 (ddd, J = 10.4, 2.7, 1.3 Hz, 1H), 4.21 (t, J = 1.8 Hz, 2H), 4.14 (t, J = 1.8 Hz, 2H), 4.06 (dt, J = 5.7, 1.3 Hz, 2H), 3.39 (s, 3H). ^{13}C NMR (75 MHz, $CDCl_3$) δ 134.0 (CH), 117.9 (CH_2), 82.5 (C), 82.2 (C), 70.7 (CH_2), 60.0 (CH_2), 57.6 (CH_3), 57.4 (CH_2). HRMS (ESI, MeOH) calcd. for $C_8H_{12}O_2$ $[M + Na]^+$: 163.1820; Found: 163.0736.

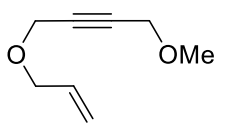

3.1.2.5. Synthesis of enynes 1b (Z = NR)

3.1.2.5.1. General procedure C for the synthesis of enynes:

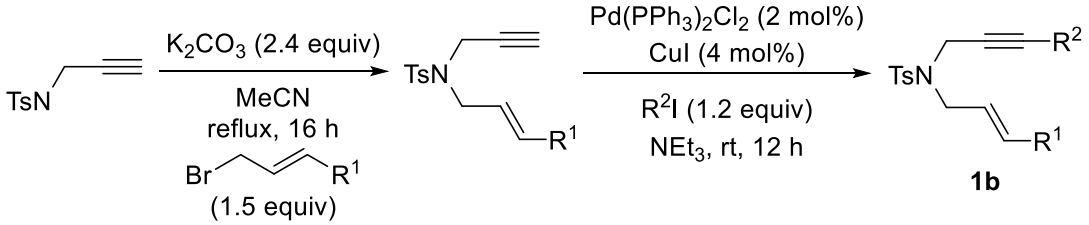

Step 1: 4-Methyl-*N*-(prop-2-yn-1-yl)benzenesulfonamide (1 equiv, 28.7 mmol), K_2CO_3 (2.4 equiv, 60.1 mmol) and acetonitrile (0.4 M) were added to a sealed tube. Then, allyl bromide (1.5 equiv, 43.1 mmol) was added and the reaction mixture was heated under reflux overnight. Then, the mixture was cooled to rt, the salts were filtered and the solvent was evaporated. The enyne was purified by column chromatography using cyclohexane/EtOAc 95:5 as an eluent. [132]

Step 2: Under an argon atmosphere, the enyne resulting from the previous step (1 equiv, 4 mmol), the iodoarene (1.2 equiv) and triethylamine (0.4 M) were added to a round bottom flask. Then, $Pd(PPh_3)_2Cl_2$ (2 mol%) and CuI (4 mol%) were added, and the mixture was stirred overnight at rt. The mixture was treated with a saturated $NaHCO_3$ solution and then was extracted with ethyl acetate (3 × 20 mL). The combined organic layers were washed with brine and dried over anhydrous $MgSO_4$. The solvent was removed under vacuum and the product was purified by column chromatography (cyclohexane/EtOAc, 95:5).[113]

[131] D. Banti, E. Groaz, M. North, *Tetrahedron* **2004**, *60*, 8043–8052.
[113] G.-Y. Lin, C.-Y. Yang, R.-S. Liu, *J. Org. Chem.* **2007**, *72*, 6753–6757.
[132] S.-K- Kang, T.G. Baik, A. N. Kulak, Y.-H. Ha, Y. Lim, J. Park, *J. Am. Chem. Soc.* **2000**, *122*, 11529–11530.

3.1.2.5.2. General procedure D for the synthesis of enynes

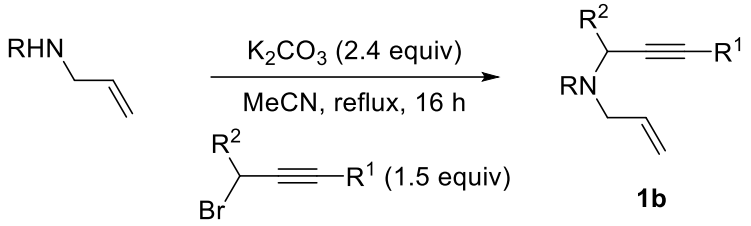

N-allyl-4-methylbenzenesulfonamide (1 equiv, 3.3 mmol), K_2CO_3 (2.4 equiv, 8.0 mmol) and acetonitrile (0.4 M) were added to a sealed tube. The corresponding propargyl bromide (1.5 equiv, 5.0 mmol) was added and the reaction mixture was heated under reflux overnight. Then, the mixture was cooled to rt, the salts were filtered and the solvent was evaporated. The product was purified by column chromatography using cyclohexane/EtOAc 95:5 as an eluent.[132]

***N*-Allyl-4-methyl-*N*-(prop-2-yn-1-yl)benzenesulfonamide (1ba)**:[64] The product was obtained following the *General procedure C* as a white solid in 96% yield (1.7 g). ^{1}H NMR (300 MHz, $CDCl_3$) δ 7.73 (d, J = 8.3 Hz, 2H), 7.30 (d, J = 8.3 Hz, 2H), 5.73 (ddt, J = 16.5, 10.0, 6.5 Hz, 1H), 5.32 – 5.25 (m, 1H), 5.26 – 5.16 (m, 1H), 4.09 (d, J = 2.5 Hz, 2H), 3.82 (dd, J = 6.5, 1.4 Hz, 2H), 2.42 (s, 3H), 2.00 (t, J = 2.5 Hz, 1H).

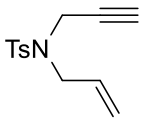

***N*-Allyl-4-methyl-*N*-(3-phenylprop-2-yn-1-yl)benzenesulfonamide (1bb)**:[67] The product was obtained following the *General procedure C* as a pale orange solid in 77% yield (997 mg). ^{1}H NMR (300 MHz, $CDCl_3$) δ 7.77 (d, J = 8.3 Hz, 2H), 7.27 – 7.21 (m, 4H), 7.06 (d, J = 7.2 Hz, 2H), 5.80 (dd, J =17.1, 10.0 Hz, 1H), 5.33 (d, J =17.1, 1H), 5.27 (d, J = 10.0 Hz, 1H), 4.31 (s, 2H), 3.89 (d, J = 6.5 Hz, 2H), 2.34 (s, 3H).

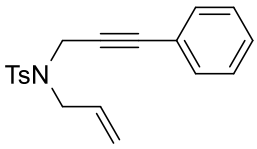

***N*-Allyl-4-methyl-*N*-(3-(*p*-tolyl)prop-2-yn-1-yl)benzenesulfonamide (1bc)**:[133] The product was obtained following the *General procedure C* as a pale yellow solid in 87% yield (1.1 g). ^{1}H NMR (300 MHz, $CDCl_3$) δ 7.77 (d, J = 8.3 Hz, 2H), 7.77 (d, J = 8.3 Hz, 2H), 7.04 (d, J = 8.0 Hz, 2H), 6.95 (d, J = 8.0 Hz, 2H), 5.80 (ddt, J = 16.9, 10.0, 6.4 Hz, 1H), 5.32 (dd, J = 16.9, 1.2 Hz, 1H), 5.26 (dd, J = 10.0, 1.2 Hz, 1H), 4.29 (s, 2H), 3.88 (d, J = 6.4 Hz, 2H), 2.35 (s, 3H), 2.32 (s, 3H).

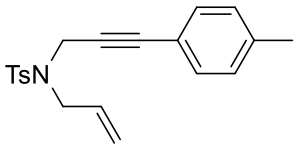

***N*-Allyl-*N*-(3-(4-methoxyphenyl)prop-2-yn-1-yl)-4-methylbenzenesulfonamide (1bd)**:[67] The product was obtained following the *General procedure C* as an orange solid in 80% yield (1.2 g). ^{1}H NMR (300 MHz, $CDCl_3$) δ 7.77 (d, J = 8.2 Hz, 2H), 7.25 (d, J = 8.2 Hz, 2H), 7.01 (d, J = 8.8 Hz, 2H), 6.76 (d, J = 8.8 Hz, 2H), 5.80 (ddt, J = 17.1, 10.1, 6.5 Hz, 1H), 5.32 (dd, J = 17.1, 1.3 Hz, 1H), 5.26 (dd, J = 10.1, 1.3 Hz, 1H), 4.29 (s, 2H), 3.88 (d, J = 6.5 Hz, 2H), 3.79 (s, 3H), 2.36 (s, 3H).

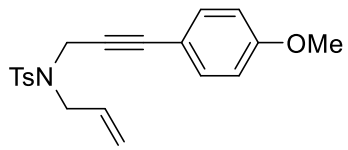

[64] (a) K. T. Sylvester, P. J. Chirik, *J. Am. Chem. Soc.* **2009**, *131*, 8772–8774.
[67] A. Lin, Z.-W. Zhang, J. Yang, *Org. Lett.* **2014**, *16*, 386–389.
[132] S.-K- Kang, T.G. Baik, A. N. Kulak, Y.-H. Ha, Y. Lim, J. Park, *J. Am. Chem. Soc.* **2000**, *122*, 11529–11530.
[133] T. Xi, Z. Lu, *J. Org. Chem.* **2016**, *81*, 8858–8866.

***N*-Allyl-*N*-(3-(4-chlorophenyl)prop-2-yn-1-yl)-4-methylbenzenesulfonamide (1be)**:[67] The

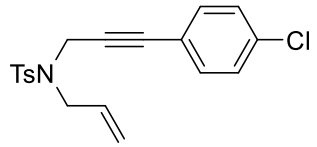

product was obtained following the *General procedure C* as an orange solid in 87% yield (1.3 g). ^{1}H NMR (300 MHz, $CDCl_3$) δ 7.77 (d, J = 8.3 Hz, 2H), 7.25 – 7.19 (m, 4H), 6.99 (d, J = 8.3 Hz, 2H), 5.79 (ddt, J = 16.6, 10.0, 6.5 Hz, 1H), 5.35 – 5.30 (m, 1H), 5.28 – 5.25 (m, 1H), 4.29 (s, 2H), 3.88 (d, J = 6.5 Hz, 2H), 2.35 (s, 3H).

***N*-Allyl-*N*-(3-(4-cyanophenyl)prop-2-yn-1-yl)-4-methylbenzenesulfonamide (1bf)**:[67] The

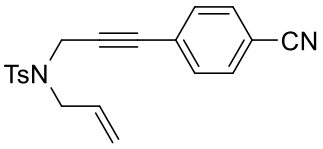

product was obtained following the *General procedure C* as an orange solid in 87% yield (612 mg). ^{1}H NMR (300 MHz, $CDCl_3$) δ 7.81 (d, J = 8.3 Hz, 2H), 7.58 (d, J = 8.4 Hz, 2H), 7.31 (d, J = 8.3 Hz, 2H), 7.15 (d, J = 8.4 Hz, 2H), 5.79 (ddt, J = 16.5, 9.9, 6.4 Hz, 1H), 5.32 (d, J = 16.5 Hz, 1H), 5.27 (d, J = 6.4 Hz, 1H), 4.32 (s, 2H), 3.88 (d, J = 6.4 Hz, 2H), 2.35 (s, 3H).

***N*-Allyl-4-methyl-*N*-(3-(4-(trifluoromethyl)phenyl)prop-2-yn-1-yl)benzenesulfonamide**

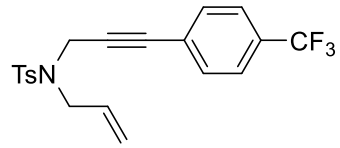

(1bg):[67] The product was obtained following the *General procedure C* as an orange solid in 89% yield (1.4 g). ^{1}H NMR (300 MHz, $CDCl_3$) δ 7.77 (d, J = 8.3 Hz, 2H), 7.50 (d, J = 8.1 Hz, 2H), 7.26 (d, J = 8.3 Hz, 2H), 7.16 (d, J = 8.1 Hz, 2H), 5.80 (ddt, J = 17.0, 10.0, 6.4 Hz, 1H), 5.35 (dd, J = 17.0, 1.4 Hz, 1H), 5.25 (d, J = 10.0, 1.4 Hz, 1H), 4.32 (s, 2H), 3.89 (dt, J = 6.5, 1.4 Hz, 2H), 2.34 (s, 3H).

***N*-(3-(4-acetylphenyl)prop-2-yn-1-yl)-*N*-allyl-4-methylbenzenesulfonamide (1bh)**:[134]

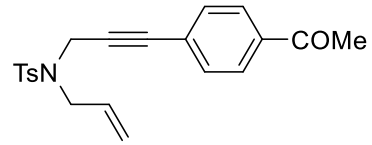

The product was obtained following the *general procedure D* as an orange solid in 89% yield (1.4 g). ^{1}H NMR (300 MHz, $CDCl_3$) δ 7.84 – 7.75 (m, 4H), 7.25 (d, J = 8.3 Hz, 2H), 7.14 (d, J = 8.3 Hz, 2H), 5.79 (ddt, J = 16.4, 9.9, 6.4 Hz, 1H), 5.37 – 5.23 (m, 1H), 4.32 (s, 2H), 3.88 (d, J = 6.4 Hz, 2H), 2.58 (d, J = 1.8 Hz, 3H), 2.34 (s, 3H).

***N*-Allyl-4-methyl-*N*-(3-(pyridin-2-yl)prop-2-yn-1-yl)benzenesulfonamide (1bi)**: The

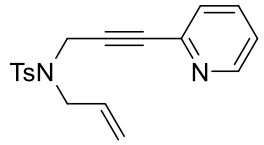

product was obtained following the *General procedure C* as a yellow oil in 56% yield (340 mg). ^{1}H NMR (300 MHz, $CDCl_3$) δ 8.52 (d, J = 4.5 Hz, 1H), 7.78 (d, J = 8.0 Hz, 2H), 7.58 (tq, J = 7.8, 0.9 Hz, 1H), 7.25 – 7.19 (m, 3H), 7.00 (d, J = 7.8 Hz, 1H), 5.78 (ddt, J = 16.6, 10.0, 6.4 Hz, 1H), 5.30 (ddd, J = 13.6, 10.0, 0.9 Hz, 2H), 4.33 (s, 2H), 3.91 (d, J = 6.3 Hz, 2H), 2.31 (s, 3H). ^{13}C NMR (75 MHz, $CDCl_3$) δ 149.7 (CH), 143.4 (C), 142.1 (C), 135.8 (CH), 135.7 (C), 131.7 (CH), 129.4 (2 × CH), 127.6 (2 × CH), 126.8 (CH), 122.9 (CH), 119.9 (CH_2), 84.9 (C), 81.7 (C), 49.2 (CH_2), 36.4 (CH_2), 21.2 (CH_3). HRMS (ESI, MeOH) calcd. for $C_{18}H_{28}N_2O_2S$ [M + H]$^+$: 327.2980; Found: 327.1154.

***N*-Allyl-*N*-(4-methoxybut-2-yn-1-yl)-4-methylbenzenesulfonamide (1bj)**: To a solution of

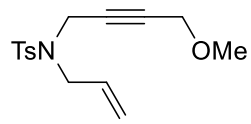

N-allyl-4-methyl-*N*-(prop-2-yn-1-yl)benzenesulfonamide (2.2 mmol) in dry THF (0.5 M) at – 78 °C, *n*-BuLi (1.6 M in hexanes, 2.4 mmol) was added dropwise within 10 min, and the mixture was stirred for 30 min. Then, paraformaldehyde (2.6 mmol) was added and the reaction mixture was stirred at room temperature until complete consumption of the starting material. Then, iodomethane (3.4 mmol) was added and the reaction mixture was stirred for 12 h. The

[67] A. Lin, Z.-W. Zhang, J. Yang, *Org. Lett.* **2014**, *16*, 386–389.
[134] Y. Tang, L. Deng, Y. Zhang, G. Dong, J. Chen, Z. Yang, *Org. Lett.* **2005**, *7*, 1657–1659.

reaction was quenched with saturated solution of NH_4Cl and extracted with EtOAc, washed with brine and dried over anhydrous $MgSO_4$. The solvent was removed under vacuum and the enyne was purified by column chromatography using cyclohexane/EtOAc 95:5 as an eluent. The product was obtained as a pale yellow oil in 51% yield (320 mg). ^{1}H NMR (300 MHz, $CDCl_3$) δ 7.58 (d, J = 8.3 Hz, 2H), 7.15 (d, J = 8.3 Hz, 2H), 5.58 (ddt, J = 16.5, 10.0, 6.4 Hz, 1H), 5.18 – 5.10 (m, 1H), 5.10 – 5.04 (m, 1H), 3.98 (s, 2H), 3.67 (dd, J = 4.0, 2.1 Hz, 4H), 3.03 (s, 3H), 2.26 (s, 3H). ^{13}C NMR (75 MHz, $CDCl_3$) δ 143.5 (C), 136.0 (C), 132.0 (CH), 129.4 (2 × CH), 127.7 (2 × CH), 119.8 (CH_2), 81.4 (C), 79.0 (C), 59.5 (CH_2), 57.3 (CH_3), 49.1 (CH_2), 36.1 (CH_2), 21.4 (CH_3). HRMS (ESI, MeOH) calcd. for $C_{15}H_{19}NO_3S$ $[M + H]^+$: 294.3810; Found: 294.1158.

***N*-(But-2-en-1-yl)-4-methyl-*N*-(prop-2-yn-1-yl)benzenesulfonamide:**[135] An isomeric mixture (*E*/*Z*, 1:4) was obtained following the *General procedure C* as a white solid in 95% yield (2.4 g). ^{1}H NMR (300 MHz, $CDCl_3$) δ 7.73 (d, J = 8.3 Hz, 2H), 7.29 (d, J = 8.3 Hz, 2H), 5.80 – 5.62 (m, 1H), 5.41 – 5.31 (m, 1H), 4.08 (d, J = 2.5 Hz, 2H), 3.88 (d, J = 7.1 Hz, 0.4H *cis*-), 3.75 (d, J = 6.8 Hz, 1.6H *trans*-), 2.42 (s, 3H), 1.99 (d, J = 2.5 Hz, 1H), 1.69 (t, J = 6.4 Hz, 3H).

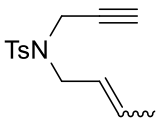

***N*-(But-2-en-1-yl)-4-methyl-*N*-(3-phenylprop-2-yn-1-yl)benzenesulfonamide (1bk)**:[135] An isomeric mixture (*E*/*Z*, 1:4) was obtained following the *General procedure C* as an orange solid in 84% yield (647 mg). ^{1}H NMR (300 MHz, $CDCl_3$) δ 7.77 (d, J = 8.3 Hz, 2H), 7.25 (d, J = 8.3, 2H), 7.24 – 7.23 (m, 3H), 7.11 – 7.01 (d, J = 6.6 Hz, 2H), 5.84 – 5.66 (m, 1H), 5.52 – 5.35 (m, 1H), 4.29 (s, 2H), 3.95 (d, J = 7.2 Hz, 0.4H *cis*-), 3.82 (d, J = 6.8 Hz, 1.6H *trans*-), 2.33 (s, 3H), 1.73 (t, J = 6.8 Hz, 3H).

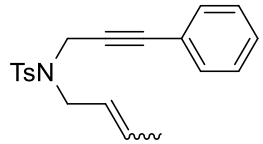

***N*-(But-3-en-1-yl)-4-methyl-*N*-(prop-2-yn-1-yl)benzenesulfonamide**:[136] The product was obtained following the *General procedure C* as a white solid in 88% yield (3.4 g). ^{1}H NMR (300 MHz, $CDCl_3$) δ 7.72 (d, J = 8.2 Hz, 2H), 7.29 (d, J = 8.2 Hz, 2H), 5.77 (ddt, J = 17.0, 10.1, 6.7 Hz, 1H), 5.16 – 4.99 (m, 2H), 4.14 (d, J = 2.4 Hz, 1H), 3.26 (t , J = 7.0 Hz, 2H), 2.42 (s, 3H), 2.34 (q, J = 7.0 Hz, 2H), 2.03 (t, J = 2.4 Hz, 1H).

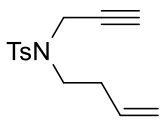

***N*-(But-3-en-1-yl)-4-methyl-*N*-(3-phenylprop-2-yn-1-yl)benzenesulfonamide (1bl)**:[136] The product was obtained following the *General procedure C* as a pale brown solid in 90% yield (1.1 g). ^{1}H NMR (300 MHz, $CDCl_3$) δ 7.77 (d, J = 8.2 Hz, 2H), 7.26 – 7.19 (m, 5H), 7.10 – 7.02 (m, 2H), 5.81 (ddt, J = 16.9, 10.1, 6.8 Hz, 1H), 5.17 – 5.05 (m, 2H), 4.35 (s, 2H), 3.33 (t , J = 7.2 Hz, 2H), 2.40 (q, J = 7.2 Hz, 2H), 2.34 (s, 3H).

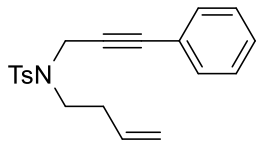

***N*-allyl-*N*-(3-phenylprop-2-yn-1-yl)aniline (1bm)**:[126] The product was obtained following the G*eneral procedure C* as a brown oil in 58% yield (420 mg). ^{1}H NMR (300 MHz, $CDCl_3$) δ 7.39 (dd, J = 6.7, 3.1 Hz, 2H), 7.30 – 7.23 (m, 5H), 6.91 (d, J = 7.9 Hz, 2H), 6.79 (t, J = 7.3 Hz, 1H), 5.94 (ddt, J = 17.2, 10.3, 5.1 Hz, 1H), 5.31 (dq, J = 17.2, 1.7 Hz, 1H), 5.21 (dq, J = 10.3, 1.7 Hz, 1H), 4.24 (s, 2H), 4.04 (d, J = 5.1 Hz, 2H).

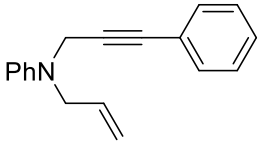

[126] S. C. Berk, R. B. Grossman, S. L. Buchwald, *J. Am. Chem. Soc.* **1994**, *116*, 8593–8601.
[135] X. Deng, S.-F. Ni, Z.-Y- Han, Y.-Q. Guan, H. Lv, L. Dang, X.M. Zhang, *Angew. Chem. Int. Ed.* **2016**, *55*, 6295–6299.
[136] J. H. Park, S. Min Kim, Y. K. Chung, *Chem. Eur. J.* **2011**, *17*, 10852–10856.

***N*-Allyl-*N*-(but-2-yn-1-yl)-4-methylbenzenesulfonamide (1bn)**:[64a] The product was obtained following the *General procedure D* as a white solid in 90% yield (785 mg).[1]H NMR (300 MHz, $CDCl_3$) δ 7.74 (d, J = 8.1 Hz, 2H), 7.32 – 7.27 (d, J = 8.1 Hz, 2H), 5.73 (ddt, J = 16.4, 10.0, 6.4 Hz, 1H), 5.30 – 5.25 (m, 1H), 5.24 – 5.23 (m, 1H), 4.02 (d, J = 2.4 Hz, 2H), 3.79 (d, J = 6.4 Hz, 2H), 2.42 (s, 3H), 1.54 (t, J = 2.4 Hz, 3H).

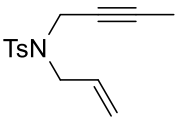

***N*-Allyl-4-methyl-*N*-(pent-2-yn-1-yl)benzenesulfonamide (1bo):**[137] The product was obtained following the *General procedure D* as a white solid in 94% yield (622 mg). [1]H NMR (300 MHz, $CDCl_3$) δ 7.74 (d, J = 8.4 Hz, 2H), 7.29 (d, J = 8.4 Hz, 2H), 5.74 (ddt, J = 16.4, 9.9, 6.4 Hz, 1H), 5.37 – 5.12 (m, 2H), 4.05 (t, J = 2.1 Hz, 2H), 3.80 (d, J = 6.4 Hz, 2H), 2.42 (s, 3H), 1.91 (qt, J = 7.5, 2.1 Hz, 2H), 0.90 (t, J = 7.5 Hz, 3H).

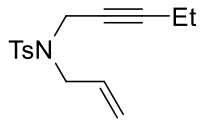

***N*-Allyl-*N*-(hex-2-yn-1-yl)-4-methylbenzenesulfonamide (1bp):**[138] The product was obtained following the *General procedure D* as a yellow oil in 72% yield (873 mg). [1]H NMR (300 MHz, $CDCl_3$) δ 7.74 (d, J = 8.3 Hz, 2H), 7.28 (d, J = 8.3 Hz, 2H), 5.75 (ddt, J = 16.5, 10.0, 6.4 Hz, 1H), 5.32 – 5.19 (m, 2H), 4.06 (t, J = 2.2 Hz, 2H), 3.81 (d, J = 6.4 Hz, 2H), 2.42 (s, 3H), 1.88 (tt, J = 7.0, 2.2 Hz, 2H), 1.28 (quin, J = 7.3 Hz, 1H), 0.81 (t, J = 7.3 Hz, 3H).

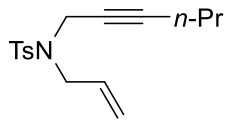

***N*-Allyl-*N*-(hept-2-yn-1-yl)-4-methylbenzenesulfonamide (1bq):**[128] The product was obtained following the *General procedure D* as a pale yellow oil in 59% yield (745 mg). [1]H NMR (300 MHz, $CDCl_3$) δ 7.74 (d, J = 8.3 Hz, 2H), 7.29 (d, J = 8.3 Hz, 2H), 5.75 (ddt, J = 16.5, 10.0, 6.4 Hz, 1H), 5.31 – 5.17 (m, 2H), 4.06 (t, J = 2.1 Hz, 2H), 3.80 (d, J = 6.4 Hz, 2H), 2.42 (s, 3H), 1.96 – 1-87 (m, 2H), 1.23 (dd, J = 7.0, 3.4 Hz, 4H), 0.84 (t, J = 7.0 Hz, 3H).

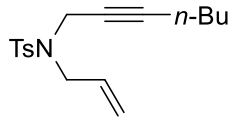

***N*-Allyl-4-methyl-*N*-(non-2-yn-1-yl)benzenesulfonamide (1br):** The product was obtained following the *General procedure D* as a yellow oil in 63% yield (881 mg). [1]H NMR (300 MHz, $CDCl_3$) δ 7.73 (d, J = 8.4 Hz, 2H), 7.28 (d, J = 8.4 Hz, 2H), 5.74 (ddt, J = 16.6, 9.9, 6.5 Hz, 1H), 5.32 – 5.18 (m, 2H), 4.06 (t, J = 2.1 Hz, 2H), 3.80 (d, J = 6.5 Hz, 2H), 2.42 (s, 3H), 1.95 – 1.79 (m, 2H), 1.25 (dd, J = 14.5, 7.6 Hz, 8H), 0.88 (t, J = 6.9 Hz, 3H). [13]C NMR (75 MHz, $CDCl_3$) δ 143.2 (C), 136.4 (C), 132.3 (CH), 129.4 (2 × CH), 127.9 (2 × CH), 119.6 (CH_2), 86.4 (C), 72.4 (C), 49.0 (CH_2), 36.4 (CH_2), 31.3 (CH_2), 28.5 (CH_2), 28.4 (CH_2), 22.6 (CH_2), 21.5 (CH_3), 18.5 (CH_2), 14.1 (CH_3). HRMS (ESI, MeOH) calcd. for $C_{19}H_{27}NO_2S$ $[M]^+$: 333.4900; Found: 333.1748.

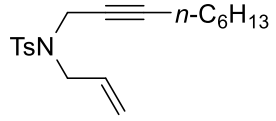

***N*-Allyl-4-methyl-*N*-(undec-2-yn-1-yl)benzenesulfonamide (1bs):** The product was obtained following the *General procedure D* as a yellow oil in 84% yield (433 mg). [1]H NMR (300 MHz, $CDCl_3$) δ 7.74 (d, J = 8.1 Hz, 2H), 7.28 (d, J = 8.1 Hz, 2H), 5.75 (ddt, J = 16.5, 10.0, 6.5 Hz, 1H), 5.34 – 5.14 (m, 2H), 4.05 (s, 2H), 3.80 (d, J = 6.5 Hz, 2H), 2.42 (s, 3H), 1.94 – 1.85 (m, 2H), 1.34 – 1.15 (m, 12H), 0.89 (t, J = 6.8 Hz, 3H). [13]C NMR (75 MHz, $CDCl_3$) δ 143.2 (C), 136.3 (C), 132.2 (CH), 129.3 (2 × CH), 127.8 (2 × CH), 119.5 (CH_2), 86.3 (C), 72.3 (C), 48.9 (CH_2), 36.4 (CH_2), 31.8 (CH_2), 29.2 (CH_2), 29.0 (CH_2), 28.8 (CH_2), 28.4 (CH_2),

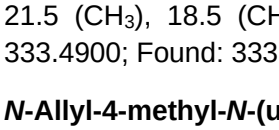

[64] (a) K. T. Sylvester, P. J. Chirik, *J. Am. Chem. Soc.* **2009**, *131*, 8772–8774.
[128] T. Morimoto, K. Fuji, K. Tsutsumi, K. Kakiuchi, *J. Am. Chem. Soc.* **2002**, 124, 3806–3807.
[137] D. A. Candito, M. Lautens, *Synlett* **2011**, 1987–1992.
[138] M. E. Krafft, L. V. R. Boñaga, J. A. Wright, C. Hirosawa, *J. Org. Chem.* **2002**, *67*, 1233–1246.

22.6 (CH_2), 21.5 (CH_3), 18.4 (CH_2), 14.1 (CH_3). HRMS (ESI, MeOH) calcd. for $C_{21}H_{31}NO_2S$ $[M + H]^+$: 362.5440; Found: 362.2142.

***N*-Allyl-*N*-(3-cyclopentylprop-2-yn-1-yl)-4-methylbenzenesulfonamide (1bt):** The

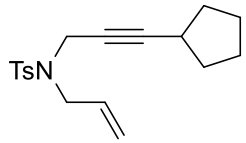

product was obtained following the *General procedure D* as a colorless oil in 17% yield (194 mg). ^{1}H NMR (300 MHz, $CDCl_3$) δ 7.73 (d, J = 8.3 Hz, 2H), 7.29 (d, J = 8.3 Hz, 2H), 5.75 (ddt, J = 16.5, 10.2, 6.4 Hz, 1H), 5.25 (ddt, J = 11.6, 10.2, 1.3 Hz, 2H), 4.07 (d, J = 2.1 Hz, 2H), 3.80 (d, J = 6.4 Hz, 2H), 2.42 (s, 3H), 2.34 (tt, J = 7.4, 2.1 Hz 1H), 1.79 – 1.64 (m, 2H), 1.63 – 1.41 (m, 4H), 1.36 – 1.19 (m, 2H). ^{13}C NMR (75 MHz, $CDCl_3$) δ 143.4 (C), 136.5 (C), 132.4 (CH), 129.5 (2 × CH), 128.0 (2 ×CH), 119.7 (CH_2), 90.8 (C), 72.0 (C), 49.0 (CH_2), 36.6 (CH_2), 33.6 (2 × CH_2), 30.0 (CH), 25.0 (2 × CH_2), 21.6 (CH_3). HRMS (ESI, MeOH) calcd. for $C_{18}H_{23}NO_2S$ $[M + Na]^+$: 340.1449; Found: 340.1327.

***N*-Allyl-4-methyl-*N*-(3-(trimethylsilyl)prop-2-yn-1-yl)benzenesulfonamide (1bu)**:[64a] The

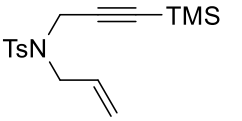

product was obtained following the *General procedure D* as a white solid in 65% yield (296 mg). ^{1}H NMR (300 MHz, $CDCl_3$) δ 7.74 (d, J = 6.7 Hz, 2H), 7.29 (d, J = 6.7 Hz, 2H), 5.75 (m, 1H), 5.27 (t, J = 13.0 Hz, 2H), 4.10 (s, 2H), 3.82 (d, J = 6.3 Hz, 2H), 2.42 (s, 3H), -0.01 (d, J = 1.1 Hz, 9H).

***N*-Allyl-*N*-(dodec-3-yn-2-yl)-4-methylbenzenesulfonamide (1bv):** The product was

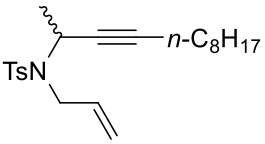

obtained following the *General procedure D* as a colorless oil in 28% yield (339 mg). ^{1}H NMR (300 MHz, $CDCl_3$) δ 7.73 (d, J = 8.3 Hz, 2H), 7.27 (d, J = 8.3 Hz, 2H), 5.93 (dddd, J = 17.1, 10.2, 6.9, 4.8 Hz, 1H), 5.25 (dd, J = 17.1, 1.6 Hz, 1H), 5.12 (dd, J = 10.2, 1.6 Hz, 1H), 4.91 – 4.81 (m, 1H), 3.88 (dd, J = 16.4, 4.8 Hz, 1H), 3.71 (dd, J = 16.4, 6.9 Hz, 1H), 2.41 (s, 3H), 1.94 (dt, J = 6.9, 3.3 Hz, 2H), 1.39 (d, J = 7.1 Hz, 3H), 1.32 – 1.15 (m, 12H), 0.89 (t, J = 6.9 Hz, 3H). ^{13}C NMR (75 MHz, $CDCl_3$) δ 143.1 (C), 136.6 (C), 136.3 (CH), 129.3 (2 × CH), 127.7 (2 × CH), 116.7 (CH_2), 85.8 (C), 77.5 (C), 47.2 (CH_2), 46.8 (CH), 31.9 (CH_2), 29.2 (CH_2), 29.1 (CH_2), 28.8 (CH_2), 28.4 (CH_2), 23.2 (CH_3), 22.7 (CH_2), 21.5 (CH_3), 18.4 (CH_2), 14.1 (CH_3). HRMS (ESI, MeOH) calcd. for $C_{22}H_{33}NO_2S$ $[M + Na]^+$: 398.2232; Found: 398.2127.

***N*-Allyl-*N*-(but-2-yn-1-yl)aniline (1bw)**:[139] The product was obtained following the *General*

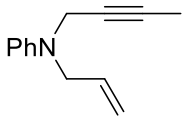

procedure D as a colorless oil in 84% yield (265 mg). ^{1}H NMR (300 MHz, $CDCl_3$) δ 7.25 (t, J = 8.1 Hz, 2H), 6.84 (d, J = 8.1 Hz, 2H), 6.76 (t, J = 7.3 Hz, 1H), 5.89 (ddd, J = 15.4, 10.2, 5.1 Hz, 1H), 5.31 – 5.10 (m, 2H), 3.97 (s, 3H), 1.80 (s, 3H).

***N*-Allyl-*N*-(but-2-yn-1-yl)benzamide (1bx)**:[83] The product was obtained following the

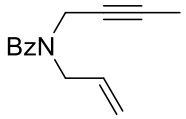

General procedure D as a colorless oil in 52% yield (612 mg). ^{1}H NMR (300 MHz, $CDCl_3$) δ 7.60 – 7.35 (m, 5H), 5.99 – 5.66 (m, 1H), 5.29 – 5.16 (m, 2H), 4.25 (br s, 2H), 4.03 – 3.89 (m, 2H), 1.85 (s, 3H).

***N*-Allyl-4-methyl-*N*-(1-phenylbut-2-yn-1-yl)benzenesulfonamide (1by)**: To a solution of

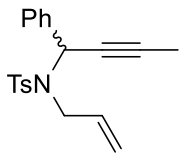

N-allyl-4-methylbenzenesulfonamide (1.8 mmol), 1-phenylbut-2-yn-1-ol (1.5 mmol) and triphenylphosphine (1.8 mmol) in THF (4 mL), DIAD (1.8 mmol) was added at 0 °C. Then, the mixture was stirred at room temperature for 5 h until complete consumption of the sulfonamide. The solvent was removed under vacuum and the product was purified by column chromatography on

[64] (a) K. T. Sylvester, P. J. Chirik, *J. Am. Chem. Soc.* **2009**, *131*, 8772–8774.
[83] J. B. Diccianni, T. Heitmann, T. Diao, *J. Org. Chem.* **2017**, *82*, 6895–6903.
[139] S. J. Sturla, S. L. Buchwald, *J. Org. Chem.* **1999**, *64*, 5547–5550.

silica gel using cyclohexane/EtOAc 95:5 as an eluent. The product was obtained as a colorless oil in 43% yield (221 mg). ^{1}H NMR (300 MHz, $CDCl_3$) δ 7.81 (d, J = 8.3 Hz, 2H), 7.57 (dd, J = 7.0, 1.3 Hz, 2H), 7.32 (dd, J = 8.3, 2.9 Hz, 5H), 6.03 (d, J = 2.0 Hz, 1H), 5.41 (ddt, J = 16.2, 10.1, 6.5 Hz, 1H), 4.82 (dd, J = 16.2, 1.4 Hz, 1H), 4.75 (dd, J = 10.1, 1.4 Hz, 1H), 3.64 (qd, J = 16.2, 6.5 Hz, 2H), 2.45 (s, 3H), 1.69 (s, 3H). ^{13}C NMR (75 MHz, $CDCl_3$) δ 143.3 (C), 137.1 (C), 136.5 (C), 134.7 (CH), 129.3 (2 × CH), 128.4 (2 × CH), 128.3 (2 × CH), 128.2 (CH), 128.1 (2 × CH), 116.7 (CH_2), 84.6 (C), 73.7 (C), 54.0 (CH), 48.0 (CH_2), 21.6 (CH_3), 3.4 (CH_3). HRMS (ESI, MeOH) calcd. for $C_{20}H_{21}NO_2S$ [M + Na]$^+$: 362.4530; Found: 362.1182.

***N*-(But-2-yn-1-yl)-*N*-(but-3-en-2-yl)-4-methylbenzenesulfonamide (1bz)**:[140] To a solution of *N*-(but-2-yn-1-yl)-4-methylbenzenesulfonamide (1.9 mmol), but-3-en-2-ol (2.3 mmol) and triphenylphosphine (2.3 mmol) in THF (4 mL), DIAD (2.3 mmol) was added at 0 °C. Then, the mixture was stirred at rt for 5 h until complete consumption of the sulfonamide. The solvent was removed under vacuum and the product was purified by column chromatography on silica gel using cyclohexane/EtOAc 95:5 as an eluent. The product was obtained as a colorless oil in 82% yield (438 mg). ^{1}H NMR (300 MHz, $CDCl_3$) δ 7.80 (d, J = 8.3 Hz, 2H), 7.27 (d, J = 8.3 Hz, 2H), 5.83 – 5.70 (m, 1H), 5.15 (d, J = 1.7 Hz, 1H), 5.11 (ddd, J = 7.1, 1.7, 1.0 Hz, 1H), 4.61 – 4.49 (m, 1H), 4.07 (dq, J = 18.2, 2.4 Hz, 1H), 3.82 (dq, J = 18.2, 2.4 Hz, 1H), 2.42 (s, 3H), 1.67 (t, J = 2.4 Hz, 3H), 1.25 (d, J = 7.0 Hz, 3H).

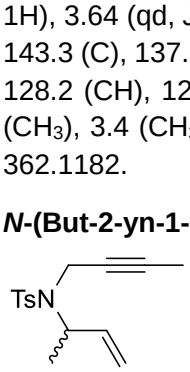

3.1.2.6. Synthesis of enynes 1c (Z = C(CO$_2$Me)$_2$) and 1d (Z = C(CH$_2$OR)$_2$)

3.1.2.6.1. General procedure E for synthesis of enynes

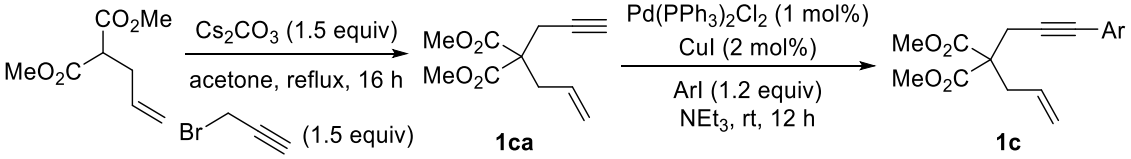

Step 1: Dimethyl 2-allylmalonate (1 equiv, 29.0 mmol), Cs_2CO_3 (1.5 equiv, 43.5 mmol) and acetone (0.4 M) were added to a sealed tube. Then, propargyl bromide (1.5 equiv, 43.5 mmol) was added and the reaction mixture was heated under reflux overnight. Then, the mixture was cooled to room temperature, the salts were filtered and the solvent was evaporated. The compound was purified by column chromatography using cyclohexane/EtOAc 95:5.[141]

Step 2: The corresponding iodoarene (1.2 equiv.) and triethylamine (0.4 M) were added to a round bottom flask. Then, $Pd(PPh_3)_2Cl_2$ (1 mol%) and CuI (2 mol%) were added, and the mixture was stirred for 5 min. Finally, the enyne resulting from the previous step (**1ca**, 1 equiv) was added and the mixture was stirred overnight at room temperature. The reaction mixture was treated with a saturated $NaHCO_3$ solution and then it was extracted with ethyl acetate (3 × 20 mL). The combined organic layers were washed with brine and dried over anhydrous $MgSO_4$. The solvent was removed under vacuum and the product was purified by column chromatography (cyclohexane/EtOAc, 95:5).[113]

[140] D. E. Kim, S. H. Park, Y. H. Choi, S.-G. Lee, D. Moon, J. Seo, N. Jeong, *Chem. Asian J.* **2011**, *6*, 2009–2014.
[141] J. W. Faller, P. P. Fontaine, *J. Organomet. Chem.* **2006**, *691*, 1912–1918.

Dimethyl 2-allyl-2-(prop-2-yn-1-yl)malonate (1ca):[74] The product was obtained following the *General procedure E* as a colorless oil in 94% yield (5.7 g). ^{1}H NMR (300 MHz, $CDCl_3$) δ 5.62 (ddt, J = 17.5, 10.0, 7.5 Hz, 1H), 5.24 – 5.15 (m, 1H), 5.14 (d, J = 10.0 Hz, 1H), 3.74 (s, 6H), 2.86 – 2.78 (m, 4H), 2.02 (t, J = 2.7 Hz, 1H).

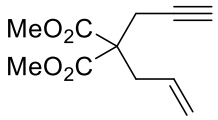

Dimethyl 2-allyl-2-(but-2-yn-1-yl)malonate (1cb):[142] The product was obtained following the *step 1 of General procedure E*, using 1-bromobut-2-yne as starting material, as a pale yellow oil in 92% yield (1.2 g). ^{1}H NMR (300 MHz, $CDCl_3$) δ 5.63 (ddt, J = 17.4, 10.0, 7.5 Hz, 1H), 5.16 (dd, J = 17.4, 1.6 Hz, 1H), 5.11 (dd, J = 10.0, 1.6 Hz, 1H), 3.73 (s, 6H), 2.78 (d, J = 7.5 Hz, 2H), 2.74 (q, J = 2.5 Hz, 2H), 1.76 (t, J = 2.5 Hz, 3H).

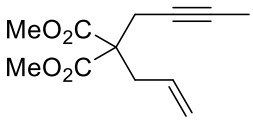

Dimethyl 2-allyl-2-(3-phenylprop-2-yn-1-yl)malonate (1cc):[143] The product was obtained following the *General procedure E* as a brown oil in 87% yield (1.2 g). ^{1}H NMR (300 MHz, $CDCl_3$) δ 7.37 (dd, J = 6.7, 3.0 Hz, 2H), 7.30 – 7.27 (dd , J = 6.7, 3.0 Hz, 3H), 5.68 (ddt, J = 17.1, 10.1 7.6 Hz, 1H), 5.21 (d, J = 17.1 Hz, 1H), 5.15 (d, J = 10.1 Hz, 1H), 3.76 (s, 6H), 3.02 (s, 2H), 2.87 (d, J = 7.6 Hz, 2H).

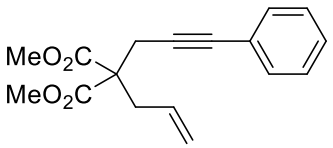

Dimethyl 2-allyl-2-(3-(3-methoxyphenyl)prop-2-yn-1-yl)malonate (1cd):[144] The product was obtained following the *General procedure E* as a brown oil in 62% yield (468 mg). ^{1}H NMR (300 MHz, $CDCl_3$) δ 7.19 (t, J = 7.9 Hz, 1H), 6.97 (d, J = 7.9 Hz, 1H), 6.92 – 6.81 (m, 2H), 5.68 (dd, J = 17.1, 9.8 Hz, 1H), 5.30 – 5.14 (m, 2H), 3.79 (s, 3H), 3.76 (s, 6H), 3.02 (s, 2H), 2.87 (d, J = 7.5 Hz, 2H).

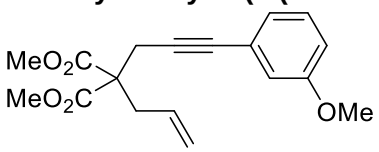

Dimethyl 2-allyl-2-(3-(4-methoxyphenyl)prop-2-yn-1-yl)malonate (1ce):[144] The product was obtained following the *General procedure E* as a brown solid in 67% yield (1.0 g). ^{1}H NMR (300 MHz, $CDCl_3$) δ 7.30 (d, J = 8.2 Hz, 2H), 6.81 (d, J = 8.2 Hz, 2H), 5.69 (ddt, J = 17.0, 10.0, 7.6 Hz, 1H), 5.20 (d, J = 17.0 Hz, 1H), 5.14 (d, J = 10.0 Hz, 1H), 3.80 (s, 3H), 3.76 (s, 6H), 3.00 (s, 2H), 2.87 (d, J = 7.6 Hz, 2H).

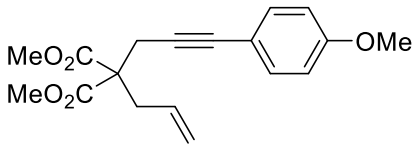

Dimethyl 2-allyl-2-(3-(4-cyanophenyl)prop-2-yn-1-yl)malonate (1cf):[144] The product was obtained following the *General procedure E* as a pale yellow solid in 84% yield (1.25 g). ^{1}H NMR (300 MHz, $CDCl_3$) δ 7.57 (d, J = 8.3 Hz, 2H), 7.44 (d, J = 8.3 Hz, 2H), 5.75 – 5.57 (m, 1H), 5.28 – 5.11 (m, 2H), 3.76 (s, 6H), 3.04 (s, 2H), 2.84 (d, J = 7.4 Hz, 2H).

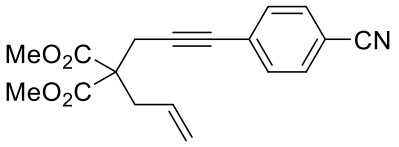

Dimethyl 2-allyl-2-(3-(4-(trifluoromethyl)phenyl)prop-2-yn-1-yl)malonate (1cg):[74] The product was obtained following the *General procedure E* as an orange oil in 98% yield (330 mg). ^{1}H NMR (300 MHz, $CDCl_3$) δ 7.48 (d, J = 8.3 Hz, 2H), 7.41 (d, J = 8.3 Hz, 2H), 5.62 (ddt, J = 17.0, 10.0, 7.5 Hz, 1H), 5.15 (dd,

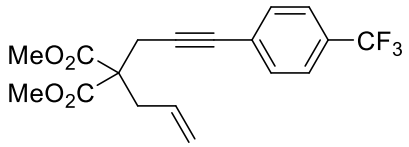

[74] Z. Chai, H.-F. Wang, G. Zhao, *Synlett* **2009**, 1785–1790.
[113] G.-Y. Lin, C.-Y. Yang, R.-S. Liu, *J. Org. Chem.* **2007**, *72*, 6753–6757.
[142] C. Gryparis, C. Efe, C. Raptis, I. N. Lykakis, M. Stratakis, *Org. Lett.* **2012**, *14*, 2956–2959.
[143] Z.-L- Lu, E. Neumann, A. Pfaltz, *Eur. J. Org. Chem.* **2007**, 4189–4192.
[144] A. Escribano-Cuesta, P. Pérez-Galán, E. Herrero-Gómez, M. Sekine, A. A. C. Braga, F. Maseras, A. M. Echavarren, *Org. Biomol. Chem.* **2012**, *10*, 6105–6111.

J = 17.0, 1.3 Hz, 1H), 5.10 (dd, *J* = 10.0, 1.3 Hz, 1H), 3.71 (s, 6H), 2.98 (s, 2H), 2.80 (d, *J* = 7.5 Hz, 2H).

Dimethyl 2-allyl-2-(3-(4-nitrophenyl)prop-2-yn-1-yl)malonate (1ch):[144] The product was obtained following the *General procedure E* as a light brown solid in 89% yield (1.4 g). ^{1}H NMR (300 MHz, $CDCl_3$) δ 8.16 (d, *J* = 8.8 Hz, 2H), 7.51 (d, *J* = 8.8 Hz, 1H), 5.67 (ddt, *J* = 14.4, 10.0, 7.4 Hz, 1H), 5.21 (d, *J* = 14.4 Hz, 1H), 5.17 (d, *J* = 10.0 Hz, 1H), 3.77 (s, 6H), 3.06 (s, 2H), 2.86 (d, *J* = 7.4 Hz, 2H).

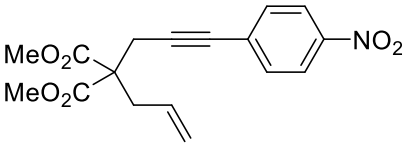

Dimethyl 2-(but-2-en-1-yl)-2-(3-phenylprop-2-yn-1-yl)malonate (1ci):[145] A isomeric mixture (*E*/*Z*, 1:4) was obtained following the *General procedure E*, using dimethyl 2-(prop-2-yn-1-yl)malonate and 1-bromobut-2-ene as starting materials, as an orange oil in 75% yield (1.0 g). ^{1}H NMR (300 MHz, $CDCl_3$) δ 7.44 – 7.33 (m, 2H), 7.30 – 7.27 (m, 3H), 5.63 (dd, *J* = 15.0, 6.5 Hz, 1H), 5.28 (dtt, *J* = 15.0, 7.5, 1.5 Hz, 1H), 3.76 (s, 6H), 3.00 (s, 2H), 2.91 (d, *J* = 7.5 Hz, 0.4H *cis*-), 2.80 (d, *J* = 7.5 Hz, 1.6H *trans*-), 1.67 (d, *J* = 6.5 Hz, 3H).

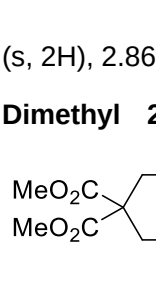

3.1.2.6.2. General procedure F for synthesis of enynes

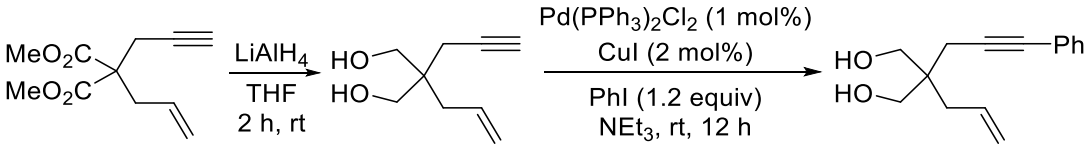

Step 1: To a solution of dimethyl 2-allyl-2-(prop-2-yn-1-yl)malonate (5.5 mmol) in anhydrous THF (0.13 M), $LiAlH_4$ (11 mmol, 1 M in THF) was added dropwise. The resulting mixture was stirred during 2 h. Then, the mixture was cooled to 0 °C and water was added dropwise. The mixture was extracted with EtOAc, the combined organic layers were washed with brine and dried over anhydrous $MgSO_4$. The solvent was removed under vacuum and the product was used without further purification. The resulting 2-allyl-2-(prop-2-yn-1-yl)propane-1,3-diol was arylated by Sonogashira reaction following the *General procedure for the synthesis of propargylic alcohols.*[146]

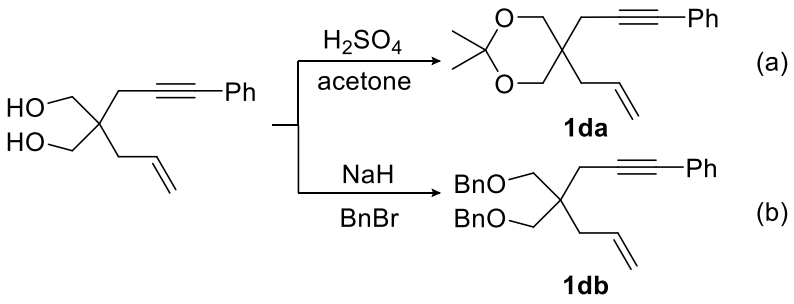

[74] Z. Chai, H.-F. Wang, G. Zhao, *Synlett* **2009**, 1785–1790.
[144] A. Escribano-Cuesta, P. Pérez-Galán, E. Herrero-Gómez, M. Sekine, A. A. C. Braga, F. Maseras, A. M. Echavarren, *Org. Biomol. Chem.* **2012**, *10*, 6105–6111.
[145] O. Buisine, C. Aubert, M. Malacria, *Chem. Eur. J.* **2001**, *7*, 3517–3525.
[146] J. H. Park, Y. Cho, Y. K. Chung, *Angew. Chem. Int. Ed*. **2010**, *49*, 5138–5141.

Step 2a: To a solution of 2-allyl-2-(3-phenylprop-2-yn-1-yl)propane-1,3-diol (1.1 mmol) in acetone (0.5 M), H_2SO_4 (0.2 mL) was added dropwise until the solution was acid. The resulting mixture was stirred during 2 h. Then, the mixture was cooled to 0 °C and NaOH solution was added dropwise. The mixture was extracted with EtOAc, the combined organic layers were washed with brine and dried over anhydrous $MgSO_4$. The solvent was removed under vacuum and the product was purified by column chromatography (cyclohexane/EtOAc, 95:5).[146]

Step 2b: the experimental procedure of this step is described in the *General procedure A.*

2-Allyl-2-(3-phenylprop-2-yn-1-yl)propane-1,3-diol:[146] 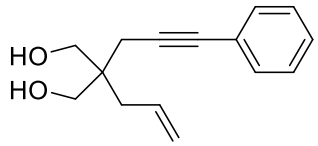 The product was obtained following the step 1 of the *General procedure F* as a colorless oil in 90% yield (821 mg). ^{1}H NMR (300 MHz, $CDCl_3$) δ 7.44 – 7.36 (m, 2H), 7.32 – 7.27 (m, 3H), 5.89 (ddt, *J* = 17.6, 10.0, 7.6 Hz, 1H), 5.16 (dd, *J* = 12.5, 10.0 Hz, 2H), 3.73 (t, *J* = 5.7 Hz, 4H), 2.48 (s, 2H), 2.23 (d, *J* = 7.6 Hz, 2H), 2.15 (t, *J* = 5.7 Hz, 2H).

5-Allyl-2,2-dimethyl-5-(3-phenylprop-2-yn-1-yl)-1,3-dioxane (1da):[146] 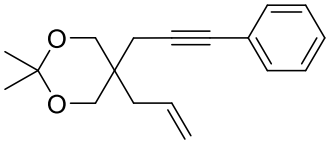 The product was obtained following the step 2a of the *General procedure F* as a yellow oil in 51% yield (153 mg). ^{1}H NMR (300 MHz, $CDCl_3$) δ 7.41 – 7.38 (m, 2H), 7.32 – 7.26 (m, 3H), 5.81 (dq, *J* = 10.0, 7.6 Hz, 1H), 5.22 – 5.10 (m, 2H), 3.80 – 3.66 (m, 4H), 2.60 (s, 2H), 2.23 (d, *J* = 7.6 Hz, 2H), 1.44 (s, 6H).

(((2-Allyl-2-(3-phenylprop-2-yn-1-yl)propane-1,3-diyl)bis(oxy))bis(methylene))dibenzene (1db):[146] 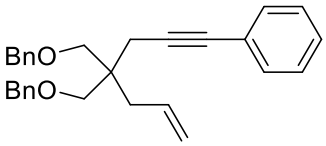 The product was obtained following the *General procedure A*, using 2-allyl-2-(3-phenylprop-2-yn-1-yl)propane-1,3-diol and (bromomethyl)benzene as starting materials, as a yellow oil in 73% yield (324 mg). ^{1}H NMR (300 MHz, $CDCl_3$) δ 7.37 – 7.30 (m, 9H), 7.28 (d, *J* = 3.6 Hz, 6H), 5.84 (ddt, *J* = 17.6, 10.0, 7.6 Hz, 1H), 5.11 (dd, *J* = 10.0, 6.1 Hz, 2H), 4.53 (s, 4H), 3.52 – 3.40 (m, 4H), 2.50 (s, 2H), 2.31 (d, *J* = 7.6 Hz, 2H).

3.1.2.7. Synthesis of enynes 1e (Z = CH_2)

3.1.2.7.1. General procedure G for the synthesis of enynes

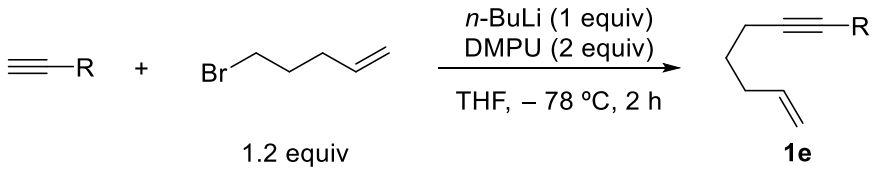

To a solution of the corresponding alkyne (9.8 mmol) in dry THF (0.5 M) at – 78 °C, *n*-BuLi (1.6 M in hexanes, 9.8 mmol) was added dropwise within 10 min, and the mixture was stirred for 30 min. Then, 5-bromopent-1-ene (11.8 mmol) and DMPU (19.6 mmol) were added and the reaction mixture was stirred for 2 h at rt. The reaction mixture was quenched with saturated solution of NH_4Cl and extracted with EtOAc, washed with brine and dried over

[146] J. H. Park, Y. Cho, Y. K. Chung, *Angew. Chem. Int. Ed*. **2010**, *49*, 5138–5141.

anhydrous $MgSO_4$. The solvent was removed under vacuum and the enyne was purified by column chromatography using cyclohexane as an eluent.[147]

Hept-6-en-1-yn-1-ylbenzene (1ea):[148] The product was obtained following the *General procedure G*, using phenylacetylene as starting alkyne, as a pale yellow oil in 74% yield (1.3 g). ^{1}H NMR (300 MHz, $CDCl_3$) δ 7.40 (dd, J = 6.5, 3.2 Hz, 2H), 7.28 (dd, J = 5.0, 2.0 Hz, 3H), 5.84 (ddt, J = 17.0, 10.2, 6.7 Hz, 1H), 5.07 (ddd, J = 17.0, 3.5, 1.6 Hz, 1H), 5.01 (ddt, J = 10.2, 3.5, 1.6 Hz, 1H), 2.43 (t, J = 7.1 Hz, 2H), 2.23 (dt, J = 7.1, 1.3 Hz, 2H), 1.70 (quin, J = 7.1 Hz, 2H).

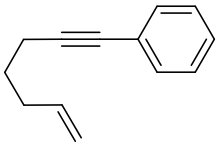

1-(Hept-6-en-1-yn-1-yl)-4-methylbenzene (1eb):[148] The product was obtained following the *General procedure G*, using 4-ethynyltoluene as starting alkyne, as a pale yellow oil in 76% yield (1.2 g). ^{1}H NMR (300 MHz, $CDCl_3$) δ 7.29 (d, J = 8.1 Hz, 2H), 7.09 (d, J = 8.1 Hz, 2H), 5.84 (ddt, J = 17.0, 10.2, 6.7 Hz, 1H), 5.07 (ddd, J = 17.0, 3.5, 1.6 Hz, 1H), 5.03 – 4.97 (ddt, J = 10.2, 3.5, 1.1 Hz, 1H), 2.41 (t, J = 7.1 Hz, 2H), 2.33 (s, 3H), 2.27 – 2.17 (qt, J = 7.1, 1.1 Hz, 2H), 1.70 (p, J = 7.1 Hz, 2H). [149]

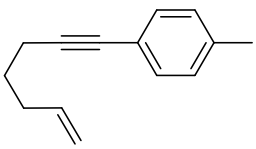

1-Fluoro-4-(hept-6-en-1-yn-1-yl)benzene (1ec):**Error! Bookmark not defined.** The product was obtained following the *General procedure G*, using 1-ethynyl-4-fluorobenzene as starting alkyne, as a colorless oil in 68% yield (214 mg). ^{1}H NMR (300 MHz, $CDCl_3$) δ 7.37 (dd, J = 8.8, 5.4 Hz, 2H), 6.97 (t, J = 8.8 Hz, 2H), 5.83 (ddt, J = 16.9, 10.1, 6.7 Hz, 1H), 5.11 – 5.04 (m, 1H), 5.01 (dd, J = 10.1, 0.9 Hz, 1H), 2.41 (t, J = 7.3 Hz, 2H), 2.22 (dd, J = 14.1, 7.3 Hz, 2H), 1.70 (quint, J = 7.3 Hz, 2H). ^{13}C NMR (75 MHz, $CDCl_3$) δ 163.9 (d, J = 248.1 Hz, C-F), 138.0 (CH), 133.5 (d, J = 8.2 Hz, 2 × CH), 120.2 (d, J = 3.5 Hz, C), 115.7 (2 × CH), 115.4 (CH_2), 89.7 (C), 80.0 (C), 33.0 (CH_2), 28.0 (CH_2), 18.9 (CH_2). ^{19}F NMR (282 MHz, $CDCl_3$) δ – 112.38. HRMS (TOF EI, MeOH) calcd. for $C_{13}H_{13}F$ $[M]^+$: 188.1001; Found: 188.1005.

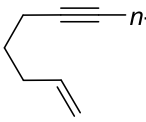

Hept-6-en-1-yn-1-ylbenzene (1ed):[148] The product was obtained following the *General procedure G*, using 1-hexyne as starting alkyne, as a colorless oil in 97% yield (540 mg). ^{1}H NMR (300 MHz, $CDCl_3$) δ 5.80 (ddt, J = 17.0, 10.2, 6.7 Hz, 1H), 5.06 (ddd, J = 17.0, 3.5, 1.6 Hz, 1H), 4.95 (ddt, J = 11.2, 2.2, 1.2 Hz, 1H), 2.21 – 2.07 (m, 6H), 1.57 (dt, J = 13.7, 6.7 Hz, 2H), 1.50 – 1.33 (m, 4H), 0.91 (t, J = 7.1 Hz, 3H).

[147] N. Topolovčan, I. Panov, M. Kotora, *Synlett* **2016**, *27*, 432–436.
[148] N. Topolovčan, I. Panov, M. Kotora, *Eur. J. Org. Chem.* **2015**, 2868–2878.

3.1.2.8. Synthesis of enynes 1f

3.1.2.8.1. General procedure for the synthesis of **1fa**

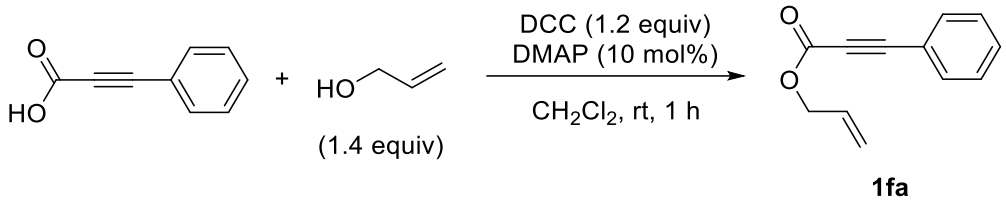

1fa

To a solution of 3-phenylpropiolic acid (6.8 mmol) and allyl alcohol (9.5 mmol) in CH_2Cl_2 (22 mL), a solution of DCC (8.2 mmol) and DMAP (0.7 mmol) in CH_2Cl_2 (5 mL) was added dropwise at 0 °C. The mixture was stirred for 1 h at rt. The solvent was removed under vacuum and the enyne was purified by column chromatography using cyclohexane/EtOAc 98:2.

Allyl 3-phenylpropiolate (1fa):[149] The product was obtained as a pale yellow oil in 92% yield (1.1 g). ^{1}H NMR (300 MHz, $CDCl_3$) δ 7.62 – 7.57 (m, 2H), 7.49 – 7.42 (m, 1H), 7.41 – 7.34 (m, 2H), 5.98 (ddt, *J* = 17.1, 10.4, 5.9 Hz, 1H), 5.41 (ddd, *J* = 17.1, 2.8, 1.2 Hz, 1H), 5.32 (ddd, *J* = 10.4, 2.4, 1.2 Hz, 1H), 4.73 (dt, *J* = 5.9, 1.2 Hz, 2H).

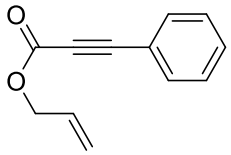

3.1.2.8.2. General procedure for the synthesis of **1fb**

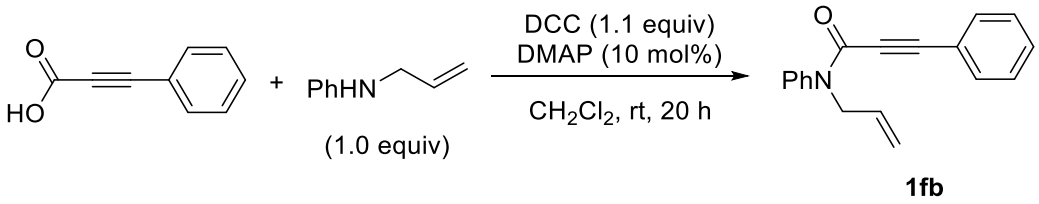

1fb

To a solution of 3-phenylpropiolic acid (6.8 mmol) in CH_2Cl_2 (15 mL), a solution of DCC (7.5 mmol) and DMAP (0.7 mmol) in CH_2Cl_2 (10 mL) was added dropwise at – 10 °C. *N*-phenylbut-3-en-1-amine (6.8 mmol) was then added and the mixture was stirred for 20 h at rt. The solid was filtered off and the filtrated was washed with 0.1 N HCl (10 mL) and dried over anhydrous $MgSO_4$. The solvent was removed under vacuum and the enyne was purified by column chromatography using cyclohexane/EtOAc 9:1 as an eluent.

***N*-Allyl-*N*,3-diphenylpropiolamide (1fb)**:[150] The product was obtained as a pale yellow solid in 69% yield (1.2 g). ^{1}H NMR (300 MHz, $CDCl_3$) δ 7.41 (t, *J* = 7.5 Hz, 3H), 7.33 (m, 3H), 7.23 (t, *J* = 7.5 Hz, 2H), 7.14 – 7.07 (m, 2H), 5.90 (ddt, *J* = 16.1, 9.9, 6.2 Hz, 1H), 5.22 – 5.13 (m, 2H), 4.42 (d, *J* = 6.2 Hz, 2H). [151]

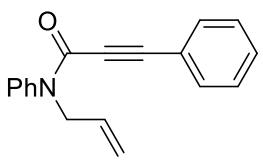

[149] T. Tsujihara, K. Takenaka, K. Onitsuka, M. Hatanaka, H. Sasai, *J. Am. Chem. Soc.* **2009**, *131*, 3452–3453.
[150] M.-B. Zhou, W.-T. Wei, Y.-X. Xie, Y. Lei, J.-H. Li, *J. Org. Chem.* **2010**, *75*, 5635–5642.

3.1.2.9. General procedure for the synthesis of enynones 1g

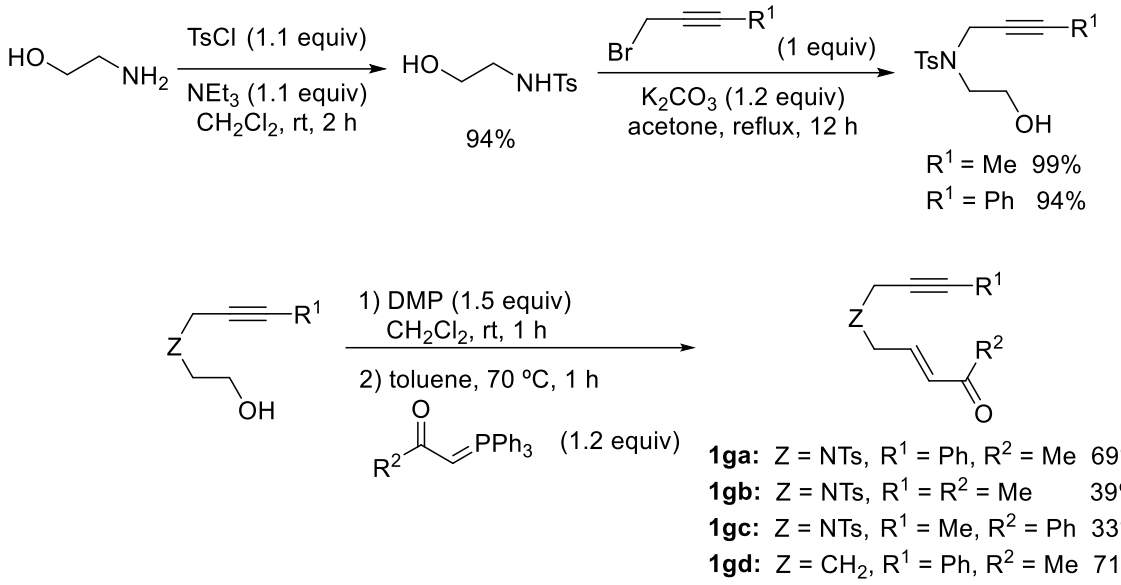

Step 1: To a solution of ethanolamine (1 equiv, 16.4 mmol) and *p*-toluenesulfonyl chloride (1.1 equiv, 18.0 equiv) in CH_2Cl_2 (0.45 M) at 0 °C, triethylamine (1.1 equiv) was added dropwise. The mixture was allowed to warm to room temperature and was stirred for 2 h. The reaction was quenched with H_2O and extracted with CH_2Cl_2. The combined organic layers were washed with brine and dried over anhydrous $MgSO_4$. Solvent was removed under vacuum and the residue was purified by column chromatography in silica gel using cyclohexane/AcOEt 1:1 as an eluent.[121]

Step 2: The reaction was performed using ethanolamine (1 equiv, 10.7 mmol), K_2CO_3 (1.2 equiv, 12.8 mmol) in acetone (0.5 M) and following the *General Procedure D*. The residue was purified by column chromatography in silica gel using cyclohexane/EtOAc 7:3 as an eluent.

Step 3: To a solution of the corresponding alcohol (1 equiv) in CH_2Cl_2 at 0 °C, DMP (1.5 equiv) was added. The resulting mixture was stirred at that temperature for 5 min and for another 30 min at room temperature. Then, the reaction was quenched with a solution of $Na_2S_2O_3$ and $NaHCO_3$ (5 mL) and extracted with EtOAc. The combined organic layer was washed with brine, dried over anhydrous $MgSO_4$ and filtered. The filtrate was concentrated under reduced pressure. The residue was dissolved in toluene (0.2 M) and the commercially available phosphorus ylide (1.2 equiv) was added. Then, the mixture was heated to 70 °C for 1 h. The solvent was evaporated under vacuum and the residue was purified by column chromatography in silica gel using cyclohexane/EtOAc 9:1 as an eluent.[151]

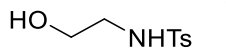

***N*-(2-Hydroxyethyl)-4-methylbenzenesulfonamide**:[121] The product was obtained following the *Step 1* as a white solid in 94% yield (3.33 g). ^{1}H NMR (300 MHz, $CDCl_3$) δ 7.75 (d, J = 8.3 Hz, 2H), 7.30 (d, J = 8.3 Hz, 2H), 5.40 (br s, 1H), 3.68 (d, J = 4.7 Hz, 2H), 3.07 (d, J = 4.7 Hz, 2H), 2.57 (br s, 1H), 2.42 (s, 3H).

[121] A. R. O. Venning, M. R. Kwiatkowski, J. E. Roque Peña, B. C. Lainhart, A. A. Guruparan, E. J. Alexanian, *J. Am. Chem. Soc.* **2017**, *139*, 11595–11600.
[151] Z. Yu, L. Liu, J. Zhang, *Chem. Eur. J.* **2016**, *22*, 8488–8492.

***N*-(2-Hydroxyethyl)-4-methyl-*N*-(3-phenylprop-2-yn-1-yl)benzenesulfonamide**:[152] The

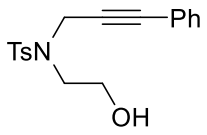

product was obtained following the *Step 2* as a yellow solid in 94% yield (1.29 g). ^{1}H NMR (300 MHz, $CDCl_3$) δ 7.79 (d, J = 8.3 Hz, 2H), 7.39 – 7.18 (m, 5H), 7.09 (d, J = 8.3 Hz, 2H), 4.42 (s, 2H), 3.84 (dd, J = 10.8, 5.5 Hz, 2H), 3.42 (t, J = 5.2 Hz, 2H), 2.35 (s, 3H), 2.22 (t, J = 5.9 Hz, 1H).

***N*-(But-2-yn-1-yl)-*N*-(2-hydroxyethyl)-4-methylbenzenesulfonamide**:[152] The product was

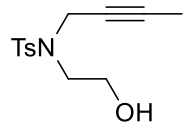

obtained following the *Step 2* as a yellow solid in 99% yield (2.89 g). ^{1}H NMR (300 MHz, $CDCl_3$) δ 7.75 (d, J = 8.3 Hz, 2H), 7.30 (d, J = 8.3 Hz, 2H), 4.16 – 4.06 (m, 2H), 3.77 (t, J = 5.2 Hz, 2H), 3.32 (t, J = 5.2 Hz, 2H), 2.43 (s, 3H), 1.88 (t, J = 2.5 Hz, 1H), 1.59 (t, J = 2.4 Hz, 3H).

(*E*)-4-Methyl-*N*-(4-oxopent-2-en-1-yl)-*N*-(3-phenylprop-2-yn-1-yl)benzenesulfonamide

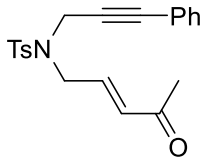

(1ga):[152] The product was obtained following the *Step 3* as a yellow oil in 69% yield (434 mg). ^{1}H NMR (300 MHz, $CDCl_3$) δ 7.78 (d, J = 8.3 Hz, 2H), 7.34 – 7.19 (m, 5H), 7.08 (dd, J = 8.3, 1.6 Hz, 2H), 6.71 (dt, J = 16.0, 5.8 Hz, 1H), 6.31 – 6.24 (dt, J = 16.0, 1.4 Hz 1H), 4.31 (s, 2H), 4.07 (d, J = 5.8 Hz, 2H), 2.36 (s, 3H), 2.25 (s, 3H).

(*E*)-*N*-(But-2-yn-1-yl)-4-methyl-*N*-(4-oxopent-2-en-1-yl)benzenesulfonamide (1gb): The

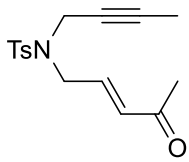

product was obtained following the *Step 3* as a yellow oil in 39% yield (675 mg). ^{1}H NMR (300 MHz, $CDCl_3$) δ 7.77 (d, J = 8.2 Hz, 2H), 7.25 (d, J = 8.2 Hz, 2H), 7.01 (d, J = 8.8 Hz, 2H), 6.76 (d, J = 8.8 Hz, 2H), 5.80 (ddt, J = 17.1, 10.1, 6.5 Hz, 1H), 5.32 (dd, J = 17.1, 1.3 Hz, 1H), 5.26 (dd, J = 10.1, 1.3 Hz, 1H), 4.29 (s, 2H), 3.88 (d, J = 6.5 Hz, 2H), 3.79 (s, 3H), 2.36 (s, 3H). ^{13}C NMR (75 MHz, $CDCl_3$) δ 197.9 (C), 143.7 (C), 140.9 (CH), 135.6 (C), 132.8 (CH), 129.4 (2 × CH), 127.7 (2 × CH), 82.3 (C), 71.2 (C), 47.5 (CH_3), 37.4 (CH_3), 27.0 (CH_2), 21.4 (CH_2), 3.1 (CH_3). HRMS (ESI, MeOH) calcd. for $C_{16}H_{19}NO_3S$ [M + H]$^+$: 306.1086; Found: 306.1162.

(*E*)-*N*-(But-2-yn-1-yl)-4-methyl-*N*-(4-oxo-4-phenylbut-2-en-1-yl)benzenesulfonamide

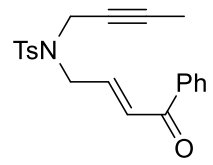

(1gc):[152] The product was obtained following the *Step 3* as a yellow oil in 33% yield (683 mg). ^{1}H NMR (300 MHz, $CDCl_3$) δ 7.91 (dd, J = 8.3, 1.3 Hz, 2H), 7.76 (d, J = 8.3 Hz, 2H), 7.61 – 7.55 (m, 1H), 7.47 (dd, J = 8.0, 6.7 Hz, 2H), 7.31 (d, J = 8.0 Hz, 2H), 7.08 (dt, J = 15.4, 1.4 Hz, 1H), 6.87 (dt, J = 15.4, 5.4 Hz, 1H), 4.08 (d, J = 4.8 Hz, 4H), 2.42 (s, 3H), 1.58 (t, J = 2.3 Hz, 3H).

***(E)*-9-Phenylnon-3-en-8-yn-2-one (1gd)**:[103] The product was obtained following the *General*

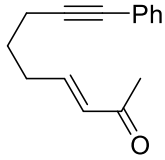

procedure for the synthesis of propargylic alcohols, using 5-hexyn-1-ol and iodobenzene, followed by *Step 3* as a light brown oil in 71% yield (259 mg). ^{1}H NMR (300 MHz, $CDCl_3$) δ 7.39 (dd, J = 6.6, 3.0 Hz, 2H), 7.31 – 7.27 (m, 3H), 6.84 (dt, J = 15.9, 6.9 Hz, 1H), 6.14 (d, J = 15.9 Hz, 1H), 2.47 (t, J = 7.0 Hz, 2H), 2.44 – 2.38 (m, 2H), 2.25 (s, 3H), 1.79 (p, J = 7.0 Hz, 2H).

[103] C. Wu, J. Liao, S. Ge, *Angew. Chem. Int. Ed.* **2019**, 58, 8882–8886.
[151] Z. Yu, L. Liu, J. Zhang, *Chem. Eur. J.* **2016**, *22*, 8488–8492.

CHAPTER 2:

Fe-catalyzed hydroborylative cyclization of enynes

3.2. CHAPTER 2

3.2.1. Goal

During the last years, our group has contributed to the development of Pd-catalyzed hydroborylative cyclization reactions of polyunsaturated compounds, avoiding the use of organohalides and Li and Mg nucleophiles.[90–96] However, this methodology shows some drawbacks, as the use of diboron derivatives B_2pin_2 (that leads to the loss of one B unit) and the impossibility to tune the catalysts properties since it takes place in the absence of added ligands.

Encouraged by the Co-catalyzed hydroborylative cyclization of enynes described by Lu and co-workers (*see* ***Scheme I.55***),[100] we turned our attention to the possibility of using iron complexes to catalyze this reaction. In this way, we could achieve a more economical and less toxic proccess for the synthesis of organoboranes and, moreover, we could envision the discovery of novel activation pathways.

3.2.2. Precedents

Hydroboration of unsaturated species is one of the most employed methods for the synthesis of boryl derivatives. Catalysis of this reaction with noble metals, such as Pd, Ir, Ru and Rh, has been vastly used. However, the use of these precious metals presents many drawbacks. In this field, the employment of the first-row transition metals has led to the development of efficient and inexpensive base-metal systems. Due to their low cost, high earth-abundance and minimal environmental impact, iron has received significant attention during the last years.[152]

3.2.2.1. Fe-catalyzed hydroboration of dienes

The first iron-catalyzed hydroboration of olefinic substrates was described by Ritter and co-workers.[153] The use of an iron complex with a bidentate nitrogen ligand, Mg as reductant and pinacolborane allows the hydroboration of several 2-substituted-1,3-dienes with good yields (**Scheme 2.1**). The regioselectivity of the hydroboration is sensitive to the substituent on the imine nitrogen of the catalyst, which controls the formation of either the linear or the branched boronate. However, internal dienes do not react under the optimal conditions.

---

[90] J. Marco-Martínez, V. López-Carrillo, E. Buñuel, R. Simancas, D. J. Cárdenas, *J. Am. Chem. Soc.* **2007**, *129*, 1874–1875.
[91] V. Pardo-Rodríguez, E. Buñuel, D. Collado-Sanz, D. J. Cárdenas, *Chem. Commun.* **2012**, *48*, 10517–10519.
[92] A. Martos-Redruejo, R. López-Durán, E. Buñuel, D. J. Cárdenas, *Chem. Commun.* **2014**, *50*, 10094–10097.
[93] J. Marco-Martínez, E. Buñuel, R. López-Durán, D. J. Cárdenas, *Chem. Eur. J.* **2011**, *17*, 2734–2741.
[94] J. Marco-Martínez, E. Buñuel, R. Muñoz-Rodríguez, D. J. Cárdenas, *Org. Lett.* **2008**, *10*, 3619–3621.
[95] R. López-Durán, A. Martos-Redruejo, E. Buñuel, V. Pardo-Rodríguez, D. J. Cárdenas, *Chem. Commun.* **2013**, *49*, 10691–10693.
[96] V. Pardo-Rodríguez, J. Marco-Martínez, E. Buñuel, D. J. Cárdenas, *Org. Lett.* **2009**, *11*, 4548–4551.
[100] T. Xi, Z. Lu, *ACS Catal.* **2017**, *7*, 1181–1185.
[152] (a) *Iron Catalysis in Organic Chemistry*, (Ed. B. Plietker), Wiley-VCH, Weinheim, **2008**. (b) I. Bauer, H.-J. Knölker, *Chem. Rev.* **2015**, *115*, 3170–3387. (c) M. D. Greenhalgh, A. S. Jones, S. P. Thomas, *ChemCatChem* **2015**, *7*, 190–222.
[153] J. Y. Wu, B. Moreau, T. Ritter, *J. Am. Chem. Soc.* **2009**, *131*, 12915–12917.

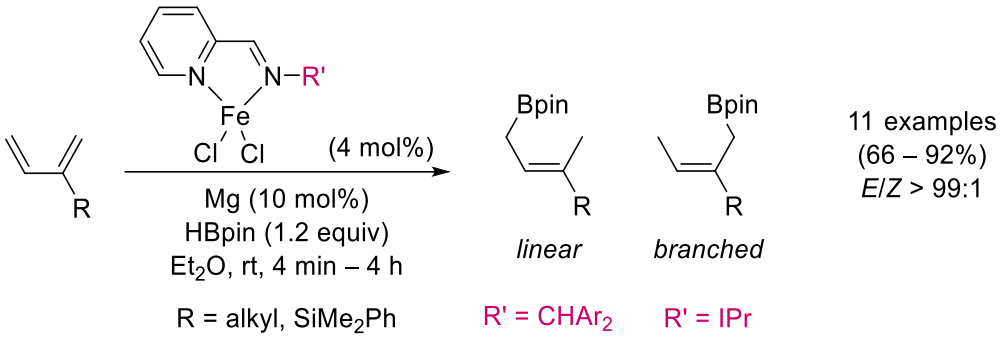

Scheme 2.1. Fe-catalyzed hydroboration of 1,3-dienes.

The proposed mechanism starts with the reduction of the iron precatalyst and coordination of the diene. Then, an oxidative addition of the HBpin takes place to obtain an intermediate iron complex which can undergo a migratory insertion of the alkene into the Fe–H or Fe–B bond. Finally, π-σ rearrangement followed by a reductive elimination furnishes the observed allylboronate (**Figure 2.1**).

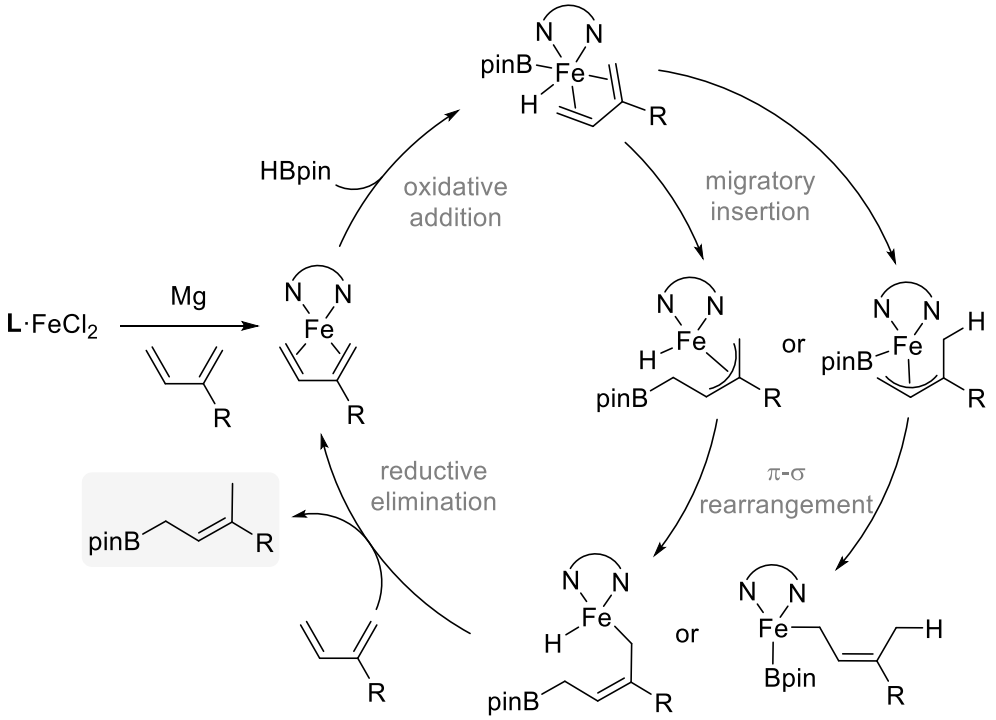

Figure 2.1. Proposed mechanism for the Fe-catalyzed hydroboration of 1,3-dienes.

Few years later, Huang and co-workers described the synthesis of (*Z*)-allylboronates by the regioselective Fe-catalyzed hydroboration of 1-aryl-substituted-1,3-dienes.[154] In this study, both internal and terminal dienes effectively yield the corresponding allylboronates (**Scheme 2.2**). The active catalyst is *in situ* generated by reaction of the iron(II) complex with $NaBHEt_3$. The proposed reaction pathway is the same as the suggested by Ritter.

[154] Y. Cao, Y. Zhang, L. Zhang, D. Zhang, X. Leng, Z. Huang, *Org. Chem. Front.* **2014**, *1*, 1101–1106.

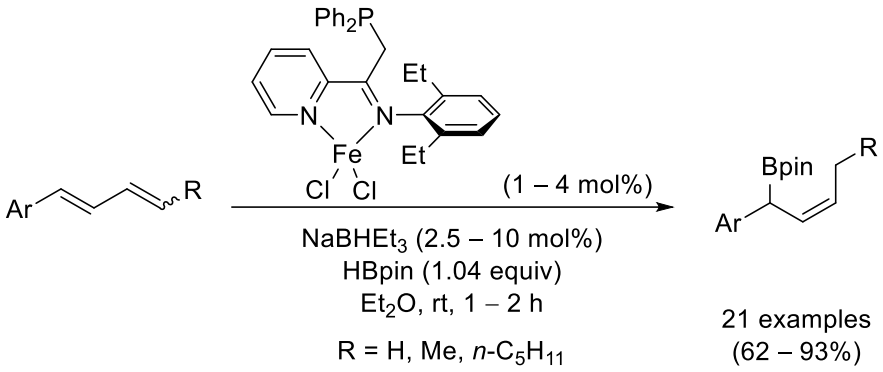

Scheme 2.2. Fe-catalyzed hydroboration of dienes described by Huang.

3.2.2.2. Fe-catalyzed hydroboration of alkenes

Fernández and Gulyás described the first example of an iron-catalyzed hydroboration of alkenes. The combination of a simple iron(II) salt with PPh_3 allows the β-borylation of electron-deficient olefins in quantitative yields (**Scheme 2.3**).[155] The reaction seems to take place through the preactivation of the substrate by the Lewis acidic iron salt, promoting the boryl-addition.

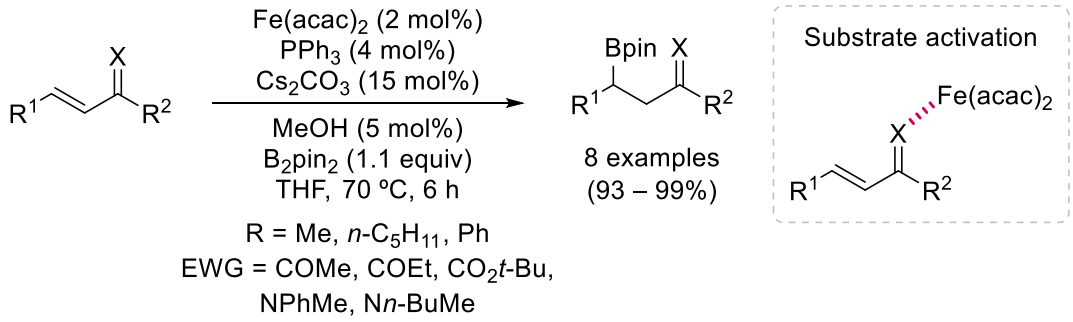

Scheme 2.3. Fe-catalyzed hydroboration of electron-deficient alkenes.

In 2013, Huang described the hydroboration reaction of alkenes using a PNN iron pincer complex (**Scheme 2.4**).[156] The catalytic system shows an exclusive regioselectivity to the *anti*-Markovnikov hydroboration of the alkene, obtaining the corresponding alkylboronates with excellent yields in a short reaction time. The reaction also needs the addition of $NaBHEt_3$, although in a very low catalytic load.

[155] A. Bonet, C. Sole, H. Gulyás, E. Fernández, *Chem. Asian J.* **2011**, *6*, 1011–1014.
[156] (a) L. Zhang, D. Peng, X. Leng, Z. Huang, *Angew. Chem. Int. Ed.* **2013**, *52*, 3676–3680. (b) L. Zhang, Z. Huang, *Synlett* **2013**, *24*, 1745–1747.

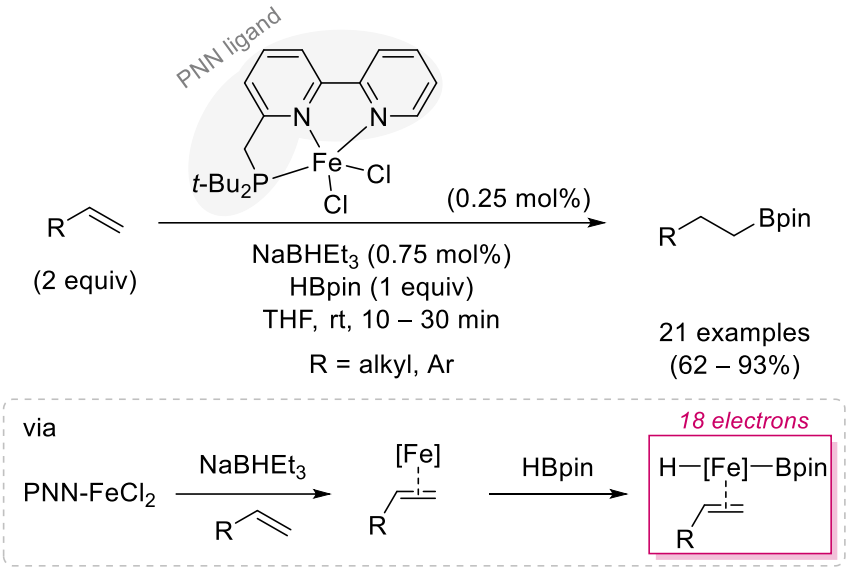

Scheme 2.4. Fe-catalyzed hydroboration of alkenes described by Huang.

Noticeably, the previous Ritter iron complex does not work under these reaction conditions. Tridentate ligands are essential for the reaction to take place. The authors propose such a ligand would induce a less electrophilic iron center and may allow easy access to a 18 electron Fe(II) boryl hydride species, which is a potential key intermediate in other catalytic alkene hydroborations.

Simultaneously, Chirik described the hydroboration of alkenes by a bis(iminopyridine) (BIP) iron(0) dinitrogen-based system.[157] No other additives are required, and both internal and terminal alkenes react with excellent yields in solvent-free conditions (**Scheme 2.5**).

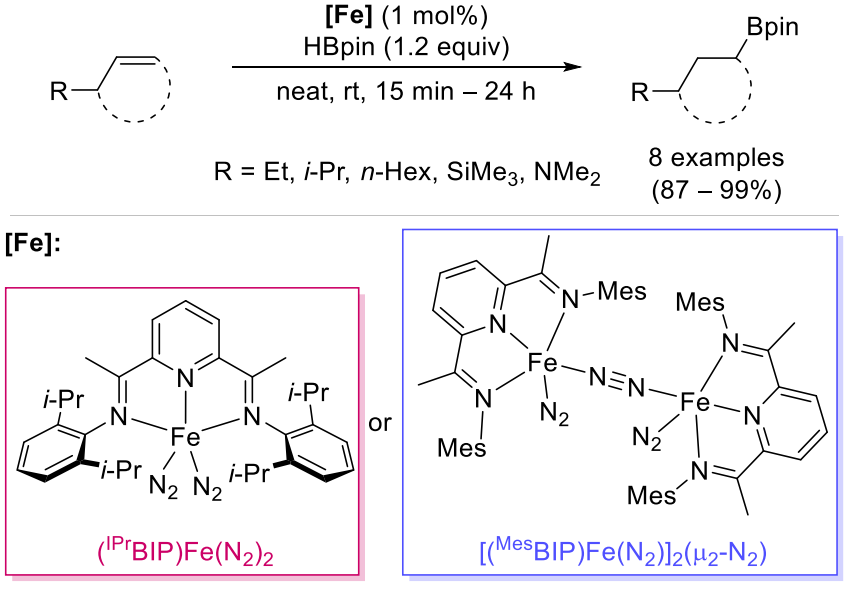

Scheme 2.5. BIP-Fe-catalyzed hydroboration of alkenes.

Thomas and co-workers performed this type of reaction by choosing a BIP ligand, a simple iron salt, an activating agent and pinacolborane in smooth reaction conditions (**Scheme**

[157] J. V. Obligacion, P. J. Chirik, *Org. Lett.* **2013**, *15*, 2680–2683.

2.6).[158] This system performs the *anti*-Markovnikov hydroboration of a broad variety of alkenes, showing a high functional group tolerance.

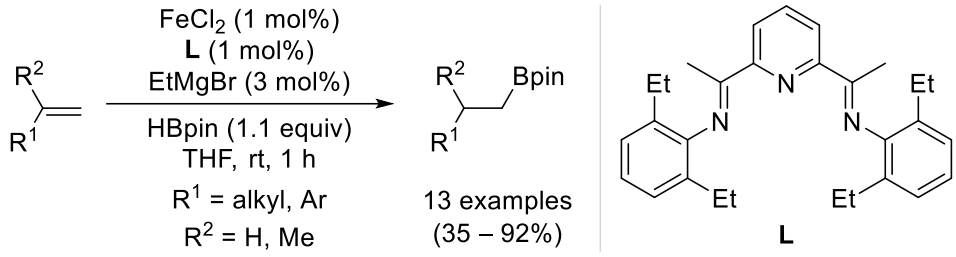

Scheme 2.6. Fe-catalyzed hydroboration of alkenes described by Thomas.

Comparing to the previous reported highly-air and moisture sensitive precatalyst, this system simplifies practical requirements since the active catalyst is *in situ* generated by reaction of $FeCl_2$/BIP with the organomagnesium reagent. The authors propose an active Fe(I) species by quantifying the formation of the homocoupling product of the nucleophile.

Thomas also describes the hydroboration of alkenes using the same type of BIP ligand with an iron(II) tetrafluoroborate salt in the absence of an external activator.[159] The key step of this methodology is the endogeneous activation of the precatalyst by counterion dissociation, generating fluoride which indirectly activates the system by reaction with HBpin (**Scheme 2.7**). Formation of BF_3 and FBpin was detected by NMR spectroscopy.

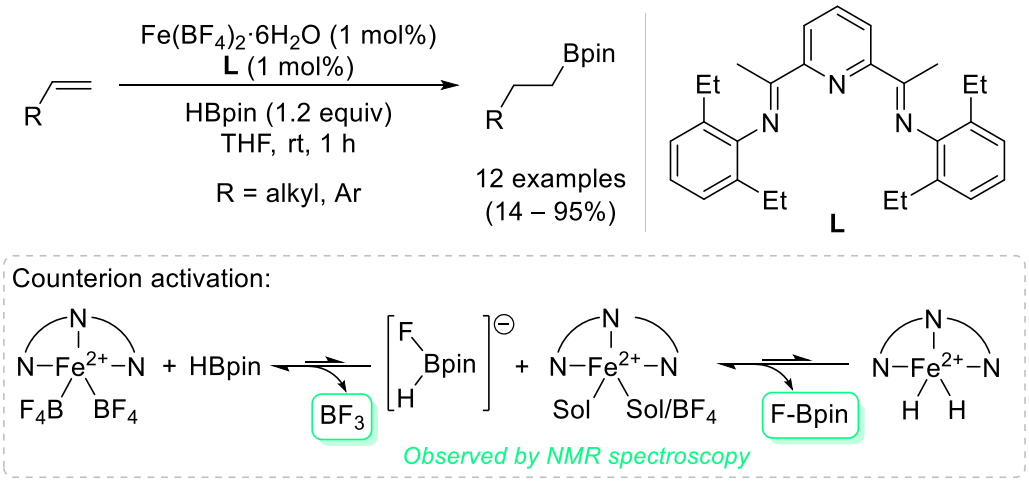

Scheme 2.7. Hydroboration of alkenes by counterion activation.

Lu group has described various hydroboration reactions of alkenes by using novel oxazoline imino(piridine) ligands (OIP). Iron(II) complexes based on this kind of ligands have allowed the development of an asymmetric *anti*-Markovnikov hydroboration of alkenes with high yields and excellent enantioselectivities (**Scheme 2.8**).[160]

[158] M. D. Greenhalgh, S. P. Thomas, *Chem. Commun.* **2013**, *49*, 11230–11232.
[159] R. Agahi, A. J. Challinor, N. B. Carter, S. P. Thomas, *Org. Lett.* **2019**, *21*, 993–997.
[160] J. Chen, T. Xi, Z. Lu, *Org. Lett.* **2014**, *16*, 6452–6455.

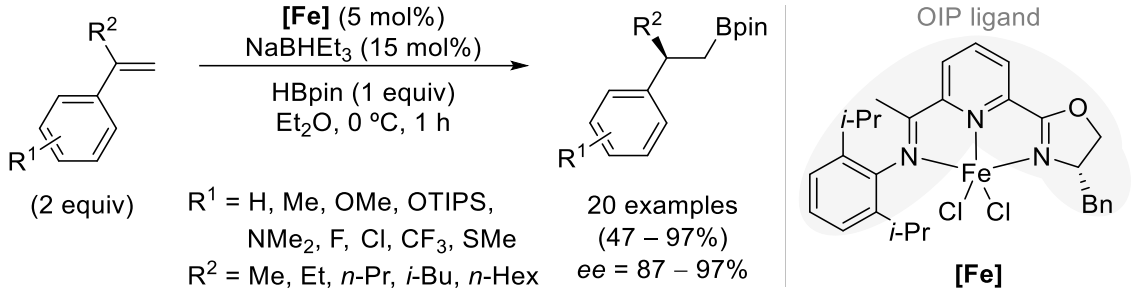

Scheme 2.8. Asymmetric Fe-catalyzed hydroboration of alkenes.

This methodology has been extended to alkenylcyclopropanes as well, using similar reaction conditions.[161] In this study, Lu and co-workers describe an iron-catalyzed Markovnikov-type hydroboration *via* selective C–C bond cleavage (**Scheme 2.9**). The proposed mechanism involves an iron hydride as the active species for the transformation.

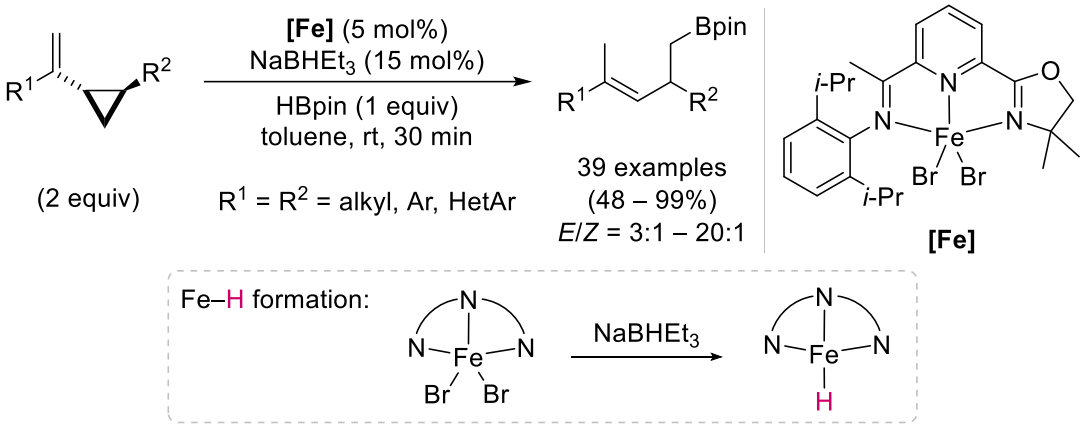

Scheme 2.9. Fe-catalyzed hydroboration of alkenylcyclopropanes.

The substitution of the imine moiety by an amide group in the ligand structure affords the Markovnikov-selective hydroboration of styrenes. Using pinacolborane and catalytic amounts of simple iron(II) chloride, $NaBHEt_3$ and OPPA ligand (oxazolinylphenyl picolinamide), the corresponding alkylboronates are obtained in moderate to high yields (**Scheme 2.10**).[162]

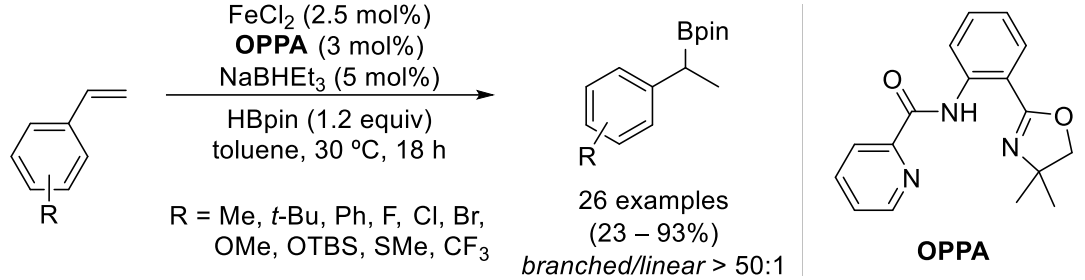

Scheme 2.10. Fe-catalyzed Markovnikov-selective hydroboration of styrenes.

Another example of iron-catalyzed Markovnikov hydroboration of alkenes has been described by Webster.[163] The suitable choice of the substituent in the ligand allows to

[161] C. Chen, X. Shen, J. Chen, Z. Lu, *Org. Lett.* **2017**, *19*, 5422–5425.
[162] X. Chen, Z. Cheng, Z. Lu, *Org. Lett.* **2017**, *19*, 969–971.
[163] M. Espinal-Viguri, C. R. Woof, R. L. Webster, *Chem. Eur. J.* **2016**, *22*, 11605–11608.

modulate the regioselectivity of the hydroboration of several alkenes and alkynes (**Scheme 2.11**). The reaction proceeds in mild conditions, without reducing agents or additives, and furnishes the corresponding boryl derivatives in high yields.

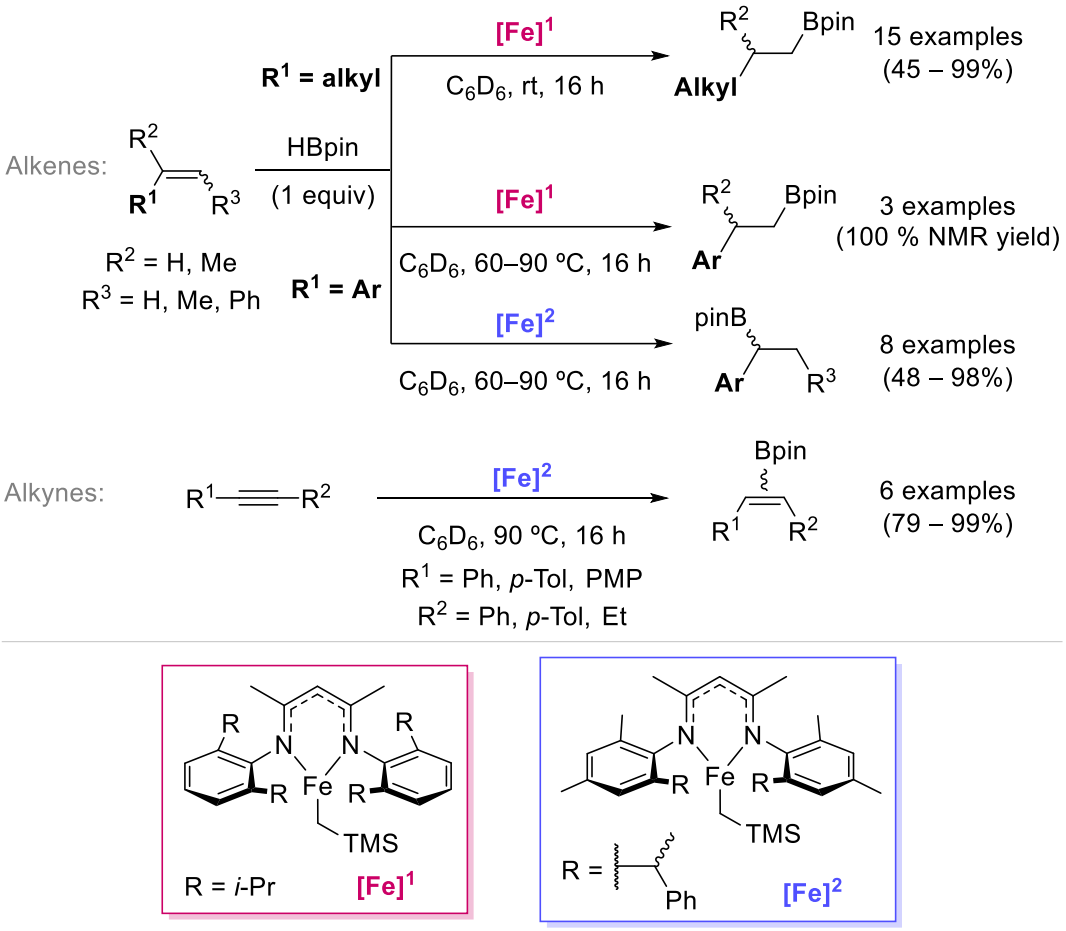

Scheme 2.11. Fe-catalyzed hydroboration of alkenes and alkynes described by Webster.

Stoichiometric experiments suggest that the catalytic cycle proceed *via* an iron hydride, and kinetic studies demonstrate that the reaction is first order in alkene, HBpin and the iron complex.

Notably, the use of NHC ligands along with iron precatalyst has allowed the development of efficient procedures. Sortais, Darcel and co-workers described the first (NHC)Fe-catalyzed *anti*-Markovnikov hydroboration of several alkenes, requiring UV irradiation in neat conditions (**Scheme 2.12**).[164] Presumably, an oxidative addition of HBpin takes place by UV-assisted decoordination of a CO ligand.

[164] J. Zheng, J.-B. Sortais, C. Darcel, *ChemCatChem* **2014**, *6*, 763–766.

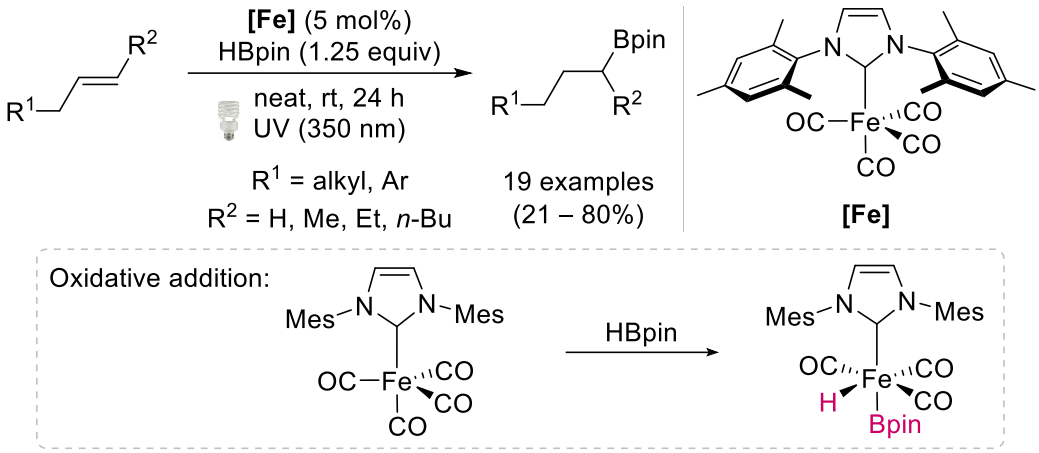

Scheme 2.12. (NHC)Fe-catalyzed hydroboration of alkenes.

Thomas designed new NHC ligands with a coordinating group in the structure, in order to enable an internal activation of the iron catalyst without the need for an external activator. These novel ligands efficiently perform the hydroboration of alkenes and orient the reactivity toward both regioselectivities, Markovnikov and *anti*-Markovnikov (**Scheme 2.13**).[165] Mechanistic experiments and reaction monitoring by ESI-MS hint the reaction proceeds through alkene hydrometallation by an iron-hydride complex.

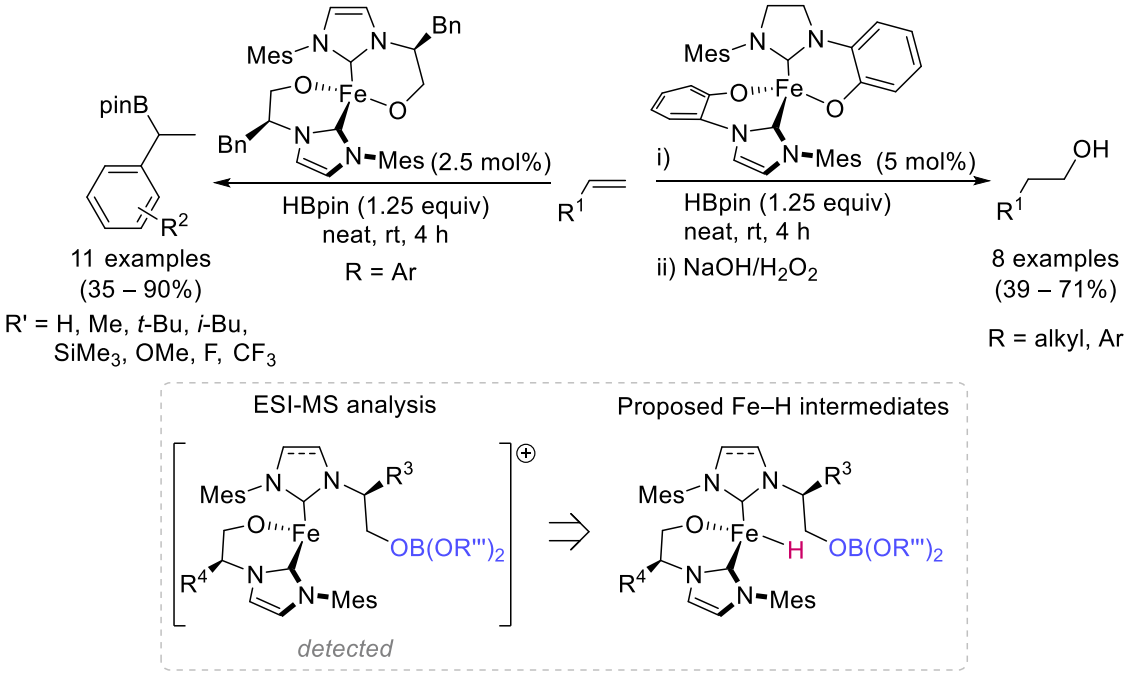

Scheme 2.13. (NHC)Fe-catalyzed hydroboration of alkenes described by Thomas.

Design and synthesis of new pincer ligands for the hydroboration of unsaturated species has been also developed by Szymczak.[166] Alkylation of a remote site on the ligand backbone effectively provides a more electrophilic complex, displaying higher reaction rate and distinct regioselectivity in the hydroboration process (**Scheme 2.14**).

[165] A. J. MacNair, C. R. P. Millet, G. S. Nichol, A. Ironmonger, S. P. Thomas, *ACS Catal.* **2016**, *6*, 7217–7221.
[166] K.-N. T. Tseng, J. W. Kampf, N. K. Szymczak, *ACS Catal.* **2015**, *5*, 411–415.

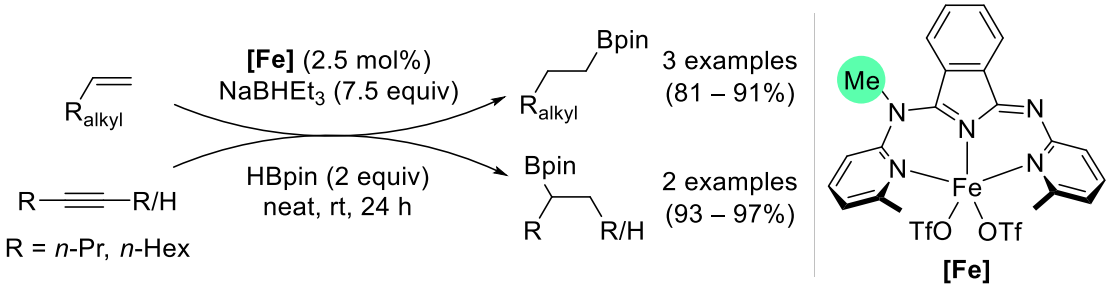

Scheme 2.14. Alteration of ligand backbone for olefin hydroboration.

Sydora, Stradiotto, Turculet and co-workers described the isomerization-hydroboration of branched aliphatic alkenes using modified Co and Fe complexes with *N*-phosphinoamidinate ligands, obtaining the terminal boronate in all the examples (**Scheme 2.15**).[167]

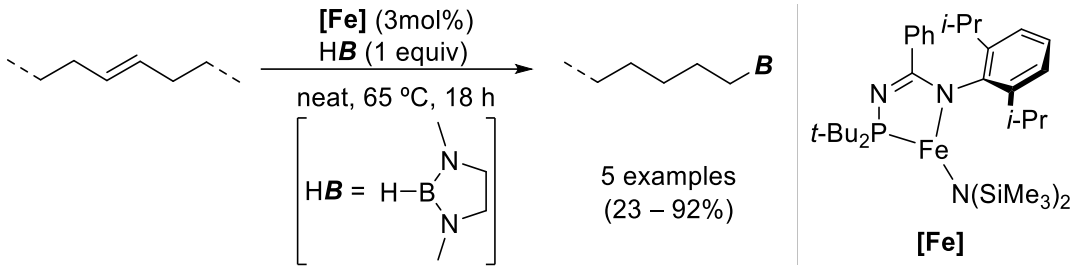

Scheme 2.15. Fe-catalyzed isomerization-hydroboration of alkenes.

A ligand-free methodology for the hydroboration of styrene derivatives has been developed by Zhou group.[168] A simple and inexpensive iron salt, such as $FeCl_2$, catalyzes the hydroboration reaction with excellent yields. However, one boryl unit is lost during the process since B_2pin_2 along with a base are required (**Scheme 2.16**).

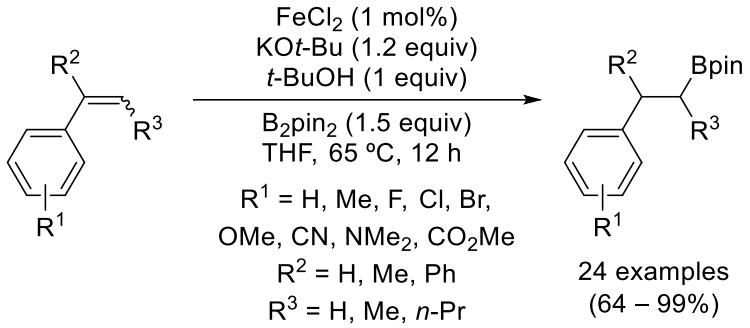

Scheme 2.16. Fe-catalyzed ligand-free hydroboration of styrenes.

A putative mechanism is shown in **Figure 2.2**. First, the addition of an anionic Bpin, derived from the reaction between B_2pin_2 and the base, to the starting Fe complex takes place. Then, the alkene inserts in the Fe–B bond towards the *anti*-Markovnikov observed regioselectivity. Finally, this iron intermediate is protonated with *t*-BuOH to generate the desired boronate and the iron catalyst.

[167] T. Ogawa, A. J. Ruddy, O. L.Sydora, M. Stradiotto, L. Turculet, *Organometallics* **2017**, *36*, 417–423.
[168] Y. Liu, Y. Zhou, H. Wang, J. Qu, *RSC Adv.* **2015**, *5*, 73705–73713.

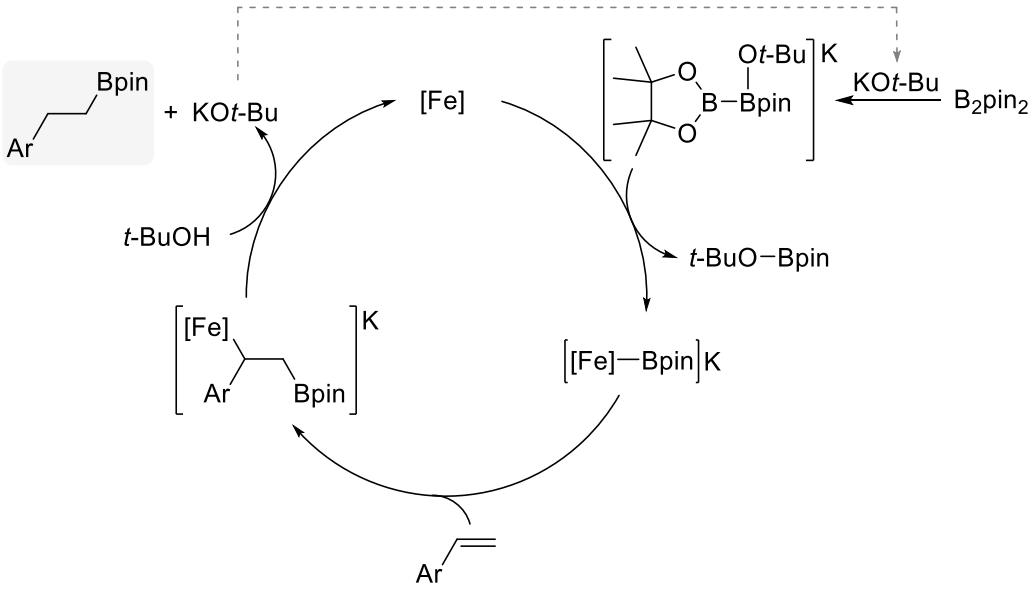

Figure 2.2. Putative mechanism Fe-catalyzed ligand-free hydroboration of styrenes.

The iron-catalyzed dehydrogenative borylation process, considered as a "deleterious" pathway in hydroboration reactions, has been optimized by Ge and co-workers. Catalytic system involves a Fe(0) salt, pinacolborane and hydrogen acceptors, such as norbornene (nbe). The reaction shows a broad scope regarding styrene derivatives, affording alkenylboronates with high yields (**Scheme 2.17**).[169] In addition, the authors perform different one-pot procedures for the borylation/functionalization of starting vinylarenes.

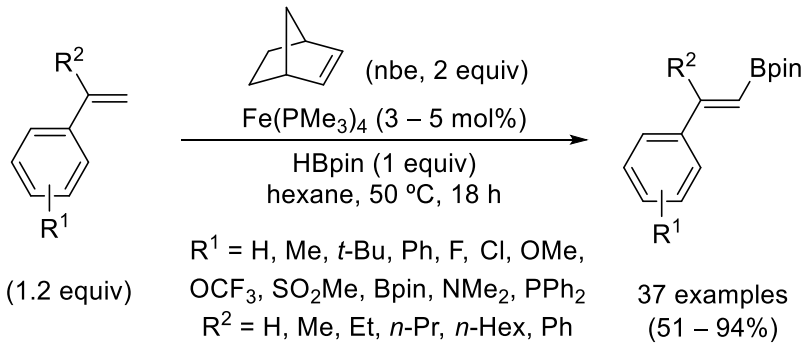

Scheme 2.17. Fe-catalyzed dehydrogenative borylation of alkenes.

The proposed catalytic cycle for this reaction begins with the oxidative addition of HBpin to the Fe(0) catalyst. Then, *syn*-insertion of alkene into the Fe–B bond followed by *β*-hydrogen elimination releases the alkenylboronate. Finally, the hydrogen acceptor generates the catalytically active Fe(0) species (**Figure 2.3**).

[169] C. Wang, C. Wu, S. Ge, *ACS Catal.* **2016**, *6*, 7585–7589.

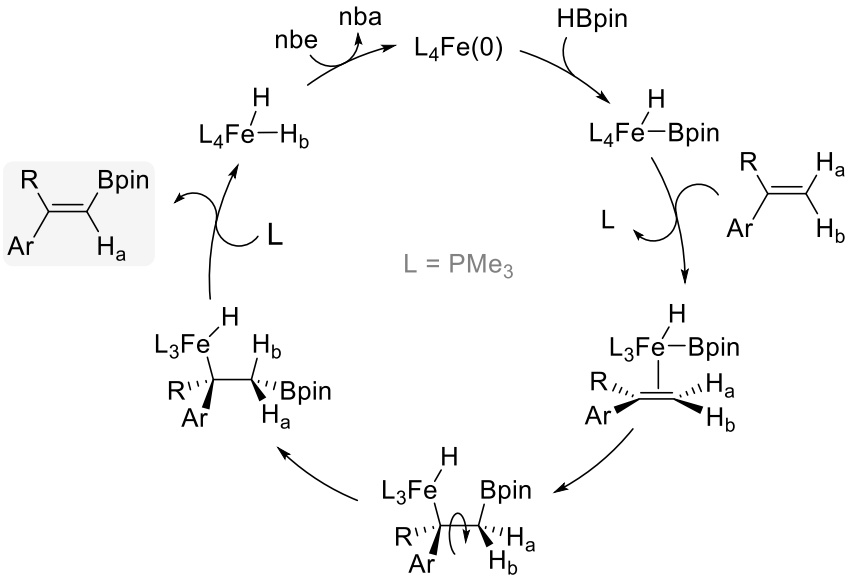

Figure 2.3. Proposed catalytic cycle for the dehydrogenative borylation.

3.2.2.3. Fe-catalyzed hydroboration of alkynes

Apart from the mentioned work described by Webster (*vide supra*),[163] other studies about hydroboration of alkynes using Fe-based catalyst have been reported in the literature.

In 2013, Enthaler described the hydroboration of alkynes with HBpin using $Fe_2(CO)_9$ as reaction catalyst. The system works well with terminal alkynes, affording regio- and stereoselectively *anti*-Markovnikov (*E*)-alkenylboronates (**Scheme 2.18**).[170] However, complex mixtures of isomers are obtained when internal and non-symmetrical alkynes are used. The authors propose a similar reaction pathway as the previously suggested by Ritter (*see* **Figure 2.1**).

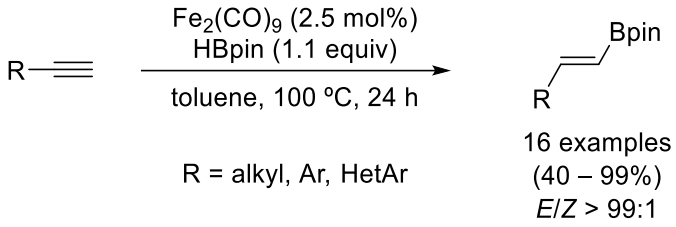

Scheme 2.18. Fe-catalyzed hydroboration of alkynes described by Enthaler.

The combination of simple $FeCl_3$ or iron nanoparticles with B_2pin_2 also performs the hydroboration of alkynes towards the exclusively formation of (*E*)-alkenylboronates with high yields (**Scheme 2.19**).[171] When iron nanoparticles are used as reaction catalyst, it can be recovered by using an external magnetic field, and can be recycled up to 6 times without significant loss of catalytic activity.

[163] M. Espinal-Viguri, C. R. Woof, R. L. Webster, *Chem. Eur. J.* **2016**, *22*, 11605–11608.
[170] M. Haberberger, S. Enthaler, *Chem. Asian J.* **2013**, *8*, 50–54.
[171] V. S. Rawat, B. Sreedhar, *Synlett* **2014**, *25*, 1132–1136.

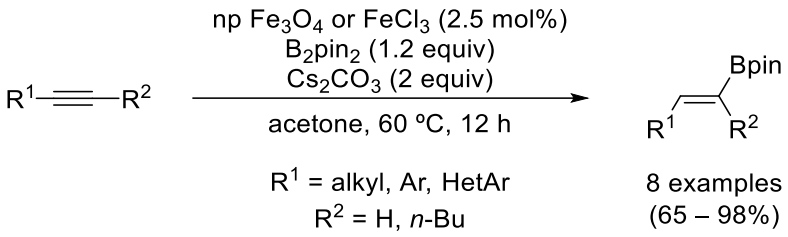

Scheme 2.19. Fe-catalyzed hydroboration of alkynes described by Sreedhar.

Kirchner and co-workers synthetized new PNP pincer-type ligands in order to design novel iron complexes for the hydroboration of alkynes.[172] Fortunately, this kind of complexes performs the reaction in a chemo-, regio- and stereoselective manner, affording an unusual *Z*-configuration of final boronates with excellent yields (**Scheme 2.20**).

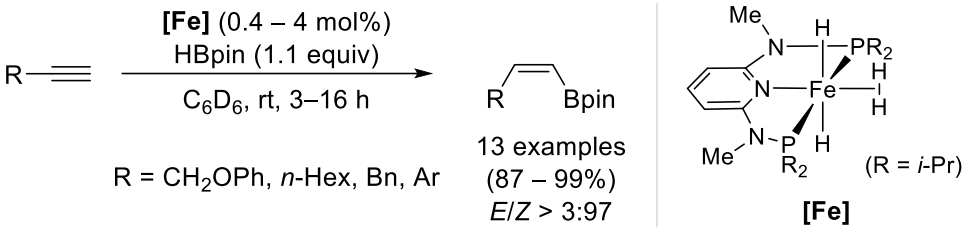

Scheme 2.20. PNP-Fe-catalyzed hydroboration of alkynes.

Simultaneously, Nishibayashi group also described the PNP-Fe-catalyzed *anti*-Markovnikov hydroboration of mainly aromatic-substituted alkynes.[173] In this case, *E*-selectivity is obtained with high yields (**Scheme 2.21**). The reaction pathway seems to involve an iron-boryl species as the key intermediate, since the corresponding (PNP)Fe-Bpin is isolated and tested as catalyst.

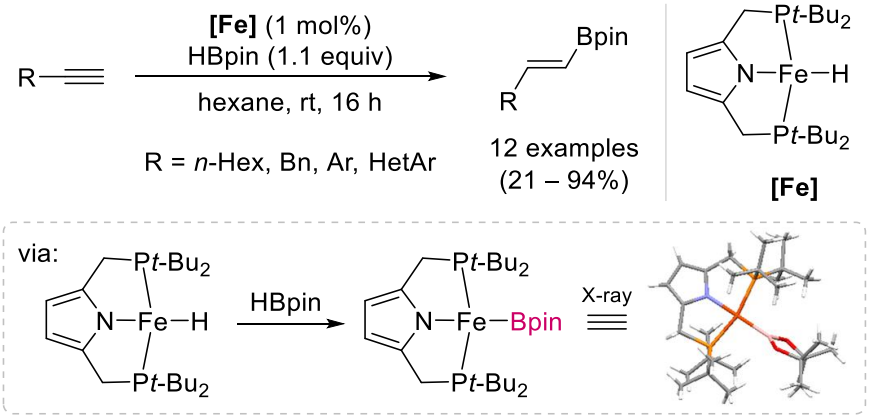

Scheme 2.21. Fe-catalyzed hydroboration of alkynes described by Nishibayashi.

[172] N. Gorgas, L. G. Alves, B. Stöger, A. M. Martins, L. F. Veiros, K. Kirchner, *J. Am. Chem. Soc.* **2017**, *139*, 8130–8133.
[173] K. Nakajima, T. Kato, Y. Nishibayashi, *Org. Lett.* **2017**, *19*, 4323–4326.

3.2.3. Results

We begin the study of the Fe-catalyzed hydroborylative cyclization reaction choosing the previously synthetized enyne **1aa** as the model starting substrate, pinacolborane as the boron reagent and simple iron(II) bromide as the iron source. Based on the different examples of Fe-catalyzed hydroboration described in the literature, we suggested that the use of PyBox-type ligand should be a suitable choice to evaluate initial reaction conditions, since several tridentate nitrogen ligands have been employed (*vide supra*). Furthermore, we envisioned that an external additive might be necessary to activate the iron complex prior to the addition of all the substrates. Taking into account the activation of some Co[174] and Fe[175] complexes, organomagnesium and organolithium reagents were used for the alkylation of the initial halogen-metal complexes. Thus, we chose MeMgCl as activating agent to begin with this study.

We performed the reaction shown in **Scheme 2.22** with the initially chosen condiitions. Preactivation step of Fe/L with MeMgCl, and addition of enyne and HBpin were carried out at 0 ºC, and then the reaction mixture was stirred at room temperature. A mixture of two regioisomers derived from the hydroboration of the alkyne moiety (**2aa'** and **2aa''**) along with the desired cyclic borylated product **2aa** were obtained, albeit in low yield.

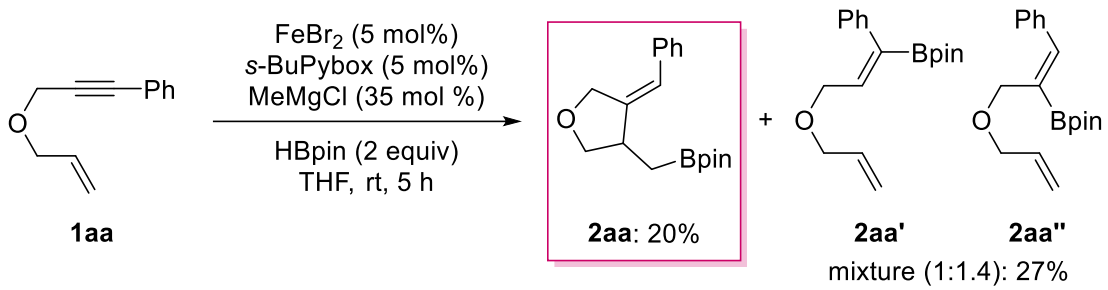

Scheme 2.22. Initial assay for the Fe-catalyzed borylation of model enyne.

Encouraged by this result, we then evaluated different ligands (**Scheme 2.23**). Unfortunately, the same mixture of hydroboration products was detected by GC/MS techniques in most cases. Tpy and bathocuproine also afforded **2aa** in low yields. In contrast, we were pleased to find that the use of biquinoline afforded cyclic alkylboronate **2aa** as the unique reaction product in 37% yield with complete conversion of enyne **1aa**.

[174] V. C. Gibson, M. J. Humphries, K. P. Tellmann, D. F. Wass, A. J. P. White, D, J. Williams, *Chem. Commun.* **2001**, 2252–2253.
[175] (a) J. Cámpora, A. M. Naz, P. Palma, E. Álvarez, *Organometallics* **2005**, *24*, 4878–4881. (b) A. M. Tondreau, J. M. Darmon, B. M. Wile, S. K. Floyd, E. Lobkovsky, P. J. Chirik, *Organometallics* **2009**, *28*, 3928–3940.

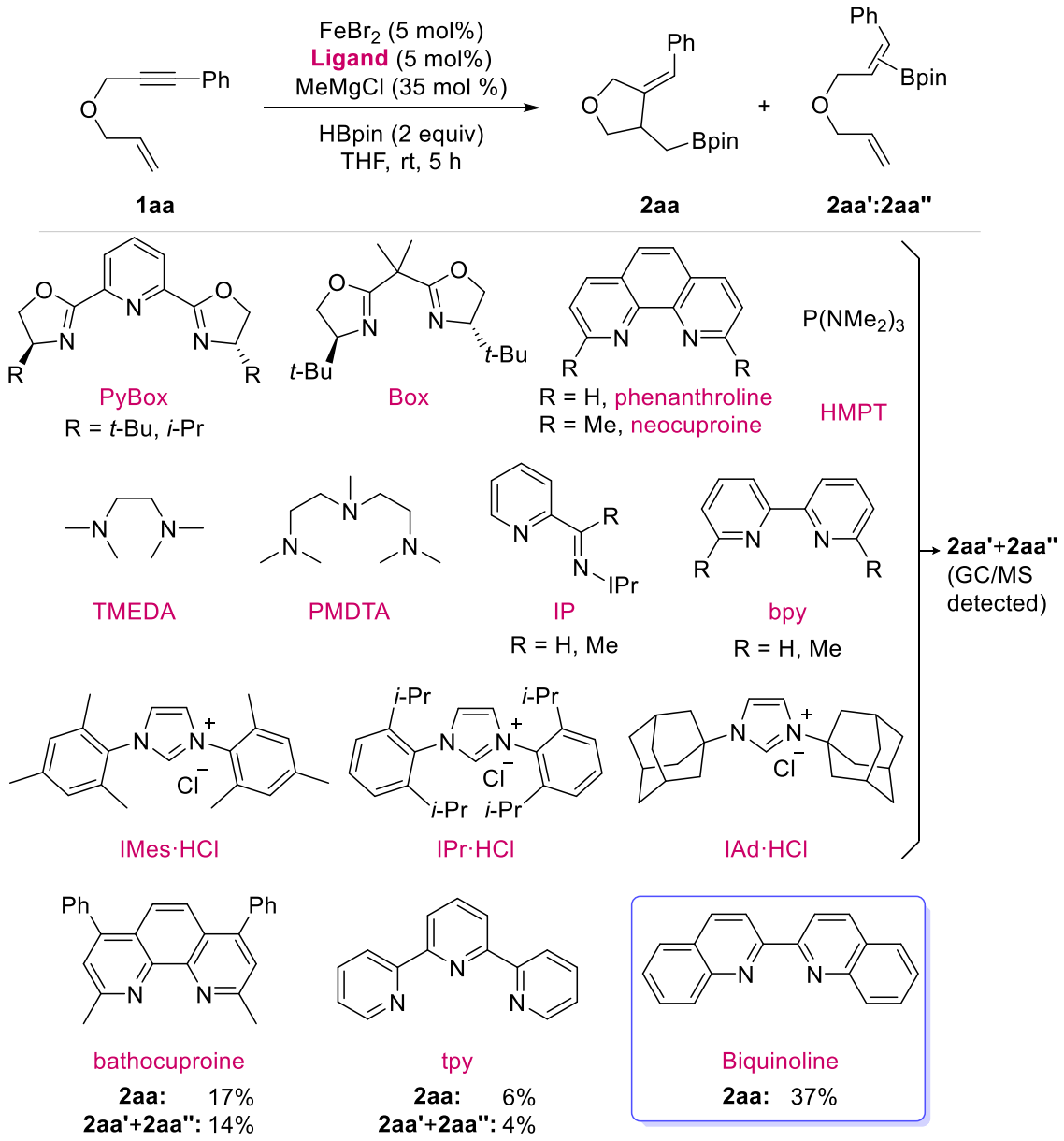

Scheme 2.23. Ligand screening.

Then, we optimized the reaction conditions by modifying different parameters, such us temperature, iron source, amounts of additional reagents and solvent (**Scheme 2.24**). Noticeably, addition of sodium borohydride only furnishes a mixture of alkyne hydroboration products in low yield. Different organomagnesium reagents can be employed as additives, such us (1,3-dioxan-2-ylethyl)magnesium bromide. Pinacolborane equivalents could be reduced to 1.5 without a significant decrease of the reaction yield. The use of MeMgCl in a lower amount was key for the reaction effectiveness, showing a dark green solution in the initial activation step. Since some boronates tend to decompose during isolation process, we established a short and fast purification by column chromatographic, which leads to an appreciable increase of the reaction yield (from 65% to 77%). In short, we found that the most convenient catalyst is generated by reaction of $FeBr_2$ (5 mol%), 2,2'-biquinoline (5 mol%) and MeMgCl (10 mol%) in dioxane at room temperature, affording **2aa** in 77% yield with complete conversion in 5 h. It is worth to mention that the higher the amount of ligand, the lower the reaction rate, and even reaction inhibition was observed when 3 equiv of biquinoline, in relation to $FeBr_2$, were used.

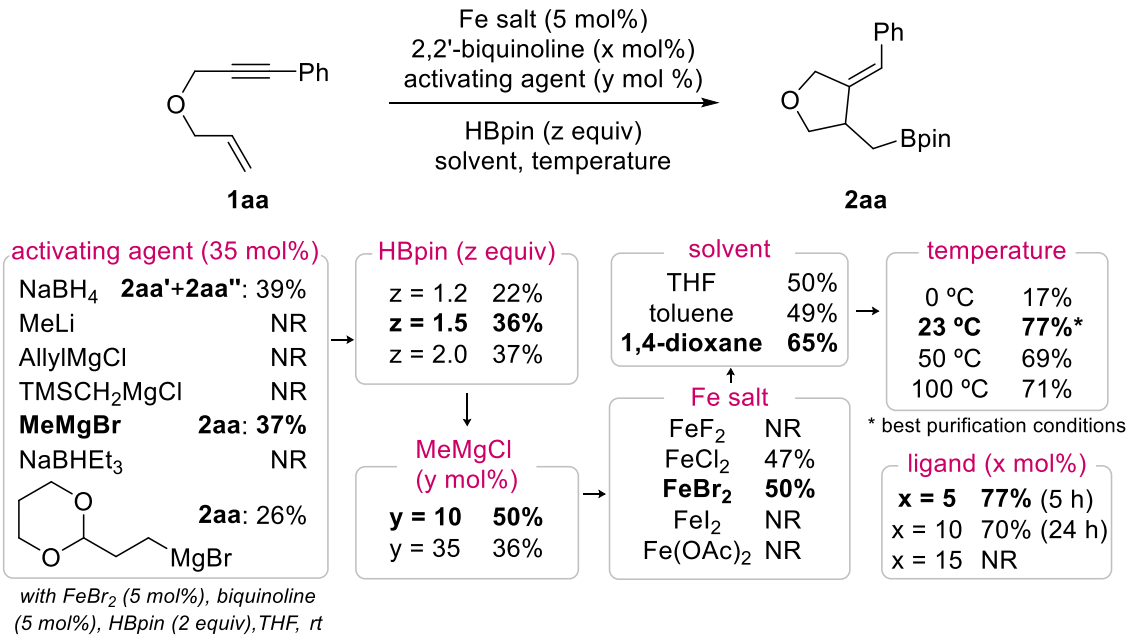

Scheme 2.24. Optimization of reaction conditions.

Under the optimized conditions, the structural scope was evaluated with a wide variety of 1,6-enynes to give borylated carbo- and heterocycles (**Scheme 2.25**). Particularly, aryl ring on the alkyne may hold a variety of substituents with very different electronic properties, ranging from MeO to CN and CF_3 (**2aa**–**af**, **2bb**–**bf**). Carbocycles are also accessible (**2da**–**db**, **2ea**–**eb**) and there is no need for the substrate to bear a quaternary center to enhance Thorpe–Ingold effect and provide good results (**2ea**). Alkynes with substituents other than aromatic rings were also suitable reaction partners (**2ap**, **2bj**, **2bn**). Moreover, additional substitution on the internal carbon of the alkene also afforded the expected boronate albeit in moderate yield (**2ao**). The reaction also tolerates substitution in the propargyl carbon, although no stereocontrol on the formation of the new stereogenic center was observed (**2ag**).

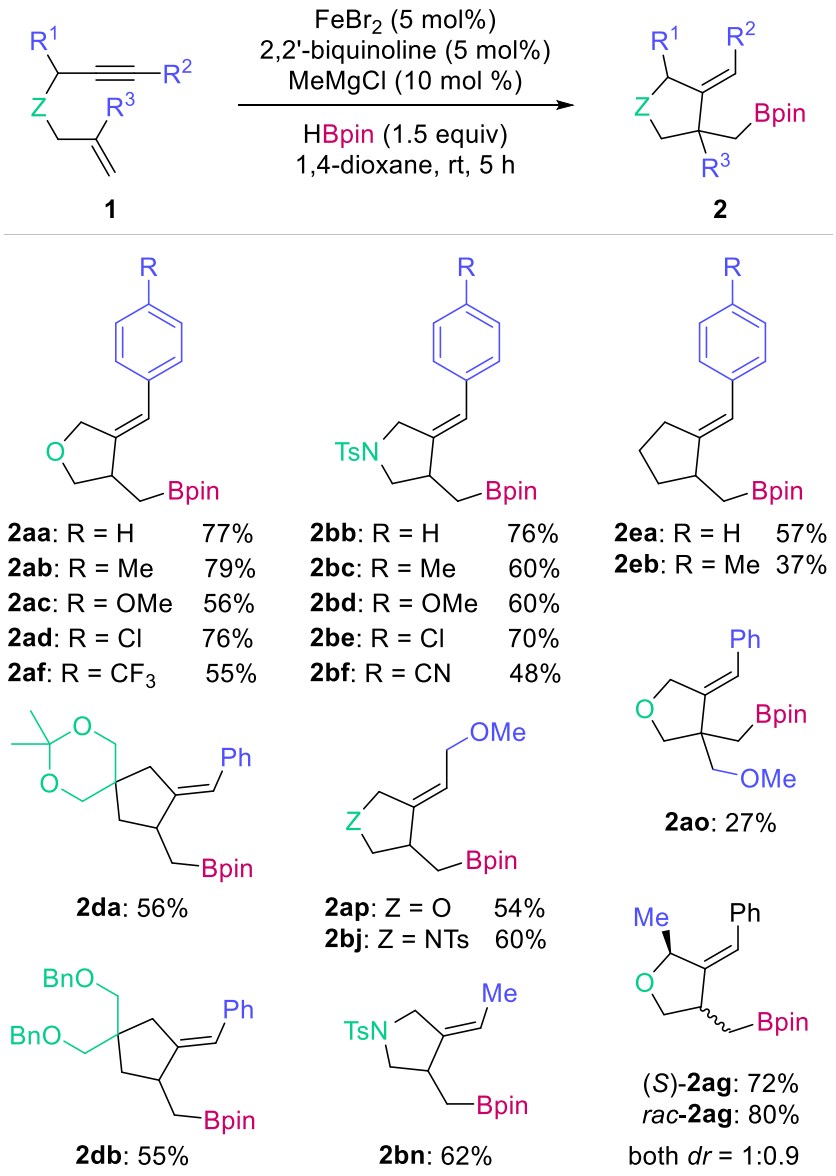

Scheme 2.25. Reaction scope.

Nevertheless, the reaction also shows some limitations regarding the enyne structure, e.g., the desired products were not observed when the distal carbon of the alkene is substituted with either Me or Ph groups for O and NTs tethered substrates (**1k-l**, **1bk**). Likewise, when a malonate derivative was used (**1cc**), a primary alcohol derived from reductive decarboxylation of the diester group was obtained in low yield (**Scheme 2.26**). Thus, ester group is not compatible with the use of Grignard reagent as an additive, as expected.

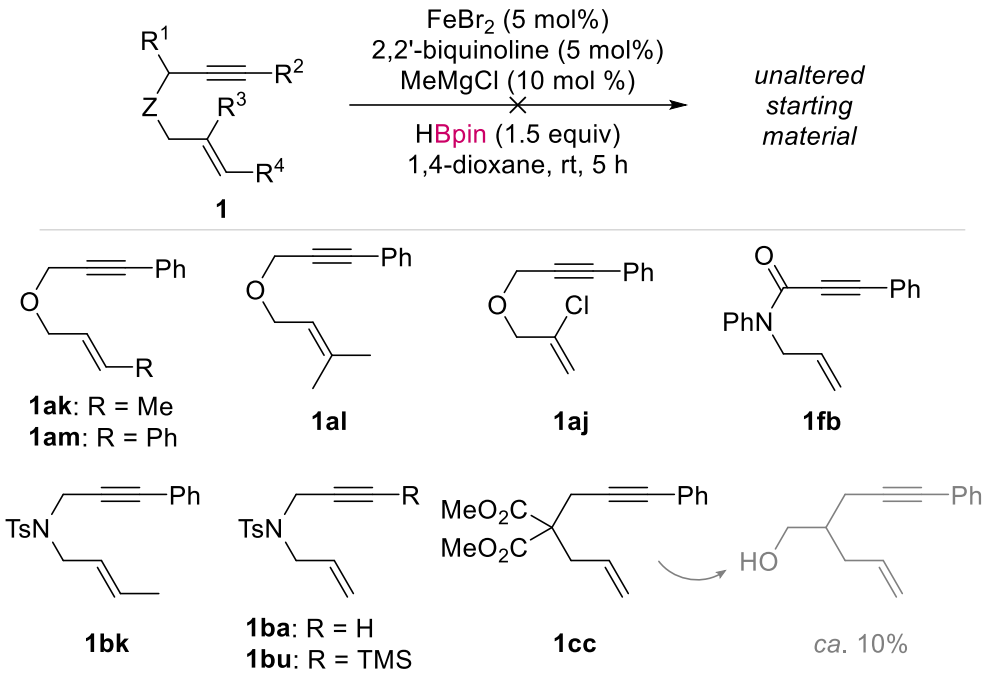

Scheme 2.26. Reaction limitations.

To illustrate the reactivity and potential applicability of the borylated products, we performed some transformations on the boronates (**Scheme 2.27**). Thus, two O and NTs heterocycles were oxidized to the corresponding alcohols in high yields (**3**) or transformed into the synthetically useful trifluoroborate salts (**4**), that are convenient nucleophiles for Suzuki cross-coupling (**5**). However, the latter reaction proceeded with low yields.

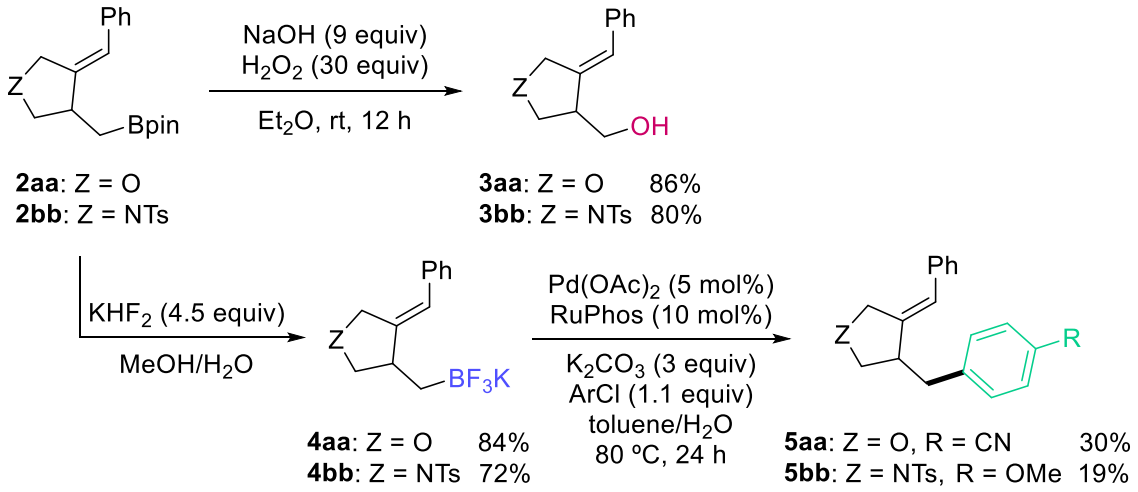

Scheme 2.27. Functionalization of alkylboronates **2**.

We were interested in getting insight into the reaction mechanism for this novel transformation, and performed some experiments with this aim. Thus, simple alkene as allylphenylether, that contains an electronically similar double bond, did not react and we recovered the unchanged starting substrate (equation 1, **Scheme 2.28**). Instead, the reaction of alkynes afforded hydroboration compounds in poor yields (equations 2 and 3, **Scheme 2.28**). Therefore, enyne activation seems to proceed through initial alkyne functionalization.

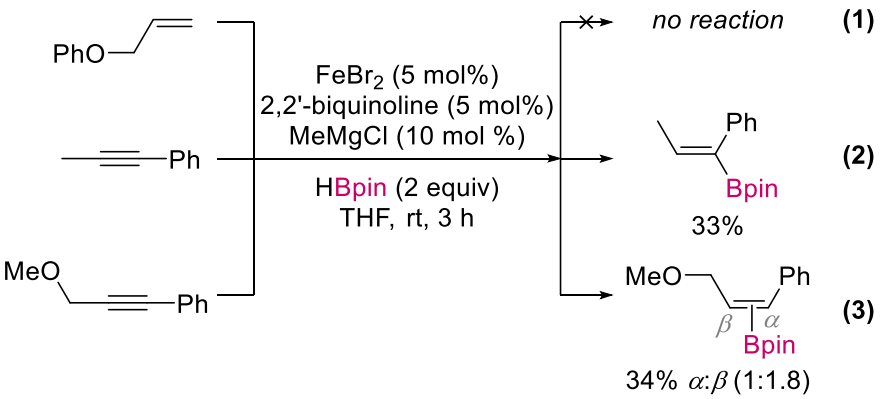

Scheme 2.28. Reaction of simple alkenes and alkynes.

Moreover, the reaction of **1aa** with 100 mol% $FeBr_2$/biquinoline and 200 mol% MeMgCl, followed by quenching with DCl in D_2O did not afford the expected dideuterated cyclic product, only the unaltered starting enyne was observed (**Scheme 2.29**). Therefore, an oxidative cyclometalation does not seem to take place as the initial step of the reaction mechanism.

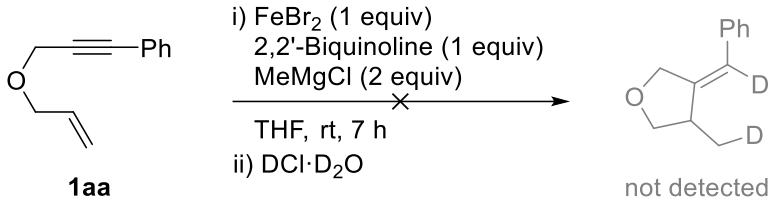

Scheme 2.29. Oxidative cyclometalation attempt.

On the other hand, we tried to determine the oxidation state of the active species. The participation of a Grignard reagent in the activation process of the Fe salt could imply reduction of the Fe(II) precatalyst by homocoupling of the nucleophile to generate Fe(0). However, reaction of an equimolar mixture of $FeBr_2$ and 2,2'-biquinoline with two different Grignard reagents afforded a low yield of homocoupling non-volatile compound (entry 1) , or even no coupling at all (entry 2), suggesting that Fe does not get reduced and that the catalytically active complex is a Fe(II) one (**Table 2.1**). Furthermore, reduction products derived from the organomagnesium reagent were detected in low amounts.

Table 2.1. Determination of the oxidation state.

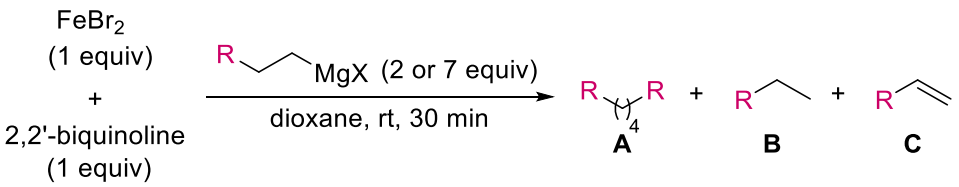

Entry	R =	X =	Yield **A**	Yield **B**	Yield **C**
1	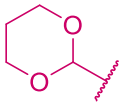	Br	9%[a]	0%	7%[b]
2	Ph	Cl	0%	6%[b]	3%[b]

[a] Isolated yield. [b] Yield determined by internal standard (TMS, 0.22 equiv).

Moreover, the use of just 1 equivalent of MeMgCl in relation to iron salt did not afford a catalytically active system, what points to a dialkyl–Fe(II) complex as a competent catalytic species in the dark green solution obtained by reaction of $FeBr_2$, 2,2'-biquinoline, and 2 equivalents of MeMgCl. This solution seems to react with HBpin to afford MeBpin, since we were able to detect it by GC-MS in low intensity due to its presumably formation in catalytic amounts (top, **Figure 2.4**). We also detected the same borylated compound when (1,3-dioxan-2-ylethyl)magnesium bromide was used (bottom).

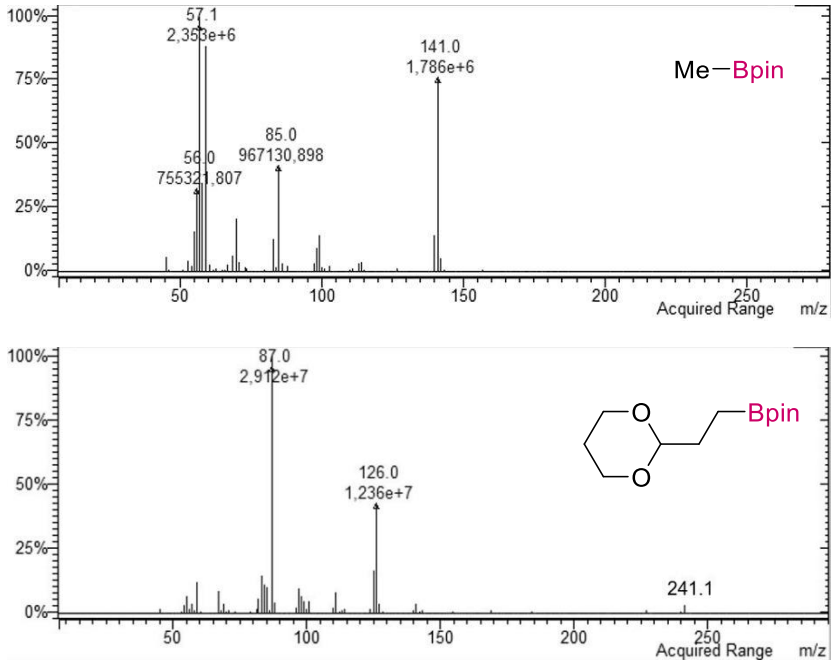

Figure 2.4. Mass spectra of RBpin.

With these results in hand, we performed DFT calculations in order to explore the reactivity of model (NN)$FeMe_2$ (**I**, (NN) = 2,2'-biquinoline) and find a feasible reaction pathway from this putative model catalyst, whose intermediacy is strongly suggested by the experimental results mentioned above. Initial calculations using different spin states pointed to singlet derivatives as the most stable ones. Enyne **1ea** was chosen as model substrate in order to simplify the calculations. Results are summarized in **Scheme 2.30**.

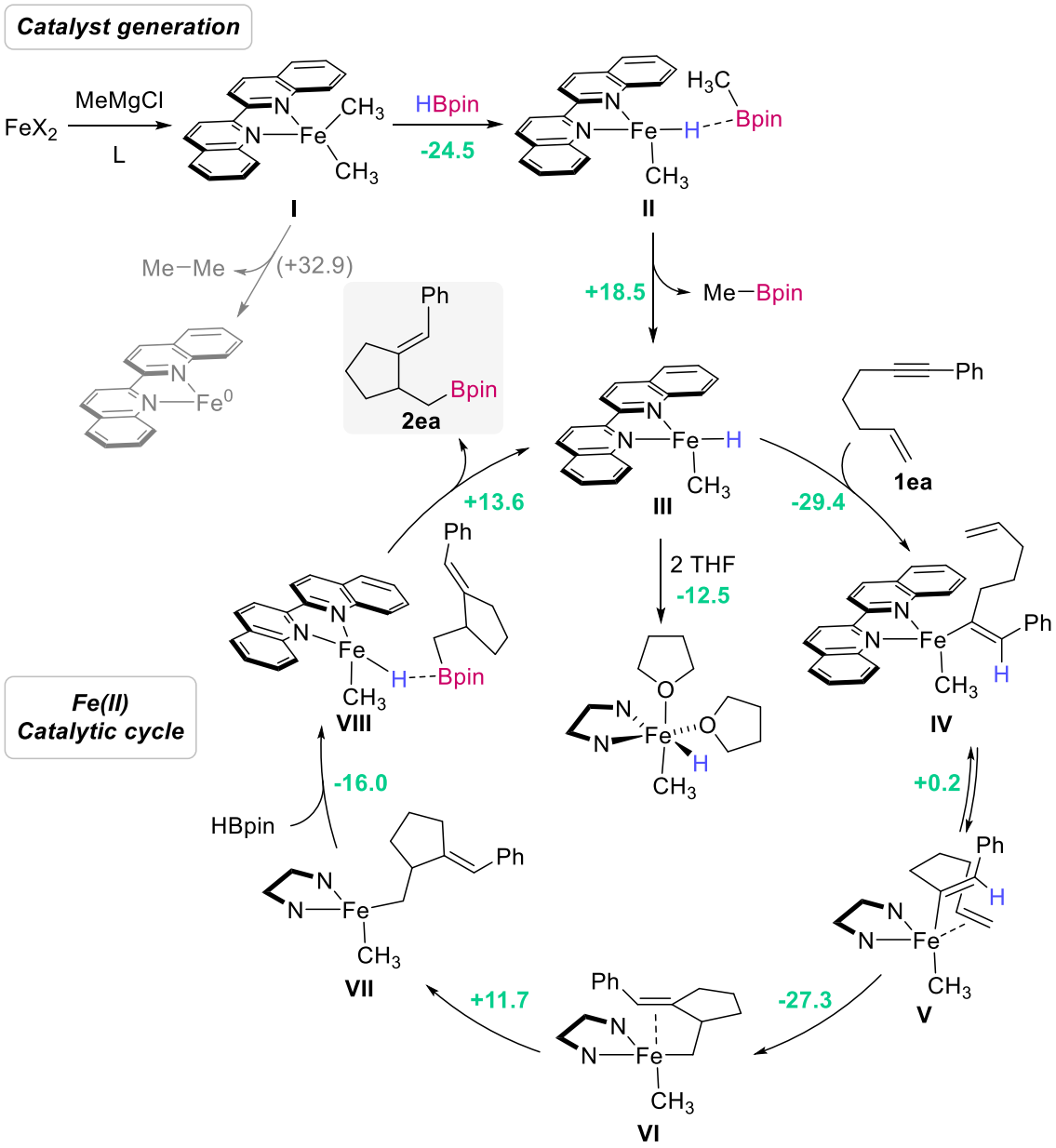

Scheme 2.30. Mechanistic proposal by DFT calculations. ΔG (kcal mol^{-1}) calculated at M06-2X/6-31G(d) (C,H,B,N,O), LANL2DZ (Fe) level in gas phase. Calculated activation energies are shown in brackets.

Interestingly, initial σ-bond metathesis reaction of **I** with HBpin proceeds downhill (ΔG = –24.5 kcal mol^{-1}) without an activation barrier (a, **Figure 2.5**). In contrast, C–C reductive elimination to Fe(0) cannot take place, since it shows a very high activation energy (32.9 kcal mol^{-1}, top in grey, **Scheme 2.30**). The corresponding MeBpin-(NN)Fe(H)Me adduct (**II**) that forms upon σ-metathesis would dissociate MeBpin (+18.5 kcal mol^{-1}) to give the active catalyst **III**.[176] It is expected that coordinatively unsaturated **III** gets stabilized by solvent. The calculated stabilization energy upon coordination of two molecules of THF is –12.5 kcal mol^{-1} (**Scheme 2.30**, center) and therefore it drives the formation of the alkyl(hydride)Fe complex to

[176] The corresponding stereoisomer complex containing H, Me groups in *trans* arrangement was computed to be 0.5 kcal mol^{-1} less stable, as expected considering the strong *trans*-influence of these ligands. *Cis* derivatives show the adequate arrangement to accommodate the entering borane.

completion. We then studied the interaction of **III** with the enyne through the alkyne group, according to the experimental results. No transition state could be located for either alkyne coordination or for the hydrometalation of the alkyne. A study of the potential energy surface for the coordination and insertion of the alkyne into the Fe–H bond confirmed the absence of activation barrier for this step (b, **Figure 2.5**). The resulting alkenylFe(II) intermediate **IV** is formed in an exoergic fashion and the resulting complex is further stabilized by coordination of the alkene (**V**), what is necessary for the next step to occur. Albeit we could not locate a transition state for the carbometalation of the alkene, calculations indicate that this step proceeds with low activation energy (*ca*. 4.7 kcal mol^{-1}, c, **Figure 2.5**) to provide alkylFe complex **VI**. Finally, dissociation of the resulting C–C double bond (**VI** to **VII**) allows gathering of a second HBpin molecule to cleave the C(sp^3)–Fe bond, furnishing the final compound by meaning an exoergic and again barrierless σ-bond metathesis reaction, regenerating the active catalyst upon dissociation of **VIII**.

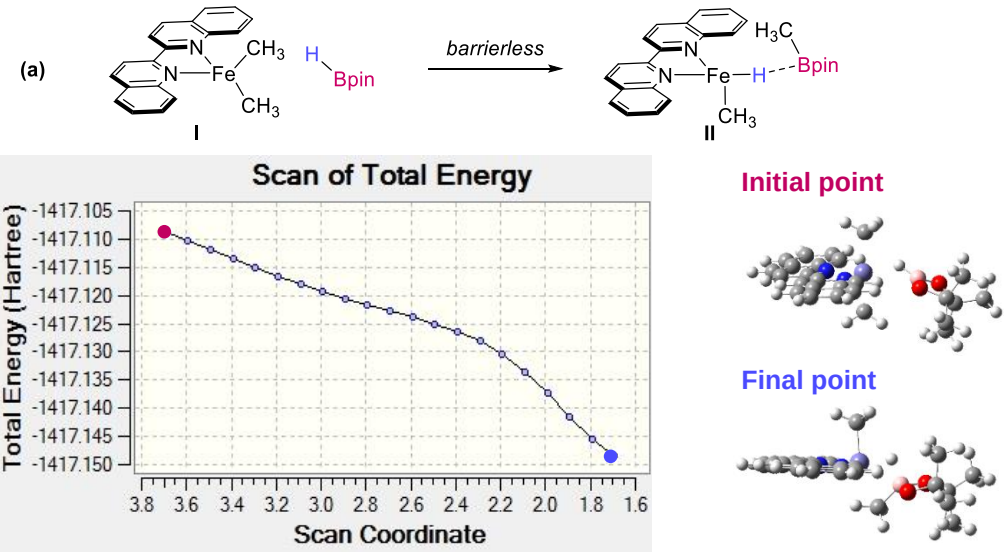

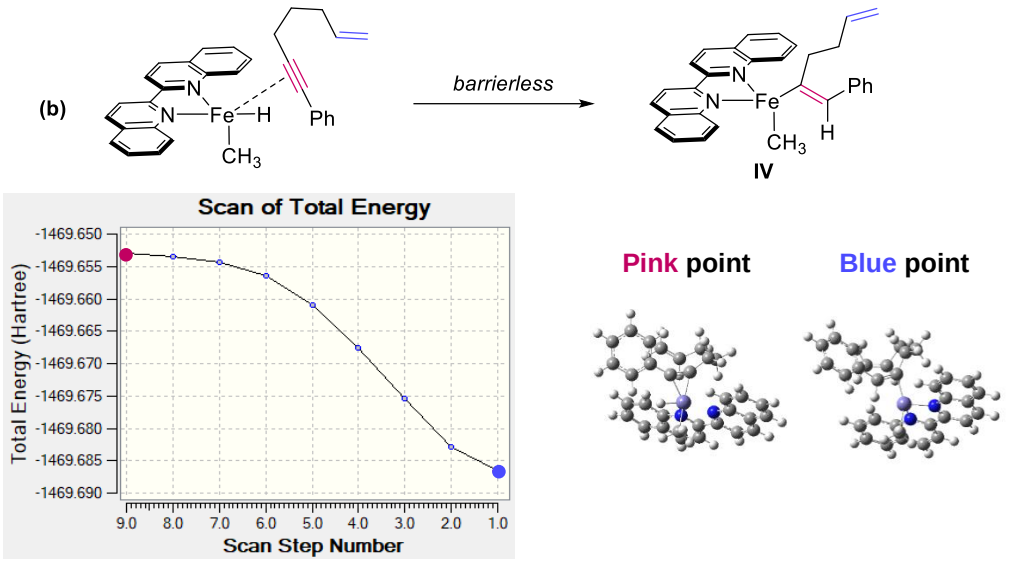

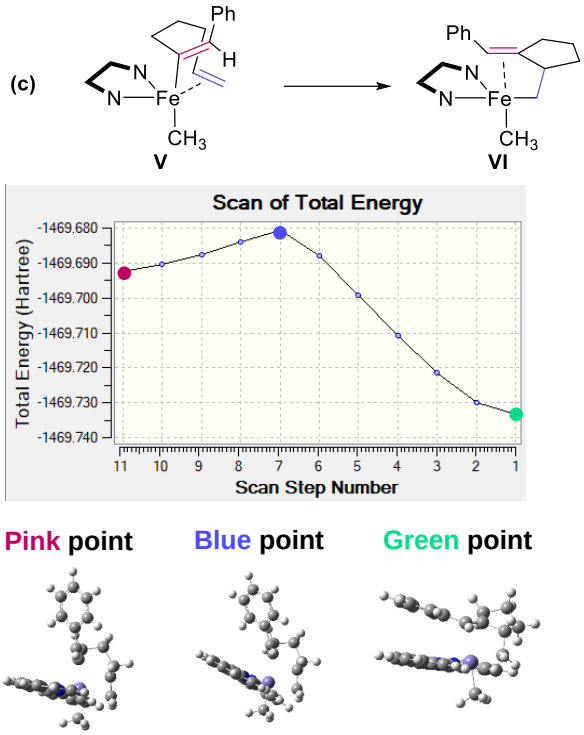

Figure 2.5. Scanning of the potential energy surface for (a) σ-metathesis through Me–B distance, (b) alkyne hydrometallation, (c) alkene carbometalation.

The proposed reaction pathway shows extremely low activation energies for all steps, what makes it feasible and highly likely (total energy balance: ΔG = –53.2 kcal mol^{-1}). Formation of dialkyl-Fe intermediate, suggested by experiments, is key to this process, since it readily reacts with HBpin to afford a hydride complex highly reactive towards the alkyne moiety. The subsequent steps are very fast and allow a facile regeneration of the active species. Intermediate diorgano-Fe complexes are stable towards reductive elimination due to the high activation energy of this process. Alkyl spectator ligands have been also found in Zn-promoted reactions,[177] and even more reactive C(sp^2)–Fe bonds have been proposed to remain intact through catalytic cycles in cross-coupling reactions.[178]

Based on the novelty of this Fe-catalyst, we thought of studying the reaction mechanism in depth in order to confirm and propose a more accurate reaction pathway. Since Neidig group has published very recently an extensive mechanistic study of the Fe-catalyzed Kumada-type alkyl–alkyl cross-coupling reaction,[179] previously developed by our research group,[180] we suggested the collaboration between both groups might be the better way to achieve our purpose. Thus, during my short stay in Rochester, we evaluated the Fe catalytically active solution for the hydroborylative cyclation reaction by different techniques: X-ray diffraction, Mössbauer spectroscopy and EPR spectroscopy.

[177] M. Kahnes, H. Görls, L. González, M. Westerhausen, *Organometallics* **2010**, *29*, 3098–3108.
[178] R. B. Bedford, P. B. Brenner, E. Carter, P. M. Cogswell, M. F. Haddow, J. N. Harvey, D. M. Murphy, J. Nunn, C. H. Woodall, *Angew. Chem. Int. Ed.* **2014**, *53*, 1804–1808.
[179] V. E. Fleischauer, S. B. Muñoz, P. G. N. Neate, W. W. Brennessel, M. L. Neidig, *Chem. Sci.* **2018**, *9*, 1878–1891.
[180] M. Guisán-Ceinos, F. Tato, E. Buñuel, P. Calle, D. J. Cárdenas, *Chem. Sci.* **2013**, *4*, 1098–1104.

First, different attempts of crystallization of the species present in the green active solution ($FeBr_2(THF)_2$, biquinoline, MeMgBr)[181] were carried out. We succeeded at isolating and identifying four different iron species as is illustrated in **Figure 2.6**. Furthermore, we also isolated the precatalyst (biquinoline)$FeBr_2$ obtained by simple stirring of $FeBr_2$ with the ligand in THF and filtration of the resultant light green solid. However, we failed to isolate the proposed iron hydride intermediate (**III** in **Scheme 2.30**), because no suitable crystals were obtained.

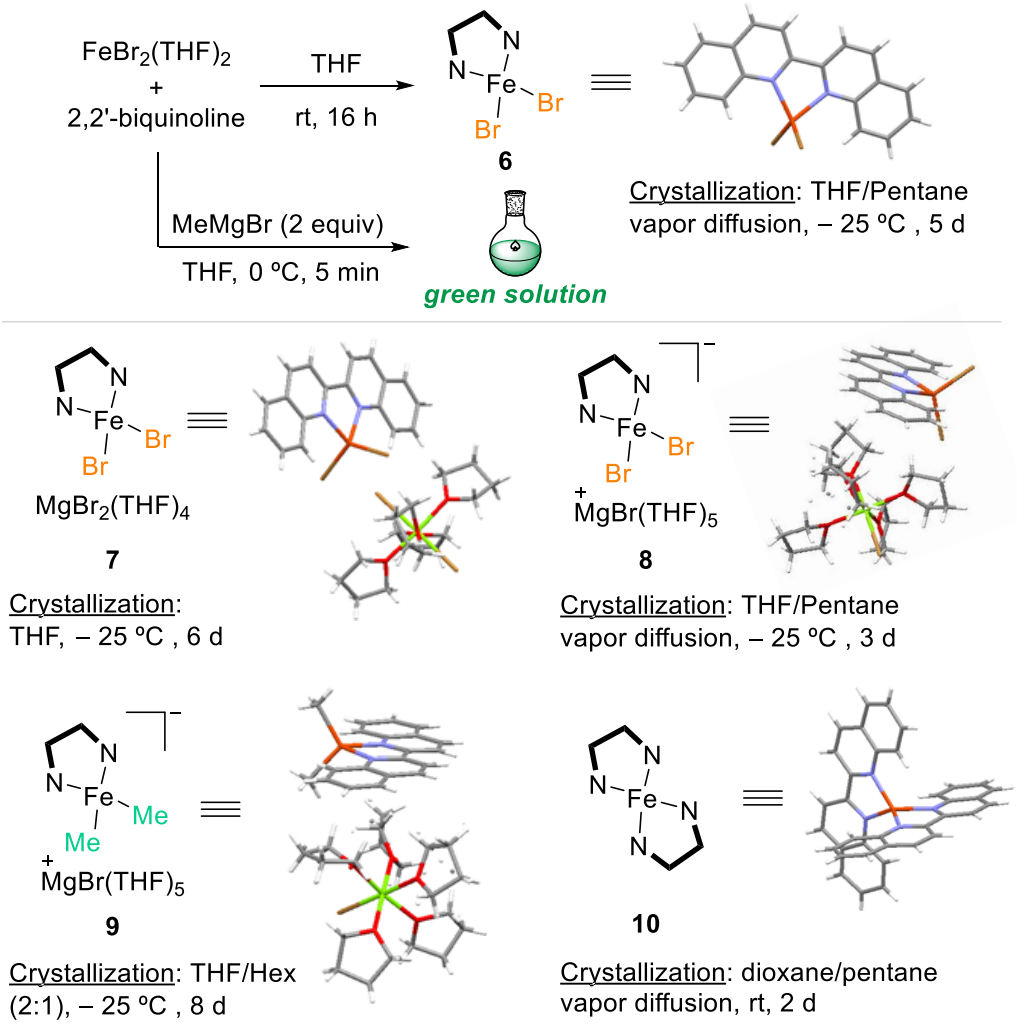

Figure 2.6. Isolated and crystallized iron structures.

The starting iron precatalyst (biquinoline)$FeBr_2$ was crystallized as simple complex in the absence of MeMgBr (**6**) and as magnesium adduct in catalytic conditions (**7**). Complex **8** shows similar connectivity to **7**, but it has anionic character corresponding to a formal Fe(I) derivative. Dimethyl-Fe complex (**9**) does not correspond to the active compound we previously proposed, since it is again a formal Fe(I) compound. Likewise, using dioxane as reaction solvent we crystallized a formal (biquinoline)$_2$Fe(0) complex (**10**). These results suggest that Grignard reagent acts as the activating agent by alkylation of the iron precatalyst and that reduction of iron may take place. However, this fact is in contrast with our previous experimental studies where the reduction of the iron species in not necessary to be proposed.

[181] $FeBr_2(THF)_2$ was used instead of commercially available $FeBr_2$ because small amounts of metallic Fe(0) are present and can interfere by broadening the spectra signals. MeMgBr was used instead of MeMgCl in order to minimize the number of different halogen-Fe species formed in solution.

It is important to note that the Fe(I) complexes that we have been able to crystallize are ionic compounds that may easily precipitate compared to the putative neutral dialkyl-Fe(II) species. Therefore, we do not think that the isolated species are catalytically competent. Nevertheless, we cannot discard these Fe(I) species as the true catalysts. They could be formed under the catalytic reaction conditions and compete with Fe(II) complexes. However, the lack of appreciable formation of organic compounds from the Grignard reagent oxidation, and the high activity of the Fe(II) catalysts suggested by the extremely low reactions barrier, makes it unnecessary to propose reduction of Fe prior to hydroborylative cyclization.

Nevertheless, the formation and isolation of the above-mentioned reduced Fe complexes deserve some discussion. The presence of bis(imino)pyridine ligands facilitate the reduction of Fe(II) species, since they act as “redox active” or “redox non-innocent” ligands. This is due to the ability of these structures to act as π acceptors from the metal center.[182] In many cases, the term “non-innocent” has become synonymous with situations where the formal oxidation state differs from the experimentally determined oxidation state.[183] The electron-reservoir function of the ligand tolerates the metal to maintain its most common or most stable oxidation state by delivering or accepting the electron density associated with the multielectron transformation. As an example, Chirik studied the catalysis of [2+2] cycloaddition of dienes with a (BIP)Fe complex (**Figure 2.7**).[184] Although the overall reaction is a formal reduction (the C=C double bonds are converted to single bonds), no oxidation state changes occur at the metal. The required electrons to form the C–C single bonds are supplied by the ligand. Similarly, the reductive elimination of the product does not form Fe(0) but reduces the ligand again. Therefore, the iron complex is viewed as a hybrid between low-spin Fe(0) and Fe(II) oxidation states.

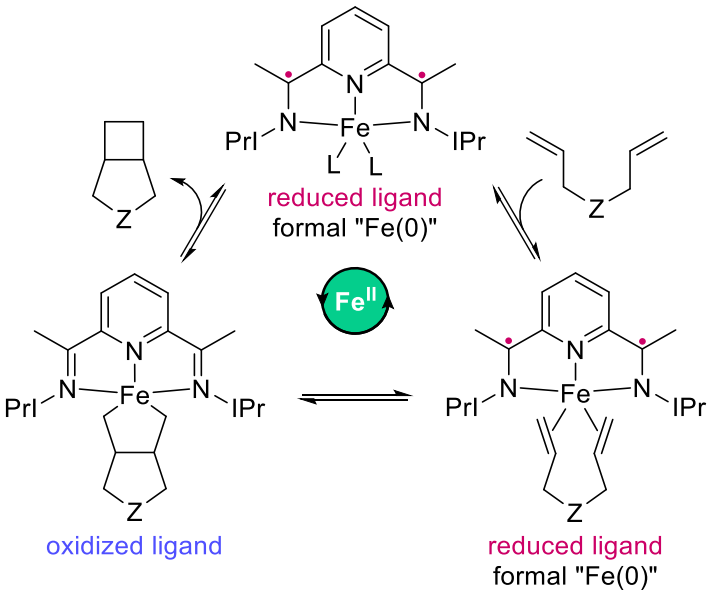

Figure 2.7. Redox non-innocent ligands in Fe catalysis.

[182] (a) S. C. Bart, K. Chłopek, E. Bill, M. W. Bouwkamp, E. Lobkovsky, F. Neese, K. Wieghardt, P. J. Chirik, *J. Am. Chem. Soc.* **2006**, *128*, 13901–13912. (b) D. Zhu, I. Thapa, I. Korobkov, S. Gambarotta, P. H. M. Budzelaar, *Inorg. Chem.* **2011**, *50*, 9879–9887. (c) S. C. E. Stieber, C. Milsmann, J. M. Hoyt, Z. R. Turner, K. D. Finkelstein, K. Wieghardt, S. DeBeer, P. J. Chirik, *Inorg. Chem.* **2012**, *51*, 3770−3785. (d) V. Lyaskovskyy, B. de Bruin, *ACS Catal.* **2012**, *2*, 270−279. (e) J. M. Darmon, R. P. Yu, S. P. Semproni, Z. R. Turner, S. C. E. Stieber, S. DeBeer, P. J. Chirik, *Organometallics* **2014**, *33*, 5423−5433.

[183] P. J. Chirik, *Inorg. Chem.* **2011**, *50*, 9737–9740.

[184] (a) M. W. Bouwkamp, A. C. Bowman, E. Lobkovsky, P. J. Chirik, *J. Am. Chem. Soc.* **2006**, *128*, 13340−13341. (b) P. J. Chirik, K. Wieghardt, *Science* **2010**, *327*, 794−795.

Considering the bidentate nitrogen ligand we used, we may better described the formally Fe(I) anionic complexes as Fe(II) species where the electron is delocalized in the ligand (**Figure 2.8**).

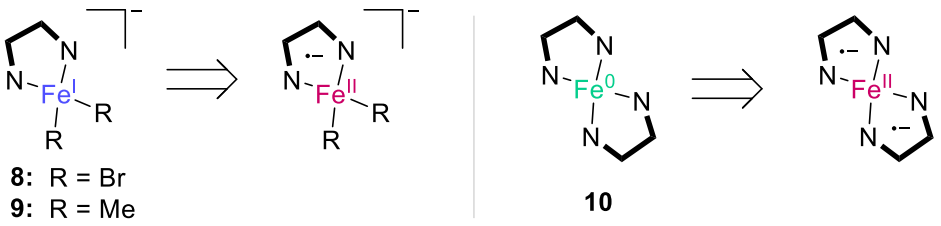

Figure 2.8. Fe(II) anionic complexes based on redox non-innocent ligand.

Moreover, we analyzed the green active solution by quantitative EPR spectroscopy (**Figure 2.9**). Although an active signal is obtained corresponding to a S = ½ species, which could mean the presence of Fe(I) complexes, it represents less than 10% of the total sample.[185]

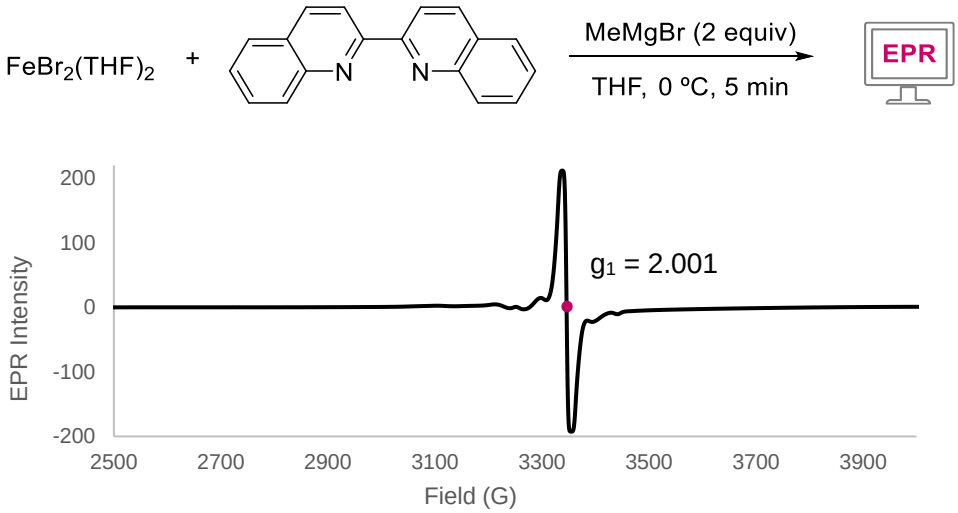

Figure 2.9. EPR spectra of catalytically active solution.

In the same manner, we performed cyclic voltammetry on a solution of precatalyst **6** [(biquinoline)$FeBr_2$] to measure its reduction potential with the aim of using a suitable reductant and evaluate the hydroborylative cyclization reaction under those conditions. Thus, the experiment was carried out in THF, with N(*n*-Bu)$_4PF_6$ for the blank solution and ferrocene for the potential correction, obtaining the value of $E_{red}(Ag/AgNO_3)$ = –1.355 V (top, **Figure 2.10**). Taking into account the described standard reduction potential values,[186] we chose Mg(s) as putative reductant ($E_{red}(Mg^{2+}\rightarrow Mg)$ = –2.37 V) to evaluate our reaction, but no alkylboronate **2aa** was detected (bottom, **Figure 2.10**), in accord with the intermediacy of Fe(II) catalytic species.

[185] A 5 mM MeOH/EtOH (9:1) solution of $CuSO_4 \cdot 5H_2O$ was used as internal standard for the quantitative EPR.
[186] P. Vanýsek, *Handbook of Chemistry and Physics* 91st Edition, (Ed. W. M. Haynes), CRC, **2010**.

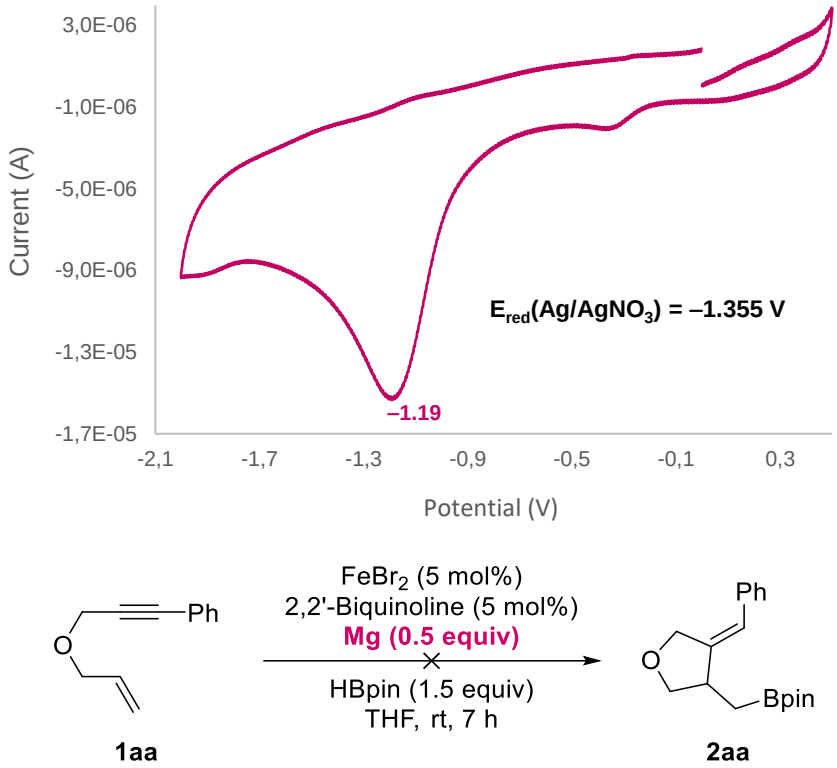

Figure 2.10. Cyclic voltammetry of precatalyst **6** (top). Hydroborylative cyclization reaction with Mg as reductant (bottom).

Then, we turned into Mössbauer spectroscopy. Mössbauer spectroscopy involves the recoil-free absorption of γ-rays for transitions between nuclear ground and excited states in a Mössbauer active nucleus. While numerous nuclei are amenable to Mössbauer spectroscopy (e.g. ^{119}Sn, ^{197}Au), ^{57}Fe Mössbauer spectroscopy is by far the most widely utilized due to factors including the natural abundance and stability of ^{57}Fe, the use of a source material with a reasonable half-life (^{57}Co, half-life ~270 days) and the excited state lifetime properties of the ^{57}Fe excited state enabling well-resolved absorption features. Due to recoil effects from the absorption (or emission) of γ radiation in a free atom or molecule, a non-zero recoil-free fraction is required restricting Mössbauer measurements to solid or frozen solution samples. Due to the narrow linewidths for ^{57}Fe Mössbauer transitions observed, small changes in the Mössbauer transitions due to interactions between the nucleus and its surrounding environment can be observed, manifested as hyperfine interactions. Three hyperfine interactions contribute to Mössbauer spectra: (i) monopole interaction (leading to the isomer shift), (ii) magnetic dipole interaction (leading to the magnetic splitting), and (iii) electric quadrupole interaction (leading to the quadrupole splitting). The isomer shift (δ) arises from Coulombic interaction between the nucleus and surrounding electrons, where the *s*-electrons can penetrate the nucleus (left, **Figure 2.11**). The shift provides information regarding changes in the electron density of the Mössbauer active nucleus. Information from the isomer shift can provide insight into the oxidation state and spin state of a given compound. Quadrupole splitting (ΔE_Q) occurs when a Mössbauer nucleus has a measurable electric quadrupole moment due to a nonspherical nuclear charge distribution, as is the case for ^{57}Fe, which interacts with the local electric field gradient around the nucleus to remove the degeneracy of the M_I levels of the excited state (left, **Figure 2.11**). Quadrupole splitting is observed as a doublet in the absence of a magnetic interaction and provides additional insight into symmetry, oxidation state, and spin state of a compound (right, **Figure 2.11**). The

magnetic hyperfine interaction (ΔE_M) occurs when a nucleus has a magnetic dipole moment that interacts with a magnetic field (internal or applied). However, magnetic hyperfine splitting is not observed in most iron catalyzed cross-coupling Mössbauer studies, which are performed in the absence of an applied external magnetic field.[187]

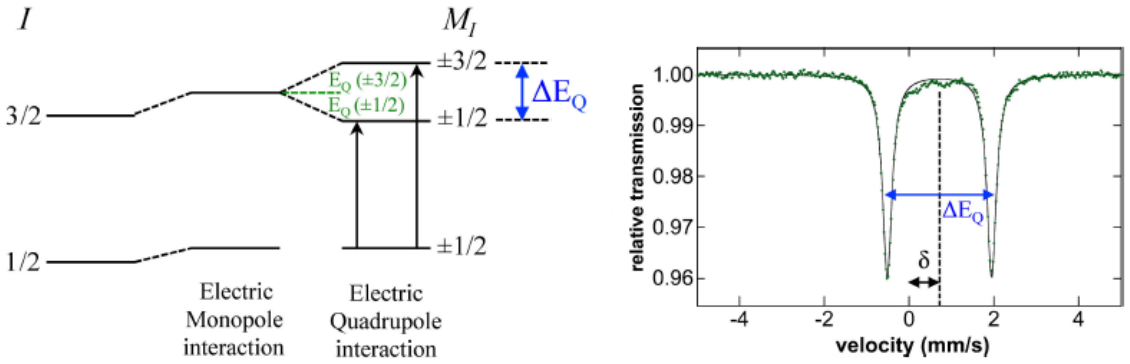

Figure 2.11. Fundamental of Mössbauer spectroscopy.

Mössbauer spectroscopy is a powerful tool for studying iron catalyzed cross-coupling systems, as all iron species are observable regardless of spin or oxidation state. Thus, this method enables the identification and quantification of all the iron species formed *in situ* in frozen solution measurements. However, the low natural abundance of ^{57}Fe (2.1%) requires enrichment of iron salts or precatalyst samples with ^{57}Fe for studies of iron speciation at catalytically relevant concentrations. Importantly, the two parameters obtained from a zerofield Mössbauer experiment (isomer shift and quadrupole splitting) are unique for each iron compound in a mixture. Lastly, the use of freeze-quenched, time-resolved Mössbauer studies of reactions enables the study of the evolution of iron speciation as a function of time and reaction temperature, as well as detailed studies correlating iron speciation changes to product and side product formation in reaction studies with electrophile, even at very short reaction times.

With the aim of identifying all the iron species that formed the catalytically active dark green solution, first it is necessary to isolate each of them and record its spectra. Despite we crystallized several species, we were not able to reproduce their crystallization in enough amount to perform the solid Mössbauer spectroscopy,[188] except for complex **6** (top, **Figure 2.12**). Besides, we carried out the spectra of the *in situ* formation of the precatalyst **6** in THF with ^{57}Fe-enriched sample (bottom, **Figure 2.12**), showing similar isomer shift and quadrupole splitting.

[187] S. H. Carpenter, M. L. Neidig, *Isr. J. Chem.* **2017**, *57*, 1106–1116.
[188] When the established conditions were used for crystallization of complexes **8** and **9**, suitable isolated samples were not obtained for Mössbauer spectroscopy, instead mixture-crystallization of both complexes or a LFe(Me)Br intermediate was observed.

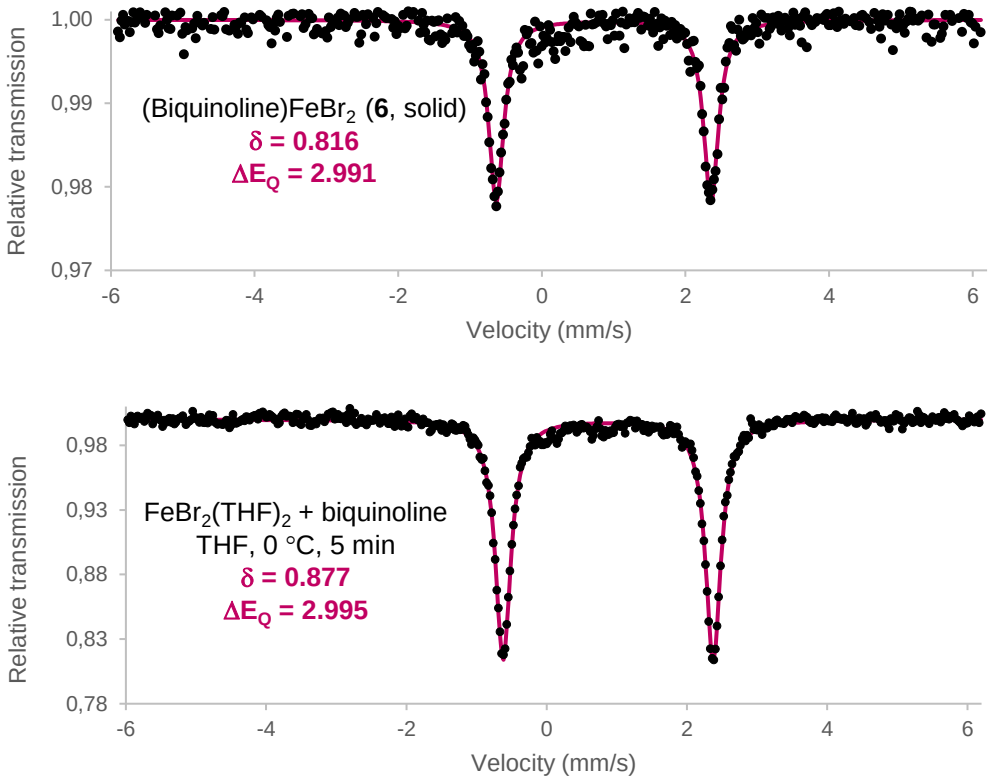

Figure 2.12. Mössbauer spectra of complex **6** in solid-state (top) and in solution (bottom).

Furthermore, using $^{57}FeBr_2$ we were able to obtain single enriched crystals of complex **10** to perform the Mössbauer spectroscopy by dissolving them in anhydrous THF (**Figure 2.13**).

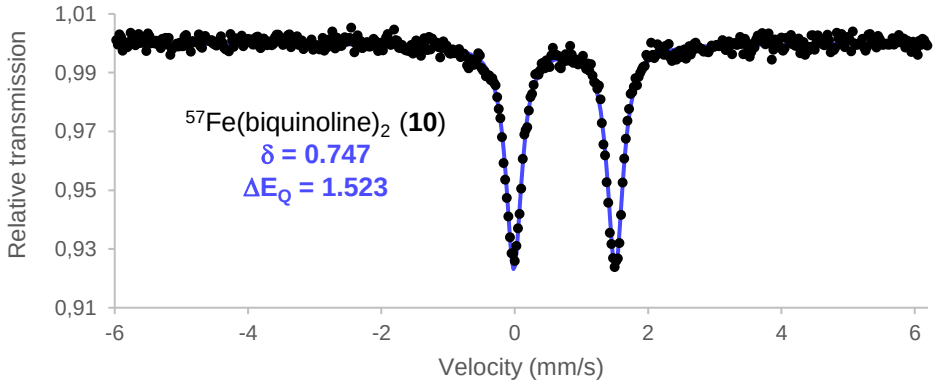

Figure 2.13. Mössbauer spectra of complex **10**.

Later, we evaluated the active solution with this technique, requiring the use of small amount of enriched $^{57}FeBr_2$ along with $FeBr_2(THF)_2$ as aforementioned. When equimolar mixture of Fe/ligand/MeMgBr is used, an incomplete conversion of the precatalyst **6** is observed after few minutes, but new species appears (yellow, **Figure 2.14**). This result supports that the reaction requires at least 2 equiv of MeMgBr to take place, and the new species could be the monoalkylated (biquinoline)Fe(Me)Br.

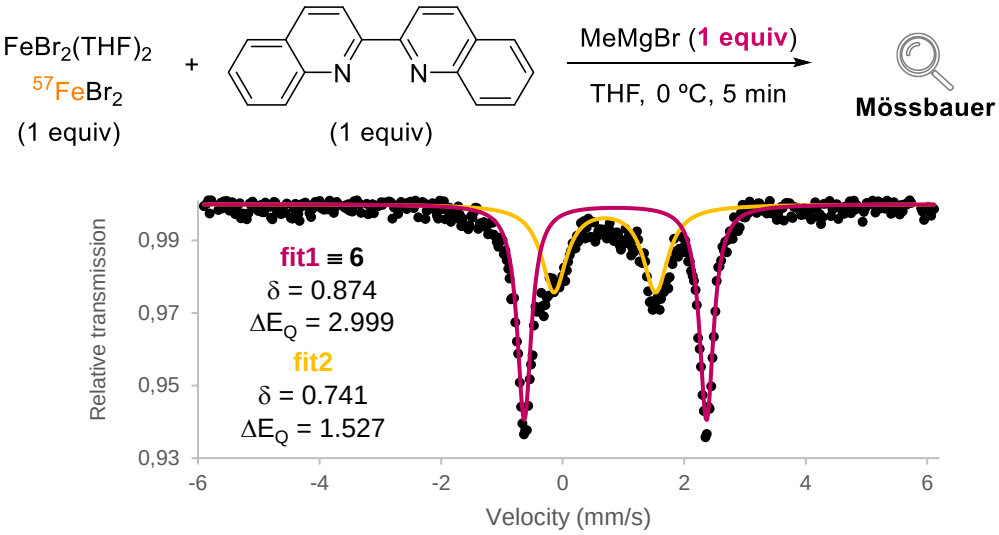

Figure 2.14. Mössbauer spectra with 1 equiv of MeMgBr.

On the other hand, when 2 equiv of MeMgBr were used, we observed complete consumption of precatalyst **6** and formation of mainly two different species in Mössbauer spectra (**Figure 2.15**). The **green** one represents about 80% of existing Fe species, which presumably is the dimethylFe complex, but it has not been identified yet. Similar spectra were recorded when reaction temperature was lowered to – 25 ºC.

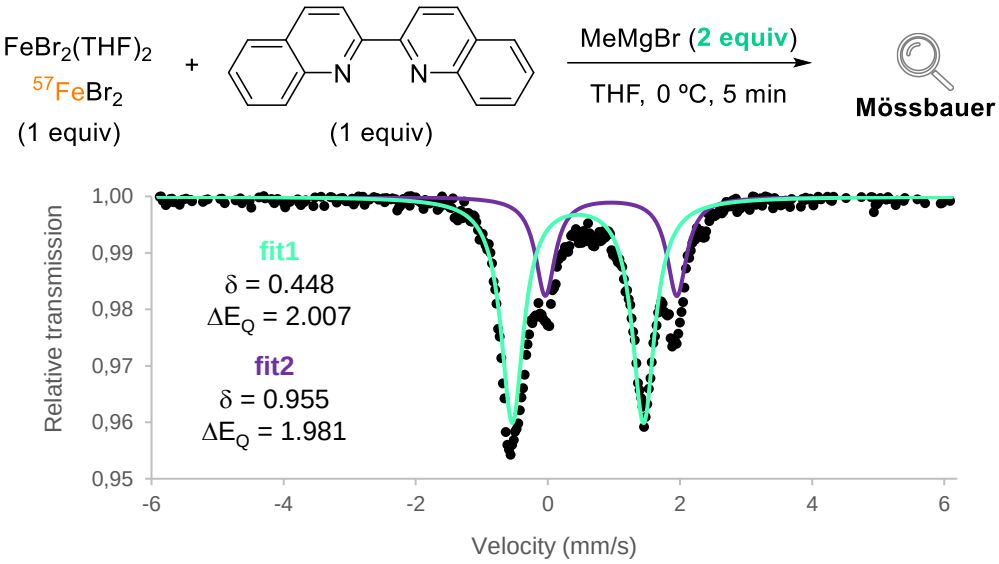

Figure 2.15. Mössbauer spectra with 2 equiv of MeMgBr.

Although there is a major iron species in Mössbauer spectra of catalytic conditions, the catalytically active solution involves formation of more than one Fe complex. Further experiments are necessary for comprehension of the reaction mechanism, such us solid-Mössbauer spectroscopy of isolated Fe complexes in order to unequivocally identify every signal, and Mössbauer spectroscopy in catalytic conditions in the presence of HBpin and/or enyne. In addition, we cannot ensure that we have isolated and identified all the existing Fe species, more crystallization attempts might be carry out. Nevertheless, these preliminary results are compatible with our proposal of a dialkyl-Fe complex as the key precatalyst formed by reaction of the Fe salt with the alkylmagnesium reagent.

3.2.4. Experimental section

3.2.4.1. Materials and methods

General considerations have been described in *Experimental section* of *Chapter 1*. Additionally, pinacolborane (HBpin) and methylmagnesium chloride (3.0 M solution in THF) were purchased from Sigma-Aldrich Co. 2,2-Biquinoline was purchased from Fluorochem Co. The other commercially available chemicals were purchased and used as received without further purifications. The hydroborylative cyclization reactions were carried out under argon atmosphere in anhydrous 1,4-dioxane stored over activated molecular sieves 4 Å (VWR) and Ar-degassed. The molarities of the Grignard reagents were checked immediately before use.[189] In some ^{13}C NMR spectra, the carbon atoms bonded to the boron atoms were not observed due to line broadening.[190]

Solid samples for ^{57}Fe Mössbauer spectroscopy were performed on isolated complexes based on natural abundance of ^{57}Fe or from ^{57}Fe-enriched samples of isolated complexes. Frozen solution samples for ^{57}Fe Mössbauer spectroscopy were prepared from $^{57}FeBr_2$ and $FeBr_2(THF)_2$. $FeBr_2(THF)_2$ was used instead of commercially available $FeBr_2$ to avoid the presence of metallic iron traces. All samples were prepared in an inert atmosphere glovebox with a liquid nitrogen fill port to freeze each sample at 77 K within the glovebox. Each sample was loaded into a Delrin Mössbauer sample cup for measurements and loaded under liquid nitrogen. Low temperature ^{57}Fe Mössbauer measurements were performed using a See Co. MS4 Mössbauer spectrometer integrated with a Janis SVT-400T He/N_2 cryostat for measurements at 80 K or 5 K. All Mössbauer spectra were fit using the program WMoss (See Co).

3.2.4.2. Ligand synthesis

3.2.4.2.1. PyBox ligands

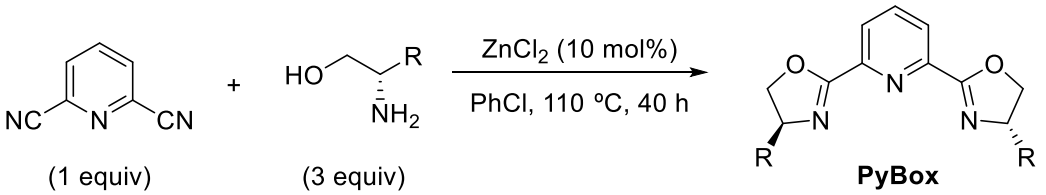

Pyridine-2,6-dinitrile (1 equiv, 5.7 mmol), (2*S*,3*S*)-isoleucinol or (*S*)-*tert*-leucinol (3 equiv, 17 mmol) and anhydrous $ZnCl_2$ (0.1 equiv, 0.57 mmol) were added to a sealed tube. Then, chlorobenzene (0.9 M, 20 mL) was added and the reaction mixture was stirred at 110 ºC for 40 h. Then, the solution was passed through a short pad of silica gel (CH_2Cl_2 and EtOAc) and the filtrate was concentrated under vacuum. The residue was purified by column chromatography in silica gel using CH_2Cl_2/EtOAc (4:1) as an eluent. The product was crystallized from hot hexane/EtOAc (20:1).[191]

[189] A. Krasovskiy, P. Knochel, *Synthesis* **2006**, *5*, 890–891.
[190] A. Datta, A. Köllhofer, H. Plenio, *Chem. Commun.* **2004**, 1508–1509.
[191] J. Zhou, G. C. Fu, *J. Am. Chem. Soc.* **2003**, *125*, 14726–14727.

2,6-Bis((*S*)-4-(*sec*-butyl)-4,5-dihydrooxazol-2-yl)pyridine (*s*-BuPyBox):[189] The ligand was obtained as a white solid in 45% yield (846 mg). ^{1}H NMR (300 MHz, $CDCl_3$) δ 8.22 (d, J = 7.8 Hz, 2H), 7.85 (t, J = 7.8 Hz, 1H), 4.58 – 4.39 (m, 2H), 4.33 – 4.18 (m, 4H), 1.80 – 1.57 (m, 4H), 1.25 (dt, J = 14.9, 7.4 Hz, 2H), 0.96 (t, J = 7.3 Hz, 6H), 0.88 (d, J = 6.7 Hz, 6H).

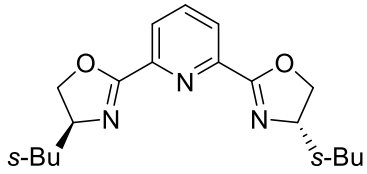

2,6-Bis((*S*)-4-(*tert*-butyl)-4,5-dihydrooxazol-2-yl)pyridine (*t*-BuPyBox):[192] The ligand was obtained as a white solid in 50% yield (465 mg). ^{1}H NMR (300 MHz, $CDCl_3$) δ 8.26 (d, J = 7.8 Hz, 2H), 7.85 (t, J = 7.8 Hz, 1H), 4.48 (dd, J = 10.3, 8.9 Hz, 2H), 4.32 (t, J = 8.6 Hz, 2H), 4.11 (dd, J = 10.3, 8.6 Hz, 2H), 0.96 (s, 19H).

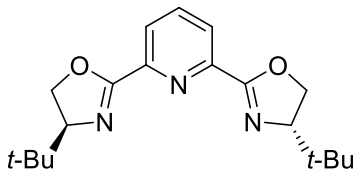

3.2.4.2.2. Iminopyridine ligands (IP)

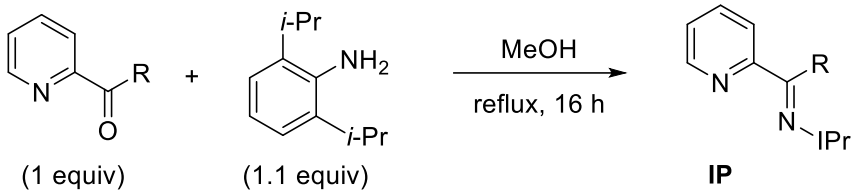

Pyridine derivative (1 equiv, 4.7 mmol) and MeOH (5 mL) were added to a round bottom flask equipped with stir bar. Then, 2,6-diisopropylaniline (1.1 equiv, 5.1 mmol) was added and the mixture was stirred at reflux overnight. Then, the solvent was removed under vacuum and the residue was purified by column chromatography in silica gel using CyHex/EtOAc (95:5) as an eluent. The product was crystallized from Et_2O.[193]

(*E*)-*N*-(2,6-Diisopropylphenyl)-1-(pyridin-2-yl)methanimine:[193] The ligand was obtained as a light yellow solid in 29% yield (363 mg). ^{1}H NMR (300 MHz, $CDCl_3$) δ 8.74 (d, J = 4.2 Hz, 1H), 8.31 (s, 1H), 8.27 (d, J = 7.9 Hz, 1H), 7.86 (t, J = 7.7 Hz, 1H), 7.42 (dd, J = 7.0, 5.5 Hz, 1H), 7.21 – 7.07 (m, 3H), 2.97 (dt, J = 13.7, 6.9 Hz, 2H), 1.18 (d, J = 6.9 Hz, 12H).

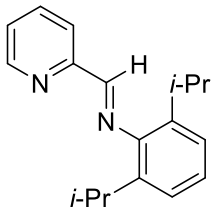

(*E*)-*N*-(2,6-Diisopropylphenyl)-1-(pyridin-2-yl)ethan-1-imine:[193] The ligand was obtained as a yellow solid in 58% yield (622 mg). ^{1}H NMR (300 MHz, $CDCl_3$) δ 8.68 (d, J = 4.3 Hz, 1H), 8.36 (d, J = 8.0 Hz, 1H), 7.82 (td, J = 7.7, 1.8 Hz, 1H), 7.39 (dd, J = 6.9, 5.4 Hz, 1H), 7.19 – 7.02 (m, 3H), 2.75 (hept, J = 6.9 Hz, 2H), 2.21 (s, 3H), 1.15 (d, J = 6.9 Hz, 12H).

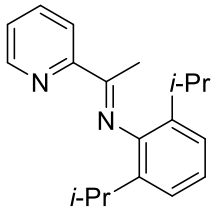

[192] S. E. Schaus, E. N. Jacobsen, *Org. Lett.* **2000**, *2*, 1001–1004.
[193] C. Bianchini, H. M. Lee, G. Mantovani, A. Meli, W. Oberhauser, *New J. Chem.* **2002**, *26*, 387–397.

3.2.4.3. General procedure for Fe-catalyzed hydroborylative cyclization of enynes

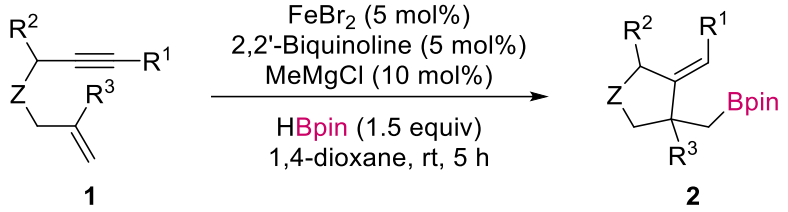

1 **2**

A vial was charged with $FeBr_2$ (4.3 mg, 0.02 mmol), 2,2'-biquinoline (5.1 mg, 0.02 mmol), and a stir bar in air. The vial was sealed by a septum and backfilled with Ar. Then, anhydrous and Ar-degassed 1,4-dioxane (2 mL) was added. The resulting mixture was stirred at 23 °C for 5 minutes and then cooled in an ice bath. Afterwards, 0.04 mmol of methylmagnesium chloride solution in THF (molarity was previously checked following the procedure reported) was added dropwise at 0 °C until the solution turns green. Then, the corresponding enyne **1** (0.4 mmol) and HBpin (87 µl, 0.6 mmol) were added at 0 °C and the reaction mixture was stirred for 5 h at room temperature. When complete consumption of the enyne was verified by TLC, the solvent was evaporated under vacuum and the product was purified by column chromatography in silica gel.

(*Z*)-2-((4-Benzylidenetetrahydrofuran-3-yl)methyl)-4,4,5,5-tetramethyl-1,3,2-dioxaborolane (2aa): The compound was purified by column chromatography (cyclohexane/EtOAc, 95:5) and was obtained as a yellow oil in 77% yield (93 mg). ^{1}H NMR (300 MHz, $CDCl_3$) δ 7.33 (t, J = 7.3 Hz, 2H), 7.20 (t, J = 7.3 Hz, 1H), 7.12 (d, J = 7.3 Hz, 2H), 6.33 (d, J = 2.3 Hz, 1H), 4.63 (dd, J = 14.1, 1.8 Hz, 1H), 4.55 (dt, J = 14.1, 1.8 Hz, 1H), 4.11 (t, J = 7.8 Hz, 1H), 3.44 (t, J = 7.8 Hz, 1H), 3.10 – 2.94 (m, 1H), 1.25 (d, J = 2.6 Hz, 12H), 1.19 (d, J = 5.9 Hz, 1H), 1.00 (dd, J = 15.9, 8.4 Hz, 1H). ^{13}C NMR (75 MHz, $CDCl_3$) δ 147.1 (C), 137.6 (C), 128.5 (2 × CH), 127.9 (2 × CH), 126.4 (CH), 119.9 (CH), 83.3 (2 × C), 74.2 (CH_2), 70.2 (CH_2), 41.2 (CH), 25.0 (2 × CH_3), 24.8 (2 × CH_3), 14.2 (br m, CH_2-B). HRMS (ESI, MeOH) calcd. for $C_{18}H_{25}BO_3$ [M + H]$^+$: 301.2050; Found: 301.1974.

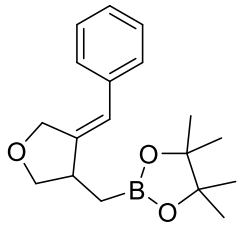

(*Z*)-4,4,5,5-Tetramethyl-2-((4-(4-methylbenzylidene)tetrahydrofuran-3-yl)methyl)-1,3,2-dioxaborolane (2ab): The compound was purified by column chromatography (cyclohexane/EtOAc, 95:5) and was obtained as a yellow oil in 79% yield (98 mg). ^{1}H NMR (300 MHz, $CDCl_3$) δ 7.14 (d, J = 8.0 Hz, 2H), 7.03 (d, J = 8.0 Hz, 1H), 6.32 (d, J = 2.1 Hz, 2H), 4.68 (d, J = 14.0, 1.8 Hz, 1H), 4.61 (d, J = 14.0, 1.8 Hz, 1H), 4.11 (t, J = 7.8 Hz, 1H), 3.46 (t, J = 7.8 Hz, 1H), 3.04 (dd, J = 14.0, 7.1 Hz, 1H), 2.34 (s, 3H), 1.26 (d, J = 2.6 Hz, 12H), 1.20 (d, J = 5.9 Hz, 1H), 1.02 (dd, J = 15.9, 8.3 Hz, 1H). ^{13}C NMR (75 MHz, $CDCl_3$) δ 146.0 (C), 136.1 (C), 134.8 (C), 129.2 (2 × CH), 127.9 (2 × CH), 119.7 (CH), 83.3 (2 × C), 74.2 (CH_2), 70.2 (CH_2), 41.2 (CH), 25.0 (2 × CH_3), 24.8 (2 × CH_3), 21.1 (CH_3), 14.0 (br m, CH_2-B). HRMS (ESI, MeOH) calcd. for $C_{19}H_{27}BO_3$ [M + H]$^+$: 315.2320; Found: 315.2126.

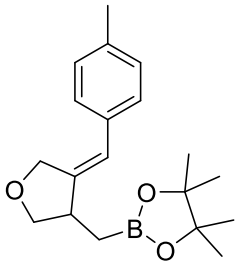

(*Z*)-2-((4-(4-Methoxybenzylidene)tetrahydrofuran-3-yl)methyl)-4,4,5,5-tetramethyl-1,3,2-dioxaborolane (2ac): 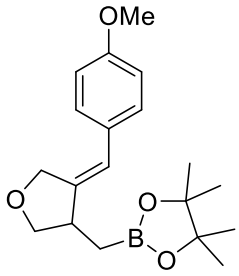
The compound was purified by column chromatography (cyclohexane/EtOAc,, 95:5) and was obtained as a pale yellow oil in 56% yield (74 mg). ^{1}H NMR (300 MHz, $CDCl_3$) δ 7.05 (d, J = 8.7 Hz, 2H), 6.86 (d, J = 8.7 Hz, 2H), 6.27 (d, J = 2.2 Hz, 1H), 4.65 (d, J = 14.0 Hz, 1H), 4.59 (t, J = 14.0, 1.9 Hz, 1H), 4.08 (t, J = 8.0 Hz, 1H), 3.78 (s, 3H), 3.43 (t, J = 8.0 Hz, 1H), 3.07 – 2.93 (m, 1H), 1.24 (d, J = 2.6 Hz, 12H), 1.22 – 1.15 (m, 1H), 0.98 (dd, J = 15.9, 8.3 Hz, 1H). ^{13}C NMR (75 MHz, $CDCl_3$) δ 158.2 (C), 144.7 (C), 130.5 (C), 129.2 (2 × CH), 119.3 (CH), 114.0 (2 × CH), 83.3 (2 × C), 74.2 (CH_2), 70.2 (CH_2), 55.3 (CH_3), 41.1 (CH), 25.0 (2 × CH_3), 24.8 (2 × CH_3), 14.1 (br m, CH_2-B). HRMS (ESI, MeOH) calcd. for $C_{19}H_{27}BO_4$ [M + Na]$^+$: 353.2310; Found: 353.1898.

(*Z*)-2-((4-(4-Chlorobenzylidene)tetrahydrofuran-3-yl)methyl)-4,4,5,5-tetramethyl-1,3,2-dioxaborolane (2ad): 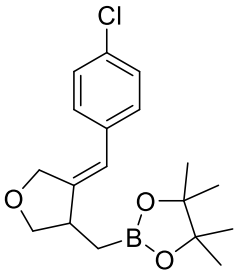
The compound was purified by column chromatography (cyclohexane/EtOAc, 95:5) and was obtained as a yellow oil in 76% yield (101 mg). ^{1}H NMR (300 MHz, $CDCl_3$) δ 7.21 (d, J = 8.4 Hz, 2H), 6.96 (d, J = 8.4 Hz, 2H), 6.21 (d, J = 2.0 Hz, 1H), 4.64 (dd, J = 14.1, 2.0 Hz, 1H), 4.56 (dt, J = 14.1, 2.0 Hz, 1H), 4.03 (t, J = 8.0 Hz, 1H), 3.38 (t, J = 8.0 Hz, 1H), 2.99 – 2.90 (m, 1H), 1.17 (d, J = 2.6 Hz, 12H), 1.11 (d, J = 5.8 Hz, 1H), 0.93 (dd, J = 15.9, 8.3 Hz, 1H). ^{13}C NMR (75 MHz, $CDCl_3$) δ 148.0 (C), 136.1 (C), 132.1 (C), 129.1 (2 × CH), 128.6 (2 × CH), 118.8 (CH), 83.4 (2 × C), 74.1 (CH_2), 70.1 (CH_2), 41.3 (CH), 25.0 (2 × CH_3), 24.8 (2 × CH_3), 13.9 (br m, CH_2-B). HRMS (ESI, MeOH) calcd. for $C_{18}H_{24}BClO_3$ [M + H]$^+$: 357.6470; Found: 357.1538.

(*Z*)-4,4,5,5-Tetramethyl-2-((4-(4-(trifluoromethyl)benzylidene)tetrahydrofuran-3-yl)methyl)-1,3,2-dioxaborolane (2af): 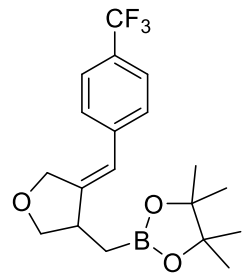
The compound was purified by column chromatography (cyclohexane/EtOAc, 95:5) and was obtained as a yellow oil in 55% yield (81 mg). ^{1}H NMR (300 MHz, $CDCl_3$) δ 7.58 (d, J = 8.2 Hz, 2H), 7.21 (d, J = 8.2 Hz, 2H), 6.37 (d, J = 2.3 Hz, 1H), 4.68 (d, J = 14.1 Hz, 1H), 4.61 (dt, J = 14.1, 8.2 Hz, 1H), 4.12 (t, J = 8.1 Hz, 1H), 3.47 (t, J = 8.1 Hz, 1H), 3.11 – 2.99 (m, 1H), 1.25 (d, J = 2.7 Hz, 12H), 1.19 (d, J = 5.8 Hz, 1H), 1.02 (dd, J = 16.0, 8.3 Hz, 1H). ^{13}C NMR (75 MHz, $CDCl_3$) δ 150.4 (C), 141.1 (C), 128.5 (C), 128.1 (4 × CH), 125.5 (q, J = 3.8 Hz, CF_3), 118.9 (CH), 83.5 (2 × C), 74.2 (CH_2), 70.2 (CH_2), 41.5 (CH), 25.0 (2 × CH_3), 24.9 (2 × CH_3), 14.0 (br m, CH_2-B). HRMS (ESI, MeOH) calcd. for $C_{19}H_{24}BF_3O_3$ [M + H]$^+$: 368.2032; Found: 368.1721.

2-(((5*S*)-4-((*Z*)-Benzylidene)-5-methyltetrahydrofuran-3-yl)methyl)-4,4,5,5-tetramethyl-1,3,2-dioxaborolane (2ag): 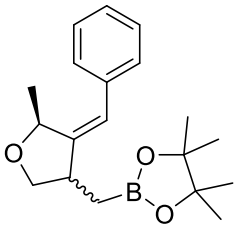
The compound was purified by column chromatography (cyclohexane/EtOAc, 95:5) and a mixture of two diastereomers (1:0.9) was obtained as a yellow oil in 80% yield (100 mg). ^{1}H NMR (300 MHz, $CDCl_3$, **mixture**) δ 7.31 (t, J = 7.3 Hz, 2H **diast1** + 2 H **diast2**), 7.20 (dd, J = 13.9, 7.3 Hz, 3H **diast1** + 3H **diast2**), 6.33 (s, 1H **diast1**), 6.24 (s, 1H **diast2**), 5.16 (qd, J = 6.7, 2.4 Hz, 1H **diast1**), 5.08 (q, J = 6.4 Hz, 1H **diast2**), 4.17 (t, J = 7.7 Hz, 1H **diast2**), 4.02 (dd, J = 8.3, 7.1 Hz, 1H **diast1**), 3.60 (t, J = 7.8 Hz, 1H **diast1**), 3.36 (dd, J = 9.2, 8.3 Hz, 1H **diast2**), 3.08 – 3.05 (m, 1H **diast2**), 3.00 – 2.95 (m, 1H **diast1**), 1.27 (s, 6H **diast1**), 1.25 (s, 6 H **diast1** + 12H **diast2**), 1.19 (dd, J = 11.7, 5.9 Hz, 1H **diast1** + 1H **diast2**), 1.08 (dd, J = 16.0, 8.8 Hz, 1H **diast1**), 0.91 (dd, J = 16.0, 8.5 Hz, 1H **diast2**). ^{13}C NMR (75 MHz,

$CDCl_3$, **mixture**) *δ* 151.8 (C **diast1**), 151.2 (C **diast2**), 137.3 (C **diast1**), 137.2 (C **diast2**), 128.4 (2 × CH **diast1**), 128.3 (2 × CH **diast2**), 126.4 (CH **diast1**), 126.3 (CH **diast2**), 120.1 (CH **diast1**), 119.7 (CH **diast2**), 83.3 (C **diast1**), 83.2 (C **diast2**), 75.7 (2 × CH **diast1** + **diast2**), 72.9 (CH_2 **diast2**), 71.8 (CH_2 **diast1**), 42.1 (CH **diast1**), 40.4 (CH **diast2**), 25.0 (2 × CH_3 **diast1**), 24.9 (2 × CH_3 **diast1**), 24.8 (2 × CH_3 **diast2**), 24.8 (2 × CH_3 **diast2**), 19.6 (CH_3 **diast1**), 18.7 (CH_3 **diast2**), 15.3 (br m, CH_2-B **diast1**), 12.3 (br m, CH_2-B **diast2**). HRMS (ESI, MeOH) calcd. for $C_{19}H_{27}BO_3$ [M + Na]$^+$: 337.2126; Found: 337.1843.

(*Z*)-2-((4-Benzylidene-3-(methoxymethyl)tetrahydrofuran-3-yl)methyl)-4,4,5,5-tetramethyl-1,3,2-dioxaborolane (2ao): The compound was purified by column chromatography (cyclohexane/EtOAc, 95:5) and was obtained as a yellow oil in 27% yield (33 mg). ^{1}H NMR (300 MHz, $CDCl_3$) *δ* 7.39 – 7.22 (m, 5H), 7.15 (m, 5H), 6.26 (s, 1H), 4.74 (dd, *J* = 14.1, 2.4 Hz, 1H), 4.62 (dd, *J* = 14.1, 2.4 Hz, 1H), 4.07 – 3.97 (m, 1H), 3.75 (d, *J* = 8.8 Hz, 1H), 3.38 – 3.30 (m, 4H), 3.18 (d, *J* = 8.8 Hz, 1H), 1.27 (d, *J* = 15.4 Hz, 1H), 1.19 (s, 12H), 1.05 (d, *J* = 15.4 Hz, 1H). ^{13}C NMR (75 MHz, $CDCl_3$) *δ* 147.9 (C), 137.6 (C), 128.6 (2 × CH), 128.2 (2 × CH), 126.7 (CH), 120.7 (CH), 83.1 (2 × C), 78.8 (CH_2), 75.4 (CH_2), 71.0 (CH_2), 59.2 (CH_3), 49.9 (C), 25.0 (2 × CH_3), 24.9 (2 × CH_3), 18.1 (br m, CH_2-B). HRMS (ESI, MeOH) calcd. for $C_{20}H_{29}BO_4$ [M + Na]$^+$: 367.2580; Found: 367.2070.

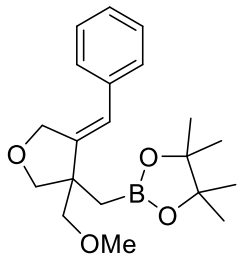

(*Z*)-2-((4-(2-Methoxyethylidene)tetrahydrofuran-3-yl)methyl)-4,4,5,5-tetramethyl-1,3,2-dioxaborolane (2ap): The compound was purified by column chromatography (cyclohexane/EtOAc, 9:1) and was obtained as a colorless oil in 54% yield (57 mg). ^{1}H NMR (300 MHz, $CDCl_3$) *δ* 5.48 – 5.37 (m, 1H), 4.41 (d, *J* = 13.7 Hz,1), 4.34 (d, *J* = 13.7 Hz, 1H), 4.08 (t, *J* = 8.0 Hz, 1H), 3.85 (d, *J* = 6.6 Hz, 2H), 3.36 (t, *J* = 8.0 Hz, 1H), 3.31 (s, 3H), 2.84 – 2.80 (m, 1H), 1.24 (s, 12H), 1.12 (dd, *J* = 16.0, 5.7 Hz, 1H), 0.86 (dd, *J* = 16.0, 8.7 Hz, 1H). ^{13}C NMR (75 MHz, $CDCl_3$) *δ* 148.7 (C), 115.4 (CH), 83.4 (2 × C), 74.9 (CH_2), 70.0 (CH_2), 69.1 (CH_2), 57.9 (CH_3), 39.8 (CH), 25.0 (2 × CH_3), 24.9 (2 × CH_3), 13.8 (br m, CH_2-B). HRMS (ESI, MeOH) calcd. for $C_{14}H_{25}BO_4$ [M + Na]$^+$: 291.1600; Found: 291.1736.

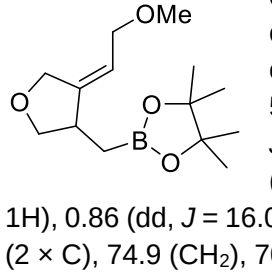

(*Z*)-3-Benzylidene-4-((4,4,5,5-tetramethyl-1,3,2-dioxaborolan-2-yl)methyl)-1-tosylpyrrolidine (2bb):[100] The compound was purified by column chromatography (cyclohexane/EtOAc, 9:1) and was obtained as a brown solid in 76% yield (139 mg). M.p. = 125 – 127 °C. ^{1}H NMR (300 MHz, $CDCl_3$) *δ* 7.72 (d, *J* = 8.2 Hz, 2H), 7.39 – 7.28 (m, 3H), 7.24 – 7.22(m, 2H), 7.12 (d, *J* = 7.6 Hz, 2H), 6.24 (d, *J* = 2.4 Hz, 1H), 4.26 (dd, *J* = 14.8, 1.6 Hz, 1H), 3.99 (dt, *J* = 14.8, 1.6 Hz, 1H), 3.64 (dd, *J* = 8.8, 7.3 Hz, 1H), 2.96 (m, 1H), 2.80 (t, *J* = 8.8 Hz, 1H), 2.41 (s, 3H), 1.19 (d, *J* = 5.7 Hz, 12H), 1.11 (dd, *J* = 16.0, 5.7 Hz, 1H), 0.93 (dd, *J* = 16.0, 8.1 Hz, 1H).

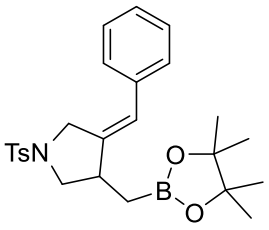

[100] T. Xi, Z. Lu, *ACS Catal.* **2017**, *7*, 1181–1185.

(*Z*)-3-(4-Methylbenzylidene)-4-((4,4,5,5-tetramethyl-1,3,2-dioxaborolan-2-yl)methyl)-1-tosylpyrrolidine (2bc): The compound was purified by column chromatography (cyclohexane/EtOAc, 9:1) and was obtained as an orange solid in 60% yield (103 mg). M.p. = 125 – 127 °C. ^{1}H NMR (300 MHz, $CDCl_3$) δ 7.72 (d, J = 8.1 Hz, 2H), 7.29 (d, J = 8.1 Hz, 2H), 7.13 (d, J = 8.0 Hz, 2H), 7.01 (d, J = 8.0 Hz, 2H), 6.21 (d, J = 1.8 Hz, 1H), 4.25 (d, J = 14.6 Hz, 1H), 3.99 (d, J = 14.6 Hz, 1H), 6.63 (t, 7.8 Hz, 1H), 2.97 (quin, J = 6.7 Hz 1H), 2.81 (t, J = 8.7 Hz, 1H), 2.39 (s, 3H), 2.33 (s, 3H), 1.18 (d, J = 5.9 Hz, 12H), 1.11 (dd, J = 16.0, 5.6 Hz, 1H), 0.94 (dd, J = 16.0, 8.0 Hz, 1H). ^{13}C NMR (75 MHz, $CDCl_3$) δ 143.5 (C), 141.3 (C), 136.7 (C), 133.9 (C), 133.2 (C), 129.7 (2 × CH), 129.3 (2 × CH), 128.1 (2 × CH), 127.8 (2 × CH), 121.8 (CH), 83.4 (2 × C), 53.7 (CH_2), 50.9 (CH_2), 40.3 (CH), 24.9 (2 × CH_3), 24.8 (2 × CH_3), 21.5 (CH_3), 21.2 (CH_3), 14.1 (br m, CH_2-B). HRMS (ESI, MeOH) calcd. for $C_{26}H_{34}BNO_4S$ $[M]^+$: 468.4310; Found: 468.2374.

(*Z*)-3-(4-Methoxybenzylidene)-4-((4,4,5,5-tetramethyl-1,3,2-dioxaborolan-2-yl)methyl)-1-tosylpyrrolidine (2bd): The compound was purified by column chromatography (cyclohexane/EtOAc, 9:1) and was obtained as a brown solid in 60% yield (107 mg). M.p. = 157 – 159 °C ^{1}H NMR (300 MHz, $CDCl_3$) δ 7.72 (d, J = 8.5 Hz, 2H), 7.30 (d, J = 8.5 Hz, 2H), 7.06 (d, J = 8.8 Hz, 2H), 6.87 (d, J = 8.8 Hz, 2H), 6.17 (d, J = 2.6 Hz, 1H), 4.23 (d, J = 14.5 Hz, 1H), 3.97 (dd, J = 14.6, 2.6 Hz, 1H), 3.81 (s, 3H), 3.62 (dd, J = 8.6, 7.6 Hz, 1H), 3.05 – 2.90 (m, 1H), 2.79 (t, J = 8.6 Hz, 1H), 2.41 (s, 3H), 1.18 (d, J = 5.8 Hz, 12H), 1.11 (dd, J = 16.0, 5.5 Hz, 1H), 0.93 (dd, J = 16.0, 8.0 Hz, 1H). ^{13}C NMR (75 MHz, $CDCl_3$) δ 158.5 (C), 143.5 (C), 140.1 (C), 133.2 (C), 129.7 (2 × CH), 129.5 (C), 129.4 (2 × CH), 127.8 (CH), 121.4 (2 × CH), 114.0 (2 × CH), 83.4 (2 × C), 55.3 (CH_3), 53.7 (CH_2), 50.8 (CH_2), 40.3 (CH), 24.9 (2 × CH_3), 24.8 (2 × CH_3), 21.5 (CH_3), 14.1 (br m, CH_2-B). HRMS (ESI, MeOH) calcd. for $C_{26}H_{34}BNO_5S$ $[M + H]^+$: 484.2251; Found: 484.2327.

(*Z*)-3-(4-Chlorobenzylidene)-4-((4,4,5,5-tetramethyl-1,3,2-dioxaborolan-2-yl)methyl)-1-tosylpyrrolidine (2be): The compound was purified by column chromatography (cyclohexane/EtOAc, 9:1) and was obtained as an orange solid in 70% yield (140 mg). M.p. = 147 – 149 °C. ^{1}H NMR (300 MHz, $CDCl_3$) δ 7.71 (d, J = 8.4 Hz, 2H), 7.30 (dd, J = 8.4, 3.0 Hz, 4H), 7.04 (d, J = 8.4 Hz, 2H), 6.18 (d, J = 2.5 Hz, 1H), 4.21 (dd, J = 14.9, 1.6 Hz, 1H), 3.94 (d, J = 14.9, 1.6 Hz, 1H), 3.64 (dd, J = 8.9, 7.3 Hz, 2H), 2.97 (m, 1H), 2.80 (t, J = 8.9 Hz, 1H), 2.41 (s, 3H), 1.18 (d, J = 5.7 Hz, 12H), 1.11 (dd, J = 16.1, 5.7 Hz, 1H), 0.93 (dd, J = 16.1, 8.1 Hz, 1H). ^{13}C NMR (75 MHz, $CDCl_3$) δ 143.6 (C), 143.3 (C), 135.2 (C), 133.0 (C), 132.6 (C), 129.7 (2 × CH), 129.3 (2 × CH), 128.7 (2 × CH), 127.8 (2 × CH), 120.9 (CH), 83.4 (2 × C), 53.6 (CH_2), 50.8 (CH_2), 40.4 (CH), 24.9 (2 × CH_3), 24.7 (2 × CH_3), 21.5 (CH_3), 13.9 (br m, CH_2-B). HRMS (ESI, MeOH) calcd. for $C_{25}H_{31}BClNO_4S$ $[M + H]^+$: 488.1755; Found: 488.1828.

(*Z*)-4-((4-((4,4,5,5-Tetramethyl-1,3,2-dioxaborolan-2-yl)methyl)-1-tosylpyrrolidin-3-ylidene)methyl)benzonitrile (bf): 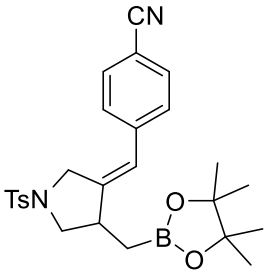

The compound was purified by column chromatography (cyclohexane/EtOAc, 9:1) and was obtained as an orange oil in 48% yield (91 mg). ^{1}H NMR (300 MHz, $CDCl_3$) δ 7.72 (d, J = 8.2 Hz, 2H), 7.61 (d, J = 8.4 Hz, 2H), 7.32 (d, J = 8.2 Hz, 2H), 7.19 (d, J = 8.4 Hz, 2H), 6.26 (d, J = 2.4 Hz, 1H), 4.24 (dd, J = 15.1, 1.9 Hz, 1H), 3.96 (dt, J = 15.1, 1.9 Hz, 1H), 3.66 (dd, J = 9.0, 7.4 Hz, 1H), 3.05 – 2.96 (m, 1H), 2.82 (t, J = 9.0 Hz, 1H), 2.42 (s, 3H), 1.18 (d, J = 4.4 Hz, 12H), 1.11 (dd, J = 16.1, 5.5 Hz, 1H), 0.93 (dd, J = 16.1, 8.1 Hz, 1H). ^{13}C NMR (75 MHz, $CDCl_3$) δ 146.9 (C), 143.8 (C), 141.2 (C), 132.9 (C), 132.4 (2 × CH), 129.8 (2 × CH), 128.5 (2 × CH), 127.8 (2 × CH), 120.7 (CH), 118.8 (C), 110.3 (C), 83.5 (2 × C), 53.5 (CH_2), 50.9 (CH_2), 40.7 (CH), 24.9 (2 × CH_3), 24.7 (2 × CH_3), 21.6 (CH_3), 14.0 (br m, CH_2-B). HRMS (ESI, MeOH) calcd. for $C_{26}H_{31}BN_2O_4S$ [M + H]$^+$: 479.2098; Found: 479.2161.

(*Z*)-3-(2-Methoxyethylidene)-4-((4,4,5,5-tetramethyl-1,3,2-dioxaborolan-2-yl)methyl)-1-tosylpyrrolidine (2bj): 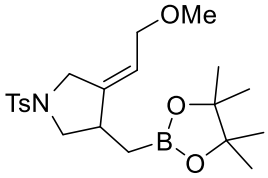

The compound was purified by column chromatography (cyclohexane/EtOAc, 9:1) and was obtained as an orange oil in 60% yield (93 mg). ^{1}H NMR (300 MHz, $CDCl_3$) δ 7.70 (d, J = 8.2 Hz, 2H), 7.32 (d, J = 8.2 Hz, 2H), 5.35 (ddd, J = 6.4, 4.5, 2.4 Hz, 1H), 3.95 (d, J = 14.4 Hz, 1H), 3.80 (d, J = 6.4 Hz, 2H), 3.72 (d, J = 14.4 Hz, 1H), 3.63 (dd, J = 8.4, 6.4 Hz, 1H), 2.79 (m, 1H), 2.70 (t, J = 8.7 Hz, 1H), 2.43 (s, 3H), 1.19 (d, J = 1.5 Hz, 12H), 1.04 (dd, J = 16.1, 5.1 Hz, 1H), 0.77 (dd, J = 16.1, 8.4 Hz, 1H). ^{13}C NMR (75 MHz, $CDCl_3$) δ 144.4 (C), 143.6 (C), 132.8 (C), 129.7 (2 × CH), 127.9 (2 × CH), 117.9 (CH), 83.4 (2 × C), 69.6 (CH_2), 58.1 (CH_3), 54.4 (CH_2), 49.6 (CH_2), 38.8 (CH), 24.9 (2 × CH_3), 24.8 (2 × CH_3), 21.6 (CH_3), 13.6 (br m, CH_2-B). HRMS (ESI, MeOH) calcd. for $C_{21}H_{32}BNO_5S$ [M + Na]$^+$: 444.3590; Found: 444.1966.

(*Z*)-3-Ethylidene-4-((4,4,5,5-tetramethyl-1,3,2-dioxaborolan-2-yl)methyl)-1-tosylpyrrolidine (2bn): 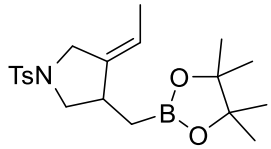

The compound was purified by column chromatography (cyclohexane/EtOAc, 9:1) and was obtained as a yellow oil in 62% yield (94 mg). ^{1}H NMR (300 MHz, $CDCl_3$) δ 7.69 (d, J = 8.2 Hz, 2H), 7.30 (d, J = 8.2 Hz, 2H), 5.25 – 5.08 (m, 1H), 3.86 (d, J = 14.1 Hz, 1H), 3.64 (dd, J = 14.1, 5.0 Hz, 1H), 3.58 (d, J = 1.4 Hz, 1H), 2.70 (q, J = 8.4 Hz, 2H), 2.40 (s, 3H), 1.48 (dd, J = 6.8, 1.1 Hz, 3H), 1.15 (d, J = 4.7 Hz, 12H), 0.96 (dd, J = 16.0, 4.7 Hz, 1H), 0.74 (dd, J = 16.0, 7.4 Hz, 1H). ^{13}C NMR (75 MHz, $CDCl_3$) δ 143.4 (C), 141.1 (C), 133.1 (C), 129.6 (2 × CH), 127.9 (2 × CH), 115.8 (CH), 83.3 (2 × C), 54.9 (CH_2), 49.8 (CH_2), 38.5 (CH), 24.9 (2 × CH_3), 24.7 (2 × CH_3), 21.6 (CH_3), 14.4 (CH_3), 13.6 (br m, CH_2-B). HRMS (ESI, MeOH) calcd. for $C_{20}H_{30}BNO_4S$ [M + H]$^+$: 392.3330; Found: 392.2061.

(*E*)-2-((3-Benzylidene-8,8-dimethyl-7,9-dioxaspiro[4.5]decan-2-yl)methyl)-4,4,5,5-tetramethyl-1,3,2-dioxaborolane (2da): 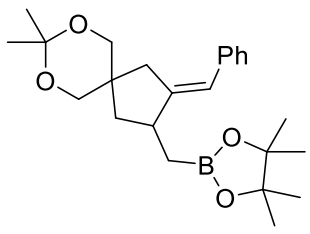

The compound was purified by column chromatography (cyclohexane/EtOAc, 95:5) and was obtained as a yellow oil in 56% yield (45 mg). ^{1}H NMR (300 MHz, $CDCl_3$) δ 7.34 – 7.27 (m, 4H), 7.21 – 7.11 (m, 1H), 6.26 (q, J = 2.2 Hz, 1H), 3.74 – 3.50 (m, 4H), 2.85 – 2.82 (m, 1H), 2.77 (d, J = 17.3 Hz, 1H), 2.48 (d, J = 17.3 Hz, 1H), 2.02 (dd, J = 12.5, 7.9 Hz, 1H), 1.43 (s, 3H), 1.41 (s, 3H), 1.37 – 1.31 (m, 1H), 1.24 (d, J = 1.2 Hz, 12H), 1.16 (dd, J = 15.7, 5.1 Hz, 1H), 0.98 (dd, J = 15.7, 8.0 Hz, 1H). ^{13}C NMR (75 MHz, $CDCl_3$) δ 149.1 (C), 138.6 (C), 128.4 (2 × CH), 128.3 (2 × CH), 126.0 (CH),

121.6 (CH), 98.0 (C), 83.2 (2 × C), 70.0 (CH_2), 68.4 (CH_2), 40.9 (C), 40.4 (CH_2), 39.6 (CH), 39.0 (CH_2), 25.1 (2 × CH_3), 24.9 (3 × CH_3), 23.1 (CH_3), 16.7 (br m, CH_2-B). HRMS (ESI, MeOH) calcd. for $C_{24}H_{35}BO_4$ $[M + Na]^+$: 421.3500; Found: 421.2358.

(*E*)-2-((2-Benzylidene-4,4-bis((benzyloxy)methyl)cyclopentyl)methyl)-4,4,5,5-tetramethyl-1,3,2-dioxaborolane (2db): 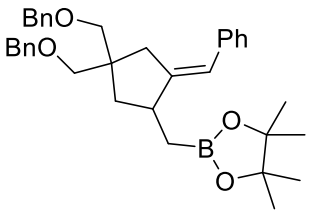

The compound was purified by column chromatography (cyclohexane/EtOAc, 98:2) and was obtained as a pale yellow oil in 55% yield (119 mg). ^{1}H NMR (300 MHz, $CDCl_3$) δ 7.32 – 7.27 (m, 15H), 6.23 (d, *J* = 2.2 Hz, 1H), 4.50 (d, *J* = 1.9 Hz, 4H), 3.47 – 3.40 (m, 4H), 2.89 (s, 1H), 2.55 (dt, *J* = 17.3, 2.2 Hz, 2H), 2.05 (dd, *J* = 12.7, 7.9 Hz, 1H), 1.24 (d, *J* = 2.1 Hz, 13H), 1.18 (d, *J* = 6.2 Hz, 1H), 0.95 (dd, *J* = 15.5, 8.2 Hz, 1H). ^{13}C NMR (75 MHz, $CDCl_3$) δ 150.4 (C), 139.1 (C), 139.0 (C), 138.8 (C), 128.5 (2 × CH), 128.4 (2 × CH), 128.2 (2 × CH), 127.6 (2 × CH), 127.5 (2 × CH), 127.5 (2 × CH), 127.4 (2 × CH), 125.8 (CH), 120.9 (CH), 83.2 (2 × C), 75.2 (CH_2), 73.4 (CH_2), 73.3 (CH_2), 72.9 (CH_2), 46.9 (C), 40.0 (CH), 39.5 (CH_2), 38.1 (CH_2), 25.1 (2 × CH_3), 24.9 (2 × CH_3), 16.7 (br m, CH_2-B). HRMS (ESI, MeOH) calcd. for $C_{35}H_{43}BO_4$ $[M]^+$: 539.5350; Found: 539.3326.

(*E*)-2-((2-Benzylidenecyclopentyl)methyl)-4,4,5,5-tetramethyl-1,3,2-dioxaborolane (2ea): 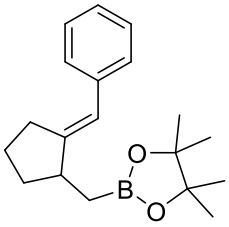

The compound was purified by column chromatography (cyclohexane/EtOAc, 98:2) and was obtained as a yellow oil in 57% yield (68 mg). ^{1}H NMR (300 MHz, $CDCl_3$) δ 7.31 (d, *J* = 4.3 Hz, 4H), 7.15 (td, *J* = 8.5, 4.3 Hz, 1H), 6.27 (d, *J* = 2.3 Hz, 1H), 2.80 – 2.51 (m, 3H), 2.07 – 1.77 (m, 3H), 1.73 – 1.51 (m, 1H), 1.26 (d, *J* = 2.3 Hz, 12H), 1.18 (dd, *J* = 15.6, 5.7 Hz, 1H), 0.95 (dd, *J* = 15.6, 8.5 Hz, 1H). ^{13}C NMR (75 MHz, $CDCl_3$) δ 152.2 (C), 139.2 (C), 128.2 (4 × CH), 125.7 (CH), 120.2 (CH), 83.2 (2 × C), 42.5 (CH), 34.5 (CH_2), 31.4 (CH_2), 25.1 (2 × CH_3), 24.9 (2 × CH_3), 24.8 (CH_2), 16.9 (br m, CH_2-B). HRMS (ESI, MeOH) calcd. for $C_{19}H_{27}BO_2$ $[M + H]^+$: 299.2330; Found: 299.2176.

(*E*)-4,4,5,5-Tetramethyl-2-((2-(4-methylbenzylidene)cyclopentyl)methyl)-1,3,2-dioxaborolane (2eb): 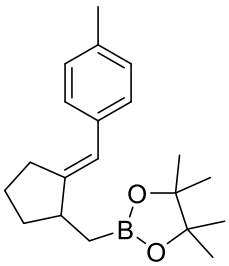

The compound was purified by column chromatography (cyclohexane/EtOAc, 98:2) and was obtained as a colorless oil in 37% yield (47 mg). ^{1}H NMR (300 MHz, $CDCl_3$) δ 7.21 (d, *J* = 8.1 Hz, 2H), 7.11 (d, *J* = 8.1 Hz, 2H), 6.23 (d, *J* = 2.3 Hz, 1H), 2.80 – 2.45 (m, 3H), 2.33 (s, 3H), 2.03 – 1.75 (m, 2H), 1.69 – 1.51 (m, 2H), 1.26 (d, *J* = 2.3 Hz, 12H), 1.19 (dd, *J* = 15.6, 5.5 Hz, 1H), 0.94 (dd, *J* = 15.6, 8.5 Hz, 1H). ^{13}C NMR (75 MHz, $CDCl_3$) δ 151.1 (C), 136.4 (C), 135.2 (C), 129.0 (2 × CH), 128.1 (2 × CH), 120.0 (CH), 83.1 (2 × C), 42.4 (CH), 34.5 (CH_2), 31.3 (CH_2), 25.1 (2 × CH_3), 24.9 (2 × CH_3), 24.8 (CH_2), 21.2 (CH_3), 16.7 (br m, CH_2-B). HRMS (ESI, MeOH) calcd. for $C_{20}H_{29}BO_2$ $[M + Na]^+$: 335.2600; Found: 335.2163.

2-(3-Phenylprop-2-yn-1-yl)pent-4-en-1-ol: 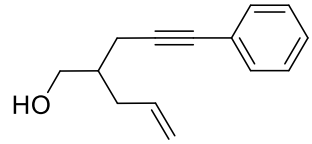

The compound was purified by column chromatography (cyclohexane/EtOAc 7:3) and was obtained as a yellow oil in 7% yield (6 mg). ^{1}H NMR (300 MHz, $CDCl_3$) δ 7.35 – 7.28 (m, 2H), 7.23 – 7.15 (m, 3H), 5.76 (ddt, *J* = 17.2, 10.1, 7.0 Hz, 1H), 5.13 – 4.94 (m, 2H), 3.65 (d, *J* = 5.2 Hz, 2H), 2.43 (t, *J* = 5.2 Hz, 2H), 2.16 (t, *J* = 7.0 Hz, 2H), 1.84 (dp, *J* = 12.6, 6.2 Hz, 1H), 1.58 (br s, 1H). ^{13}C NMR (75 MHz, $CDCl_3$) δ 136.3 (CH), 131.7 (2 × CH), 128.4 (2 × CH), 127.8 (CH), 123.9 (C), 117.0 (CH_2), 88.0 (C), 82.3 (C), 65.2 (CH_2), 40.1 (CH), 35.2

(CH_2), 21.0 (CH_2). HRMS (ESI, MeOH) calcd. for $C_{14}H_{16}O$ [M + Na]$^+$: 223.2810; Found: 223.1090.

3.2.4.4. Transformations of alkylboronates

3.2.4.5.1. General procedure for oxidation of alkylboronates

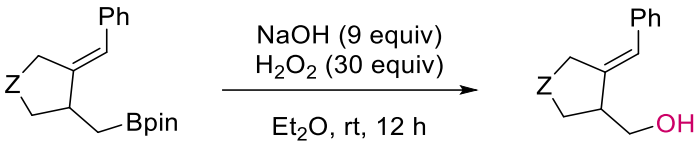

2 **3**

The corresponding alkylboronate **2** (1 equiv, 0.4 mmol) in diethylether (0.2 M, 2.5 mL) was treated with NaOH (3 N, 9 equiv) and H_2O_2 (30%, 30 equiv) at 0 °C. The mixture was stirred overnight at room temperature. The resulting suspension was extracted with diethyl ether (2 × 5 mL). The combined organic layers were washed with brine, dried over anhydrous $MgSO_4$, filtered and concentrated under vacuum. The resulting residue was purified by column chromatography to give the corresponding alcohol (cyclohexane/EtOAc 7:3 was used as an eluent).[100]

(*Z*)-(4-Benzylidenetetrahydrofuran-3-yl)methanol (3aa):[100] The product was obtained as a colorless oil in 86% yield (80 mg). ^{1}H NMR (300 MHz, $CDCl_3$) δ 7.34 (t, J = 7.3 Hz, 2H), 7.22 (t, J = 7.3 Hz, 1H), 7.13 (d, J = 7.3 Hz, 2H), 6.44 (d, J = 1.8 Hz, 1H), 4.68 (dt, J = 14.1, 2.0 Hz, 1H), 4.57 (dd, J = 14.1, 2.0 Hz, 1H), 3.94 (qd, J = 8.9, 5.1 Hz, 2H), 3.73 (d, J = 6.2 Hz, 1H), 3.09 – 2.97 (m, 1H), 2.19 (br s, 1H).

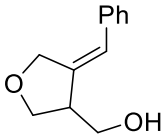

(*Z*)-(4-Benzylidene-1-tosylpyrrolidin-3-yl)methanol (3bb):[100] The product was obtained as a white solid in 80% yield (78 mg). ^{1}H NMR (300 MHz, $CDCl_3$) δ 7.73 (d, J = 8.2 Hz, 2H), 7.35 (m, 4H), 7.26 (m, 1H), 7.14 (d, J = 8.2 Hz, 2H), 6.37 (s, 1H), 4.22 (d, J = 14.8 Hz, 1H), 4.02 (d, J = 14.8 Hz, 1H), 3.65 (t, J = 5.6 Hz, 2H), 3.38 (dd, J = 9.6, 4.0 Hz, 1H), 3.28 (dd, J = 9.6, 6.8 Hz, 1H), 2.99 (m, 1H), 2.42 (s, 3H), 1.70 (t, J = 5.6 Hz, 1H).

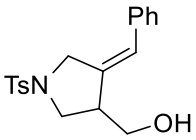

3.2.4.5.2. General procedure for the synthesis of trifluoroborates salts

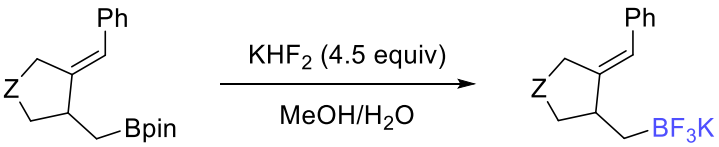

2 **4**

The corresponding alkylboronate **2** (1 equiv, 0.4 mmol) was dissolved in methanol (0.2 M, 2 mL). Then, KHF_2 (4.5 equiv, 4.5 M in water) was added dropwise to the solution. The reaction mixture was stirred at 23 °C for 1.5 h. Then, the solvent was removed under vacuum and the solid residue was triturated with acetone (20 mL). The liquid phase was filtered, and the

[100] T. Xi, Z. Lu, *ACS Catal.* **2017**, *7*, 1181–1185.

residual inorganic salts were washed with additional acetone. The combined solutions were concentrated under vacuum to give white solids. The solids were washed with diethyl ether (3 × 20 mL) to remove pinacol and dried under vacuum, affording the desired product.[100]

Potassium (*Z*)-((4-benzylidenetetrahydrofuran-3-yl)methyl)trifluoroborate (4aa): The

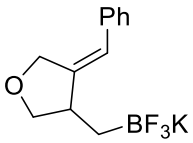

product was obtained as a white solid in 84 % yield (94 mg). ^{1}H NMR (300 MHz, d^{6}-DMSO) δ 7.32 (t, J = 7.5 Hz, 2H), 7.16 (dd, J = 11.3, 7.5 Hz, 3H), 6.24 (d, J = 2.1 Hz, 1H), 4.57 (d, J = 14.4 Hz, 1H), 4.37 (d, J = 14.4 Hz, 1H), 3.97 (dd, J = 8.1, 7.9 Hz, 1H), 3.16 (t, J = 8.8 Hz, 1H), 2.62 (m, 1H), 0.60 – 0.45 (m, 1H), 0.06 – -0.15 (m, 1H). ^{13}C NMR (75 MHz, DMSO-d^{6}) δ 150.7 (C), 137.8 (C), 128.4 (2 × CH), 127.6 (2 × CH), 125.7 (CH), 117.6 (CH), 74.2 (CH_2), 69.4 (2 × CH_2), 43.0 (q, J = 2.3 Hz, CH). ^{19}F NMR (282 MHz, DMSO-d^{6}) δ – 136.24. HRMS (ESI, MeCN) calcd. for $C_{12}H_{13}BF_3KO$ [M - K]$^{+}$: 241.0397; Found: 241.1026.

Potassium (*Z*)-3-benzylidene-1-tosyl-4-((trifluoroboranyl)methyl)pyrrolidine (4bb):[100]

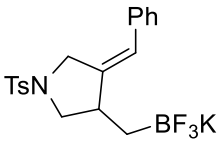

The product was obtained as a white solid in 72 % yield (79 mg). ^{1}H NMR (300 MHz, d^{6}-DMSO) δ 7.66 (d, J = 7.9 Hz, 2H), 7.37 (m, 4H), 7.18 (m, 3H), 6.22 (s, 1H), 4.19 (d, J = 15.4 Hz, 1H), 3.76 (d, J = 15.4 Hz, 1H), 3.55 (d, J = 7.7 Hz, 1H), 2.37 (s, 3H), 0.48 (br s, 1H), –0.20 (br s, 1H).

3.2.4.5.3. General procedure for Suzuki-Miyaura Cross-Coupling Reaction

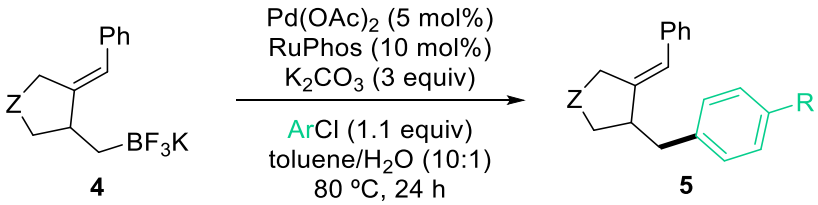

A vial was charged with $Pd(OAc)_2$ (0.02 mmol), RuPhos (0.04 mmol), 4-chlorobenzonitrile (0.4 mmol), the corresponding potassium trifluoroborate compound **4** (0.4 mmol) and K_2CO_3 (1.2 mmol). The vial was sealed by a septum, dried under vacuum and backfilled with Ar. To the vial, toluene (2 mL) and H_2O (0.2 mL) were added, and then the reaction was heated to 80 °C for 24 h. The reaction mixture was allowed to cool to room temperature. The organic layer was separated, and the aqueous layer was washed with EtOAc. The combined organic solutions were concentrated under vacuum and the residue was purified by silica gel column chromatography to yield the product.[18e]

(*Z*)-4-((4-Benzylidenetetrahydrofuran-3-yl)methyl)benzonitrile (5aa): The product was

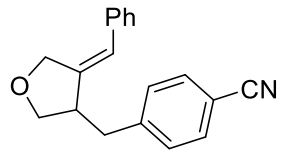

obtained as a yellow oil in 30 % yield (15 mg). ^{1}H NMR (300 MHz, $CDCl_3$) δ 7.61 (d, J = 8.2 Hz, 2H), 7.39 – 7.29 (m, 4H), 7.22 (d, J = 7.4 Hz, 1H), 7.10 (d, J = 7.4 Hz, 2H), 6.23 (s, 1H), 4.70 (d, J = 14.3 Hz, 1H), 4.62 (dd, J = 14.3, 1.8 Hz, 1H), 3.84 (dd, J = 8.6, 6.0 Hz, 1H), 3.65 (dd, J = 8.6, 4.4 Hz, 1H), 3.11 (s, 1H), 3.04 (d, J = 6.0 Hz, 1H), 2.85 (dd, J = 13.1, 8.6 Hz, 1H). ^{13}C NMR (75 MHz, $CDCl_3$) δ 145.6 (C), 143.6 (C), 137.0

[18] (e) S. D. Dreher, S.-E. Lim, D. L. Sandrock, G. A. Molander, *J. Org. Chem.* **2009**, *74*, 3626–3631.
[100] T. Xi, Z. Lu, *ACS Catal.* **2017**, *7*, 1181–1185.

(C), 132.4 (2 × CH), 130.0 (2 × CH), 128.7 (2 × CH), 128.1 (2 × CH), 127.1 (CH), 122.0 (CH), 119.0 (C), 110.5 (C), 72.1 (CH_2), 70.3 (CH_2), 47.0 (CH_3), 39.9 (CH_2).

(*Z*)-3-Benzylidene-4-(4-methoxybenzyl)-1-tosylpyrrolidine (5bb): The product was obtained as a yellow oil in 19 % yield (7 mg). 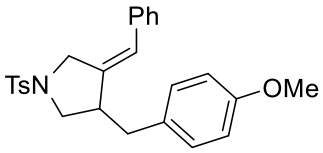

^{1}H NMR (300 MHz, $CDCl_3$) *δ* 7.69 (d, *J* = 8.2 Hz, 2H), 7.37 – 7.32 (m, 5H), 7.12 (d, *J* = 7.5 Hz, 2H), 7.06 (d, *J* = 8.5 Hz, 2H), 6.83 (d, *J* = 8.5 Hz, 2H), 6.23 (s, 1H), 4.21 (d, *J* = 14.7 Hz, 1H), 4.08 (d, *J* = 14.7 Hz, 1H), 3.80 (s, 3H), 3.17 (dd, *J* = 9.1, 6.7 Hz, 1H), 3.06 (dd, *J* = 9.1, 4.9 Hz, 1H), 3.05 – 2.97 (m, 1H), 2.90 (dd, *J* = 13.5, 5.5 Hz, 1H), 2.61 (dd, *J* = 13.5, 9.1 Hz, 1H), 2.42 (s, 3H). ^{13}C NMR (75 MHz, $CDCl_3$) δ 158.4 (C), 143.8 (C), 140.1 (C), 136.6 (C), 133.1 (C), 131.3 (C), 130.1 (2 × CH), 129.9 (2 × CH), 128.7 (2 × CH), 128.2 (2 × CH), 127.9 (2 × CH), 127.2 (CH), 123.5 (CH), 114.1 (2 × CH), 55.4 (CH_3), 51.6 (CH_2), 50.9 (CH_2), 47.0 (CH), 38.9 (CH_2), 21.7 (CH_3). HRMS (ESI, MeOH) calcd. for $C_{26}H_{27}NO_3S$ $[M]^+$: 433.5660; Found: 433.1706.

3.2.4.5. Mechanistic studies

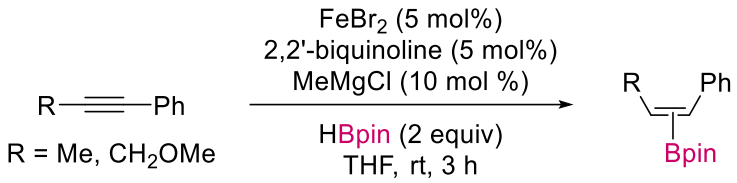

(*Z*)-4,4,5,5-Tetramethyl-2-(1-phenylprop-1-en-1-yl)-1,3,2-dioxaborolane:[194] The compound was obtained following the *general procedure for hydroborylative cyclization*. The product was purified by column chromatography (cyclohexane/EtOAc, 95:5) and was obtained as a yellow oil in 33% yield (32 mg). 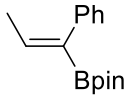

^{1}H NMR (300 MHz, $CDCl_3$) *δ* 7.40 – 7.35 (m, 2H), 7.25 – 7.13 (m, 3H), 6.72 (q, *J* = 7.0 Hz, 1H), 1.77 (d, *J* = 7.0 Hz, 3H), 1.32 (s, 3H), 1.27 (s, 12H).

(*Z*)-2-(3-Methoxy-1-phenylprop-1-en-1-yl)-4,4,5,5-tetramethyl-1,3,2-dioxaborolane (A) and **(*Z*)-2-(3-methoxy-1-phenylprop-1-en-2-yl)-4,4,5,5-tetramethyl-1,3,2-dioxaborolane (B)**: The mixture (A/B, 1:1.9) was obtained following the *general procedure for hydroborylative cyclization*. The product was purified by column chromatography (cyclohexane/EtOAc, 95:5) and was obtained as a yellow oil in 34% yield (38 mg). 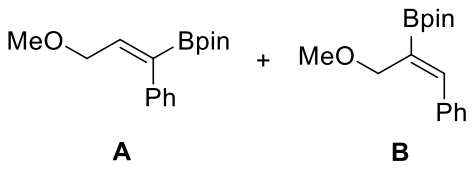

A **B**
^{1}H NMR (300 MHz, $CDCl_3$, **mixture**) *δ* 7.44 – 7.21 (m, 5H **A**), 7.41 – 7.23 (m, 5H **B**), 7.10 – 7.05 (m, 1H **B**), 6.62 (t, *J* = 6.0 Hz, 1H **A**), 4.08 (s, 2H **B**), 3.98 (d, *J* = 6.0 Hz, 2H **A**), 3.31 (d, *J* = 3.5 Hz, 3H **B**), 3.21 (s, 3H **A**), 1.26 (s, 12H **B**), 1.21 (s, 12H **A**).

3.2.4.6. EPR

All samples for EPR spectroscopy were prepared in an inert atmosphere glovebox equipped with a liquid nitrogen fill port to enable sample freezing to 77 K within the glovebox. EPR samples were prepared in 4 mm OD Suprasil quartz EPR tubes from Wilmad Labglass. Samples for spin integration utilised high precision suprasil quartz tubes to allow for direct

[194] Y. D. Bidal, F. Lazreg, C. S. J. Cazin, *ACS Catal.* **2014**, *4*, 1564–1569.

comparison of intensities between different samples. X-band EPR spectra were recorded on a Bruker EMXplus spectrometer equipped with a 4119HS cavity and an Oxford ESR-900 helium flow cryostat. The instrumental parameters employed for all samples were as follows: 1 mW power; time constant 41 ms; modulation amplitude 8 G; 9.38 GHz; modulation frequency 100 kHz; temperature 10 K.

For quantitative EPR, a 5mM MeOH/EtOH (9:1) solution of $CuSO_4 \cdot 5H_2O$ was used as internal standard. The corresponding Fe sample was prepared at the same concentration, showing its integral = 14853.943, corresponding to *ca*. 10%.

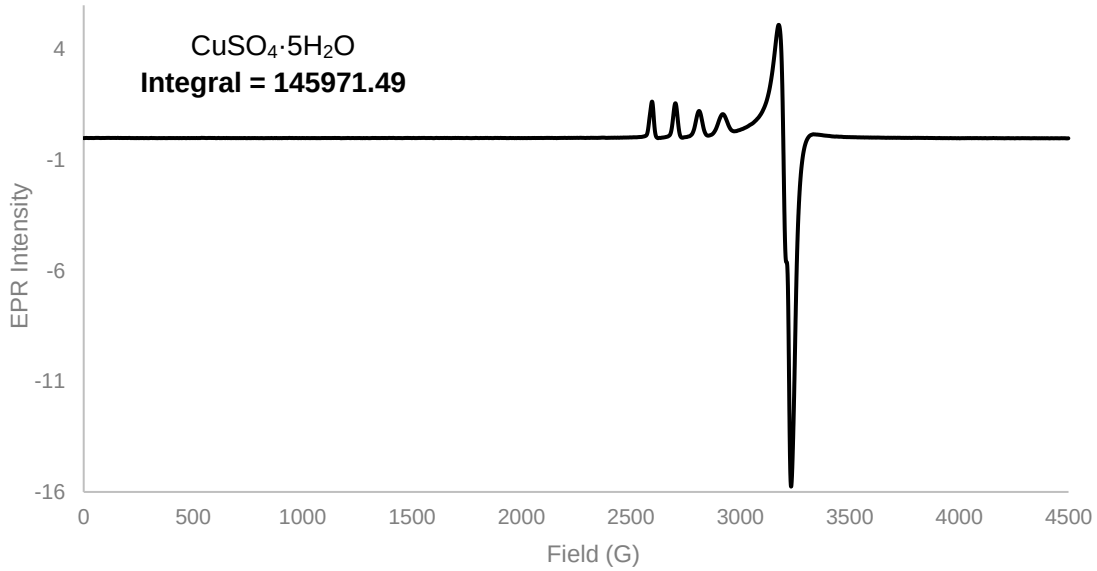

3.2.4.7. Cyclic voltammetry

The sample for Cyclic Voltammetry was measured in a potentiostat/galvanostat Autolab PGSTAT30. Experimental system involves a counter electrode (CE) of platinum, working electrode (WE) of carbon and reference electrode (RE) of $Ag/AgNO_3$. A 0.1 M solution of $N(n\text{-}Bu)_4PF_6$ in THF was used as blank solution. Solid ferrocene was added to the problem sample for potential correction in the square wave (SW) voltammogram.

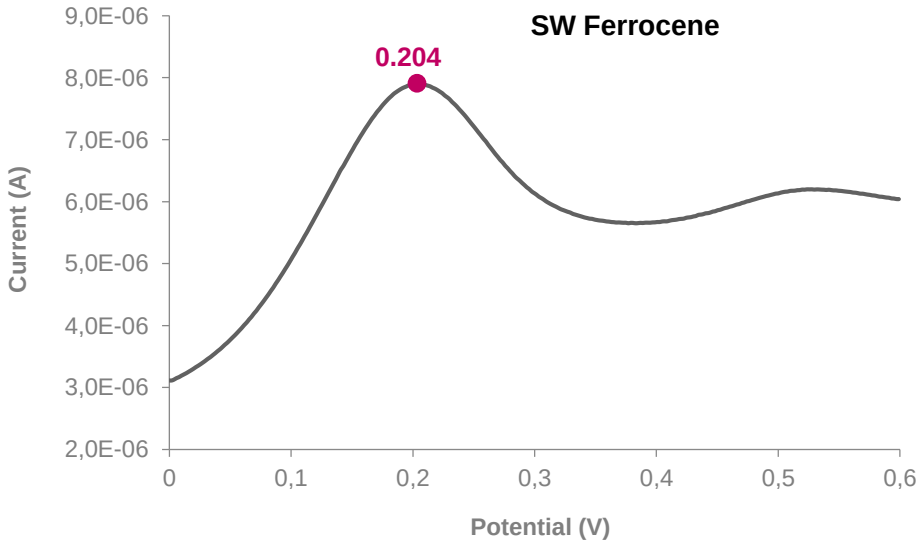

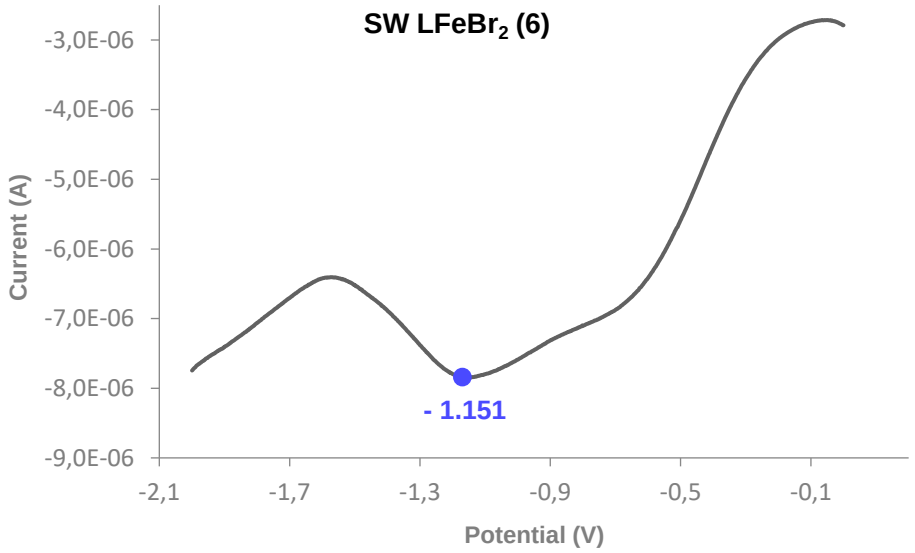

$$\boldsymbol{E_{red}(correction)} = E_{red}(Fe\ sample) - E_{red}(ferrocene) = \boldsymbol{-1.355\ V}$$

3.2.4.8. Mössbauer spectroscopy

$FeBr_2(THF)_2$ was prepared by simple stirring of $FeBr_2$ in THF at room temperature for 24 h in the glovebox. Then, metallic traces were removed with the stir bar, THF was removed and the light brown solid was dried under vacuum.

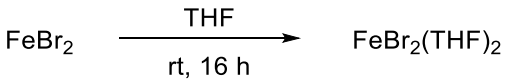

Table 2.2. Values of different fit species of Mössbauer spectra.

	fit1	fit2	fit1	fit2
δ	0.869	0.695	0.448	0.955
ΔE_Q	2.999	1.674	2.007	1.981
γ	0.281	0.500	0.385	0.336
Rel. Area	0.573	0.404	0.686	0.288
	Figure 2.14		**Figure 2.15**	

CHAPTER 3:

Ni-catalyzed hydroborylative cyclization of enynes

3.3. CHAPTER 3

3.3.1. Goal

After the success in the development of the Fe-catalyzed hydroborylative cyclization of enynes described in *Chapter 2*, and taking into account the renaissance of first-row transition metal-catalyzed reactions of synthetic interest, we were interested in the study of nickel catalysis in this context, in order to further expand the interest of this metal in the development of a broad range of innovative reactions.[195]

Regarding the recent Ni-catalyzed hydroborylative cyclization of enynes described by Cheng and Hsieh (*see* ***Scheme I.60***),[104] this reaction shows some limitations related to the use of a diboron reagent (meaning in the loss of one boryl unit during the process) and the restricted structural scope (specific enynes are required for the reaction to take place). Thus, we aimed to develop a more general and atom-economical Ni-catalyzed methodology for the synthesis of organoboronates by using HBpin as the boron source.

3.3.2. Precedents

Nickel complexes also play an essential role in the catalysis of the hydroboration of unsaturated species. In the literature, we find different Ni-based catalytic systems that efficiently perform the hydroboration of alkenes, alkynes and dienes, which involve novel activation pathways.

3.3.2.1. Ni-catalyzed hydroboration of alkenes

In 1994, Kabalka and co-workers published the first Ni-catalyzed hydroboration reaction.[196] A heterogeneous catalyst based on activated nickel powder affords the *anti*-Markovnikov selective hydroboration of some alkenes using catecholborane as the borylation agent (**Scheme 3.1**).

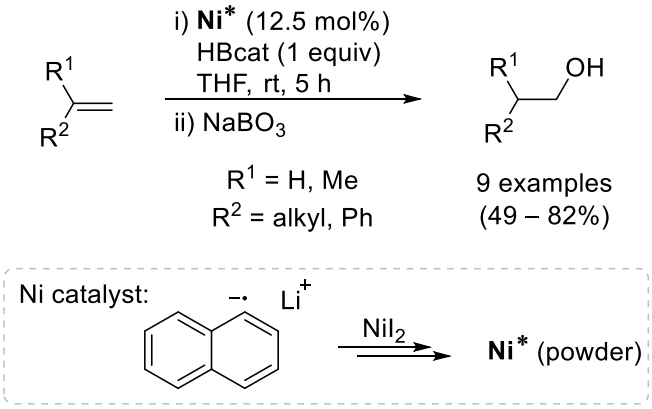

Scheme 3.1. The first described Ni-catalyzed hydroboration reaction.

Few years later, Srebnik tested Ni and Rh complexes for the hydroboration of alkenes and alkynes, showing the effectiveness of both catalysts with different olefins (**Scheme 3.**2).[197]

[104] J.-C. Hsieh, Y.-C. Hong, C.-M. Yang, S. Mannathan, C.-H. Cheng, *Org. Chem. Front.* **2017**, *4*, 1615–1619.
[195] S. Z. Tasker, E. A. Standley, T. F. Jamison, *Nature* **2014**, *509*, 299–309.
[196] G. W. Kabalka, C. Narayana, N. K. Reddy, *Synthetic Commun.* **1994**, *24*, 1019–1023.
[197] S. Pereira, M. Srebnik, *Tetrahedron Lett.* **1996**, *37*, 3283–3286.

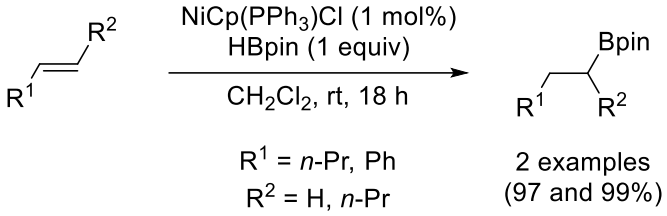

Scheme 3.2. Ni-catalyzed hydroboration of alkenes described by Srebnik.

Yorimitsu and Oshima studied the catalysis of the hydroboration of α,β-unsaturated esters and amides with Ni(0) complexes and phosphine ligands (**Scheme 3.3**).[198] Despite the reaction shows a broad scope and affords good yields, bis(pinacolato)diboron is used in the reaction and only one boryl unit is incorporated into the structure.

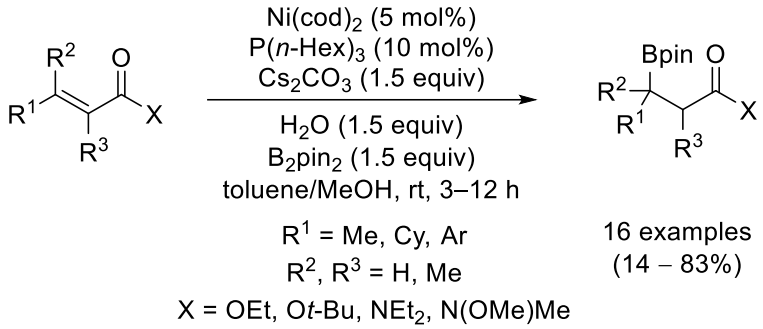

Scheme 3.3. Ni-catalyzed hydroboration of α,β-unsaturated species.

The reaction pathway begins with the coordination of the Ni(0) starting complex to the alkene followed by the coordination of the carbonyl moiety to the diboron reagent. The Lewis acidity of the boron promotes the formation of a π-allyl complex which undergoes transmetalation of one boryl unit. Finally, reductive elimination and protonolysis of the boryl enolate with MeOH close the catalytic cycle and yield the corresponding boronate (**Figure 3.1**).

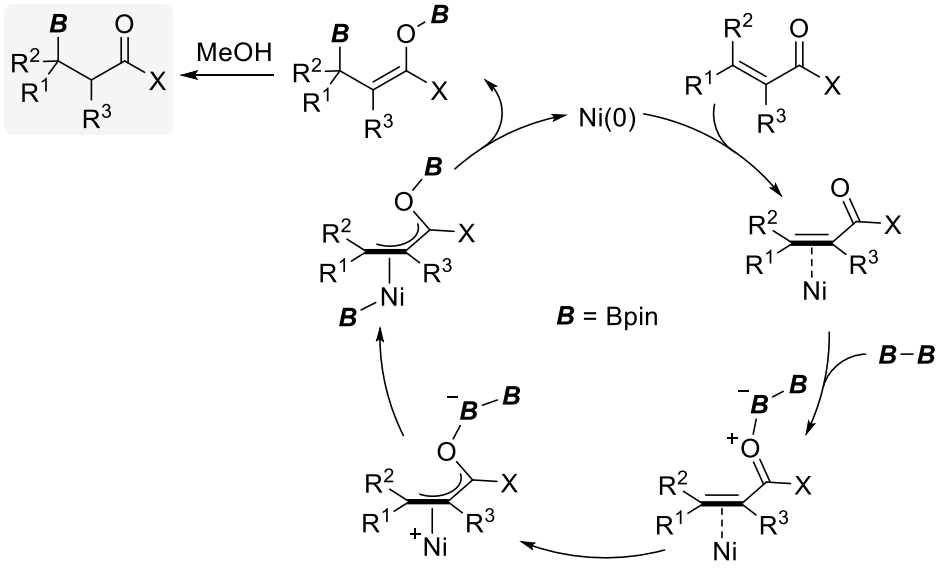

Figure 3.1. Plausible catalytic cycle for the hydroboration of α,β-unsaturated species.

[198] K. Hirano, H. Yorimitsu, K. Oshima, *Org. Lett.* **2007**, *9*, 5031−5033.

They also applied this methodology to vinylcyclopropanes, which undergo Ni-catalyzed borylative ring opening to yield allylic boronates with excellent *E*-selectivity (**Scheme 3.4**).[199] The authors propose a similar mechanism than the one previously described.

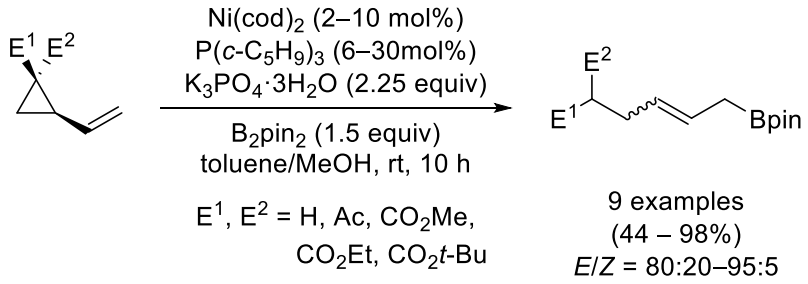

Scheme 3.4. Ni-catalyzed borylative ring opening of vinylcyclopropanes.

Another example of Ni-catalyzed borylative ring opening was performed by Pineschi.[200] Several vinyl epoxides and aziridines were tested under the optimal reaction conditions, followed by one-pot oxidation or reaction with aldehydes (**Scheme 3.5**).

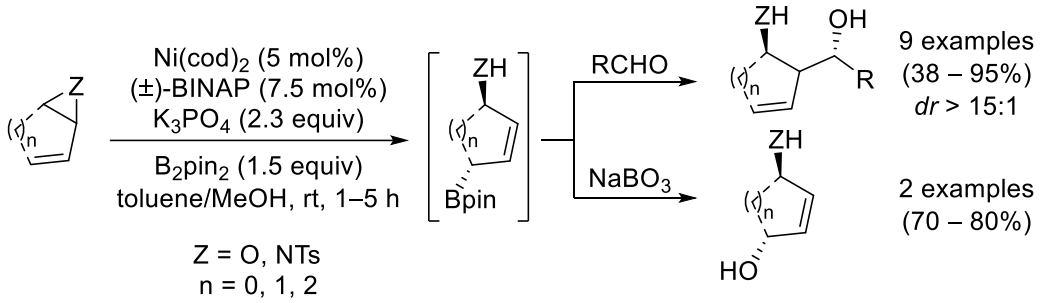

Scheme 3.5. Ni-catalyzed borylative ring opening described by Pinechi.

Fernández and co-workers developed an efficient asymmetric version of the hydroboration of α,β-unsaturated esters for the synthesis of alkylboronates with high yields and excellent enantioselectivities (**Scheme 3.6**).[201] The proposed reaction mechanism is similar to that proposed by Oshima *et al*.

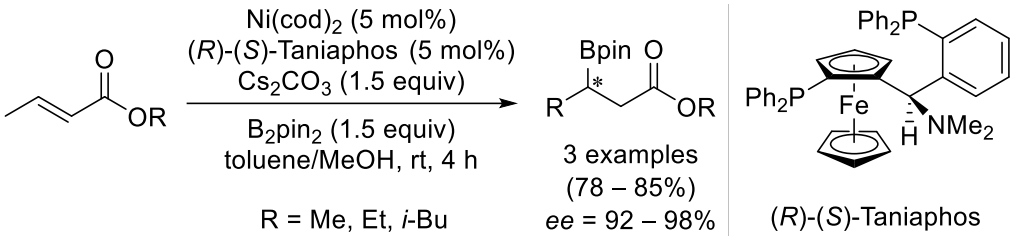

Scheme 3.6. Ni-catalyzed hydroboration reaction described by Fernández.

Schomaker group found that heteroleptic nickel complexes catalyze the Markovnikov-selective hydroboration of styrenes.[202] They envisioned that the *trans* effect of the NHC

[199] Y. Sumida, H. Yorimitsu, K. Oshima, *Org. Lett.* **2008**, *10*, 4677−4679.
[200] S. Crotti, F. Bertolini, F. Macchia, M. Pineschi, *Org. Lett.* **2009**, *11*, 3762−3765.
[201] V. Lillo, M. J. Geier, S. A. Wescott, E. Fernández, *Org. Biomol. Chem.* **2009**, *7*, 4674−4676.
[202] E. E. Touney, R. V. Hoveln, C. T. Buttke, M. D. Freidberg, I. A. Guzei, J. M. Schomaker, *Organometallics* **2016**, *35*, 3436–3439.

ligand could increase the rate of the phosphine dissociation. Indeed, the process works in high yields with good functional group compatibility (**Scheme 3.7**)

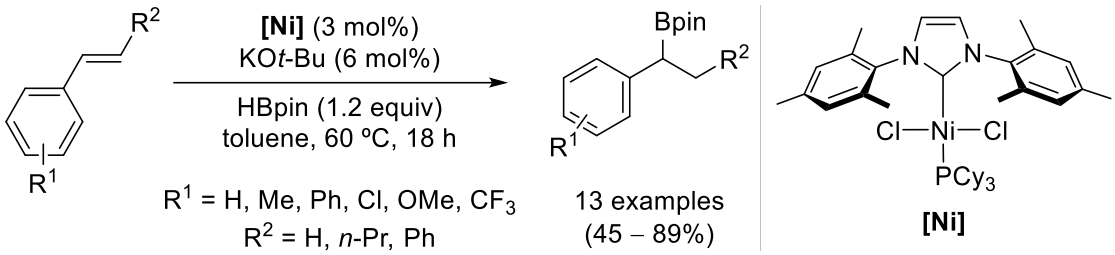

Scheme 3.7. Ni-catalyzed Markovnikov-selective hydroboration of alkenes.

The Ni(II) precatalyst is proposed to be reduced by HBpin to generate the catalytically active Ni(0) species. Dissociation of the phosphine ligand promotes the oxidative addition of HBpin, followed by the alkene insertion into the Ni–H bond. Finally, reductive elimination produces the new C–B bond and regenerates the Ni(0) catalyst (**Figure 3.2**).

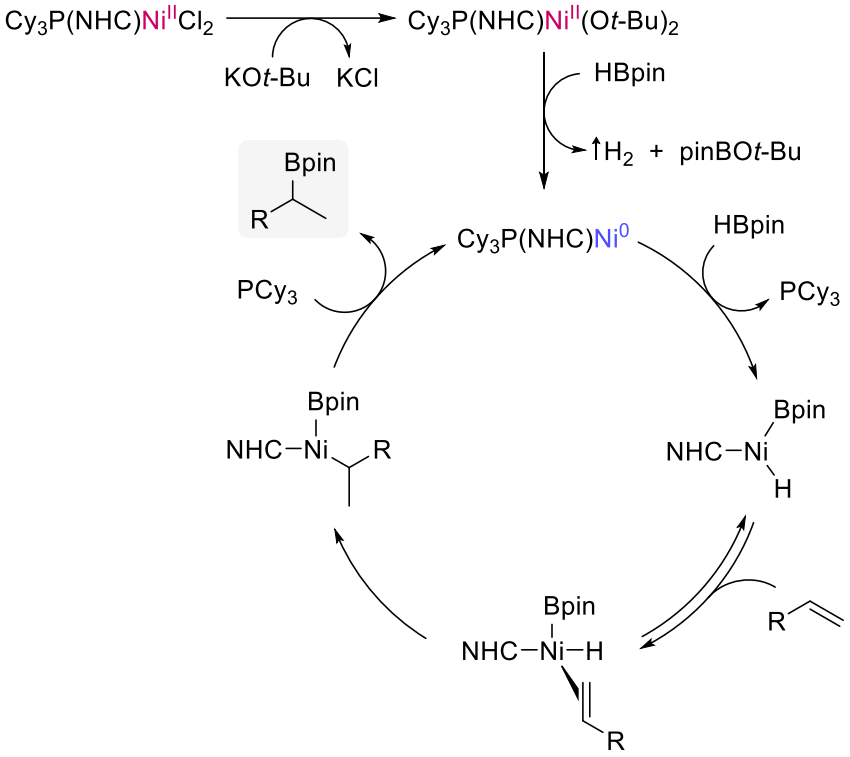

Figure 3.2. Proposed catalytic cycle for the Ni-catalyzed hydroboration of styrenes.

Wang and Ye performed the Ni-catalyzed hydroboration of aliphatic and aromatic alkenes with B_2pin_2 in the absence of an external base.[203] They proposed the alcoholic solvent, which acts as the hydrogen source, accelerates the reaction and makes unnecessary the use of stoichiometric amounts of base. The reaction takes place with moderate to high yields (**Scheme 3.8**).

[203] J.-F. Li, Z.-Z. Wei, Y.-Q. Wang, M. Ye, *Green Chem.* **2017**, *19*, 4498–4502.

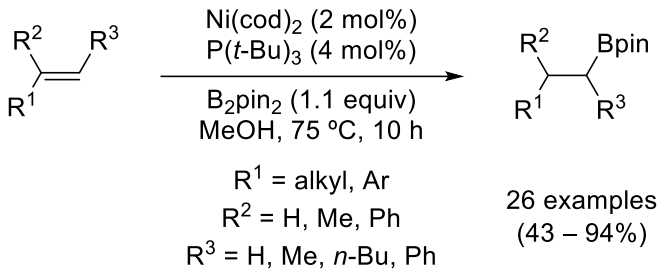

Scheme 3.8. Base-free Ni-catalyzed hydroboration of alkenes.

The proposed catalytic cycle starts with the oxidative addition of B_2pin_2 to the Ni(0) precatalyst. Then, insertion of the alkene in the Ni–B bond followed by transmetalation with MeOH results in a Ni-hydride intermediate. Finally, reductive elimination regenerates the active Ni(0) species and delivers the desired alkylboronate.

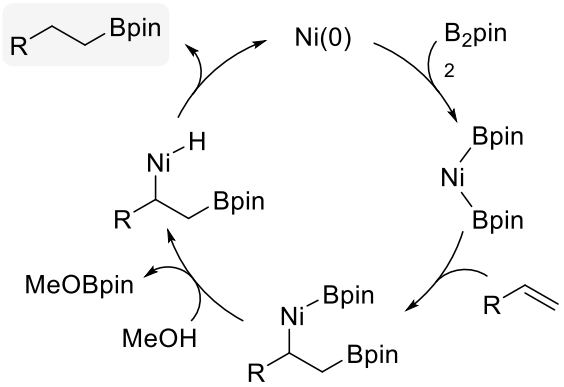

Figure 3.3. Putative reaction mechanism proposed by Wang and Ye.

Kamei described the *anti*-Markovnikov Ni-catalyzed hydroboration of several styrenes.[204] The use of water instead of other alcohols as solvent provides the best results (**Scheme 3.9**). The authors propose a similar mechanism to that proposed by Wang and Ye (*see above*).

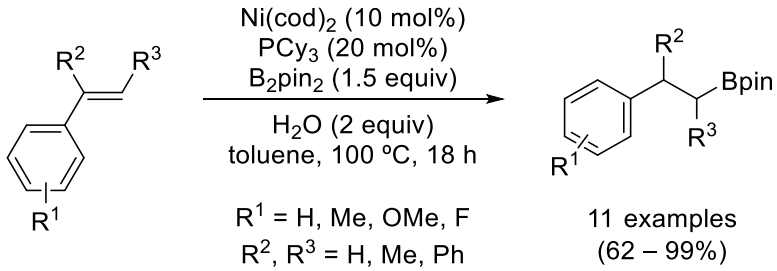

Scheme 3.9. Ni-catalyzed hydroboration of styrenes described by Kamei.

Recently, Mandal and co-workers employed non-innocent ligands in Ni-complexes for the catalytic hydroboration of styrenes. The reaction smoothly proceeds to yield Markovnikov hydroboration products in short reaction times (**Scheme 3.10**).[205]

[204] T. Kamei, S. Nishino, T. Shimada, *Tetrahedron Lett.* **2018**, *59*, 2896–2899.
[205] G. Vijaykumar, M. Bhunia, S. K. Mandal, *Dalton Trans.* **2019**, *48*, 5779–5784.

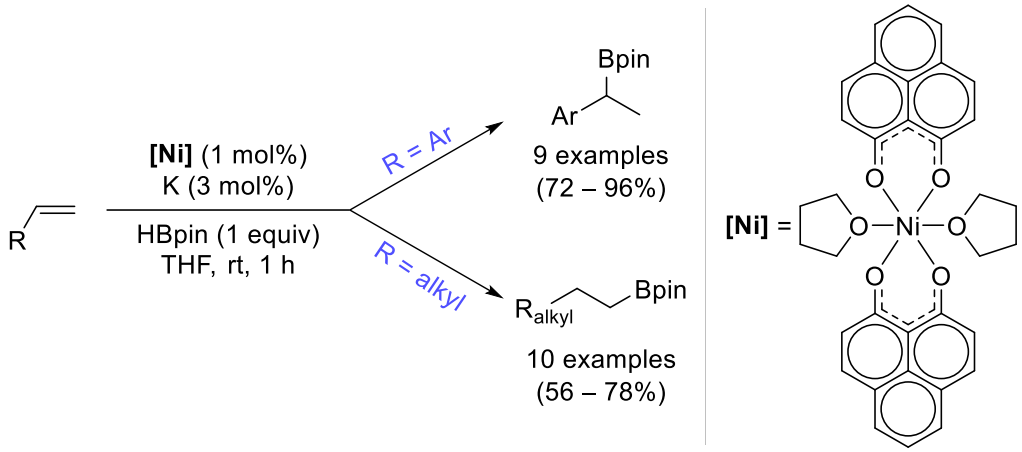

Scheme 3.10. Non-innocent ligand-based nickel catalyst.

This ligand acts as an electron reservoir, promoting the reaction to follow a radical pathway that takes place through a single electron transfer (SET), leading to the cleavage of the B–H bond (**Figure 3.4**).

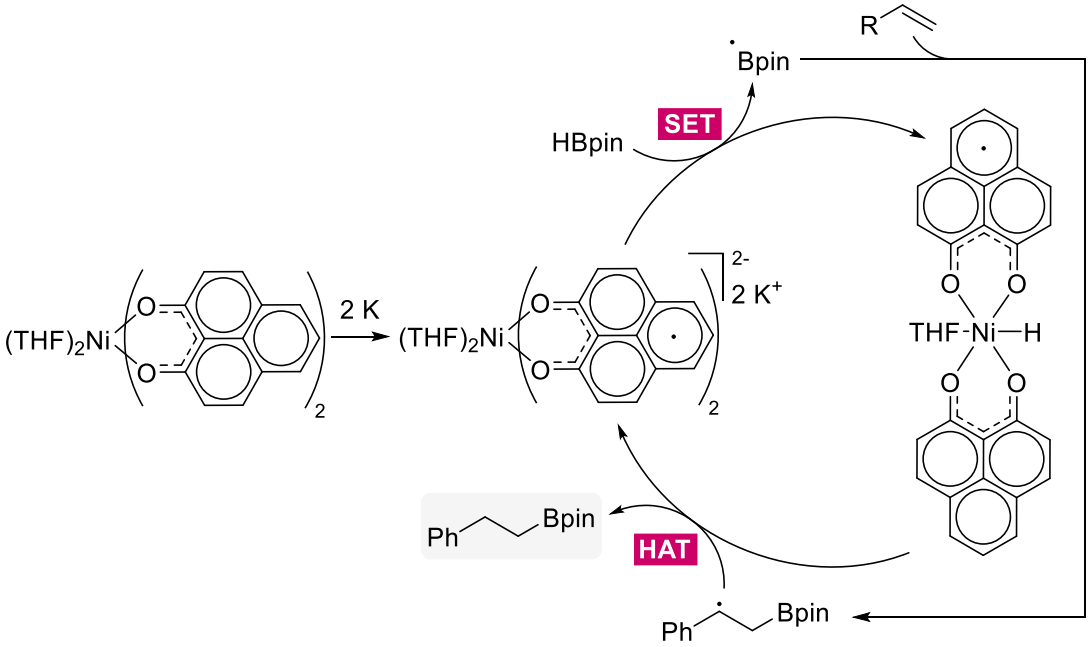

Figure 3.4. Proposed radical pathway for the Ni-catalyzed hydroboration of styrenes.

3.3.2.2. Ni-catalyzed hydroboration of alkynes

The methodology described by Srebnik for the nickel-catalyzed hydroboration of alkenes (*vide supra*) was also applied to terminal alkynes.[197] The reaction smoothly proceeds to the hydroboration on the distal position, affording alkenylboronates in quantitative yields (**Scheme 3.11**).

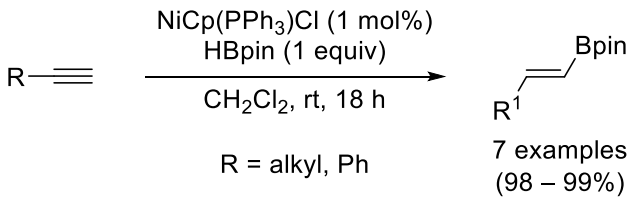

Scheme 3.11. Ni-catalyzed hydroboration of alkynes described by Srebnik.

Zaidlewicz an co-workers performed the chemoselective Ni-catalyzed hydroboration of 1,3-enynes.[206] The use of a phosphine-based Ni(II) complex with catecholborane led to the formation of alkenylboronates with good yields (**Scheme 3.12**).

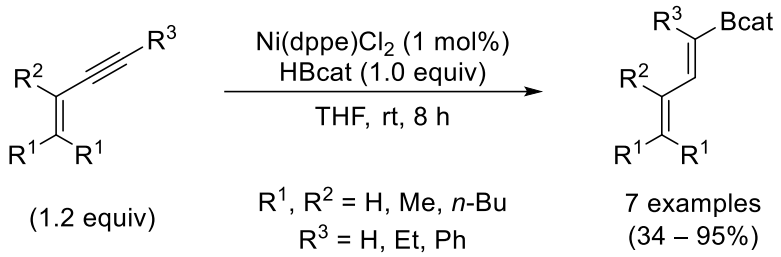

Scheme 3.12. Ni-catalyzed hydroboration of 1,3-enynes.

This group also extended the hydroboration reaction to simple and functionalized alkynes.[207] This methodology requires mild reaction conditions and yields alkenylboronates with excellent regioselectivity in the case of terminal alkynes (**Scheme 3.13**).

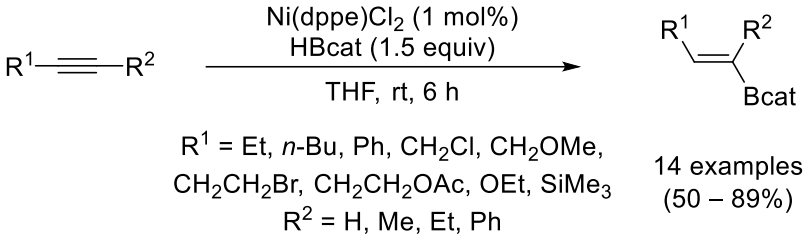

Scheme 3.13. Ni-catalyzed hydroboration of functionalized alkynes.

3.3.2.3. Ni-catalyzed hydroboration of dienes

Zaidlewicz also describes the Ni-catalyzed 1,2-hydroboration of conjugated dienes where the borylation takes places in the terminal carbon of the alkene (**Scheme 3.14**).[208]

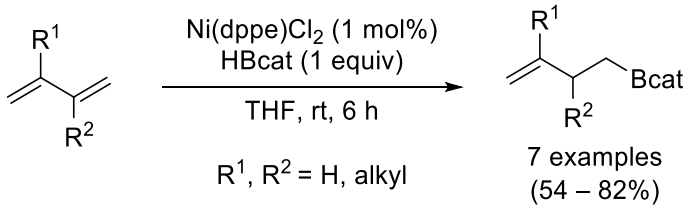

Scheme 3.14. The first described Ni-catalyzed hydroboration of 1,3-dienes.

In 2010, Morken and co-workers carried out the 1,4-hydroboration of 1,3-dienes using Ni(0)/PCy_3 catalysis.[209] The reaction leads to the regio- and stereoselective synthesis of allylboronates with good yields (**Scheme 3.15**). In the case of internal alkenes, borylation occurs at the less hindered carbon of the diene.

[197] S. Pereira, M. Srebnik, *Tetrahedron Lett.* **1996**, *37*, 3283–3286.
[206] M. Zaidlewicz, J. Meller, *Collect. Czech. Chem. Commun.* **1999**, *64*, 1049–1056.
[207] M. Zaidlewicz, J. Meller, *Main Group Met. Chem.* **2000**, *23*, 765–772.
[208] M. Zaidlewicz, J. Meller, *Tetrahedron Lett.* **1997**, *38*, 7279–7282.
[209] R. J. Ely, J. P. Morken, *J. Am. Chem. Soc.* **2010**, *132*, 2534–2535.

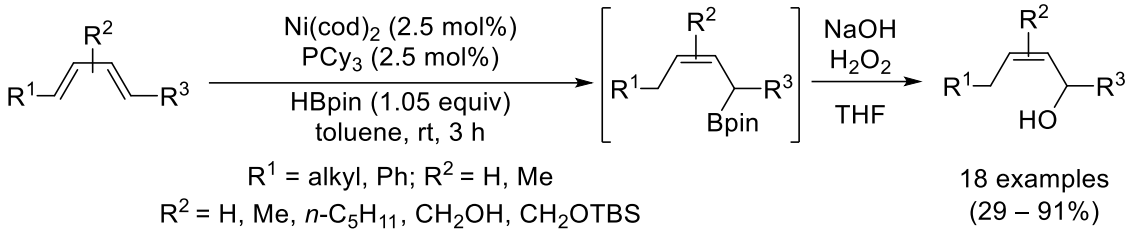

Scheme 3.15. Ni-catalyzed 1,4-hydroboration of dienes.

The reaction pathway involves an initial coordination or oxidative cyclometalation of the starting Ni(0) complex with the diene followed by reaction with HBpin to afford a π-allyl complex, which undergoes reductive elimination to yield the observed boronate (**Figure 3.5**).

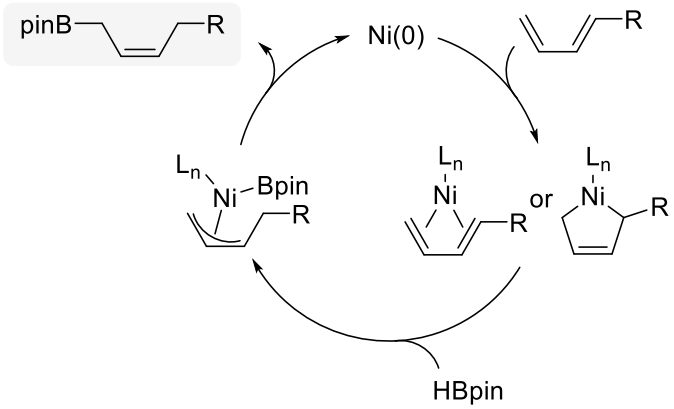

Figure 3.5. Plausible mechanism for the 1,4-hydroboration of conjugated dienes.

Few years later, the same research group described the diastereoselective version of this reaction for the synthesis of chiral dienols (**Scheme 3.16**).[210] Besides, they performed further functionalization of the structure by different processes such us oxidation, homologation and protodeboronation.

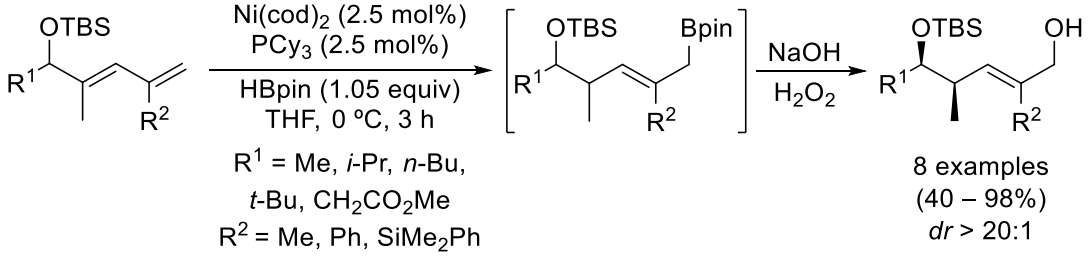

Scheme 3.16. Ni-catalyzed hydroboration of dienes for the synthesis of dienols.

[210] R. J. Ely, Z. Yu, J. P. Morken, *Tetrahedron Lett.* **2015**, *56*, 3402–3405.

3.3.3. Results

We began our study by extrapolating the previously optimized reaction conditions for the Fe-catalyzed hydroborylative cyclization (*Chapter 2*) to a similar Ni system. Thus, we evaluated the reaction between enyne **1aa**, pinacolborane, $NiCl_2$, biquinoline and different activating agents (**Scheme 3.17**). However, no borylated compounds were detected in the reaction crude, and we observed either unaltered starting enyne or decomposition.

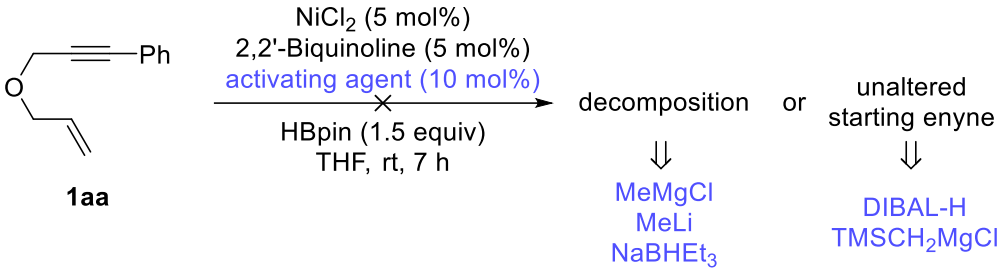

Scheme 3.17. Inicial attempts.

As it can be seen in the literature mentioned above, the usually employed catalytic systems involve a Ni(0) precatalyst, generally $Ni(cod)_2$, and phosphine ligands. Therefore, we tested this kind of conditions with our enyne and pinacolborane. After an extensive ligand screening, also including nitrogen-based ligands, we found that only when Xantphos was used a mixture of borylated compounds were obtained in moderate overall yield (**Scheme 3.18**). With the rest of ligands, only the unreacted enyne was observed. Additionally, terpyridine furnished the hydroboration product **2aa'** detected in the Fe-system, albeit in low yield. It is important to mention that, in contrast with the previously developed Fe-system, three different boronates were obtained, comprising two alkylboronates (**2aa** and **12aa**) and one alkenylboronate (**11aa**). The corresponding reduced cyclic compound (**13aa**) was also observed, but in low amounts. Our aim was then not only to try to increase the reaction yield, but also to study and, hopefully, to try to control the regioselectivity of the reaction.

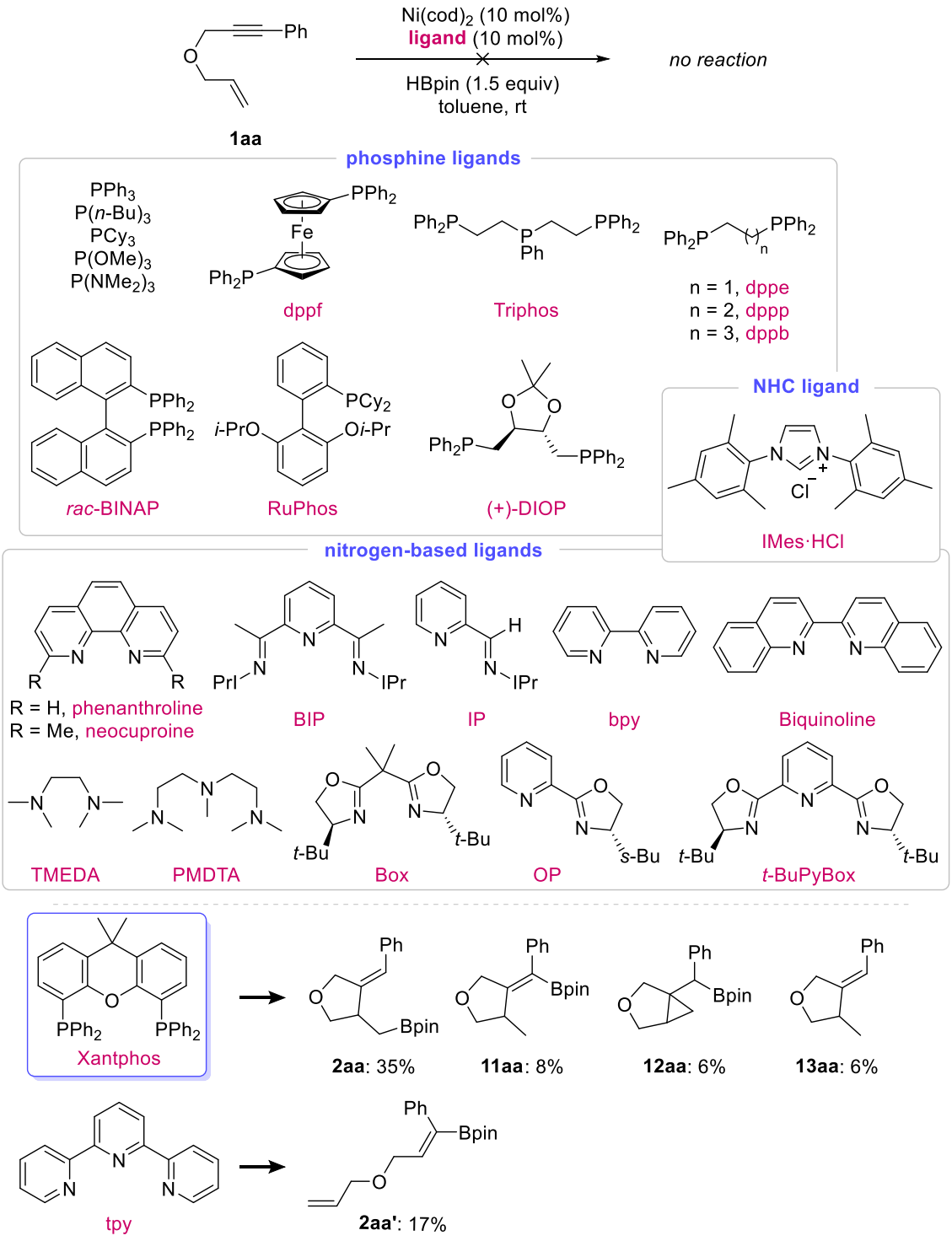

Scheme 3.18. Ligand screening.

Encouraged by the positive result, we next evaluated different reaction parameters to optimize the reaction. First, we reduced the catalyst loading and tested different Ni sources (**Table 3.1**). Similar results were obtained with 5 mol% of $Ni(cod)_2$/Xantphos mixture (entry 2). Ni(II) salts did not work under these conditions (entry 4 – 8), except for $Ni(acac)_2$, which slightly improves **2aa** yield (entry 3). Additionally, we checked whether the reaction worked in the absence of Xantphos (entry 9), with negative result, as expected.

Table 3.1. Optimization of Ni salt and catalyst loading.

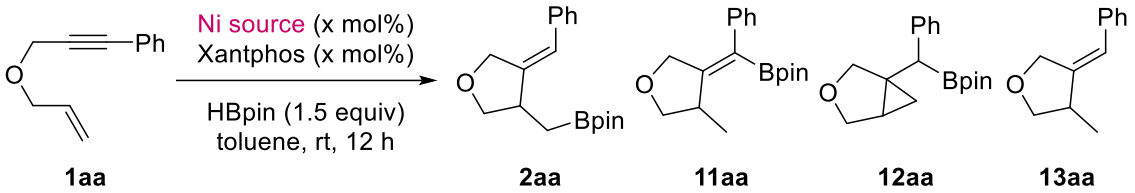

1aa **2aa** **11aa** **12aa** **13aa**

Entry	Ni source	x mol%	Yield (%)[a]			
			2aa	**11aa**	**12aa**	**13aa**
1[b]	$Ni(cod)_2$	10	35	8	6	6
2[b]	$Ni(cod)_2$	5	36	9	6	6
3[b]	**$Ni(acac)_2$**	**5**	38	9	7	3
4	$NiCl_2$	5	–	–	–	–
5	$Ni(Py)_4Cl_2$	5	–	–	–	traces
6	$Ni(PPh_3)_2Cl_2$	5	–	–	–	–
7	$NiCl_2$·glyme	5	–	–	–	–
8	$Ni(OAc)_24H_2O$	5	–	–	–	traces
9[c]	$Ni(acac)_2$	5	–	–	–	–

[a] Isolated yield. [b] Time reaction was 7 h. [c] No Xantphos was used.

Since no Ni(II) precatalyst was able to perform the hydroborylative cyclization reaction, except $Ni(acac)_2$, we envisioned that the use of an reducing agent might offer a different approach to carry out this process (**Table 3.2**). Indeed, we obtained similar reaction yield when MeMgCl (10 mol%) was added with $Ni(Py)_4Cl_2$ as Ni source (entry 1). However, the addition of MeMgCl with the rest of the Ni(II) complexes did not afford positive results (entry 2 – 4).

Table 3.2. Screening the performance of different Ni(II) salts in the presence of MeMgCl.

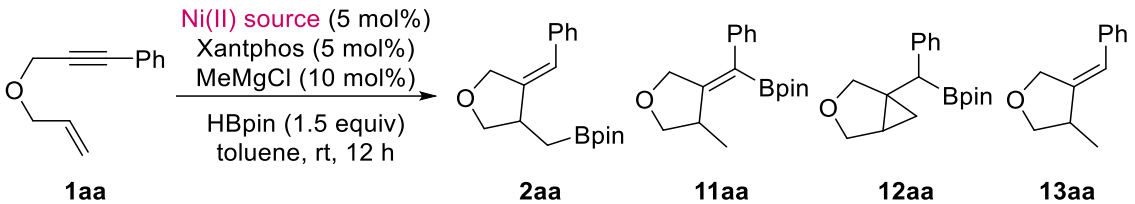

1aa **2aa** **11aa** **12aa** **13aa**

Entry	Ni(II) source	Yield (%)[a]			
		2aa	**11aa**	**12aa**	**13aa**
1	$Ni(Py)_4Cl_2$	33	7	9	–
2	$NiCl_2$	22	4	–	3
3	$Ni(PPh_3)_2Cl_2$	17	4	1	–
4	$NiCl_2$·glyme	18	5	–	3

[a] Isolated yield.

In the same way, we tested the influence of an activating agent for the reaction catalyzed by $Ni(acac)_2$ (**Table 3.3**). Unfortunately, no increase of reaction yield was observed.

Table 3.3. Screening of activating agents with $Ni(acac)_2$.

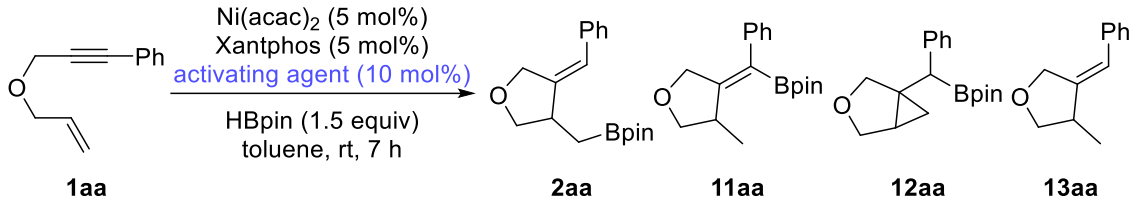

1aa **2aa** **11aa** **12aa** **13aa**

Entry	Activating agent	Yield (%)[a]			
		2aa	**11aa**	**12aa**	**13aa**
1	MeMgCl	31	3	1	2
2	$NaBHEt_3$	28	3	4	11
3	DIBAL-H	32	8	10	4

[a] Isolated yield.

Since we are interested in developing green and eco-friendly synthetic methods, and addition of reducing agents hardly improved the reaction performance, we dismissed the addition of any external agent and continue with the study employing $Ni(acac)_2$ and Xantphos as the catalytic system. Next, we evaluated different reaction conditions, comprising temperature, solvent and Ni/L ratio (**Table 3.4**). We concluded that toluene is the best solvent to carry out this transformation (entry 1) and the use of higher ligand amount does not improve the reaction yield (entry 3).

Table 3.4. Other parameters optimization.

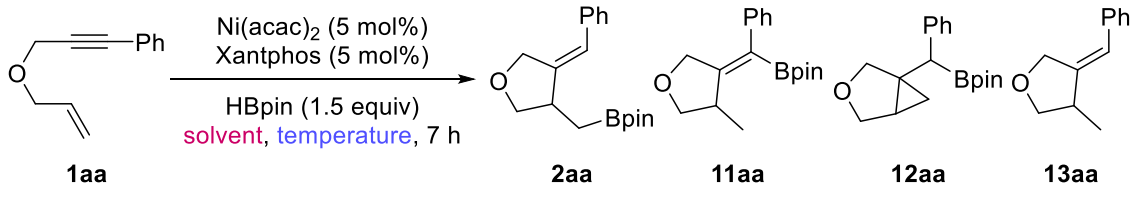

1aa **2aa** **11aa** **12aa** **13aa**

Entry	solvent	temperature	Yield (%)[a]			
			2aa	**11aa**	**12aa**	**13aa**
1	toluene	rt	38	9	7	3
2	toluene	50 °C	32	9	9	7
3[b]	toluene	rt	27	3	7	3
4	THF	rt	34	7	6	16
5	*i*-Pr_2O	rt	37	6	7	6
6	1,4-dioxane	rt	30	8	5	16
7	DMF	rt	31	–	5	15
8	xylene	rt	25	4	5	6

[a] Isolated yield. [b] 10 mol% of Xantphos was used.

Finally, other ligands structurally similar to Xantphos were evaluated in order to get better results (**Scheme 3.19**).

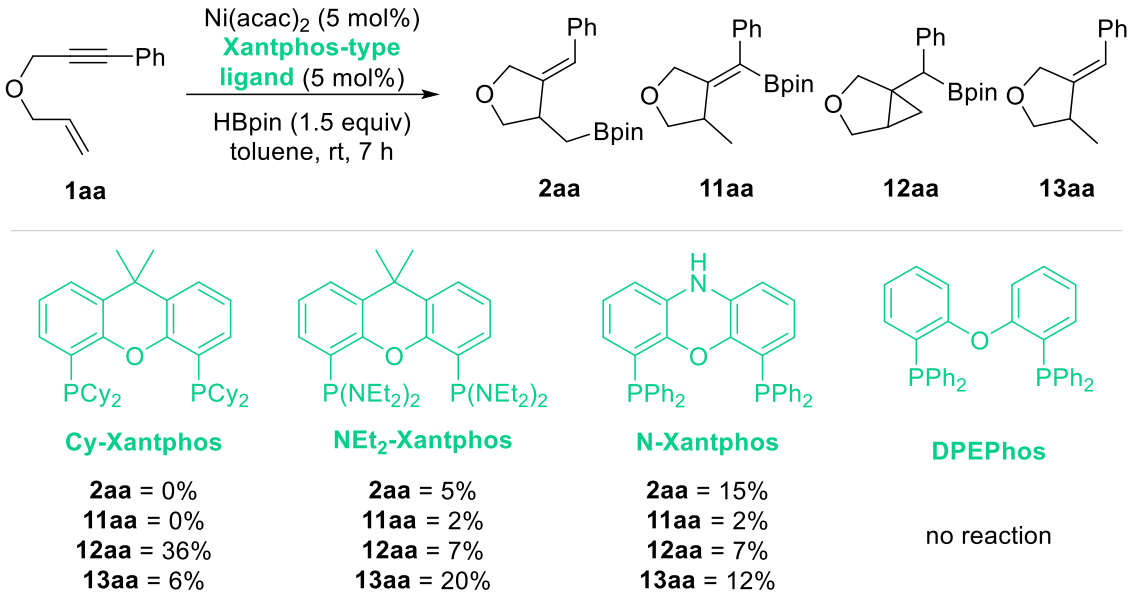

Scheme 3.19. Xantphos-type ligands screening.

Despite our efforts, we were not able to improve the reaction effectiveness. Thus, we assumed that the optimal reaction conditions comprise the use of $Ni(acac)_2$ (5 mol%) and Xantphos (5 mol%) in toluene at room temperature, yielding the alkylboronate **2aa** as the major reaction product (38% yield).

Later, we decided to study the structural scope of this transformation. To our delight, when we extended the reaction to a wide variety of different substrates containing an aryl ring on the alkyne, much better yields were obtained. Interestingly, with this kind of aryl derivatives, only alkylboronates (**2**) were formed. The reaction shows a broad scope, tolerating different tethering groups between the alkene and the alkyne, as well as a wide variety of substituents on the aromatic ring (**Scheme 3.20**). Thus, for ether derivatives, electron donating (Me and OMe) and electron withdrawing (Cl, CN and CF_3) groups on the aryl ring gave the corresponding alkylboronates (**2aa**-**af**). Better yields were observed for the sulfonamide derivatives (**2bb**-**bh**), for the malonate compounds (**2cc**-**2cg**) and for quaternary carbon-containing precursor species (**2da**-**db**). The presence of a ketone group conjugated to the alkyne effectively afforded borylated cyclopentanones (**2fa**-**fb**). 1,7-Enynes gave the corresponding six membered ring derivatives albeit in low yields (**2ah** and **2bl**), probably due to entropic reasons. This may also be the case for CH_2-connected compounds (**2ea**-**eb**) that lack a potential Thorpe–Ingold effect. There does not seem to be a correlation between the yields and the electron richness of the ring. The reaction also takes place with pyridine derivative **1bi** (**2bi**). The smooth reaction conditions render this process compatible with haloarene, acetal, ester, sulfonamide, nitrile, and ketone groups. However, the presence of a chloro motif in the aromatic ring afforded poorer yields (**2ad** and **2be**), probably due to the well-known ability of Ni to activate C(sp^2)-Cl bonds.[211] In addition, the reaction can be scale

[211] (a) C. Chena, L.-M. Yang, *Tetrahedron Lett.* **2007**, *48*, 2427–2430. (b) S. Ge, J. F. Hartwig, *J. Am. Chem. Soc.* **2011**, *133*, 16330–16333. (c) S. Bajo, G. Laidlaw, A. R. Kennedy, S. Sproules, D. J. Nelson, *Organometallics* **2017**, *36*, 1662–1672. (d) G. Gao, Y. Fu, M. Li, B. Wang, B. Zheng, S. Hou, P. J. Walsh, *Adv. Synth. Catal.* **2017**, *359*,

to 1 mmol with better results (**2cc**, yield in brackets). The configuration of the C–C double bond in products **2** is in accordance with the occurrence of a *cis*-selective carbometalation involving an intermediate complex with, at least, coordinated alkyne.

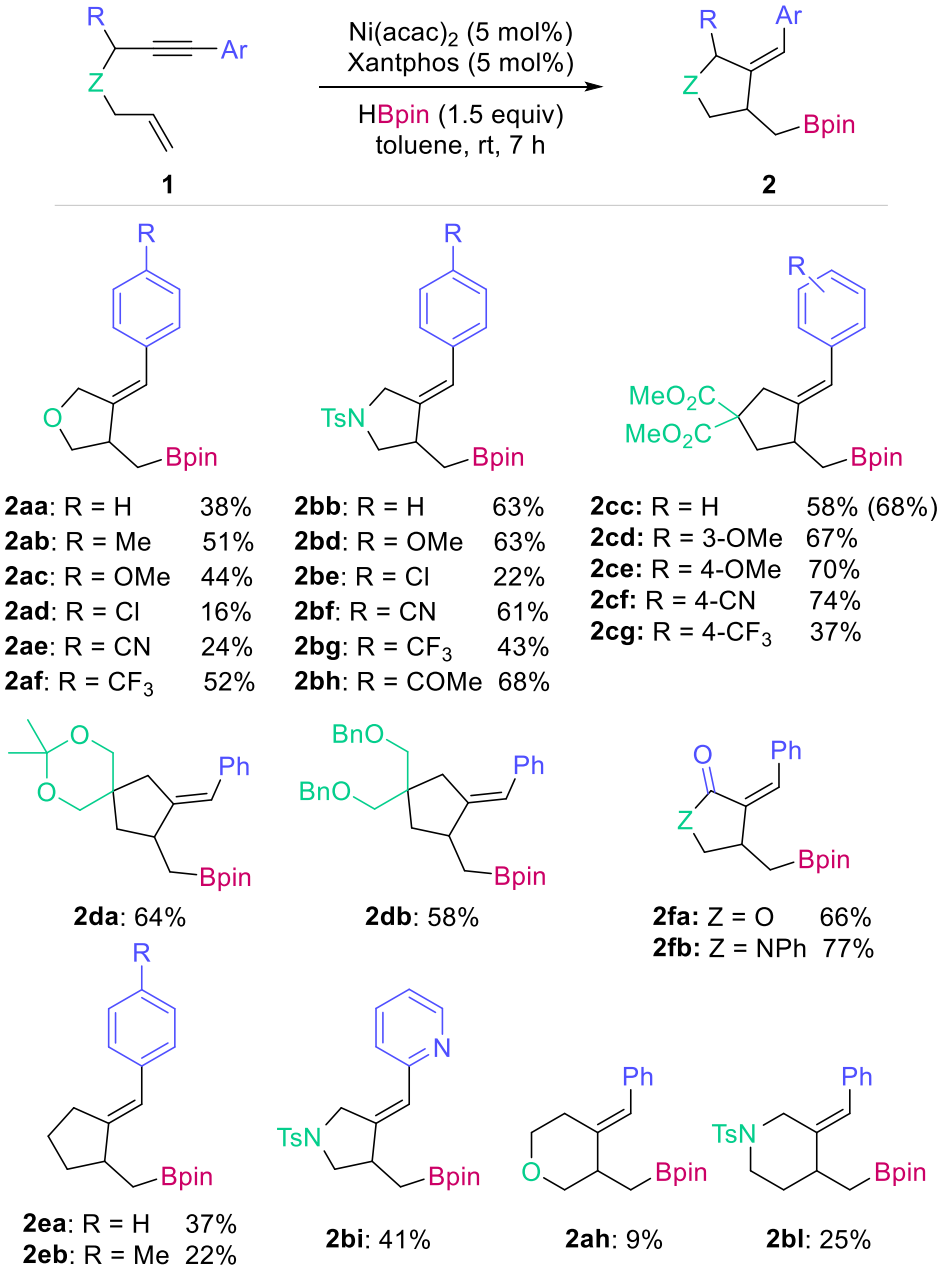

Scheme 3.20. Reaction scope for the hydroborlative cyclization of aryl-substituted enynes.

Interestingly, the regioselectivity of the reaction changes completely when alkyl-substituted alkynes, such as enyne **1bn**, are subjected to the reaction conditions (**Scheme 3.21**). In this case, the boryl group incorporates into the external alkyne carbon affording a cyclic alkenylboronate in high yield (**11bn**).

2890–2894. (e) C. M. Lavoie, R. McDonald, E. R. Johnson, M. Stradiotto, *Adv. Synth. Catal.* **2017**, *359*, 2972–2980. (f) R. S. Sawatzky, M. J. Ferguson, M. Stradiotto, *Synlett* **2017**, *28*, 1586–1591.

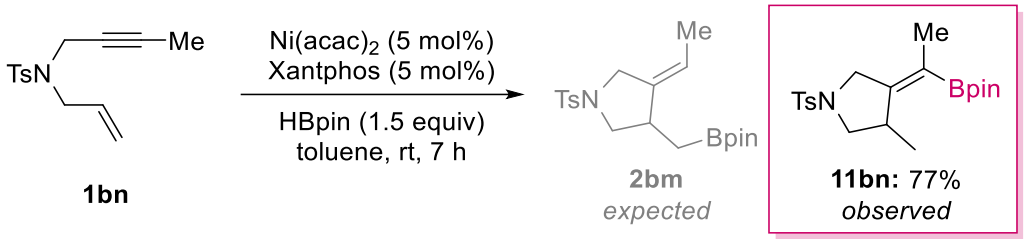

Scheme 3.21. Hydroborylative cyclization of alkyl-substituted enyne **1bn**.

Therefore, we decided to evaluate the scope of several alkyl-subtituted enynes (**Scheme 3.22**). The highest yields were observed for the formation of pyrrolidine compounds, showing different substituents on the tethering N atom. Thus, substrates with tosyl (**11bn**-**bs**), phenyl (**11bw**) and benzoyl (**11bx**) groups provided good to excellent results. In contrast, ether and malonate derivatives furnished poor yields (**11an** and **11cb**). The presence of a stereogenic center on the propargylic or allylic positions resulted in fully diastereoselective reactions (**11by** and **11bz**). The relative configuration of the new stereogenic centers in **11by** could be determined by single crystal X-ray diffraction, revealing *trans* arrangements for Ph and Me groups. The presence of a Me substituent on the allylic carbon (**1bz**) afforded a vicinal dimethyl product with both methyl groups in a *trans* configuration (**11bz**), as determined on the basis of NMR analysis.

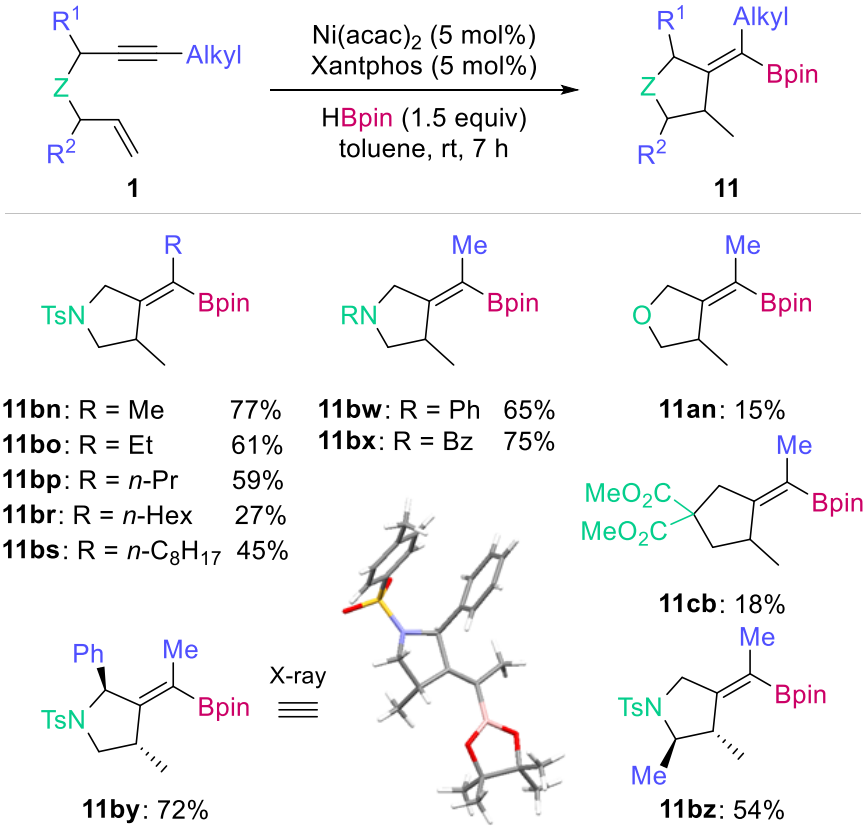

Scheme 3.22. Structural scope of alkenylboronates **11**.

The configuration of the new C–C double bond was confirmed by X-ray diffraction of **11by** (**Scheme 3.22**). Previous nOe measurements suggested the same configuration as well (**Figure 3.6**).

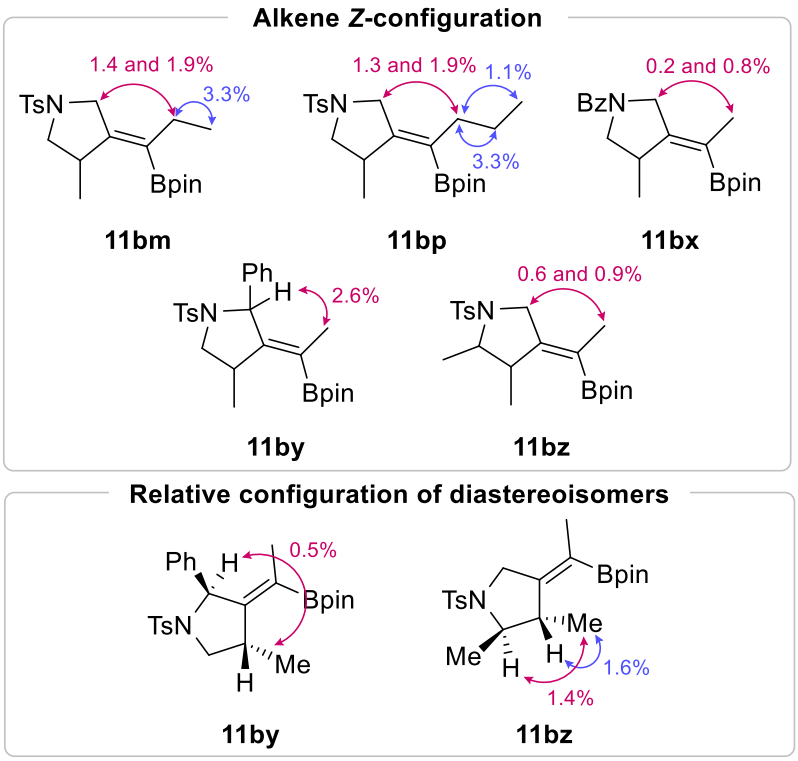

Figure 3.6. nOe measurements of some alkenylboronates **11**.

In contrast to the above mentioned results, we were not able to find the desired cyclized alkyl- or alkenylboronates for substrates containing an alkene conjugated to a ketone group, in spite of this kind of substrates constituted the optimal enynes for the hydroborylative cyclization described by Hsieh and Cheng.[104] Noticeably, the reaction of enones **1g** under our optimized conditions led to the formation of reductive cyclization derivatives (**13**) in moderate yields, without incorporation of the boryl fragment (HBpin acts as a reducing agent). In this case, the same kinds of products are obtained for both aryl- (**13ga** and **13gd**) and alkyl-substituted (**13gb** and **13gc**) alkynes. NTs and methylene could be used as tethering groups (**Scheme 3.23**).

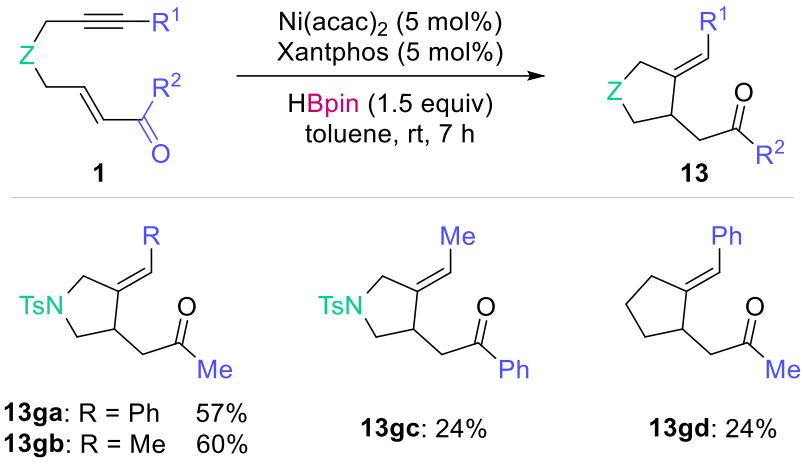

Scheme 3.23. Reaction with enynes bearing enones (**1g**).

The formation of compounds **13g** probably involves the generation of a boron enolate that is hydrolyzed during the reaction work-up, rather than the incorporation of a second hydride, since the reaction requires less than 2 equiv of HBpin (**Figure 3.7**).

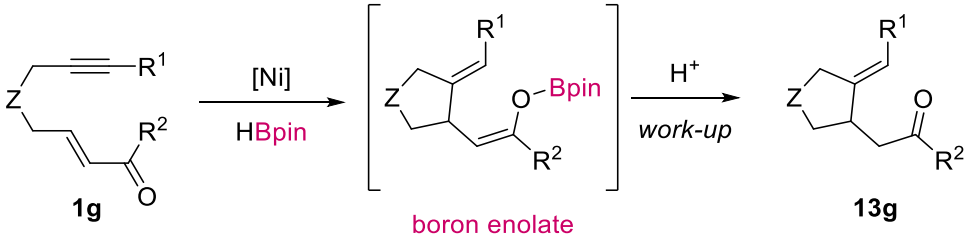

Figure 3.7. Putative formation of boron enolate.

Unfortunately, the reaction scope is limited to unsubstituted alkenes, since several enynes with substitution in the internal (**1ai**, **1aj**, **1ao**) or distal (**1ak**, **1al**) carbon of the alkene did not work under optimal conditions. Enynes with terminal alkyne (**1ba**, **1ca**) did not afford the desired boronates either (**Scheme 3.24**). The nitrophenyl moiety of enyne **1ch** was reduced under reaction conditions to the corresponding aniline derivative in moderate yield.

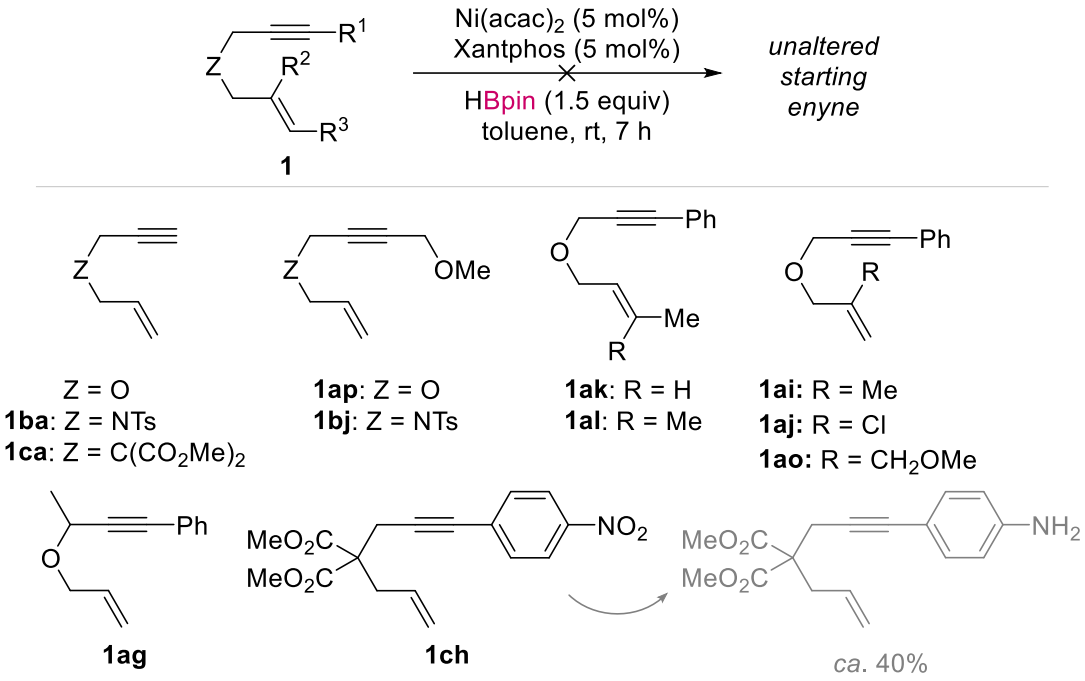

Scheme 3.24. Scope limitations.

Then, we performed derivatization reactions on the obtained alkyl- and alkenylboronates to illustrate the synthetic utility of our method. Thus, alkylboronates **2** can be oxidized to the corresponding alcohols (**3**) in good yields (**Scheme 3.25**). On the other hand, treatment with potassium bifluoride gave rise to the corresponding potassium trifluoroborate salts (**4**), which are usually the more convenient nucleophiles for Suzuki cross-coupling reactions of alkyl nucleophiles. As an example, we performed the reaction of **4cc** with *p*-chlorobenzonitrile to obtain the corresponding coupling compound **5cc** in high yield (78%).

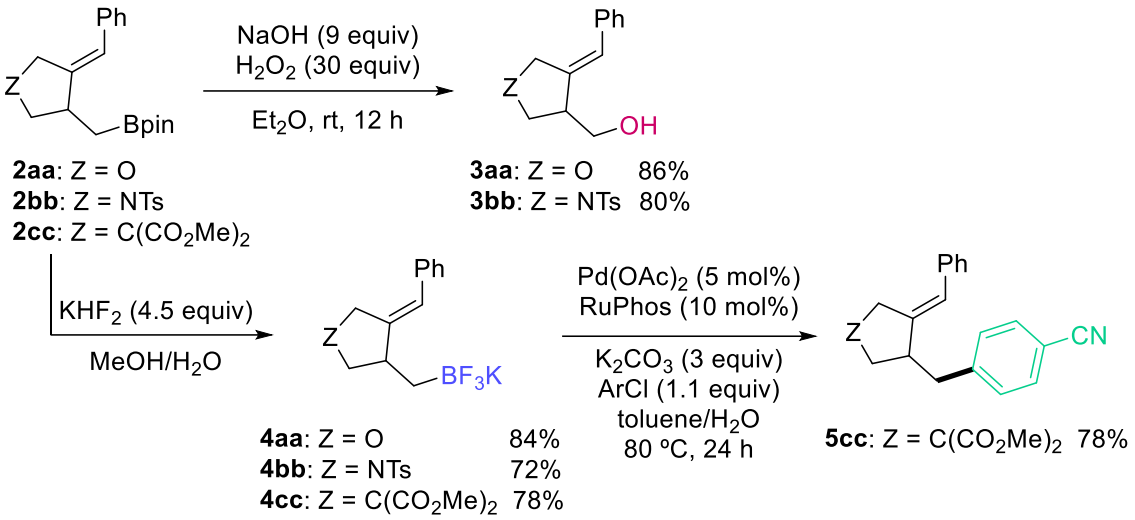

Scheme 3.25. Functionalization of alkylboronates **2**.

Alkenylboronate **11bn** can be oxidized as well to give the expected ketone **14bn**. Finally, direct Suzuki cross-coupling reaction with two iodoarenes allowed the preparation of the expected stereo-defined aryl–alkenyl derivatives **15bn** and **16bn** in quantitative yields (**Scheme 3.26**). The above-mentioned reactions show the usefulness of the boron compounds in the context of the preparation of unsymmetrical exocyclic ketones and in the preparation of stereo-defined tetra-substituted alkenes.

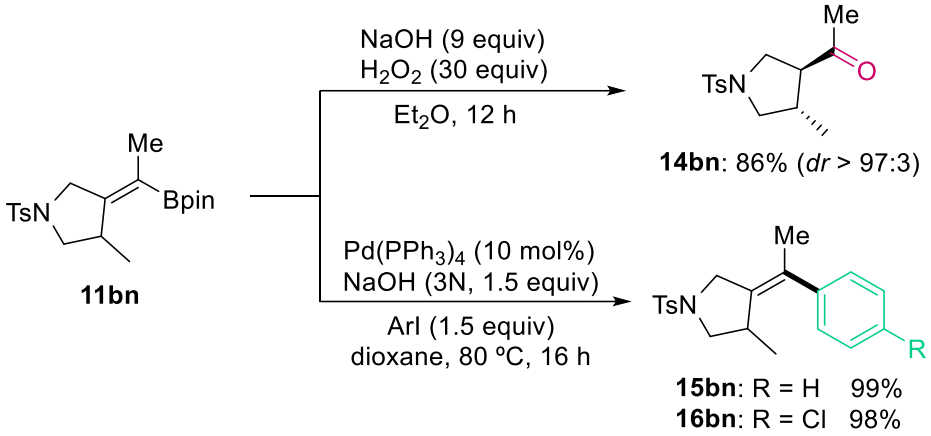

Scheme 3.26. Functionalization of alkenylboronate **11bn**.

We were interested in the determination of the reaction pathway of this Ni-catalyzed hydroborylative cyclization. In contrast to previously reported Ni-catalyzed borylative cyclization, involving B_2pin_2, no transmetalation reaction is expected in this case. Both computational and experimental mechanistic studies were undertaken in order to determine the actual activation mechanism of HBpin and the enyne by the catalyst, to derive a feasible complete reaction pathway and to explain the observed regioselectivity.

We firstly examined the reactivity of simple alkenes or alkynes under the optimized reaction conditions. No product was observed in any case, which suggested that the presence of both alkene and alkyne is necessary for the reaction to start (**Scheme 3.27**).

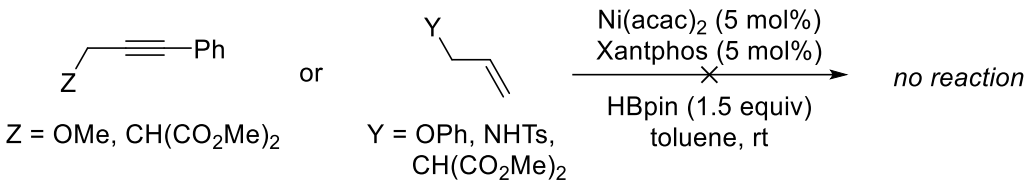

Scheme 3.27. Reaction with simple alkenes and alkynes.

With the aim of determining the oxidation state of the catalytically active species, we carried out some experiments with stoichiometric amounts of the nickel precursor. Thus, the reaction of enyne **1aa** with 1 equiv of HBpin in the presence of 100 mol% $Ni(acac)_2$/Xantphos does not take place. We need to add two additional equivalents of HBpin in order to achieve complete conversion (equation 1, **Scheme 3.28**). This result suggests that reduction of the Ni(II) precatalyst to Ni(0) is necessary for the reaction to proceed. In fact, we observed complete consumption of the enyne **1aa** when 1 equiv of $Ni(cod)_2$/Xantphos was used in the presence of just 1 equiv of HBpin (equation 2, **Scheme 3.28**).

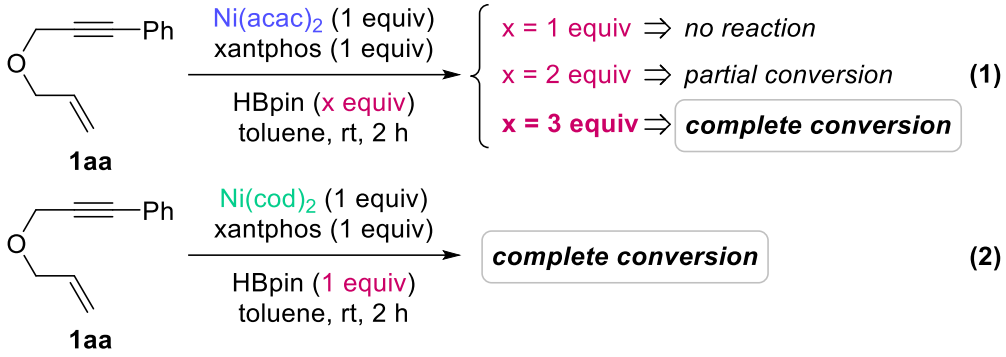

Scheme 3.28. Determination of the oxidation state of the catalyst.

This result further supports that the catalytically active species is a Ni(0) complex and that HBpin acts as the reducing agent when using $Ni^{II}(acac)_2$. Moreover, the reaction of $Ni(acac)_2$ and Xantphos with 2 equiv of HBpin in toluene (top, **Figure 3.8**) takes place at room temperature with H_2 evolution to give a brick-red precipitate of previously described complex $Ni(Xantphos)_2$.[212] The same brick-red precipitate was obtained by equimolar reaction of $Ni(cod)_2$ and Xantphos (bottom, **Figure 3.8**).

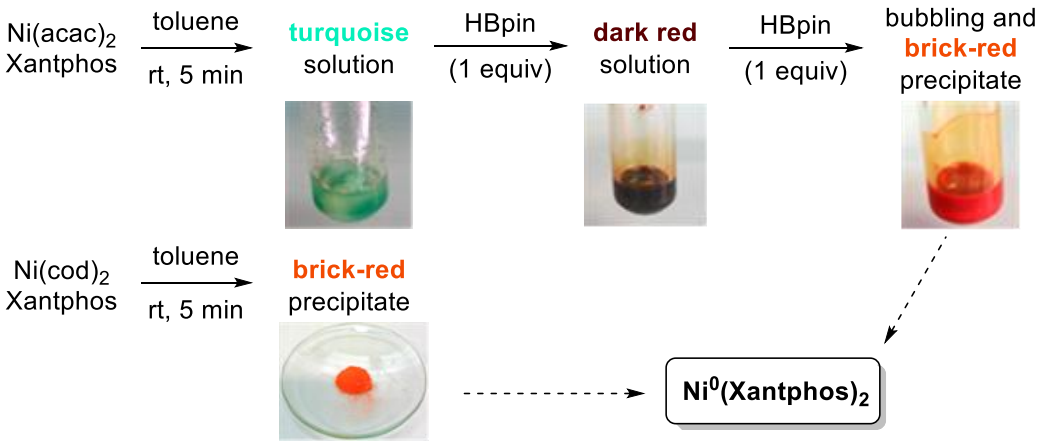

Figure 3.8. Qualitative studies for determining the oxidation state.

[212] N. D. Staudaher, R. M. Stolley, J. Louie, *Chem. Commun.* **2014**, *50*, 15577–15580.

Comparing the ^{31}P-NMR spectra of the brick-red precipitate in d^8-THF with a related Ni(ThiXantphos)$_2$ complex in d^8-toluene,[213] a similar peak pattern is observed (**Figure 3.9**).

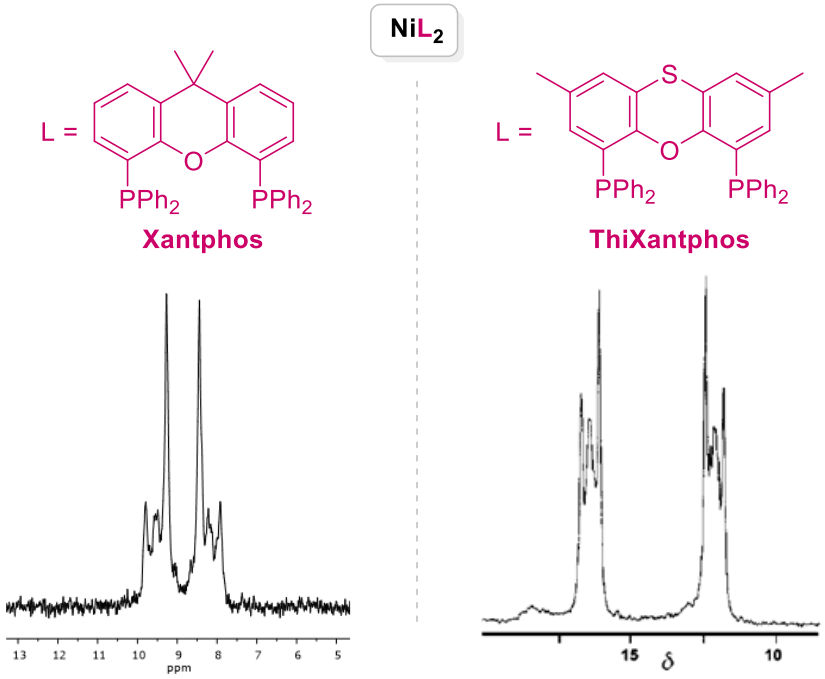

Figure 3.9. Experimental (left) *vs* reported (right) ^{31}P-NMR spectra of NiL$_2$.

The complex observed signal is caused by a highly asymmetric geometry of the bis(chelate) complex NiL$_2$, probably due to the rigid, non-planar butterfly structure of the Xantphos-based ligands. Thus, there are at least two different coordination modes, which make the phosphorus nuclei P$_a$ and P$_b$ magnetically inequivalent (**Figure 3.10**).

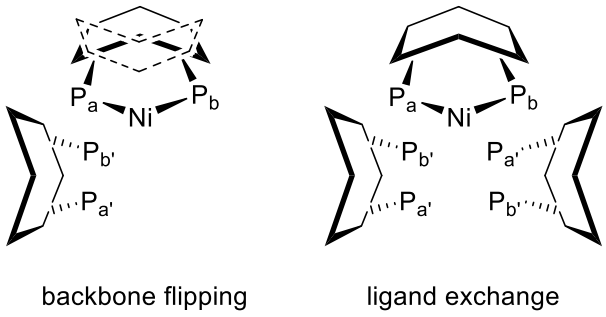

Figure 3.10. Butterfly structure of NiL$_2$.

Although Ni(Xantphos)$_2$ was formed in the stoichiometric experiments, we believe that this coordinatively saturated complex is not the actual reaction catalyst and could constitute the catalyst resting state. Formation of these bis(chelate) complexes is generally considered detrimental to catalysis, since these species are very stable and catalytically inactive in some transformations.[213] Furthermore, other study reported the effectiveness of Ni(Xantphos)$_2$ to serve as a viable precatalyst, where an initial ligand displacement of one Xantphos occurs and subsequently it is replaced by another ligand or the reaction substrate.[212] In addition, Ni(cod)(Xantphos) may be also present in the reaction medium.

[213] W. Goertz, W. Keim, D. Vogt, U. Englert, M. D. K. Boele, L. A. van der Veen, P. C. J. Kamerc, P. W. N. M. van Leeuwen, *J. Chem. Soc., Dalton Trans.* **1998**, 2981–2988.

Interestingly, the reaction of $Ni(acac)_2$, Xantphos and 1 equiv. of HBpin produced a dark red solution (shown in **Figure 3.8**) which afforded a NMR signal at – 9.95 ppm, that could match with a nickel hydride intermediate (top, **Figure 3.11**).[214] This Ni-hydride can react with another equivalent of HBpin to generate a Ni-dihydride, which would experience a reductive elimination to generate H_2 and Ni(0) (bottom, **Figure 3.11**) as qualitative experiments suggest.

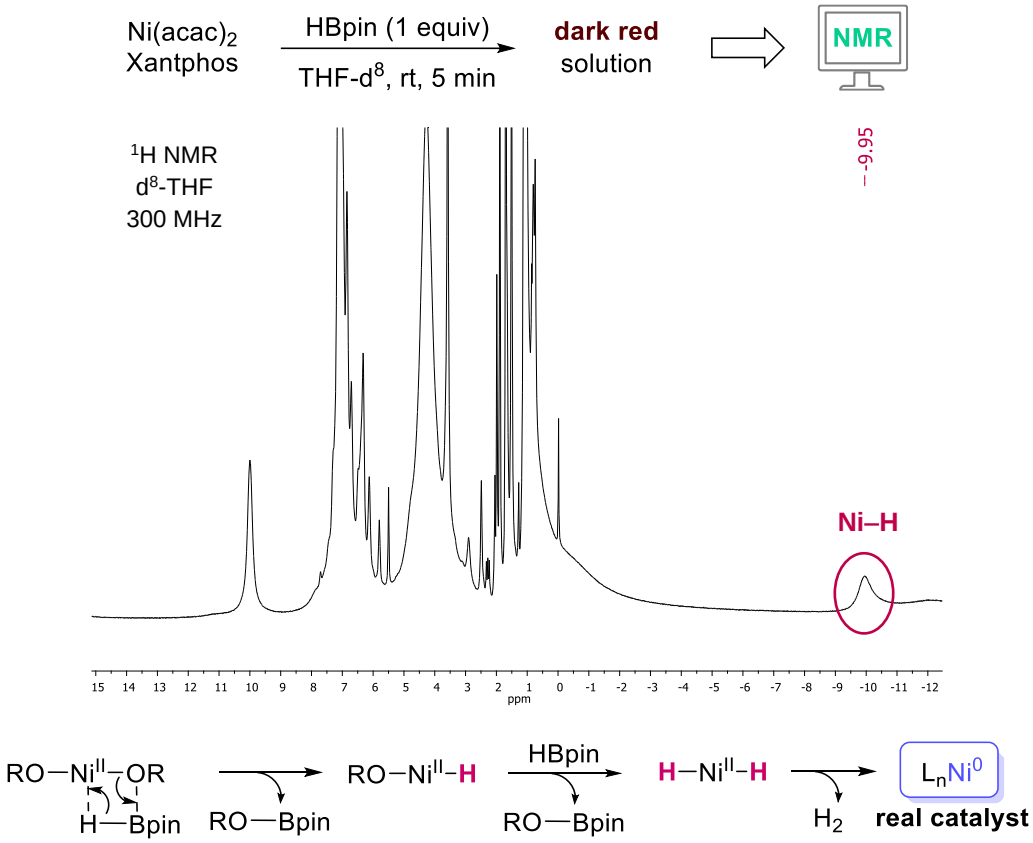

Figure 3.11. Detection of a presumable Ni-hydride intermediate.

Finally, the reaction of **1bb** with 100 mol% $Ni(cod)_2$/Xantphos, followed by quenching with DCl in D_2O afforded dideuterated cyclic product d^2-**13bb** in 30% yield. (**Scheme 3.29**). Therefore, nickelacyclopentene formed by oxidative cyclometalation seems to be a reaction intermediate.

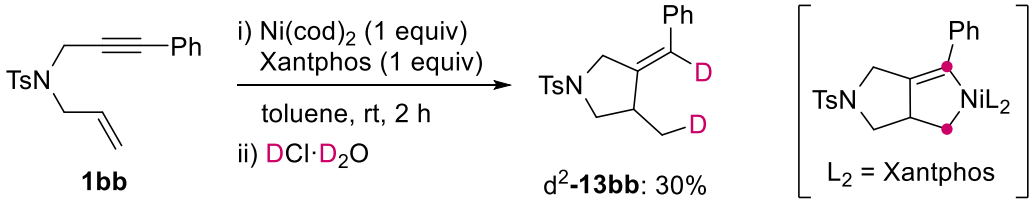

Scheme 3.29. Deuteration experiment.

[212] N. D. Staudaher, R. M. Stolley, J. Louie, *Chem. Commun.* **2014**, *50*, 15577–15580.
[213] W. Goertz, W. Keim, D. Vogt, U. Englert, M. D. K. Boele, L. A. van der Veen, P. C. J. Kamerc, P. W. N. M. van Leeuwen, *J. Chem. Soc., Dalton Trans.* **1998**, 2981–2988.
[214] (a) J. Breitenfeld, R. Scopelliti, X. Hu, *Organometallics* **2012**, *31*, 2128–2136. (b) N. A. Eberhardt, H. Guan, *Chem. Rev.* **2016**, *116*, 8373–8426. (c) F. Zhou, J. Zhu, Y. Zhang, S. Zhu, *Angew. Chem. Int. Ed.* **2018**, *57*, 4058–4062.

With these results in hand, we performed a detailed computational study at the DFT level to derive a complete reaction pathway. The full structure of the Xantphos ligand, without any simplification, was used for the calculations. Although the experiments clearly pointed to initial formation of a nickelacycle, we explored the feasibility of the oxidative addition of HBpin to Ni(Xantphos) (**I**). This process resulted to be endoergic (14.2 kcal mol^{-1}, equation 1, **Scheme 3.30**). Likewise, hydronickelation of alkyne was also computed, but a high activation energy was obtained (32.5 kcal mol^{-1}, equation 2, **Scheme 3.30**).

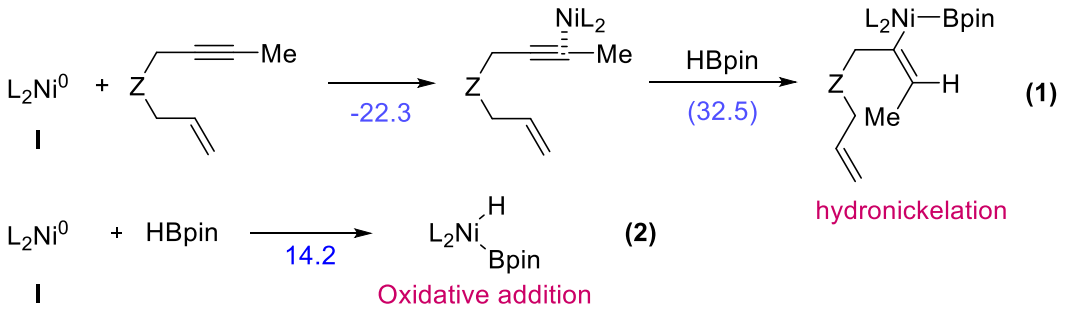

Scheme 3.30. Computed alternative disregarded reaction pathways. Δ*G* (kcal mol^{-1}) are calculated in toluene (PCM) at 6-31G(d) (C,H,N,P,O,B), LANL2DZ (Ni) level. Calculated activation energies in toluene are shown in brackets. L_2 = Xantphos.

Therefore, we centered our efforts in the study of the activation of the enyne to give the putative metalacycle, as well as its evolution to the final products (**Scheme 3.31**). Initial coordination of enyne to Ni(xantphos) (**I**) would afford intermediate **II**, which would evolve through oxidative cyclometalation to Ni(II) metalacycle **III**. Then, we considered the reaction of this key intermediate with HBpin by oxidative addition of the B–H bond to Ni(II). However, we were not able to locate any structure corresponding to a Ni(IV) complex (bottom center, **Scheme 3.31**). Alternatively, activation of the boron hydride may take place through σ-bond metathesis, with participation of H–B and Ni–C bonds. Subsequent reductive elimination would account for the formation of the final products.

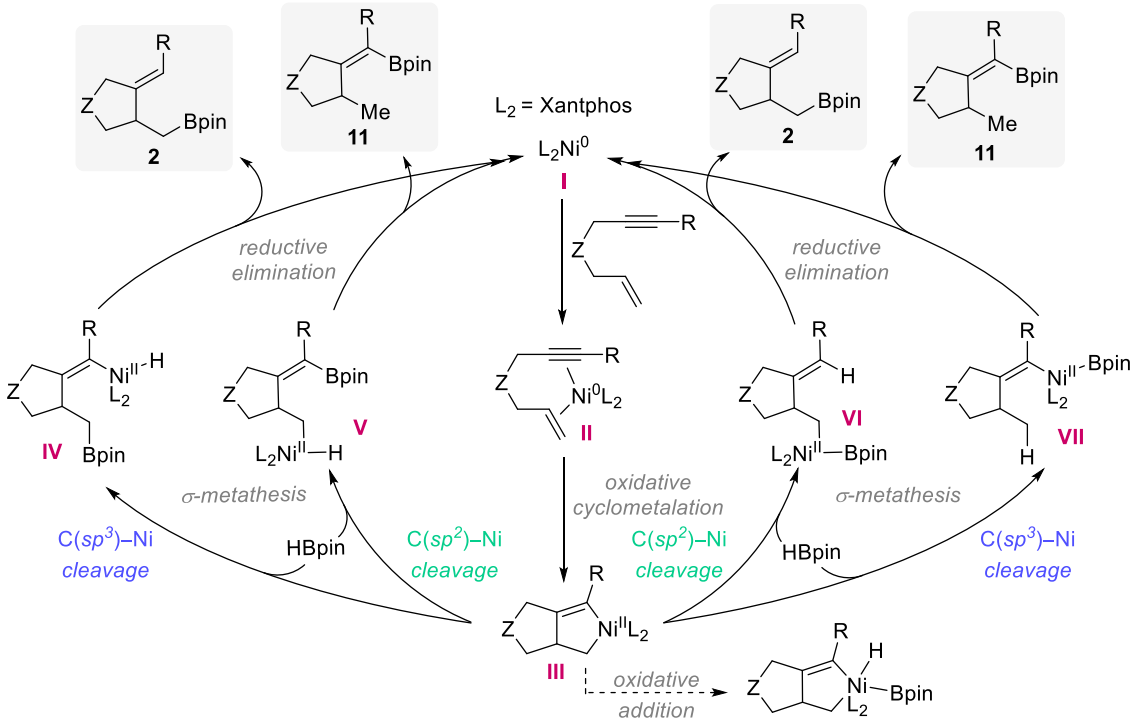

Scheme 3.31. Possible reaction pathways.

It is important to note that, in principle, σ-metathesis may involve either the alkenyl–Ni or the alkyl–Ni bonds. Additionally, this process could proceed in two different fashions to afford either Ni–H and C–B bonds or Ni–B and C–H bonds (**Scheme 3.32**).

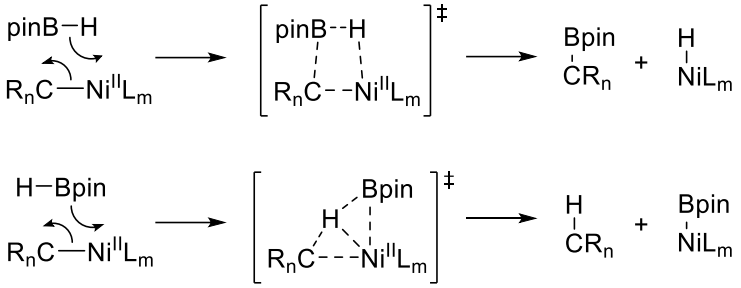

Scheme 3.32. Possible σ-bond metathesis involving Ni–C and B–H bonds.

Therefore, there are four possible pathways for the formation of both the alkylboronate **2** and the alkenylboronate **11**, depending firstly on the kind of Ni–C bond involved in the metathesis and on the chemoselectivity of this reaction. We have calculated all the possible intermediates and transition states for model enynes containing methyl and phenyl groups as substituents on the alkyne, in order to determine the most favorable pathways and obtain insight into the origin of the observed regioselectivity.

We considered methylamine derivatives **A** and **B** as the model enynes for the computational study (top and bottom, respectively, **Scheme 3.33**). The coordination of both enynes to Ni(xantphos) (**I**) to give **IIa** and **IIb** is strongly favored in spite of the entropy loss, and it is especially exoergic for the aryl-substituted derivative **B** (−25.1 and −33.5 kcal mol^{-1}, respectively). Subsequent formation of metalacycle **IIIa** by oxidative cyclometalation from **IIa** is practically thermoneutral and proceeds through a low barrier (E_a = 14.5 kcal mol^{-1}). The analogous reaction involving the phenyl-substituted derivative (**B**) that gives rise to **IIIb** shows a similar barrier (15.9 kcal mol^{-1}). In this case, the reaction is slightly endergonic (+3.4 kcal mol^{-1}). These two-step processes are thermodynamically very favorable. Therefore, the Ni catalyst seems to activate the enyne prior to the reaction with HBpin.

Then, we explored the feasibility of the oxidative addition of HBpin to the Ni(II) metalacycles **III**. The expected octahedral Ni(IV) complexes that would be formed in this reaction were not located. Instead, we found species resulting from C–B or C–H bond formation. Thus, evolution of complexes **III** does not seem to involve B–H bond oxidative addition to give a Ni(IV) intermediate.

Consequently, we explored the different kinds of σ-bond metathesis reactions involving HBpin and **IIIa** and **IIIb** that can be proposed in principle. These processes involve a Ni–C bond and the H–B bond. Taking into account that both Ni–C(sp^2) and Ni–C(sp^3) bonds can participate in the reaction and that either of them may evolve in two different ways to give Ni–B or Ni–H bonds along with the boronate, there are four possible reaction pathways from every metalacycle (**Scheme 3.33**).

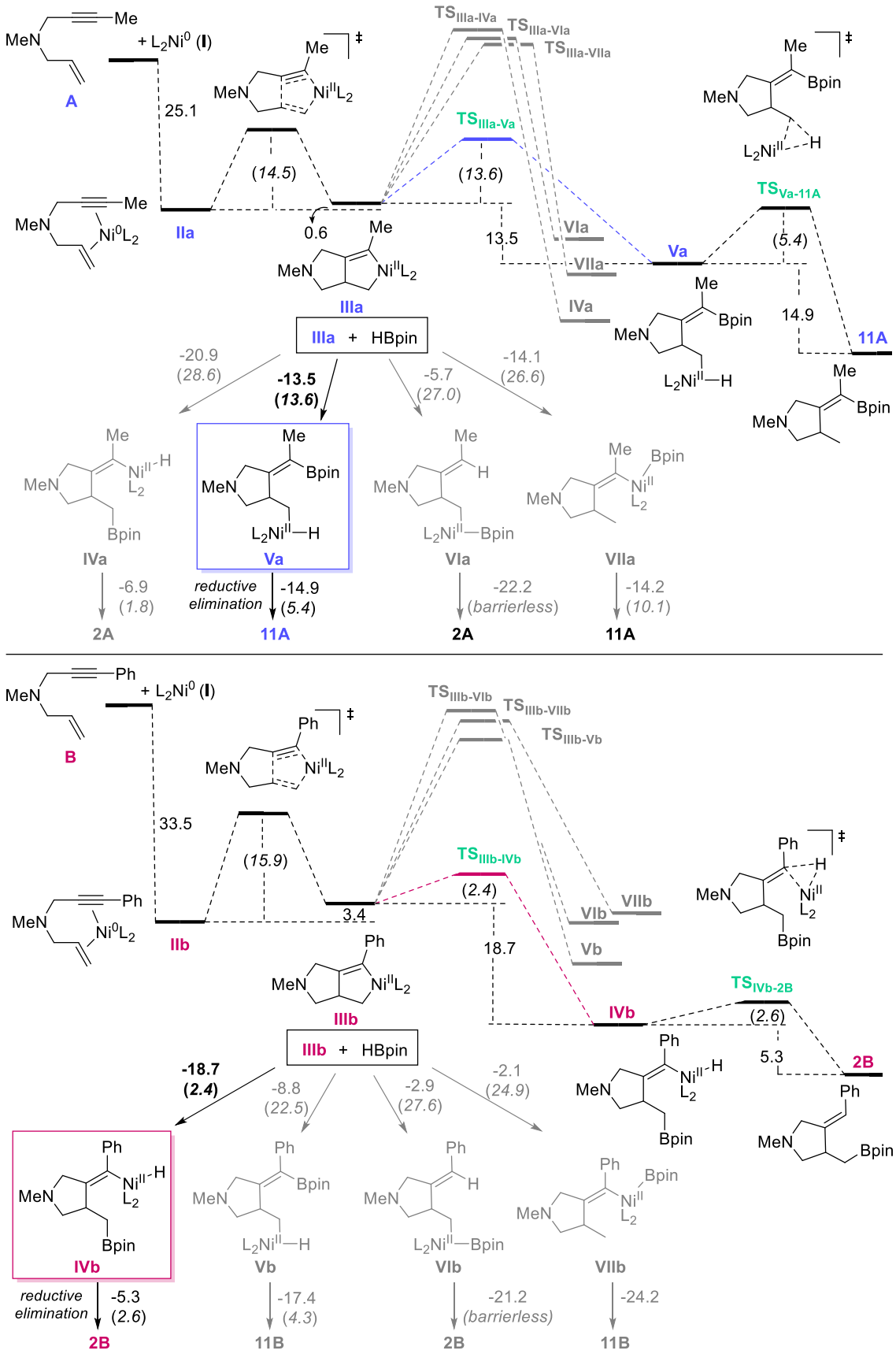

Scheme 3.33. Computed reaction profile for the methyl- (**A**, top) and phenyl-substituted (**B**, bottom) alkyne. Δ*G* (kcal mol^{-1}) values are calculated in toluene (PCM) at the 6-31G(d) (C,H,N,P,O,B), LANL2DZ (Ni) level. Calculated activation energies in toluene are shown in brackets. L_2 = Xantphos.

We were able to obtain the structures of the corresponding transition states for all the possible metathesis reactions from **IIIa** (top) and **IIIb** (bottom). The activation energies for the reactions of **IIIa** with HBpin are high (E_a > 25 kcal mol^{-1}), which would not take place at room temperature, except for the reaction involving the cleavage of the alkenyl–Ni bond to give the corresponding complex containing an alkyl–Ni hydride (**Va**) and an alkenylboronate (**11A**). This complex is formed exoergically (−13.5 kcal mol^{-1}) with a low activation energy (13.6 kcal mol^{-1}). Subsequent Ni–H reductive elimination from this compound is highly exothermic (and kinetically irrelevant, E_a = 5.4 kcal mol^{-1}) and leads to the observed product **11A**. Therefore, the computational data perfectly match the regioselectivity observed for the reaction of the methyl-substituted alkyne. Moreover, calculations for the σ-metathesis from the Ph-substituted metalacycle **IIIb** are also in agreement with the formation of the experimentally observed product, the alkylboronate (**2**). In this case, the most favorable process corresponds to the cleavage of the alkyl–Ni bond, with the same regioselectivity as that previously found: the formation of an intermediate Ni–H complex (**IVb**). The activation energy is even lower for this reaction (2.4 kcal mol^{-1}), whereas those for the alternative processes are far much slower (E_a > 22 kcal mol^{-1}). Reductive eliminations of either C–H (**IVb**-**Vb**) or C–B (**VIb**-**VIIb**) bonds to give Ni(0) are fast and exothermic reactions and do not affect the reaction kinetics. According to the computed reaction profile, oxidative cyclometalation is the rate-limiting step for this reaction for the substrates bearing aryl-substituted alkynes. For the methyl-substituted derivatives, this cannot be definitively stated, due to the similar activation energy found for the σ-bond metathesis.

Transition states corresponding to the two possible metathesis reactions leading to Ni–H complexes **IV** and **V** show the expected four-membered geometry. As an example, the transition state from **IIIa** to **Va** is depicted in **Figure 3.12** (top). Noticeably, the transition states for the alternative processes, leading to boryl–Ni complexes **VIa** and **VIIa**, show a nearly linear C–H–B arrangement in the H atom transfer from B to C, with short Ni–H distances, suggesting a metal–hydride interaction along the reaction coordinate (**Figure 3.12**, the second structure shows the transition state that would lead to **VIa**). It is important to note that the activation energy for this different kind of σ-metathesis reaction is similar to that found for the non-preferred pathways involving the formation of C–B and Ni–H bonds (**IVa**). Therefore, although the formation of Ni–boryl complexes is not competitive in this case, it constitutes a feasible pathway that could operate in other Ni-catalyzed reactions.

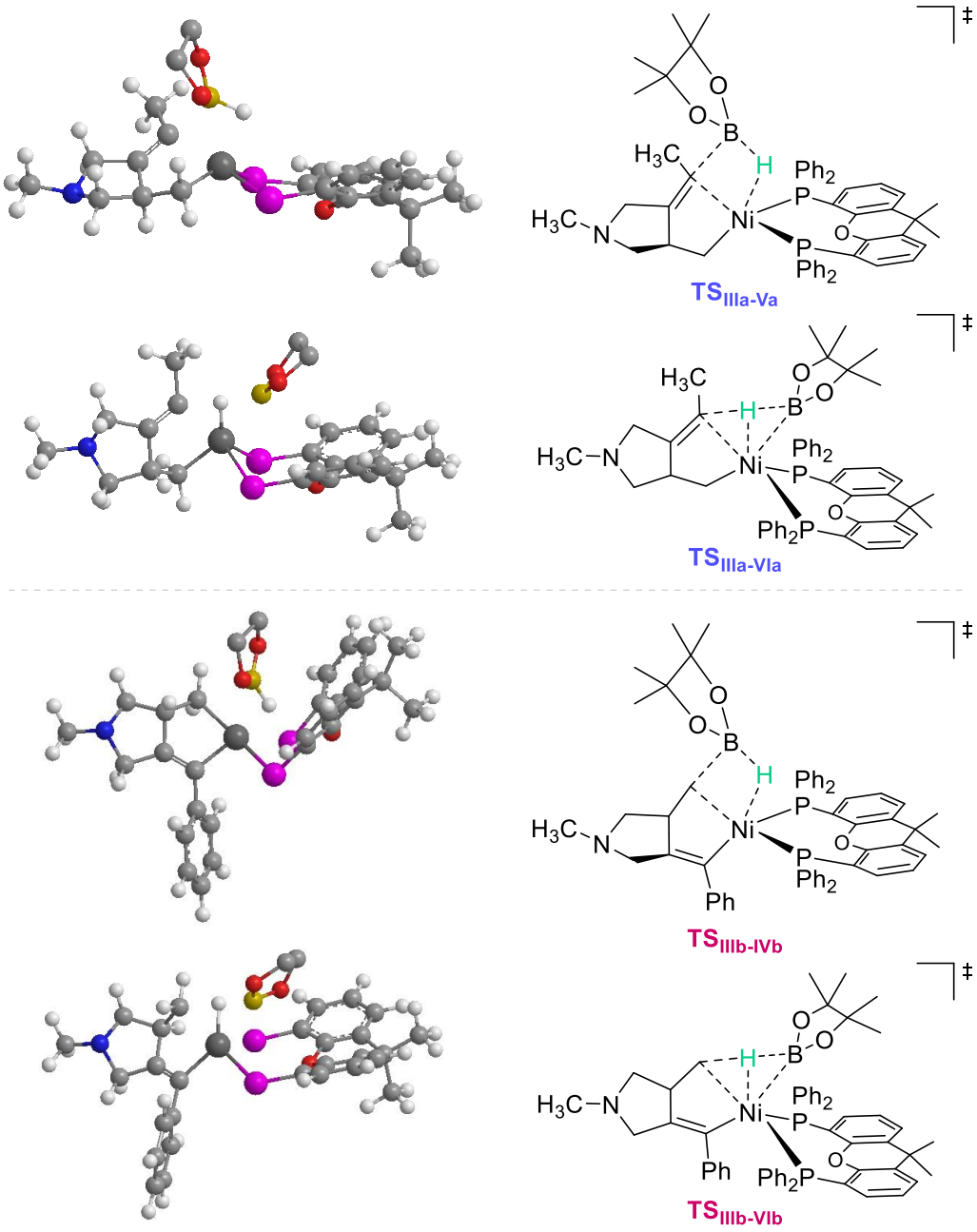

Figure 3.12. Structure of calculated transition states. From **IIIa** (top). From **IIIb** (bottom). Phenyl groups of Xantphos and methyls of Bpin have been omitted for clarity in the 3D representations.

Careful investigation of the structure of all the transition states calculated for the different metathesis reactions points to the steric hindrance as the reason for the observed regioselectivity. Frontier orbitals of different TS through formation of Ni hydrides intermediates do not show important differences (**Figure 3.13**).

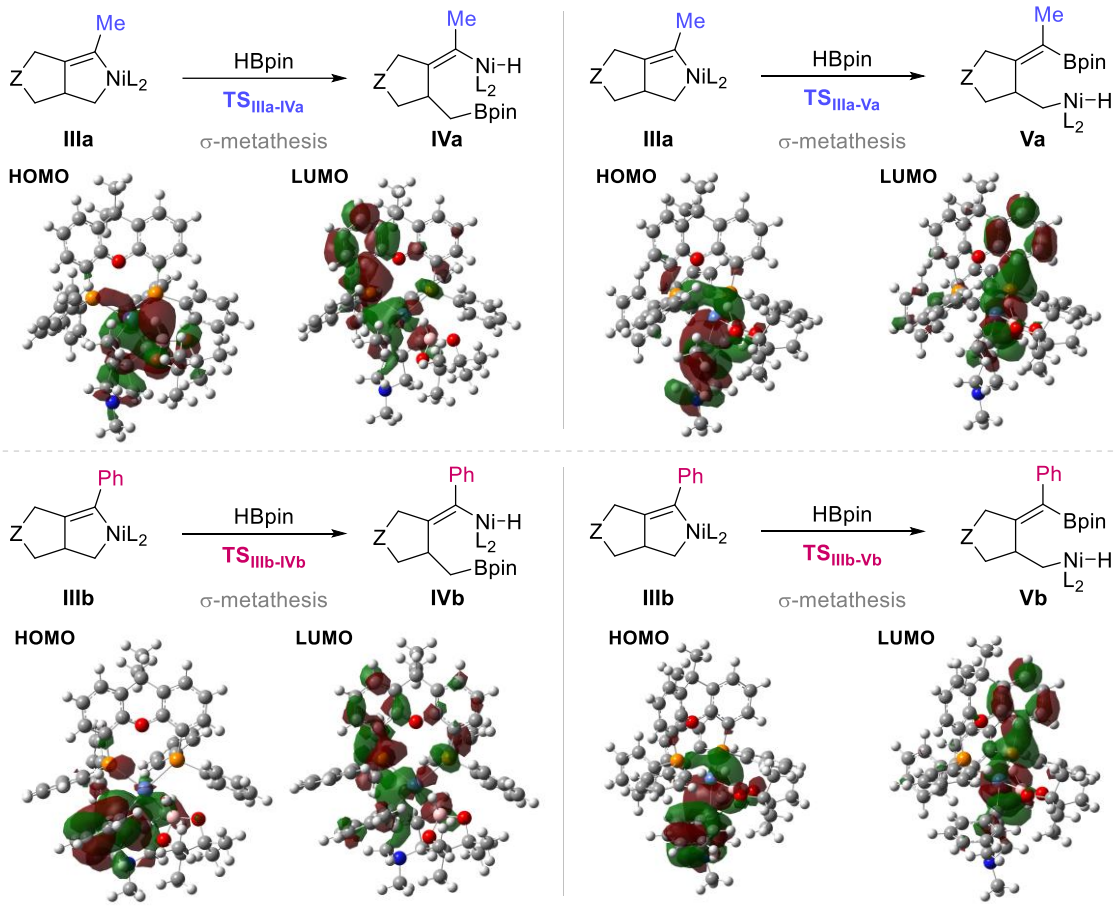

Figure 3.13. Frontier orbitals of TS through formation of Ni hydrides.

The special structure of Xantphos, along with the steric encumbrance exerted by the methyl groups of the pinacol fragment and the aryl on the alkyne, conditions the approach of HBpin to the nickelacycle (**Figure 3.14**).

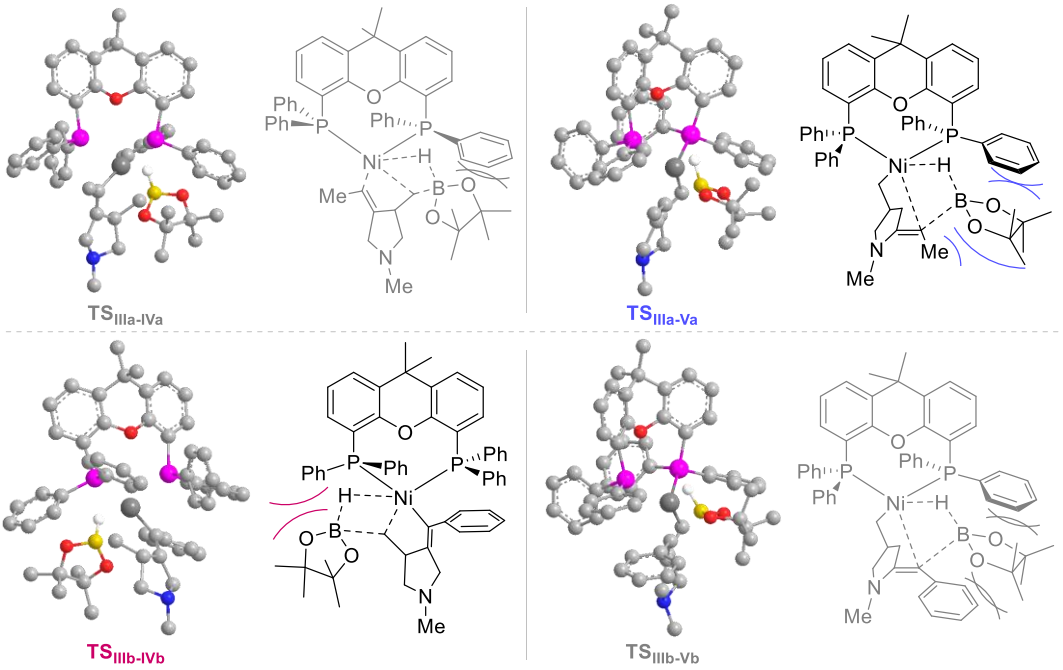

Figure 3.14. Steric hindrance observed in TS through formation of Ni hydrides. H atoms have been omitted for clarity in the 3D representations.

The common feature of the preferred transition states is that they show comparatively shorter Ni–H distances and a longer Ni–P distance with respect to the P atom *cis* to the carbon involved in the metathesis (**Table 3.5**). This fact suggests that the accessibility of the lowest energy transition states requires an effective Ni–H interaction (entries 2 and 3).

Table 3.5. Relevant bond distances (Å) for transition states leading to Ni hydrides through σ-metathesis reaction of **IIIa** and **IIIb** with HBpin.[a]

Entry		Ni–P[b]	Ni–P	Ni–C	Ni–H	B–C[c]	B–H
1	**IIIa**–**IVa**	2.493	2.532	2.174	1.993	2.133	1.237
2	**IIIa**–**Va**	2.317	**2.723**	2.184	**1.895**	2.033	1.256
3	**IIIb**–**IVb**	2.434	**2.985**	2.050	**1.693**	2.397	1.233
4	**IIIb**–**Vb**	2.344	2.725	2.261	1.912	2.095	1.243

[a] Data corresponding to the lowest energy transition states. [b] P atom *trans* to the C involved in the C–B formation. [c] Distances to the C atom involved in metathesis.

In conclusion, we can propose the catalytic cycle illustrated in **Figure 3.15**. Thus, the reaction begins with the oxidative cyclometalation of the enyne, which might be the rate-limiting step for this process with an activation barrier about 15 kcal mol^{-1}. Then, exoergic σ-metathesis with HBpin takes place, involving the cleavage of the Ni–C(sp^2) bond with Ph-substituted alkynes (cycle A) and the Ni–C(sp^3) bond with Me-substituted alkynes (cycle B). Both metathesis reactions lead to the formation of Ni-hydride intermediates, which undergo a final reductive elimination with low activation energies to regioselectively yield the observed alkyl- or alkenylboronates.

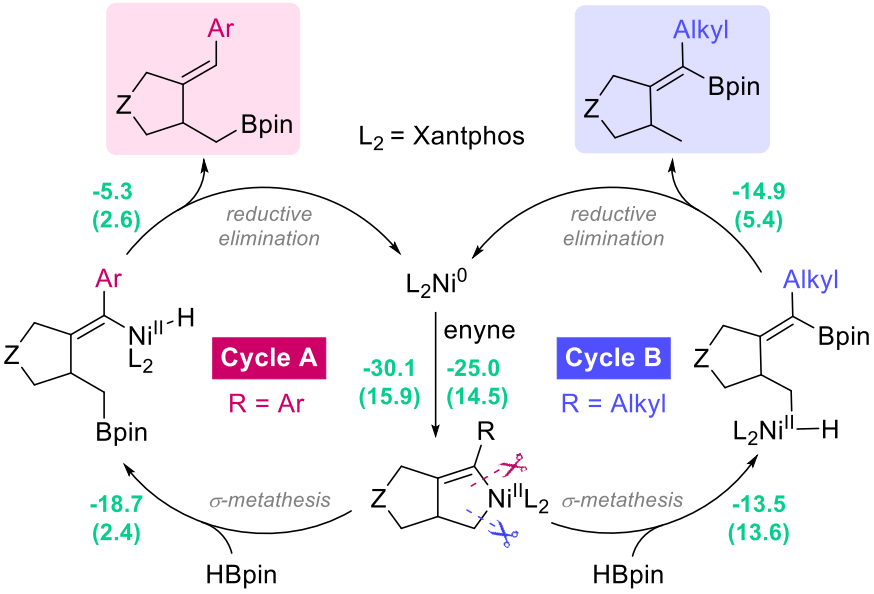

Figure 3.15. Proposed catalytic cycles. Δ*G* (kcal mol^{-1}) and activation energies (in brackets) are shown in green.

3.3.4. Experimental section

3.3.4.1. Materials and methods

General considerations have been described in *Experimental section* of *Chapter 1*. Additionally, $Ni(cod)_2$, $Ni(acac)_2$, pinacolborane and Xantphos were purchased from Sigma-Aldrich Co. The other commercially available chemicals were purchased and used as received without further purifications. The hydroborylative cyclization reactions were carried out under argon atmosphere in anhydrous toluene stored over activated molecular sieves 4 Å (VWR) and Ar-degassed.

3.3.4.2. Ligand synthesis

3.3.4.2.1. (Oxazoline)pyridine ligand (OP)

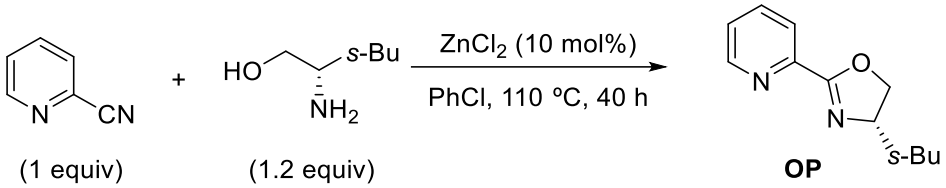

(1 equiv) (1.2 equiv) **OP**

2-Pyridinecarbonitrile (1 equiv, 9.6 mmol), (2*S*,3*S*)-isoleucinol (1.2 equiv, 11.5 mmol) and anhydrous $ZnCl_2$ (0.1 equiv, 0.96 mmol) were added to a sealed tube. Then, chlorobenzene (0.3 M, 30 mL) was added and the reaction mixture was stirred at 110 ºC for 40 h. Then, the solution was passed through a short pad of silica gel (CH_2Cl_2 and EtOAc) and the filtrate was concentrated under vacuum. The residue was purified by column chromatography in silica gel using CH_2Cl_2/EtOAc (4:1) as an eluent.[215]

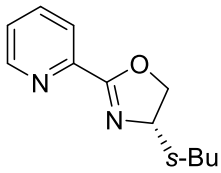

(*S*)-4-((*R*)-*sec*-Butyl)-2-(pyridin-2-yl)-4,5-dihydrooxazole (OP):[215] The ligand was obtained as a yellow oil in 50% yield (978 mg). ^{1}H NMR (300 MHz, $CDCl_3$) δ 8.70 (dd, J = 4.8, 0.9 Hz, 1H), 8.05 (dd, J = 7.9, 0.9 Hz, 1H), 7.77 (td, J = 7.9, 1.7 Hz, 1H), 7.41 – 7.32 (m, 1H), 4.49 (dd, J = 8.6, 7.2 Hz, 1H), 4.33 – 4.15 (m, 2H), 1.82 – 1.59 (m, 2H), 1.33 – 1.17 (m, 1H), 0.96 (t, J = 7.4 Hz, 3H), 0.89 (d, J = 6.7 Hz, 3H).

3.3.4.2.2. Bis(imino)pyridine ligands (IP)

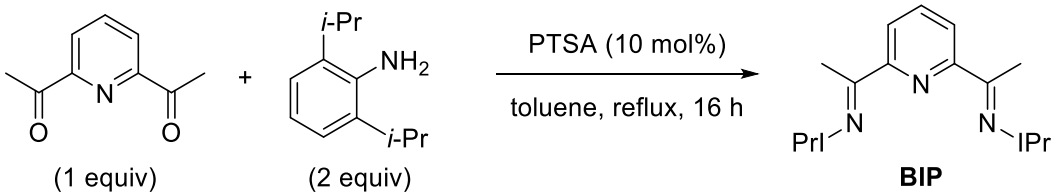

(1 equiv) (2 equiv) **BIP**

2,6-Diacetylpyridine (1 equiv, 1 mmol) and 2,6-diisopropylaniline (2 equiv, 2 mmol) were added to a sealed tube equipped with stir bar. Then, toluene (9 mL) and catalytic amount of *p*-toluenesulfonic acid (0.1 equiv, 19 mg) were added and the mixture was stirred at reflux overnight. Then, the solvent was removed under vacuum and the obtained yellow solid was washed with hexane and Et_2O to afford the product.[216]

[215] C. Bolm, K. Weickhardt, M. Zehnder, T. Ranff, *Chem. Ber.* **1991**, *124*, 1173–1180.
[216] P. M. Cheung, R. F. Berger, L. N. Zakharov, J. D. Gilbertson, *Chem. Commun.* **2016**, *52*, 4156–4159.

(1*E*,1'*E*)-1,1'-(Pyridine-2,6-diyl)bis(*N*-(2,6-diisopropylphenyl)ethan-1-imine) (BIP):[216]

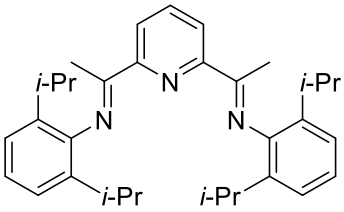

The ligand was obtained as a light yellow solid in 54% yield (259 mg). ^{1}H NMR (300 MHz, $CDCl_3$) δ 8.57 (d, J = 7.6 Hz, 1H), 8.15 (d, J = 7.5 Hz, 1H), 7.95 (t, J = 7.6 Hz, 1H), 7.24 – 7.04 (m, 6H), 2.83 – 2.66 (m, 4H), 2.27 (s, 6H), 1.28 – 1.10 (m, 24H).

3.3.4.3. General procedure for Ni-catalyzed hydroborylative cyclization of enynes

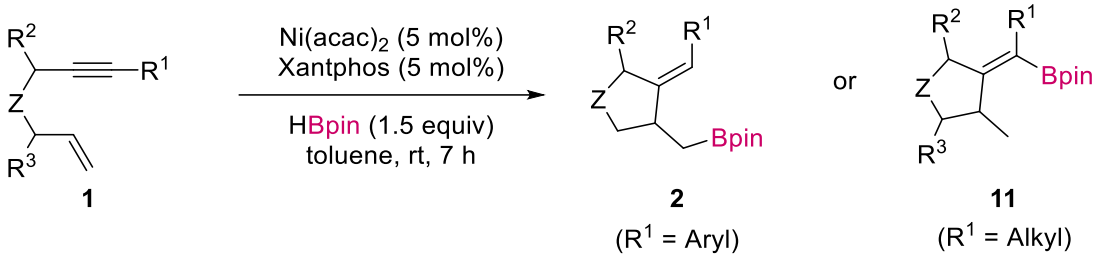

A vial was charged with $Ni(acac)_2$ (5.1 mg, 0.02 mmol), Xantphos (11.6 mg, 0.02 mmol), the corresponding enyne **1** (0.4 mmol) and a stir bar in air. The vial was sealed by a septum and backfilled with Ar. Then, anhydrous and Ar-degassed toluene (2 mL) and HBpin (87 µl, 0.6 mmol) were added. The resulting mixture was stirred for 7 h at room temperature. When complete consumption of the enyne was verified by TLC, the solvent was evaporated under vacuum and the product was purified by column chromatography in silica gel.

Alkylboronates (2)

(*Z*)-2-((4-Benzylidenetetrahydrofuran-3-yl)methyl-4,4,5,5-tetramethyl-1,3,2-dioxaborolane (2aa):

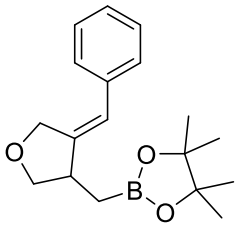

The compound was purified by column chromatography (cyclohexane/EtOAc, 95:5) and was obtained as a yellow oil in 38% yield (46 mg). ^{1}H NMR (300 MHz, $CDCl_3$) δ 7.33 (t, J = 7.3 Hz, 2H), 7.20 (t, J = 7.3 Hz, 1H), 7.12 (d, J = 7.3 Hz, 2H), 6.33 (d, J = 2.3 Hz, 1H), 4.63 (dd, J = 14.1, 1.8 Hz, 1H), 4.55 (dt, J = 14.1, 1.8 Hz, 1H), 4.11 (t, J = 7.8 Hz, 1H), 3.44 (t, J = 7.8 Hz, 1H), 3.10 – 2.94 (m, 1H), 1.25 (d, J = 2.6 Hz, 12H), 1.19 (d, J = 5.9 Hz, 1H), 1.00 (dd, J = 15.9, 8.4 Hz, 1H). ^{13}C NMR (75 MHz, $CDCl_3$) δ 147.1 (C), 137.6 (C), 128.5 (2 × CH), 127.9 (2 × CH), 126.4 (CH), 119.9 (CH), 83.3 (2 × C), 74.2 (CH_2), 70.2 (CH_2), 41.2 (CH), 25.0 (2 × CH_3), 24.8 (2 × CH_3), 14.2 (br m, CH_2-B). HRMS (ESI, MeOH) calcd. for $C_{18}H_{25}BO_3$ $[M + H]^+$: 301.2050; Found: 301.1974.

(*Z*)-4,4,5,5-Tetramethyl-2-((4-(4-methylbenzylidene)tetrahydrofuran-3-yl)methyl)-1,3,2-dioxaborolane (2ab):

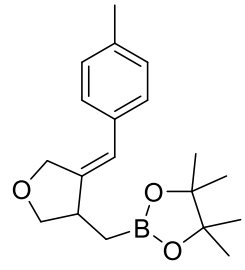

The compound was purified by column chromatography (cyclohexane/EtOAc, 95:5) and was obtained as a yellow oil in 51% yield (64 mg). ^{1}H NMR (300 MHz, $CDCl_3$) δ 7.14 (d, J = 8.0 Hz, 2H), 7.03 (d, J = 8.0 Hz, 1H), 6.32 (d, J = 2.1 Hz, 2H), 4.68 (d, J = 14.0, 1.8 Hz, 1H), 4.61 (d, J = 14.0, 1.8 Hz, 1H), 4.11 (t, J = 7.8 Hz, 1H), 3.46 (t, J = 7.8 Hz, 1H), 3.04 (dd, J = 14.0, 7.1 Hz, 1H), 2.34 (s, 3H), 1.26 (d, J = 2.6 Hz, 12H), 1.20 (d, J = 5.9 Hz, 1H), 1.02 (dd, J = 15.9, 8.3 Hz, 1H). ^{13}C NMR (75 MHz, $CDCl_3$) δ 146.0 (C), 136.1 (C), 134.8 (C), 129.2 (2 × CH), 127.9 (2 × CH), 119.7 (CH), 83.3 (2 × C), 74.2 (CH_2), 70.2 (CH_2), 41.2 (CH), 25.0 (2 × CH_3), 24.8 (2 × CH_3), 21.1 (CH_3), 14.0 (br m, CH_2-B). HRMS (ESI, MeOH) calcd. for $C_{19}H_{27}BO_3$ $[M + H]^+$: 315.2320; Found: 315.2126.

(*Z*)-2-((4-(4-Methoxybenzylidene)tetrahydrofuran-3-yl)methyl)-4,4,5,5-tetramethyl-1,3,2-dioxaborolane (2ac): The compound was purified by column chromatography (cyclohexane/EtOAc, 95:5) and was obtained as a pale yellow oil in 44% yield (58 mg). ^{1}H NMR (300 MHz, $CDCl_3$) δ 7.05 (d, J = 8.7 Hz, 2H), 6.86 (d, J = 8.7 Hz, 2H), 6.27 (d, J = 2.2 Hz, 1H), 4.65 (d, J = 14.0 Hz, 1H), 4.59 (t, J = 14.0, 1.9 Hz, 1H), 4.08 (t, J = 8.0 Hz, 1H), 3.78 (s, 3H), 3.43 (t, J = 8.0 Hz, 1H), 3.07 – 2.93 (m, 1H), 1.24 (d, J = 2.6 Hz, 12H), 1.22 – 1.15 (m, 1H), 0.98 (dd, J = 15.9, 8.3 Hz, 1H). ^{13}C NMR (75 MHz, $CDCl_3$) δ 158.2 (C), 144.7 (C), 130.5 (C), 129.2 (2 × CH), 119.3 (CH), 114.0 (2 × CH), 83.3 (2 × C), 74.2 (CH_2), 70.2 (CH_2), 55.3 (CH_3), 41.1 (CH), 25.0 (2 × CH_3), 24.8 (2 × CH_3), 14.1 (br m, CH_2-B). HRMS (ESI, MeOH) calcd. for $C_{19}H_{27}BO_4$ [M + Na]$^+$: 353.2310; Found: 353.1898.

(*Z*)-2-((4-(4-Chlorobenzylidene)tetrahydrofuran-3-yl)methyl)-4,4,5,5-tetramethyl-1,3,2-dioxaborolane (2ad): The compound was purified by column chromatography (cyclohexane/EtOAc, 95:5) and was obtained as a yellow oil in 16% yield (21 mg). ^{1}H NMR (300 MHz, $CDCl_3$) δ 7.21 (d, J = 8.4 Hz, 2H), 6.96 (d, J = 8.4 Hz, 2H), 6.21 (d, J = 2.0 Hz, 1H), 4.64 (dd, J = 14.1, 2.0 Hz, 1H), 4.56 (dt, J = 14.1, 2.0 Hz, 1H), 4.03 (t, J = 8.0 Hz, 1H), 3.38 (t, J = 8.0 Hz, 1H), 2.99 – 2.90 (m, 1H), 1.17 (d, J = 2.6 Hz, 12H), 1.11 (d, J = 5.8 Hz, 1H), 0.93 (dd, J = 15.9, 8.3 Hz, 1H). ^{13}C NMR (75 MHz, $CDCl_3$) δ 148.0 (C), 136.1 (C), 132.1 (C), 129.1 (2 × CH), 128.6 (2 × CH), 118.8 (CH), 83.4 (2 × C), 74.1 (CH_2), 70.1 (CH_2), 41.3 (CH), 25.0 (2 × CH_3), 24.8 (2 × CH_3), 13.9 (br m, CH_2-B). HRMS (ESI, MeOH) calcd. for $C_{18}H_{24}BClO_3$ [M + H]$^+$: 357.6470; Found: 357.1538.

(*Z*)-4,4,5,5-Tetramethyl-2-((4-(4-(trifluoromethyl)benzylidene)tetrahydrofuran-3-yl)methyl)-1,3,2-dioxaborolane (2af): The compound was purified by column chromatography (cyclohexane/EtOAc, 95:5) and was obtained as a yellow oil in 52% yield (76 mg). ^{1}H NMR (300 MHz, $CDCl_3$) δ 7.58 (d, J = 8.2 Hz, 2H), 7.21 (d, J = 8.2 Hz, 2H), 6.37 (d, J = 2.3 Hz, 1H), 4.68 (d, J = 14.1 Hz, 1H), 4.61 (dt, J = 14.1, 8.2 Hz, 1H), 4.12 (t, J = 8.1 Hz, 1H), 3.47 (t, J = 8.1 Hz, 1H), 3.11 – 2.99 (m, 1H), 1.25 (d, J = 2.7 Hz, 12H), 1.19 (d, J = 5.8 Hz, 1H), 1.02 (dd, J = 16.0, 8.3 Hz, 1H). ^{13}C NMR (75 MHz, $CDCl_3$) δ 150.4 (C), 141.1 (C), 128.5 (C), 128.1 (4 × CH), 125.5 (q, J = 3.8 Hz, CF_3), 118.9 (CH), 83.5 (2 × C), 74.2 (CH_2), 70.2 (CH_2), 41.5 (CH), 25.0 (2 × CH_3), 24.9 (2 × CH_3), 14.0 (br m, CH_2-B). HRMS (ESI, MeOH) calcd. for $C_{19}H_{24}BF_3O_3$ [M + H]$^+$: 368.2032; Found: 368.1721.

(*Z*)-4-((4-((4,4,5,5-Tetramethyl-1,3,2-dioxaborolan-2-yl)methyl)dihydrofuran-3(2*H*)-ylidene)methyl)benzonitrile (1ae): The compound was purified by column chromatography (cyclohexane/EtOAc, 95:5) and was obtained as a white solid in 24% yield (31 mg). M.p. = 108 – 110 °C. ^{1}H NMR (300 MHz, $CDCl_3$) δ 7.61 (d, J = 8.4 Hz, 2H), 7.18 (d, J = 8.4 Hz, 2H), 6.35 (q, J = 2.3 Hz, 1H), 4.67 (dd, J = 14.7, 1.6 Hz, 1H), 4.59 (dt, J = 14.7, 2.2 Hz, 1H), 4.14 (t, J = 7.4 Hz, 1H), 3.47 (t, J = 8.1 Hz, 1H), 3.11 – 2.98 (m, 1H), 1.24 (d, J = 2.9 Hz, 12H), 1.18 (dd, J = 16.0, 5.8 Hz, 1H), 1.01 (dd, J = 16.0, 8.4 Hz, 1H). ^{13}C NMR (75 MHz, $CDCl_3$) δ 152.1 (C), 142.1 (C), 132.4 (2 × CH), 128.4 (2 × CH), 119.1 (C), 118.8 (CH), 109.8 (C), 83.6 (2 × C), 74.2 (CH_2), 70.3 (CH_2), 41.7 (CH), 25.1 (2 × CH_3), 24.9 (2 × CH_3), 14.0 (br m, CH_2-B). HRMS (ESI, MeOH) calcd. for $C_{19}H_{24}BNO_3$ [M + Na]$^+$: 348.2150; Found: 348.1754.

(*E*)-2-((4-Benzylidenetetrahydro-2*H*-pyran-3-yl)methyl)-4,4,5,5-tetramethyl-1,3,2-dioxaborolane (2ah): 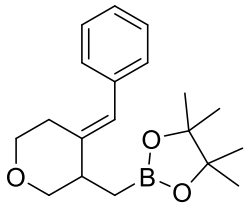 The compound was purified by column chromatography (cyclohexane/EtOAc, 98:2) and was obtained as a yellow oil in 9% yield (11 mg). ^{1}H NMR (300 MHz, $CDCl_3$) δ 7.30 (t, J = 7.3 Hz, 2H), 7.22 – 7.15 (m, 3H), 6.34 (s, 1H), 3.87 (dd, J = 10.7, 4.0 Hz, 1H), 3.73 – 3.64 (m, 1H), 3.63 – 3.54 (m, 1H), 3.42 (dd, J = 10.7, 7.0 Hz, 1H), 2.74 – 2.57 (m, 2H), 2.43 – 2.32 (m, 1H), 1.23 (s, 12H), 1.15 (dd, J = 15.6, 8.0 Hz, 1H), 0.96 (dd, J = 15.6, 7.2 Hz, 1H). ^{13}C NMR (75 MHz, $CDCl_3$) δ 142.6 (C), 138.0 (C), 129.1 (2 × CH), 128.2 (2 × CH), 126.2 (CH), 122.0 (CH), 83.3 (2 × C), 75.5 (CH_2), 69.2 (CH_2), 40.9 (CH), 29.4 (CH_2), 25.1 (2 × CH_3), 25.0 (2 × CH_3), 12.5 (br m, CH_2-B). HRMS (ESI, MeOH) calcd. for $C_{19}H_{27}BNO_3$ $[M + Na]^+$: 337.2320; Found: 337.1951.

(*Z*)-3-Benzylidene-4-((4,4,5,5-tetramethyl-1,3,2-dioxaborolan-2-yl)methyl)-1-tosylpyrrolidine (2bb):[100] 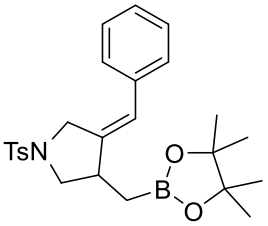 The compound was purified by column chromatography (cyclohexane/EtOAc, 9:1) and was obtained as a brown solid in 63% yield (114 mg). M.p. = 125 – 127 °C. ^{1}H NMR (300 MHz, $CDCl_3$) δ 7.72 (d, J = 8.2 Hz, 2H), 7.39 – 7.28 (m, 3H), 7.24 – 7.22(m, 2H), 7.12 (d, J = 7.6 Hz, 2H), 6.24 (d, J = 2.4 Hz, 1H), 4.26 (dd, J = 14.8, 1.6 Hz, 1H), 3.99 (dt, J = 14.8, 1.6 Hz, 1H), 3.64 (dd, J = 8.8, 7.3 Hz, 1H), 2.96 (m, 1H), 2.80 (t, J = 8.8 Hz, 1H), 2.41 (s, 3H), 1.19 (d, J = 5.7 Hz, 12H), 1.11 (dd, J = 16.0, 5.7 Hz, 1H), 0.93 (dd, J = 16.0, 8.1 Hz, 1H).

(*Z*)-3-(4-Methoxybenzylidene)-4-((4,4,5,5-tetramethyl-1,3,2-dioxaborolan-2-yl)methyl)-1-tosylpyrrolidine (2bd): 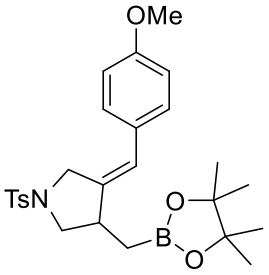 The compound was purified by column chromatography (cyclohexane/EtOAc, 9:1) and was obtained as a brown solid in 63% yield (120 mg). M.p. = 157 – 159 °C. ^{1}H NMR (300 MHz, $CDCl_3$) δ 7.72 (d, J = 8.5 Hz, 2H), 7.30 (d, J = 8.5 Hz, 2H), 7.06 (d, J = 8.8 Hz, 2H), 6.87 (d, J = 8.8 Hz, 2H), 6.17 (d, J = 2.6 Hz, 1H), 4.23 (d, J = 14.5 Hz, 1H), 3.97 (dd, J = 14.6, 2.6 Hz, 1H), 3.81 (s, 3H), 3.62 (dd, J = 8.6, 7.6 Hz, 1H), 3.05 – 2.90 (m, 1H), 2.79 (t, J = 8.6 Hz, 1H), 2.41 (s, 3H), 1.18 (d, J = 5.8 Hz, 12H), 1.11 (dd, J = 16.0, 5.5 Hz, 1H), 0.93 (dd, J = 16.0, 8.0 Hz, 1H). ^{13}C NMR (75 MHz, $CDCl_3$) δ 158.5 (C), 143.5 (C), 140.1 (C), 133.2 (C), 129.7 (2 × CH), 129.5 (C), 129.4 (2 × CH), 127.8 (CH), 121.4 (2 × CH), 114.0 (2 × CH), 83.4 (2 × C), 55.3 (CH_3), 53.7 (CH_2), 50.8 (CH_2), 40.3 (CH), 24.9 (2 × CH_3), 24.8 (2 × CH_3), 21.5 (CH_3), 14.1 (br m, CH_2-B). HRMS (ESI, MeOH) calcd. for $C_{26}H_{34}BNO_5S$ $[M + H]^+$: 484.2251; Found: 484.2327.

(*Z*)-3-(4-Chlorobenzylidene)-4-((4,4,5,5-tetramethyl-1,3,2-dioxaborolan-2-yl)methyl)-1-tosylpyrrolidine (2be): 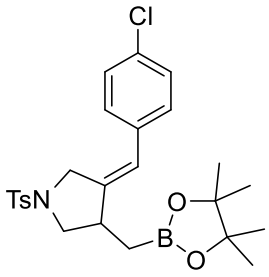 The compound was purified by column chromatography (cyclohexane/EtOAc, 9:1) and was obtained as an orange solid in 22% yield (43 mg). M.p. = 147 – 149 °C. ^{1}H NMR (300 MHz, $CDCl_3$) δ 7.71 (d, J = 8.4 Hz, 2H), 7.30 (dd, J = 8.4, 3.0 Hz, 4H), 7.04 (d, J = 8.4 Hz, 2H), 6.18 (d, J = 2.5 Hz, 1H), 4.21 (dd, J = 14.9, 1.6 Hz, 1H), 3.94 (d, J = 14.9, 1.6 Hz, 1H), 3.64 (dd, J = 8.9, 7.3 Hz, 2H), 2.97 (m, 1H), 2.80 (t, J = 8.9 Hz, 1H), 2.41 (s, 3H), 1.18 (d, J = 5.7 Hz, 12H), 1.11 (dd, J = 16.1, 5.7 Hz, 1H), 0.93 (dd, J = 16.1, 8.1 Hz, 1H). ^{13}C NMR (75 MHz, $CDCl_3$) δ 143.6 (C), 143.3 (C), 135.2 (C), 133.0 (C), 132.6 (C), 129.7 (2 × CH), 129.3 (2 × CH), 128.7 (2 × CH), 127.8 (2 × CH), 120.9 (CH), 83.4 (2 × C), 53.6 (CH_2), 50.8 (CH_2), 40.4 (CH), 24.9 (2 × CH_3), 24.7 (2 × CH_3), 21.5 (CH_3),

[100] T. Xi, Z. Lu, *ACS Catal.* **2017**, *7*, 1181–1185.

13.9 (br m, CH_2-B). HRMS (ESI, MeOH) calcd. for $C_{25}H_{31}BClNO_4S$ [M + H]$^+$: 488.1755; Found: 488.1828.

(*Z*)-4-((4-((4,4,5,5-Tetramethyl-1,3,2-dioxaborolan-2-yl)methyl)-1-tosylpyrrolidin-3-ylidene)methyl)benzonitrile (2bf): The compound was purified by column chromatography (cyclohexane/EtOAc, 9:1) and was obtained as an orange oil in 61% yield (116 mg). ^{1}H NMR (300 MHz, $CDCl_3$) δ 7.72 (d, J = 8.2 Hz, 2H), 7.61 (d, J = 8.4 Hz, 2H), 7.32 (d, J = 8.2 Hz, 2H), 7.19 (d, J = 8.4 Hz, 2H), 6.26 (d, J = 2.4 Hz, 1H), 4.24 (dd, J = 15.1, 1.9 Hz, 1H), 3.96 (dt, J = 15.1, 1.9 Hz, 1H), 3.66 (dd, J = 9.0, 7.4 Hz, 1H), 3.05 – 2.96 (m, 1H), 2.82 (t, J = 9.0 Hz, 1H), 2.42 (s, 3H), 1.18 (d, J = 4.4 Hz, 12H), 1.11 (dd, J = 16.1, 5.5 Hz, 1H), 0.93 (dd, J = 16.1, 8.1 Hz, 1H). ^{13}C NMR (75 MHz, $CDCl_3$) δ 146.9 (C), 143.8 (C), 141.2 (C), 132.9 (C), 132.4 (2 × CH), 129.8 (2 × CH), 128.5 (2 × CH), 127.8 (2 × CH), 120.7 (CH), 118.8 (C), 110.3 (C), 83.5 (2 × C), 53.5 (CH_2), 50.9 (CH_2), 40.7 (CH), 24.9 (2 × CH_3), 24.7 (2 × CH_3), 21.6 (CH_3), 14.0 (br m, CH_2-B). HRMS (ESI, MeOH) calcd. for $C_{26}H_{31}BN_2O_4S$ [M + H]$^+$: 479.2098; Found: 479.2161.

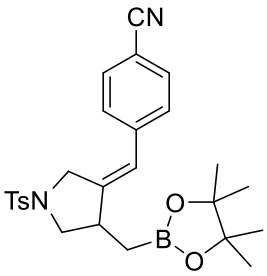

(*Z*)-3-((4,4,5,5-Tetramethyl-1,3,2-dioxaborolan-2-yl)methyl)-1-tosyl-4-(4-(trifluoromethyl)benzylidene)pyrrolidine (2bg): The compound was purified by column chromatography (cyclohexane/EtOAc, 9:1) and was obtained as a brown solid in 43% yield (90 mg). M.p. = 112 – 114 °C. ^{1}H NMR (300 MHz, $CDCl_3$) δ 7.71 (d, J = 8.1 Hz, 2H), 7.56 (d, J = 8.1 Hz, 2H), 7.30 (d, J = 8.1 Hz, 2H), 7.20 (d, J = 8.1 Hz, 2H), 6.28 (s, 1H), 4.24 (d, J = 14.9 Hz, 1H), 3.97 (d, J = 14.9 Hz, 1H), 3.65 (t, J = 8.2 Hz, 1H), 3.07 – 2.93 (m, 1H), 2.83 (t, J = 8.7 Hz, 1H), 2.39 (s, 3H), 1.17 (d, J = 5.0 Hz, 12H), 1.09 (dd, J = 13.6, 5.0 Hz, 1H), 0.96 (dd, J = 16.1, 7.9 Hz, 1H). ^{13}C NMR (75 MHz, $CDCl_3$) δ 145.5 (C), 143.7 (C), 140.3 (C), 140.2 (C), 133.0 (C), 129.9 (2 × CH), 129.8 (2 × CH), 128.3 (2 × CH), 127.9 (2 × CH), 125.5 (q, J = 3.6 Hz, CF_3), 120.9 (CH), 83.5 (2 × C), 53.6 (CH_2), 50.9 (CH_2), 40.5 (CH), 24.9 (2 × CH_3), 24.7 (2 × CH_3), 21.5 (CH_3), 14.3 (br m, CH_2-B). HRMS (ESI, MeCN) calcd. for $C_{26}H_{31}BF_3NO_4S$ [M + Na]$^+$: 544.4022; Found: 544.1914.

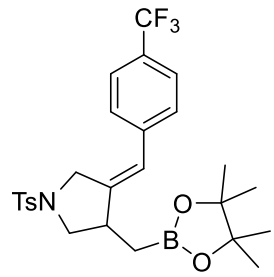

(*Z*)-1-(4-((4-((4,4,5,5-Tetramethyl-1,3,2-dioxaborolan-2-yl)methyl)-1-tosylpyrrolidin-3-ylidene)methyl)phenyl)ethan-1-one (2bh): The compound was purified by column chromatography (cyclohexane/EtOAc, 9:1) and was obtained as a light brown solid in 68% yield (68 mg). M.p. = 61 – 63 °C. ^{1}H NMR (300 MHz, $CDCl_3$) δ 7.92 (d, J = 8.4 Hz, 2H), 7.72 (d, J = 8.3 Hz, 2H), 7.31 (d, J = 8.0 Hz, 2H), 7.19 (d, J = 8.3 Hz, 2H), 6.28 (d, J = 2.3 Hz, 1H), 4.27 (dd, J = 14.8, 1.4 Hz, 1H), 3.99 (dt, J = 4.3, 1.9 Hz, 1H), 3.66 (dd, J = 9.0, 7.5 Hz, 1H), 3.07 – 2.95 (m, 1H), 2.82 (t, J = 8.7 Hz, 1H), 2.60 (s, 3H), 2.41 (s, 3H), 1.18 (d, J = 5.5 Hz, 12H), 1.12 (dd, J = 16.0, 5.5 Hz, 1H), 0.96 (dd, J = 16.0, 8.0 Hz, 1H). ^{13}C NMR (75 MHz, $CDCl_3$) δ 197.5 (C), 145.7 (C), 143.7 (C), 141.4 (C), 135.4 (C), 133.0 (C), 129.8 (2 × CH), 128.7 (2 × CH), 128.2 (2 × CH), 127.9 (2 × CH), 121.3 (C), 83.5 (2 × C), 53.6 (CH_2), 51.0 (CH_2), 40.7 (CH), 26.6 (CH_3), 24.9 (2 × CH_3), 24.8 (2 × CH_3), 21.6 (CH_3), 14.0 (br m, CH_2-B). HRMS (ESI, MeOH) calcd. for $C_{27}H_{34}BNO_5S$ [M + Na]$^+$: 518.4410; Found: 518.2144.

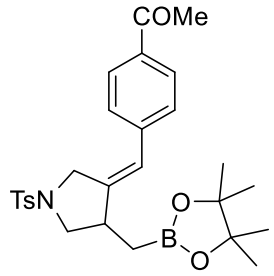

(*Z*)-2-((4-((4,4,5,5-Tetramethyl-1,3,2-dioxaborolan-2-yl)methyl)-1-tosylpyrrolidin-3-ylidene)methyl)pyridine (2bi): 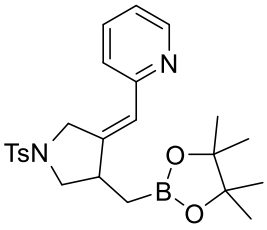

The compound was purified by column chromatography (cyclohexane/EtOAc, 9:1) and was obtained as a brown oil in 41% yield (64 mg). ^{1}H NMR (300 MHz, $CDCl_3$) δ 8.57 (s, 1H), 7.74 (d, J = 8.0 Hz, 2H), 7.65 – 7.47 (m, 1H), 7.28 (d, J = 8.0 Hz, 2H), 7.14 – 6.97 (m, 2H), 6.23 (d, J = 2.1 Hz, 1H), 4.55 (t, J = 14.2 Hz, 1H), 4.33 (t, J = 16.1 Hz, 1H), 3.70 – 3.51 (m, 1H), 3.04 – 2.94 (m, 1H), 2.82 – 2.68 (m, 1H), 2.38 (s, 3H), 1.18 (d, J = 5.4 Hz, 12H), 1.12 (dd, J = 16.0, 5.4 Hz, 1H), 0.92 (dd, J = 16.0, 8.5 Hz, 1H). ^{13}C NMR (75 MHz, $CDCl_3$) δ 155.8 (C), 149.5 (CH), 148.4 (C), 143.4 (C), 136.2 (CH), 133.2 (C), 129.7 (2 × CH), 128.0 (2 × CH), 123.5 (CH), 120.8 (CH), 120.4 (CH), 83.5 (2 × C), 53.7 (CH_2), 52.7 (CH_2), 40.4 (CH), 24.9 (2 × CH_3), 24.8 (2 × CH_3), 21.6 (CH_3), 14.1 (br m, CH_2-B). HRMS (ESI, MeOH) calcd. for $C_{24}H_{31}BN_2O_4S$ [M + H]$^+$: 455.3920; Found: 455.2157.

(*Z*)-3-Benzylidene-4-((4,4,5,5-tetramethyl-1,3,2-dioxaborolan-2-yl)methyl)-1-tosylpiperidine (2bl): 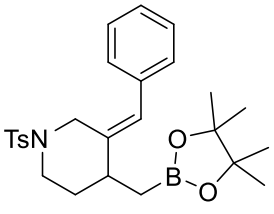

The compound was purified by column chromatography (cyclohexane/EtOAc, 95:5) and was obtained as a brown oil in 26% yield (23 mg). ^{1}H NMR (300 MHz, $CDCl_3$) δ 7.58 (d, J = 8.2 Hz, 2H), 7.34 (t, J = 7.4 Hz, 3H), 7.30 – 7.30 (m, 5H), 6.39 (s, 1H), 4.31 (d, J = 12.4 Hz, 1H), 3.62 – 3.50 (m, 1H), 3.18 (d, J = 12.4 Hz, 1H), 2.88 – 2.78 (m, 1H), 2.42 (s, 3H), 1.97 – 1.84 (m, 1H), 1.61 – 1.47 (m, 2H), 1.22 (s, 12H), 1.11 (dd, J = 15.7, 7.5 Hz, 1H), 0.88 (dd, J = 15.7, 7.3 Hz, 1H). ^{13}C NMR (75 MHz, $CDCl_3$) δ 143.5 (C), 138.5 (C), 136.9 (C), 133.4 (C), 129.7 (2 × CH), 129.1 (2 × CH), 128.5 (2 × CH), 128.0 (2 × CH), 126.9 (CH), 124.5 (CH), 83.4 (2 × C), 47.0 (CH_2), 45.7 (CH_2), 38.2 (CH), 34.5 (CH_2), 25.0 (4 × CH_3), 21.6 (CH_3), 14.8 (br m, CH_2-B). HRMS (ESI, MeOH) calcd. for $C_{26}H_{34}BNO_4S$ [M + Na]$^+$: 490.4310; Found: 490.2205.

Dimethyl (*E*)-3-benzylidene-4-((4,4,5,5-tetramethyl-1,3,2-dioxaborolan-2-yl)methyl)cyclopentane-1,1-dicarboxylate (2cc):[90] 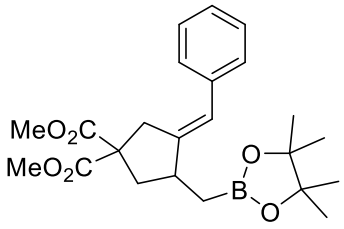

The compound was purified by column chromatography (cyclohexane/EtOAc, 9:1) and was obtained as a brown oil in 58% yield (93 mg). ^{1}H NMR (300 MHz, $CDCl_3$) δ 7.35 – 7.28 (m, 4H), 7.18 (t, J = 6.8 Hz, 1H), 6.25 (q, J = 2.3 Hz, 1H), 3.73 (s, 3H), 3.71 (s, 3H), 3.37 (d, J = 17.6 Hz, 1H), 3.20 (dt, J = 17.6, 2.5 Hz, 1H), 2.95 – 2.84 (m, 1H), 2.65 (ddd, J = 12.7, 7.2, 1.3 Hz, 1H), 1.89 (d , J = 12.7, 11.5 Hz, 1H), 1.24 (s, 12H), 1.18 (dd, J = 15.8, 7.7 Hz, 1H), 1.01 (dd, J = 15.8, 5.8 Hz, 1H).

Dimethyl (*E*)-3-(3-methoxybenzylidene)-4-((4,4,5,5-tetramethyl-1,3,2-dioxaborolan-2-yl)methyl)cyclopentane-1,1-dicarboxylate (2cd): 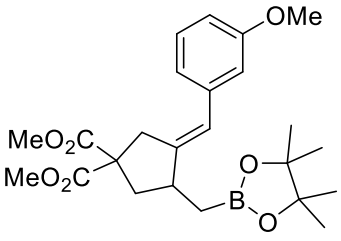

The compound was purified by column chromatography (cyclohexane/EtOAc, 9:1) and was obtained as a brown oil in 67% yield (119 mg). ^{1}H NMR (300 MHz, $CDCl_3$) δ 7.21 (t, J = 7.9 Hz, 1H), 6.87 (d, J = 7.9 Hz, 1H), 6.80 (s, 1H), 6.72 (dd, J = 7.9, 2.3 Hz, 1H), 6.22 (d, J = 2.0 Hz, 1H), 3.78 (s, 3H), 3.70 (d, J = 1.6 Hz, 6H), 3.36 (d, J = 17.5 Hz, 1H), 3.19 (dt, J = 17.5, 2.1 Hz, 1H), 2.95 – 2.83 (m, 1H), 2.63 (dd, J = 12.7, 7.2 Hz, 1H), 1.89 (t, J = 12.0 Hz, 1H), 1.23 (s, 12H), 1.16 (dd, J = 15.7, 5.6 Hz, 1H), 1.00 (dd, J = 15.7, 7.7 Hz, 1H). ^{13}C NMR (75

[90] J. Marco-Martínez, V. López-Carrillo, E. Buñuel, R. Simancas, D. J. Cárdenas, *J. Am. Chem. Soc.* **2007**, *129*, 1874–1875.

MHz, $CDCl_3$) δ 172.3 (C), 172.3 (C), 159.5 (C), 147.1 (C), 139.5 (C), 129.2 (CH), 121.5 (CH), 121.0 (CH), 114.1 (CH), 111.6 (CH), 83.2 (2 × C), 59.1 (C), 55.2 (CH_3), 52.8 (CH_3), 52.7 (CH_3), 41.2 (CH_2), 40.5 (CH), 39.0 (CH_2), 25.0 (2 × CH_3), 24.8 (2 × CH_3), 16.0 (br m, CH_2-B). HRMS (ESI, MeOH) calcd. for $C_{24}H_{33}BO_7$ [M + Na]$^+$: 467.3310; Found: 467.2222.

Dimethyl (*E*)-3-(4-methoxybenzylidene)-4-((4,4,5,5-tetramethyl-1,3,2-dioxaborolan-2-yl)methyl)cyclopentane-1,1-dicarboxylate (2ce): 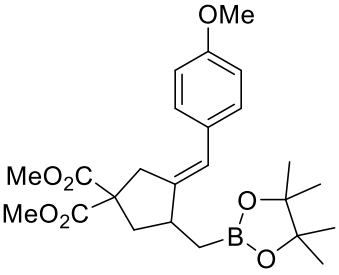

The compound was purified by column chromatography (cyclohexane/EtOAc, 95:5) and was obtained as a brown oil in 70% yield (123 mg). ^{1}H NMR (300 MHz, $CDCl_3$) δ 7.20 (d, *J* = 8.6 Hz, 2H), 6.84 (d, *J* = 8.6 Hz, 2H), 6.17 (d, *J* = 2.0 Hz, 1H), 3.77 (s, 3H), 3.69 (s, 6H), 3.32 (d, *J* = 17.4 Hz, 1H), 3.15 (dt, *J* = 17.4, 2.4 Hz, 1H), 2.94 – 2.82 (m, 1H), 2.62 (ddd, *J* = 12.6, 7.2, 1.0 Hz, 1H), 1.87 (t, *J* = 12.0 Hz, 1H), 1.22 (s, 12H), 1.14 (dd, *J* = 15.7, 5.8 Hz, 1H), 0.98 (dd, *J* = 15.7, 7.7 Hz, 1H). ^{13}C NMR (75 MHz, $CDCl_3$) δ 172.3 (2 × C), 158.0 (C), 144.4 (C), 130.9 (C), 129.5 (2 × CH), 120.9 (CH), 113.7 (2 × CH), 83.1 (2 × C), 59.1 (C), 55.2 (CH_3), 52.8 (CH_3), 52.7 (CH_3), 41.2 (CH_2), 40.4 (CH), 38.8 (CH_2), 25.0 (2 × CH_3), 24.7 (2 × CH_3), 15.7 (br m, CH_2-B). HRMS (ESI, MeCN) calcd. for $C_{24}H_{33}BO_7$ [M + Na]$^+$: 467.3310; Found: 467.2216.

Dimethyl (*E*)-3-(4-cyanobenzylidene)-4-((4,4,5,5-tetramethyl-1,3,2-dioxaborolan-2-yl)methyl)cyclopentane-1,1-dicarboxylate (2cf): 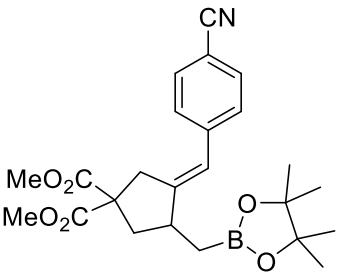

The compound was purified by column chromatography (cyclohexane/EtOAc, 9:1) and was obtained as a light brown oil in 74% yield (123 mg). ^{1}H NMR (300 MHz, $CDCl_3$) δ 7.59 (d, *J* = 8.4 Hz, 1H), 7.34 (d, *J* = 8.4 Hz, 1H), 6.26 (d, *J* = 2.3 Hz, 1H), 3.74 (s, 3H), 3.72 (s, 3H), 3.34 (d, *J* = 17.6 Hz, 1H), 3.18 (dt, *J* = 17.6, 2.6 Hz, 1H), 2.98 – 2.87 (m, 1H), 2.66 (dd, *J* = 12.2, 6.8 Hz, 1H), 1.91 (dd, *J* = 12.6, 11.6 Hz, 1H), 1.23 (d, *J* = 2.1 Hz, 12H), 1.17 (dd, *J* = 15.8, 5.7 Hz, 1H), 1.02 (dd, *J* = 15.8, 7.7 Hz, 1H). ^{13}C NMR (75 MHz, $CDCl_3$) δ 172.0 (C), 171.9 (C), 151.4 (C), 142.6 (C), 132.1 (2 × CH), 128.7 (2 × CH), 120.4 (CH), 119.1 (C), 109.3 (C), 83.3 (2 × C), 59.0 (C), 52.9 (CH_3), 52.8 (CH_3), 40.8 (CH), 39.1 (CH_2), 24.9 (2 × CH_3), 24.7 (2 × CH_3), 15.6 (br m, CH_2-B). HRMS (ESI, MeOH) calcd. for $C_{24}H_{30}BO_6$ [M + Na]$^+$: 462.3150; Found: 462.2076.

Dimethyl (*E*)-3-((4,4,5,5-tetramethyl-1,3,2-dioxaborolan-2-yl)methyl)-4-(4-(trifluoromethyl)benzylidene)cyclopentane-1,1-dicarboxylate (2cg):[101] 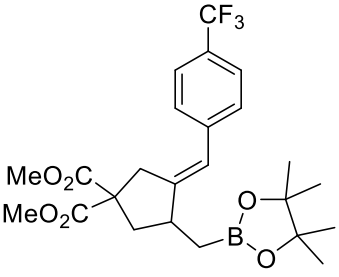

The compound was purified by column chromatography (cyclohexane/EtOAc, 95:5) and was obtained as a brown oil in 37% yield (35 mg). ^{1}H NMR (300 MHz, $CDCl_3$) δ 7.56 (d, *J* = 8.2 Hz, 2H), 7.36 (d, *J* = 8.2 Hz, 2H), 6.28 (d, *J* = 2.2 Hz, 1H), 3.73 (s, 6H), 3.72 (s, 6H), 3.35 (d, *J* = 17.6 Hz, 1H), 3.19 (dt, *J* = 17.6, 2.5 Hz, 1H), 3.02 – 2.83 (m, 1H), 2.66 (ddd, *J* = 12.6, 7.3, 1.3 Hz, 1H), 1.92 (dd, *J* = 12.6, 11.5 Hz, 1H), 1.24 (d, *J* = 1.8 Hz, 6H), 1.17 (dd, *J* = 15.9, 5.8 Hz, 1H), 1.03 (dd, *J* = 15.9, 7.7 Hz, 1H).

[101] S. Yu, C. Wu, S. Ge, *J. Am. Chem. Soc.* **2017**, *139*, 6526–6529.

(*E*)-2-((3-Benzylidene-8,8-dimethyl-7,9-dioxaspiro[4.5]decan-2-yl)methyl)-4,4,5,5-tetramethyl-1,3,2-dioxaborolane (2da): The compound was purified by column chromatography (cyclohexane/EtOAc, 95:5) and was obtained as a yellow oil in 64% yield (51 mg). ^{1}H NMR (300 MHz, $CDCl_3$) δ 7.34 – 7.27 (m, 4H), 7.21 – 7.11 (m, 1H), 6.26 (q, *J* = 2.2 Hz, 1H), 3.74 – 3.50 (m, 4H), 2.85 – 2.82 (m, 1H), 2.77 (d, *J* = 17.3 Hz, 1H), 2.48 (d, *J* = 17.3 Hz, 1H), 2.02 (dd, *J* = 12.5, 7.9 Hz, 1H), 1.43 (s, 3H), 1.41 (s, 3H), 1.37 – 1.31 (m, 1H), 1.24 (d, *J* = 1.2 Hz, 12H), 1.16 (dd, *J* = 15.7, 5.1 Hz, 1H), 0.98 (dd, *J* = 15.7, 8.0 Hz, 1H). ^{13}C NMR (75 MHz, $CDCl_3$) δ 149.1 (C), 138.6 (C), 128.4 (2 × CH), 128.3 (2 × CH), 126.0 (CH), 121.6 (CH), 98.0 (C), 83.2 (2 × C), 70.0 (CH_2), 68.4 (CH_2), 40.9 (C), 40.4 (CH_2), 39.6 (CH), 39.0 (CH_2), 25.1 (2 × CH_3), 24.9 (3 × CH_3), 23.1 (CH_3), 16.7 (br m, CH_2-B). HRMS (ESI, MeOH) calcd. for $C_{24}H_{35}BO_4$ $[M + Na]^+$: 421.3500; Found: 421.2358.

(*E*)-2-((2-Benzylidene-4,4-bis((benzyloxy)methyl)cyclopentyl)methyl)-4,4,5,5-tetramethyl-1,3,2-dioxaborolane (2db): The compound was purified by column chromatography (cyclohexane/EtOAc, 98:2) and was obtained as a pale yellow oil in 58% yield (124 mg). ^{1}H NMR (300 MHz, $CDCl_3$) δ 7.32 – 7.27 (m, 15H), 6.23 (d, *J* = 2.2 Hz, 1H), 4.50 (d, *J* = 1.9 Hz, 4H), 3.47 – 3.40 (m, 4H), 2.89 (s, 1H), 2.55 (dt, *J* = 17.3, 2.2 Hz, 2H), 2.05 (dd, *J* = 12.7, 7.9 Hz, 1H), 1.24 (d, *J* = 2.1 Hz, 13H), 1.18 (d, *J* = 6.2 Hz, 1H), 0.95 (dd, *J* = 15.5, 8.2 Hz, 1H). ^{13}C NMR (75 MHz, $CDCl_3$) δ 150.4 (C), 139.1 (C), 139.0 (C), 138.8 (C), 128.5 (2 × CH), 128.4 (2 × CH), 128.2 (2 × CH), 127.6 (2 × CH), 127.5 (2 × CH), 127.5 (2 × CH), 127.4 (2 × CH), 125.8 (CH), 120.9 (CH), 83.2 (2 × C), 75.2 (CH_2), 73.4 (CH_2), 73.3 (CH_2), 72.9 (CH_2), 46.9 (C), 40.0 (CH), 39.5 (CH_2), 38.1 (CH_2), 25.1 (2 × CH_3), 24.9 (2 × CH_3), 16.7 (br m, CH_2-B). HRMS (ESI, MeOH) calcd. for $C_{35}H_{43}BO_4$ $[M]^+$: 539.5350; Found: 539.3326.

(*E*)-2-((2-Benzylidenecyclopentyl)methyl)-4,4,5,5-tetramethyl-1,3,2-dioxaborolane (2ea): The compound was purified by column chromatography (cyclohexane/EtOAc, 98:2) and was obtained as a yellow oil in 37% yield (49 mg). ^{1}H NMR (300 MHz, $CDCl_3$) δ 7.31 (d, *J* = 4.3 Hz, 4H), 7.15 (td, *J* = 8.5, 4.3 Hz, 1H), 6.27 (d, *J* = 2.3 Hz, 1H), 2.80 – 2.51 (m, 3H), 2.07 – 1.77 (m, 3H), 1.73 – 1.51 (m, 1H), 1.26 (d, *J* = 2.3 Hz, 12H), 1.18 (dd, *J* = 15.6, 5.7 Hz, 1H), 0.95 (dd, *J* = 15.6, 8.5 Hz, 1H). ^{13}C NMR (75 MHz, $CDCl_3$) δ 152.2 (C), 139.2 (C), 128.2 (4 × CH), 125.7 (CH), 120.2 (CH), 83.2 (2 × C), 42.5 (CH), 34.5 (CH_2), 31.4 (CH_2), 25.1 (2 × CH_3), 24.9 (2 × CH_3), 24.8 (CH_2), 16.9 (br m, CH_2-B). HRMS (ESI, MeOH) calcd. for $C_{19}H_{27}BO_2$ $[M + H]^+$: 299.2330; Found: 299.2176.

(*E*)-4,4,5,5-Tetramethyl-2-((2-(4-methylbenzylidene)cyclopentyl)methyl)-1,3,2-dioxaborolane (2eb): The compound was purified by column chromatography (cyclohexane/EtOAc, 98:2) and was obtained as a colorless oil in 22% yield (28 mg). ^{1}H NMR (300 MHz, $CDCl_3$) δ 7.21 (d, *J* = 8.1 Hz, 2H), 7.11 (d, *J* = 8.1 Hz, 2H), 6.23 (d, *J* = 2.3 Hz, 1H), 2.80 – 2.45 (m, 3H), 2.33 (s, 3H), 2.03 – 1.75 (m, 2H), 1.69 – 1.51 (m, 2H), 1.26 (d, *J* = 2.3 Hz, 12H), 1.19 (dd, *J* = 15.6, 5.5 Hz, 1H), 0.94 (dd, *J* = 15.6, 8.5 Hz, 1H). ^{13}C NMR (75 MHz, $CDCl_3$) δ 151.1 (C), 136.4 (C), 135.2 (C), 129.0 (2 × CH), 128.1 (2 × CH), 120.0 (CH), 83.1 (2 × C), 42.4 (CH), 34.5 (CH_2), 31.3 (CH_2), 25.1 (2 × CH_3), 24.9 (2 × CH_3), 24.8 (CH_2), 21.2 (CH_3),

16.7 (br m, CH_2-B). HRMS (ESI, MeOH) calcd. for $C_{20}H_{29}BO_2$ $[M + Na]^+$: 335.2600; Found: 335.2163.

(*Z*)-3-Benzylidene-4-((4,4,5,5-tetramethyl-1,3,2-dioxaborolan-2-yl)methyl)dihydrofuran-2(3*H*)-one (2fa): 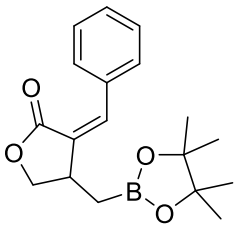 The compound was purified by column chromatography (cyclohexane/EtOAc, 95:5) and was obtained as a colorless oil in 66% yield (83 mg). ^{1}H NMR (300 MHz, $CDCl_3$) δ 7.81 (d, J = 7.8 Hz, 2H), 7.43 – 7.29 (m, 3H), 6.92 (d, J = 2.1 Hz, 1H), 4.54 (t, J = 8.4 Hz, 1H), 3.98 (dd, J = 8.7, 6.5 Hz, 1H), 3.39 (d, J = 6.5 Hz, 1H), 1.25 (d, J = 2.1 Hz, 12H), 1.13 (dd, J = 16.1, 8.3 Hz, 2H). ^{13}C NMR (75 MHz, $CDCl_3$) δ 169.2 (C), 138.6 (CH), 133.8 (C), 130.7 (2 × CH), 130.4 (C), 129.3 (CH), 128.1 (2 × CH), 83.7 (2 × C), 72.1 (CH_2), 38.3 (CH), 25.0 (2 × CH_3), 24.8 (2 × CH_3), 15.9 (br m, CH_2-B). HRMS (ESI, MeCN) calcd. for $C_{18}H_{23}BO_4$ $[M + Na]^+$: 337.1880; Found: 337.1588.

(*Z*)-3-Benzylidene-1-phenyl-4-((4,4,5,5-tetramethyl-1,3,2-dioxaborolan-2-yl)methyl)pyrrolidin-2-one (2fb): 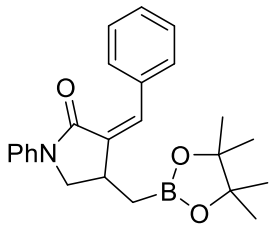 The compound was purified by column chromatography (cyclohexane/EtOAc, 95:5) and was obtained as a pale yellow oil in 77% yield (120 mg). ^{1}H NMR (300 MHz, $CDCl_3$) δ 7.82 (d, J = 7.1 Hz, 2H), 7.68 (dd, J = 8.6, 0.9 Hz, 2H), 7.41 – 7.27 (m, 5H), 7.15 (t, J = 7.4 Hz, 1H), 6.80 (d, J = 2.1 Hz, 1H), 4.06 (dd, J = 9.2, 8.2 Hz, 1H), 3.56 (dd, J = 9.2, 5.3 Hz, 1H), 3.35 – 3.20 (m, 1H), 1.37 (dd, J = 16.1, 5.6 Hz, 1H), 1.26 (s, 12H), 1.20 (dd, J = 16.1, 8.4 Hz, 1H). ^{13}C NMR (75 MHz, $CDCl_3$) δ 166.1 (C), 139.9 (C), 137.5 (C), 134.7 (C), 134.6 (CH), 130.5 (2 × CH), 128.7 (2 × CH), 128.3 (CH), 127.8 (2 × CH), 124.5 (CH), 120.1 (2 × CH), 83.5 (2 × C), 53.2 (CH_2), 34.7 (CH), 25.0 (2 × CH_3), 24.8 (2 × CH_3), 17.3 (br m, CH_2-B). HRMS (ESI, MeOH) calcd. for $C_{24}H_{28}BNO_3$ $[M + H]^+$: 390.3020; Found: 390.2226.

Alkenylboronates (11)

(*Z*)-4,4,5,5-Tetramethyl-2-(1-(4-methyldihydrofuran-3(2*H*)-ylidene)ethyl)-1,3,2-dioxaborolane (11an):[101] 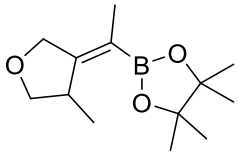 The compound was purified by column chromatography (cyclohexane/EtOAc, 98:2) and was obtained as a colorless oil in 15% yield (29 mg). ^{1}H NMR (300 MHz, $CDCl_3$) δ 4.48 (d, J = 15.0 Hz, 1H), 4.23 (d, J = 15.0 Hz, 1H), 3.80 (dd, J = 8.3, 5.2 Hz, 1H), 3.71 (d, J = 8.3 Hz, 1H), 3.22 (quin, J = 6.5 Hz 1H), 1.61 (d, J = 0.9 Hz, 3H), 1.27 (d, J = 1.1 Hz, 12H), 1.12 (d, J = 7.0 Hz, 3H). ^{13}C NMR (75 MHz, $CDCl_3$) δ 161.9 (C), 83.1 (2 × C), 76.1 (CH_2), 70.7 (CH_2), 38.6 (CH), 25.2 (2 × CH_3), 24.8 (2 × CH_3), 21.1 (CH_3), 16.9 (CH_3).

(*Z*)-3-Methyl-4-(1-(4,4,5,5-tetramethyl-1,3,2-dioxaborolan-2-yl)ethylidene)-1-tosylpyrrolidine (11bn):[100] 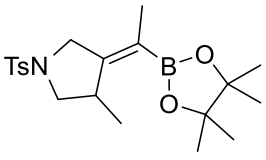 The compound was purified by column chromatography (cyclohexane/EtOAc, 9:1) and was obtained as a white solid in 71% yield (108 mg). ^{1}H NMR (300 MHz, $CDCl_3$) δ 7.69 (d, J = 8.2 Hz, 2H), 7.31 (d, J = 8.2 Hz, 2H), 4.05 (dd, J = 15.6, 1.2 Hz, 1H), 3.49 (dd, J = 15.6, 1.2 Hz, 1H), 3.27 (t, J = 8.2 Hz, 2H), 2.95 (dd, J = 8.9, 6.1 Hz, 1H), 2.40 (s, 3H), 1.55 (s, 3H), 1.20 (s, 12H), 1.10 (d, J = 6.1 Hz, 3H).

[100] T. Xi, Z. Lu, *ACS Catal.* **2017**, *7*, 1181–1185.
[101] S. Yu, C. Wu, S. Ge, *J. Am. Chem. Soc.* **2017**, *139*, 6526–6529.

(*Z*)-3-Methyl-4-(1-(4,4,5,5-tetramethyl-1,3,2-dioxaborolan-2-yl)propylidene)-1-tosylpyrrolidine (11bo): 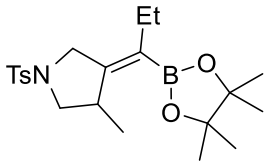

The compound was purified by column chromatography (cyclohexane/EtOAc, 95:5) and was obtained as a white solid in 61% yield (92 mg). M.p. = 132 – 134 °C. ^{1}H NMR (300 MHz, $CDCl_3$) δ 7.69 (d, J = 8.0 Hz, 2H), 7.31 (d, J = 8.0 Hz, 2H), 4.09 (d, J = 15.3 Hz, 1H), 3.56 (d, J = 15.3 Hz, 1H), 3.25 (t, J = 7.4 Hz, 2H), 2.96 (dd, J = 8.6, 6.4 Hz, 1H), 2.41 (s, 3H), 1.93 (q, J = 7.4 Hz, 2H), 1.21 (s, 12H), 1.09 (d, J = 6.9 Hz, 3H), 0.86 (t, J = 7.4 Hz, 3H). ^{13}C NMR (75 MHz, $CDCl_3$) δ 155.5 (C), 143.6 (C), 132.5 (C), 129.7 (2 × CH), 128.0 (2 × CH), 83.1 (2 × C), 55.1 (CH_2), 50.1 (CH_2), 37.7 (CH), 25.4 (CH_2), 25.0 (2 × CH_3), 24.7 (2 × CH_3), 21.9 (CH_3), 21.6 (CH_3), 13.9 (CH_3). HRMS (ESI, MeOH) calcd. for $C_{21}H_{32}BNO_4S$ [M + H]$^+$: 406.3600; Found: 406.2220.

(*Z*)-3-Methyl-4-(1-(4,4,5,5-tetramethyl-1,3,2-dioxaborolan-2-yl)butylidene)-1-tosylpyrrolidine (11bp): 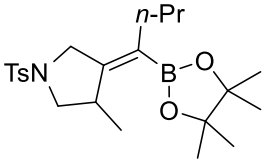

The compound was purified by column chromatography (cyclohexane/EtOAc, 95:5) and was obtained as a colorless oil in 59% yield (47 mg). ^{1}H NMR (300 MHz, $CDCl_3$) δ 7.69 (d, J = 8.1 Hz, 2H), 7.31 (d, J = 8.1 Hz, 2H), 4.09 (d, J = 15.3 Hz, 1H), 3.58 (d, J = 15.3 Hz, 1H), 3.26 (d, J = 8.6 Hz, 1H), 2.96 (dd, J = 8.9, 6.2 Hz, 1H), 2.41 (s, 3H), 1.90 (t, J = 7.6 Hz, 2H), 1.28 (dd, J = 14.8, 7.4 Hz, 2H), 1.21 (s, 12H), 1.09 (d, J = 7.0 Hz, 3H), 0.82 (t, J = 7.4 Hz, 3H). ^{13}C NMR (75 MHz, $CDCl_3$) δ 156.0 (C), 143.6 (C), 132.6 (C), 129.7 (2 × CH), 128.0 (2 × CH), 83.1 (2 × C), 55.2 (CH_2), 50.4 (CH_2), 37.8 (CH), 34.3 (CH_2), 25.0 (2 × CH_3), 24.7 (2 × CH_3), 22.7 (CH_2), 22.0 (CH_3), 21.6 (CH_3), 14.2 (CH_3). HRMS (ESI, MeOH) calcd. for $C_{22}H_{34}BNO_4S$ [M + H]$^+$: 420.3870; Found: 420.2372.

(*Z*)-3-Methyl-4-(1-(4,4,5,5-tetramethyl-1,3,2-dioxaborolan-2-yl)heptylidene)-1-tosylpyrrolidine (11br): 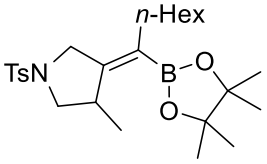

The compound was purified by column chromatography (cyclohexane/EtOAc, 95:5) and was obtained as a colorless oil in 27% yield (21 mg). ^{1}H NMR (300 MHz, $CDCl_3$) δ 7.70 (d, J = 8.2 Hz, 2H), 7.31 (d, J = 8.2 Hz, 2H), 4.09 (d, J = 15.3 Hz, 1H), 3.57 (d, J = 15.3 Hz, 1H), 3.27 (d, J = 9.1 Hz, 2H), 2.96 (dd, J = 8.9, 6.1 Hz, 1H), 2.42 (s, 3H), 1.95 – 1.88 (m, 2H), 1.31 – 1.23 (m, 8H), 1.21 (s, 12H), 1.09 (d, J = 7.0 Hz, 3H), 0.87 (t, J = 6.7 Hz, 3H). ^{13}C NMR (75 MHz, $CDCl_3$) δ 155.6 (C), 143.6 (C), 132.6 (C), 129.7 (2 × CH), 128.0 (2 × CH), 83.1 (2 × C), 55.2 (CH_2), 50.4 (CH_2), 37.8 (CH), 32.3 (CH_2), 31.9 (CH_2), 29.5 (CH_2), 29.4 (CH_2), 25.0 (2 × CH_3), 24.7 (2 × CH_3), 22.7 (CH_2), 21.9 (CH_3), 21.6 (CH_3), 14.2 (CH_3). HRMS (ESI, MeOH) calcd. for $C_{25}H_{40}BNO_4S$ [M + H]$^+$: 462.2771; Found: 462.2843.

(*Z*)-3-Methyl-4-(1-(4,4,5,5-tetramethyl-1,3,2-dioxaborolan-2-yl)nonylidene)-1-tosylpyrrolidine (11bs): 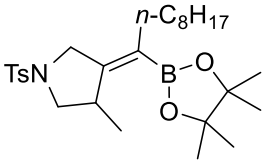

The compound was purified by column chromatography (cyclohexane/EtOAc, 95:5) and was obtained as a colorless oil in 45% yield (51 mg). ^{1}H NMR (300 MHz, $CDCl_3$) δ 7.70 (d, J = 8.0 Hz, 2H), 7.31 (d, J = 8.0 Hz, 2H), 4.09 (d, J = 15.3 Hz, 1H), 3.57 (d, J = 15.3 Hz, 1H), 3.25 (t, J = 8.8 Hz, 2H), 2.96 (dd, J = 8.8, 6.1 Hz, 1H), 2.42 (s, 3H), 1.90 (d, J = 6.7 Hz, 1H), 1.21 (br s, 25H), 1.09 (d, J = 7.0 Hz, 3H), 0.89 (t, J = 6.8 Hz, 3H). ^{13}C NMR (75 MHz, $CDCl_3$) δ 155.6 (C), 143.6 (C), 132.6 (C), 129.7 (2 × CH), 128.1 (2 × CH), 83.2 (2 × C), 55.2 (CH_2), 50.4 (CH_2), 37.8 (CH), 32.3 (CH_2), 32.0 (CH_2), 29.7 (CH_2), 29.5 (CH_2), 29.3 (CH_2), 25.0 (2 × CH_3), 24.7 (2 × CH_3), 22.8 (CH_2), 22.0 (CH_3), 21.6 (CH_3), 14.3 (CH_3). HRMS (ESI, MeOH) calcd. for $C_{27}H_{44}BNO_4S$ [M]$^+$: 490.5220; Found: 490.3175.

(*Z*)-3-Methyl-1-phenyl-4-(1-(4,4,5,5-tetramethyl-1,3,2-dioxaborolan-2-yl)ethylidene)pyrrolidine (11bw): 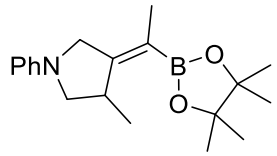

The compound was purified by column chromatography (cyclohexane/EtOAc, 9:1) and was obtained as a colorless oil in 65% yield (82 mg). ^{1}H NMR (300 MHz, $CDCl_3$) δ 7.30 – 7.22 (m, 2H), 6.71 (t, *J* = 7.3 Hz, 1H), 6.65 (d, *J* = 7.8 Hz, 2H), 4.18 (d, *J* = 16.0 Hz, 1H), 3.76 (d, *J* = 16.0 Hz, 1H), 3.54 – 3.40 (m, 1H), 3.32 – 3.22 (m, 2H), 1.73 (s, 3H), 1.29 (d, *J* = 2.3 Hz, 12H), 1.19 (d, *J* = 7.0 Hz, 2H). ^{13}C NMR (75 MHz, $CDCl_3$) *δ* 160.2 (C), 148.8 (C), 129.3 (2 × CH), 116.4 (CH), 112.4 (2 × CH), 83.1 (2 × C), 77.4 (C), 55.5 (CH_2), 52.2 (CH_2), 37.6 (CH), 25.2 (2 × CH_3), 24.9 (2 × CH_3), 23.1 (CH_3), 17.1 (CH_3). HRMS (ESI, MeOH) calcd. for $C_{19}H_{28}BNO_2$ $[M + H]^+$: 314.2480; Found: 314.2275.

(*Z*)-(3-Methyl-4-(1-(4,4,5,5-tetramethyl-1,3,2-dioxaborolan-2-yl)ethylidene)pyrrolidin-1-yl)(phenyl)methanone (11bx): 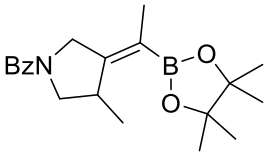

The compound was purified by column chromatography (cyclohexane/EtOAc, 9:1) and was obtained as a colorless oil in 75% yield (102 mg). ^{1}H NMR (300 MHz, $CDCl_3$) *δ* 7.52 – 7.45 (m, 2H), 7.43 – 7.37 (m, 3H), 4.56 (d, *J* = 18.5 Hz, 1H), 4.13 (d, *J* = 18.5 Hz, 1H), 4.12 – 3.90 (m, 1H), 3.61 (dd, *J* = 10.6, 6.1 Hz, 1H), 3.40 – 3.19 (m, 1H), 1.70 (s, 3H), 1.24 (d, *J* = 2.1 Hz, 12H), 1.02 (d, *J* = 7.0 Hz, 1H). ^{13}C NMR (75 MHz, $CDCl_3$) *δ* 170.1 (C), 157.0 (C), 136.7 (C), 129.9 (2 × CH), 128.4 (2 × CH), 127.3 (2 × CH), 83.2 (2 × C), 56.7 (CH_2), 49.0 (CH_2), 38.2 (CH), 25.1 (2 × CH_3), 24.8 (2 × CH_3), 21.6 (CH_3), 17.0 (CH_3). HRMS (ESI, MeOH) calcd. for $C_{20}H_{28}BNO_3$ $[M]^+$: 342.2580; Found: 342.2238.

(*Z*)-4-Methyl-2-phenyl-3-(1-(4,4,5,5-tetramethyl-1,3,2-dioxaborolan-2-yl)ethylidene)-1-tosylpyrrolidine (11by): 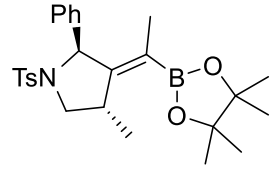

The compound was purified by column chromatography (cyclohexane/EtOAc, 95:5) and was obtained as a white solid in 72% yield (68 mg). M.p. = 144 – 146 °C. ^{1}H NMR (300 MHz, $CDCl_3$) *δ* 7.20 – 7.11 (m, 7H), 6.97 (d, *J* = 8.0 Hz, 2H), 5.59 (br s, 1H), 3.57 – 3.41 (m, 3H), 2.29 (s, 3H), 1.27 (s, 3H), 1.24 (d, *J* = 4.6 Hz, 12H), 1.15 (d, *J* = 6.2 Hz, 3H). ^{13}C NMR (75 MHz, $CDCl_3$) *δ* 161.7 (C), 142.3 (C), 140.5 (C), 137.3 (C), 129.1 (2 × CH), 128.9 (2 × CH), 128.3 (2 × CH), 127.4 (CH), 126.9 (2 × CH), 83.3 (2 × C), 66.4 (CH), 54.2 (CH_2), 38.4 (CH), 25.2 (2 × CH_3), 24.8 (2 × CH_3), 23.4 (CH_3), 21.5 (CH_3), 18.1 (CH_3). HRMS (ESI, MeOH) calcd. for $C_{26}H_{34}BNO_4S$ $[M + Na]^+$: 490.4310; Found: 490.2184.

(*Z*)-2,3-Dimethyl-4-(1-(4,4,5,5-tetramethyl-1,3,2-dioxaborolan-2-yl)ethylidene)-1-tosylpyrrolidine (11bz): 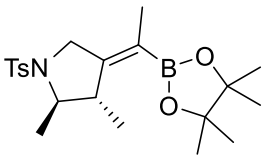

The compound was purified by column chromatography (cyclohexane/EtOAc, 95:5) and was obtained as a colorless oil in 54% yield (42 mg). ^{1}H NMR (300 MHz, $CDCl_3$) *δ* 7.75 (d, *J* = 8.2 Hz, 2H), 7.28 (d, *J* = 8.2 Hz, 2H), 4.04 (dd, *J* = 15.6, 1.0 Hz, 1H), 3.88 (dt, *J* = 15.6, 1.4 Hz, 1H), 3.69 (q, *J* = 6.5 Hz, 1H), 2.93 (q, *J* = 7.0 Hz, 1H), 2.40 (s, 3H), 1.60 (s, 3H), 1.21 (d, *J* = 2.5 Hz, 12H), 1.15 (d, *J* = 6.5 Hz, 3H), 0.67 (d, *J* = 7.0 Hz, 3H). ^{13}C NMR (75 MHz, $CDCl_3$) *δ* 156.8 (C), 143.2 (C), 136.7 (C), 129.7 (2 × CH), 127.3 (2 × CH), 83.2 (2 × CH), 63.7 (CH), 49.1 (CH_2), 45.6 (CH), 25.0 (2 × CH_3), 24.8 (2 × CH_3), 21.9 (CH_3), 21.6 (CH_3), 21.2 (CH_3), 17.1 (CH_3). HRMS (ESI, MeOH) calcd. for $C_{21}H_{32}BNO_4S$ $[M + H]^+$: 406.3600; Found: 406.2221.

Dimethyl (*E*)-3-methyl-4-(1-(4,4,5,5-tetramethyl-1,3,2-dioxaborolan-2-yl)ethylidene)cyclopentane-1,1-dicarboxylate (11cb):[99] The compound was purified by column chromatography (cyclohexane/EtOAc, 95:5) and was obtained as a colorless oil in 18% yield (25 mg). ^{1}H NMR (300 MHz, $CDCl_3$) δ 3.74 (s, 3H), 3.70 (s, 3H), 3.27 – 3.23 (m, 1H), 3.16 (d, *J* = 17.8 Hz, 1H), 2.88 (d, *J* = 17.8 Hz, 1H), 2.57 (dd, *J* = 13.3, 8.3 Hz, 1H), 2.09 (dd, *J* = 13.3, 3.1 Hz, 1H), 1.67 (d, *J* = 1.2 Hz, 3H), 1.24 (s, 12H), 1.00 (d, *J* = 7.1 Hz, 3H).

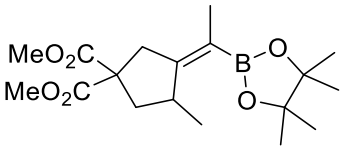

Reductive cyclization products (13)

(*Z*)-3-Benzylidene-4-methyltetrahydrofuran (13aa):[65] The compound was purified by column chromatography (cyclohexane/EtOAc 95:5) and was obtained as a yellow oil in 7% yield (5 mg). ^{1}H NMR (300 MHz, $CDCl_3$) δ 7.35 (t, *J* = 7.4 Hz, 2H), 7.21 (t, *J* = 7.4 Hz, 1H), 7.15 (d, *J* = 7.2 Hz, 2H), 6.30 (dd, *J* = 4.7, 2.3 Hz, 1H), 4.71 (d, *J* = 14.1 Hz, 1H), 4.62 (dt, *J* = 14.1, 2.2 Hz, 1H), 4.59 (d, *J* = 2.2 Hz, 1H), 3.39 (t, *J* = 8.0 Hz, 1H), 3.03 – 2.83 (m, 1H), 1.23 (d, *J* = 6.8 Hz, 3H).

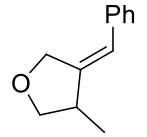

(*Z*)-1-(4-Benzylidene-1-tosylpyrrolidin-3-yl)propan-2-one (13ga): The compound was purified by column chromatography (cyclohexane/EtOAc 9:1) and was obtained as a brown oil in 57% yield (84 mg). ^{1}H NMR (300 MHz, $CDCl_3$) δ 7.71 (d, *J* = 8.2 Hz, 2H), 7.38 – 7.30 (m, 4H), 7.11 (d, *J* = 7.3 Hz, 2H), 6.26 (s, 1H), 4.24 (d, *J* = 15.0 Hz, 1H), 3.97 (dd, *J* = 15.0, 2.3 Hz, 1H), 3.36 (dd, *J* = 9.4, 6.8 Hz, 1H), 3.24 (s, 1H), 3.04 (dd, *J* = 9.4, 4.4 Hz, 1H), 2.71 (dd, *J* = 10.2, 6.9 Hz, 2H), 2.42 (s, 3H), 2.16 (s, 3H). ^{13}C NMR (75 MHz, $CDCl_3$) δ 206.7 (C), 143.9 (C), 139.6 (C), 136.3 (C), 132.7 (C), 129.9 (2 × CH), 128.7 (2 × CH), 128.1 (2 × CH), 127.8 (2 × CH), 127.3 (CH), 123.5 (CH), 52.3 (CH_2), 50.5 (CH_2), 47.4 (CH_2), 39.9 (CH), 30.3 (CH_3), 21.6 (CH_3). HRMS (ESI, MeOH) calcd. for $C_{21}H_{23}NO_3S$ [M + H]$^+$: 370.4790; Found: 370.1484.

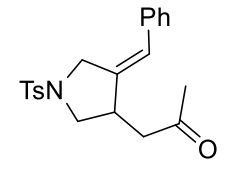

(*Z*)-1-(4-Ethylidene-1-tosylpyrrolidin-3-yl)propan-2-one (13gb):[217] The compound was purified by column chromatography (cyclohexane/EtOAc 9:1) and was obtained as a yellow oil in 60% yield (37 mg). ^{1}H NMR (300 MHz, $CDCl_3$) δ 7.71 (d, *J* = 8.3 Hz, 2H), 7.34 (d, *J* = 8.3 Hz, 2H), 5.27 – 5.22 (m, 1H), 3.85 (d, *J* = 14.0 Hz, 1H), 3.65 (d, *J* = 14.0 Hz, 1H), 3.36 (dd, *J* = 9.2, 6.6 Hz, 1H), 3.06 – 2.97 (s, 1H), 2.93 (dd, *J* = 9.2, 5.2 Hz, 1H), 2.60 – 2.48 (m, 2H), 2.44 (s, 3H), 2.12 (s, 3H), 1.54 – 1.50 (m, 3H).

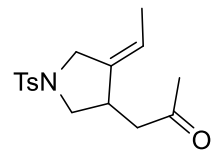

(*Z*)-2-(4-Ethylidene-1-tosylpyrrolidin-3-yl)-1-phenylethan-1-one (13gc): The compound was purified by column chromatography (cyclohexane/EtOAc 9:1) and was obtained as a yellow oil in 69% yield (51 mg). ^{1}H NMR (300 MHz, $CDCl_3$) δ 7.88 (d, *J* = 7.4 Hz, 2H), 7.70 (d, *J* = 8.1 Hz, 2H), 7.56 (t, *J* = 7.4 Hz, 1H), 7.44 (t, *J* = 7.6 Hz, 2H), 7.30 (d, *J* = 8.1 Hz, 2H), 5.42 – 5.21 (m, 1H), 3.89 (d, *J* = 14.0 Hz, 1H), 3.72 (d, *J* = 14.0 Hz, 1H), 3.47 (dd, *J* = 9.5, 6.8 Hz, 1H), 3.25 – 3.15 (m, 1H), 3.10 – 2.90 (m, 3H), 2.40 (s, 3H), 1.53 (d, *J* = 6.8 Hz, 3H). ^{13}C NMR (75 MHz, $CDCl_3$) δ 198.3 (C), 143.7 (C), 138.8 (C), 136.7 (C), 133.4 (CH), 132.7 (C), 129.8 (2 × CH), 128.7 (2 × CH), 128.1 (2 × CH), 127.9 (2 × CH), 117.8 (CH), 53.7

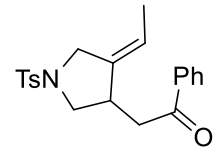

[65] T. Xi, X. Chen, H. Zhang, Z. Lu, *Synthesis* **2016**, *48*, 2837–2844.
[99] R. E. Kinder, R. A. Widenhoefer, *Org. Lett.* **2006**, *8*, 1967–1969.
[217] J. E. Lee, S. H. Hong, Y. K. Chung, *Tetrahedron Lett.* **1997**, *38*, 1781–1784.

(CH_2), 49.5 (CH_2), 42.6 (CH_2), 38.4 (CH), 21.6 (CH_3), 14.6 (CH_3). HRMS (ESI, MeOH) calcd. for $C_{21}H_{23}NO_3S$ $[M + H]^+$: 370.4790; Found: 370.1483.

(*E*)-1-(2-Benzylidenecyclopentyl)propan-2-one (13gd): The compound was purified by column chromatography (cyclohexane/EtOAc 95:5) and was obtained as a colorless oil in 24% yield (11 mg). ^{1}H NMR (300 MHz, $CDCl_3$) δ 7.33 – 7.27 (m, 4H), 7.21 – 7.14 (m, 1H), 6.22 (q, J = 2.3 Hz, 1H), 3.12 – 2.97 (m, 1H), 2.80 (dd, J = 16.6, 4.9 Hz, 1H), 2.69 – 2.38 (m, 3H), 2.20 (s, 3H), 2.00 (dt, J = 11.7, 6.8 Hz, 1H), 1.90 – 1.76 (m, 1H), 1.74 – 1.55 (m, 1H), 1.35 – 1.22 (m, 1H). ^{13}C NMR (75 MHz, $CDCl_3$) δ 208.4 (C), 149.2 (C), 138.6 (C), 128.3 (2 × CH), 128.2 (2 × CH), 126.1 (CH), 121.1 (CH), 49.3 (CH_2), 41.7 (CH), 32.5 (CH_2), 31.5 (CH_2), 30.6 (CH_3), 25.0 (CH_2). HRMS (ESI, MeOH) calcd. for $C_{15}H_{18}O$ $[M + H]^+$: 214.1358; Found: 214.1351.

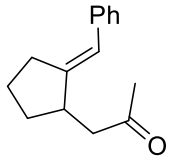

Other substrates

(*Z*)-2-(3-(Allyloxy)-1-phenylprop-1-en-1-yl)-4,4,5,5-tetramethyl-1,3,2-dioxaborolane (2aa'): The compound was purified by column chromatography (cyclohexane/EtOAc 9:1) and was obtained as a yellow oil in 17% yield (20 mg). ^{1}H NMR (300 MHz, $CDCl_3$) δ 7.35 – 7.21 (m, 3H), 7.14 (d, J = 8.1 Hz, 2H), 6.70 (t, J = 6.0 Hz, 1H), 5.86 (ddd, J = 16.2, 10.5, 5.5 Hz, 1H), 5.22 (d, J = 17.0 Hz, 1H), 5.13 (d, J = 10.3 Hz, 1H), 4.10 (d, J = 6.0 Hz, 2H), 3.92 (d, J = 5.4 Hz, 2H), 1.27 (s, 12H).

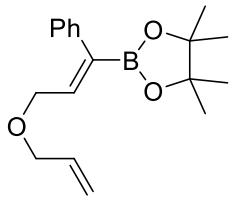

2-((3-Oxabicyclo[3.1.0]hexan-1-yl)(phenyl)methyl)-4,4,5,5-tetramethyl-1,3,2-dioxaborolane (12aa): The compound was purified by column chromatography (cyclohexane/EtOAc 9:1) and was obtained as a yellow oil in 36% yield (44 mg). ^{1}H NMR (300 MHz, $CDCl_3$) δ 7.25 – 7.08 (m, 5H), 3.78 (d, J = 1.3 Hz, 2H), 3.69 (q, J = 8.0 Hz, 2H), 2.55 (s, 1H), 1.56 – 1.48 (m, 1H), 1.23 (d, J = 4.0 Hz, 12H), 0.71 – 0.51 (m, 2H). ^{13}C NMR (75 MHz, $CDCl_3$) δ 140.8 (C), 136.1 (C), 129.2 (2 × CH), 128.3 (2 × CH), 125.7 (CH), 72.4 (CH_2), 70.1 (CH_2), 33.1 (br s, CH-B), 30.6 (C), 24.7 (2 × CH_3), 24.5 (2 × CH_3), 22.6 (CH), 12.9 (CH_2). (^{13}C-NMR was assigned from a mixture of **12aa** + **2aa**).

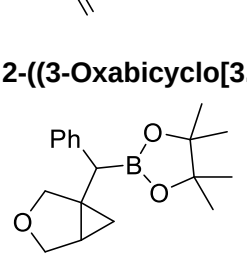

3.3.4.4. Transformations of boronates

3.3.4.4.1. General procedure for oxidation of boronates

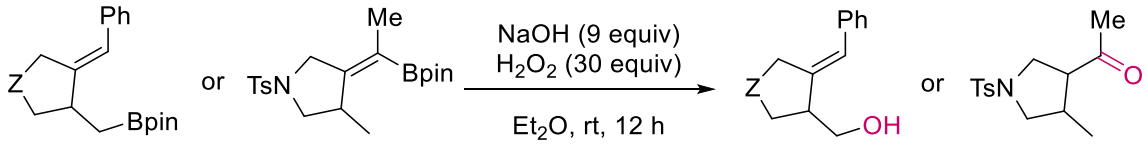

2 **11bn** **3** **14bn**

The corresponding boronate **2** or **11bn** (1 equiv, 0.4 mmol) dissolved in diethyl ether (0.2 M, 2.5 mL) was treated with NaOH (3 N, 9 equiv) and H_2O_2 (30%, 30 equiv) at 0 °C. The mixture was stirred overnight at room temperature. The resulting suspension was extracted with diethyl ether (2 × 5 mL). The combined organic layers were washed with brine, dried over anhydrous $MgSO_4$, filtered and concentrated under vacuum. The resulting residue was

purified by column chromatography to give the corresponding alcohol or ketone (cyclohexane/EtOAc 7:3 was used as an eluent).[100]

(*Z*)-(4-Benzylidenetetrahydrofuran-3-yl)methanol (3aa):[100] The product was obtained as a colorless oil in 86% yield (80 mg). ^{1}H NMR (300 MHz, $CDCl_3$) δ 7.34 (t, J = 7.3 Hz, 2H), 7.22 (t, J = 7.3 Hz, 1H), 7.13 (d, J = 7.3 Hz, 2H), 6.44 (d, J = 1.8 Hz, 1H), 4.68 (dt, J = 14.1, 2.0 Hz, 1H), 4.57 (dd, J = 14.1, 2.0 Hz, 1H), 3.94 (qd, J = 8.9, 5.1 Hz, 2H), 3.73 (d, J = 6.2 Hz, 1H), 3.09 – 2.97 (m, 1H), 2.19 (br s, 1H).

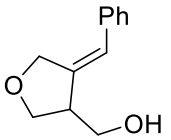

(*Z*)-(4-Benzylidene-1-tosylpyrrolidin-3-yl)methanol (3bb):[100] The product was obtained as a white solid in 80% yield (78 mg). ^{1}H NMR (300 MHz, $CDCl_3$) δ 7.73 (d, J = 8.2 Hz, 2H), 7.35 (m, 4H), 7.26 (m, 1H), 7.14 (d, J = 8.2 Hz, 2H), 6.37 (s, 1H), 4.22 (d, J = 14.8 Hz, 1H), 4.02 (d, J = 14.8 Hz, 1H), 3.65 (t, J = 5.6 Hz, 2H), 3.38 (dd, J = 9.6, 4.0 Hz, 1H), 3.28 (dd, J = 9.6, 6.8 Hz, 1H), 2.99 (m, 1H), 2.42 (s, 3H), 1.70 (t, J = 5.6 Hz, 1H).

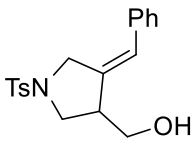

1-(4-Methyl-1-tosylpyrrolidin-3-yl)ethan-1-one (14bn):[99] The product (*dr* > 97:3) was obtained as a colorless oil in 83% yield (59 mg). ^{1}H NMR (300 MHz, $CDCl_3$) δ 7.69 (d, *J* = 8.1 Hz, 2H), 7.32 (d, *J* = 8.1 Hz, 1H), 3.55 (dd, *J* = 10.0, 8.0 Hz, 1H), 3.39 (dd, *J* = 9.7, 7.7 Hz, 1H), 3.29 (dd, *J* = 10.0, 8.0 Hz, 1H), 2.87 (dd, *J* = 9.7, 7.7 Hz, 1H), 2.66 (q, *J* = 8.1 Hz, 1H), 2.43 (s, 3H), 2.30 (dt, *J* = 14.5, 7.2 Hz, 1H), 2.12 (s, 3H), 1.02 (d, *J* = 6.7 Hz, 3H).

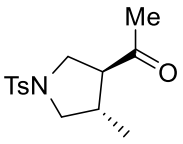

3.3.4.4.2. General procedure for the synthesis of trifluoroborates salts

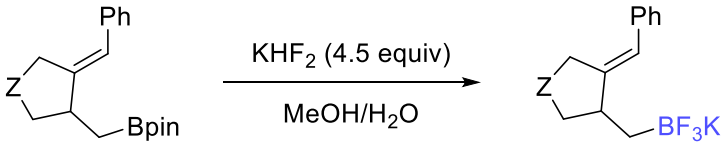

2 **4**

The corresponding alkylboronate **2** (1 equiv, 0.4 mmol) was dissolved in methanol (0.2 M, 2 mL). Then, KHF_2 (4.5 equiv, 4.5 M aqueous solution) was added dropwise to the solution. The reaction mixture was stirred at 23 °C for 1.5 h. Then, the solvent was removed under vacuum and the solid residue was triturated with acetone (20 mL). The liquid phase was filtered, and the residual inorganic salts were washed with additional acetone. The combined solutions were concentrated under vacuum to give white solids. The solids were washed with diethyl ether (3 × 20 mL) to remove pinacol and dried under vacuum, affording the desired product.[100]

Potassium (*Z*)-((4-benzylidenetetrahydrofuran-3-yl)methyl)trifluoroborate (4aa): The product was obtained as a white solid in 84 % yield (94 mg). ^{1}H NMR (300 MHz, d^6-DMSO) δ 7.32 (t, J = 7.5 Hz, 2H), 7.16 (dd, J = 11.3, 7.5 Hz, 3H), 6.24 (d, J = 2.1 Hz, 1H), 4.57 (d, J = 14.4 Hz, 1H), 4.37 (d, J = 14.4 Hz,

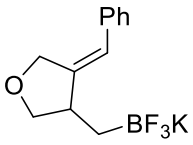

[99] R. E. Kinder, R. A. Widenhoefer, *Org. Lett.* **2006**, *8*, 1967–1969.
[100] T. Xi, Z. Lu, *ACS Catal.* **2017**, *7*, 1181–1185.

1H), 3.97 (dd, J = 8.1, 7.9 Hz, 1H), 3.16 (t, J = 8.8 Hz, 1H), 2.62 (m, 1H), 0.60 – 0.45 (m, 1H), 0.06 – -0.15 (m, 1H). ^{13}C NMR (75 MHz, DMSO-d^6) δ 150.7 (C), 137.8 (C), 128.4 (2 × CH), 127.6 (2 × CH), 125.7 (CH), 117.6 (CH), 74.2 (CH_2), 69.4 (2 × CH_2), 43.0 (q, J = 2.3 Hz, CH). ^{19}F NMR (282 MHz, DMSO-d^6) δ – 136.24. HRMS (ESI, MeCN) calcd. for $C_{12}H_{13}BF_3KO$ [M - K]$^+$: 241.0397; Found: 241.1026.

Potassium (*Z*)-3-benzylidene-1-tosyl-4-((trifluoroboranyl)methyl)pyrrolidine (4bb):[100]

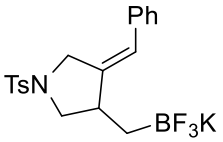

The product was obtained as a white solid in 72 % yield (79 mg). ^{1}H NMR (300 MHz, d^6-DMSO) δ 7.66 (d, J = 7.9 Hz, 2H), 7.37 (m, 4H), 7.18 (m, 3H), 6.22 (s, 1H), 4.19 (d, J = 15.4 Hz, 1H), 3.76 (d, J = 15.4 Hz, 1H), 3.55 (d, J = 7.7 Hz, 1H), 2.37 (s, 3H), 0.48 (br s, 1H), –0.20 (br s, 1H).

Potassium dimethyl (*E*)-3-benzylidene-4-((trifluoroboranyl)methyl)cyclopentane-1,1-dicarboxylate (4cc):

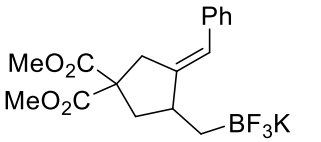

The product was obtained as a light brown solid in 78 % yield (79 mg). M.p. = 70 – 72 °C. ^{1}H NMR (300 MHz, d^6-DMSO) *δ* 7.32 (t, *J* = 7.6 Hz, 2H), 7.25 (d, *J* = 7.3 Hz, 2H), 7.16 (t, *J* = 7.0 Hz, 1H), 6.22 (d, *J* = 2.1 Hz, 1H), 3.64 (s, 3H), 3.63 (s, 3H), 3.57 (t, *J* = 7.1 Hz, 1H), 3.19 (d, *J* = 17.5 Hz, 1H), 2.95 (d, *J* = 17.5 Hz, 1H), 2.60 – 2.54 (m, 1H), 1.62 (t, *J* = 12.1 Hz, 1H), 0.68 – 0.52 (m, 1H), 0.01 – -0.18 (m, 1H). ^{13}C NMR (75 MHz, DMSO) *δ* 172.1 (2 × C), 150.3 (C), 138.3 (C), 128.2 (2 × CH), 127.9 (2 × CH), 125.6 (CH), 119.5 (CH), 58.4 (C), 52.6 (CH_3), 52.5 (CH_3), 42.0 (CH), 41.4 (CH_2), 38.4 (CH_2) ^{19}F NMR (282 MHz, DMSO-d^6) δ – 135.35. HRMS (ESI, MeOH) calcd. for $C_{17}H_{19}BF_3KO_4$ [M - K]$^-$: 355.2385; Found: 355.1335.

3.3.4.4.3. General procedure for Suzuki Cross-Coupling Reaction of alkylboronate

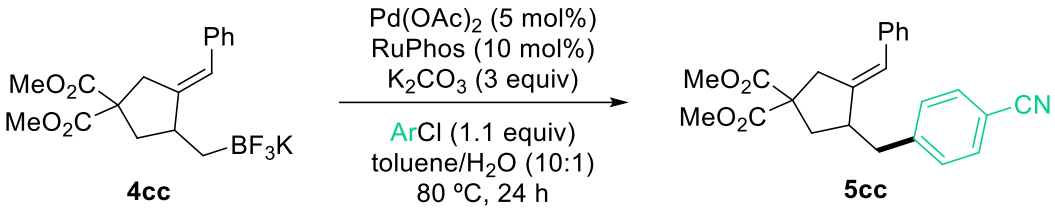

A vial was charged with $Pd(OAc)_2$ (0.02 mmol), RuPhos (0.04 mmol), 4-chlorobenzonitrile (0.4 mmol), the potassium trifluoroborate compound **4cc** (0.4 mmol) and K_2CO_3 (1.2 mmol). The vial was sealed by a septum, dried under vacuum and backfilled with Ar. To the vial, toluene (2 mL) and H_2O (0.2 mL) were added, and then the reaction was heated to 80 °C for 24 h. The reaction mixture was allowed to cool to rt. The organic layer was separated, and the aqueous layer was washed with EtOAc. The combined organic layers were concentrated under vacuum and purified by silica gel column chromatography to yield the product.[18e]

Dimethyl (*E*)-3-benzylidene-4-(4-cyanobenzyl)cyclopentane-1,1-dicarboxylate (5cc):

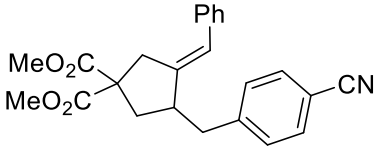

The compound was purified by column chromatography (cyclohexane/EtOAc, 95:5) and was obtained as a colorless oil in 79% yield (46 mg). ^{1}H NMR (300 MHz, $CDCl_3$) *δ* 7.60 (d, *J* = 8.0 Hz, 2H), 7.39 – 7.33 (m, 4H), 7.31 – 7.19 (m, 3H), 6.32 (s, 1H), 3.73 (s, 3H), 3.68 (s, 3H), 3.38 (d, *J* = 17.5

[18] (e) S. D. Dreher, S.-E. Lim, D. L. Sandrock, G. A. Molander, *J. Org. Chem.* **2009**, *74*, 3626–3631.
[100] T. Xi, Z. Lu, *ACS Catal.* **2017**, *7*, 1181–1185.

Hz, 1H), 3.28 – 3.15 (m, 2H), 3.12 – 3.04 (m, 1H), 2.69 (dd, *J* = 13.0, 9.4 Hz, 1H), 2.37 (dd, *J* = 13.0, 7.3 Hz, 1H), 1.85 (dd, *J* = 13.0, 10.0 Hz, 1H). ^{13}C NMR (75 MHz, $CDCl_3$) *δ* 172.0 (C), 171.9 (C), 145.9 (C), 143.6 (C), 137.5 (C), 132.4 (2 × CH), 129.9 (2 × CH), 128.5 (4 × CH), 126.7 (CH), 123.3 (CH), 119.0 (C), 110.3 (C), 59.1 (C), 53.0 (2 × CH_3), 45.4 (CH), 40.9 (CH_2), 39.2 (CH_2), 38.8 (CH_2). HRMS (ESI, MeOH) calcd. for $C_{24}H_{23}NO_4$ [M + H]$^+$: 390.4510; Found: 390.1707.

3.3.4.4.4. General procedure for Suzuki Cross-Coupling Reaction of alkenylboronates.

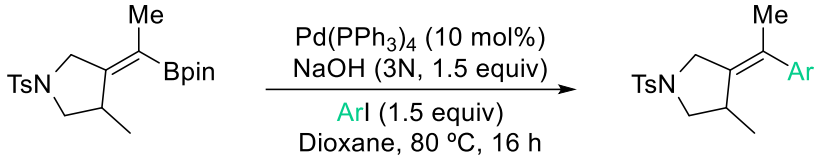

11bn **15-16bn**

A vial was charged with $Pd(PPh_3)_4$ (0.07 mmol), iodobenzene (1.05 mmol) and the alkenylboronate **11bn** (0.7 mmol). The vial was sealed by a septum, dried under vacuum and backfilled with Ar. To the vial, dioxane (3.7 mL) and NaOH (3 M, 0.35 mL) were added, and then the reaction was heated to 80 °C for 16 h. The reaction mixture was allowed to cool to rt. The solvent was removed under vacuum and the product was purified by column chromatography in silica gel (cyclohexane/EtOAc, 9:1).[101]

(*E*)-3-Methyl-4-(1-phenylethylidene)-1-tosylpyrrolidine (15bn): The product was obtained as a brown oil in 99% yield (52 mg). ^{1}H NMR (300 MHz, $CDCl_3$) *δ* 7.75 (d, *J* = 8.0 Hz, 2H), 7.36 (d, *J* = 8.0 Hz, 2H), 7.31 – 7.25 (m, 1H), 7.23 – 7.21 (m, 2H), 7.07 (d, *J* = 7.8 Hz, 2H), 4.02 (d, *J* = 14.0 Hz, 1H), 3.80 (d, *J* = 14.0 Hz, 1H), 3.17 (dd, *J* = 9.2, 6.5 Hz, 1H), 3.06 (dd, *J* = 9.2, 2.5 Hz, 1H), 2.87 – 2.71 (m, 1H), 2.45 (s, 3H), 1.85 (s, 3H), 0.76 (d, *J* = 6.9 Hz, 3H). ^{13}C NMR (75 MHz, $CDCl_3$) *δ* 143.7 (C), 142.9 (C), 136.4 (C), 133.0 (C), 129.9 (C), 129.8 (2 × CH), 128.4 (2 × CH), 128.0 (2 × CH), 127.0 (2 × CH), 126.8 (CH), 55.6 (CH_2), 50.6 (CH_2), 35.8 (CH), 22.0 (CH_3), 21.7 (CH_3), 19.4 (CH_3). HRMS (ESI, MeOH) calcd. for $C_{20}H_{23}NO_2S$ [M + H]$^+$: 342.4690; Found: 342.1511.

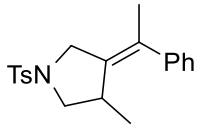

(*E*)-3-(1-(4-Chlorophenyl)ethylidene)-4-methyl-1-tosylpyrrolidine (16bn): The product was obtained as a yellow oil in 98% yield (44 mg). ^{1}H NMR (300 MHz, $CDCl_3$) *δ* 7.74 (d, *J* = 8.1 Hz, 2H), 7.35 (d, *J* = 8.1 Hz, 2H), 7.25 (d, *J* = 8.3 Hz, 2H), 7.00 (d, *J* = 8.3 Hz, 2H), 4.00 (d, *J* = 14.1 Hz, 1H), 3.77 (d, *J* = 14.1 Hz, 1H), 3.16 (dd, *J* = 9.2, 6.4 Hz, 1H), 3.06 (dd, *J* = 9.2, 2.6 Hz, 1H), 2.85 – 2.66 (m, 1H), 2.45 (s, 3H), 1.82 (s, 3H), 0.76 (d, *J* = 6.9 Hz, 3H). ^{13}C NMR (75 MHz, $CDCl_3$) *δ* 143.7 (C), 141.3 (C), 137.2 (C), 133.0 (C), 132.6 (C), 129.8 (2 × CH), 129.0 (2 × CH), 128.8 (C), 128.7 (2 × CH), 128.0 (2 × CH), 55.6 (CH_2), 50.6 (CH_2), 35.8 (CH), 21.9 (CH_3), 21.7 (CH_3), 19.4 (CH_3). HRMS (ESI, MeOH) calcd. for $C_{20}H_{22}ClNO_2S$ [M + H]$^+$: 376.9110; Found: 376.1116.

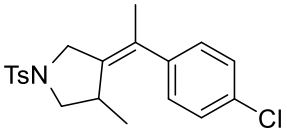

[101] S. Yu, C. Wu, S. Ge, *J. Am. Chem. Soc.* **2017**, *139*, 6526–6529.

3.3.4.5. Mechanistic studies

3.3.4.5.1. Deuteration experiment

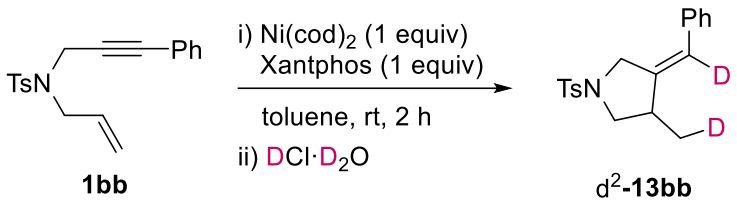

1bb **d²-13bb**

A vial was charged with $Ni(cod)_2$ (55 mg, 0.2 mmol), Xantphos (116 mg, 0.2 mmol), the enyne **1bb** (0.2 mmol) and a stir bar in air. The vial was sealed by a septum, dried under vacuum and backfilled with Ar. Then, anhydrous and Ar-degassed toluene (1 mL) was added, and the resulting mixture was stirred for 2 h at room temperature. DCl in D_2O (2 mL) was added and the reaction mixture was stirred for 5 min. Then, the reaction was extracted with EtOAc (2 × 5 mL). The combined organic layers were washed with brine, dried over anhydrous $MgSO_4$, filtered and concentrated under vacuum. The resulting residue was purified by column chromatography (cyclohexane/EtOAc 95:5 was used as an eluent).

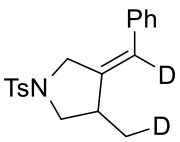

(*Z*)-3-(Methyl-*d*)-4-(phenylmethylene-*d*)-1-tosylpyrrolidine (d²-13bb): The product was obtained as a yellow oil in 30% yield (20 mg). ^1H NMR (300 MHz, $CDCl_3$) δ 7.72 (d, J = 8.2 Hz, 2H), 7.33 (dd, J = 15.4, 7.7 Hz, 5H), 7.14 (d, J = 7.2 Hz, 2H), 4.24 (d, J = 14.9 Hz, 1H), 4.05 (d, J = 14.9 Hz, 1H), 3.55 (dd, J = 8.9, 7.2 Hz, 1H), 2.95 – 2.80 (m, 1H), 2.77 – 2.67 (m, 1H), 2.41 (s, 3H), 1.17 (d, J = 6.6 Hz, 2H). ^2H NMR (77 MHz, $CDCl_3$) δ 6.26 (s, 1D), 1.18 (s, 1D). ^{13}C NMR (75 MHz, $CDCl_3$) δ 143.8 (C), 141.9 (C), 136.7 (C), 133.2 (C), 129.9 (2 × CH), 128.7 (2 × CH), 128.2 (2 × CH), 127.9 (2 × CH), 127.1 (CH), 122.2 (CD), 54.0 (CH_2), 50.9 (CH_2), 39.2 (CH), 21.7 (CH_3), 16.8 (t, J = 19.0, CH_2D). HRMS (ESI, MeCN) calcd. for $C_{19}H_{19}D_2NO_2S$ [M + Na]$^-$: 353.1419; Found: 352.1303.

3.3.4.5.2. ^{31}P-NMR experiment

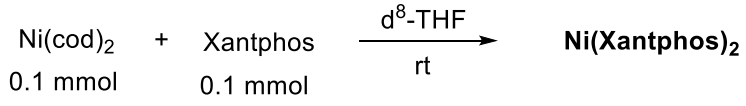

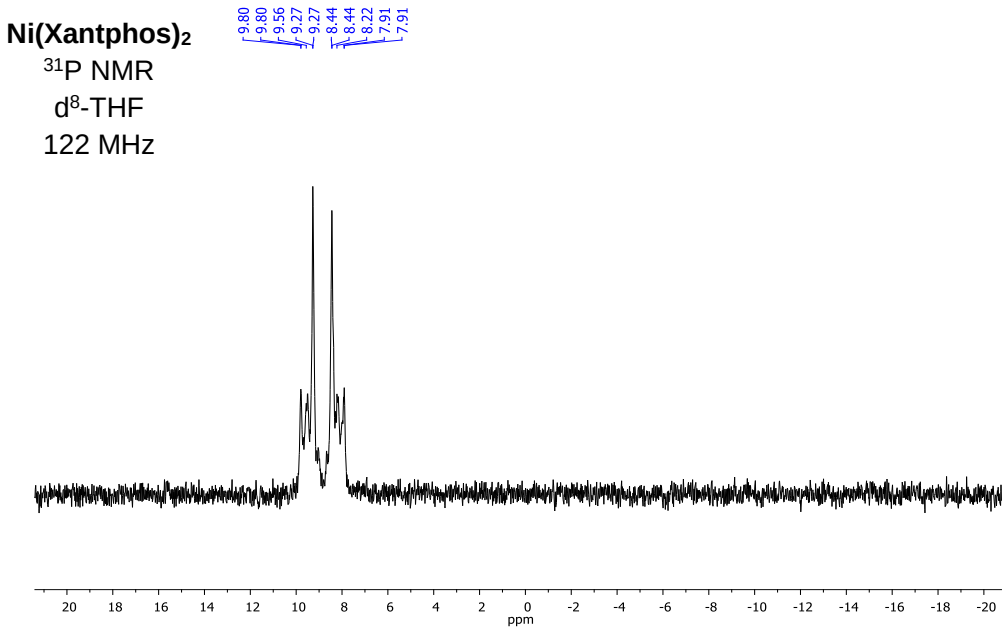

CHAPTER 4:

Ni-catalyzed diborylative cyclization of enynes

3.4. CHAPTER 4

3.4.1. Goal

Bis(boronate) compounds, which possess two boronate moieties in a single molecule, have attracted much attention as versatile building blocks for the concise synthesis of complex molecules through multiple C−C bond formation and functionalization reactions of the C−B bond. Thus, there has been a growing interest in developing direct, catalytic methods for the preparation of bis(boronate) compounds starting from simple, easily available substrates and boron sources to expand the utility of these derivatives.

Since there are no precedents in the literature of diborylative cyclization reactions, we thought that the use of Ni catalyst along with bimetallic boron compounds, such as bis(pinacolato)diboron, might be suitable for the development of diborylation and cyclization processes of polyunsaturated substrates. Furthermore, we envisioned the use of enynes as starting materials could lead to reaction products containing two different boryl units in the molecule, allowing a chemoselective functionalization of the C–B bonds.

3.4.2. Precedents

Diboration reaction of alkenes, alkynes and other unsaturated compounds for the synthesis of bis(boronates) has been performed with a variety of heavy metals,[38–41] such as Pt,[218] Rh,[219] Ir[220] and Pd.[221] These noble metals provide efficient and versatile methods, but their use involves some drawbacks regarding toxicity and economical aspects. More recently, the first-row transition metals have demonstrated to be useful for these purposes and may open up the discovery of novel activation pathways as well.[222]

3.4.2.1. Fe-catalyzed diboration

The first and only known Fe-catalyzed diboration reaction was described by Nakamura and co-workers in 2015.[223] In this study, they performed the diboration of challenging alkynes with bis(pinacolato)diboron in the presence of a simple iron salt, LiOMe and an additional borating agent (**Scheme 4.1**). In addition, they also carried out the carboboration of symmetrical alkynes by adding carbon electrophiles instead of the borylating agent.[224]

---

[38] (a) T. B. Marder, N. C. Norman, *Top. Catal.* **1998**, *5*, 63–73. (b) T. Ishiyama, N. Miyaura, *J. Organomet. Chem.* **2000**, *611*, 392–402. (c) J. Takaya, N. Iwasawa, *ACS Catal.* **2012**, *2*, 1993–2006.
[39] (a) J. Ramírez, V. Lillo, A. M. Segarra, E. Fernández, *C. R. Chimie* **2007**, *10*, 138–151. (b) J. M. Brown. B. N. Nguyen, *Science of Synthesis, 1: Stereoselective Synthesis 1* (Ed. J. G. de Vries), **2011**, 295–324.
[40] F. Zhao, X. Jia, P. Li, J. Zhao, Y. Zhou, J. Wang, H. Liu, *Org. Chem. Front.* **2017**, *4*, 2235–2255.
[41] J. Royes, A. B. Cuenca, E. Fernández, *Eur. J. Org. Chem.* **2018**, 2728–2739.
[218] (a) L. T. Kliman, S. N. Mlynarski, J. P. Morken, *J. Am. Chem. Soc.* **2009**, *131*, 13210–13211. (b) J. R. Coombs, F. Haeffner, L. T. Kliman, J. P. Morken, *J. Am. Chem. Soc.* **2013**, *135*, 11222−11231.
[219] (a) R. T. Baker, P. Nguyen, T. B. Marder, S. A. Westcott, *Angew. Chem. Int. Ed. Engl.* **1995**, *34*, 1336–1338. (b) J. B. Morgan, S. P. Miller, J. P. Morken, *J. Am. Chem. Soc.* **2003**, *125*, 8702–8703. (c) S. Trudeau, J. B. Morgan, M. Shrestha, J. P. Morken, *J. Org. Chem.* **2005**, *70*, 9538–9544.
[220] (a) C.-I. Lee, W.-C. Shih, J. Zhou, J. H. Reibenspies, O. V. Ozerov, *Angew. Chem. Int. Ed.* **2015**, *54*, 14003–14007. (b) T. Ishiyama, N. Miyaura, *Chem. Rec.* **2004**, *3*, 271–280.
[221] J. Liu, M. Nie, Q. Zhou, S. Gao, W. Jiang, L. W. Chung, W. Tang, K. Ding, *Chem. Sci.* **2017**, *8*, 5161–5165.
[222] H. Yoshida, *ACS Catal.* **2016**, *6*, 1799−1811.
[223] N. Nakagawa, T. Hatakeyama, M. Nakamura, *Chem. Eur. J.* **2015**, *21*, 4257–4261.
[224] See Chapter 5, *3.5.1.1 Fe-catalyzed carboboration.*

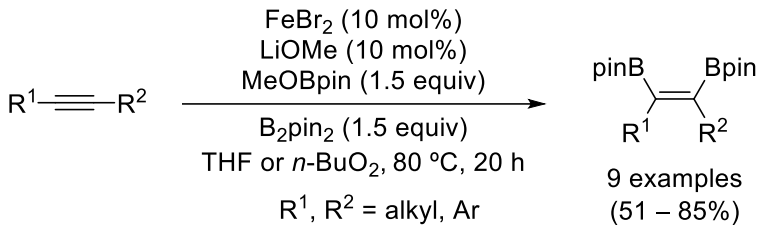

Scheme 4.1. Fe-catalyzed diboration of alkynes.

A plausible reaction mechanism is shown in **Figure 4.1**. $FeBr_2$ initially undergoes transmetalation with LiOMe to form a methoxyiron(II) intermediate, which reacts with B_2pin_2 to afford a boryliron(II) species. Then, coordination and *syn*-insertion of the alkyne into the Fe–B bond generates an alkenyliron(II), which reacts with the additional borating agent to yield the diboration product and regenerates the catalytically active Fe(II) species.

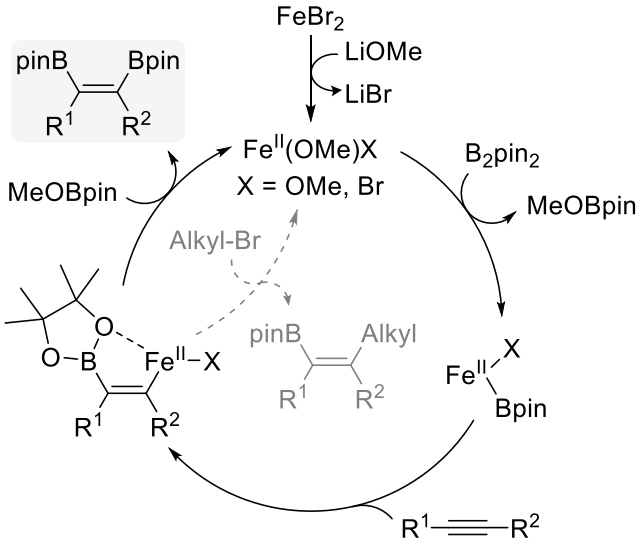

Figure 4.1 Proposed mechanism for the Fe-catalyzed diboration of alkynes.

3.4.2.2. Co-catalyzed diboration

Zuang group has described several procedures for the polyboration of unsaturated molecules by using Co-based catalysts.[225] In 2015, they performed the geminal perboration of styrenes for the synthesis of a broad array of 1,1,1-tris(boronates).[226] The reaction works with excellent yields in most cases (**Scheme 4.2**).

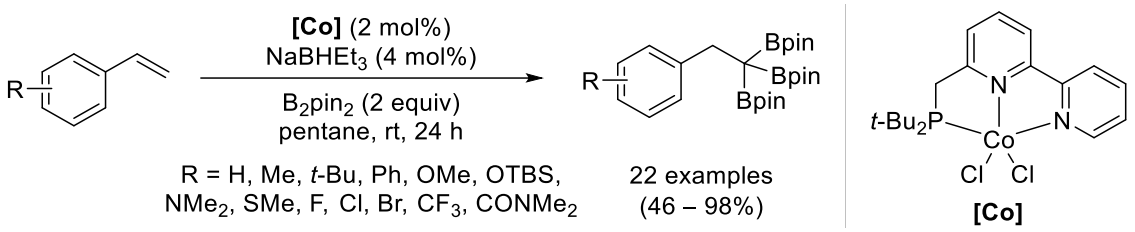

Scheme 4.2. Co-catalyzed perboration of styrenes.

[225] Z. Zuo, H. Wen, G. Liu, Z. Huang, *Synlett* **2018**, *29*, 1421–1429.
[226] L. Zhang, Z. Huang, *J. Am. Chem. Soc.* **2015**, *137*, 15600–15603.

After different mechanistic experiments, they proposed that the reaction pathway starts with the formation of a cobalt hydride by reaction with $NaBHEt_3$ (**Figure 4.2**). Upon transmetalation with B_2pin_2, it is converted into a Co(I)-boryl complex, which can experience the 1,2-insertion of the previously coordinated alkene into the Co–B bond. Then, a *β*-hydride elimination takes place to furnish an alkenylboronate intermediate and regenerates Co(I)-hydride. The former reacts again with B_2pin_2 to produce the Co-boryl species that undergoes the same process to afford a bis(boronate). Finally, the obtained bis(boronate) reacts with the Co(I)-boryl complex to perform hydroboration as final step of the catalytic cycle to obtain the desired 1,1,1-tris(boronate). Thus, the mechanism consists in a double dehydrogenative borylation along with hydroboration.

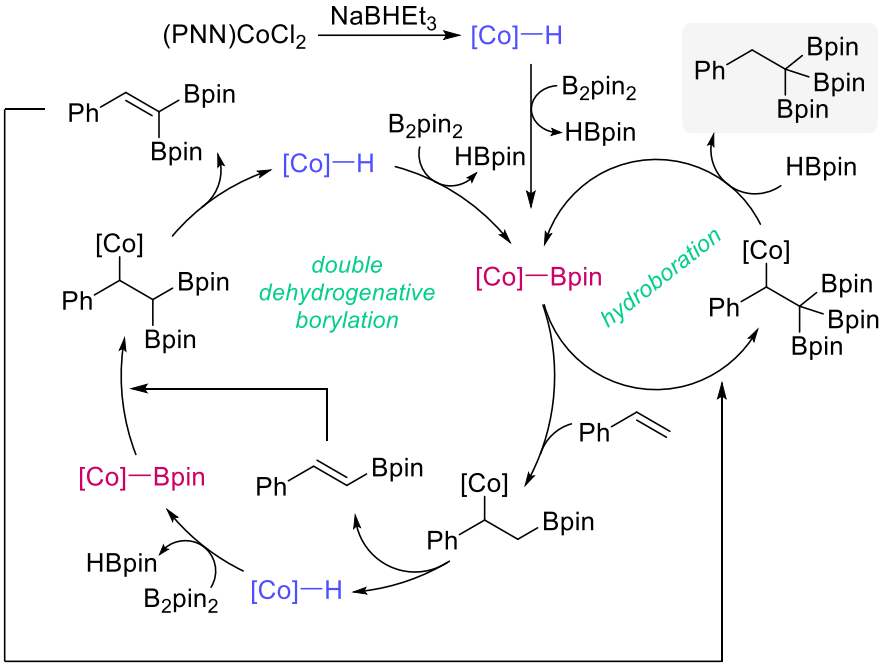

Figure 4.2. Proposed mechanism for the Co-catalyzed triboration of styrenes.

The use of OIP-type ligand-base cobalt complex allows the preparation of 1,1-diboronates from terminal alkynes. Mechanistic studies support a sequential hydroboration mechanism since the corresponding alkenylboronate is formed at the early stage of the reaction (**Scheme 4.3**).[227]

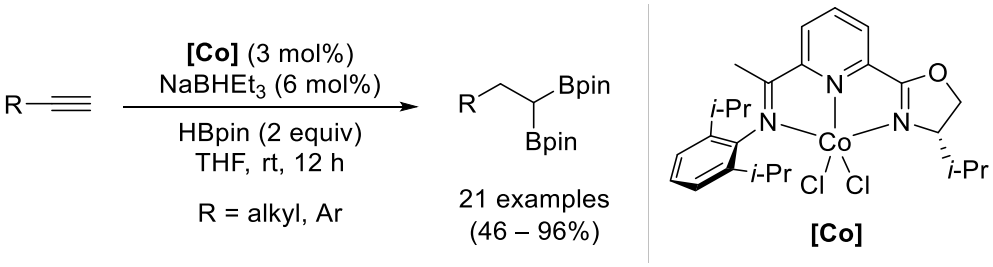

Scheme 4.3. Co-catalyzed sequential hydroboration of alkynes.

This group also developed the Co-catalyzed double dehydrogenative borylation of alkenes, observing different regioselectivity according to the substituent on the alkene.[228] Thus, when

[227] Z. Zuo, Z. Hang, *Org. Chem. Front.* **2016**, *3*, 434–438.
[228] H. Wen, L. Zhang, S. Zhu, G. Liu, Z. Huang, *ACS Catal.* **2017**, *7*, 6419–6425.

styrenes derivatives are used 1,1-diborylalkenes are obtained. On the other hand, alkylic olefins afford the 1,2-diboration product. The obtained diboronates are used in further transformations. In addition, when a lower amount of CsF is used, alkenylboronates are obtained in high yields by single dehydrogenative borylation (**Scheme 4.4**).

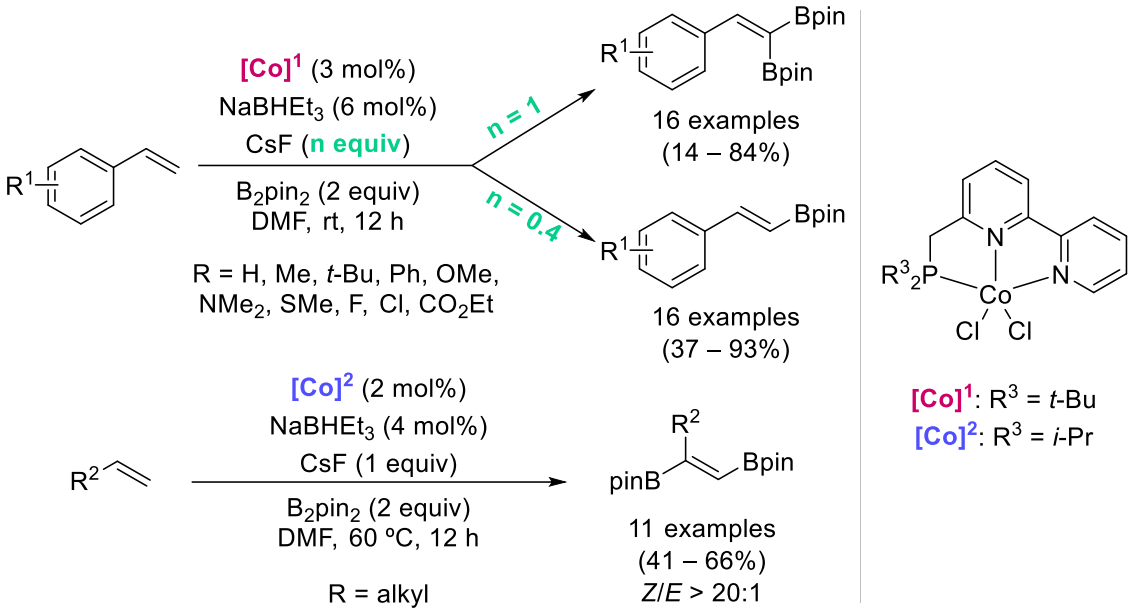

Scheme 4.4. Co-catalyzed double and single dehydrogenative borylation of alkenes.

The reaction mechanism is suggested to start with the formation of a cobalt hydride, which undergoes transmetalation with the boron source to obtain a catalytically active Co(I)-Bpin complex. This complex carries out a double dehydrogenative borylation by alkene insertion and *β*-hydride elimination to yield the observed reaction product (**Figure 4.3**).

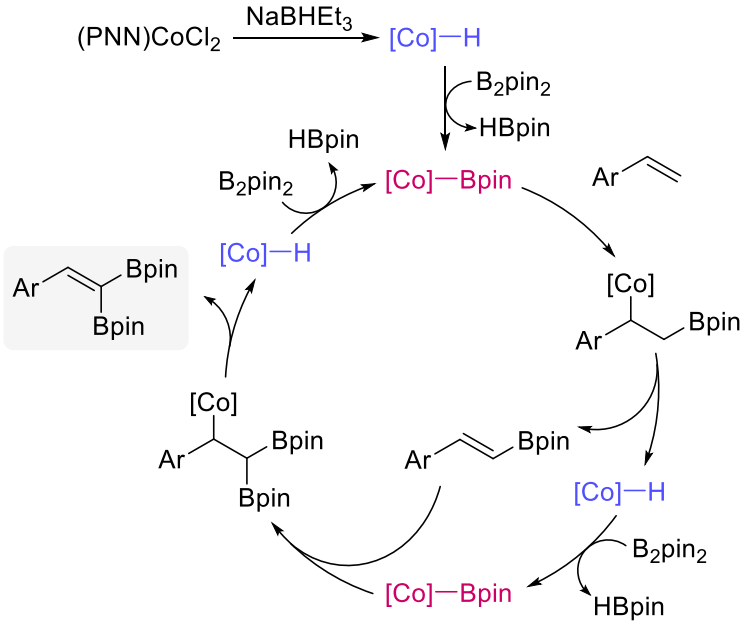

Figure 4.3. Double dehydrogenative borylation mechanistic proposal.

In 2017, Chirik and co-workers described an efficient Co-catalyzed 1,1-diboration of terminal alkynes. This methodology tolerates several functional groups and provides high yields (**Scheme 4.5**).[12e] Moreover, the resulting bis(boronates) can undergo an additional Co-

catalyzed hydroboration to give 1,1,1-triborylalkanes. The use of an unsymmetrical diboron reagent (pinB-Bdan) results in stereoselective diboration, affording trisubstituted olefins of well-defined configuration.

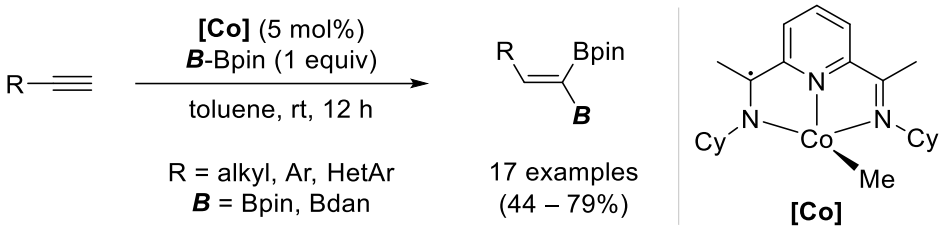

Scheme 4.5. Co-catalyzed 1,1-diboration of alkynes.

Based on previous results and deuteration experiments, the authors proposed the formation of a Co(I) acetylide as the key active species (**Figure 4.4**). This complex reacts with the diboron reagent to generate a Co-boryl complex and an alkynylboronate, which inserts into the Co–B bond. Finally, protonolysis with another alkyne unit yields the bis(boronate).

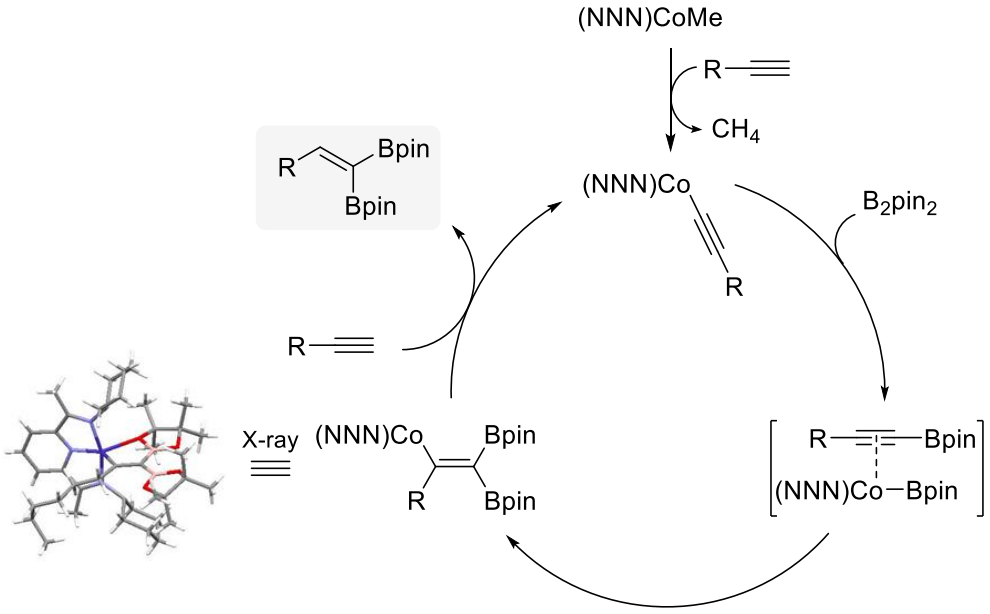

Figure 4.4. Proposed reaction mechanism for Co-catalyzed diboration of alkynes.

Petit carried out the hydroboration and 1,2-diboration of internal alkynes by a well-defined low-valent cobalt catalyst, showing moderate reaction yields (**Scheme 4.6**).[229]

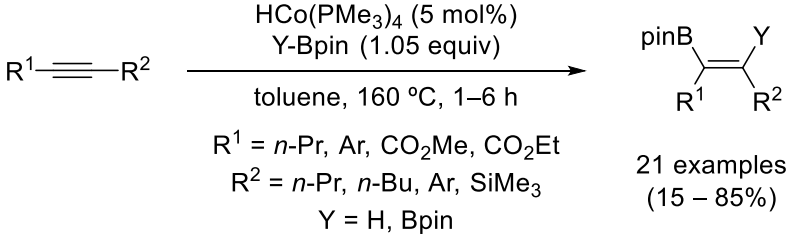

Scheme 4.6. Co-catalyzed 1,2-diboration of alkynes.

[12] (e) S. Krautwald, M. J. Bezdek, P. J. Chirik, *J. Am. Chem. Soc.* **2017**, *139*, 3868–3875.
[229] L. Ferrand, Y. Lyu, A. Rivera-Hernández, B. J. Fallon, M Amatore, C Aubert, M. Petit, *Synthesis* **2017**, *49*, 3895−3904.

Ge and co-workers broadened the Co-catalyzed *gem*-diboration reaction to 1,1-disubstituted vinylarenes.[230] The catalytic system effectively transforms the starting styrenes to bis(boronates) in high yields with a high functional group compatibility (**Scheme 4.7**).

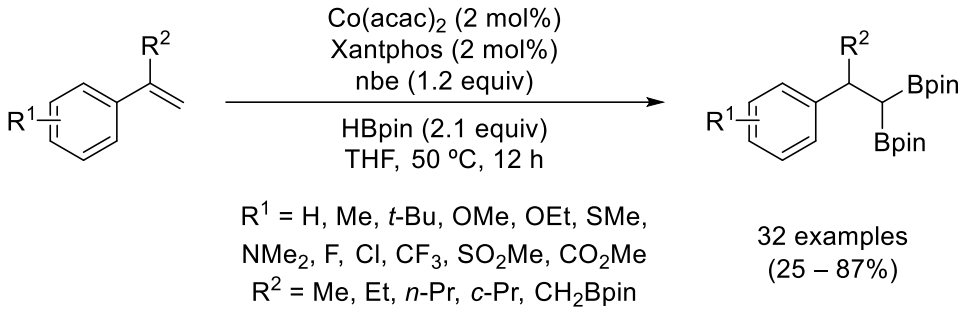

Scheme 4.7. Co-catalyzed diboration of 1,1-disubstituted vinylarenes.

Based on mechanistic studies, the authors proposed the catalytic cycle shown in **Figure 4.5**. The starting Co(II) complex reacts with $NaBHEt_3$ to generate a Co(I)-H, which undergoes the insertion of the alkene of the hydrogen acceptor (nbe). Subsequent reaction with HBpin leads to the formation of Co(I)-Bpin complex, and the alkene inserts into the Co–B bond of this intermediate. Then, tautomeration to a less hindered alkylcobalt species takes place. The resulting cobalt complex reacts with HBpin to regenerate the cobalt hydride and yields the observed product.

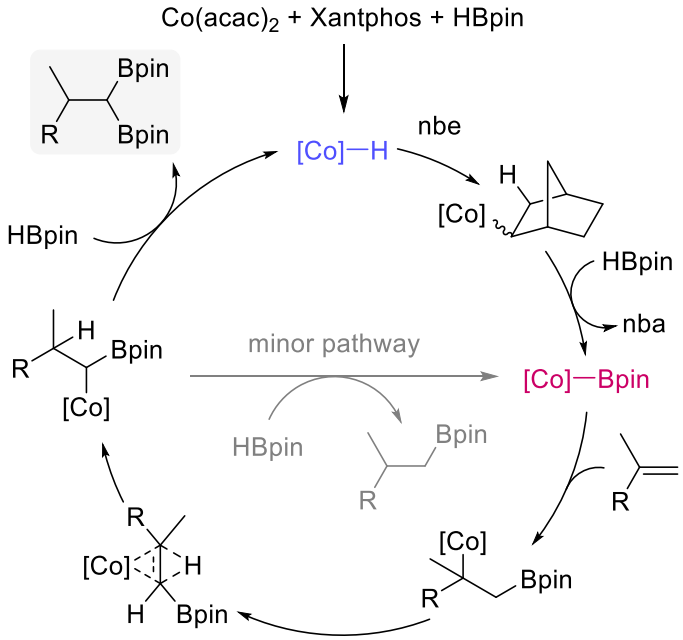

Figure 4.5. Proposed catalytic cycle for the Co-catalyzed 1,1-diboration.

An asymmetric version of this reaction was described by Ge as well.[231] A broad variety of alkenylarenes yields the desired diboronate with excellent enantioselectivities (**Scheme 4.8**). The synthetic application of the resulting *gem*-bis(boronates) was evaluated in natural product synthesis.

[230] W. J. Teo, S. Ge, *Angew. Chem. Int. Ed.* **2018**, *57*, 1654–1658.
[231] W. J. Teo, S. Ge, *Angew. Chem. Int. Ed.* **2018**, *57*, 12935–12939.

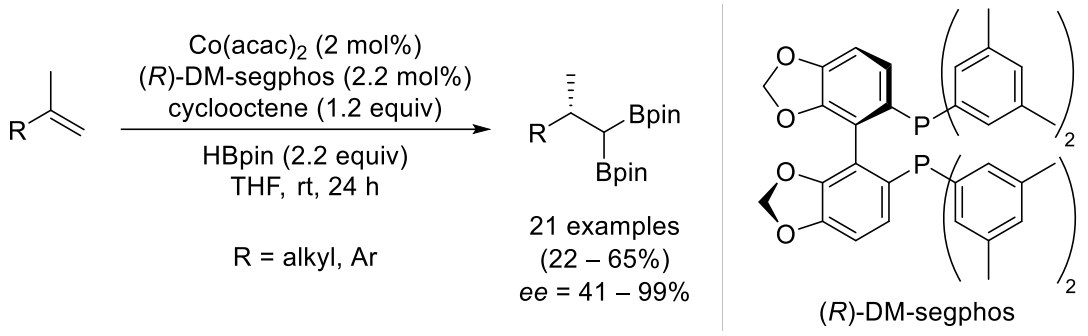

Scheme 4.8. Co-catalyzed enantioselective 1,1-diboration of styrenes.

3.4.2.3. Ni-catalyzed diboration

In 2008, Morken described the Ni-catalyzed diborylative coupling of dienes and aldehydes.[232] This reaction shows a wide scope regarding dienes and aldehydes, leading to the diastereoselective construction of diols after an oxidative quenching (**Scheme 4.9**).

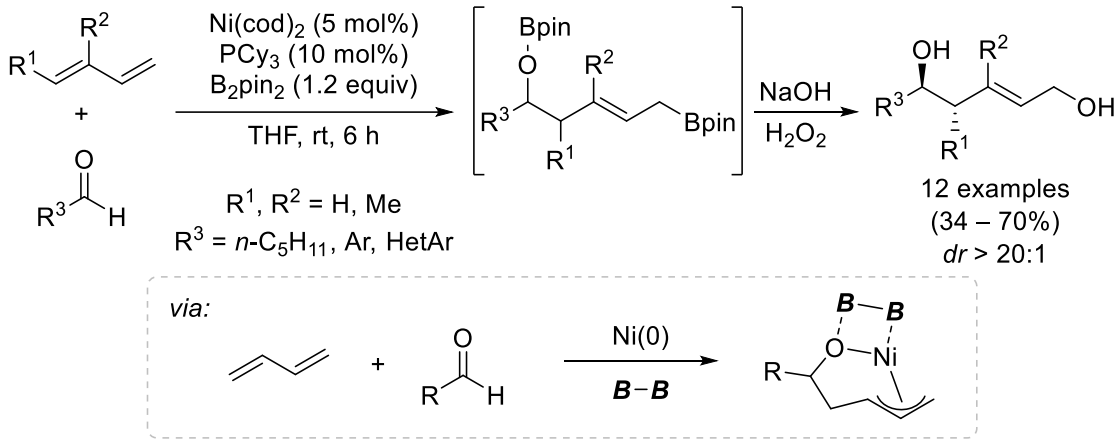

Scheme 4.9. Ni-catalyzed diborylative coupling of dienes and aldehydes.

A suitable tuning of the ligand properties allows to obtain a different regioselectivity for the same transformation.[233] Specifically, the use of $P(SiMe_3)_3$ instead of PCy_3 yields 1,3-diols with excellent diastereoselectivity (**Scheme 4.10**). A tentative hypothesis is that the large cone angle of the former ligand, combined with an ability to act as an electron acceptor, may facilitate the reductive elimination prior to isomerization process. Thus, leading to the different observed regioselectivity.

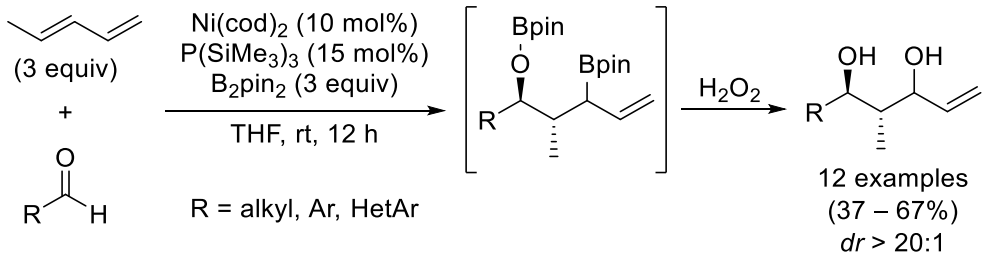

Scheme 4.10. Control of the regioselectivity by tuning the ligand properties.

[232] H. Y. Cho, J. P Morken, *J. Am. Chem. Soc.* **2008**, *130*, 16140–16141.
[233] H. Y. Cho, J. P Morken, *J. Am. Chem. Soc.* **2010**, *132*, 7576–7577.

Furthermore, the same research group has extended this procedure to ketone electrophiles, obtaining 1,3-diols in high yields with excellent levels of diastereocontrol (**Scheme 4.11**).[234] Noticeably, the regioselectivity of the reaction depends on the steric hindrance of the carbonyl substrate.

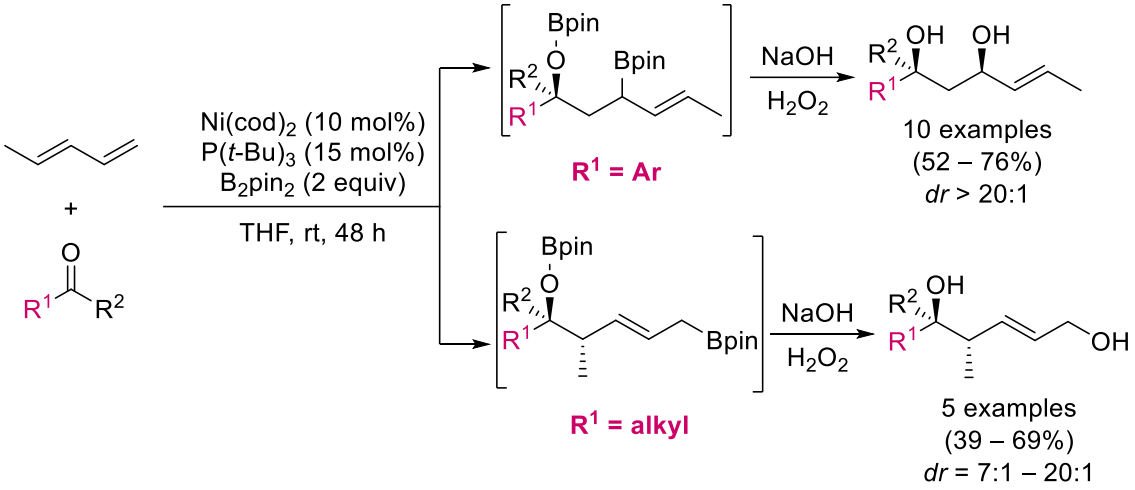

Scheme 4.11. Ni-catalyzed borylative ketone-diene coupling reaction.

Likewise, they also developed the Ni-catalyzed 1,4-selective diboration of conjugated dienes, broadening the reaction scope by including internal and sterically hindered dienes (**Scheme 4.12**).[235]

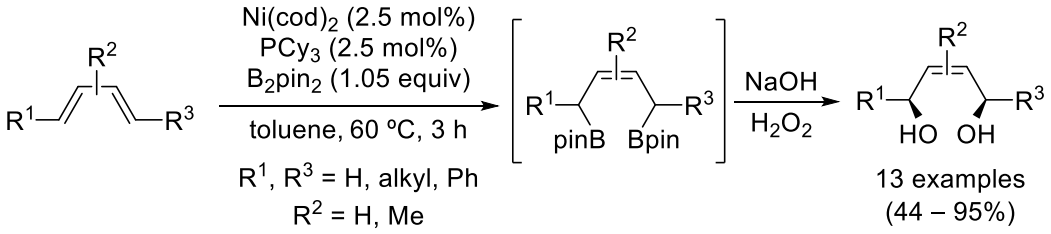

Scheme 4.12. Ni-catalyzed diboration of 1,3-dienes.

The reaction mechanism for these transformations starts with the association of the Ni(0) catalyst to the diene by coordination or cyclometalation. Subsequent reaction with B_2pin_2, followed by reductive elimination yields the observed diboronate (**Figure 4.6**).

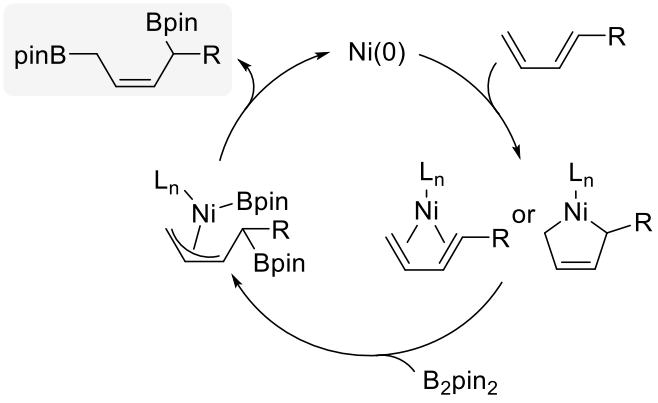

Figure 4.6. Proposed mechanism for the Ni-catalyzed diboration of dienes.

[234] H. Y. Cho, Z. Yu, J. P Morken, *Org. Lett.* **2011**, *13*, 5267–5269.
[235] R. J. Ely, J. P Morken, *Org. Lett.* **2010**, *12*, 4348–4351.

Xiao and Fu carried out the geminal Ni-catalyzed diboration of terminal alkenes.[236] Cyclohexylphosphine-based ligands are a key requirement for the reaction to take place. This procedure is compatible with a tremendous variety of alkenes, including sugar derivatives and liquid crystal materials (**Scheme 4.13**).

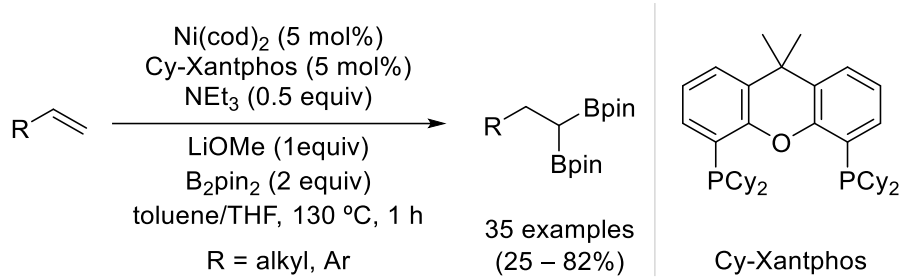

Scheme 4.13. Ni-catalyzed 1,1-diboration of alkenes.

Chirik and co-workers accomplished a novel perborylation of benzylic C–H bonds by using a α-diimine nickel bis(pivalate) complex.[237] Several substrates were effectively triborylated and used in further derivatizations for diastereoselective C–C bonds formation (**Scheme 4.14**).

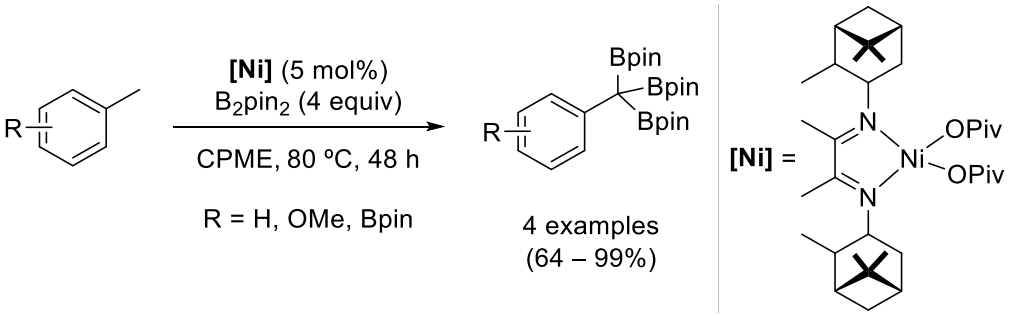

Scheme 4.14. Ni-catalyzed triborylation of benzylic substrates.

Recently, Wang and Li synthetized an efficient single-atomic-site $Pt_1/Ni(OH)_x$ catalyst for the diboration of alkenes and alkynes, showing excellent conversions to the corresponding diboronates (**Scheme 4.15**).[238]

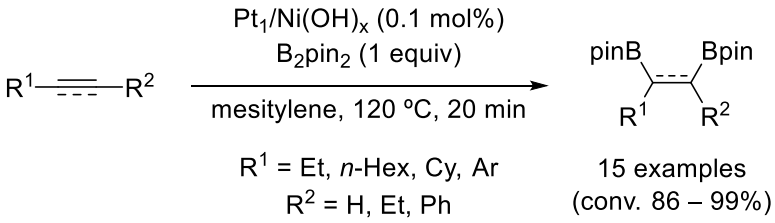

Scheme 4.15. Pt/Ni-catalyzed diboration of alkenes and alkynes.

The Ni-catalyzed vicinal diboration of alkyl bromides has been described by Lu and Fu.[239] This methodology exhibits a broad substrate scope, good functional group compatibility and regioselectivity, affording 1,2-diboronates in moderate yields (**Scheme 4.16**). Mechanistic experiments suggest that alkene intermediates are involved in the reaction mechanism.

---

[236] L. Li, T. Gong, X. Lu, B. Xiao, Y. Fu, *Nat. Commun.* **2017**, *8*, 345.
[237] W. N. Palmer, C. Zarate, P. J Chirik, *J. Am. Chem. Soc.* **2017**, *139*, 2589–2592.
[238] J. Zhang, X. Wu, W.-C. Cheong, W. Chen, R. Liu, J. Li, L. Zheng, W. Yan, L. Gu, C. Chen, Q. Peng, D. Wang, Y. Li, *Nature Commun*. **2018**, *9*, 1002.
[239] X.-X. Wang, L. Li, T.-J. Gong, B. Xiao, X. Lu, Y. Fu, *Org. Lett.* **2019**, *21*, 4298–4302.

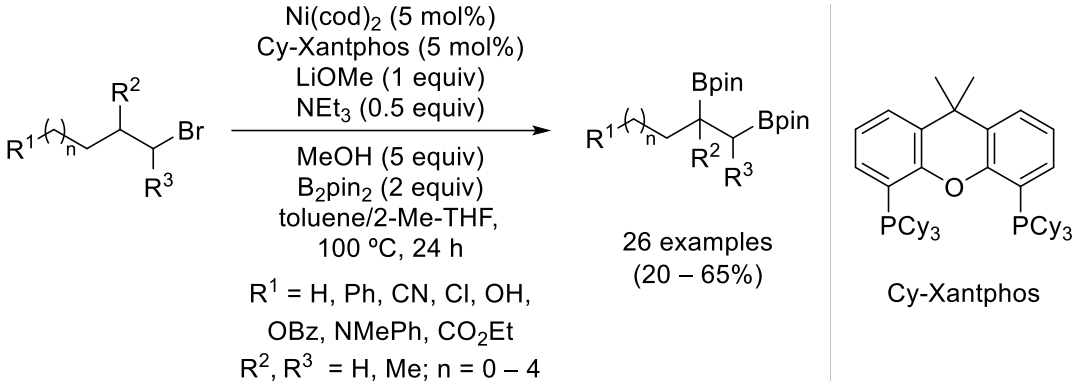

Scheme 4.16. Ni-catalyzed diboration of alkyl bromides.

3.4.2.4. Cu-catalyzed diboration

In 2006, Sadighi developed a new catalytic diboration of aldehydes using a (NHC)Cu-boryl catalyst.[240] They proposed that the insertion of the aldehyde into the Cu–B bond leads to the formation of Cu–C and B–O bonds, since they were able to isolate the corresponding copper complex containing [Cu–C–O–B] linkage (**Scheme 4.17**).

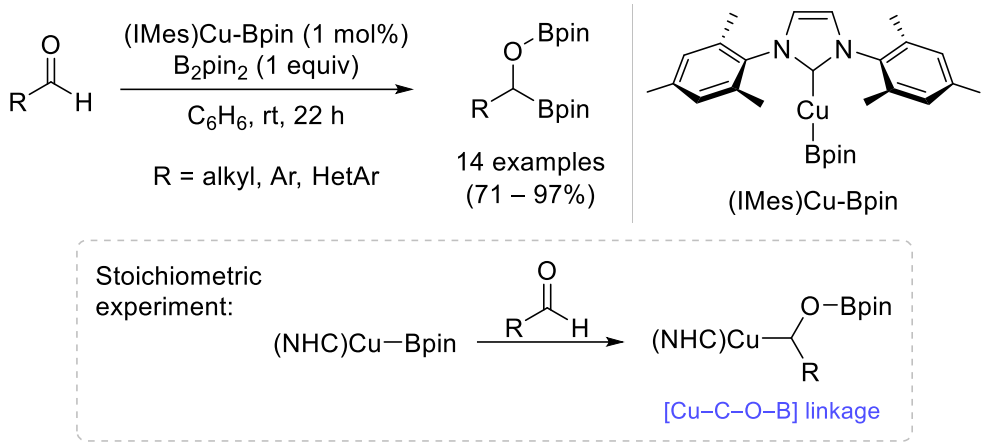

Scheme 4.17. Cu-catalyzed diboration of aldehydes.

A subsequent and extensive mechanistic study showed that the aldehyde insertion into Cu–B bond to give [Cu–O–C–B] linkage has a lower energy profile towards the formation of the [Cu–C–O–B] linkage. In addition, they proposed that the former complex undergoes a structural rearrangement to give the latter organometallic species, and that both can act as reaction catalyst (**Figure 4.7**).[241]

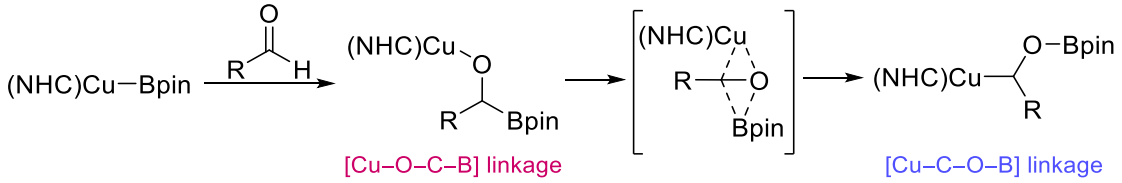

Figure 4.7. Insertion of aldehyde into Cu–B bond.

[240] D. S. Laitar, E. Y. Tsui, J. P. Sadighi, *J. Am. Chem. Soc.* **2006**, *128*, 11036–11037.
[241] H. Zhao, L. Dang, T. B. Marder, Z. Lin, *J. Am. Chem. Soc.* **2008**, *130*, 5586–5594.

Clark extend this methodology to ketones, assuming the same mechanism to that proposed by Marder and Lin (equation 1, **Scheme 4.18**).[242] In addition, they performed a direct Cu-catalyzed diboration/homologation sequence of different aldehydes (equation 2, **Scheme 4.18**).[243]

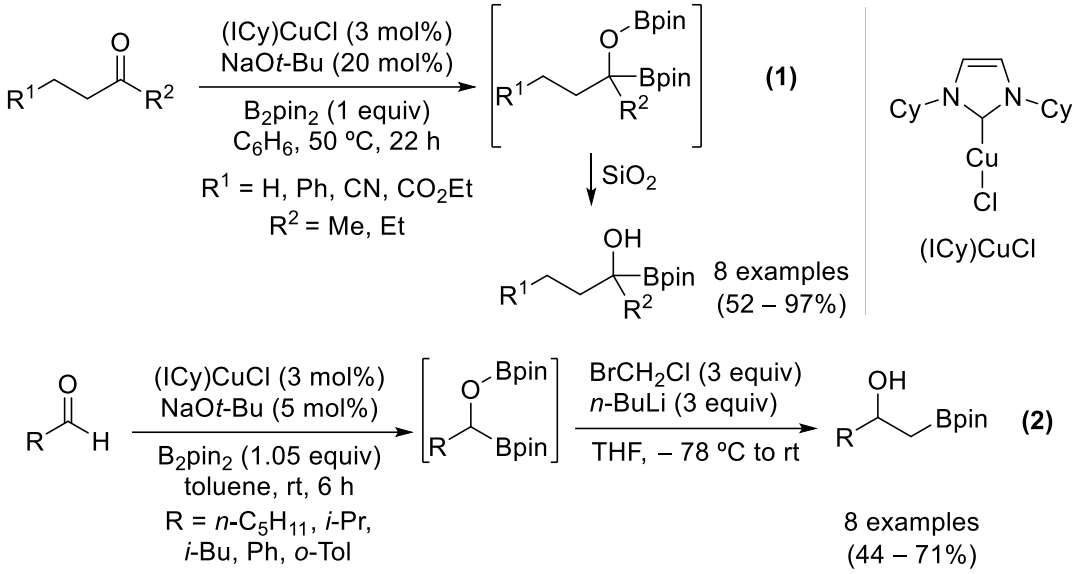

Scheme 4.18. Cu-catalyzed diboration performed by Clark.

Maseras, Pérez and Fernández described the selective 1,2-diboration of styrene by an inexpensive Cu^{I}/NHC catalytic system.[244] DFT calculations suggest that no B–B bond oxidative addition takes place, but a σ-adduct is formed and involved in the catalytic cycle (**Scheme 4.19**).

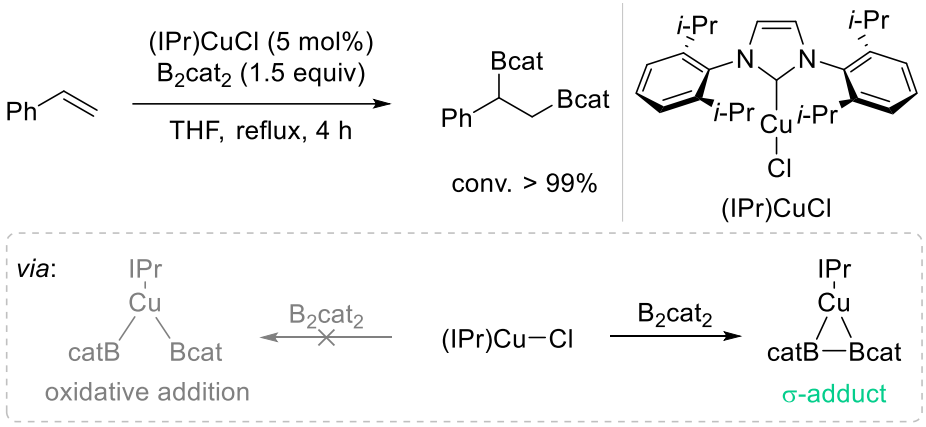

Scheme 4.19. Cu-catalyzed diboration of styrene.

The reaction pathway starts with the formation of Cu(I)-boryl species by reaction of the σ-adduct with the base. Then, the styrene inserts into the Cu–B bond with two possible regioselectivities. Finally, transmetalation with the diboron reagent regenerates the active Cu-boryl complex and yields the observed diboronate (**Figure 4.8**).

---

[242] M. L. McIntosh, C. M. Moore, T. B. Clark, *Org. Lett.* **2010**, *12*, 1996–1999.
[243] C. M. Moore, C. R. Medina, P. C. Cannamela, M. L. McIntosh, C. J. Ferber, A. J. Roering, T. B. Clark, *Org. Lett.* **2014**, *16*, 6056–6059.
[244] V. Lillo, M. R. Fructos, J. Ramírez, A. A. C. Braga, F. Maseras, M. M. Díaz-Requejo, P. J. Pérez, E. Fernández, *Chem. Eur. J.* **2007**, *13*, 2614–2621.

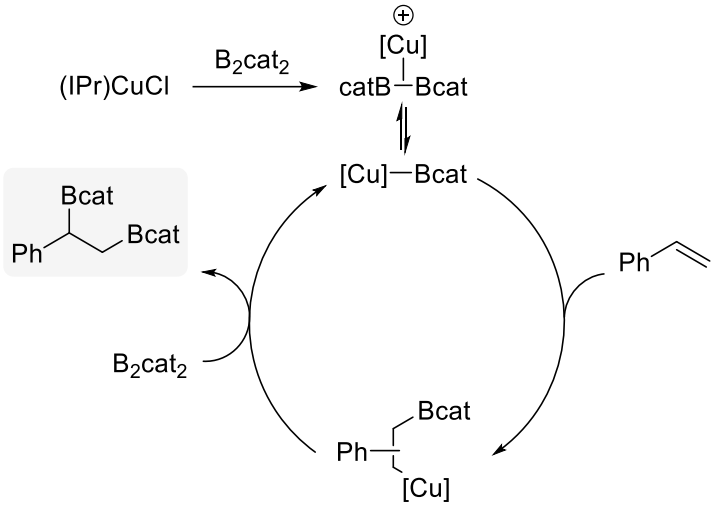

Figure 4.8. Mechanistic proposal for the Cu-catalyzed diboration of styrene.

Hoveyda and co-workers carried out the Cu-catalyzed diboration of terminal alkynes in good yields and highly enantiomeric fashion (**Scheme 4.20**).[245]

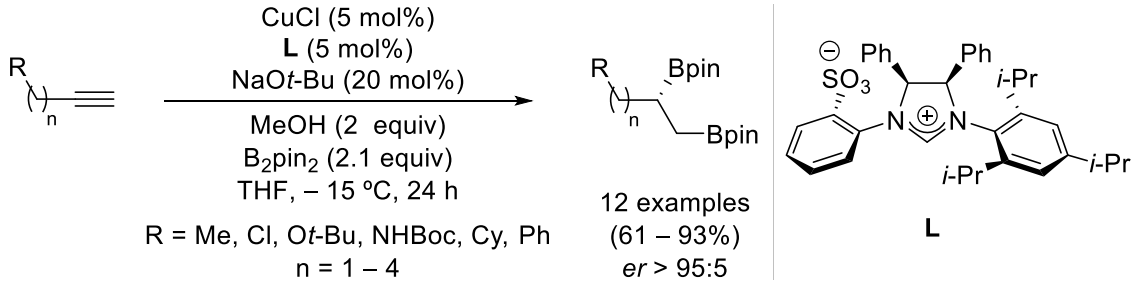

Scheme 4.20. Enantioselective Cu-catalyzed diboration of alkynes.

Few years later, Yoshida described the Cu-catalyzed diboration of internal alkynes.[246] The reaction shows a broad scope and affords 1,2-alkenyldiboronates in high yields (**Scheme 4.21**). The synthetic utility of these boron derivatives is demonstrated by drug total synthesis. A simple mechanism, based on initial formation of a Cu-boryl complex, is proposed.

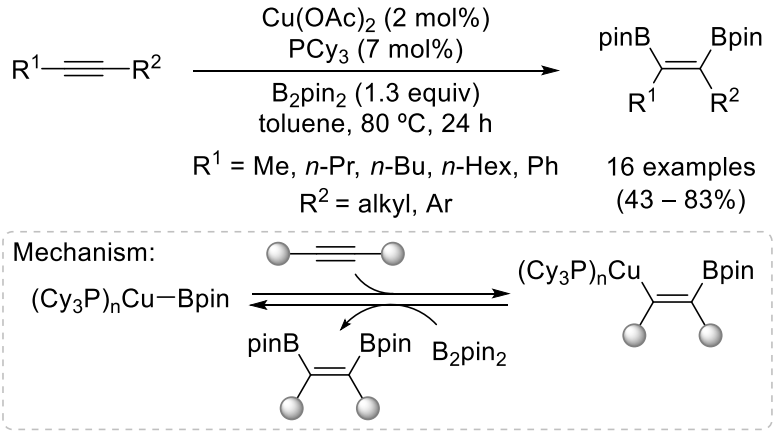

Scheme 4.21. Cu-catalyzed diboration of internal alkynes.

[245] Y. lee, H. Jang, A. H. Hoveyda, *J. Am. Chem. Soc*. **2009**, *131*, 18234–18235.
[246] H. Yoshida, S. Kawashima, Y. Takemoto, K. Okada, J. Ohshita, K. Takaki, *Angew. Chem. Int. Ed.* **2012**, *51*, 235–238.

Szabó and co-workers employed a bimetallic Pd/Cu catalysis for the borylation and diboration of propargylic substrates.[247] However, best yields are obtained in the case of propargylic epoxides when only Cu catalyst is used (**Scheme 4.22**).

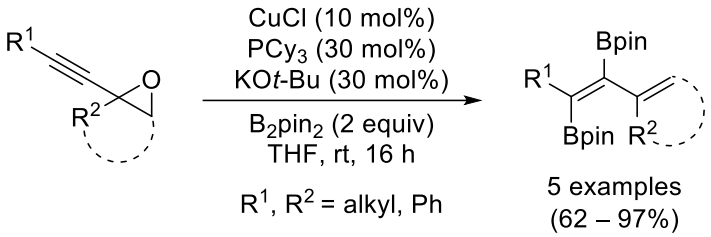

Scheme 4.22. Cu-catalyzed diboration of propargylic epoxides.

Very recently, Jin and Yamaguchi described an effective heterogeneous Cu catalyst for the mono- and diboration of styrene derivatives.[248] Alkenyl- and bis(boronates) can be obtained by a suitable choice of the metal oxide support for the Cu hydroxide catalyst, affording high yields in most cases (**Scheme 4.23**).

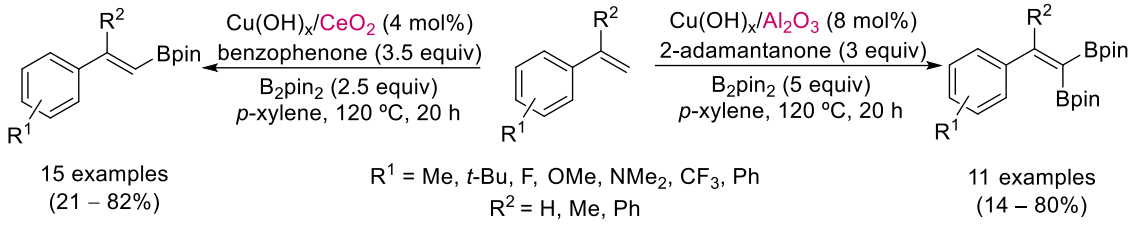

Scheme 4.23. Heterogeneous Cu catalyst for the mono- and diboration of alkenes.

The authors assume a catalytic cycle based on the formation of a catalytically active Cu-boryl species, followed by insertion of the alkene into the Cu–B bond and β-hydride elimination, yielding the monoborylated product. The Cu-boryl complex is regenerated by reaction of the resulting copper hydride with the ketone, which acts as a HBpin acceptor. The obtained alkenylboronate can undergo another dehydrogenative borylation process to afford the bis(boronate) product (**Figure 4.9**).

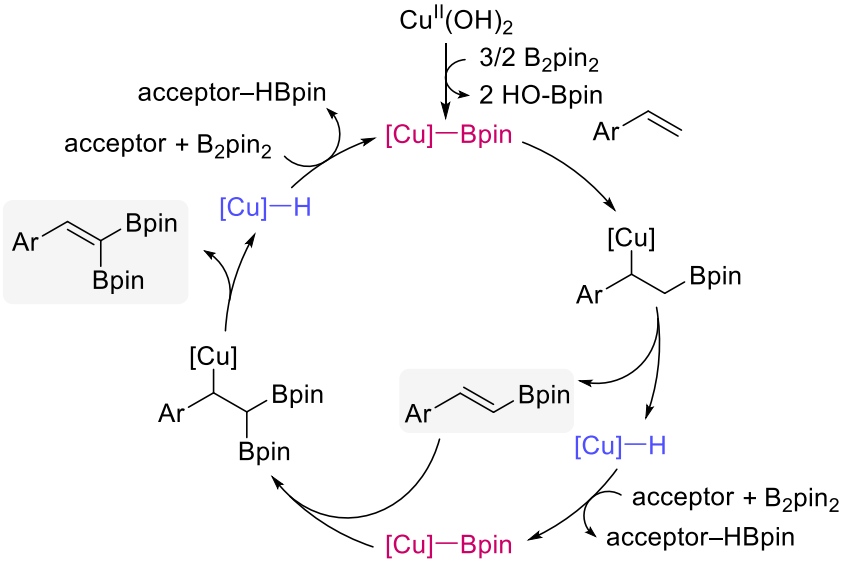

Figure 4.9. Proposed catalytic cycle for the supported Cu-catalyzed diboration of alkenes.

[247] T. S. N. Zhao, Y. Yang, T. Lessing, K. J. Szabó, *J. Am. Chem. Soc.* **2014**, *136*, 7563–7566.
[248] D. Yoshii, X. Jin, N. Mizuno, K. Yamaguchi, *ACS Catal.* **2019**, *9*, 3011–3016.

3.4.2.5. Metal-free catalyzed diboration

The transition metal-free catalyzed borylation reaction of alkynes and alkenes also offers an attractive method for generating valuable organoboron compounds.[249] Diboron reagents have been traditionally regarded as “Lewis acids”, which can react with simple Lewis base to generate Lewis acid-base adducts with a significant nucleophilic character in one of the boryl moieties. In the literature, we found different phosphine-,[250] alcoxide-,[251] salt-,[252] base-,[12g,253] amine-[254] and *N*-based ligand-catalyzed[12b,255] procedures for the diboration of unsaturated molecules.

It is worth to mention the seminal work performed by Fernández and co-workers in this field. The reaction of a base and a simple alcohol with the diboron reagent leads to the formation of a nucleophilic adduct which effectively performs the diboration of alkenes (**Scheme 4.24**).[256]

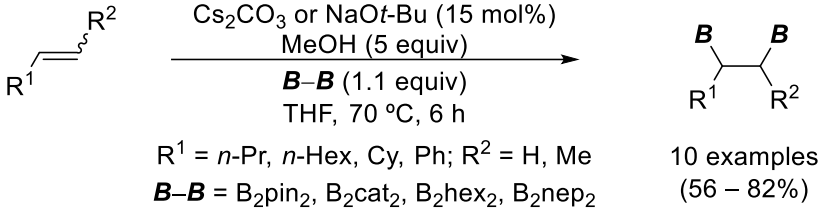

Scheme 4.24. Metal-free diboration of alkenes.

The proposed mechanism starts with the reaction between the alcohol and the base to generate an alcoxide, which activate the diboron reagent by formation of a Lewis acid-base adduct. Then, this adduct reacts with the alkene and furnishes the desired diboration product (**Figure 4.10**).

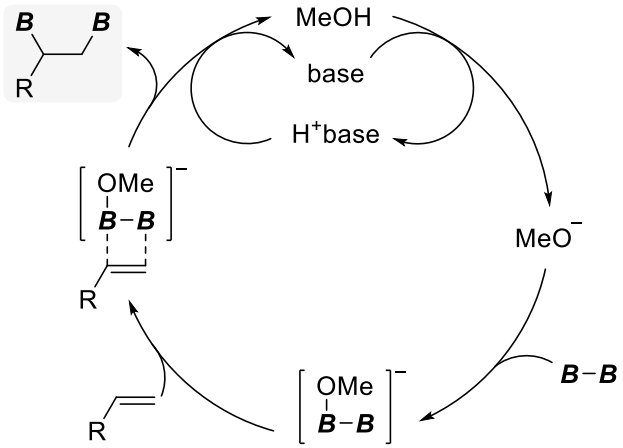

Figure 4.10. Plausible mechanism for the metal-free diboration of alkenes.

---

[12] (b) N. Miralles, J. Cid, A. B. Cuenca, J. J. Carbó, E. Fernández, *Chem. Commun.* **2015**, *51*, 1693–1696. (g) S. Peng, G. Liu, Z. Huang, *Org. Lett.* **2018**, *20*, 7363−7366.

[249] Y. Wen, C. Deng, J. Xie, X. Kang, *Molecules* **2019**, *24*, 101–116.

[250] (a) K. Nagao, H. Ohmiya, M. Sawamura *Org. Lett.* **2015**, *17*, 1304−1307. (b) A. Yoshimura, Y. Takamachi, K. Mihara, T. Saeki, S.-i. Kawaguchi, L.-B. Han, A. Nomoto, A. Ogawa, *Tetrahedron* **2016**, *72*, 7832–7838.

[251] (a) T. P. Blaisdell, T. C. Caya, L. Zhang, A. Sanz-Marco, J. P. Morken, *J. Am. Chem. Soc.* **2014**, *136*, 9264−9267. (b) L. Fang, L. Yan, F. Haeffner, J. P. Morken, *J. Am. Chem. Soc.* **2016**, *138*, 2508−2511. (c) L. Yan, Y. Meng, F. Haeffner, R. M. Leon, M. P. Crockett, J. P. Morken, *J. Am. Chem. Soc.* **2018**, *140*, 3663–3673.

[252] A. Farrea, R. Briggsa, C. Pubill-Ulldemolins, A. Bonet, *Synthesis* **2017**, *49*, 4775–4782.

[253] C. Kojima, K.-H. Lee, Z. Lin, M. Yamashita, *J. Am. Chem. Soc.* **2016**, *138*, 6662−6669.

[254] A. Farre, K. Soares, R. A. Briggs, A. Balanta, D. M. Benoit, A. Bonet, *Chem. Eur. J.* **2016**, *22*, 17552–17556.

[255] T.Ohmura, Y. Morimasa, M. Suginome, *Chem. Lett.* **2017**, *46*, 1793–1796.

[256] A. Bonet, C. Pubill-Ulldemolins, C. Bo, H. Gulyás, E. Fernández, *Angew. Chem. Int. Ed.* **2011**, *50*, 7158 –7161.

The use of chiral alcohols to activate the diboron reagent provides an opportunity to induce enantioselectivity in the diboration reaction (**Scheme 4.25**).[257] Despite the moderate enantioselectivities, this methodology represents a new strategy for inducing asymmetry in the absence of any transition metal catalyst.

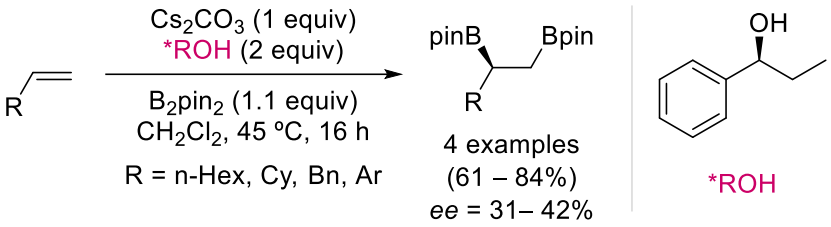

Scheme 4.25. Asymmetric alcoxide-catalyzed diboration of alkenes.

Furthermore, alcoxides also catalyzed the regioselective mixed diboration of alkenes when an unsymmetrical diboron reagent is used (**Scheme 4.26**).[12b] DFT calculations affords lower energy for the MeO-Bpin aduct towards the MeO-Bdan adduct, suggesting the activation step proceeds by reaction between the alcoxide and the Bpin moiety.

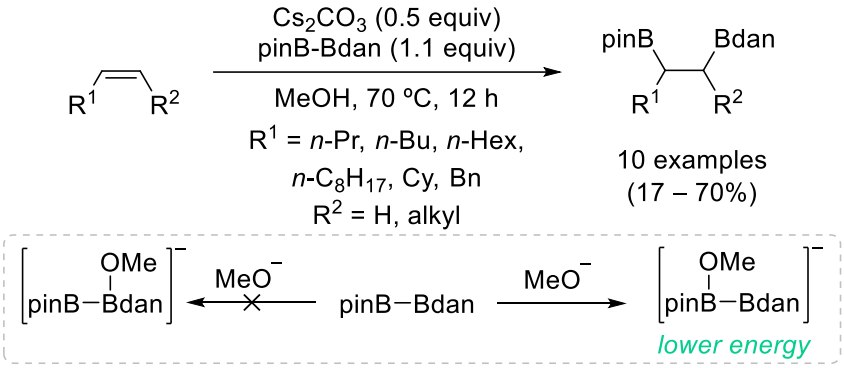

Scheme 4.26. Mixed diboration reaction of alkenes.

[12] (b) N. Miralles, J. Cid, A. B. Cuenca, J. J. Carbó, E. Fernández, *Chem. Commun.* **2015**, *51*, 1693–1696.
[257] A. Bonet, C. Sole, H. Gulyás, E. Fernández, *Org. Biomol. Chem.* **2012**, *10*, 6621–6623.

3.4.3. Results

Based on the optimal reaction conditions of the previously developed chapter (*Chapter 3*), we evaluated the diborylative cyclization reaction of enyne **1aa** with $Ni(cod)_2$/Xantphos by replacing HBpin with bis(pinacolato)diboron. Under these conditions, we were able to detect the desired bis(borylated) compound (**17aa**), but its isolation was difficult since it was impurified with B_2pin_2 and the conversion of the enyne was not complete (**Scheme 4.27**).

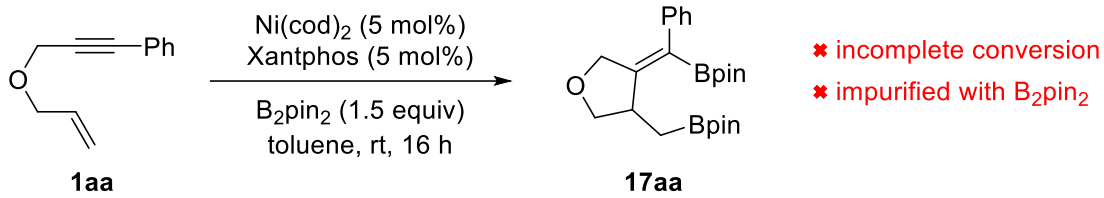

Scheme 4.27. First attempt to Ni-catalyzed diboration of enynes.

Therefore, we performed a ligand screening as we did for the reactions reported in the others chapters, but complete conversion was never achieved (**Scheme 4.28**). Among the different screened ligands, terpyridine afforded the cleanest reaction crude. Thus, we continued our study with this ligand.

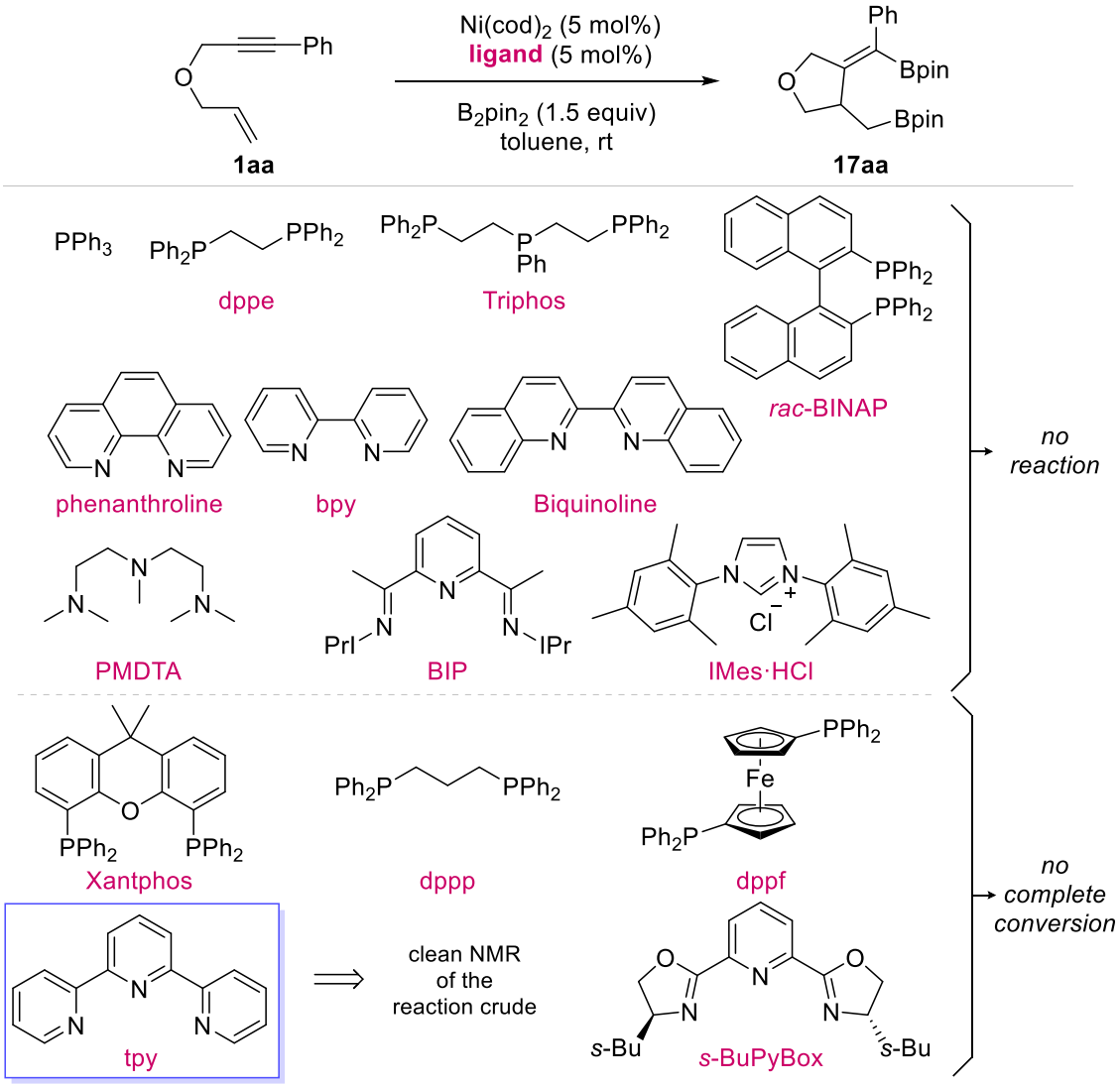

Scheme 4.28. Ligand screening.

Then, we reduced the amount of added B_2pin_2 and performed the reaction at higher temperature with the aim of completely consuming the starting enyne (**Table 4.1**). Pleasantly, we isolated the desired, pure compound **17aa** in moderate yield with a slightly excess of the diboron source (entry 3), observing that the reaction has to be performed at least at 60 ºC to afford complete conversion (entry 4).

Table 4.1. Optimization of the amount of B_2pin_2 and temperature.

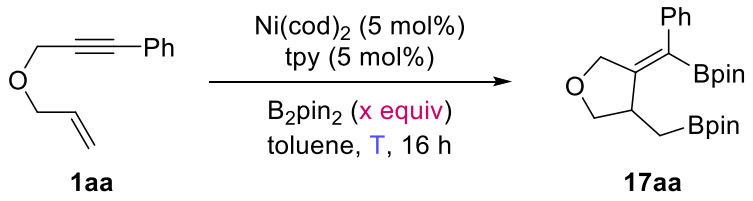

1aa **17aa**

Entry	x (equiv)	Temperature	Yield **17aa** (%)[a]
1	1.5	rt	(impure)
2	1.5	60 ºC	44% (impure)
3	1.05	60 ºC	39
4	1.05	50 ºC	incomplete conversion of **1aa**

[a] Isolated yield.

The previously tested ligands, which afford the expected product, were again evaluated under the improved reaction conditions (**Scheme 4.29**). In most cases, poor yields were obtained, except for the (dimethyl)tpy ligand, which slightly improved the reaction yield. Thus, we chose this ligand as the optimal one to continue with the optimization.

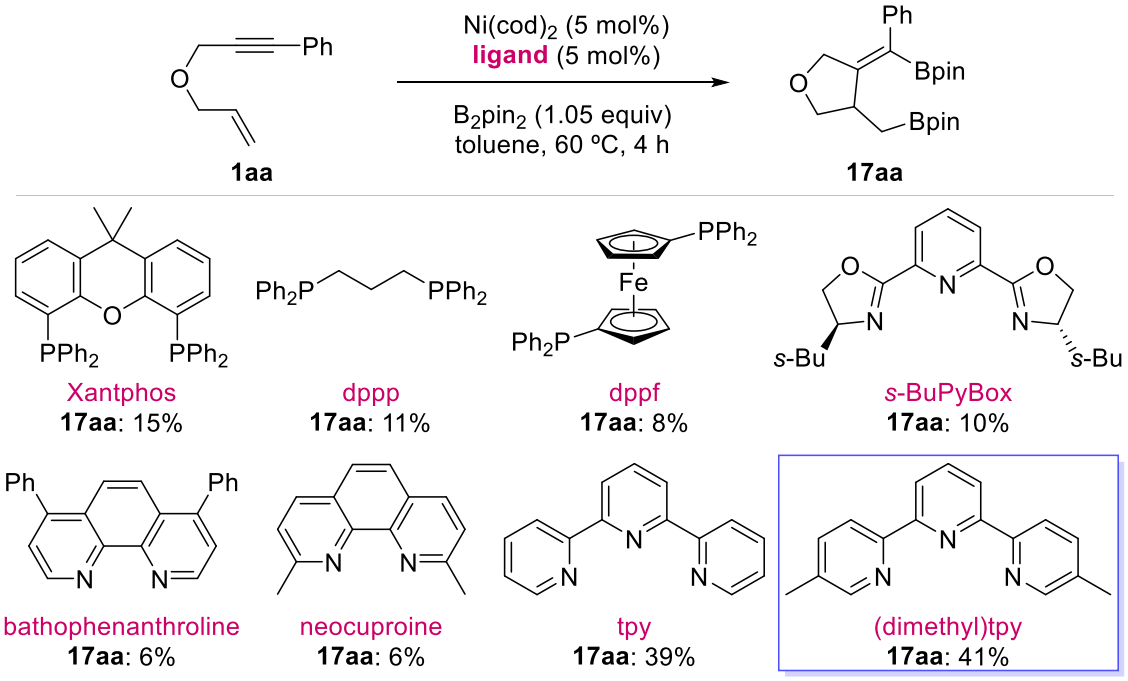

Scheme 4.29. Ligand optimization.

Finally, we studied different reaction parameters, such as solvent, Ni/L ratio and catalytic load (**Scheme 4.30**). The desired product **17aa** could be obtained in 49% yield using B_2pin_2 (1.05 equiv), $Ni(cod)_2$ (5 mol%) and 5,5''-dimethylterpyridine (5 mol%) in diisopropyl ether at 60 ºC. It is important to note that Ni(II) salts were ineffective, and led to recovery of the

unaltered starting enyne. Likewise, control experiments supports that the reaction requires the presence of both Ni source and ligand to take place.

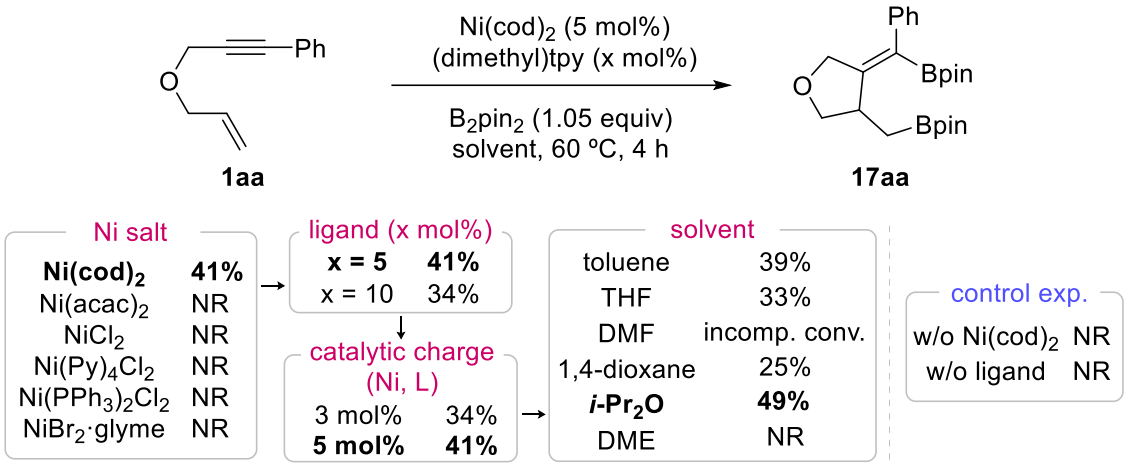

Scheme 4.30. Optimization of other parameters.

Although the yield obtained for the model reaction was moderate, the process is very general and proceeds with excellent yields for a wide variety of substrates providing boron-functionalized carbo-and heterocycles (**Scheme 4.31**). Thus, enynes containing arylalkynes afforded the corresponding products in moderate to good yields for derivatives with oxygen- (**17aa–af**), nitrogen- (**17bb–bg**, **17bm**), or malonate-derived (**17cc–cf**) within the tethering chains. The reaction tolerates a variety of functional groups with different electronic properties on the aromatic ring (Me, Cl, MeO, CN, and CF_3 in *meta*- and *para*- positions). Simple carbocycles are also accessible in good yields for substrates containing both aryl and alkyl substituents on the alkyne (**17db**, **17ea–d**). Substrates containing methyl-substituted alkynes were also effective and provided high to excellent yields, regardless of the kind of the tethering chain (**17an**, **17bn**, **17bw–bx**, **17cb**). The presence of other primary or secondary alkyl chains was also possible to give diboronates **17bo–bt**. TMS derivative **1bu** gave rise to the corresponding 1-silylalkenylboronates **17bu** in high yield. The process also tolerates substitution on the propargyl and allyl carbon atoms, affording the expected products in excellent to quantitative yields (**17bv**, **17by**, **17bz**). However, no stereocontrol on the formation of the new stereogenic center was observed. The poorest results were obtained for the reactions of enyne **17ca**, containing a terminal alkyne; and for 1,7-enyne **17ah**, which afforded the six-membered ring product in just 18% yield. We were able to obtain single crystals of compound **17cb**, that allowed us to confirm the configuration of the C–C double bond, which is in accord with the expected one for a metal-catalyzed alkyne carbometalation.

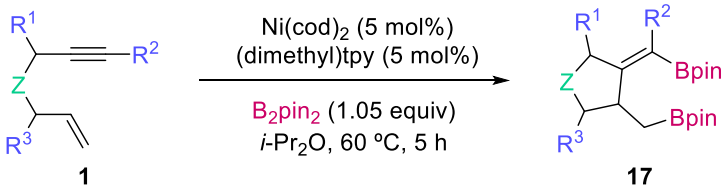

1 17

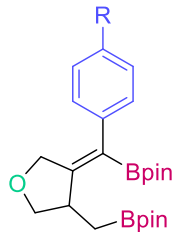

17aa: R = H 49%
17ab: R = Me 40%
17ac: R = OMe 32%
17ad: R = Cl 33%
17af: R = CF_3 16%

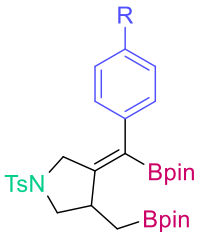

17bb: R = H 63%
17bc: R = Me 52%
17bd: R = OMe 93%
17be: R = Cl 54%
17bg: R = CF_3 61%

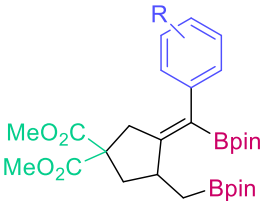

17cc: R = H 93%
17cd: R = 3-OMe 83%[a]
17ce: R = 4-OMe 42%[a]
17cf: R = 4-CN 37%

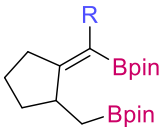

17ea: R = Ph 52%[a]
17eb: R = *p*-tol 63%[a]
17ed: R = *n*-Bu 76%

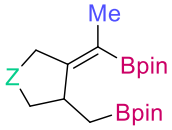

17an: Z = O 39%
17bn: Z = NPh 78%
17bw: Z = NPh 74%
17bx: Z = NBz 53%
17cb: Z = $C(CO_2Me)_2$ 96%

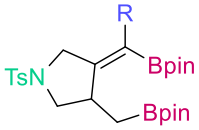

17bo: R = Et 63%
17bp: R = *n*-Pr 76%
17br: R = *n*-Hex 73%[a]
17bt: R = Cyp 74%
17bu: R = TMS 84%

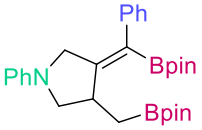

17bm: 27%

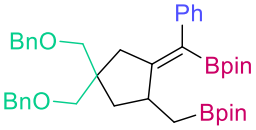

17db: 85%

X-ray

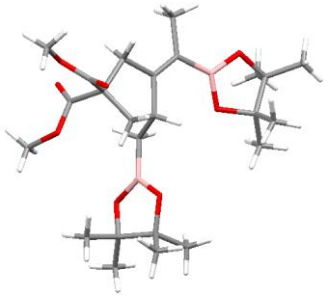

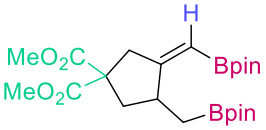

17ca: 28%

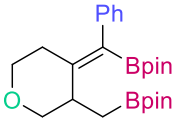

17ah: 18%

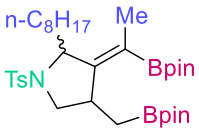

17bv: 98%
(*dr* = 1:1.7)

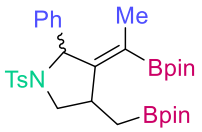

17by: 98%
(*dr* = 1:3.7)

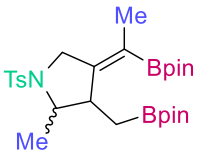

17bz: 90%
(*dr* = 1:1.2)

Scheme 4.31. Structural scope. [a] Toluene was used instead of *i*-Pr_2O.

In this system, enynes with substitution in alkene did not afford the desired bis(boronates) derivatives, even substrates containing an alkene conjugated to ketone. In addition, neither nitro- group in the aromatic ring, pyridine-subtituted alkyne nor ketone group conjugated to the alkyne afforded the desired compounds under optimal conditions (**Scheme 4.32**).

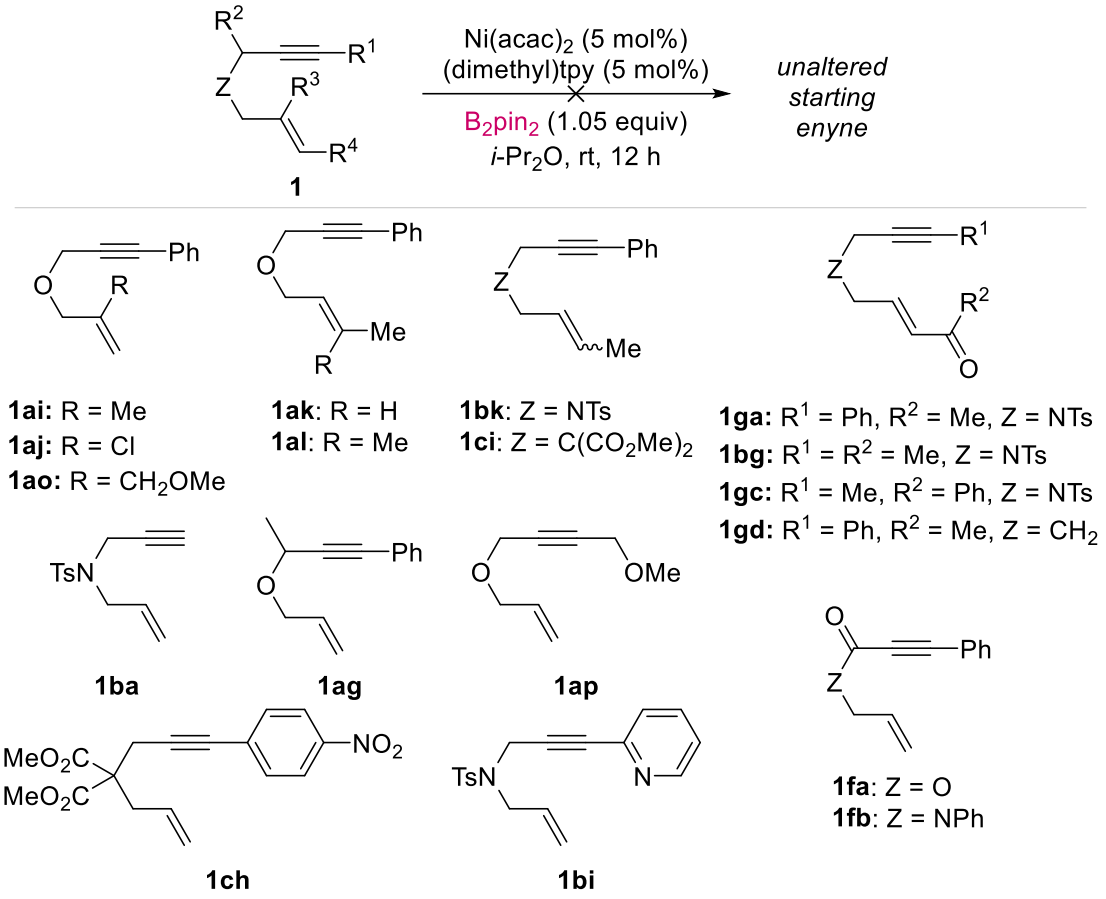

Scheme 4.32. Reaction scope limitation.

With the aim of illustrating the synthetic utility of the obtained diboronates, we performed some functionalization reactions. Thus, oxidation of both boronate groups gave the corresponding hydroxy-ketone **18bd** in high yield (top, **Scheme 4.33**). More interestingly, we succeeded at performing an orthogonal derivatization of diboronates **17cb** and **17cc** by selective Suzuki cross-coupling reactions. Firstly, we coupled the alkenylboronate moiety with iodobenzene with Pd as catalysts to obtain the corresponding alkylboronates **19**. Then, the remaining alkylboronate group was converted into the corresponding trifluoroborate salts **20**, which were used as nucleophiles in subsequent Suzuki cross-coupling reactions with 4-bromobenzonitrile to give compounds **21** (bottom, **Scheme 4.33**). We take advantage of the different reactivity of alkyl- and alkenylboronates, and there is no need to have different boryl moieties, such as Bpin and Bdan,[12] to perform a chemoselective derivatization. This orthogonal functionalization shows the usefulness of diboronates compounds as key intermediates for the preparation of well-defined tetra-substituted alkenes.

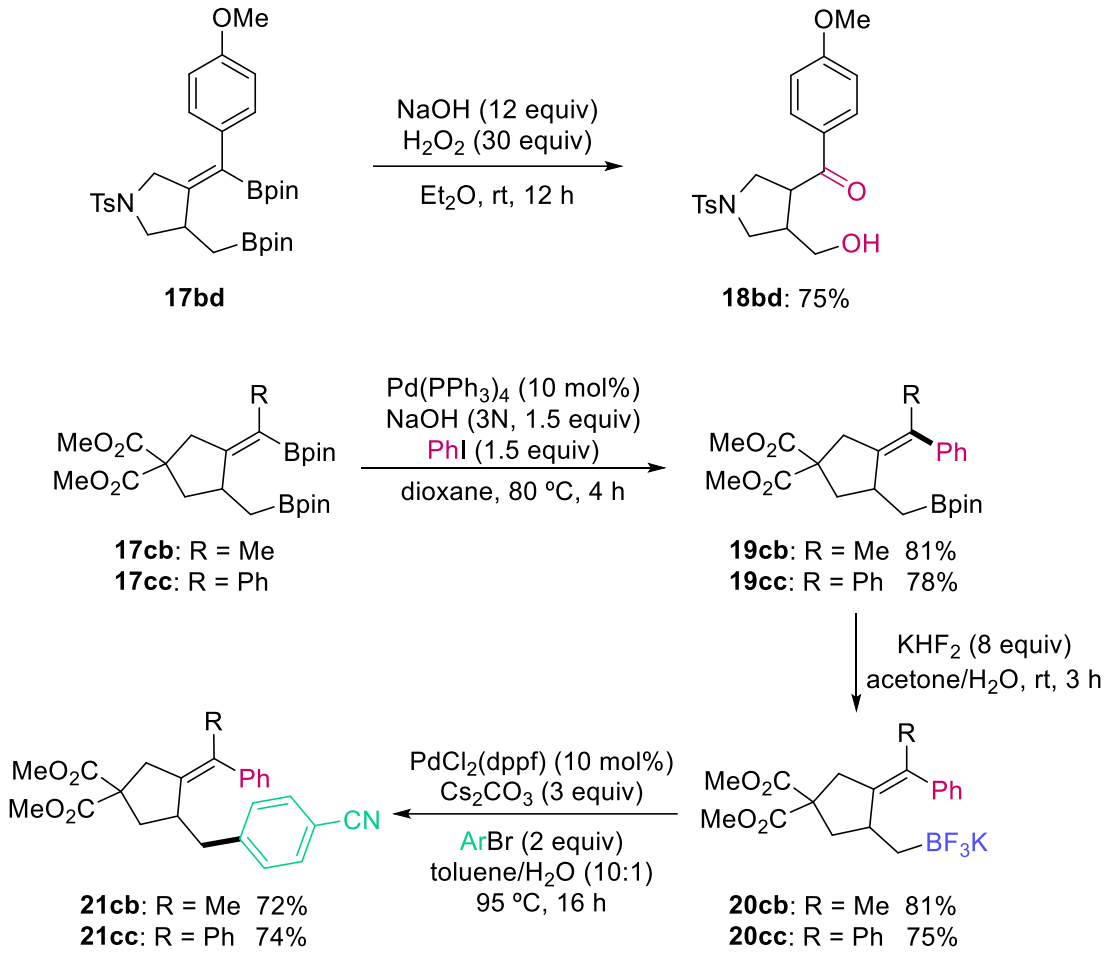

Scheme 4.33. Functionalization of bis(boronates) **17**.

In order to get insight into the reaction mechanism, we have performed some experiments. Thus, when simple alkenes or alkynes were subjected to the optimized conditions, we did not observe borylation of none of the substrates (**Scheme 4.34**). This result implies that the reaction starts with the simultaneos activation of both alkene and alkyne.

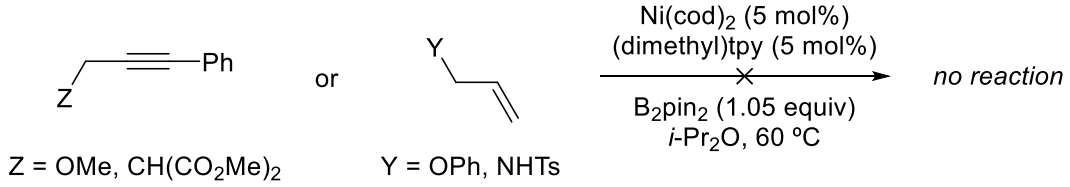

Scheme 4.34. Reaction with simple alkenes and alkynes.

On the other hand, the stoichiometric reaction of enynes **1bb** or **1cc** with $Ni(cod)_2$ and (dimethyl)tpy in the absence of diboron reagent, followed by hydrolysis with DCl in D_2O led to the corresponding dideuterated cyclic derivatives d^2-**13bb** and d^2-**13cc** in 20% and 58% yield, respectively. This result suggests the formation of an intermediate complex containing both alkyl- and alkenyl-Ni bonds.

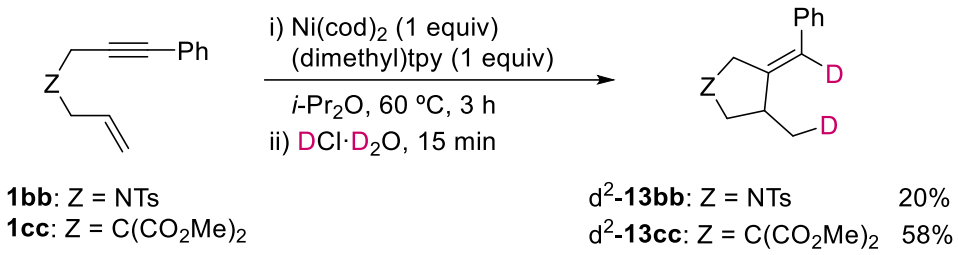

1bb: Z = NTs
1cc: Z = $C(CO_2Me)_2$

d^2-**13bb**: Z = NTs 20%
d^2-**13cc**: Z = $C(CO_2Me)_2$ 58%

Scheme 4.35. Deuteration experiment.

As we did in the Fe-catalyzed hydroborylative cyclization reaction, we sought to isolate and characterize Ni species in order to identify putative reaction intermediates. Firstly, we performed different crystallization attempts of the equimolar mixture of $Ni(cod)_2$ and tpy. After extensive experimentation, we found that a vapor diffusion of toluene/pentane at – 25 ºC afforded suitable dark blue crystals for X-ray diffraction, obtaining the crystal structure shown in **Figure 4.11**.

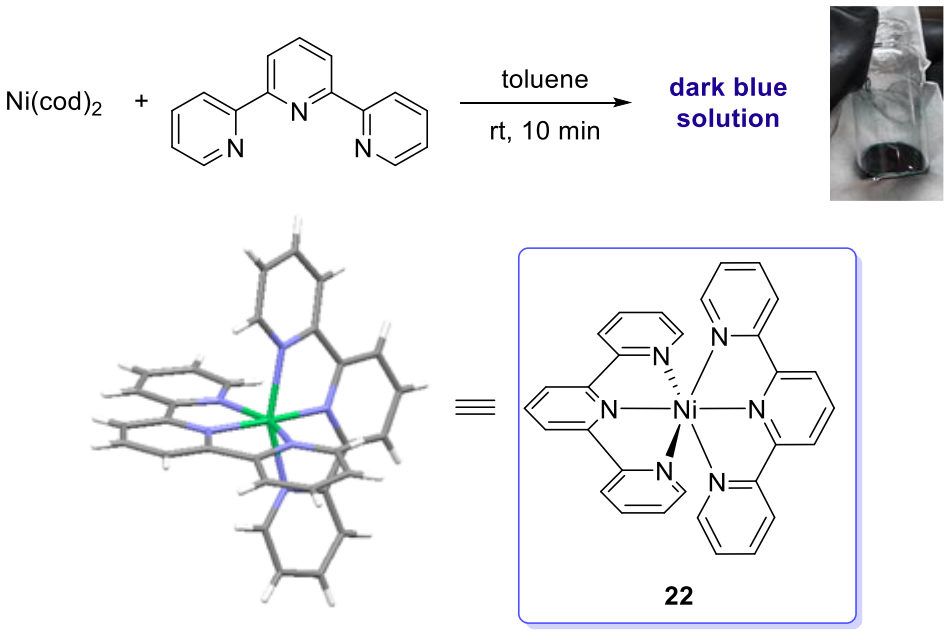

Figure 4.11. Isolation of complex **22**.

The obtained $Ni(tpy)_2$ complex (**22**) shows a distorted octahedral geometry with shorter Ni–N bond distances regarding the central nitrogen of the ligand. This complex involves a formal oxidation state of Ni(0). However, Ni(0) complexes usually present four substituents in tetrahedral arrangement. Terpyridine contains three electron-deficient pyridine heterocycles, which makes terpyridine not only a strong σ-donor but also a very good π-receptor. This nature makes tpy behave as a ‘‘non-innocent” ligand, due to delocalization of electron from metal center. When coordinating to nickel center with low oxidation state, Ni(0) for example, terpyridine stabilized the metal cation as well as enriched the electron density.[258] Thus, the formally Ni(0) complex **22** may be considered as a Ni(II) species coordinated to two radical anions (**Figure 4.12**). Depending on the number of unpaired electrons of the complex, we might have three different values for the molecule spin: (i) S = 0 or singlet, with all paired

[258] (a) G. U. Priimov, P. Moore, *Inorg. Reac. Mech.* **2003**, *5*, 21–30. (b) C. Wei, Y. He, X. Shi, Z. Song, *Coordin. Chem. Rev.* **2019**, *385*, 1–19.

electrons, (ii) S = 1 or triplet, with two unpaired electrons and (iii) S = 2 or quintet, with four unpaired electrons. DFT calculations supports that the quintet ground state is more stable than the singlet and the triplet state.

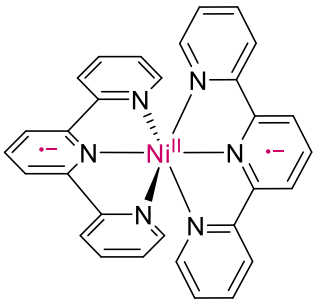

22

Figure 4.12. Complex **22** may be described as a Ni(II) complex with anionic tpy ligands.

We also recorded its ^{1}H-NMR spectra, which shows several paramagnetic signals, meaning the presence of unpaired electrons, compatible with a triple or quintet ground state (**Figure 4.13**).

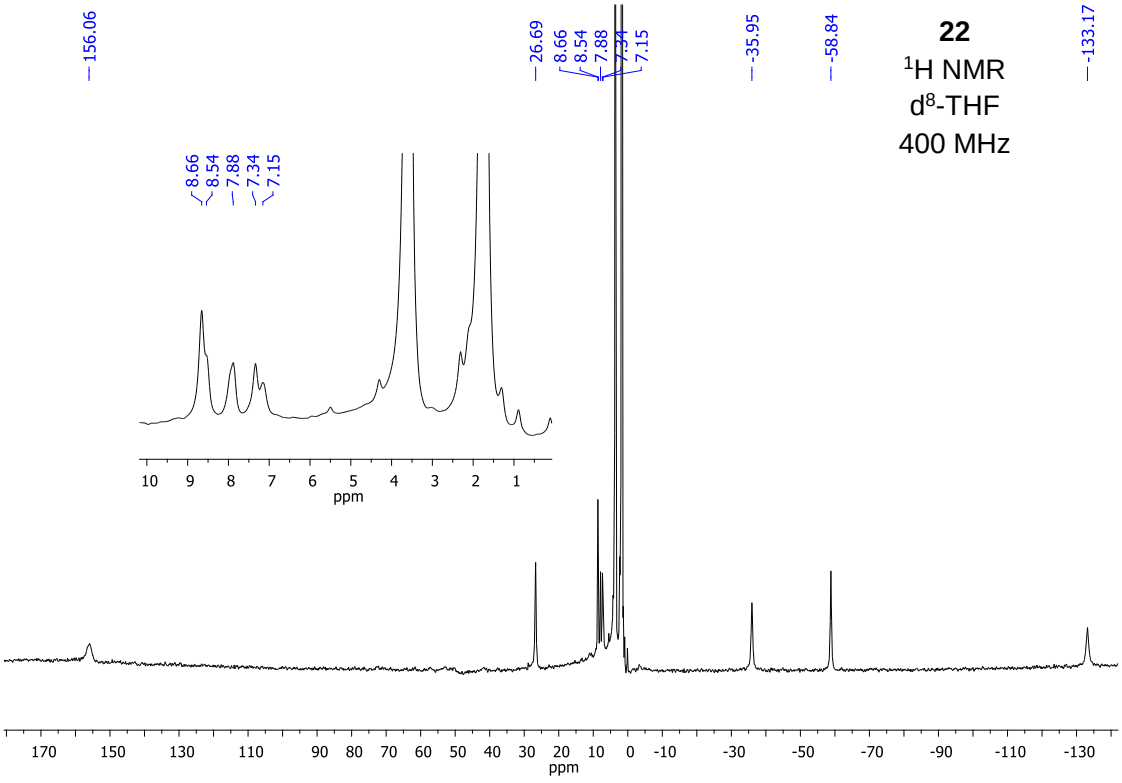

Figure 4.13. NMR spectra of isolated Ni(tpy)$_2$ (**22**) in d^8-THF.

Comparing this paramagnetic spectra with the NMR of *in situ* prepared Ni(tpy)$_2$ by reaction of tpy and Ni(cod)$_2$, we observed the same peak pattern corresponding to complex **22** (pink, **Figure 4.14**). In addition, we also detected Ni(cod)$_2$ (blue) and free cyclooctadiene ligand (green), which is in accordance with the formation of the aforementioned complex.

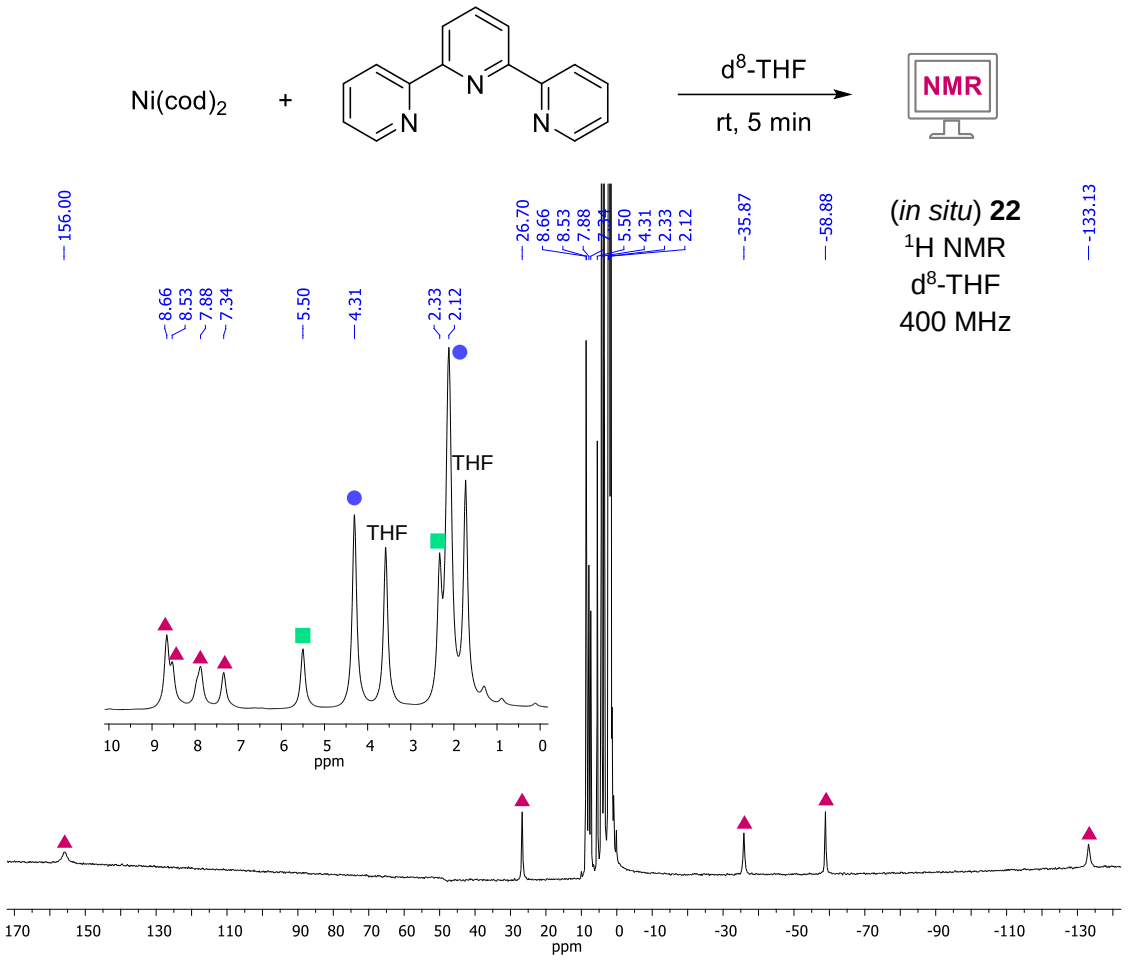

Figure 4.14. NMR spectra of *in situ* prepared $Ni(tpy)_2$.

Furthermore, we recorded quantitative EPR spectra of complex **22**, showing an active signal which could match with a S = ½ species (**Figure 4.15**). However, that signal only represents 1% of the total sample. This result suggests that the major Ni species presented in the sample has a S = 1 or 2.

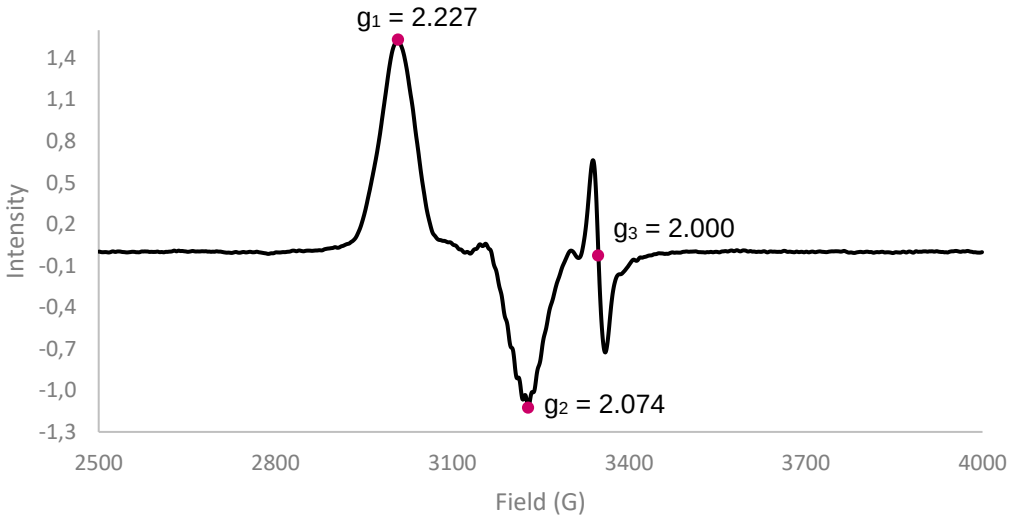

Figure 4.15. EPR spectra of complex **22**.

The Evans method uses difference in the NMR chemical shift in a solvent caused by the presence of a paramagnetic species.[259] It can be used to determine the magnetic moment of the paramagnetic species and the number of unpaired electrons present. Following this method, we measured the effective magnetic moment (μ_{eff}) of complex **22**, obtaining a value of 4.3 μB. Taking into account the described data (see **Table 4.3**, *Experimental section*), this result might involves the presence of Ni species with S = 3/2 (three unpaired electrons) or 2 (four unpaired electrons). Since there is no active, quantitative signal in EPR, a S = 3/2 complex can be disregarded. Therefore, the structure of the $Ni(tpy)_2$ complex (**22**) might entails a quintet ground state with four unpaired electrons, where two of them would be probably located in the metal center and the other two unpaired electrons would be delocalized in tpy ligands.

Based on mechanistic experiments, we had been proposed an oxidative cyclometalation of enyne as the first reaction step. Thus, we performed different crystallization attempts of an equimolar mixture of $Ni(cod)_2$, Tpy and enyne **1aa**. Succesfully, we could obtain dark red single crystals (*ca.* 9% yield) in a THF/hexane mixture (2:1).[260] X-Ray diffraction analysis revealed the structure of a fascinating bimetallic complex (**23**) containing a carbocycle and two Ni(I)-tpy units bound to alkyl and alkenyl carbon ligands (**Figure 4.16**).

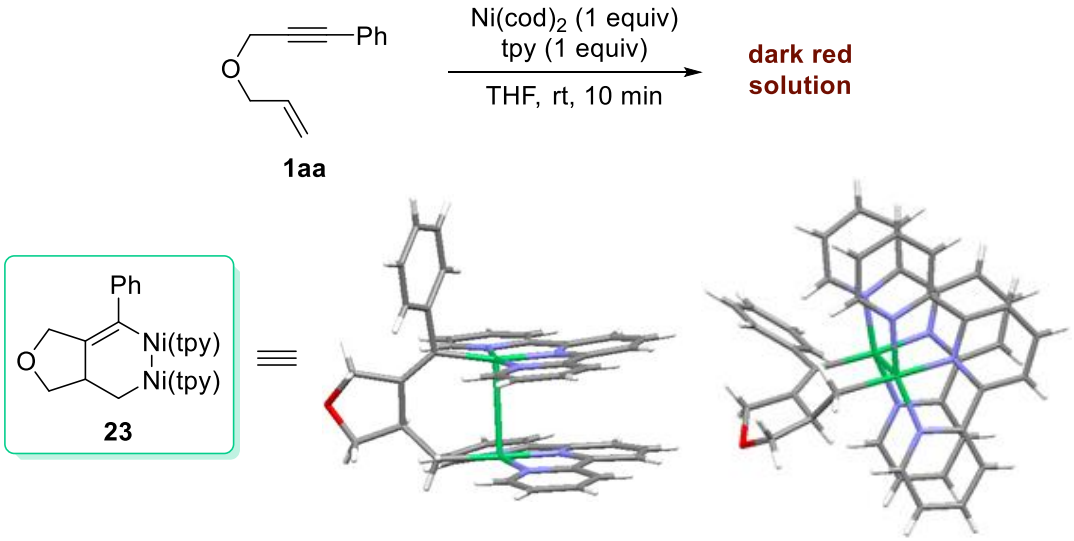

Figure 4.16. Isolation of complex **23**.

The short Ni–Ni distance (2.97 Å) indicates a strong interaction between both metals (van der Waals radius for Ni is 1.63 Å). This is reminiscent of the structure of (tpy)NiMe, in which a weaker intermolecular interaction between Ni atom was observed in the solid state (3.18 Å).[261] In the same way, we measured the effective magnetic moment of complex **23**, obtaining a μ_{eff} = 3.1 μB (**Figure 4.17**), meaning the presence of two unpaired electrons (S = 1 species).

[259] (a) D. F. Evans, *J. Chem. Soc.* **1959**, 2003–2005. (b) E. M. Schubert, *J. Chem. Educ.* **1992**, *69*, 62. (c) C. Piguet, *J. Chem. Educ.* **1997**, *74*, 815–816.
[260] Suitable crystals were also obtained from toluene/hexane or toluene/pentane mixtures (4:1), performing the reaction in toluene from the beginning.
[261] (a) T. J. Anderson, G. D. Jones, D. A. Vicic, *J. Am. Chem. Soc.* **2004**, *126*, 8100–8101. (b) G. D. Jones, C. McFarland, T. J. Anderson, D. A. Vicic, *Chem. Commun.* **2005**, 4211–4213.

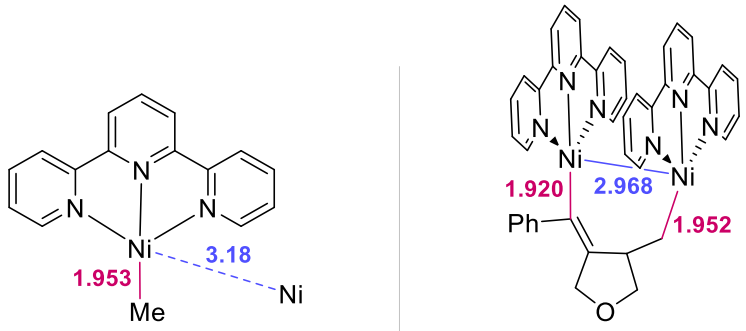

(tpy)NiMe

μ_{eff} = 1.64 μB in THF

23

μ_{eff} = 3.1 μB in THF

Figure 4.17. Comparative between (tpy)NiMe and complex **23**.

Furthermore, we recorded the quantitative EPR spectra of complex **23** (**Figure 4.18**). We observed a signal of a S = ½ species, which only represents 3.2% of the total sample. Thus, we considered that the real Ni species presented in the active solution has S = 1, according to the magnetic moment.

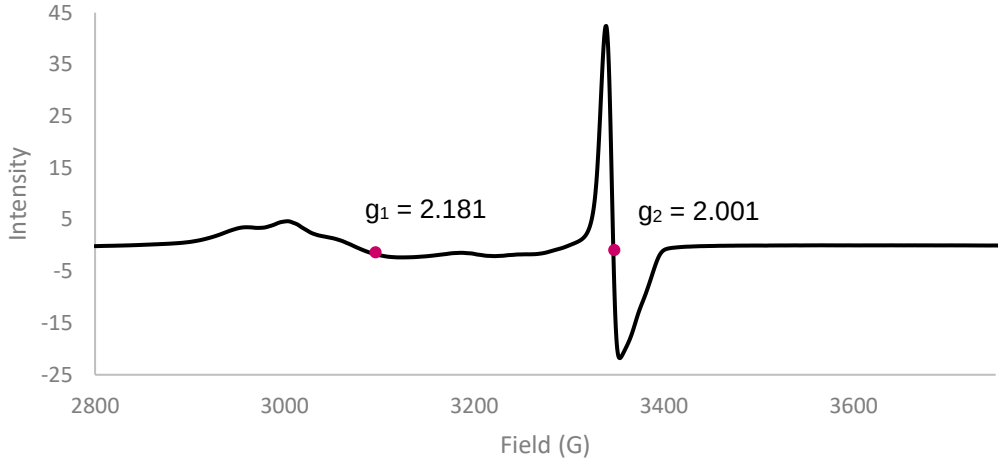

Figure 4.18. EPR spectra of complex **23**.

Both metal atoms of complex **23** are formally Ni(I), and therefore the structure of the complex corresponds to an oxidative cyclometalation with each metal increasing its oxidation state by one unit. We envisioned two possible mechanisms for the formation of **23**, and calculations at DFT level have been performed on **1aa** as a model to probe their feasibility (**Figure 4.19**).

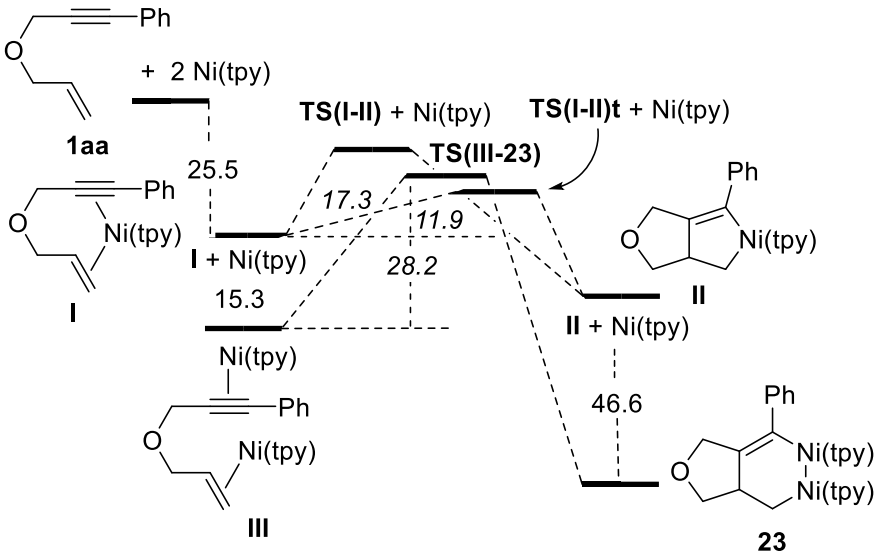

Figure 4.19. Calculated possible reaction pathways for the formation of **23**. Δ*G* (kcal mol^{-1}) are calculated with M06-2x functional, using 6-31G(d) (C,H,N,O), LANL2DZ (Ni) basis set, in diisopropyl ether (PCM) (activation energies in italics).

Thus, the process could involve the cyclization of a bimetallic precursor containing two Ni(tpy) units coordinated to each unsaturation (**III**). Formation of **III** is exoergic and its evolution to **23** would take place with a moderate activation energy (28.2 kcal mol^{-1}) compatible, within the calculation error, with a process taking place at 60 °C. Alternatively, oxidative cyclometalation could take place from a mononuclear Ni species with both the alkyne and the alkene coordinated to the metal (**I**). Activation energy for the formation of metalacycle **II** from this complex is lower (17.3 kcal mol^{-1}), albeit the corresponding transition state lies above the former mentioned one. On the other hand, a triplet transition state, **TS(I-II)t**, lying 1.1 kcal mol^{-1} below **TS(III-23)** would lead to the formation of **II**.[262] Subsequent comproportionation with Ni(tpy) would lead to the same species **23**. Complex **23** shows a triplet ground state according to its EPR spectrum and effective magnetic moment. Calculated triplet state for **23** is only 3.1 kcal mol^{-1} more stable compared to the singlet.

When we subjected complex **23** to reaction with an excess of B_2pin_2, simulating the reaction relative concentrations, bis(boronate) **17aa** was formed (41% NMR yield),[263] which could suggest that dinuclear Ni complex is a reaction intermediate. However, when a slighty excess of B_2pin_2 was used, poor yield was obtained (**Scheme 4.36**).

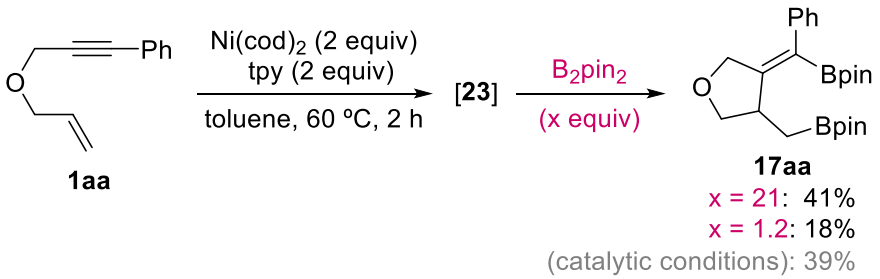

Scheme 4.36. *In situ* formation of complex **23** and subsequent reaction with B_2pin_2.

[262] DFT methods overestimate the stability of high-spin states and, therefore, the computed energy for **TS(I-II)t** is not fully reliable. (a) M. Radon, *PhysChemChemPhys* **2014**, *16*, 14479–14488. (b) D. Coskum, S. V. Jerome, R. A. Friesner, *J. Chem. Theory Comput.* **2016**, *12*, 1121–1128.

[263] TMS (0.22 equiv) was used as internal standard.

Computational and experimental results are not conclusive to decide whether the reaction takes place through monometallic intermediate **II** or by direct formation of **23**. In addition, the low energy of dinuclear complex **23** suggests that it could be a resting state rather than a reaction intermediate. Moreover, inspection of the structure of **23** makes difficult to guess how this complex could react with B_2pin_2. We have studied the interaction of **II** with the boron reagent (**Scheme 4.37**). Exploration of the potential energy surface strongly suggests that oxidative addition of the B-B bond to give a Ni(IV) intermediate does not take place. Instead, we propose a σ-bond metathesis, which may involve both Ni–C bonds to give either intermediate **IV** or **V**. Reaction involving cleavage of the alkenyl-Ni bond to provide **IV** seems more feasible, since it is exoergic (-3.4 kcal mol^{-1}), whereas formation of **V** is endoergic (+3.5 kcal mol^{-1}). Finally, downhill C–B reductive elimination would give the final diboronate **17aa** and would regenerate the Ni(0) catalyst.

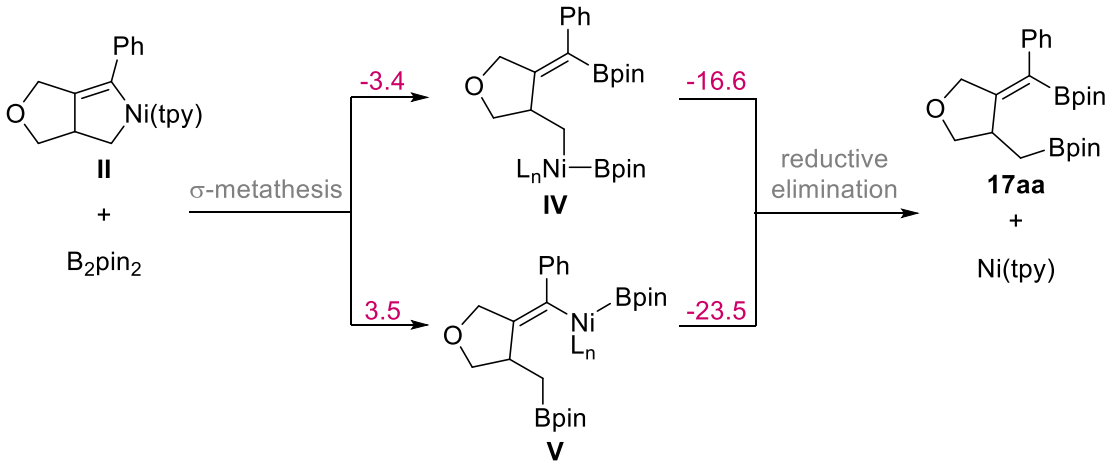

Scheme 4.37. Reaction energies for the reaction of **II** with diboron reagent. Δ*G* (kcal mol^{-1}) are calculated with M06-2x functional, using 6-31G(d) (C,H,N,O), LANL2DZ (Ni) basis set, in diisopropyl ether (PCM).

Therefore, we propose that reaction pathway begins with activation of the organic substrate prior to reaction with the borylation reagent, where a monometallic or a cooperative Ni catalysis could operate (**Figure 4.20**). Further studies to ascertain the reaction mechanism, especially regarding the activation of diboron derivatives with novel dinuclear Ni(I)-Ni(I) complexes, are underway.

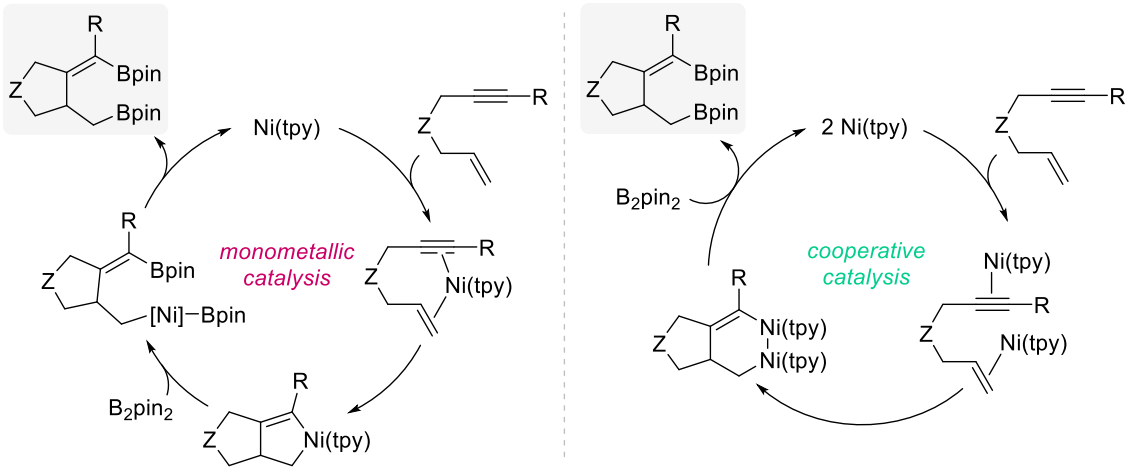

Figure 4.20. Tentative reaction mechanism proposal.

3.4.4. Experimental section

3.4.4.1. Materials and methods

General considerations have been described in *Experimental section* of *Chapter 1*. Additionally, $Ni(cod)_2$, $Ni(acac)_2$, bis(pinacolato)diboron and 2,2′:6′,2″-terpyridine were purchased from Sigma-Aldrich Co. Bis(pinacolato)diboron was recrystallized from pentane before use. The other commercially available chemicals were purchased and used as received without further purifications. The diborylative cyclization reactions were carried out under argon atmosphere in anhydrous and Ar-degassed *i*-Pr_2O purchased from Sigma-Aldrich Co.

3.4.4.2. General procedure for diborylative cyclization of enynes

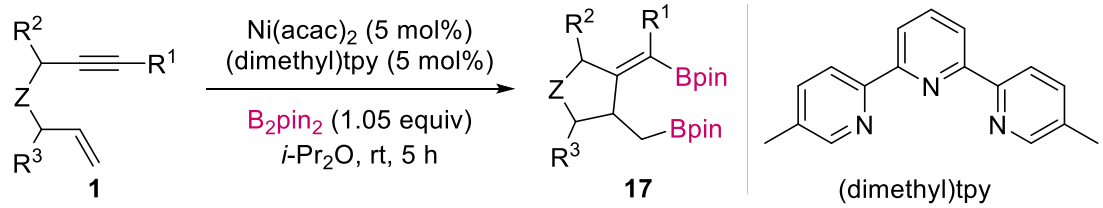

A vial was charged with $Ni(cod)_2$ (2.8 mg, 0.01 mmol), 5,5''-dimethyl-2,2':6',2''-terpyridine (2.6 mg, 0.01 mmol), B_2pin_2 (53.3 mg, 0.21 mmol), the corresponding enyne **1** (0.2 mmol) and a stir bar in air. The vial was sealed by a septum, dried under vacuum and backfilled with Ar. Then, anhydrous and Ar-degassed *i*-Pr_2O (1 mL) was added. The resulting mixture was stirred for 5 h at 60 °C. When complete consumption of the enyne was verified by TLC, the solvent was evaporated under vacuum and the product was purified by column chromatography in silica gel.

(*Z*)-4,4,5,5-Tetramethyl-2-((4-(phenyl(4,4,5,5-tetramethyl-1,3,2-dioxaborolan-2-yl)methylene)tetrahydrofuran-3-yl)methyl)-1,3,2-dioxaborolane (17aa): The compound

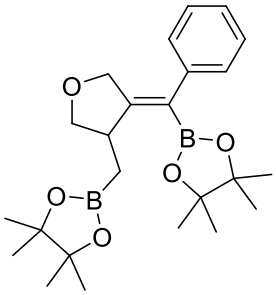

was purified by column chromatography (cyclohexane/EtOAc 95:5) and was obtained as a colorless oil in 45% yield (38 mg). ^{1}H NMR (300 MHz, $CDCl_3$) δ 7.29 (d, J = 7.1 Hz, 2H), 7.18 (d, J = 7.1 Hz, 1H), 7.12 – 7.08 (m, 2H), 4.51 (d, J = 15.0 Hz, 1H), 4.03 (d, J = 15.0 Hz, 1H), 3.89 (d, J = 8.5, 5.8 Hz, 1H), 3.75 (dd, J = 8.5, 2.2 Hz, 1H), 3.55 – 3.45 (m, 1H), 1.26 (d, J = 3.5 Hz, 24H), 1.17 (dd, J = 12.7, 6.9 Hz, 2H). ^{13}C NMR (75 MHz, $CDCl_3$) δ 164.2 (C), 142.2 (C), 128.4 (2 × CH), 128.0 (2 × CH), 126.0 (CH), 83.4 (2 × C), 83.1 (2 × CH), 74.9 (CH_2), 70.7 (CH_2), 40.2 (CH), 25.1 (2 × CH_3), 25.0 (2 × CH_3), 24.9 (2 × CH_3), 24.7 (2 × CH_3), 18.7 (br m, CH_2-B). HRMS (ESI, MeOH) calcd. for $C_{24}H_{36}B_2O_5$ $[M + Na]^+$: 449.2749; Found: 449.2648.

(*Z*)-4,4,5,5-Tetramethyl-2-((4-((4,4,5,5-tetramethyl-1,3,2-dioxaborolan-2-yl)(*p*-tolyl)methylene)tetrahydrofuran-3-yl)methyl)-1,3,2-dioxaborolane (17ab): The

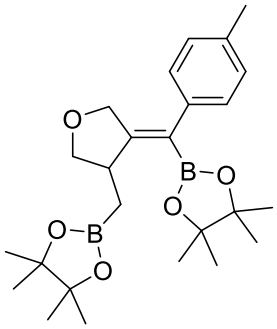

compound was purified by column chromatography (cyclohexane/EtOAc 95:5) and was obtained as a yellow oil in 40% yield (35 mg). ^{1}H NMR (300 MHz, $CDCl_3$) δ 7.08 (d, J = 7.8 Hz, 2H), 6.99 (d, J = 7.8 Hz, 2H), 4.52 (dd, J = 15.0, 1.4 Hz, 1H), 4.05 (d, J = 15.0 Hz, 1H), 3.88 (dd, J = 8.6, 6.2 Hz, 1H), 3.75 (dd, J = 8.6, 2.2 Hz, 1H), 3.54 – 3.45 (m, 1H), 2.31 (s, 3H), 1.26 (d, J = 3.9 Hz, 24H), 1.18 (dd, J = 10.7, 5.6 Hz, 2H). ^{13}C NMR (75 MHz, $CDCl_3$) δ 163.7 (C), 139.1 (C), 135.4 (C), 128.7 (2 × CH), 128.2 (2 × CH), 83.3 (2 × C), 83.1 (2 × CH), 74.8 (CH_2), 70.7 (CH_2), 40.1 (CH), 25.1 (2 × CH_3), 24.9 (2 × CH_3), 24.7 (2 × CH_3), 24.6 (2 × CH_3), 21.2 (CH_3), 18.6 (br m, CH_2-B). HRMS (ESI, MeOH) calcd. for $C_{25}H_{38}B_2O_5$ [M+ Na]$^+$: 463.2905; Found: 463.2805.

(*Z*)-2-((4-((4-Methoxyphenyl)(4,4,5,5-tetramethyl-1,3,2-dioxaborolan-2-yl)methylene)tetrahydrofuran-3-yl)methyl)-4,4,5,5-tetramethyl-1,3,2-dioxaborolane

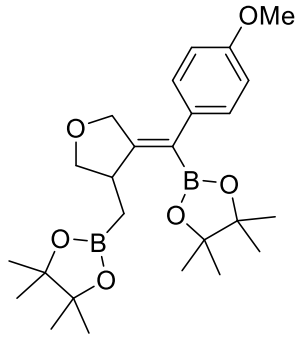

(17ac): The compound was purified by column chromatography (cyclohexane/EtOAc 95:5) and was obtained as a yellow oil in 32% yield (28 mg). ^{1}H NMR (300 MHz, $CDCl_3$) δ 7.02 (d, J = 8.6 Hz, 2H), 6.81 (d, J = 8.6 Hz, 2H), 4.52 (dd, J = 14.9, 1.2 Hz, 1H), 4.05 (d, J = 14.9 Hz, 1H), 3.88 (dd, J = 8.3, 6.0 Hz, 1H), 3.78 (s, 3H), 3.74 (dd, J = 8.6, 2.1 Hz, 1H), 3.48 (dd, J = 7.3, 3.0 Hz, 1H), 1.26 (d, J = 5.2 Hz, 24H), 1.16 (dd, J = 12.4, 6.9 Hz, 2H). ^{13}C NMR (75 MHz, $CDCl_3$) δ 163.4 (C), 157.8 (C), 134.5 (C), 129.4 (2 × CH), 113.5 (2 × CH), 83.3 (2 × C), 83.1 (2 × C), 74.8 (CH_2), 70.7 (CH_2), 55.2 (CH_3), 40.1 (CH), 25.1 (2 × CH_3), 25.0 (2 × CH_3), 24.9 (2 × CH_3), 24.7 (2 × CH_3), 18.6 (br m, CH_2-B). HRMS (ESI, MeOH) calcd. for $C_{25}H_{38}B_2O_6$ [M + Na]$^+$: 479.2854; Found: 479.2764.

(*Z*)-2-((4-((4-Chlorophenyl)(4,4,5,5-tetramethyl-1,3,2-dioxaborolan-2-yl)methylene)tetrahydrofuran-3-yl)methyl)-4,4,5,5-tetramethyl-1,3,2-dioxaborolane

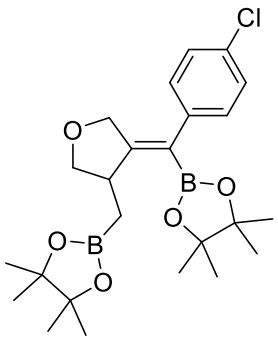

(17ad): The compound was purified by column chromatography (cyclohexane/EtOAc 95:5) and was obtained as a yellow oil in 33% yield (30 mg). ^{1}H NMR (300 MHz, $CDCl_3$) δ 7.23 (d, J = 8.4 Hz, 2H), 7.03 (d, J = 8.4 Hz, 2H), 4.46 (dd, J = 15.1, 1.3 Hz, 1H), 3.99 (d, J = 15.1 Hz, 1H), 3.87 (dd, J = 8.5, 5.8 Hz, 1H), 3.75 (dd, J = 8.5, 2.0 Hz, 1H), 3.55 – 3.44 (m, 1H), 1.25 (d, J = 2.2 Hz, 24H), 1.15 (dd, J = 13.8, 6.7 Hz, 2H). ^{13}C NMR (75 MHz, $CDCl_3$) δ 165.3 (C), 140.6 (C), 131.8 (C), 129.8 (2 × CH), 128.2 (2 × CH), 83.5 (2 × C), 83.2 (2 × C), 74.9 (CH_2), 70.7 (CH_2), 40.2 (CH), 25.1 (2 × CH_3), 25.0 (2 × CH_3), 24.9 (2 × CH_3), 24.7 (2 × CH_3), 18.6 (br m, CH_2-B). HRMS (ESI, MeOH) calcd. for $C_{24}H_{35}B_2ClO_5$ [M + Na]$^+$: 483.2359; Found: 483.2265.

(*Z*)-4,4,5,5-Tetramethyl-2-((4-((4,4,5,5-tetramethyl-1,3,2-dioxaborolan-2-yl)(4-(trifluoromethyl)phenyl)methylene)tetrahydrofuran-3-yl)methyl)-1,3,2-dioxaborolane

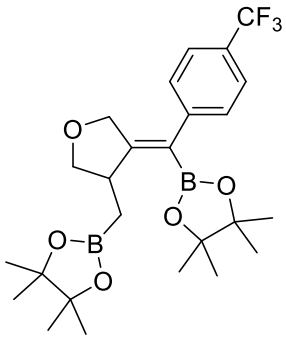

(17af): The compound was purified by column chromatography (cyclohexane/EtOAc 95:5) and was obtained as a colorless oil in 16% yield (16 mg). ^{1}H NMR (300 MHz, $CDCl_3$) δ 7.52 (d, J = 8.1 Hz, 2H), 7.20 (d, J = 8.1 Hz, 2H), 4.46 (dd, J = 15.2, 1.1 Hz, 1H), 3.98 (d, J = 15.2 Hz, 1H), 3.88 (dd, J = 8.5, 5.7 Hz, 1H), 3.77 (dd, J = 8.6, 2.1 Hz, 1H), 3.57 – 3.47 (m, 1H), 1.26 (d, J = 2.6 Hz, 24H), 1.17 (dd, J = 10.0, 2.8 Hz, 2H). ^{13}C NMR (75 MHz, $CDCl_3$) δ 166.3 (C), 146.1 (C), 128.7 (4 × CH), 125.1 (q, J = 3.8 Hz, CF_3), 83.6 (2 × C), 83.2 (2 × C), 75.0 (CH_2), 70.7 (CH_2), 40.3 (CH), 25.1 (2 × CH_3), 25.0 (2 × CH_3), 24.9 (2 × CH_3), 24.7 (2 × CH_3), 18.7 (br m, CH_2-B). ^{19}F NMR (282 MHz, $CDCl_3$) δ – 62.30. HRMS (ESI, MeOH) calcd. for $C_{25}H_{35}B_2F_3O_5$ $[M + Na]^+$: 517.2623; Found: 517.2514.

(*E*)-4,4,5,5-Tetramethyl-2-(phenyl(3-((4,4,5,5-tetramethyl-1,3,2-dioxaborolan-2-yl)methyl)tetrahydro-4*H*-pyran-4-ylidene)methyl)-1,3,2-dioxaborolane (17ah): The

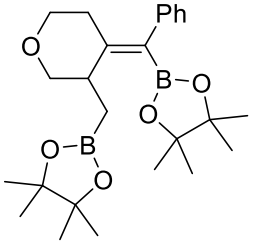

compound was purified by column chromatography (cyclohexane/EtOAc 95:5) and was obtained as a pale yellow oil in 18% yield (16 mg). ^{1}H NMR (300 MHz, $CDCl_3$) δ 7.26 (dd, J = 8.4, 6.2 Hz, 2H), 7.17 (d, J = 7.3 Hz, 1H), 7.11 – 7.04 (m, 2H), 3.89 (dd, J = 10.6, 4.3 Hz, 1H), 3.61 (ddd, J = 11.0, 2.5, 1.4 Hz, 1H), 3.27 (ddd, J = 13.3, 11.0, 2.6 Hz, 1H), 3.14 (d, J = 9.9 Hz, 1H), 2.48 – 2.34 (m, 1H), 2.20 (d, J = 14.2 Hz, 1H), 1.52 (dd, J = 16.0, 10.5 Hz, 1H), 1.25 (d, J = 2.6 Hz, 24H), 1.09 (dd, J = 16.0, 4.7 Hz, 2H). ^{13}C NMR (75 MHz, $CDCl_3$) δ 154.2 (C), 141.5 (C), 129.3 (2 × CH), 128.0 (2 × CH), 125.7 (CH), 83.4 (2 × C), 83.1 (2 × C), 73.6 (CH_2), 69.4 (CH_2), 39.4 (CH), 28.4 (CH_2), 25.1 (2 × CH_3), 25.0 (2 × CH_3), 24.9 (2 × CH_3), 24.7 (2 × CH_3), 19.3 (br m, CH_2-B). HRMS (ESI, MeOH) calcd. for $C_{25}H_{38}B_2O_5$ $[M + Na]^+$: 463.2905; Found: 463.2799.

(*Z*)-4,4,5,5-Tetramethyl-2-((4-(1-(4,4,5,5-tetramethyl-1,3,2-dioxaborolan-2-yl)ethylidene)tetrahydrofuran-3-yl)methyl)-1,3,2-dioxaborolane (17an): The compound

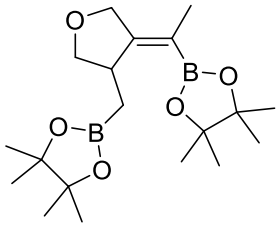

was purified by column chromatography (cyclohexane/EtOAc 95:5) and was obtained as a colorless oil in 39% yield (28 mg). ^{1}H NMR (300 MHz, $CDCl_3$) δ 4.46 (d, J = 14.8 Hz, 1H), 4.19 (d, J = 14.8 Hz, 1H), 3.77 (d, J = 3.0 Hz, 2H), 3.29 (d, J = 10.1 Hz, 1H), 1.57 (s, 3H), 1.24 (dd, J = 5.4, 2.9 Hz, 24H), 1.07 – 0.90 (m, 2H). ^{13}C NMR (75 MHz, $CDCl_3$) δ 163.2 (C), 83.0 (4 × C), 75.4 (CH_2), 70.6 (CH_2), 39.8 (CH), 25.2 (2 × CH_3), 24.9 (2 × CH_3), 24.9 (2 × CH_3), 24.8 (2 × CH_3), 18.4 (br m, CH_2-B), 16.8 (CH_3). HRMS (ESI, MeOH) calcd. for $C_{19}H_{34}B_2O_5$ $[M + Na]^+$: 387.2592; Found: 387.2488.

(Z)-3-(Phenyl(4,4,5,5-tetramethyl-1,3,2-dioxaborolan-2-yl)methylene)-4-((4,4,5,5-tetramethyl-1,3,2-dioxaborolan-2-yl)methyl)-1-tosylpyrrolidine (17bb): The compound

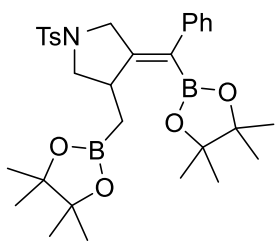

was purified by column chromatography (cyclohexane/EtOAc 9:1) and was obtained as a colorless oil in 63% yield (57 mg). ^{1}H NMR (300 MHz, $CDCl_3$) δ 7.61 (d, J = 7.9 Hz, 2H), 7.35 – 7.20 (m, 4H), 6.98 (d, J = 7.9 Hz, 2H), 4.06 (d, J = 15.7 Hz, 1H), 3.45 (d, J = 15.7 Hz, 2H), 3.52 – 3.43 (m, 1H), 3.30 (d, J = 9.6 Hz, 1H), 3.18 (dd, J = 9.6, 6.2 Hz, 1H), 2.41 (s, 3H), 1.35 – 1.13 (m, 24H), 1.06 (dd, J = 15.1, 6.7 Hz, 2H). ^{13}C NMR (75 MHz, $CDCl_3$) δ 159.2 (C), 143.4 (C),

141.5 (C), 133.0 (C), 129.7 (2 × CH), 128.2 (4 × CH), 128.0 (2 × CH), 126.3 (CH), 83.5 (2 × C), 83.3 (2 × C), 54.4 (CH_2), 51.4 (CH_2), 39.2 (CH), 25.2 (2 × CH_3), 25.0 (2 × CH_3), 24.9 (2 × CH_3), 24.7 (2 × CH_3), 21.6 (CH_3), 19.1 (br m, CH_2-B). HRMS (ESI, MeOH) calcd. for $C_{31}H_{43}B_2NO_6S$ [M + Na]$^+$: 602.2997; Found: 602.2893.

(*Z*)-3-((4,4,5,5-Tetramethyl-1,3,2-dioxaborolan-2-yl)(*p*-tolyl)methylene)-4-((4,4,5,5-tetramethyl-1,3,2-dioxaborolan-2-yl)methyl)-1-tosylpyrrolidine (17bc): The compound was purified by column chromatography (cyclohexane/EtOAc 9:1) and was obtained as a colorless oil in 52% yield (46 mg). ^{1}H NMR (300 MHz, $CDCl_3$) δ 7.61 (d, *J* = 8.0 Hz, 2H), 7.27 (d, *J* = 8.0 Hz, 2H), 7.08 (d, *J* = 7.8 Hz, 2H), 6.88 (d, *J* = 7.9 Hz, 2H), 4.07 (d, *J* = 15.6 Hz, 1H), 3.52 – 3.44 (m, 1H), 3.47 (d, *J* = 15.6 Hz, 1H), 3.29 (d, *J* = 9.5 Hz, 1H), 3.18 (dd, *J* = 9.5, 6.7 Hz, 1H), 2.41 (s, 3H), 2.33 (s, 3H), 1.24 (dd, *J* = 9.0, 6.8 Hz, 24H), 1.11 – 1.00 (m, 2H). ^{13}C NMR (75 MHz, $CDCl_3$) *δ* 158.8 (C), 143.4 (C), 138.4 (C), 135.8 (C), 133.1 (C), 129.6 (2 × CH), 129.0 (2 × CH), 128.1 (2 × CH), 128.0 (2 × CH), 83.5 (2 × C), 83.3 (2 × C), 54.3 (CH_2), 51.4 (CH_2), 39.1 (CH), 25.2 (2 × CH_3), 25.0 (2 × CH_3), 24.9 (2 × CH_3), 24.7 (2 × CH_3), 21.6 (CH_3), 21.3 (CH_3), 19.1 (br m, CH_2-B). HRMS (ESI, MeOH) calcd. for $C_{32}H_{45}B_2NO_6S$ [M + Na]$^+$: 616.3154; Found: 616.3053.

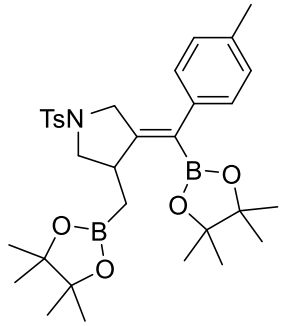

(*Z*)-3-((4-Methoxyphenyl)(4,4,5,5-tetramethyl-1,3,2-dioxaborolan-2-yl)methylene)-4-((4,4,5,5-tetramethyl-1,3,2-dioxaborolan-2-yl)methyl)-1-tosylpyrrolidine (17bd): The compound was purified by column chromatography (cyclohexane/EtOAc 9:1) and was obtained as a pale brown oil in 93% yield (114 mg). ^{1}H NMR (300 MHz, $CDCl_3$) *δ* 7.61 (d, *J* = 8.0 Hz, 2H), 7.26 (d, *J* = 8.0 Hz, 2H), 6.93 (d, *J* = 8.6 Hz, 2H), 6.81 (d, *J* = 8.6 Hz, 2H), 4.09 (d, *J* = 15.6 Hz, 1H), 3.79 (s, 3H), 3.52 – 3.44 (m, 1H), 3.48 (d, *J* = 15.6 Hz, 1H), 3.29 (d, *J* = 9.4 Hz, 1H), 3.17 (dd, *J* = 9.4, 6.7 Hz, 1H), 2.39 (s, 3H), 1.28 – 1.18 (m, 24H), 1.05 (dd, *J* = 14.9, 6.8 Hz, 2H). ^{13}C NMR (75 MHz, $CDCl_3$) *δ* 158.4 (C), 158.0 (C), 143.4 (C), 133.6 (C), 133.0 (C), 129.6 (2 × CH), 129.3 (2 × CH), 127.8 (2 × CH), 113.6 (2 × CH), 83.4 (2 × C), 83.2 (2 × C), 55.2 (CH_3), 54.2 (CH_2), 51.3 (CH_2), 39.0 (CH), 25.0 (2 × CH_3), 24.9 (2 × CH_3), 24.8 (2 × CH_3), 24.6 (2 × CH_3), 21.5 (CH_3), 19.1 (br m, CH_2-B). HRMS (ESI, MeOH) calcd. for $C_{32}H_{45}B_2NO_7S$ [M + Na]$^+$: 632.3103; Found: 632.3023.

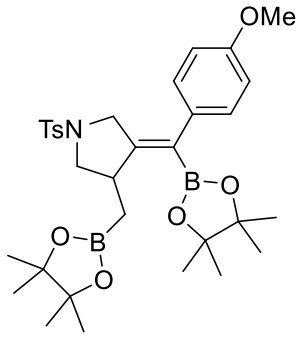

(*Z*)-3-((4-Chlorophenyl)(4,4,5,5-tetramethyl-1,3,2-dioxaborolan-2-yl)methylene)-4-((4,4,5,5-tetramethyl-1,3,2-dioxaborolan-2-yl)methyl)-1-tosylpyrrolidine (17be): The compound was purified by column chromatography (cyclohexane/EtOAc 9:1) and was obtained as a colorless oil in 54% yield (75 mg). ^{1}H NMR (300 MHz, $CDCl_3$) *δ* 7.63 (d, *J* = 8.2 Hz, 2H), 7.30 (d, *J* = 9.1 Hz, 3H), 7.27 (d, *J* = 9.1 Hz, 3H), 6.95 (d, *J* = 8.2 Hz, 2H), 4.05 (d, *J* = 15.8 Hz, 1H), 3.55 – 3.47 (m, 1H), 3.41 (d, *J* = 15.8 Hz, 1H), 3.32 (dd, *J* = 9.6, 1.8 Hz, 1H), 3.24 – 3.11 (m, 1H), 2.44 (s, 3H), 1.26 (dd, *J* = 9.7, 7.0 Hz, 24H), 1.12 – 1.07 (m, 2H). ^{13}C NMR (75 MHz, $CDCl_3$) *δ* 160.4 (C), 143.5 (C), 140.0 (C), 132.9 (C), 132.2 (C), 129.7 (2 × CH), 129.6 (2 × CH), 128.5 (2 × CH), 128.0 (2 × CH), 83.7 (2 × C), 83.3 (2 × CH), 54.4 (CH_2), 51.4 (CH_2), 39.2 (CH), 25.2 (2 × CH_3), 25.1 (2 × CH_3), 25.0 (2 × CH_3), 24.7 (2 × CH_3), 21.6 (CH_3), 19.4 (br m, CH_2-B). HRMS (ESI, MeOH) calcd. for $C_{31}H_{42}B_2ClNO_6S$ [M + Na]$^+$: 636.2607; Found: 636.2513.

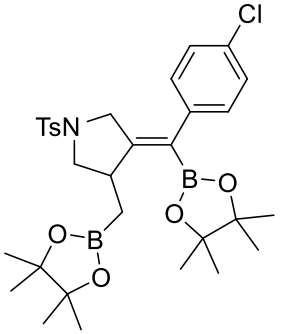

(*Z*)-3-((4,4,5,5-Tetramethyl-1,3,2-dioxaborolan-2-yl)(4-(trifluoromethyl)phenyl)methylene)-4-((4,4,5,5-tetramethyl-1,3,2-dioxaborolan-2-yl)methyl)-1-tosylpyrrolidine (17bg): 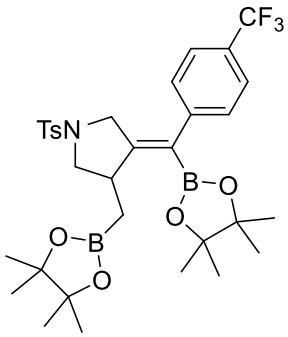 The compound was purified by column chromatography (cyclohexane/EtOAc 9:1) and was obtained as a light brown oil in 61% yield (70 mg). ^{1}H NMR (300 MHz, $CDCl_3$) δ 7.61 (d, J = 8.2 Hz, 2H), 7.53 (d, J = 8.0 Hz, 2H), 7.28 (d, J = 8.2 Hz, 3H), 7.10 (d, J = 8.0 Hz, 2H), 4.02 (d, J = 15.8 Hz, 1H), 3.60 – 3.47 (m, 1H), 3.38 (d, J = 15.8 Hz, 1H), 3.31 (d, J = 9.5 Hz, 1H), 3.18 (dd, J = 9.5, 6.7 Hz, 1H), 2.41 (s, 3H), 1.24 (dd, J = 9.0, 5.8 Hz, 24H), 1.15 – 1.04 (m, 2H). ^{13}C NMR (75 MHz, $CDCl_3$) δ 161.2 (C), 145.4 (C), 143.6 (C), 132.8 (C), 130.0 (C), 129.7 (2 × CH), 128.6 (2 × CH), 128.0 (2 × CH), 125.3 (q, J = 3.8 Hz, CF_3), 83.8 (2 × C), 83.4 (2 × C), 54.4 (CH_2), 51.4 (CH_2), 39.3 (CH), 25.2 (2 × CH_3), 25.0 (2 × CH_3), 24.9 (2 × CH_3), 24.6 (2 × CH_3), 21.6 (CH_3), 19.3 (br m, CH_2-B). ^{19}F NMR (282 MHz, $CDCl_3$) δ – 62.32. HRMS (ESI, MeOH) calcd. for $C_{32}H_{42}B_2F_3NO_6S$ [M + Na]$^+$: 670.2871; Found: 670.2758.

(*Z*)-1-Phenyl-3-(phenyl(4,4,5,5-tetramethyl-1,3,2-dioxaborolan-2-yl)methylene)-4-((4,4,5,5-tetramethyl-1,3,2-dioxaborolan-2-yl)methyl)pyrrolidine (17bm): The compound was purified by column chromatography (cyclohexane/EtOAc 9:1) and was obtained as a brown oil in 27% yield (27 mg). ^{1}H NMR (300 MHz, $CDCl_3$) δ 7.36 – 7.29 (m, 2H), 7.21 – 7.14 (m, 4H), 6.65 (t, J = 7.3 Hz, 1H), 6.52 (d, J = 7.8 Hz, 2H), 4.25 (d, J = 16.0 Hz, 1H), 3.84 – 3.72 (m, 1H), 3.54 (d, J = 16.0 Hz, 1H), 3.36 (qd, J = 9.3, 4.0 Hz, 2H), 1.29 (s, 12H), 1.27 (d, J = 1.7 Hz, 2H), 1.24 (d, J = 2.0 Hz, 12H). ^{13}C NMR (75 MHz, $CDCl_3$) δ 162.1 (C), 148.4 (C), 142.3 (C), 129.1 (2 × CH), 128.5 (2 × CH), 128.1 (2 × CH), 126.0 (CH), 116.2 (CH), 112.3 (2 × CH), 83.4 (2 × C), 83.1 (2 × CH), 54.3 (CH_2), 52.2 (CH_2), 39.2 (CH), 25.2 (2 × CH_3), 25.0 (2 × CH_3), 24.9 (2 × CH_3), 24.7 (2 × CH_3), 19.6 (br m, CH_2-B). HRMS (ESI, MeOH) calcd. for $C_{30}H_{41}B_2NO_4$ [M + H]$^+$: 502.3222; Found: 502.3287.

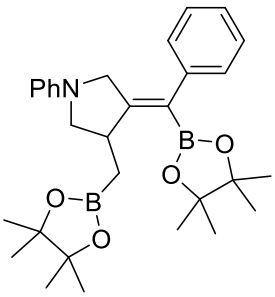

(*Z*)-3-(1-(4,4,5,5-Tetramethyl-1,3,2-dioxaborolan-2-yl)ethylidene)-4-((4,4,5,5-tetramethyl-1,3,2-dioxaborolan-2-yl)methyl)-1-tosylpyrrolidine (17bn): The compound was purified by column chromatography (cyclohexane/EtOAc 95:5) and was obtained as a colorless oil in 78% yield (81 mg). ^{1}H NMR (300 MHz, $CDCl_3$) δ 7.68 (d, J = 8.0 Hz, 2H), 7.29 (d, J = 8.0 Hz, 2H), 4.00 (d, J = 15.5 Hz, 1H), 3.49 (d, J = 15.5 Hz, 1H), 3.34 (d, J = 9.1 Hz, 1H), 3.29 – 3.24 (m, 1H), 2.39 (s, 3H), 1.53 (s, 3H), 1.21 (s, 12H), 1.18 (d, J = 1.7 Hz, 12H), 1.05 (dd, J = 16.3, 11.8 Hz, 1H), 0.85 (d, J = 15.5 Hz, 1H). ^{13}C NMR (75 MHz, $CDCl_3$) δ 158.6 (C), 143.4 (C), 132.5 (C), 129.6 (2 × CH), 128.0 (2 × CH), 83.1 (2 × C), 83.0 (2 × C), 54.8 (CH_2), 51.1 (CH_2), 38.8 (CH), 25.0 (2 × CH_3), 24.9 (2 × CH_3), 24.8 (2 × CH_3), 24.7 (2 × CH_3), 21.5 (CH_3), 19.4 (br m, CH_2-B), 16.9 (CH_3). HRMS (ESI, MeOH) calcd. for $C_{26}H_{41}B_2NO_6S$ [M + Na]$^+$: 540.2841; Found: 540.2751.

(*Z*)-3-((4,4,5,5-Tetramethyl-1,3,2-dioxaborolan-2-yl)methyl)-4-(1-(4,4,5,5-tetramethyl-1,3,2-dioxaborolan-2-yl)propylidene)-1-tosylpyrrolidine (17bo): The compound was purified by column chromatography (cyclohexane/EtOAc 9:1) and was obtained as a colorless oil in 63% yield (67 mg). ^{1}H NMR (300 MHz, $CDCl_3$) δ 7.69 (d, J = 8.1 Hz, 2H), 7.29 (d, J = 8.1 Hz, 2H), 4.05 (d, J = 15.2 Hz, 1H), 3.57 (d, J = 15.2 Hz, 1H), 3.32 (d, J = 9.1 Hz, 2H), 3.05 – 2.89 (m, 1H), 2.40 (s, 3H), 1.91 (q, J = 7.3 Hz, 2H), 1.21 (d, J = 6.0 Hz, 24H), 1.05 (dd, J = 16.2, 11.7 Hz, 2H), 0.85 (t, J = 7.5 Hz, 3H). ^{13}C NMR (75 MHz, $CDCl_3$) δ 157.0 (C), 143.5 (C), 132.3 (C), 129.6 (2 × CH), 128.1 (2 × CH), 83.1 (2 × C), 83.0 (2 × C), 54.6 (CH_2), 50.3 (CH_2), 38.8 (CH), 25.3 (CH_2), 25.0 (4 × CH_3), 24.9 (2 × CH_3), 24.7 (2 × CH_3), 21.6 (CH_3), 19.5 (br m, CH_2-B), 13.9 (CH_3). HRMS (ESI, MeOH) calcd. for $C_{27}H_{43}B_2NO_6S$ [M + Na]$^+$: 554.2997; Found: 554.2884.

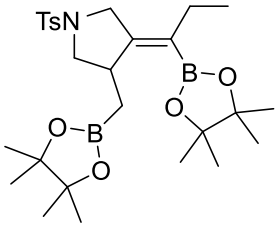

(*Z*)-3-(1-(4,4,5,5-Tetramethyl-1,3,2-dioxaborolan-2-yl)butylidene)-4-((4,4,5,5-tetramethyl-1,3,2-dioxaborolan-2-yl)methyl)-1-tosylpyrrolidine (17bp): The compound was purified by column chromatography (cyclohexane/EtOAc 9:1) and was obtained as a colorless oil in 76% yield (83 mg). ^{1}H NMR (300 MHz, $CDCl_3$) δ 7.69 (d, J = 8.2 Hz, 2H), 7.29 (d, J = 8.2 Hz, 2H), 4.05 (d, J = 15.2 Hz, 1H), 3.57 (d, J = 15.2 Hz, 1H), 3.31 (t, J = 9.8 Hz, 1H), 2.98 (dd, J = 8.6, 6.7 Hz, 1H), 2.40 (s, 3H), 1.98 – 1.78 (m, 2H), 1.27 (dd, J = 12.8, 5.3 Hz, 2H), 1.20 (d, J = 9.2 Hz, 24H), 1.05 (dd, J = 16.4, 11.7 Hz, 2H), 0.80 (t, J = 7.3 Hz, 3H). ^{13}C NMR (75 MHz, $CDCl_3$) δ 157.5 (C), 143.5 (C), 132.6 (C), 129.6 (2 × CH), 128.0 (2 × CH), 83.1 (2 × C), 83.0 (2 × C), 54.6 (CH_2), 50.5 (CH_2), 38.9 (CH), 34.1 (CH_2), 25.0 (2 × CH_3), 24.9 (4 × CH_3), 24.7 (2 × CH_3), 22.6 (CH_2), 21.6 (CH_3), 19.6 (br m, CH_2-B), 14.0 (CH_3). HRMS (ESI, MeOH) calcd. for $C_{28}H_{45}B_2NO_6S$ [M + Na]$^+$: 568.3154; Found: 568.3040.

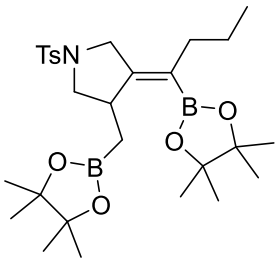

(*Z*)-3-(1-(4,4,5,5-Tetramethyl-1,3,2-dioxaborolan-2-yl)heptylidene)-4-((4,4,5,5-tetramethyl-1,3,2-dioxaborolan-2-yl)methyl)-1-tosylpyrrolidine (17br): The compound was purified by column chromatography (cyclohexane/EtOAc 9:1) and was obtained as a colorless oil in 73% yield (85 mg). ^{1}H NMR (300 MHz, $CDCl_3$) δ 7.69 (d, J = 8.1 Hz, 2H), 7.29 (d, J = 8.1 Hz, 2H), 4.05 (d, J = 15.2 Hz, 1H), 3.57 (d, J = 15.2 Hz, 1H), 3.33 (d, J = 9.2 Hz, 2H), 3.04 – 2.94 (dd, J = 8.7, 6.6 Hz, 1H), 2.40 (s, 3H), 1.97 – 1.85 (m, 2H), 1.31 – 1.24 (m, 8H), 1.20 (d, J = 8.2 Hz, 24H), 1.05 (dd, J = 16.2, 11.7 Hz, 2H), 0.86 (t, J = 6.6 Hz, 3H). ^{13}C NMR (75 MHz, $CDCl_3$) δ 157.1 (C), 143.4 (C), 132.6 (C), 129.6 (2 × CH), 128.0 (2 × CH), 83.1 (2 × C), 83.0 (2 × C), 54.6 (CH_2), 50.5 (CH_2), 38.9 (CH), 32.1 (CH_2), 31.9 (CH_2), 29.4 (CH_2), 29.2 (CH_2), 25.0 (2 × CH_3), 24.9 (2 × CH_3), 24.8 (2 × CH_3), 24.7 (2 × CH_3), 22.6 (CH_2), 21.6 (CH_3), 19.6 (br m, CH_2-B), 14.2 (CH_3). HRMS (ESI, MeOH) calcd. for $C_{31}H_{51}B_2NO_6S$ [M]$^+$: 610.3623; Found: 610.3522.

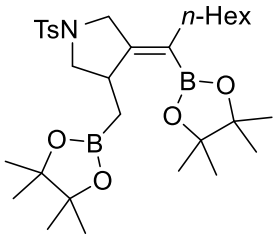

(*Z*)-3-(Cyclopentyl(4,4,5,5-tetramethyl-1,3,2-dioxaborolan-2-yl)methylene)-4-((4,4,5,5-tetramethyl-1,3,2-dioxaborolan-2-yl)methyl)-1-tosylpyrrolidine (17bt): The compound

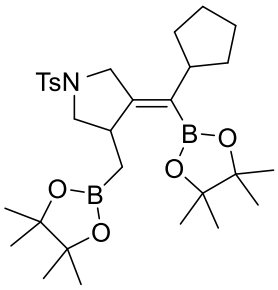

was purified by column chromatography (cyclohexane/EtOAc 9:1) and was obtained as a colorless oil in 74% yield (42 mg). ^{1}H NMR (300 MHz, $CDCl_3$) δ 7.69 (d, J = 8.1 Hz, 2H), 7.29 (d, J = 8.1 Hz, 2H), 4.06 (d, J = 14.8 Hz, 1H), 3.59 (d, J = 14.8 Hz, 1H), 3.30 (d, J = 9.2 Hz, 1H), 3.21 – 3.08 (m, 1H), 2.98 (dd, J = 8.4, 6.7 Hz, 1H), 2.41 (s, 3H), 2.35 – 2.18 (m, 1H), 1.71 – 1.55 (m, 4H), 1.55 – 1.40 (m, 4H), 1.21 (s, 24H), 1.04 (dd, J = 18.2, 6.3 Hz, 1H), 0.87 (d, J = 15.8 Hz, 1H). ^{13}C NMR (75 MHz, $CDCl_3$) δ 153.1 (C), 143.5 (C), 132.7 (C), 129.6 (2 × CH), 128.1 (2 × CH), 83.1 (2 × C), 83.0 (2 × C), 54.5 (CH_2), 50.4 (CH_2), 43.8 (CH), 38.9 (CH), 32.2 (CH_2), 31.9 (CH_2), 26.0 (CH_2), 25.8 (CH_2), 25.1 (2 × CH_3), 25.0 (2 × CH_3), 24.9 (2 × CH_3), 24.8 (2 × CH_3), 22.5 (CH_3), 21.6 (br m, CH_2-B). HRMS (ESI, MeOH) calcd. for $C_{30}H_{47}B_2NO_6S$ [M + Na]$^+$: 594.3310; Found: 594.3209.

(*Z*)-3-((4,4,5,5-Tetramethyl-1,3,2-dioxaborolan-2-yl)(trimethylsilyl)methylene)-4-((4,4,5,5-tetramethyl-1,3,2-dioxaborolan-2-yl)methyl)-1-tosylpyrrolidine (17bu): The

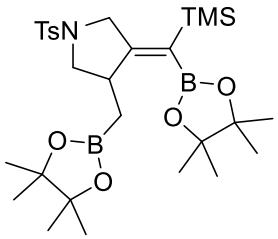

compound was purified by column chromatography (cyclohexane/EtOAc 9:1) and was obtained as a pale brown oil in 84% yield (97 mg). ^{1}H NMR (300 MHz, $CDCl_3$) δ 7.65 (d, J = 8.1 Hz, 2H), 7.29 (d, J = 8.1 Hz, 2H), 4.02 (d, J = 15.1 Hz, 1H), 3.50 (d, J = 15.1 Hz, 1H), 3.27 (d, J = 8.2 Hz, 1H), 3.04 – 2.87 (m, 2H), 2.40 (s, 3H), 1.20 (d, J = 5.2 Hz, 24H), 1.14 – 0.91 (m, 2H), 0.06 (s, 9H). ^{13}C NMR (75 MHz, $CDCl_3$) δ 166.9 (C), 143.6 (C), 132.1 (C), 129.6 (2 × CH), 128.0 (2 × CH), 83.3 (2 × C), 83.2 (2 × CH), 53.8 (CH_2), 52.3 (CH_2), 42.2 (CH), 25.1 (2 × CH_3), 25.0 (2 × CH_3), 24.9 (2 × CH_3), 24.8 (2 × CH_3), 21.5 (CH_3), 19.2 (br m, CH_2-B), 0.2 (3 × CH_3). HRMS (ESI, MeOH) calcd. for $C_{28}H_{47}B_2NO_6SSi$ [M + Na]$^+$: 598.3079; Found: 598.2983.

(*Z*)-2-Methyl-4-((4,4,5,5-tetramethyl-1,3,2-dioxaborolan-2-yl)methyl)-3-(1-(4,4,5,5-tetramethyl-1,3,2-dioxaborolan-2-yl)nonylidene)-1-tosylpyrrolidine (17bv): The

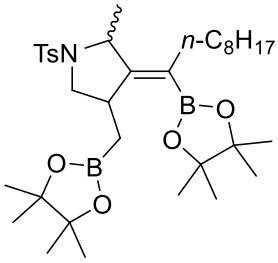

compound was purified by column chromatography (cyclohexane/EtOAc 9:1) and a mixture of two diastereomers (1:1.7, **diast1**:**diast2**) was obtained as a colorless oil in 85% yield (96 mg). ^{1}H NMR (300 MHz, $CDCl_3$) δ 7.69 (d, J = 8.5 Hz, 2H **diast2**), 7.67 (d, J = 8.3 Hz, 2H **diast1**), 7.25 (d, J = 8.5 Hz, 2H **diast2**), 7.22 (d, J = 8.3 Hz, 2H **diast1**), 4.67 (q, J = 6.2 Hz, 1H **diast1**), 4.09 (q, J = 6.4 Hz, 1H **diast2**), 3.49 (dd, J = 10.8, 6.2 Hz, 1H **diast1**), 3.33 (d, J = 9.4 Hz, 1H **diast2**), 3.21 (dd, J = 11.5, 5.7 Hz, 2H **diast1** + 1H **diast2**), 3.04 (dd, J = 8.2, 7.9 Hz, 1H **diast2**), 2.38 (s, 3H **diast2**), 2.37 (s, 3H **diast1**), 2.06 – 1.86 (m, 2H **diast1** + 2H **diast2**), 1.49 (d, J = 6.5 Hz, 3H **diast2**), 1.32 – 1.25 (m, 3H **diast1**), 1.22 – 1.15 (m, 36H **diast1** + 36H **diast2**), 0.97 (d, J = 15.8 Hz, 2H **diast2**), 0.86 (t, J = 6.6 Hz, 3H **diast1** + 3H **diast2**), 0.68 (d, J = 16.4 Hz, 1H **diast1**), 0.34 (dd, J = 16.4, 12.9 Hz, 1H **diast1**). ^{13}C NMR (75 MHz, $CDCl_3$) δ 162.1 (C **diast1**), 160.5 (C **diast2**), 143.2 (C **diast2**), 142.9 (C **diast1**), 137.7 (C **diast1**), 133.5 (C **diast2**), 129.6 (2 × CH **diast1**), 129.5 (2 × CH **diast2**), 128.0 (2 × CH **diast2**), 127.2 (2 × CH **diast1**), 83.2 (2 × C **diast2**), 83.1 (2 × C **diast1** + 2 × C **diast2**), 83.0 (2 × C **diast1**), 58.1 (CH **diast1**), 58.0 (CH **diast2**), 55.0 (CH_2 **diast2**), 51.8 (CH_2 **diast1**), 38.9 (CH **diast1**), 38.2 (CH **diast2**), 32.9 (CH_2 **diast1**), 32.0 (CH_2 **diast2**), 31.5 (CH_2 **diast1**), 30.1 (CH_2 **diast1**), 29.9 (CH_2 **diast2**), 29.8 (2 × CH_2 **diast1**), 29.6 (3 × CH_2 **diast2**), 29.5 (CH_2 **diast1**), 29.3 (CH_2 **diast1**), 29.2 (CH_2 **diast2**), 25.1 (2 × CH_3 **diast1**), 24.9 (2 × CH_3 **diast2**), 24.8 (2 × CH_3 **diast1**), 24.7 (2 × CH_3 **diast2**), 24.1 (CH_3

diast1), 22.8 (CH_2 **diast2**), 21.6 (CH_3 **diast2**), 21.1 (CH_3 **diast2**), 20.0 (br m, CH_2-B **diast1**), 18.0 (br m, CH_2-B **diast2**), 14.2 (CH_3 **diast2**). HRMS (ESI, MeOH) calcd. for $C_{34}H_{57}B_2NO_6S$ $[M + Na]^+$: 652.4093; Found: 652.4000.

(*Z*)-1-Phenyl-3-(1-(4,4,5,5-tetramethyl-1,3,2-dioxaborolan-2-yl)ethylidene)-4-((4,4,5,5-tetramethyl-1,3,2-dioxaborolan-2-yl)methyl)pyrrolidine (17bw): The compound was

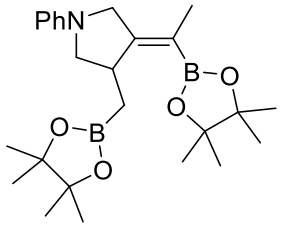

purified by column chromatography (cyclohexane/EtOAc 95:5) and was obtained as a brown solid in 74% yield (65 mg). M. p. = 109 – 111 °C. ^{1}H NMR (300 MHz, $CDCl_3$) δ 7.27 (t, J = 7.9 Hz, 3H), 6.78 – 6.61 (m, 4H), 4.19 (d, J = 15.9 Hz, 1H), 3.74 (d, J = 15.9 Hz, 1H), 3.68 – 3.59 (m, 1H), 3.42 (d, J = 9.2 Hz, 1H), 3.30 (dd, J = 9.1, 6.4 Hz, 1H), 1.75 (s, 3H), 1.31 (d, J = 3.5 Hz, 12H), 1.24 (d, J = 3.0 Hz, 12H), 1.18 – 1.09 (m, 2H). ^{13}C NMR (75 MHz, $CDCl_3$) δ 161.6 (C), 148.8 (C), 129.1 (2 × CH), 116.3 (CH), 112.6 (2 × CH), 83.0 (2 × C), 82.9 (2 × C), 54.8 (CH_2), 52.4 (CH_2), 38.8 (CH), 25.2 (2 × CH_3), 25.0 (2 × CH_3), 24.9 (2 × CH_3), 24.8 (2 × CH_3), 19.9 (br m, CH_2-B), 17.0 (CH_3). HRMS (ESI, MeOH) calcd. for $C_{25}H_{39}B_2NO_4$ $[M + H]^+$: 440.3065; Found: 440.3132.

(*Z*)-henyl(3-(1-(4,4,5,5-tetramethyl-1,3,2-dioxaborolan-2-yl)ethylidene)-4-((4,4,5,5-tetramethyl-1,3,2-dioxaborolan-2-yl)methyl)pyrrolidin-1-yl)methanone (17bx): The

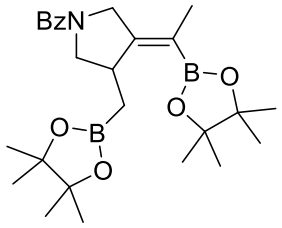

compound was purified by column chromatography (cyclohexane/EtOAc 9:1) and was obtained as a white solid in 53% yield (49 mg). M. p. = 153 – 155 °C. ^{1}H NMR (300 MHz, $CDCl_3$) δ 7.49 – 7.39 (m, 3H), 7.38 – 7.27 (m, 2H), 4.52 (d, J = 18.5 Hz, 1H), 4.05 (dd, J = 18.5, 12.1 Hz, 2H), 3.61 – 3.35 (m, 4H), 1.66 (s, 3H), 1.22 (s, 12H), 1.07 (d, J = 11.1 Hz, 12H), 0.97 – 0.89 (m, 2H). ^{13}C NMR (75 MHz, $CDCl_3$) δ 170.1 (C), 158.4 (C), 136.9 (C), 129.6 (CH), 128.2 (2 × CH), 127.3 (2 × CH), 83.0 (2 × C), 82.9 (2 × CH), 55.9 (CH_2), 49.0 (CH_2), 39.3 (CH), 25.1 (2 × CH_3), 24.9 (2 × CH_3), 24.7 (2 × CH_3), 24.6 (2 × CH_3), 18.9 (CH_3), 16.8 (br m, CH_2-B). HRMS (ESI, MeOH) calcd. for $C_{26}H_{39}B_2NO_5$ $[M + Na]^+$: 490.3014; Found: 490.2917.

(*Z*)-2-Phenyl-3-(1-(4,4,5,5-tetramethyl-1,3,2-dioxaborolan-2-yl)ethylidene)-4-((4,4,5,5-tetramethyl-1,3,2-dioxaborolan-2-yl)methyl)-1-tosylpyrrolidine (17by): The compound

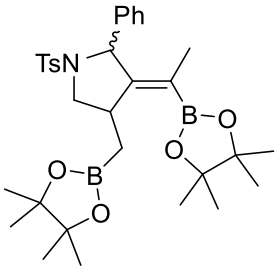

was purified by column chromatography (cyclohexane/EtOAc 9:1) and a mixture of two diastereomers (1:3.7, **diast1**:**diast2**) was obtained as a pale yellow oil in 98% yield (120 mg). M. p. = 179 – 181 °C. ^{1}H NMR (300 MHz, $CDCl_3$) δ 7.64 (d, J = 8.3 Hz, 2H **diast2**), 7.44 (d, J = 6.7 Hz, 2H **diast2**), 7.31 – 7.19 (m, 5H **diast1** + 5H **diast2**), 7.23 – 7.11 (m, 2H **diast1**), 7.01 (d, J = 8.3 Hz, 2H **diast1**), 5.59 (s, 1H **diast1**), 5.33 (s, 1H **diast2**), 3.80 (dd, J = 11.2, 7.6 Hz, 1H **diast2**), 3.74 (d, J = 3.6 Hz, 1H **diast1**), 3.62 – 3.53 (m, 1H **diast1**), 3.20 (d, J = 7.0 Hz, 1H **diast2**), 3.10 (dd, J = 11.3, 4.8 Hz, 1H **diast1** + 1H **diast2**), 2.39 (s, 3H **diast2**), 2.31 (s, 3H **diast1**), 1.47 (s, 3H **diast2**), 1.27 (s, 3H **diast1**), 1.21 (d, J = 4.5 Hz, 24H **diast1** + 24H **diast2**), 0.97 – 0.86 (m, 2H **diast1** + 2H **diast2**). ^{13}C NMR (75 MHz, $CDCl_3$) δ 163.4 (C **diast1**), 160.6 (C **diast2**), 143.1 (C **diast2**), 142.2 (C **diast1**), 140.7 (C **diast1**), 138.9 (C **diast2**), 137.3 (C **diast1**), 135.4 (C **diast2**), 129.4 (2 × CH **diast2**), 129.1 (2 × CH **diast1**), 128.8 (2 × CH **diast1**), 128.4 (2 × CH **diast2**), 128.2 (2 × CH **diast2**), 127.7 (2 × CH **diast2**), 127.3 (2 × CH **diast1** + **diast2**), 127.2 (2 × CH **diast1**), 126.8 (2 × CH **diast1**), 83.2 (2 × C **diast2**), 83.1 (2 × C **diast1** + 2 × C **diast2**), 83.0 (2 × C **diast1**), 66.5 (CH **diast1**), 66.2 (CH **diast2**), 54.8 (CH_2 **diast2**), 53.7 (CH_2 **diast1**), 39.6 (CH **diast1**), 38.1 (CH **diast2**), 25.1 (2 × CH_3 **diast1**), 25.0 (2 × CH_3 **diast1** + 2 × CH_3 **diast2**), 24.9 (2 × CH_3 **diast2**), 24.8

(2 × CH_3 **diast1** + 4 × CH_3 **diast2**), 24.7 (2 × CH_3 **diast1**), 21.6 (CH_3 **diast2**), 21.4 (CH_3 **diast1**), 20.4 (br m, CH_2-B **diast1** + CH_2-B **diast2**), 17.9 (CH_3 **diast2**), 17.8 (CH_3 **diast1**). HRMS (ESI, MeOH) calcd. for $C_{32}H_{45}B_2NO_6S$ [M + Na]$^+$: 616.3154; Found: 616.3040.

(*Z*)-2-Methyl-4-(1-(4,4,5,5-tetramethyl-1,3,2-dioxaborolan-2-yl)ethylidene)-3-((4,4,5,5-tetramethyl-1,3,2-dioxaborolan-2-yl)methyl)-1-tosylpyrrolidine (17bz): The compound was purified by column chromatography (cyclohexane/EtOAc 9:1) and a mixture of two diastereomers (1:1.2, **diast1**:**diast2**) was obtained as a colorless oil in 90% yield (96 mg). ^{1}H NMR (300 MHz, $CDCl_3$) δ 7.72 (d, *J* = 7.9 Hz, 2H **diast2**), 7.65 (d, *J* = 7.9 Hz, 2H **diast1**), 7.29 (d, *J* = 7.9 Hz, 2H **diast2**), 7.23 (d, *J* = 7.9 Hz, 2H **diast1**), 4.13 (d, *J* = 16.2 Hz, 1H **diast2**), 4.07 (d, *J* = 15.6 Hz, 1H **diast1**), 3.84 (d, *J* = 15.6 Hz, 1H **diast1**), 3.72 (q, *J* = 6.9 Hz, 1H **diast1**), 3.57 (d, *J* = 16.2 Hz, 1H **diast2**), 3.29 – 3.21 (m, 1H **diast2**), 3.09 (p, *J* = 5.9 Hz, 1H **diast2**), 2.95 (d, *J* = 12.5 Hz, 1H **diast1**), 2.39 (s, 3H **diast2**), 2.38 (s, 3H **diast1**), 1.58 (s, 3H **diast1**), 1.52 (s, 3H **diast2**), 1.40 (s, 3H **diast2**), 1.38 (s, 3H **diast1**), 1.24 – 1.17 (m, 48H **diast1** + **diast2**), 1.09 (dd, *J* = 16.0, 10.4 Hz, 1H **diast2**), 0.81 (d, *J* = 16.0 Hz, 1H **diast2**), 0.54 (d, *J* = 16.1 Hz, 1H **diast1**), 0.11 (d, *J* = 13.4 Hz, 1H **diast1**). ^{13}C NMR (75 MHz, $CDCl_3$) δ 158.3 (C **diast1**), 156.5 (C **diast2**), 143.4 (C **diast2**), 143.1 (C **diast1**), 136.3 (C **diast1**), 132.9 (C **diast2**), 129.6 (2 × CH **diast1** + 2 × CH **diast2**), 128.0 (2 × CH **diast2**), 127.3 (2 × CH **diast1**), 83.1 (2 × C **diast2**), 83.0 (2 × C **diast1** + 2 × C **diast2**), 82.9 (2 × C **diast1**), 63.2 (CH **diast1**), 60.1 (CH **diast2**), 53.2 (CH_2 **diast2**), 49.5 (CH_2 **diast1**), 46.7 (CH **diast1**), 44.3 (CH **diast2**), 25.2 (2 × CH_3 **diast1** + 2 × CH_3 **diast2**), 25.1 (2 × CH_3 **diast2**), 25.0 (2 × CH_3 **diast1**), 24.9 (2 × CH_3 **diast2**), 24.8 (2 × CH_3 **diast1**), 24.7 (2 × CH_3 **diast1**), 24.6 (2 × CH_3 **diast2**), 22.4 (CH_3 **diast1**), 21.6 (CH_3 **diast2**), 18.9 (br m, CH_2-B **diast1**), 16.9 (CH_3 **diast1**), 16.6 (CH_3 **diast2**), 16.5 (CH_3 **diast1** + CH_3 **diast2**), 15.0 (br m, CH_2-B **diast2**). HRMS (ESI, MeOH) calcd. for $C_{27}H_{43}B_2NO_6S$ [M + Na]$^+$: 554.2997; Found: 554.2903.

Dimethyl (*Z*)-3-((4,4,5,5-tetramethyl-1,3,2-dioxaborolan-2-yl)methyl)-4-((4,4,5,5-tetramethyl-1,3,2-dioxaborolan-2-yl)methylene)cyclopentane-1,1-dicarboxylate (17ca): The compound was purified by column chromatography (cyclohexane/EtOAc 9:1) and was obtained as a colorless oil in 28% yield (26 mg). ^{1}H NMR (300 MHz, $CDCl_3$) δ 5.22 (s, 1H), 3.72 (s, 3H), 3.69 (s, 3H), 3.25 (dt, *J* = 16.5, 2.2 Hz, 1H), 3.22 – 3.14 (m, 1H), 2.86 (d, *J* = 16.5 Hz, 1H), 2.71 (dd, *J* = 13.4, 8.3 Hz, 1H), 2.01 (dd, *J* = 13.4, 6.6 Hz, 1H), 1.23 (s, 24H), 0.99 (dd, *J* = 16.2, 11.2 Hz, 1H). ^{13}C NMR (75 MHz, $CDCl_3$) δ 172.6 (C), 172.1 (C), 83.0 (2 × C), 82.9 (2 × C), 59.0 (C), 52.8 (CH_3), 52.7 (CH_3), 44.6 (CH_2), 41.6 (CH_2), 38.1 (CH), 25.2 (2 × CH_3), 25.1 (2 × CH_3), 24.9 (2 × CH_3), 24.8 (2 × CH_3), 19.8 (br m, CH_2-B). HRMS (ESI, MeOH) calcd. for $C_{23}H_{38}B_2O_8$ [M + Na]$^+$: 487.2753; Found: 487.2635.

Dimethyl (*E*)-3-(1-(4,4,5,5-tetramethyl-1,3,2-dioxaborolan-2-yl)ethylidene)-4-((4,4,5,5-tetramethyl-1,3,2-dioxaborolan-2-yl)methyl)cyclopentane-1,1-dicarboxylate (17cb): The compound was purified by column chromatography (cyclohexane/EtOAc 9:1) and was obtained as a white solid in 96% yield (92 mg). M. p. = 115 – 117 °C. ^{1}H NMR (300 MHz, $CDCl_3$) δ 3.71 (s, 3H), 3.67 (s, 3H), 3.36 – 3.23 (m, 1H), 3.10 (d, *J* = 17.7 Hz, 1H), 2.87 (d, *J* = 17.7 Hz, 1H), 2.55 (dd, *J* = 13.5, 8.3 Hz, 1H), 2.16 (dd, *J* = 13.5, 4.1 Hz, 1H), 1.63 (s, 3H), 1.21 (d, *J* = 2.4 Hz, 24H), 1.05 (dd, *J* = 16.3, 3.1 Hz, 1H), 0.78

(dd, *J* = 16.3, 12.1 Hz, 1H). ^{13}C NMR (75 MHz, $CDCl_3$) *δ* 172.9 (C), 172.7 (C), 163.2 (C), 82.7 (4 × C), 58.7 (C), 52.7 (CH_3), 52.6 (CH_3), 40.9 (CH_2), 39.2 (CH_2), 38.6 (CH), 25.0 (2 × CH_3), 24.8 (4 × CH_3), 24.7 (2 × CH_3), 20.2 (br m, CH_2-B), 17.4 (CH_3). HRMS (ESI, MeOH) calcd. for $C_{24}H_{40}B_2O_8$ [M + Na]$^+$: 501.2909; Found: 501.2806.

Dimethyl (*E*)-3-(phenyl(4,4,5,5-tetramethyl-1,3,2-dioxaborolan-2-yl)methylene)-4-((4,4,5,5-tetramethyl-1,3,2-dioxaborolan-2-yl)methyl)cyclopentane-1,1-dicarboxylate (17cc): The compound was purified by column chromatography (cyclohexane/EtOAc 9:1) and was obtained as a white solid in 67% yield (72 mg). M. p. = 88 – 89 °C. ^{1}H NMR (300 MHz, $CDCl_3$) *δ* 7.25 (t, *J* = 7.4 Hz, 2H), 7.14 (d, *J* = 7.4 Hz, 1H), 7.07 (d, *J* = 7.4 Hz, 2H), 3.67 (s, 3H), 3.60 (s, 3H), 3.50 – 3.38 (m, 1H), 3.12 (d, *J* = 17.0 Hz, 1H), 2.74 (d, *J* = 17.0 Hz, 1H), 2.70 (dd, *J* = 14.2, 7.5 Hz, 1H), 2.04 (dd, *J* = 13.5, 5.8 Hz, 1H), 1.24 (d, *J* = 6.1 Hz, 24H), 1.03 (dd, *J* = 16.0, 11.3 Hz, 2H). ^{13}C NMR (75 MHz, $CDCl_3$) δ 172.6 (C), 172.2 (C), 163.9 (C), 143.1 (C), 128.8 (2 × CH), 127.8 (2 × CH), 125.5 (CH), 83.1 (2 × C), 83.0 (2 × C), 59.1 (CH_2), 52.6 (CH_3), 52.5 (CH_3), 40.7 (CH_2), 40.3 (CH_2), 38.4 (CH), 25.0 (2 × CH_3), 24.9 (2 × CH_3), 24.8 (2 × CH_3), 24.6 (2 × CH_3), 20.9 (br m, CH_2-B). HRMS (ESI, MeOH) calcd. for $C_{29}H_{42}B_2O_8$ [M + Na]$^+$: 563.3066; Found: 563.2957.

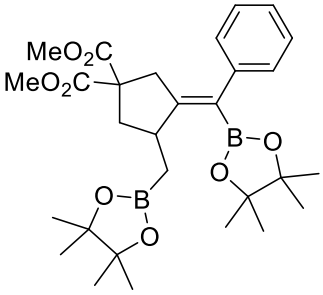

Dimethyl (*E*)-3-((3-methoxyphenyl)(4,4,5,5-tetramethyl-1,3,2-dioxaborolan-2-yl)methylene)-4-((4,4,5,5-tetramethyl-1,3,2-dioxaborolan-2-yl)methyl)cyclopentane-1,1-dicarboxylate (17cd): The compound was purified by column chromatography (cyclohexane/EtOAc 9:1) and was obtained as a colorless oil in 83% yield (95 mg). ^{1}H NMR (300 MHz, $CDCl_3$) *δ* 7.17 (t, *J* = 7.9 Hz, 1H), 6.74 – 6.60 (m, 3H), 3.77 (s, 3H), 3.68 (s, 3H), 3.62 (s, 3H), 3.51 – 3.35 (m, 1H), 3.12 (dd, *J* = 17.0, 1.8 Hz, 1H), 2.78 (d, *J* = 17.0 Hz, 1H), 2.70 (dd, *J* = 13.5, 8.4 Hz, 1H), 2.03 (dd, *J* = 13.5, 5.8 Hz, 1H), 1.27 – 1.20 (m, 24H), 1.20 (d, *J* = 3.2 Hz, 1H), 1.03 (dd, *J* = 16.1, 11.3 Hz, 1H). ^{13}C NMR (75 MHz, $CDCl_3$) *δ* 172.6 (C), 172.2 (C), 163.8 (C), 159.1 (C), 144.4 (C), 128.7 (CH), 121.3 (CH), 114.4 (CH), 111.2 (CH), 83.1 (2 × C), 82.9 (2 × C), 59.1 (C), 55.1 (CH_3), 52.6 (CH_3), 52.5 (CH_3), 40.7 (CH_2), 40.3 (CH_2), 38.4 (CH), 25.0 (2 × CH_3), 24.9 (2 × CH_3), 24.8 (2 × CH_3), 24.6 (2 × CH_3), 20.9 (br m, CH_2-B). HRMS (ESI, MeOH) calcd. for $C_{30}H_{44}B_2O_9$ [M + Na]$^+$: 593.3171; Found: 593.3057.

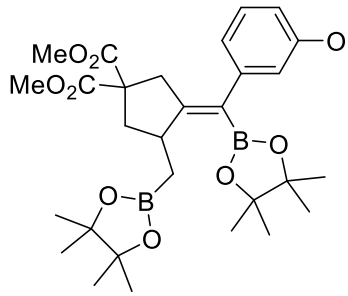

Dimethyl (*E*)-3-((4-methoxyphenyl)(4,4,5,5-tetramethyl-1,3,2-dioxaborolan-2-yl)methylene)-4-((4,4,5,5-tetramethyl-1,3,2-dioxaborolan-2-yl)methyl)cyclopentane-1,1-dicarboxylate (17ce): The compound was purified by column chromatography (cyclohexane/EtOAc 9:1) and was obtained as a colorless oil in 42% yield (48 mg). ^{1}H NMR (300 MHz, $CDCl_3$) *δ* 7.00 (d, *J* = 7.7 Hz, 2H), 6.80 (dd, *J* = 8.6, 1.4 Hz, 2H), 3.76 (s, 3H), 3.68 (s, 3H), 3.60 (s, 3H), 3.39 – 3.49 (m, 1H), 3.12 (d, *J* = 17.0 Hz, 1H), 2.76 (d, *J* = 17.0 Hz, 1H), 2.69 (dd, *J* = 15.2, 10.0 Hz, 1H), 2.02 (dd, *J* = 13.4, 5.8 Hz, 1H), 1.23 (d, *J* = 3.4 Hz, 24H), 1.26 – 1.16 (m, 1H), 1.01 (dd, *J* = 16.1, 11.3 Hz, 1H). ^{13}C NMR (75 MHz, $CDCl_3$) *δ* 172.6 (C), 172.2 (C), 163.3 (C), 157.5 (C), 135.3 (C), 129.8 (2 × CH), 113.2 (2 × CH), 83.0 (2 × C), 82.9 (2 × C), 59.1 (C), 55.1 (CH_3), 52.6 (CH_3), 52.5 (CH_3), 40.6

(CH_2), 40.2 (CH_2), 38.4 (CH), 25.0 (2 × CH_3), 24.9 (2 × CH_3), 24.8 (2 × CH_3), 24.6 (2 × CH_3), 20.8 (br m, CH_2-B). HRMS (ESI, MeOH) calcd. for $C_{30}H_{44}B_2O_9$ [M + Na]$^+$: 593.3171; Found: 593.3060.

Dimethyl (*E*)-3-((4-cyanophenyl)(4,4,5,5-tetramethyl-1,3,2-dioxaborolan-2-yl)methylene)-4-((4,4,5,5-tetramethyl-1,3,2-dioxaborolan-2-yl)methyl)cyclopentane-1,1-dicarboxylate (17cf): The compound was purified by column chromatography (cyclohexane/EtOAc 9:1) and was obtained as a light brown oil in 37% yield (42 mg). ^{1}H NMR (300 MHz, $CDCl_3$) *δ* 7.56 (d, *J* = 8.3 Hz, 2H), 7.19 (d, *J* = 8.3 Hz, 2H), 3.69 (s, 3H), 3.63 (s, 3H), 3.52 – 3.40 (m, 1H), 3.07 (dd, *J* = 16.9, 1.9 Hz, 1H), 2.74 – 2.60 (m, 2H), 2.06 (dd, *J* = 13.7, 5.9 Hz, 1H), 1.24 (d, *J* = 7.2 Hz, 24H), 1.22 – 1.18 (m, 1H), 1.11 – 0.99 (m, 1H). ^{13}C NMR (75 MHz, $CDCl_3$) *δ* 172.4 (C), 172.1 (C), 166.8 (C), 148.6 (C), 131.9 (2 × CH), 129.8 (2 × CH), 119.6 (C), 109.4 (C), 83.6 (2 × C), 83.2 (2 × C), 59.2 (C), 52.9 (CH_3), 52.8 (CH_3), 40.7 (CH_2), 40.6 (CH_2), 38.7 (CH), 25.1 (2 × CH_3), 25.0 (2 × CH_3), 24.9 (2 × CH_3), 24.7 (2 × CH_3), 20.6 (br m, CH_2-B). HRMS (ESI, MeOH) calcd. for $C_{30}H_{41}B_2NO_8$ [M + Na]$^+$: 588.3018; Found: 588.2914.

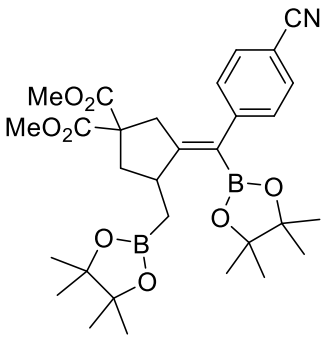

(*E*)-2-((4,4-Bis((benzyloxy)methyl)-2-((4,4,5,5-tetramethyl-1,3,2-dioxaborolan-2-yl)methyl)cyclopentylidene)(phenyl)methyl)-4,4,5,5-tetramethyl-1,3,2-dioxaborolane (17db): The compound was purified by column chromatography (cyclohexane/EtOAc 9:1) and was obtained as a colorless oil in 85% yield (115 mg). ^{1}H NMR (300 MHz, $CDCl_3$) *δ* 7.34 – 7.25 (m, 10H), 7.21 (d, *J* = 8.0 Hz, 3H), 7.14 (dd, *J* = 9.4, 8.0 Hz, 2H), 4.53 (s, 2H), 4.42 (q, *J* = 12.2 Hz, 2H), 3.47 (s, 2H), 3.45 – 3.34 (m, 1H), 3.25 (q, *J* = 9.0 Hz, 2H), 2.39 (q, *J* = 16.2 Hz, 2H), 2.10 (dd, *J* = 13.2, 8.9 Hz, 1H), 1.30 (d, *J* = 5.2 Hz, 24H), 1.14 (dd, *J* = 15.7, 11.2 Hz, 2H). ^{13}C NMR (75 MHz, $CDCl_3$) *δ* 167.4 (C), 143.6 (C), 139.1 (2 × C), 129.2 (2 × CH), 128.3 (2 × CH), 128.2 (2 × CH), 127.7 (2 × CH), 127.5 (2 × CH), 127.4 (2 × CH), 127.3 (CH), 127.2 (CH), 125.3 (CH), 83.0 (2 × C), 82.9 (2 × C), 75.1 (CH_2), 73.3 (CH_2), 73.2 (CH_2), 72.5 (CH_2), 47.3 (C), 39.1 (CH_2), 38.0 (CH), 25.2 (2 × CH_3), 25.0 (2 × CH_3), 24.9 (2 × CH_3), 24.6 (2 × CH_3), 22.4 (br m, CH_2-B). HRMS (ESI, MeOH) calcd. for $C_{41}H_{54}B_2O_6$ [M + Na]$^+$: 687.4107; Found: 687.3990.

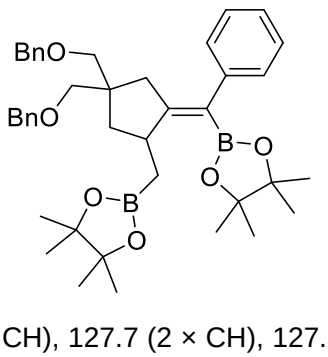

(*E*)-4,4,5,5-Tetramethyl-2-(phenyl(2-((4,4,5,5-tetramethyl-1,3,2-dioxaborolan-2-yl)methyl)cyclopentylidene)methyl)-1,3,2-dioxaborolane (17ea): The compound was purified by column chromatography (cyclohexane/EtOAc 95:5) and was obtained as a pale yellow oil in 52% yield (39 mg). ^{1}H NMR (300 MHz, $CDCl_3$) *δ* 7.30 – 7.20 (m, 2H), 7.16 – 7.09 (m, 3H), 3.40 – 3.25 (m, 1H), 2.48 – 2.34 (m, 1H), 2.14 (dt, *J* = 17.3, 7.0 Hz, 1H), 1.86 (dt, *J* = 11.1, 7.6 Hz, 1H), 1.69 (dd, *J* = 12.3, 8.0 Hz, 1H), 1.61 – 1.46 (m, 2H), 1.26 (s, 12H), 1.16 – 1.03 (m, 2H). ^{13}C NMR (75 MHz, $CDCl_3$) *δ* 169.3 (C), 143.9 (C), 129.0 (2 × CH), 127.7 (4 × CH), 125.2 (CH), 83.1 (2 × C), 82.9 (2 × C), 39.7 (CH), 33.6 (CH_2), 32.7 (CH_2), 25.1 (2 × CH_3), 25.0 (2 × CH_3), 24.9 (2 × CH_3), 24.7 (2 × CH_3), 23.7 (CH_2), 20.8 (br m, CH_2-B). HRMS (ESI, MeOH) calcd. for $C_{25}H_{38}B_2O_4$ [M + Na]$^+$: 447.2956; Found: 447.2846.

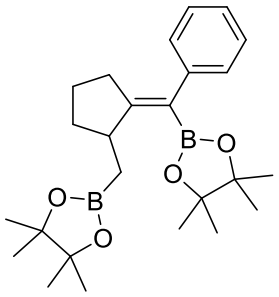

(*E*)-4,4,5,5-Tetramethyl-2-((2-((4,4,5,5-tetramethyl-1,3,2-dioxaborolan-2-yl)(p-tolyl)methylene)cyclopentyl)methyl)-1,3,2-dioxaborolane (17eb): The compound was purified by column chromatography (cyclohexane/EtOAc 95:5) and was obtained as a pale yellow oil in 63% yield (52 mg). ^{1}H NMR (300 MHz, $CDCl_3$) δ 7.08 (d, J = 8.1 Hz, 2H), 7.02 (d, J = 8.1 Hz, 2H), 3.39 – 3.29 (m, 1H), 2.47 – 2.34 (m, 1H), 2.32 (s, 3H), 2.15 (dt, J = 17.3, 6.9 Hz, 1H), 1.95 – 1.80 (m, 1H), 1.75 – 1.59 (m, 1H), 1.48 (dd, J = 9.8, 6.1 Hz, 2H), 1.27 (d, J = 1.7 Hz, 24H), 1.12 – 0.96 (m, 2H). ^{13}C NMR (75 MHz, $CDCl_3$) δ 168.9 (C), 140.8 (C), 134.5 (C), 128.9 (2 × CH), 128.5 (2 × CH), 83.0 (2 × C), 82.9 (2 × C), 39.7 (CH), 33.6 (CH_2), 32.7 (CH_2), 25.1 (2 × CH_3), 25.0 (2 × CH_3), 24.9 (2 × CH_3), 24.7 (2 × CH_3), 23.7 (CH_2), 21.3 (CH_3), 19.9 (br m, CH_2-B). HRMS (ESI, MeOH) calcd. for $C_{26}H_{40}B_2O_4$ [M + Na]$^+$: 461.3113; Found: 461.2994.

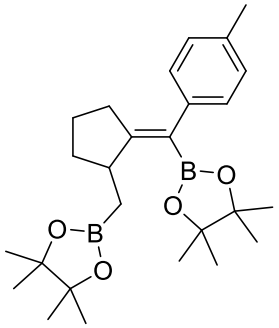

(*E*)-4,4,5,5-Tetramethyl-2-(1-(2-((4,4,5,5-tetramethyl-1,3,2-dioxaborolan-2-yl)methyl)cyclopentylidene)pentyl)-1,3,2-dioxaborolane (17ec): The compound was purified by column chromatography (cyclohexane/EtOAc 98:2) and was obtained as a colorless oil in 76% yield (61 mg). ^{1}H NMR (300 MHz, $CDCl_3$) δ 3.25 – 3.11 (m, 1H), 2.46 – 2.35 (m, 1H), 2.27 – 2.12 (m, 1H), 2.10 – 2.00 (m, 3H), 1.72 – 1.57 (m, 3H), 1.51 – 1.44 (m, 1H), 1.26 – 1.19 (m, 24H), 1.21 – 1.17 (m, 2H), 0.90 – 0.83 (m, 6H). ^{13}C NMR (75 MHz, $CDCl_3$) δ 167.2 (C), 82.7 (2 × C), 82.5 (2 × C), 39.4 (CH), 33.6 (CH_2), 32.3 (CH_2), 32.1 (CH_2), 30.6 (CH_2), 25.1 (2 × CH_3), 25.0 (2 × CH_3), 24.9 (2 × CH_3), 24.8 (2 × CH_3), 22.9 (CH_2), 22.8 (CH_2), 20.2 (br m, CH_2-B), 14.3 (CH_3). HRMS (ESI, MeOH) calcd. for $C_{23}H_{42}B_2O_4$ [M + Na]$^+$: 427.3269; Found: 427.3161.

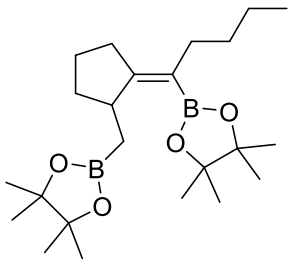

3.4.4.3. Transformations of bis(boronates)

3.4.4.3.1. General procedure for oxidation of diboronate

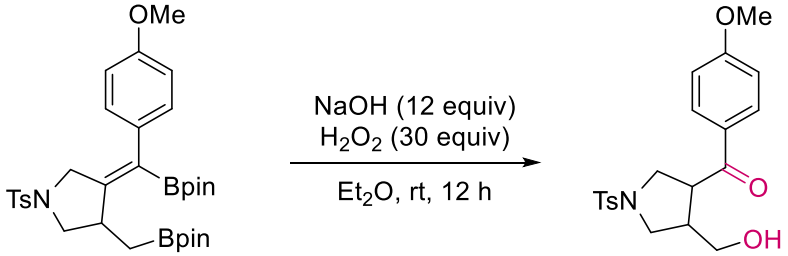

17bd **18bd**

The diboronate **17bd** (1 equiv, 0.14 mmol) in diethyl ether (0.2 M, 0.7 mL) at 0 °C was treated with NaOH (3 N, 12 equiv) and H_2O_2 (30%, 30 equiv) at 0 °C. The mixture was stirred overnight at room temperature. The resulting suspension was extracted with diethyl ether (2 × 5 mL). The combined organic layers were washed with brine, dried over anhydrous $MgSO_4$, filtered and concentrated under vacuum. The resulting residue was purified by column chromatography to give the corresponding alcohol-ketone (cyclohexane/AcOEt 1:1 was used as an eluent).[100]

[100] T. Xi, Z. Lu, *ACS Catal.* **2017**, *7*, 1181–1185.

(*Z*)-3-((4-Methoxyphenyl)(4,4,5,5-tetramethyl-1,3,2-dioxaborolan-2-yl)methylene)-4-((4,4,5,5-tetramethyl-1,3,2-dioxaborolan-2-yl)methyl)-1-tosylpyrrolidine (18bd): The

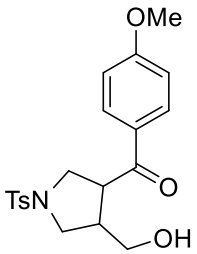

product was obtained as a pale yellow oil in 75% yield (41 mg). ^{1}H NMR (300 MHz, $CDCl_3$) δ 7.88 (d, J = 8.7 Hz, 2H), 7.69 (d, J = 8.0 Hz, 2H), 7.32 (d, J = 8.0 Hz, 2H), 6.91 (d, J = 8.7 Hz, 2H), 3.85 (s, 3H), 3.81 – 3.67 (m, 1H), 3.63 – 3.54 (s, 2H), 3.30 (d, J = 5.6 Hz, 2H), 3.24 (dd, J = 9.6, 7.3 Hz, 1H), 2.78 – 2.63 (m, 1H), 2.44 (s, 3H), 2.15 (br s, 1H). ^{13}C NMR (75 MHz, $CDCl_3$) δ 196.9 (C), 164.1 (C), 143.9 (C), 133.3 (C), 131.0 (2 × CH), 129.9 (2 × CH), 129.0 (C), 127.8 (2 × CH), 114.1 (2 × CH), 63.0 (CH_2), 55.7 (CH_3), 50.7 (CH_2), 49.8 (CH_2), 46.8 (CH), 43.7 (CH), 21.7 (CH_3). HRMS (ESI, MeOH) calcd. for $C_{20}H_{23}NO_5S$ $[M]^+$: 412.1297; Found: 412.1183.

3.4.4.3.2. General procedure for Suzuki Cross-Coupling Reaction of alkenylboronates.

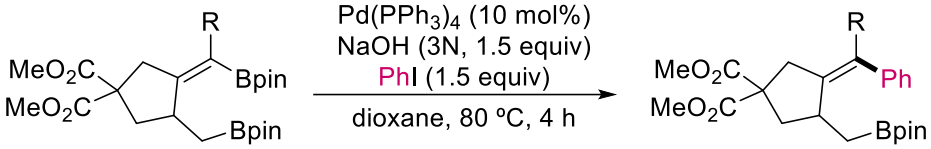

17cb: R = Me
17cc: R = Ph

19cb: R = Me
19cc: R = Ph

A vial was charged with $Pd(PPh_3)_4$ (0.07 mmol), iodobenzene (1.05 mmol) and the corresponding diboronate **17c** (0.7 mmol). The vial was sealed by a septum, dried under vacuum and backfilled with Ar. To the vial, dioxane (3.7 mL) and NaOH (3 M, 0.35 mL) were added, and then the reaction was heated to 80 °C for 16 h. The reaction mixture was allowed to cool to room temperature. The solvent was removed under vacuum and the product was purified by column chromatography in silica gel (cyclohexane/EtOAc 9:1).[101]

Dimethyl (*Z*)-3-(1-phenylethylidene)-4-((4,4,5,5-tetramethyl-1,3,2-dioxaborolan-2-yl)methyl)cyclopentane-1,1-dicarboxylate (19cb): The product was obtained as a pale

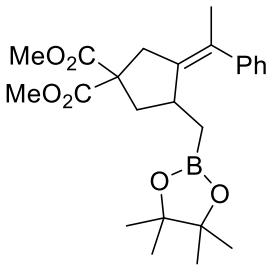

yellow oil in 81% yield (243 mg). ^{1}H NMR (300 MHz, $CDCl_3$) δ 7.29 – 7.21 (m, 3H), 7.19 – 7.08 (m, 2H), 3.75 (s, 3H), 3.73 (s, 3H), 3.05 (s, 2H), 2.58 (dd, J = 13.2, 7.9 Hz, 1H), 1.99 (dd, J = 13.2, 7.9 Hz, 1H), 1.93 (s, 3H), 1.61 – 1.53 (m, 1H), 1.15 (s, 12H), 0.57 (dd, J = 16.1, 3.4 Hz, 1H), 0.43 (dd, J = 16.1, 10.0 Hz, 1H). ^{13}C NMR (75 MHz, $CDCl_3$) δ 172.7 (C), 172.6 (C), 144.0 (C), 140.4 (C), 129.1 (C), 128.2 (2 × CH), 127.9 (2 × CH), 126.2 (CH), 82.8 (2 × C), 59.0 (C), 52.8 (CH_3), 52.7 (CH_3), 41.6 (CH_2), 39.5 (CH_2), 36.4 (CH), 25.0 (2 × CH_3), 24.7 (2 × CH_3), 22.5 (CH_3), 16.7 (br m, CH_2-B). HRMS (ESI, MeOH) calcd. for $C_{24}H_{33}BO_6$ $[M + Na]^+$: 451.2370; Found: 451.2279.

[101] S. Yu, C. Wu, S. Ge, *J. Am. Chem. Soc.* **2017**, *139*, 6526–6529.

Dimethyl 3-(diphenylmethylene)-4-((4,4,5,5-tetramethyl-1,3,2-dioxaborolan-2-yl)methyl)cyclopentane-1,1-dicarboxylate (19cc): The product was obtained as a pale yellow oil in 78% yield (267 mg). ^{1}H NMR (300 MHz, $CDCl_3$) δ 7.33 – 7.22 (m, 5H), 7.19 – 7.10 (m, 5H), 3.71 (s, 3H), 3.69 (s, 3H), 3.39 – 3.23 (m, 1H), 3.33 (d, J = 14.8 Hz, 1H), 2.92 (d, J = 15.8 Hz, 1H), 2.68 (dd, J = 11.7, 8.2 Hz, 1H), 1.95 (dd, J = 12.9, 8.7 Hz, 1H), 1.21 (d, J = 3.3 Hz, 12H), 0.74 (dd, J = 16.3, 3.7 Hz, 1H), 0.62 (dd, J = 16.3, 8.6 Hz, 1H). ^{13}C NMR (75 MHz, $CDCl_3$) δ 172.2 (C), 172.1 (C), 143.7 (C), 143.4 (C), 142.3 (C), 135.5 (C), 129.4 (2 × CH), 129.2 (2 × CH), 128.3 (2 × CH), 127.9 (2 × CH), 126.5 (CH), 126.4 (CH), 82.9 (2 × C), 77.4 (CH), 67.1 (CH_2), 59.6 (C), 52.6 (CH_3), 41.2 (CH_2), 36.7 (CH_3), 24.9 (2 × CH_3), 24.8 (2 × CH_3), 19.5 (br m, CH_2-B). HRMS (ESI, MeOH) calcd. for $C_{29}H_{35}BO_6$ $[M + Na]^+$: 513.2527; Found: 513.2411.

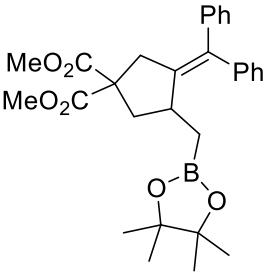

3.4.4.3.3. General procedure for the synthesis of trifluoroborate salts

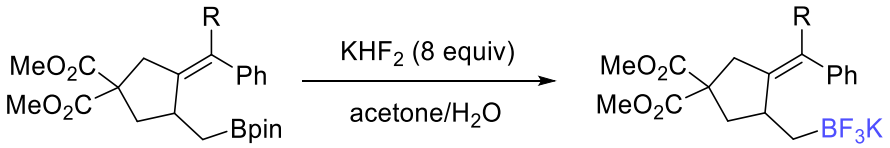

19cb: R = Me
19cc: R = Ph

20cb: R = Me
20cc: R = Ph

Alkylboronate **19c** (1 equiv, 0.4 mmol) was solved in acetone (0.4 M, 1 mL). To the solution, KHF_2 (8 equiv, 0.4 M aqueous solution) were added. The reaction mixture was stirred at 25 °C for 3 h. Then, the solvent was removed under vacuum and the solid residue was triturated with hexane (10 mL) and was washed with cold diethyl ether (3 x 10 mL) to remove pinacol and dried under vacuum, affording the desired product.

Potassium dimethyl (*Z*)-3-(1-phenylethylidene)-4-((trifluoroboranyl)methyl)cyclopentane-1,1-dicarboxylate (20cb): The product was obtained as a light brown solid in 81% yield (132 mg). M.p. = 67 – 69 °C. ^{1}H NMR (300 MHz, d^6-acetone) δ 7.22 – 7.15 (m, 2H), 7.12 (d, J = 7.0 Hz, 2H), 7.06 (t, J = 7.0 Hz, 1H), 3.62 (s, 6H), 2.98 (d, J = 16.0 Hz, 1H), 2.88 (d , J = 16.0 Hz, 1H), 2.43 (dd, J = 13.4, 8.1 Hz, 1H), 2.08 (dd, J = 13.4, 5.8 Hz, 1H), 2.01 – 1.97 (m, 1H), 1.84 (s, 3H), 0.20 – 0.04 (m, 1H), -0.01 – -0.17 (m, 1H). ^{13}C NMR (75 MHz, Acetone-d^6) δ 173.7 (C), 173.4 (C), 145.4 (C), 145.2 (2 × CH), 128.8 (2 × CH), 128.5 (2 × CH), 126.2 (CH), 125.9 (C), 59.5 (C), 52.5 (CH_3), 52.4 (CH_3), 41.5 (CH_2), 39.2 (CH_2), 38.9 (CH), 22.2 (CH_3). ^{19}F NMR (282 MHz, Acetone-d^6) δ – 138.21. HRMS (ESI, MeCN) calcd. for $C_{18}H_{21}BF_3KO_4$ $[M - K]^-$: 369.1490; Found: 369.1480.

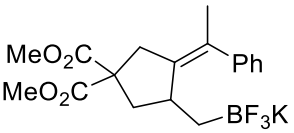

Potassium dimethyl 3-(diphenylmethylene)-4-((trifluoroboranyl)methyl)cyclopentane-1,1-dicarboxylate (20cc): The product was obtained as a light brown solid in 78% yield (147 mg). M.p. = 65 – 67 °C. ^{1}H NMR (300 MHz, d^6-acetone) δ 7.32 – 7.20 (m, 4H), 7.18 – 7.07 (m, 6H), 3.64 (s, 3H), 3.61 (s, 3H), 3.19 (d, J = 14.0 Hz, 1H), 3.15 – 3.08 (m, 1H), 2.69 (d, J = 15.7 Hz, 1H), 2.59 (dd, J = 12.9, 7.9 Hz, 1H), 2.12 (dd, J = 13.7, 6.8 Hz, 1H), 0.38 – 0.25 (m, 1H), 0.18 – 0.04 (m, 1H). ^{13}C NMR (75 MHz,

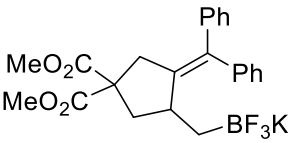

Acetone-d^6) δ 173.3 (C), 173.1 (C), 148.6 (C), 145.1 (C), 143.7 (C), 133.8 (C), 130.4 (2 × CH), 130.1 (2 × CH), 128.6 (2 × CH), 128.5 (2 × CH), 126.7 (CH), 126.6 (CH), 60.3 (C), 52.6 (CH_3), 52.5 (CH_3), 41.1 (CH_2), 40.9 (CH_2), 39.2 (CH). ^{19}F NMR (282 MHz, Acetone-d^6) δ –137.95. HRMS (ESI, MeCN) calcd. for $C_{23}H_{23}BF_3KO_4$ [M - K]$^-$: 431.1647; Found: 431.1652.

3.4.4.3.4. General procedure for Suzuki Coupling Reaction of alkyltrifluoroborates salts

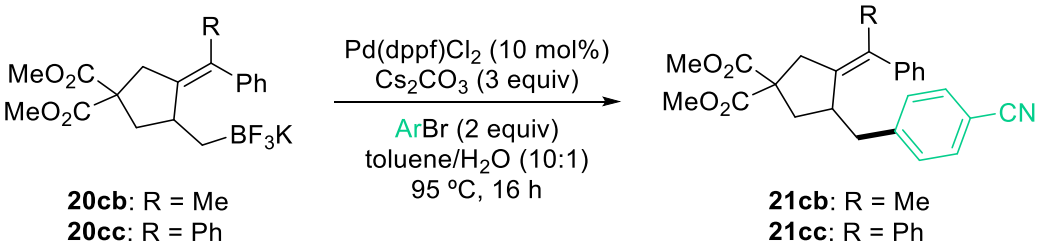

20cb: R = Me
20cc: R = Ph

21cb: R = Me
21cc: R = Ph

A vial was charged with Pd(dppf)Cl_2 (0.02 mmol), 4-bromobenzonitrile (0.4 mmol), the corresponding potassium trifluoroborate compound **20c** (0.2 mmol) and Cs_2CO_3 (0.6 mmol). The vial was sealed by a septum, dried under vacuum and backfilled with Ar. To the vial, toluene (2 mL) and H_2O (0.2 mL) were added, and then the reaction was heated to 95 °C for 16 h. The reaction mixture was allowed to cool to room temperature. The solvent was removed under vacuum and purified by silica gel column chromatography to yield the product (cyclohexane/EtOAc 95:5).[100]

Dimethyl (*Z*)-3-(4-cyanobenzyl)-4-(1-phenylethylidene)cyclopentane-1,1-dicarboxylate (21cb): 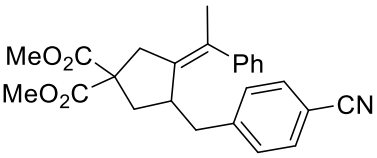

The product was obtained as a pale yellow oil in 72% yield (58 mg). ^{1}H NMR (300 MHz, $CDCl_3$) δ 7.42 (d, *J* = 8.1 Hz, 2H), 7.35 (t, *J* = 7.2 Hz, 2H), 7.29 – 7.23 (m, 1H), 7.20 – 7.14 (m, 2H), 6.83 (d, *J* = 8.1 Hz, 2H), 3.77 (s, 3H), 3.74 (s, 3H), 3.10 (s, 2H), 3.02 (d, *J* = 6.8 Hz, 1H), 2.43 (dd, *J* = 13.4, 3.8 Hz, 1H), 2.29 (dd, *J* = 13.4, 8.2 Hz, 1H), 2.11 (dd, *J* = 13.4, 11.1 Hz, 1H), 2.01 (s, 3H), 1.93 (dd, *J* = 13.4, 5.9 Hz, 1H). ^{13}C NMR (75 MHz, $CDCl_3$) δ 172.6 (C), 172.3 (C), 146.5 (C), 143.8 (C), 137.7 (C), 132.1 (2 × CH), 129.6 (2 × CH), 128.6 (2 × CH), 127.8 (2 × CH), 126.8 (CH), 119.2 (C), 109.8 (C), 59.0 (C), 53.0 (2 × CH_3), 42.8 (CH), 40.4 (CH_2), 39.1 (CH_2), 38.7 (CH_2), 22.5 (CH_3). HRMS (ESI, MeOH) calcd. for $C_{25}H_{25}NO_4$ [M + H]$^+$: 404.1784; Found: 404.1855.

Dimethyl 3-(4-cyanobenzyl)-4-(diphenylmethylene)cyclopentane-1,1-dicarboxylate (21cc): 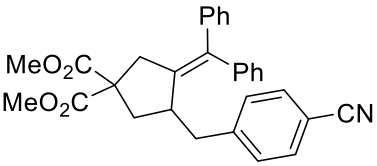

The product was obtained as a pale yellow oil in 74% yield (69 mg). ^{1}H NMR (300 MHz, $CDCl_3$) δ 7.45 (d, *J* = 8.1 Hz, 2H), 7.38 – 7.22 (m, 6H), 7.18 – 7.05 (m, 4H), 6.91 (d, *J* = 8.1 Hz, 2H), 3.73 (s, 3H), 3.66 (s, 3H), 3.50 – 3.39 (m, 1H), 3.18 (dd, *J* = 16.1, 2.1 Hz, 1H), 2.95 (dd, *J* = 16.1, 1.5 Hz, 1H), 2.61 (dd, *J* = 13.3, 4.4 Hz, 1H), 2.44 (ddd, *J* = 13.3, 8.1, 1.4 Hz, 1H), 2.34 (dd, *J* = 13.3, 10.2 Hz, 1H), 1.86 (dd, *J* = 13.3, 7.1 Hz, 1H). ^{13}C NMR (75 MHz, $CDCl_3$) δ 172.1 (C), 171.9 (C), 146.0 (C), 142.4 (C), 142.0 (C), 140.4 (C), 138.0 (C), 132.2 (2 × CH), 129.8 (2 × CH), 129.4 (2 × CH), 129.2 (2 × CH), 128.7 (2 × CH), 128.2 (2 × CH), 127.2 (CH), 127.0 (CH), 119.2 (C), 110.0 (C), 59.6 (C), 53.0 (CH_3), 52.9

[100] T. Xi, Z. Lu, *ACS Catal.* **2017**, *7*, 1181–1185.

(CH_3), 42.9 (CH), 40.6 (CH_2), 40.5 (CH_2), 38.6 (CH_2). HRMS (ESI, MeOH) calcd. for $C_{30}H_{27}NO_4$ $[M + H]^+$: 466.1940; Found: 466.2023.

3.4.4.4. Mechanistic studies

3.4.4.4.1. Deuteration experiment

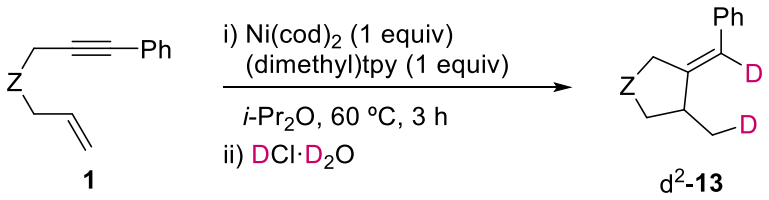

1 **d²-13**

A vial was charged with $Ni(cod)_2$ (55 mg, 0.2 mmol), (5,5''-dimethyl)tpy (52 mg, 0.2 mmol), the enyne **1** (0.2 mmol) and a stir bar in air. The vial was sealed by a septum, dried under vacuum and backfilled with Ar. Then, anhydrous and Ar-degassed diisopropyl ether (1 mL) was added, and the resulting mixture was stirred for 2 h at room temperature. DCl in D_2O (1 mL) was added and the reaction mixture was stirred for 5 min. Then, the reaction was extracted with EtOAc (2 × 5 mL). The combined organic layers were washed with brine, dried over anhydrous $MgSO_4$, filtered and concentrated under vacuum. The resulting residue was purified by column chromatography (cyclohexane/EtOAc 95:5 was used as an eluent).

(*Z*)-3-(Methyl-*d*)-4-(phenylmethylene-*d*)-1-tosylpyrrolidine (d²-13bb): The product was obtained as a yellow oil in 20% yield (13 mg). ^{1}H NMR (300 MHz, $CDCl_3$) *δ* 7.72 (d, *J* = 8.2 Hz, 2H), 7.33 (dd, *J* = 15.4, 7.7 Hz, 5H), 7.14 (d, *J* = 7.2 Hz, 2H), 4.24 (d, *J* = 14.9 Hz, 1H), 4.05 (d, *J* = 14.9 Hz, 1H), 3.55 (dd, *J* = 8.9, 7.2 Hz, 1H), 2.95 – 2.80 (m, 1H), 2.77 – 2.67 (m, 1H), 2.41 (s, 3H), 1.17 (d, *J* = 6.6 Hz, 2H). D NMR (77 MHz, $CDCl_3$) *δ* 6.26 (s, 1D), 1.18 (s, 1D). ^{13}C NMR (75 MHz, $CDCl_3$) *δ* 143.8 (C), 141.9 (C), 136.7 (C), 133.2 (C), 129.9 (2 × CH), 128.7 (2 × CH), 128.2 (2 × CH), 127.9 (2 × CH), 127.1 (CH), 122.2 (CD), 54.0 (CH_2), 50.9 (CH_2), 39.2 (CH), 21.7 (CH_3), 16.8 (t, *J* = 19.0, CH_2D). HRMS (ESI, MeCN) calcd. for $C_{19}H_{19}D_2NO_2S$ $[M + Na]^-$: 352.1419; Found: 352.1303.

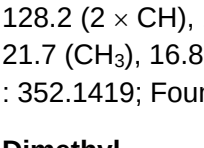

Dimethyl (*E*)-3-(methyl-*d*)-4-(phenylmethylene-*d*)cyclopentane-1,1-dicarboxylate (d²-13cc): The product was obtained as a colorless oil in 58% yield (34 mg). ^{1}H NMR (300 MHz, $CDCl_3$) *δ* 7.40 – 7.24 (m, 5H), 3.73 (d, *J* = 1.2 Hz, 6H), 3.40 (d, *J* = 17.7 Hz, 1H), 3.21 (dd, *J* = 17.7, 2.4 Hz, 1H), 2.84 – 2.70 (m, 1H), 2.61 (dd, *J* = 12.6, 7.1 Hz, 1H), 1.78 (t, *J* = 12.6 Hz, 1H), 1.21 (d, *J* = 6.1 Hz, 2H). ^{13}C NMR (75 MHz, $CDCl_3$) *δ* 172.5 (C), 172.4 (C), 146.1 (C), 138.0 (C), 128.4 (4 × CH), 126.3 (CH), 120.0 (CD), 59.2 (2 × C), 53.0 (CH_3), 52.9 (CH_3), 41.7 (CH_2), 39.2 (CH_2), 37.0 (CH), 18.1 (t, *J* = 19.2, CH_2D). HRMS (ESI, MeCN) calcd. for $C_{17}H_{18}D_2O_4$ $[M + Na]^-$: 313.1487; Found: 313.1364.

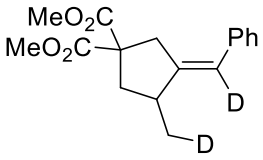

3.4.4.4.2. Generation of complex **22**

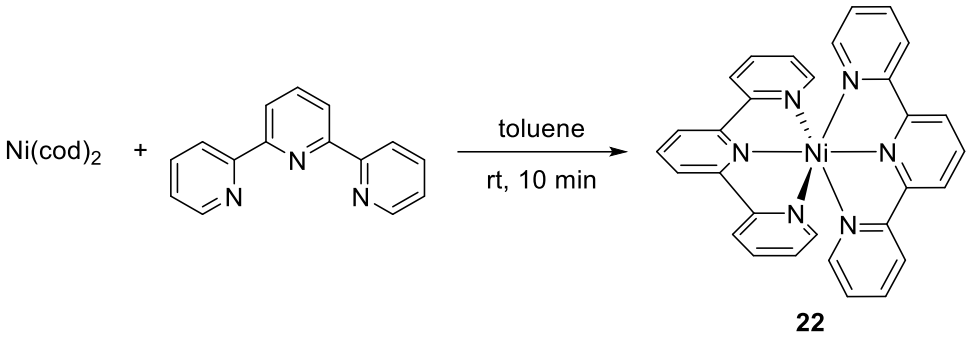

22

In a glove-box under nitrogen atmosphere, $Ni(cod)_2$ (0.04 mmol, 11 mg) and terpyridine (0.04 mmol, 9 mg) were added to a vial with a stir bar. Then, anhydrous toluene (2 mL) was added, and the mixture was stirred for 10 min at room temperature. Then, the reaction mixture was filtered through a celite pad, affording a dark blue solution. Suitable crystals of complex **22** were obtained by vapor diffusion with toluene/pentane at – 25 ºC after 24 h.

– Measurement of the effective magnetic moment of **22**

A sealed tube with THF as internal standard was introduced in the NMR tube. Then, a solution of complex **22** in THF (0.5 mL) was added. The experiment was carried out with the parameters described in **Table 4.2**.

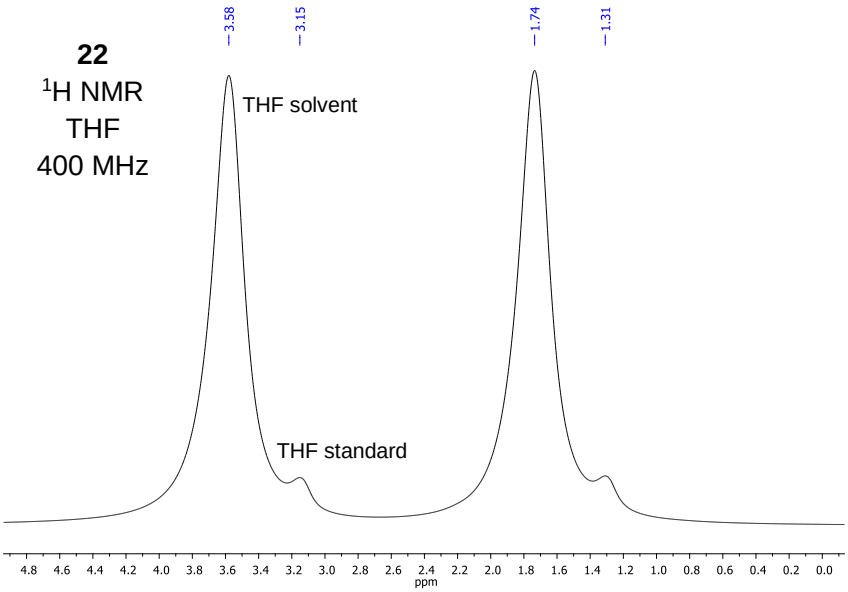

Table 4.2. Parameters used for the measurement of μ_{eff}

Parameter	Value
temperature	298
frequency shift in Hz	172.0559
spectrometer frequency in Hz	400130000
concentration in moles/L	0.01396
molecular weight in g/mol	525.2414
diamagnetic susceptibility	$- 306 \cdot 10^{-6}$

Magnetic susceptibility:[264] χ(**22**) = 6·(–49·10^{-6} (Py)) + (–12·10^{-6} (Ni)) = –306·10^{-6}

Using a difference of 0.43 ppm of signals shift, we obtained a value of μ_{eff} **= 4.3**. It could correspond to a S = 2 complex.

Table 4.3. Number of unpaired electrons and spin-only magnetic moments.

n	S	μ_{eff}
1	1/2	1.73
2	1	2.83
3	3/2	3.87
4	2	4.90
5	5/2	5.92

3.4.4.4.3. Generation of complex **23**

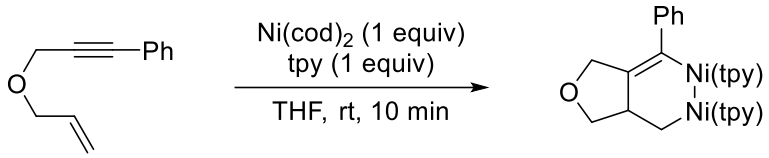

1aa **23**

In a glove-box under nitrogen atmosphere, Ni(cod)$_2$ (0.04 mmol, 11 mg), terpyridine (0.04 mmol, 9 mg) and the enyne **1aa** (0.04 mmol, 7 mg) were added to a vial with a stir bar. Then, anhydrous toluene (2 mL) was added, and the mixture was stirred for 10 min at room temperature. Then, the reaction mixture was filtered through a celite pad, affording a dark red solution. Suitable crystals of complex **23** were obtained in approximately 9% yield by adding anhydrous pentane or hexane (0.5 mL) and keeping the sample a room temperature for 5 days.

– NMR

23
^{1}H NMR
d^{8}-THF
400 MHz

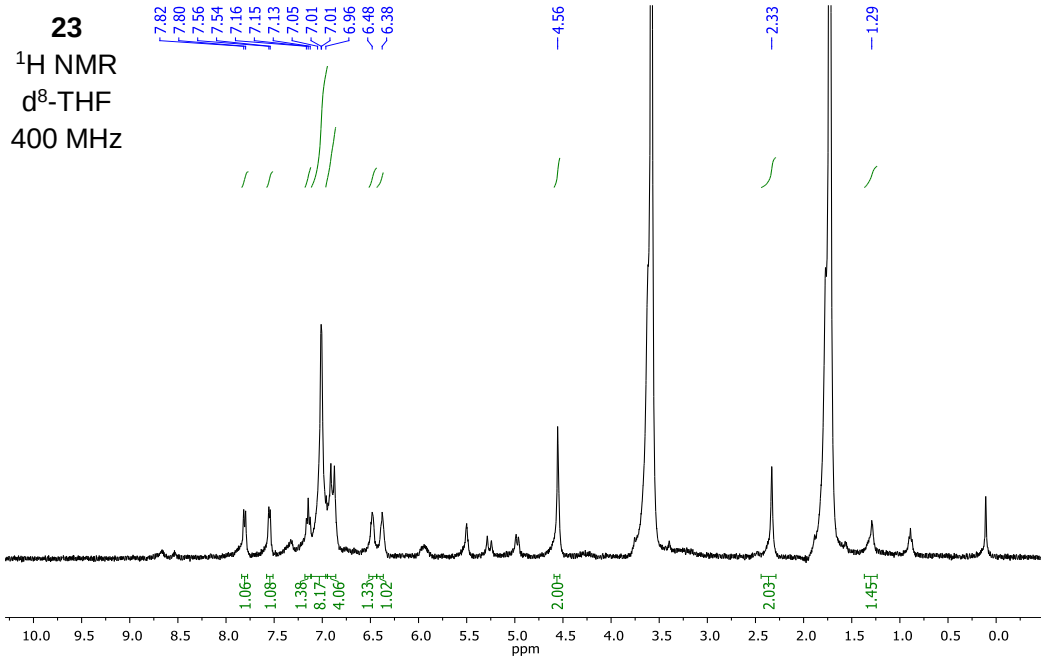

[264] G. A. Bain, J. F. Berry, *J. Chem. Educ.* **2008**, *85*, 532–536.

– Measurement of the effective magnetic moment of **23**

A sealed tube with THF as internal standard was introduced in the NMR tube. Then, a solution of complex **23** in THF (0.5 mL) was added. The experiment was carried out with the parameters described in **Table 4.4**.

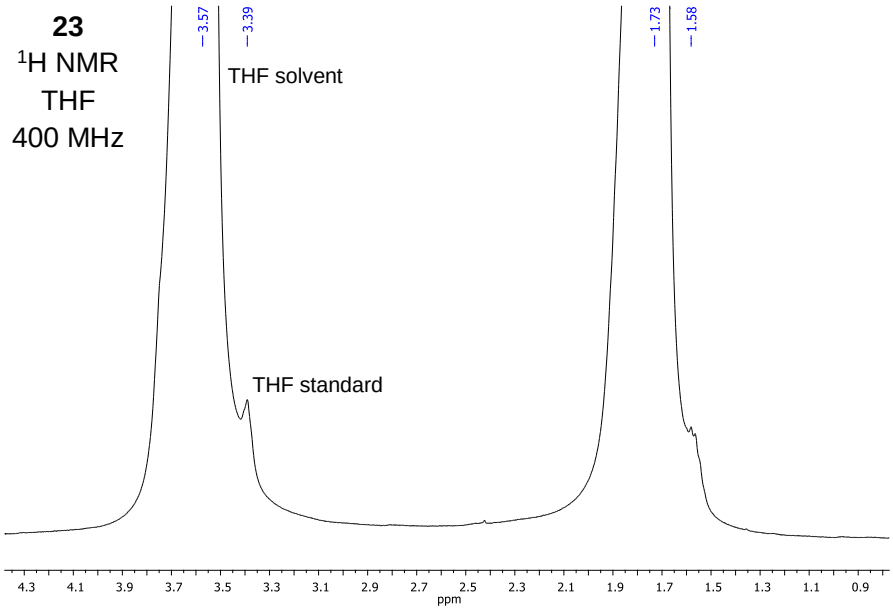

Table 4.4. Parameters used for the measurement of μ_{eff}

Parameter	**Value**
temperature	298
frequency shift in Hz	72.0234
spectrometer frequency in Hz	400130000
concentration in moles/L	0.011902
molecular weight in g/mol	756.1618
diamagnetic susceptibility	$- 414 \cdot 10^{-6}$

Magnetic susceptibility:[264] χ(**23**) = $6\cdot(-49\cdot10^{-6}$ (Py)) + $2\cdot(-12\cdot10^{-6}$ (Ni)) + $4\cdot(-6\cdot10^{-6}$ (C)) + $12\cdot(-2.93\cdot10^{-6}$ (H)) + $6\cdot(-6.24\cdot10^{-6}$ (C ring)) + $(5.5\cdot10^{-6}$ (C=C)) + $(-4.61\cdot10^{-6}$ (O ether)) = $-414\cdot10^{-6}$

Using a difference of 0.18 ppm of signals shift, we obtained a value of μ_{eff} **= 3.1**. It could correspond to a S = 1 complex.

[264] G. A. Bain, J. F. Berry, *J. Chem. Educ.* **2008**, *85*, 532–536.

CHAPTER 5:

Ni-catalyzed carboborylative cyclization of enynes

3.5. CHAPTER 5

3.5.1. Goal

In order to explore new possibilities concerning borylative cyclizations, we considered the use of organoboronates as boron source for the reaction, instead of the more commonly used HBpin and B_2pin_2 boron reagents, with the aim of discovering a novel and powerful way for the synthesis of complex structures bearing new carbon and boron moieties in one single step. In particular, we envisioned that carboborylative cyclization of enynes using Ni-based catalytic system would allow the activation of the C–B bond of the boron source and would lead to the synthesis of complex, cyclic boronates in a full atom-economical, efficient fashion.

3.5.2. Precedents

Among the different methods reported for the synthesis of organoboronates, carboboration is one of the most commonly used, since it leads to the concomitant formation of C–C and C–B bonds in one synthetic operation. Several transition metal-catalyzed[265] as well as metal-free[266] systems have been described. However, to the best of our knowledge, carboborylative cyclization reactions have no precedent in the literature.

3.5.1.1. Fe-catalyzed carboboration

Along with the previously mentioned Fe-catalyzed diboration reaction of alkynes (*see* ***Scheme 4.1***), Nakamura and co-workers described the carboboration of 4-octyne using B_2pin_2 and alkyl bromides (**Scheme 5.1**).[223]

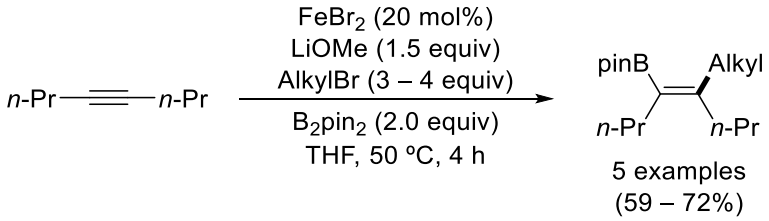

Scheme 5.1. Fe-catalyzed carboboration of alkynes.

The proposed reaction mechanism is similar to the diboration process, but in this case the alkenyliron(II) intermediate reacts with the alkyl bromide instead of an additional boron reagent (**Figure 5.1**). They proposed that carboboration step with the alkyl bromide involves homolytic cleavage of the C–Br bond with concomitant formation of radical species.

[223] N. Nakagawa, T. Hatakeyama, M. Nakamura, *Chem. Eur. J.* **2015**, *21*, 4257–4261.
[265] (a) M. Suginome, *Chem. Rec.* **2010**, *10*, 348–358. (b) R. Barbeyron, E. Benedetti, J. Cossy, J.-J. Vasseur, S. Arseniyadis, M. Smietana, *Tetrahedron* **2014**, *70*, 8431–8452.
[266] (a) G. Kehr, G. Erker, *Chem. Commun.* **2012**, *48*, 1839–1850. (b) G. Kehr, G. Erker, *Chem. Sci.* **2016**, *7*, 56–65.

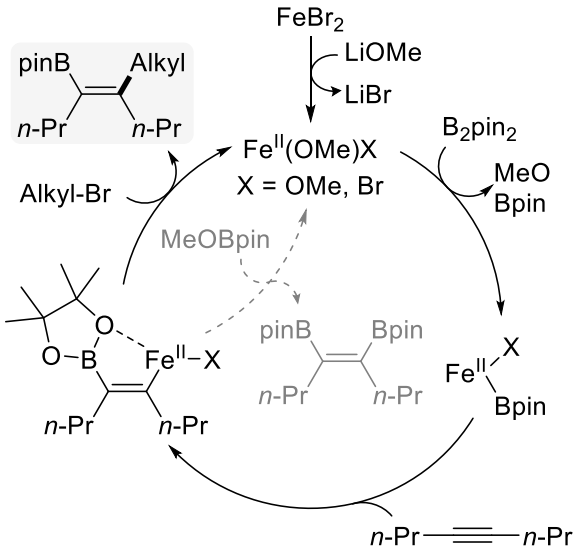

Figure 5.1. Proposed mechanism for Fe-catalyzed carboboration of alkynes.

3.5.1.2. Ni-catalyzed carboboration

Suginome group has described several examples of Ni-catalyzed carboboration reactions. In 2005, they performed intramolecular *trans*-alkynylboration of alkynes *via* activation of a B–Cl bond.[267] The catalytic system requires Ni(0) precatalyst, phosphine ligands and alkynylstannanes reagents as organic group donor (**Scheme 5.2**).

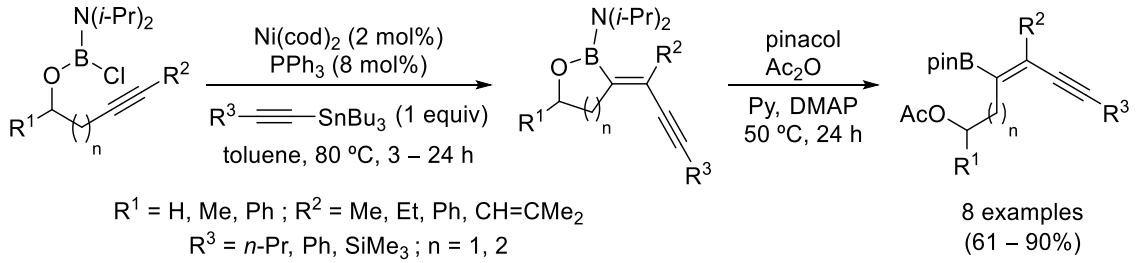

Scheme 5.2. Ni-catalyzed alkynylboration of alkynes.

The proposed mechanism starts with the oxidative addition of the B–Cl bond to Ni(0) complex, followed by insertion of the triple bond into the Ni–B bond in a *cis*-addition manner. Then, a *cis* to *trans* isomerization (regarding the relative position of Ni and B atoms) takes place probably due to the considerable steric repulsion of the *iso*-propyl groups on the nitrogen atom. The resultant *trans*-alkenyl-Ni complex, which was characterized by X-ray spectroscopy, undergoes transmetalation with the organotin reagent to afford the carboboration product by a final reductive elimination stage (**Figure 5.2**).

[267] A. Yamamoto, M. Suginome, *J. Am. Chem. Soc.* **2005**, *127*, 15706–15707.

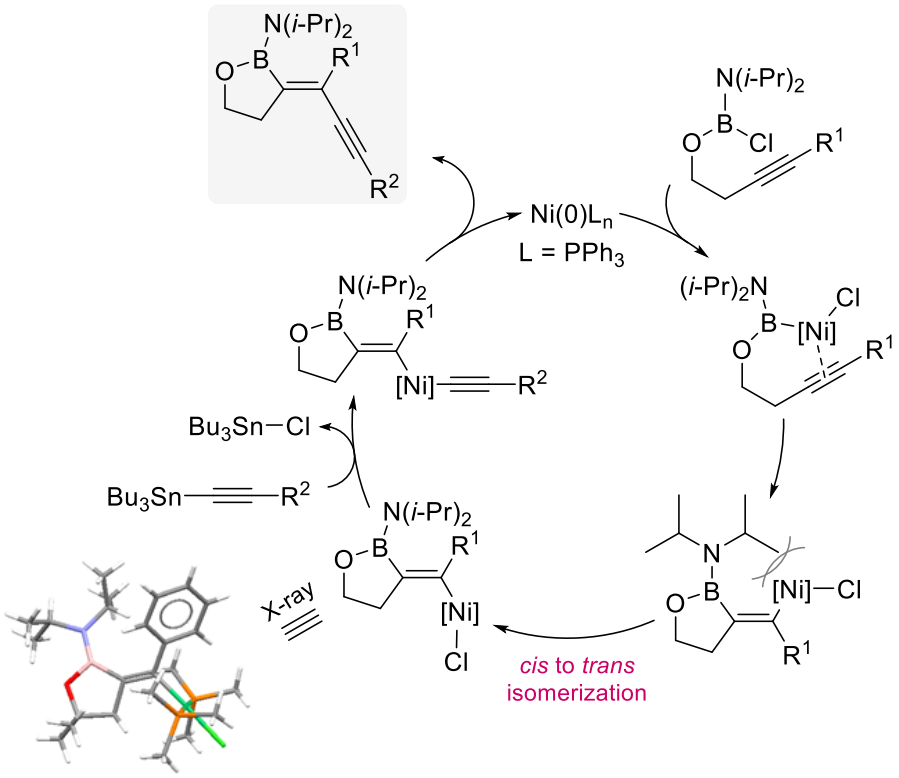

Figure 5.2. Proposed mechanism for the Ni-catalyzed alkynylboration of alkynes.

Subsequent studies broadened this methodology by using alkenylstannane and organozirconium reagents, obtaining *trans*-carboboration in all cases as well.[268]

In 2006, they performed the Ni-catalyzed carboboration of alkynes by a direct activation of the C–B bond of alkynylboronates (**Scheme 5.3**).[269] The reaction mechanism is not clear, but they assume that the reaction may proceed through oxidative addition of the C–B bond to the starting Ni(0) complex.

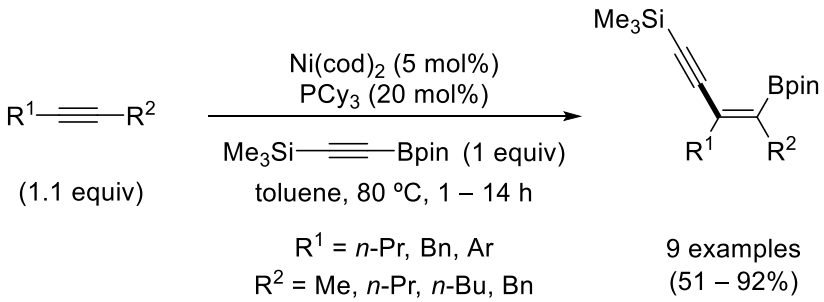

Scheme 5.3. Ni-catalyzed carboboration of alkynes.

Cheng and co-workers have rencently developed a three-component system for the Ni-catalyzed borylative coupling of alkynes and enones.[270] This methodology affords alkenylboronates with high yields in a regio- and stereoselective manner (**Scheme 5.4**).

[268] M. Daini, A. Yamamoto, M. Suginome, *Asian J. Org. Chem.* **2013**, *2*, 968–976.
[269] M. Suginome, M. Shirakura, A. Yamamoto, *J. Am. Chem. Soc.* **2006**, *128*, 14438–14439.
[270] S. Mannathan, M. Jeganmohan, C.-H. Cheng, *Angew. Chem. Int. Ed.* **2009**, *48*, 2192–2195.

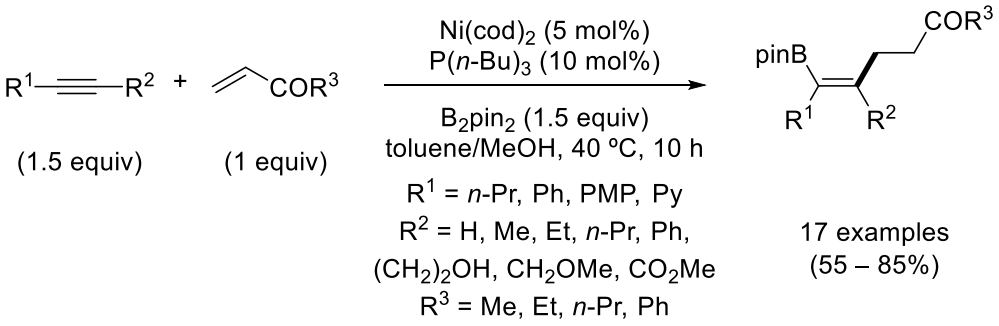

Scheme 5.4. Ni-catalyzed borylative coupling of alkynes and enones.

A possible catalytic reaction mechanism for this reaction is shown in **Figure 5.3**. Chemoselective coordination of the alkyne and enone to the initial Ni(0) complex takes place, followed by a regioselective oxidative metalation step. The resulting nickelacyclopentene is protonated by reaction with MeOH to afford an alkenyl-Ni(II) intermediate, which undergoes transmetalation with B_2pin_2. Finally, reductive elimination yields the observed borylated compound and regenerates the active Ni(0) catalyst. However, an alternative mechanism involving oxidative addition of the diboron compound to Ni(0), sequential insertion of both the alkyne and the enone into the Ni–B bonds and a final protonation by MeOH cannot be ruled out.

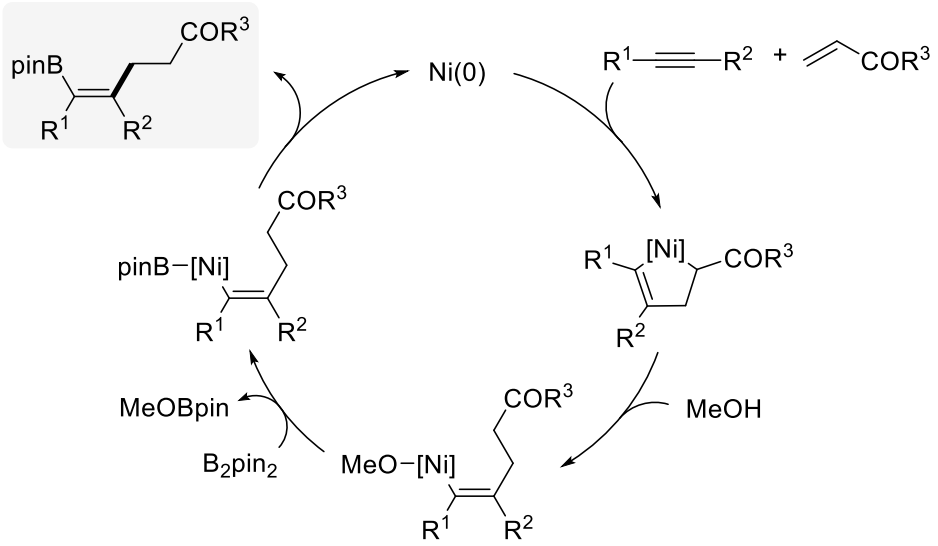

Figure 5.3. Proposed mechanism for three-component system Ni-catalyzed carboboration.

A different approach for the development of carboboration reaction of unsaturated species is based on the ability of Ni complexes to activate C–X bonds (X = Cl, Br, I or OTs). Thus, Semba and Nakao described a cooperative Ni/Cu catalysis for the carboboration of activated alkenes, such us styrene derivatives, where it is demonstrated both metals are required for the reaction to take place (**Scheme 5.5**).[271]

[271] K. Semba, Y. Ohtagaki, Y. Nakao, *Org. Lett.* **2016**, *18*, 3956–3959.

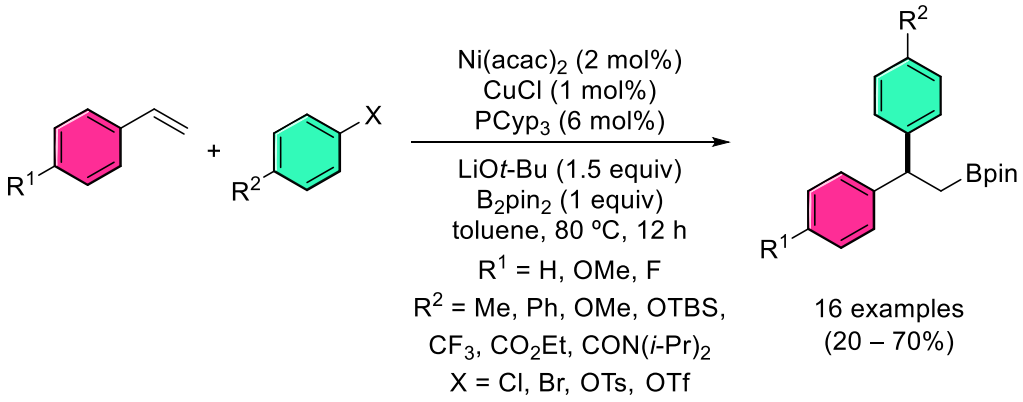

Scheme 5.5. Dual Ni/Cu-catalyzed carboboration of activated alkenes.

The reaction mechanism starts with oxidative addition of ArX to *in situ* generated Ni(0) complex. Transmetalation between the resultant Ni(II) complex and alkylcopper, which should be generated from borylcupration of the alkene in the Cu cycle, followed by reductive elimination would afford the observed product and regenerate the catalytically active Ni(0) species from the Ni cycle (**Figure 5.4**).

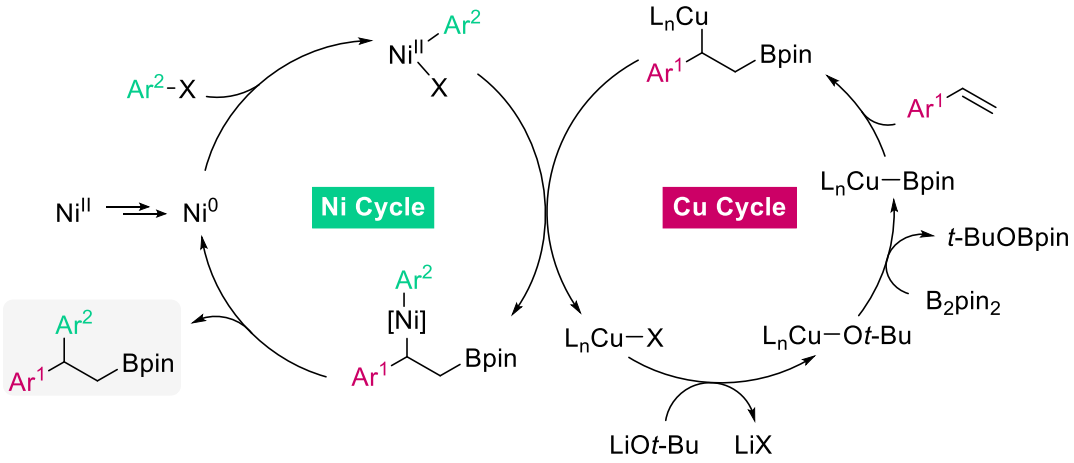

Figure 5.4. Plausible mechanism for the Ni/Cu-catalyzed carboboration of activated alkenes.

Few years later, Brown described a complementary methodology for the carboboration of unactivated alkenes with bromoarenes, but in this case, only a Ni-based complex (without external ligands) is necessary for the reaction catalysis (**Scheme 5.6**).[272] The reaction shows a broad scope regarding both substrates with moderate yields and excellent diastereoselectivity. The utility of the resulting alkylboronates is also demonstrated.

[272] K. M. Logan, S. R. Sardini, S. D. White, M. K. Brown, *J. Am. Chem. Soc.* **2018**, *140*, 159–162.

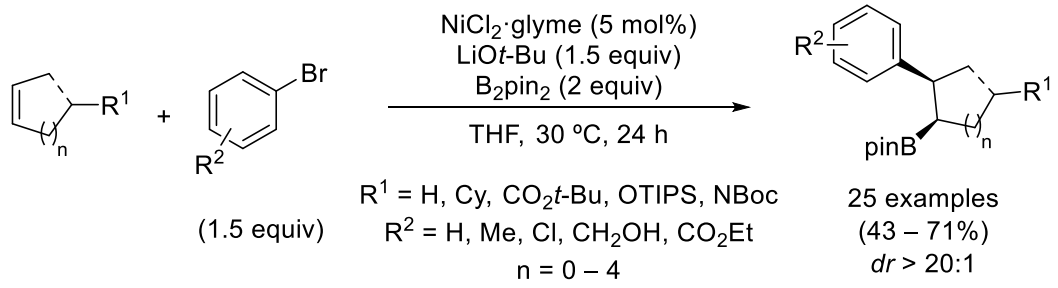

Scheme 5.6. Ni-catalyzed carboboration of unactivated alkenes.

Based on mechanistic experiments, authors proposed the mechanism begins with the formation of a boryl-Ni complex, which can undergo insertion of the alkene into the Ni–B bond, followed by reaction with bromoarene to close the catalytic cycle and afford the observed product (**Figure 5.5**).

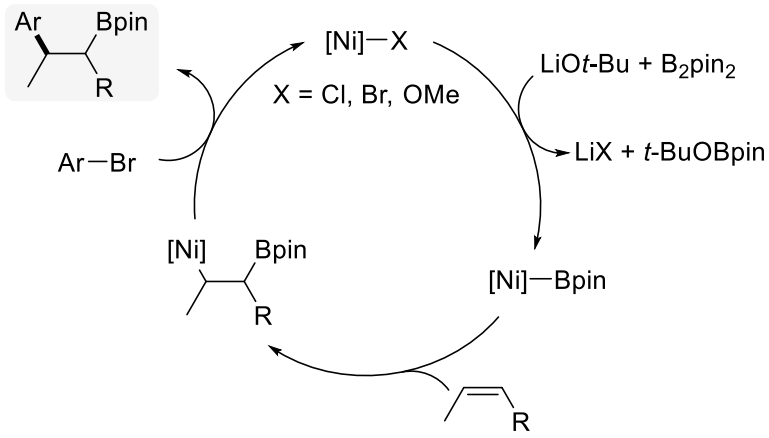

Figure 5.5. Possible catalytic cycle for Ni-catalyzed carboboration of alkenes.

A subsequent study expands the reaction scope to monosubstituted and 1,1-disubstituted alkenes.[273] Very similar reaction conditions are used, but the addition of 20 equivalents of DMA is required, for both suppressing the formation of regioisomers and enhancing the desired product yield (**Scheme 5.7**).

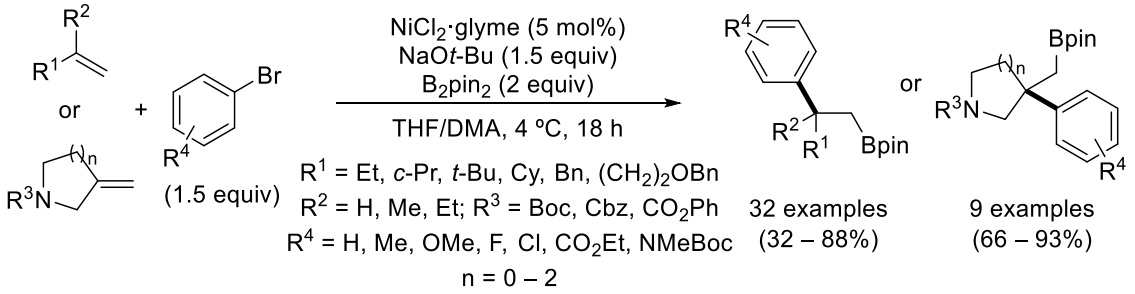

Scheme 5.7. Ni-catalyzed arylboration of unactivated alkenes.

[273] S. R. Sardini, A. L. Lambright, G. K. Trammel, H. M. Omer, P. Liu, M. K. Brown, *J. Am. Chem. Soc.* **2019**, *141*, 9391–9400.

Mechanistic studies were performed using both computational and experimental techniques, supporting a Ni(I)/Ni(III) catalytic cycle where an oxidative addition of bromoarene to an alkenyl-Ni intermediate takes place (**Figure 5.6**).

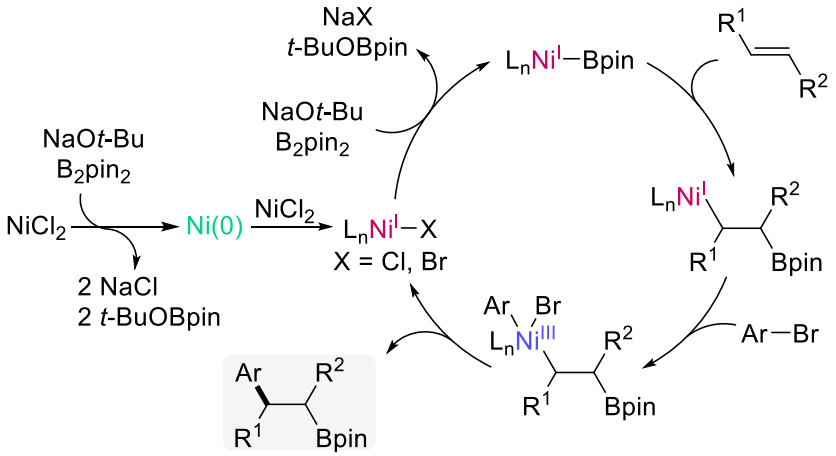

Figure 5.6. Proposed Ni(I)/Ni(III) catalytic cycle.

Furthermore, Brown described the Ni-catalyzed arylboration reaction of a wide range of trisubstituted alkenes, affording one single diastereomer in good yields (top, **Scheme 5.8**).[274] In addition, a regiodivergent arylboration of 1,2-disubstituted alkenylarenes is observed depending on the reaction solvent (bottom). A similar Ni(I)/Ni(III) catalytic cycle to that proposed by the same authors seems to take place in this reaction.

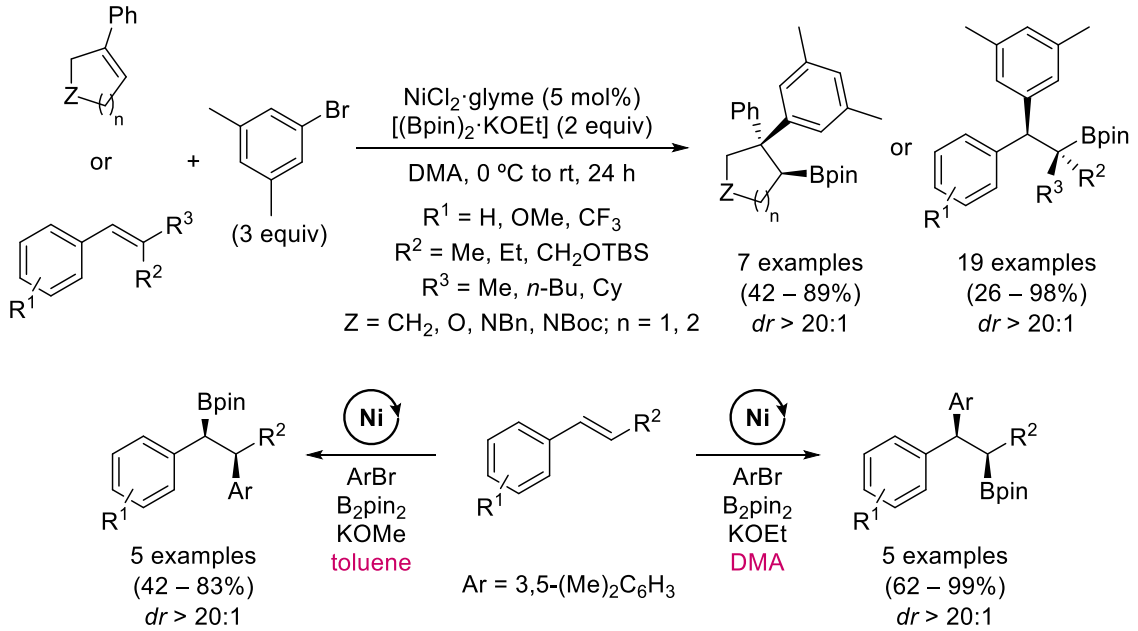

Scheme 5.8. Ni-catalyzed arylboration of trisubstituted alkenes (top) and regiodivergent arylboration of 1,2-substituted alkenylarenes (bottom).

Very recently, Yin and co-workers have studied the Ni-catalyzed migratory arylboration of styrene derivatives, leading to primary alkylboronates where the carbon moiety is incorporated in benzylic position (**Scheme 5.9**).[275] The catalytic system employs a non

[274] L.-A. Chen, A. R. Lear, P. Gao, M. K. Brown, *Angew. Chem. Int. Ed.* **2019**, *58*, 10956–10960.
[275] W. Wang, C. Ding, Y. Li, Z. Li, Y. Li, L. Peng, G. Yin, *Angew. Chem. Int. Ed.* **2019**, *58*, 4612–4616.

common nitrogen bis(chelate) ligand, but it tolerates several functional groups and performs the reaction with good yields in most cases. A similar reaction mechanism to that proposed by Brown seems to take place in this methodology, including a reversible chain-walking process prior to the reductive elimination step.

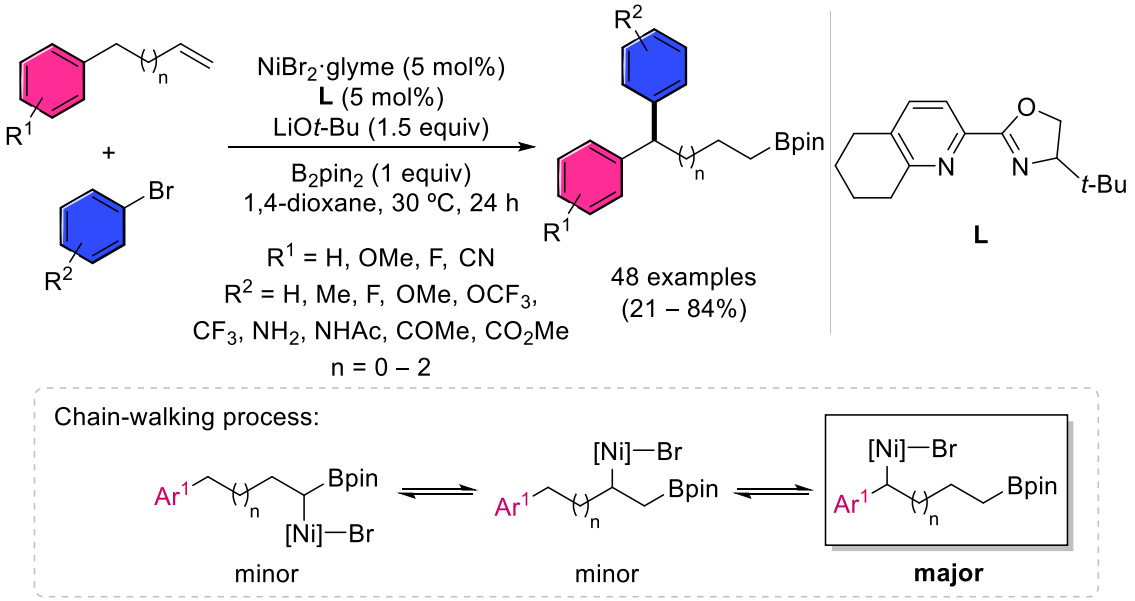

Scheme 5.9. Ni-catalyzed migratory carboboration of alkenes.

Furthermore, Ni-catalyzed 1,1-carboboration have been also described by Yin and co-workers.[276] They found that Ni(II) complex and pyridyl carboxamide-type ligand enable geminal carboboration of terminal alkenes using bromoalkene derivatives (**Scheme 5.10**). The same reaction pathway than the previous study is proposed, being favored the 1,2-nickel migration (left structure in **Scheme 5.9**).

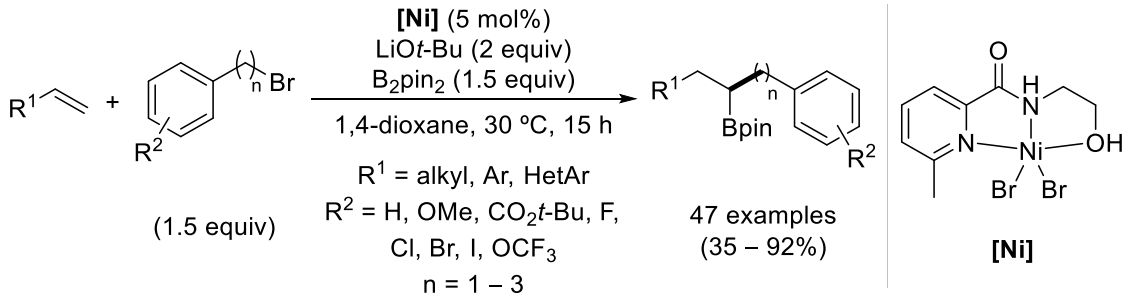

Scheme 5.10. Ni-catalyzed 1,1-carboboration of alkenes.

3.5.1.3. Cu-catalyzed carboboration

During the last decades, a huge number of Cu-catalyzed carboboration reactions have been described in the literature.[277] These methodologies are based on the inherent reactivity of the β-borylcopper intermediate formed during the Cu-catalyzed hydroboration reactions. Thus, several authors envisaged that the use of a suitable carbon electrophile for trapping the aforementioned Cu complex would lead to a carboboration reaction. A general plausible

[276] Y. Li, H. Pang, D. Wu, Z. Li, W. Wang, H. Wei, Y. Fu, G. Yin, *Angew. Chem. Int. Ed.* **2019**, *58*, 8872–8876.
[277] (a) J. Yun, *Asian J. Org. Chem.* **2013**, *2*, 1016–1025. (b) T. Fujihara, K. Semba, J. Terao, Y. Tsuji, *Catal. Sci. Technol.* **2014**, *4*, 1699–1709. (c) Y. Shimizu, M. Kanai, *Tetrahedron Lett.* **2014**, *55*, 3727–3737.

reaction mechanism for this process is shown in **Figure 5.7**, where the borylcupration step of unsaturated species triggers the reaction. Generally, NHC and phosphine ligands are commonly employed for these transformations.

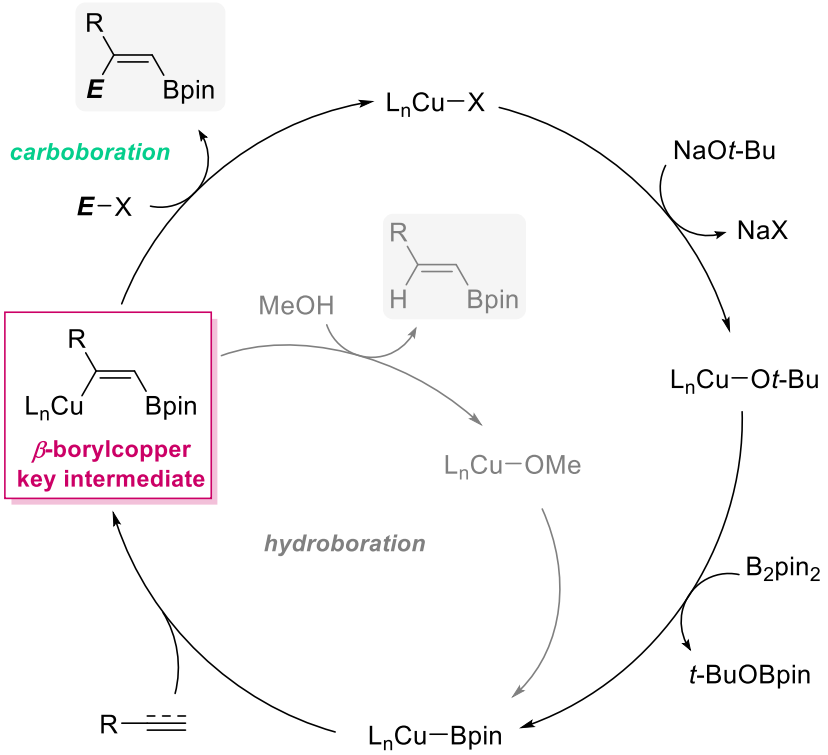

Figure 5.7. Proposed mechanism for Cu-catalyzed carboboration reactions.

In 2012, Tortosa described the first example of Cu-catalyzed carboboration of alkynes, leading to the synthesis of tri- and tetrasubstituted vinylboronates.[278] This novel methodology proceeds with high regioselectivity and *syn*-stereoselectivity, affording the methylboration of both terminal and internal alkynes in high yields (**Scheme 5.11**). In addition, allyl iodide and benzyl bromide were used as carbon electrophiles for the carboboration reaction.

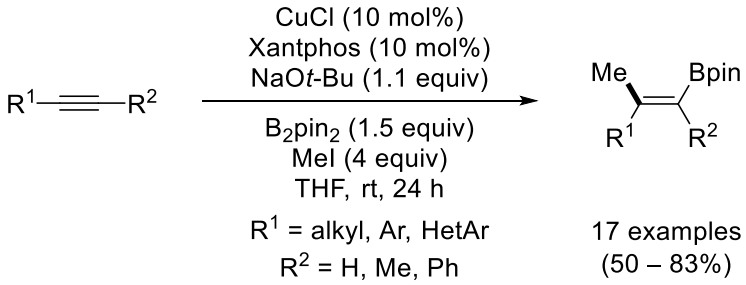

Scheme 5.11. Cu-catalyzed carboboration of alkynes described by Tortosa.

Following studies described different reaction conditions for the methylboration of alkynes, comprising a regioselective (NHC)Cu-catalyzed reaction in air,[194] an inter- and intramolecular methodology where the (NHC)Cu(I) complex is deeply encapsulated in the cavity of a

[194] Y. D. Bidal, F. Lazreg, C. S. J. Cazin, *ACS Catal.* **2014**, *4*, 1564–1569.
[278] R. Alfaro, A. Parra, J. Alemán, J. L. García Ruano, M. Tortosa, *J. Am. Chem. Soc.* **2012**, *134*, 15165–15168.

cyclodextrin[279] and an efficient ligand-free system.[280] Likewise, an enantiomeric version of the Cu-catalyzed methylboration of alkenes has been accomplished, showing its utility in drug synthesis.[281]

Independently, Yoshida and co-workers developed a three-component Cu-catalyzed system for the carboboration of alkynes[282] and alkenes.[283] In particular, phosphine ligand or NHC-based catalyst are required for the borylative coupling of alkynes or alkenes, respectively, with benzyl chlorides (**Scheme 5.12**).

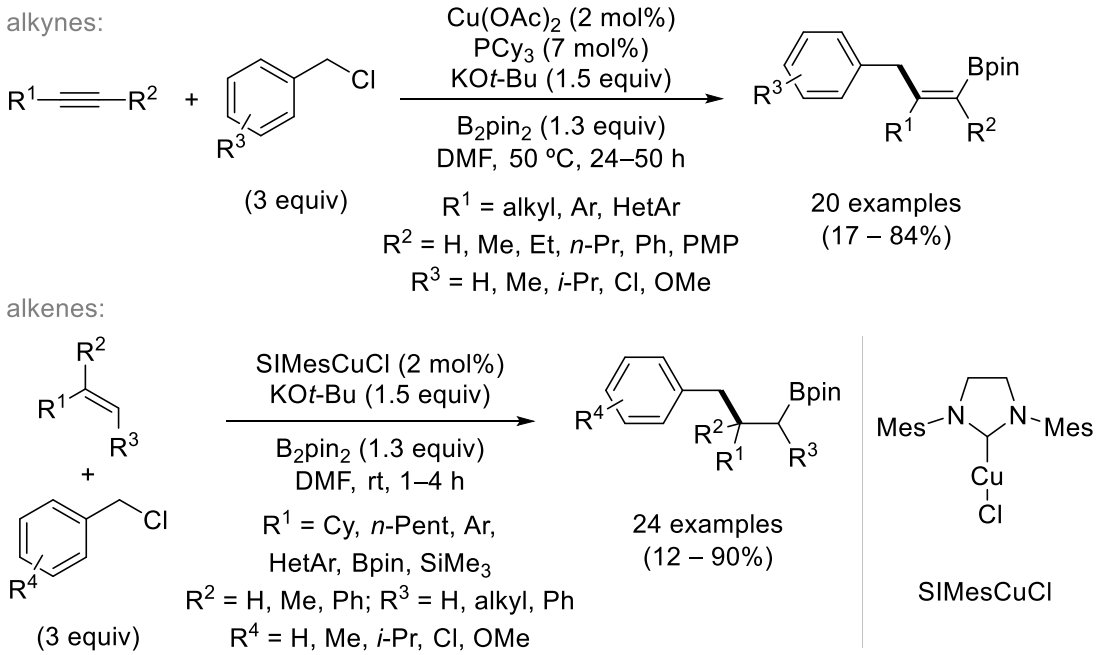

Scheme 5.12. Cu-catalyzed carboboration of alkenes and alkynes.

Additionally, they described alkylboration of alkenes with unsymmetrical diboron reagent (pinB–Bdan), where the Bdan moiety is sole, regioselectively installed into terminal carbon (**Scheme 5.13**).[284]

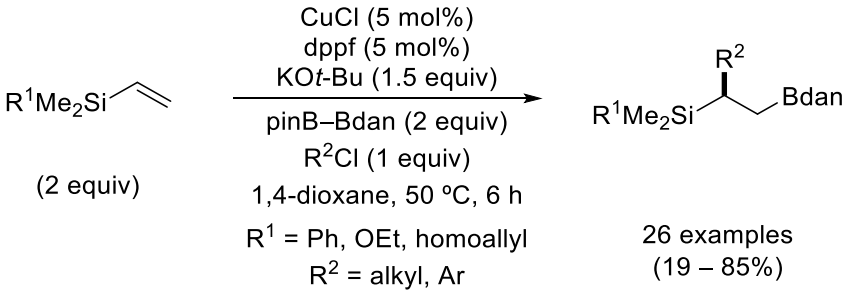

Scheme 5.13. Cu-catalyzed carboboration of alkenes with pinB–Bdan.

[279] Z. Wen, Y. Zhang, S. Roland, M. Sollogoub, *Eur. J. Org. Chem.* **2019**, 2682–2687.
[280] S. Liu, X. Zeng, B. Xu, *Adv. Synth. Catal.* **2018**, *360*, 3249–3253.
[281] B. Chen, P. Cao, Y. Liao, M. Wang, J. Liao, *Org. Lett.* **2018**, *20*, 1346–1349.
[282] H. Yoshida, I. Kageyuki, K. Takaki, *Org. Lett.* **2013**, *15*, 952–955.
[283] I. Kageyuki, H. Yoshida, K. Takaki, *Synthesis* **2014**, *46*, 1924–1932.
[284] I. Kageyuki, I. Osaka, K. Takaki, H. Yoshida, *Org. Lett.* **2017**, *19*, 830–833.

In 2016, Kanai group reported Cu-catalyzed regio- and stereoselective alkylboration of dialkylsubstituted internal alkynes by the design of a π-accepting (NHC)Cu catalyst, obtaining alkenylboronates in high yields (**Scheme 5.14**).[285]

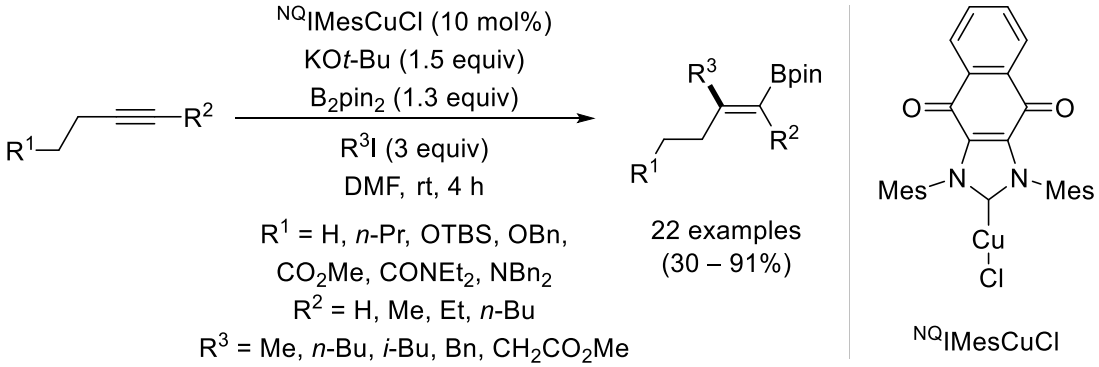

Scheme 5.14. Cu-catalyzed alkylboration of dialkylsubstituted alkynes.

A diastereoselective version of this reaction was described by Zhong.[286] This system allows the allylboration of α,β-unsaturated carboxylic esters to produce well-defined quaternary centers (**Scheme 5.15**).

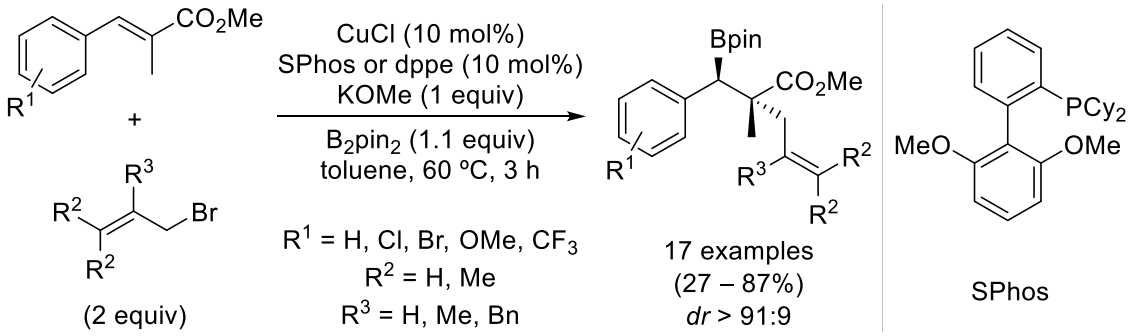

Scheme 5.15. Cu-catalyzed diastereoselective allylboration.

Arylboration of alkynes has also been accomplished. Thus, Brown applied the conditions of his Cu-catalyzed cross-coupling of boronic esters and aryl iodides to perform the carboboration of internal alkynes with high yields and regioselectivity (**Scheme 5.16**).[287]

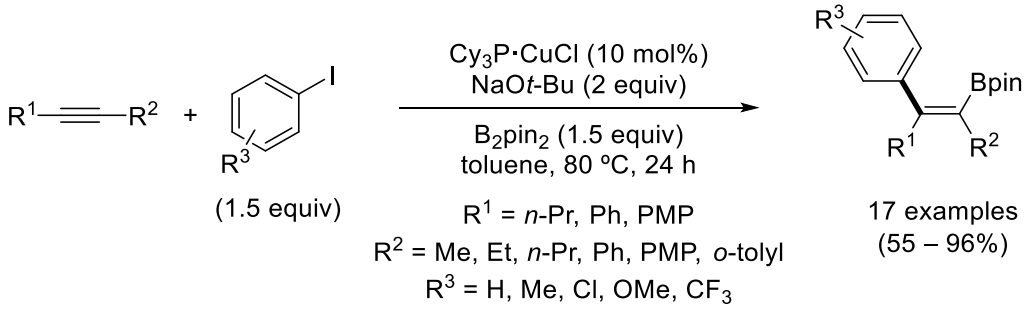

Scheme 5.16. Cu-catalyzed arylboration of alkynes.

[285] T. Itoh, Y. Shimizu, M. Kanai, *J. Am. Chem. Soc.* **2016**, *138*, 7528–7531.
[286] Y.-J. Zuo, Z. Zhong, Y. Fan, X. Li, X. Chen, Y. Chang, R. Song, X. Fu, A. Zhang, C.-M. Zhong, *Org. Biomol. Chem.* **2018**, *16*, 9237–9242.
[287] Y. Zhou, W. You, K. B. Smith, M. K. Brown, *Angew. Chem. Int. Ed.* **2014**, *53*, 3475–3479.

Fu, Xiao and co-workers also contributed to this kind of reaction by describing ligand-controlled regiodivergent systems for the alkylboration of terminal alkenes[288] and alkynes.[289] Suitable tuning of the ligand properties allows the synthesis of both Markovnikov and *anti*-Markovnikov products (**Scheme 5.17**). Further mechanistic studies show that the regioselectivity-determining step is the migratory insertion of the olefin in both cases. For alkenes, the steric hindrance of Xantphos ligand triggers the *anti* or *syn* addition of the double bond.[290] In the case of alkynes, the *anti*-Markovnikov regioselectivity is due to the steric effect of the bulky dppbz ligand. In contrast, electronic effect becomes the main factor of selectivity with DMAP, because of the strong complexation of DMAP with Cu metal center.[291]

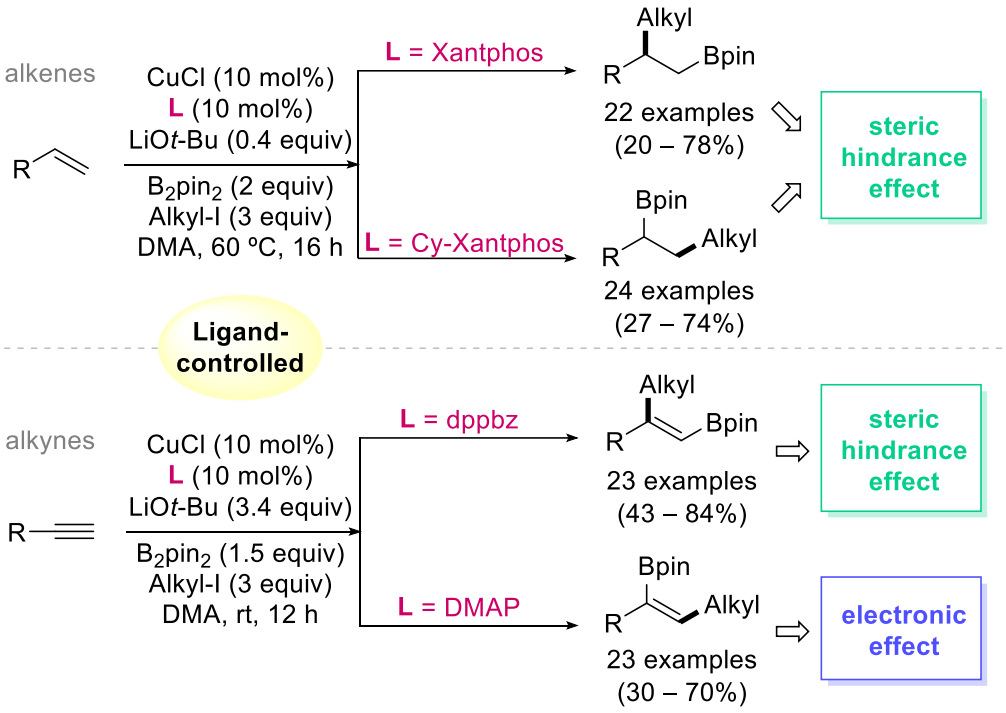

Scheme 5.17. Ligand-controlled regiodivergent Cu-catalyzed carboboration reaction.

Another interesting strategy to accomplish the carboboration of unsaturated molecules is based on synergistic catalysis of Pd/Cu systems. This procedure takes advantage of the reactivity of both metals: copper reacts with boron reagent through formation of the well-known β-borylcopper key intermediate, and palladium catalyzes the cross-coupling step with haloarene. The commonly accepted mechanism for this reaction consists in a dual catalytic cycle as is illustrated in **Figure 5.8**. In most cases, copper catalyst employed NHC ligands and palladium catalysts, phosphine ligands.

[288] W. Su, T.-J. Gong, X. Lu, M.-Y. Xu, C.-G. Yu, Z.-Y. Xu, H.-Z. Yu, B. Xiao, Y. Fu, *Angew. Chem. Int. Ed.* **2015**, *54*, 12957–12961.
[289] W. Su, T.-J. Gong, Q. Zhang, Q. Zhang, B. Xiao, Y. Fu, *ACS Catal.* **2016**, *6*, 6417–6421.
[290] Z.-Y. Xu, Y.-Y. Jiang, W. Su, H.-Z- Yu, Y. Fu, *Chem. Eur. J.* **2016**, *22*, 14611–14617.
[291] Q. Zhang, M. Li, J.-Q. Liu, H.-Z Yu, *J. Organomet. Chem.* **2018**, *871*, 48–55.

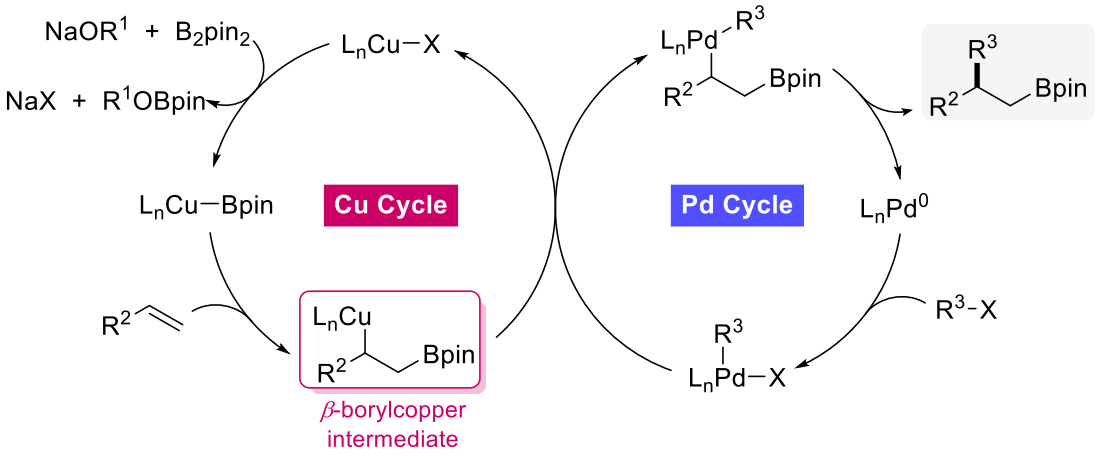

Figure 5.8. General mechanism for Pd/Cu cooperative catalysis.

It is noteworthy to mention the different studies reported by Brown,[292] Semba and Nakao[293] groups. They described numerous 1,2- and 1,1-arylboration of alkenes, alkynes and dienes in a regio-, enantio- and diastereoselective manner, synthesizing versatile organoboronates in good to high yields (**Scheme 5.18**).

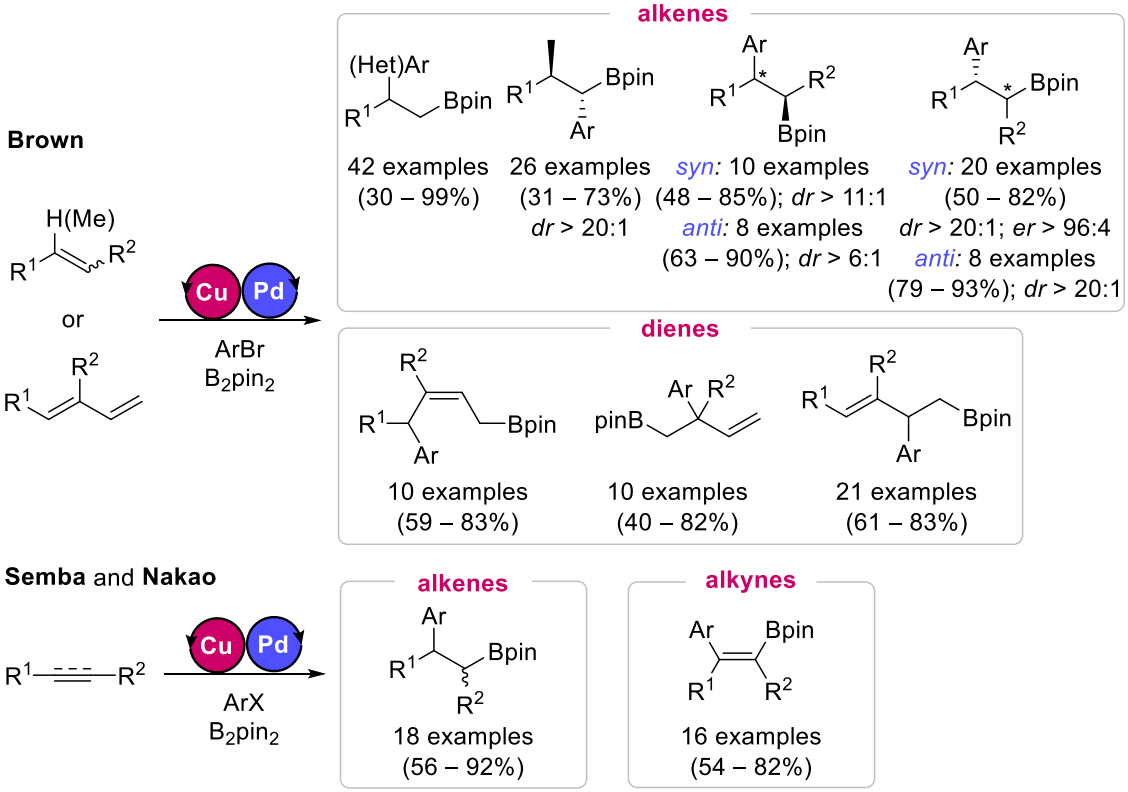

Scheme 5.18. Pd/Cu-catalyzed carboboration reactions.

[292] (a) K. B. Smith, K. M. Logan, W. You, M. K. Brown, *Chem. Eur. J.* **2014**, *20*, 12032–12036. (b) K. M. Logan, K. B. Smith, M. K. Brown, *Angew. Chem. Int. Ed.* **2015**, *54*, 5228–5231. (c) K. B. Smith, M. K. Brown, *J. Am. Chem. Soc.* **2017**, *139*, 7721–7724. (d) S. R. Sardini, M. K. Brown, *J. Am. Chem. Soc.* **2017**, *139*, 9823–9826. (e) K. M. Logan, M. K. Brown, *Angew. Chem. Int. Ed.* **2017**, *56*, 851–855. (f) A. M. Bergmann, S. K. Dorn, K. B. Smith, K. M. Logan, M. K. Brown, *Angew. Chem. Int. Ed.* **2019**, *58*, 1719–1723. (g) Y. Huang, M. K. Brown, *Angew. Chem. Int. Ed.* **2019**, *58*, 6048–602.

[293] (a) K. Semba, Y. Nakao, *J. Am. Chem. Soc.* **2014**, *136*, 7567–7570. (b) K. Semba, M. Yoshizawa, Y. Ohtagaki, Y. Nakao, *Bull. Chem. Soc. Jpn.* **2017**, *90*, 1340–1343.

Very recently, Lalic carried out the Pd/Cu-catalyzed reductive 1,1-arylboration of alkynes.[294] The catalytic system uses HBpin instead of diboron reagent, leading to the synthesis of alkylboronates in high yields (**Scheme 5.19**).

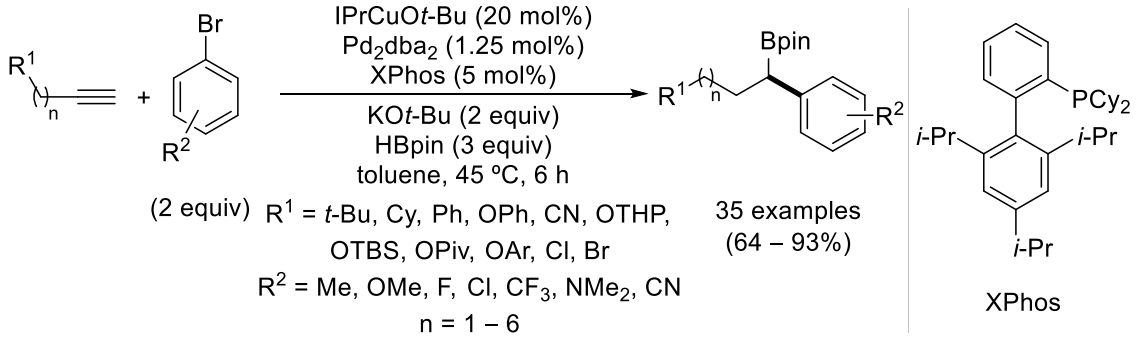

Scheme 5.19. Pd/Cu-catalyzed reductive carboboration described by Lalic.

The proposed reaction pathway for this reaction slightly differs from the general dual catalytic cycle. Authors propose the reaction takes place through a first hydroboration step, followed by a second hydrocupration of the resultant alkenylboronate and a final Pd-catalyzed arylation coupling process (**Figure 5.9**).

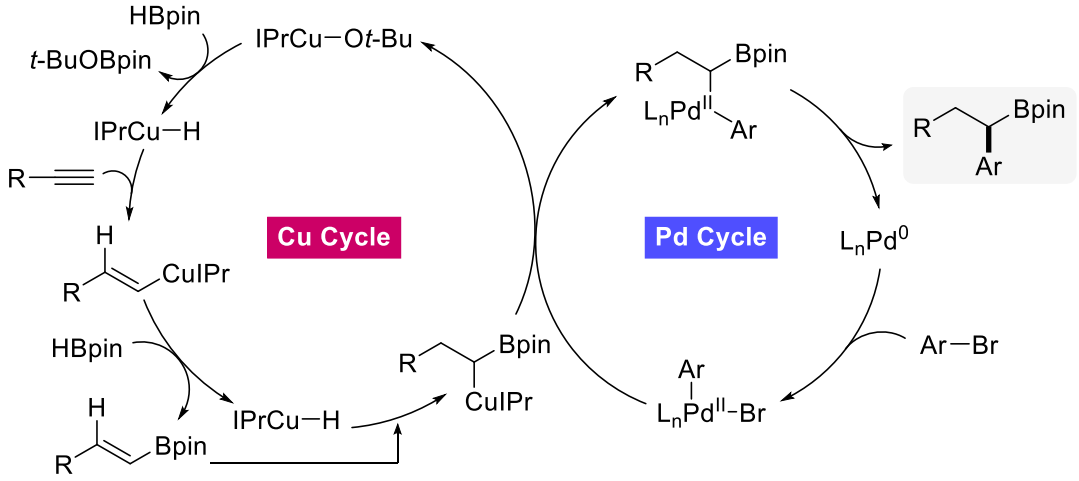

Figure 5.9. Catalytic cycle for Pd/Cu-catalyzed reductive carboboration of alkynes.

[294] M. K. Armstrong, G. Lalic, *J. Am. Chem. Soc.* **2019**, *141*, 6173–6179.

3.5.3. Results

Taking into account the Ni-catalyzed carboboration reaction of alkynes with alkynylboronates described by Suginome (*see* ***Scheme 5.3***), we sought to evaluated such reaction conditions with enynes.

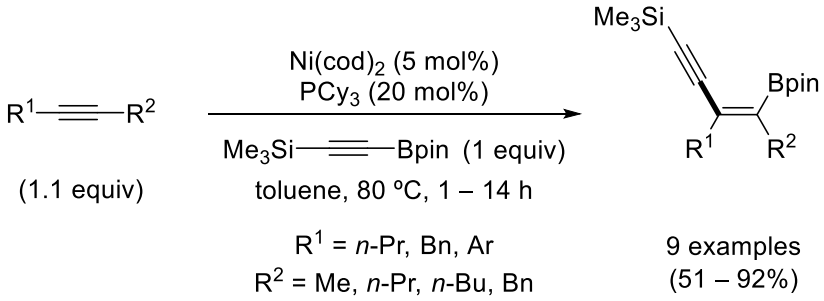

Scheme 5.3. Ni-catalyzed carboboration of alkynes.

Specifically, when unsymmetrical alkynes bearing aromatic and alkylic substituents were evaluated, good regioselectivity was obtained through insertion of Bpin moiety into alkyl-substituted carbon (**Scheme 5.20**).

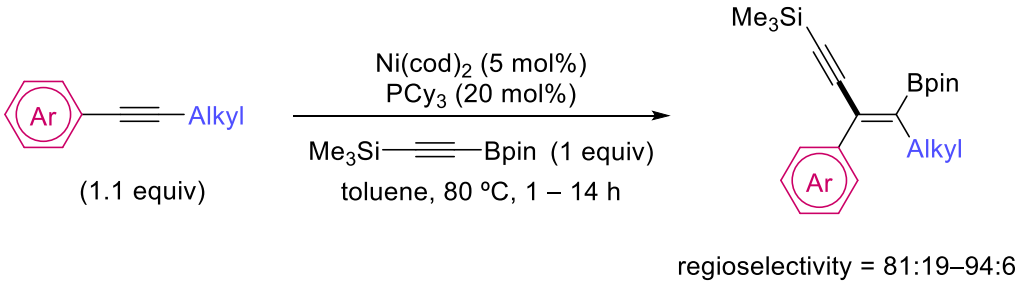

Scheme 5.20. Observed regioselectivity in Suginome method.

Since the reaction is proposed to take place through oxidative addition of C(*sp*)–B bond to the starting Ni(0) complex, we envisioned such a regioselectivity would lead to an alkenyl-Ni intermediate with the ability to perform the cyclization process prior to the borylation step when enynes are used (**Scheme 5.21**).

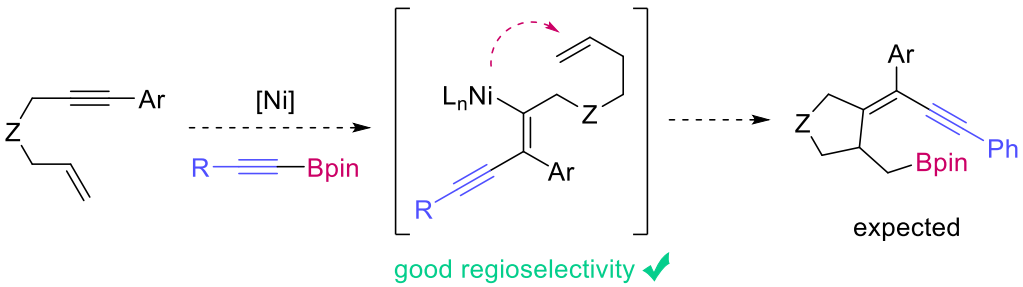

Scheme 5.21. Hypothesis of carboborylative cyclization reaction.

We began our study testing the model enyne **1aa** with (phenylethynyl)boronate (**24**) under described reaction conditions (**Scheme 5.22**), but no borylated compounds were detected. Instead, we observed decomposition of starting enyne.

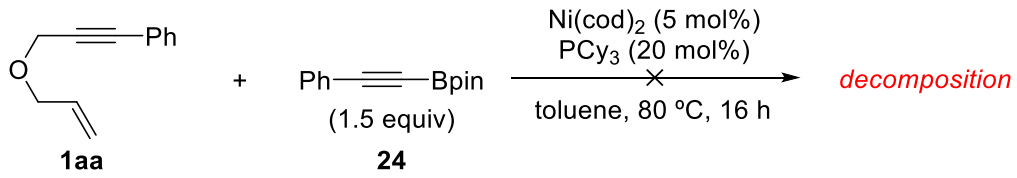

Scheme 5.22. First attempt.

We also tried the reaction by adding the enyne to a $Ni(cod)_2/PCy_3$/**24** mixture in toluene at different rates: (i) rapid addition and (iii) slow addition with a syringe pump for 1.5 h. However, the same decomposed reaction crude was observed.

Then, we evaluated different temperatures, but similar results were obtained (top, **Scheme 5.23**). In addition, we tested a Ni(II) source with several activating agents (bottom). But again, just decomposition of enyne **1aa** was detected.

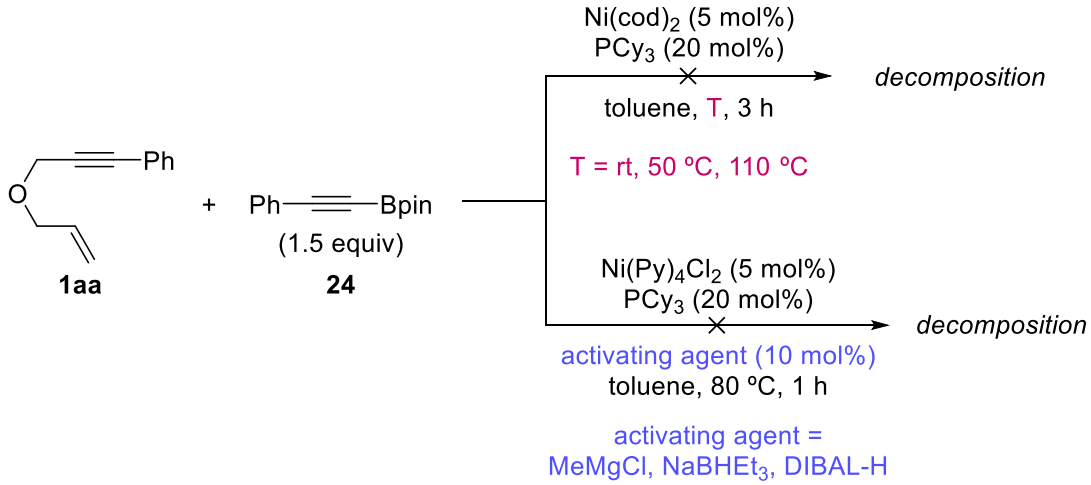

Scheme 5.23. Temperatures and Ni(II) source screening.

Since no borylated derivate could be observed under the described reaction conditions, we decided to evaluate different ligands (**Scheme 5.24**). In most cases, decomposition or unaltered starting enyne were observed. In contrast, when Xantphos was used, we isolated the corresponding propargylic alcohol (derived from enyne **1aa**) and the product derived from allylation of the alkynyl moiety of the starting alkynylboronate **24**.

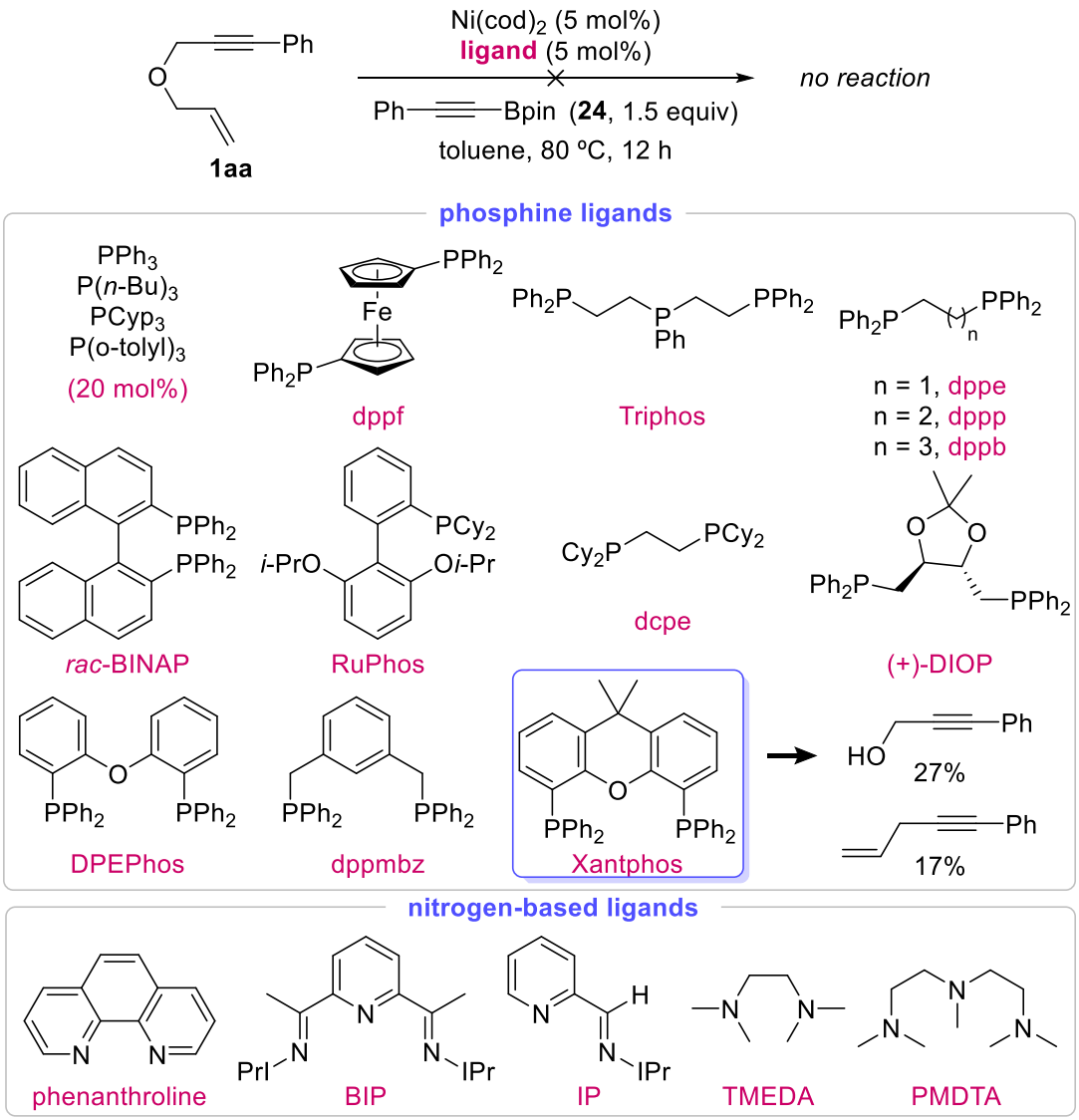

Scheme 5.24. Ligand screening.

These results suggested that the model enyne **1aa** is not a suitable substrate under this reaction conditions, because the C(allyl)–O bond can be activated by Ni catalyst, favoring side reactions instead of the pursued carboborylative cyclization.

Therefore, we evaluated other enynes with different connectors, such as nitrogen-, malonate- and carbon-tethered enynes (**Scheme 5.25**). No reaction was observed in any case. Instead, starting enyne was recovered.

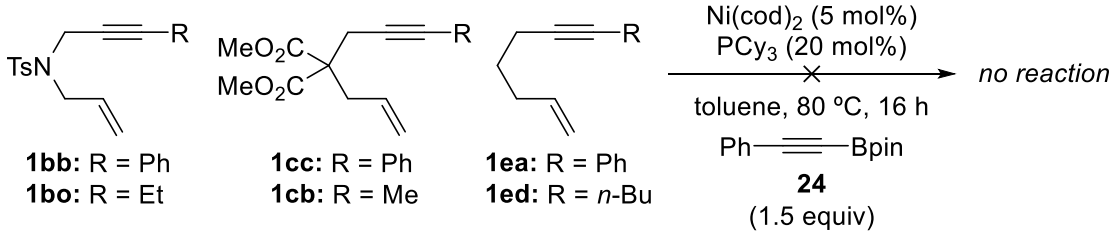

Scheme 5.25. Enynes screening.

Regarding the Suginome method, the alkynylboronate bearing a trimethylsilyl group (**25**) afforded better yields comparing to other tested alkynylboronates. Thus, we moved to evaluate the optimal conditions with this alkynylboronate (**25**) and enyne **1ea**. When the enyne was present in the reaction medium from the beginning, or when it was rapidly added to the mixture of the rest of the reagents, we only observed oligomerization products derived from the enyne. In contrast, slow addition of enyne **1ea** by a syringe pump for 1 h, led to complete suppression of oligomerization, and surprisingly afforded the unexpected compound **26ea** in 82% yield (**Scheme 5.26**). Formation of **26ea** involves the formation of two C–C bonds and one C–B bond in just one synthetic operation, affording a complex fused-bicyclic structure with two non-conjugated double bonds. The expected isomer which would result by carboborylative cyclization similar to those already described (**27ea**) was not detected.

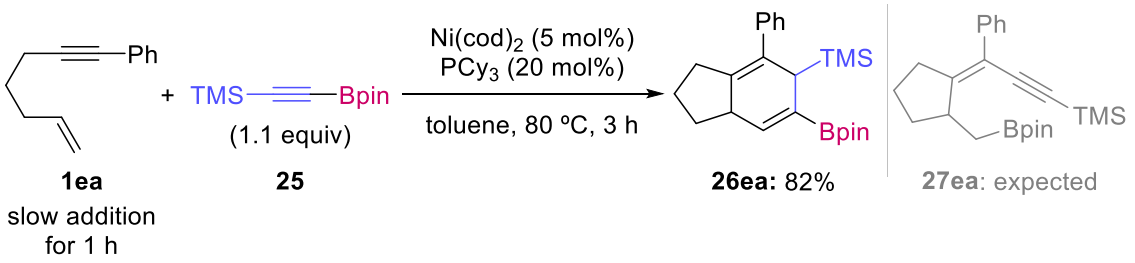

Scheme 5.26. Reaction with enyne **1ea**.

Encouraged by this result, we sought to optimize the reaction yield. Firstly, we tested again several ligands under described reaction conditions by slow addition of enyne **1ea**. However, we cannot improved the reaction yield. In most cases, the reaction did not work (**Scheme 5.27**).

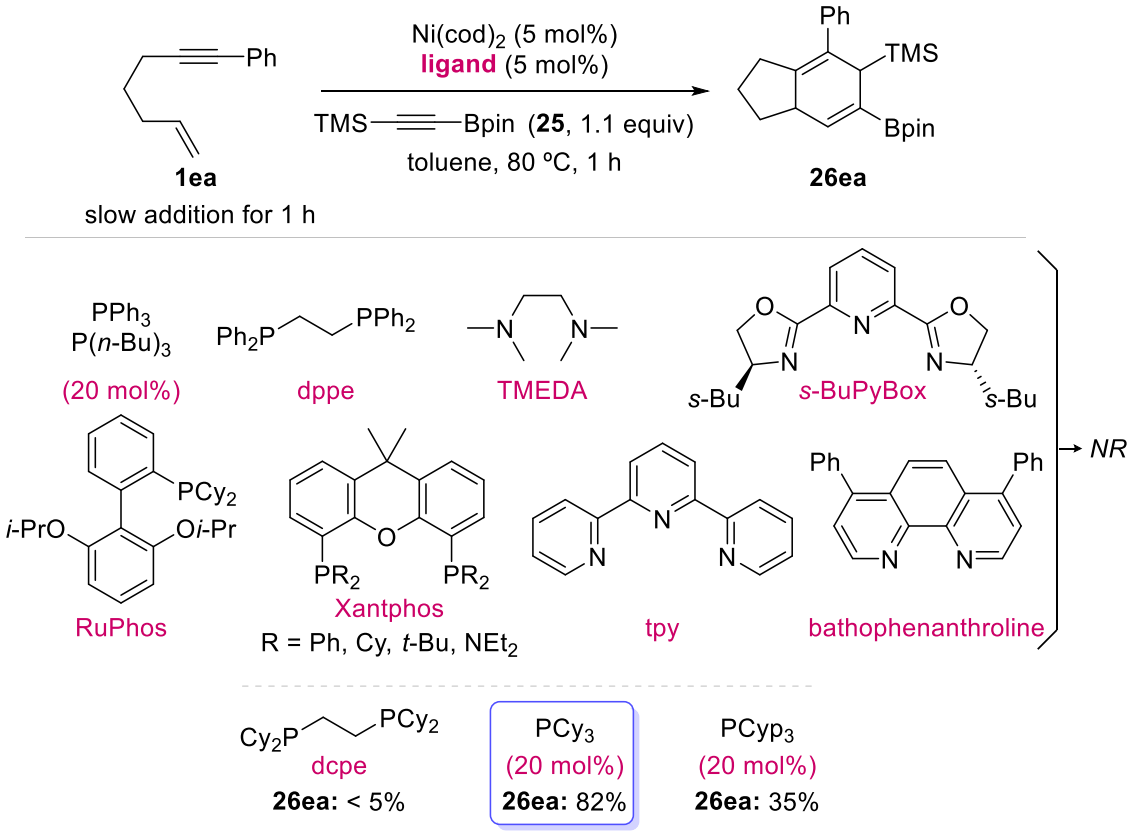

Scheme 5.27. Ligand screening with enyne **1ea**.

Further experimentation using different reaction conditions, such us temperature, rate of addition, Ni/ligand ratio and solvent, was carried out, but neither the yield of **26ea** increased nor other carboborylation products were observed (**Scheme 5.28**). Noticeably, Ni(II) salts were ineffective, and led to recovery of the unaltered starting enyne. Control experiments show that the reaction does not take place in the absence of $Ni(cod)_2$ nor PCy_3.

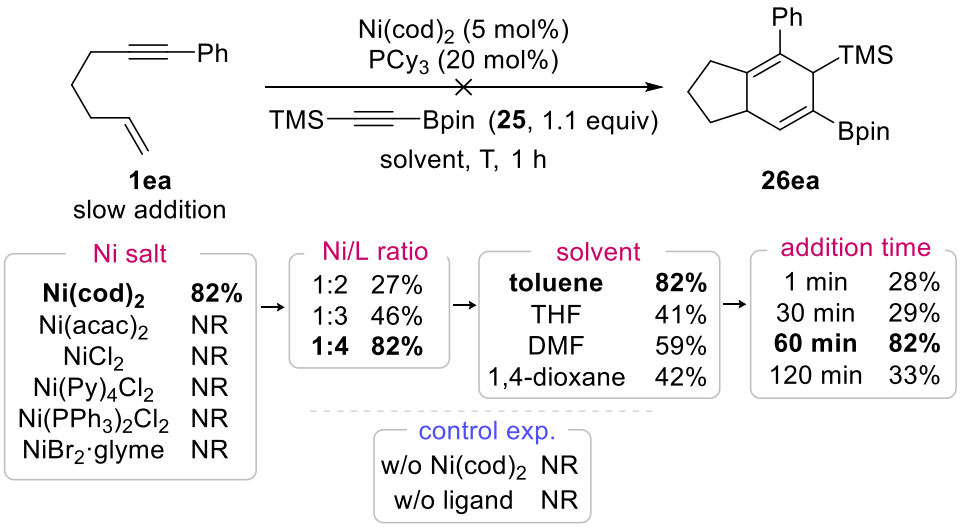

Scheme 5.28. Another parameters optimization.

With the optimal conditions in hand, we evaluated the scope of the reaction (**Scheme 5.29**). The expected isomer (**27**) was not observed in any case. Several 1,6-enynes with both aryl and alkyl-substituted alkynes effectively performed the carboborylative cyclization reaction. The best results were obtained with enynes containing simple alkyl tethering chains (**26ea-ed**) bearing different substituents in the aromatic ring in *para* position (Me and F). Therefore, a quaternary center that would presumably favor the reaction by Thorpe-Ingold effect is not required for the cyclization to occur. Nitrogen- and malonate-tethered substrates also work with good yields (**26bd**, **26ce**), although worse results were obtained for oxygen derivative **26aa** and for the preparation of lactam **26fb**. The latter product allowed us to obtain single crystals that helped us to confirm the observed structure of compounds **26**. Interestingly, single diastereisomers are formed in these compounds, which present two stereogenic centers in 1,4-positions, which suggests a highly stereoselective reaction mechanism. Substrates containing internal alkynes with different distal substituents, such as Me (**26bw**, **26cb**), Et (**26bo**) and Bu (**26bq**, **26ed**), led to the desired products in poor to excellent yields regardless the enyne connector. It is important to note that the longer chain (Bu) derivative affords lower yield in comparison with the ethyl-substituted analogue (22% for **26bq** vs 99% for **26bo**). Enyne **1ba**, bearing a terminal alkyne in the structure gave the reaction in moderate yield (**26ba**). An internal alkene was also evaluated, affording the expected compound **26ci**, albeit in low yield. This method could be also extended to a 1,7-enyne, leading to the formation of two fused 6-membered rings in moderate yield (**26bl**). Finally, substitution in allylic and propargylic positions was evaluated. Thus, enynes **1by** and **1bz** afforded the corresponding compounds **26by** and **26bz**, respectively, in good yields as diastereomeric mixtures. Again, we successfully crystallized compound **26bz** to completely confirm the proposed structure for the fused-bicycle. When we performed the reaction with enyne **1ai**, which has the internal carbon of the alkene substituted with a methyl group, the unreactive starting enyne was recovered.

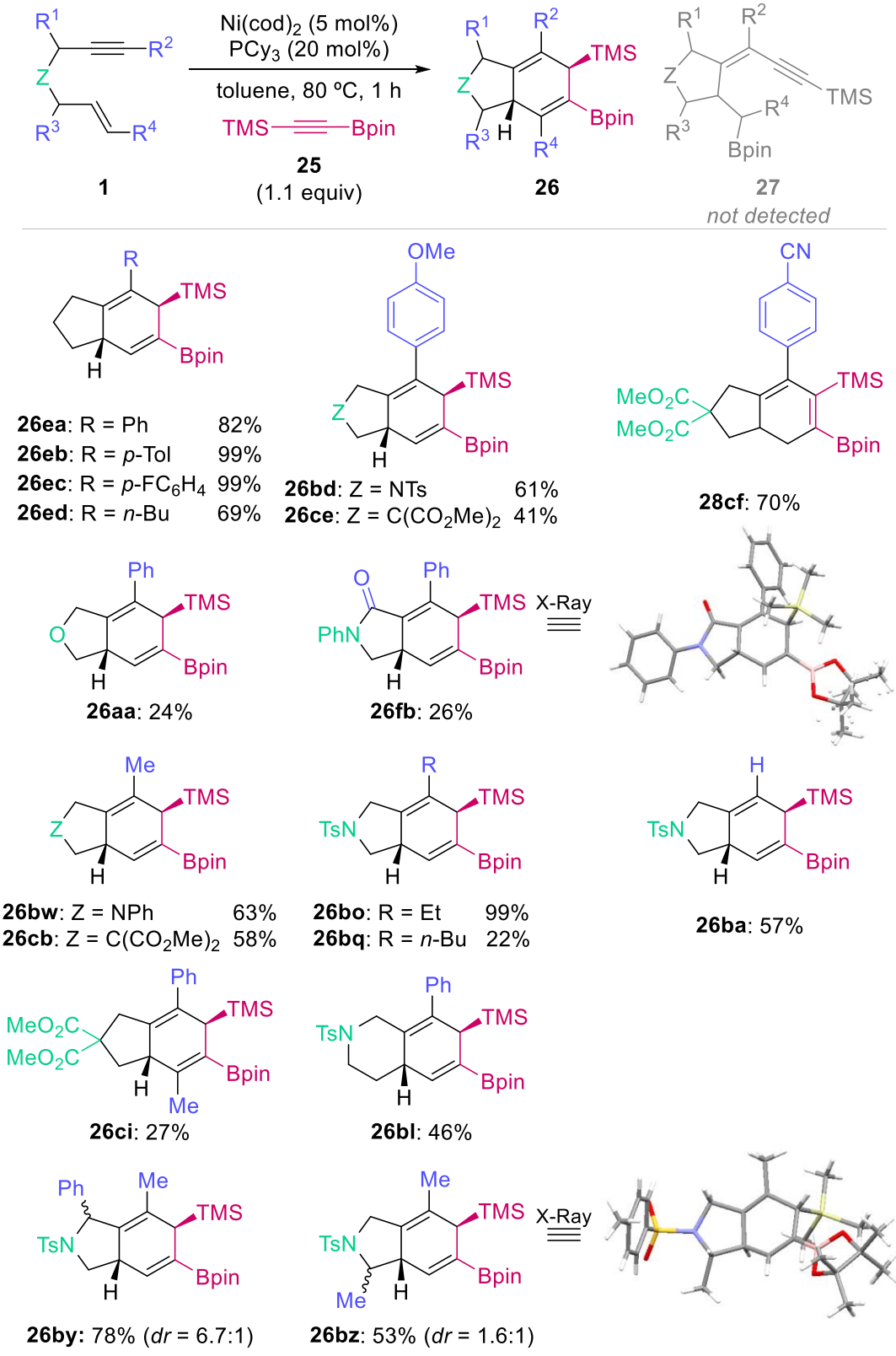

Scheme 5.29. Structural scope.

Noticeably, enyne **1g**, bearing a *p*-CN substituent on the aryl ring, exclusively afforded the conjugated 1,3-diene **28cf** in high yield. Initially, this behavior could result from isomerization of the initial product. In fact, we have observed that compounds **26** are not very stable and tend to evolve through different pathways, involving conjugation of double bonds,

aromatization and deborylative-aromatization of the 6-membered ring, which made difficult their purification and characterization. We were able to identify and characterize some of these products such as **29bd** and **29ea** (**Scheme 5.30**). The former was obtained when we tried to crystallize compound **26bd** under air. Formation of compound **29bd** involves deborylation (probably by hydrolysis) followed by 1,2-migration of TMS. This process has been previously reported in other arylsilanes, and it is proposed to take place through a cationic pathway triggered by protonation of the aromatic ring, which is favored by the stabilizing effect of Si, and driven by the release of steric hindrance.[295]

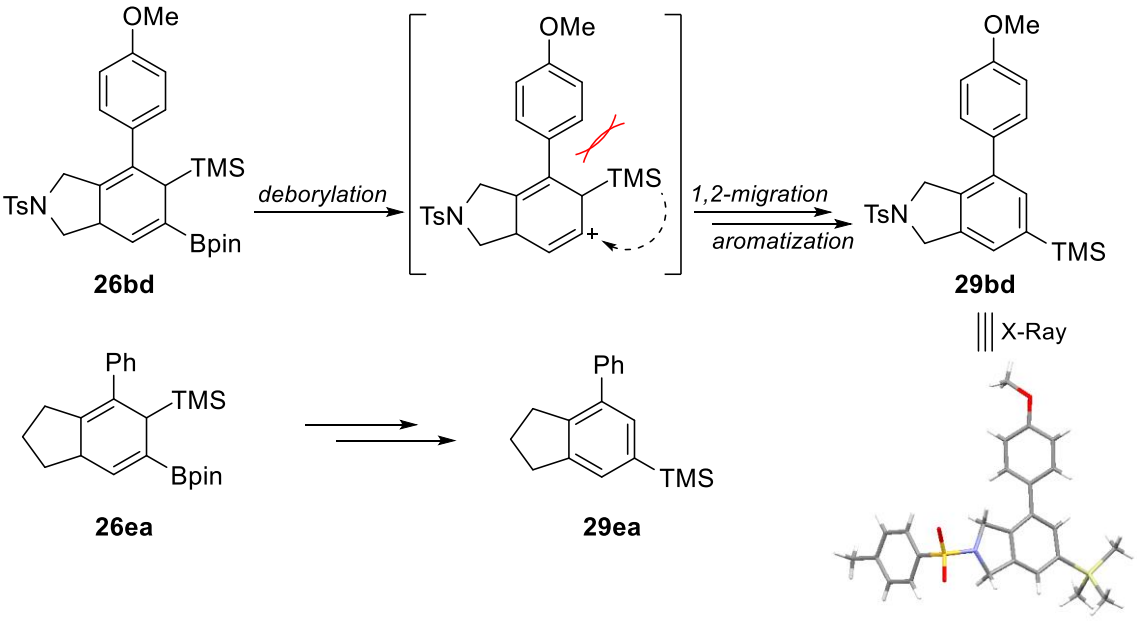

Scheme 5.30. Transformations of compounds **26**.

In contrast to the reactivity observed for the enynes shown above, the reaction of enones **1gb** and **1gc** under similar conditions led to cyclic ketones **30gb** and **30gc**, respectively, in which only the alkyne moiety from the boronate was incorporated to the structure (**Scheme 5.31**).

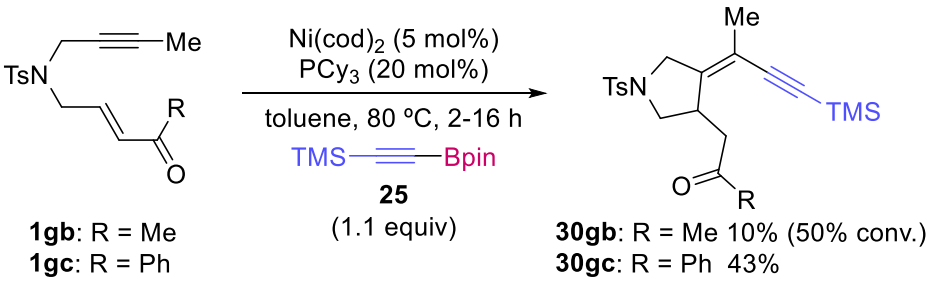

Scheme 5.31. Carbocyclization of enones **1g**.

Although we have no experimental evidence, formation of compounds **30** might take place by generation of a Ni-enolate complex, followed by transmetalation of alkynyl to the metal, insertion of the alkyne into the alkynyl-Ni bond and reductive elimination (left, **Figure 5.10**).[296]

[295] (a) D. Seyferth, D. L. White, *J. Am. Chem. Soc.* **1972**, *94*, 3132–3138. (b) D. Seyferth, S. C. Vick, *J. Organomet. Chem.* **1977**, *141*, 173–187. (c) B. Becker, A. Herman, W. Wojnowski, *J. Organomet. Chem.* **1980**, *193*, 293–297. (d) T. Shimizu, S. Morisako, Y. Yamamoto, A. Kawachi, *Heteroatom Chem.* **2018**, *29*, e21434.
[296] S. Ikeda, Y. Sato, *J. Am. Chem. Soc.* **1994**, *116*, 5975–5976.

An alternative initial C–B bond activation, two subsequent consecutive insertions of the alkyne and alkene, and a final hydrolysis of an intermediate boron enolate during the reaction work-up would also explain these structures (right, **Figure 5.10**). Nevertheless, oxidative addition is not probably operating in this case (see below).

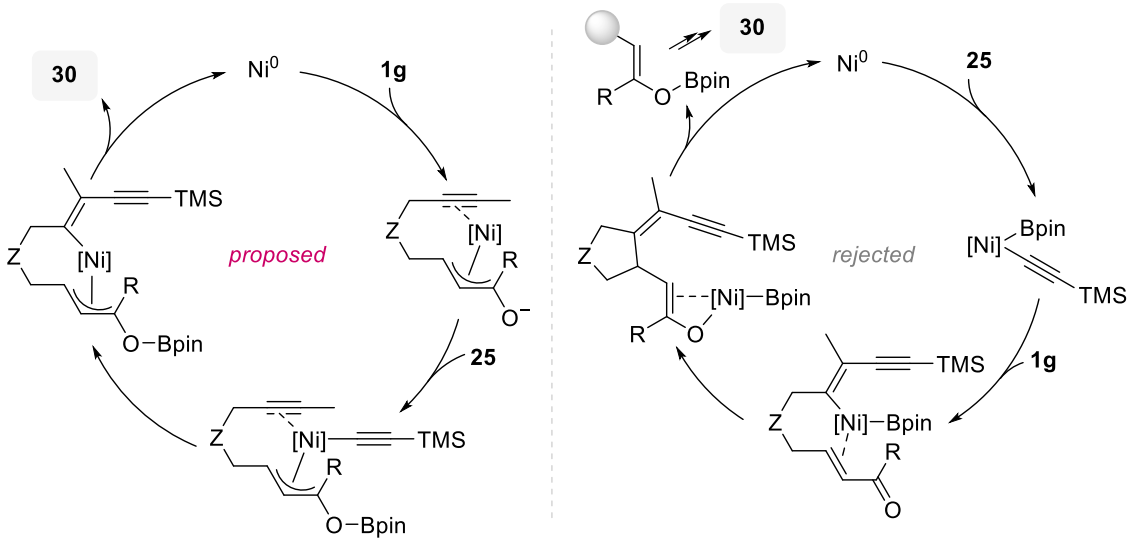

Figure 5.10. Plausible pathways for the formation of **30**.

We tried to extend the reaction to other alkynylboronates, bearing Ph, *p*-Tol or *n*-Hex instead of TMS group. Firstly, we carried out their synthesis as is illustrated in **Scheme 5.32**, affording the expected alkynylboronates in excellent yields.

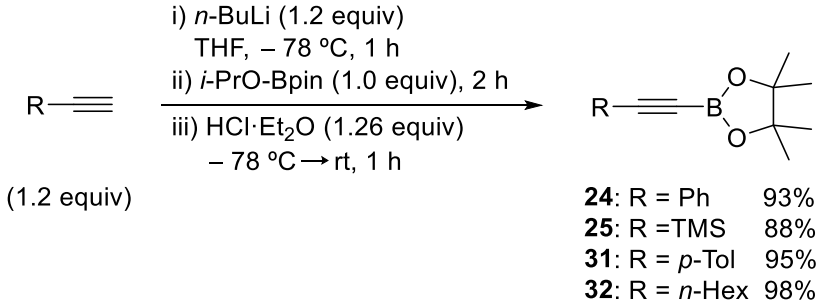

Scheme 5.32. Synthesis of alkynylboronates.

Unfortunately, when we carried out the catalytic reaction with these alkynylboronates, the desired products were not obtained. Although boron and alkyne moieties seem to be incorporated, we observed the formation of complex mixtures of several isomers as well as decomposition products (**Scheme 5.33**).

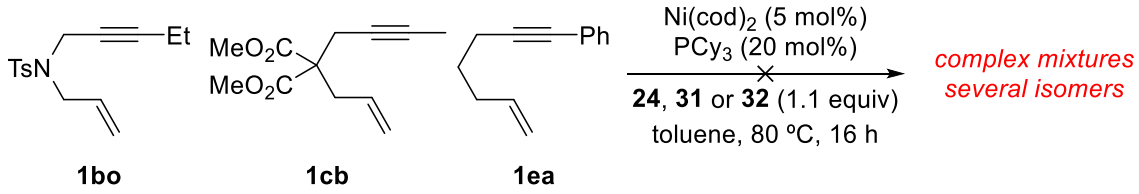

Scheme 5.33. Abortive attempts with other alkynylboronates.

Additionally, we evaluated other ligands with alkynylboronate **24**, but the same complex mixtures were observed in all cases (**Scheme 5.34**).

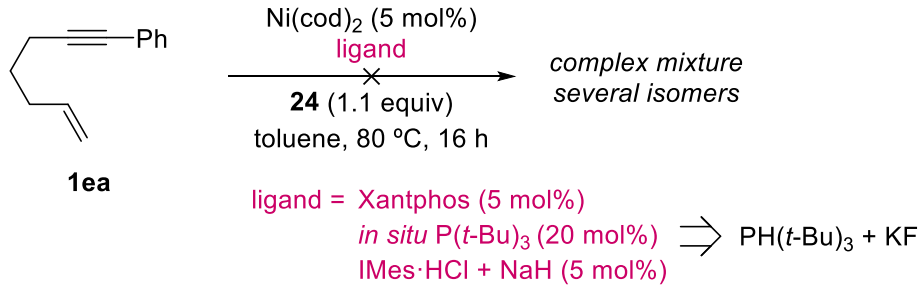

Scheme 5.34. Reaction conditions screening with **24**.

As we did with the reactions shown in previous chapters, we wanted to illustrated the utility of the resulting borylated compounds **26**. However, when we performed the oxidation of the boron moiety, we did not observed the expected results. Along with the formation of the corresponding ketone group by oxidation of alkenylboronate, we also observed the loss of the TMS group (**Scheme 5.35**). Starting from compound **26bd**, we directly observed the conjugated α,β-unsaturated ketone (**33bd**). In contrast, a non-conjugated ketone (**34ea**) was obtained with compound **26ea**. Such double bond conjugation was partially observed in **34ea** as time passes along with oxidation in γ position (**35ea**). That type of oxidation has been previously reported in other α,β-unsaturated ketone in the presence of an oxidant, where O_2 afforded the best results.[297]

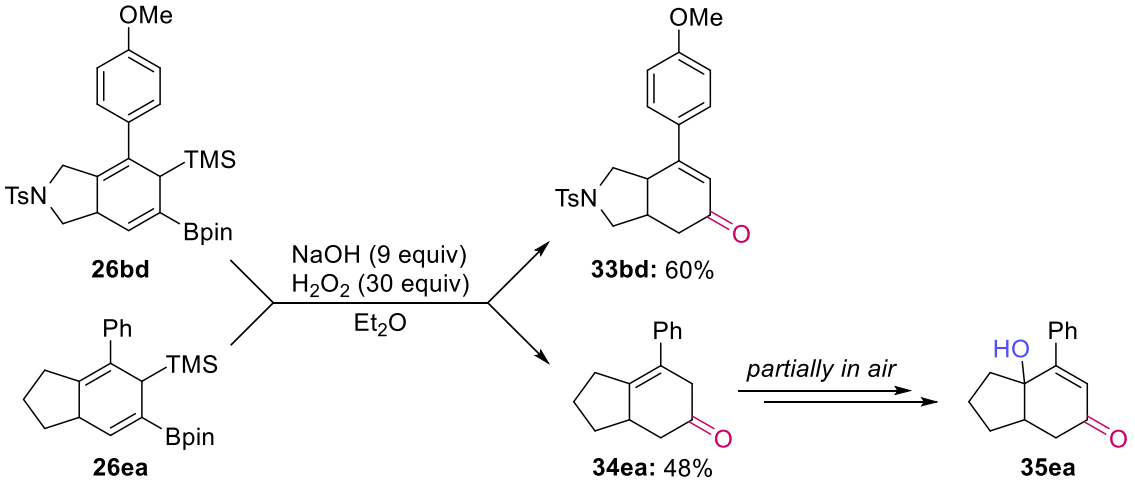

Scheme 5.35. Oxidative conditions with compounds **26**.

On the other hand, we sought to functionalize the incorporated silyl moiety in compounds **26** under Fleming-Tamao oxidation conditions (**Scheme 5.36**). Instead, we obtained a mixture of desilylated-oxidation products, comprising the previously detected ketones (**34**–**35ea**) and a phenol derivative (**36ea**), in poor yields.

[297] A. L. García-Cabeza, R. Marín-Barrios, R. Azarken, F. J. Moreno-Dorado, M. J. Ortega, H. Vidal, J. M. Gatica, G. M. Massanet, F. M. Guerra, *Eur. J. Org. Chem.* **2013**, 8307–8314.

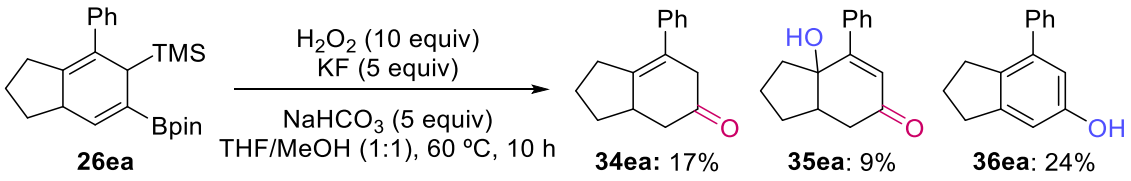

Scheme 5.36. Fleming-Tamao oxidation.

Although we did not succeed in the controlled functionalization of Bpin and TMS substituents, we believed these compounds are interesting molecules and further optimization of reaction conditions may lead to useful transformations.

With the aim of getting insight into the reaction mechanism, and to propose a reasonable pathway for the formation of compounds **26**, we performed additional experiments. We tested our optimal reaction conditions with simple alkynes and alkenes (**Scheme 5.37**). Thus, when we used 4-octyne as substrate, the previously described carboborylation compound **37** was obtained (top). Structurally similar alkenes did not react under optimal conditions (middle). Surprisingly, when styrene was employed, borylated compound **7** was obtained in moderate yield (bottom).

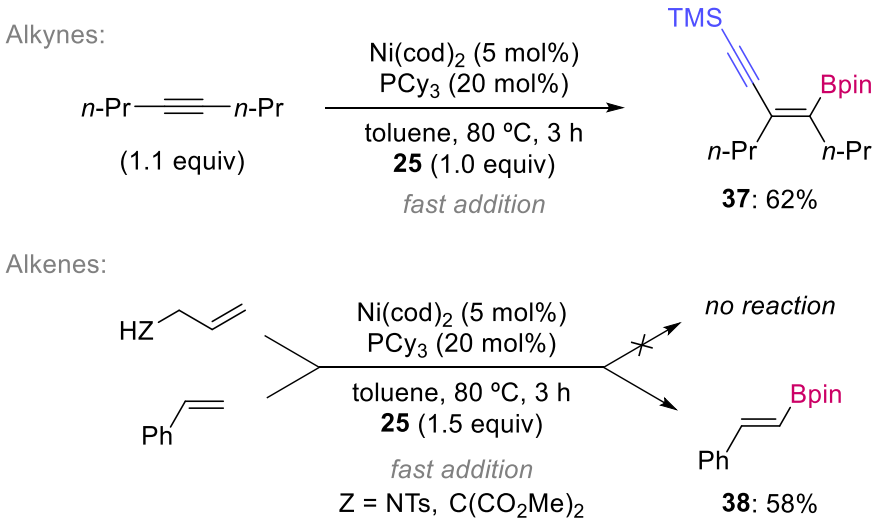

Scheme 5.37. Reaction with simple alkenes and alkynes.

Both results are consistent with an initial C–B bond activation. In fact, terminal alkynes such as phenylacetylene and ethynyltrimethylsilane (lacking the boryl group) afforded only oligomerization products (**Scheme 5.38**).

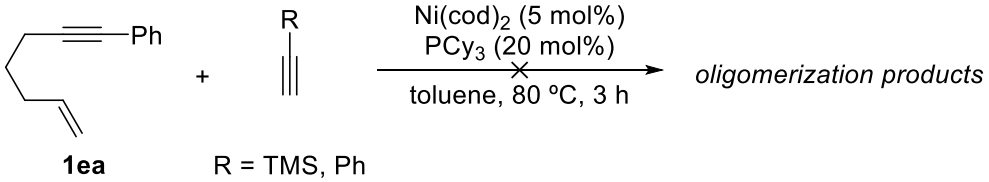

Scheme 5.38. Reaction with terminal alkynes.

On the other hand, we have demonstrated that Ni/Xantphos (*Chapter 3*) and Ni/tpy (*Chapter 4*) systems are able to activate enynes by coordination to both the alkene and alkyne followed by oxidative cyclometalation. In order to evaluate the feasibility of this process in this case, we performed a stoichiometric reaction between $Ni(cod)_2$, PCy_3 and the enyne **1ea**, without

the alkynylboronate. After hydrolyzing the reaction mixture with DCl·D_2O, the expected dideuterated cyclic compound was not detected, only oligomerization of enyne was observed (**Scheme 5.39**). Therefore, oxidative cyclometalation does not seem to take place under the reaction conditions.

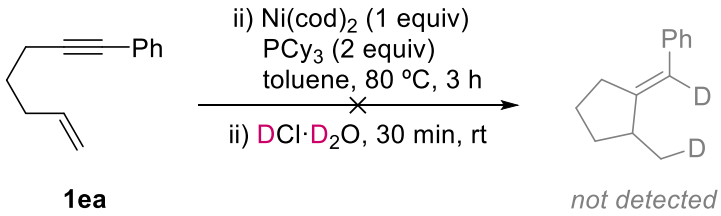

Scheme 5.39. Deuteration experiment.

In addition, we studied the catalytic system in the absence of the enyne by ^{31}P- and ^{11}B-NMR. Comparison of the ^{31}P-NMR spectrum of a mixture of Ni/PCy_3 (1:4) in toluene- d^8 with that of a mixture of Ni/PCy_3/**25** (1:4:1) stirred at 80 ºC for 5 minutes, indicates the formation of a new species showing a signal at 20.7 ppm. The same signal is observed when the mixture is stirred at 23 °C for 2 h (**Figure 5.11**).[298]

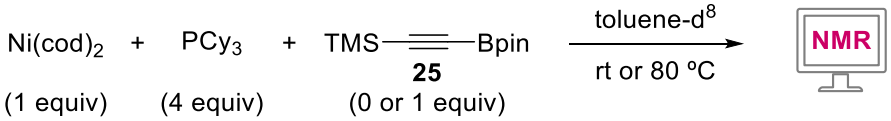

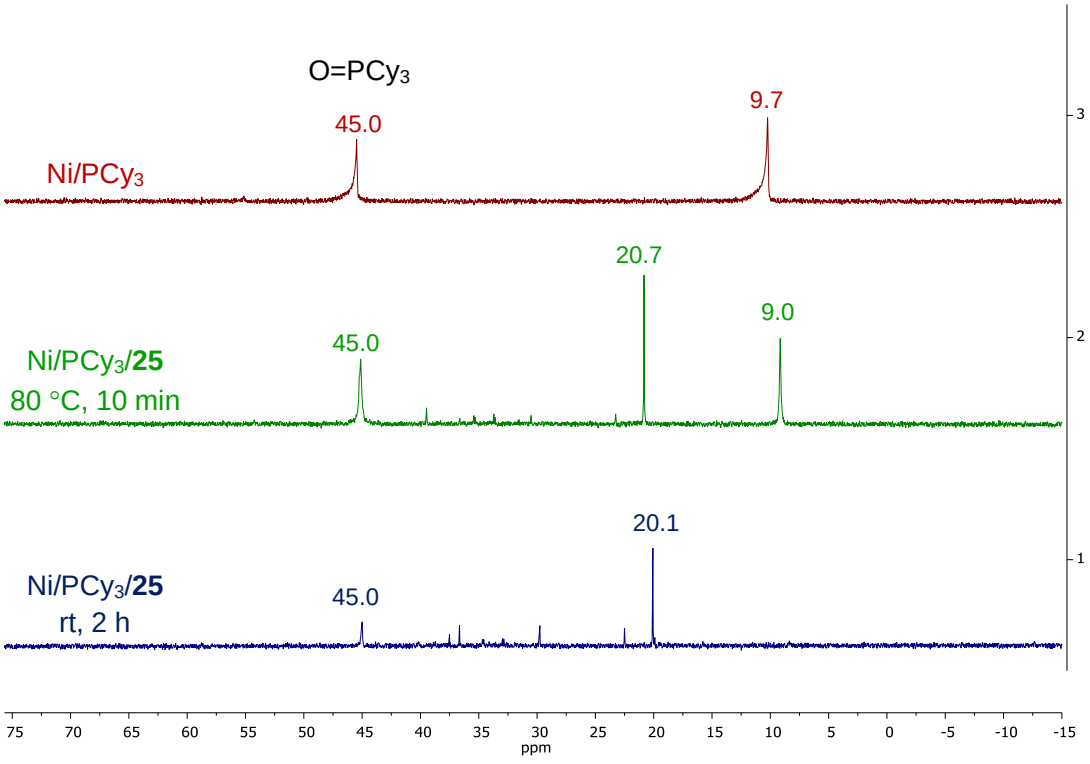

Figure 5.11. ^{31}P-NMR spectra of Ni/PCy_3 (top) and Ni/PCy_3/**25** (80 ºC, middle; rt, bottom).

[298] Big amounts of tricyclohexylphosphine oxide were observed, because of the ease of tricyclohexylphosphine to oxidize. We used its signal as an internal standard for the spectra.

On the other hand, the ^{11}B-NMR spectrum of a mixture of Ni/PCy$_3$/**25** (1:2:1) stirred for 10 min at 23 °C, shows two signals at 21.9 and 29.5 ppm, and unreacted alkynylboronate **25** (23.5 ppm). When heating this solution for 10 min at 80 ºC, we only observed the signal at 21.9 ppm (**Figure 5.12**).

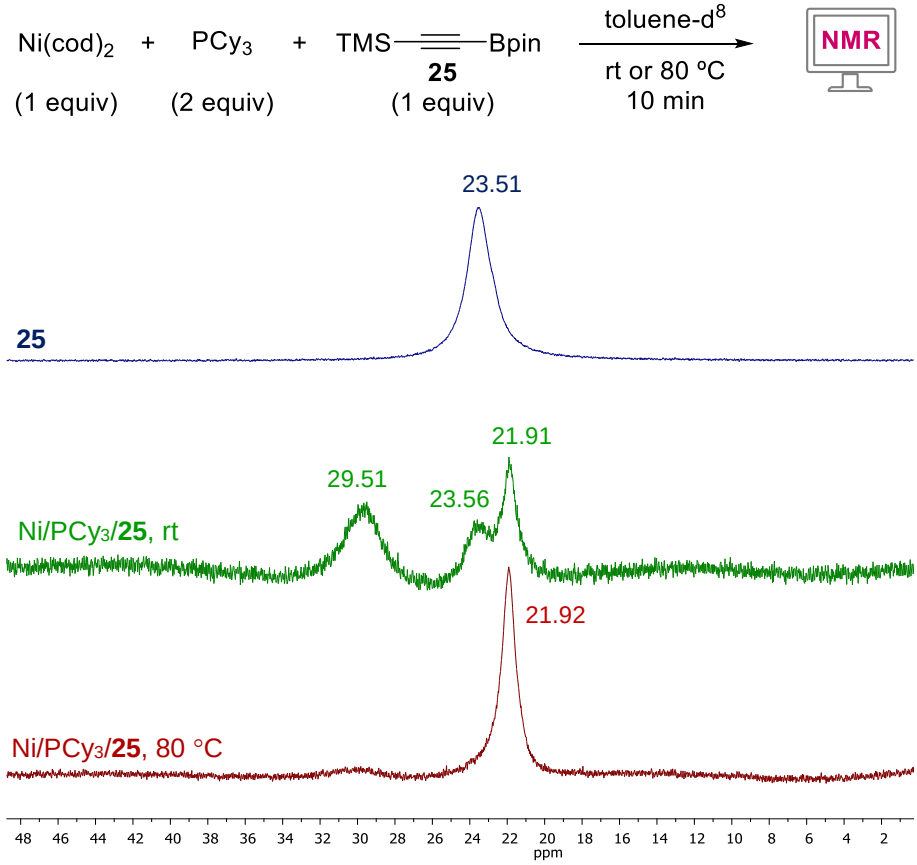

Figure 5.12. ^{11}B-NMR spectra of **25** (top) and Ni/PCy$_3$/**25** (rt, middle; 80 ºC, bottom).

These results suggest that the alkyne interacts with the precatalyst affording a new species, but the small shift observed is probably due to alkyne coordination rather than oxidative addition of the C–B to Ni(0) proposed by Suginome for the alkynylborylation of alkynes.[269]

The formation of non-conjugated cyclic dienes from the reaction substrates is challenging from a mechanistic point of view. For this reason we studied computationally at DFT level the thermodynamic stability of some of the observed reaction products (**26ec**, **26bo**, and "**26cf"**), compared with the corresponding conjugated dienes (**28**). Interestingly, the observed 1,4-dienes (**26**) are more stable (5 to 8 kcal mol^{-1} in terms of ΔG), probably due to the release upon deconjugation of the high steric strain that exists in the conjugated diene between the coplanar SiMe$_3$, Bpin, and the substituent of the alkyne.

The above-mentioned experiments lead to disregard both the oxidative addition of C–B bond to Ni, and the formation of a nickelacyclopentadiene by oxidative cyclometalation of the coordinated enyne. Instead, we propose an initial oxidative cyclometalation involving the alkyne groups present in **25** and the enyne (**1**), after previous coordination to Ni(0) (**Figure 5.13**). The resulting nickelacyclopentadiene would evolve by carbometalation of the alkene and subsequent reductive elimination to afford a 1,3-diene and regenerating the Ni(0) species. In fact, we could isolate such kind of derivative in one case (**28cf**). An off-cycle isomerization involving a 1,3-hydrogen migration would lead to the observed products. Nevertheless, we have no explanation for the lack of isomerization of **28cf**.

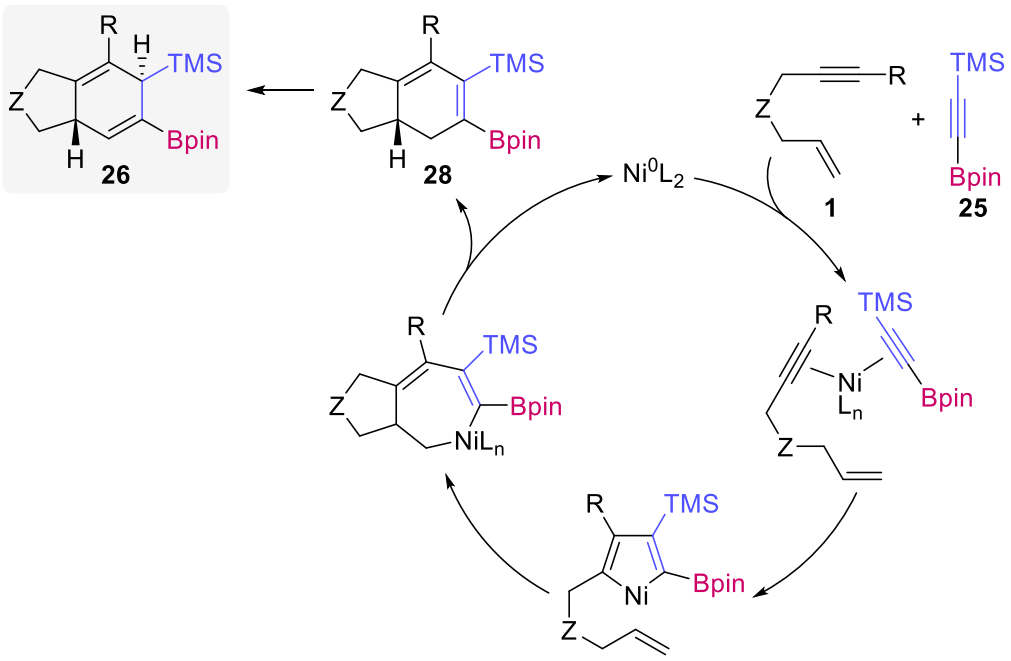

Figure 5.13. Proposed reaction mechanism.

Finally, we synthetized the dideuterated enyne d^2-**1ea** (72% D incorporation) in the terminal position of the alkene. The carboborylative cyclization reaction under the optimized conditions led to compound d^2-**26ea** in 80% yield with the expected deuterium distribution (**Scheme 5.40**). This result further supports the mechanistic proposal.

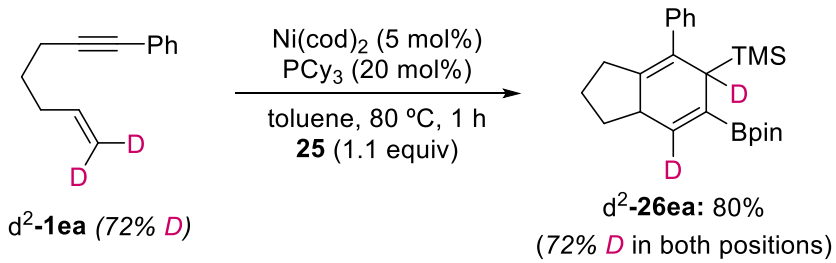

Scheme 5.40. Reaction with dideuterated enyne d^2-**1ea**.

In conclusion, we have described the first carboborylative cyclization reaction of enynes, furnishing novel bicyclic structures from simple starting materials, such as enynes and alkynylboronates, in a complete atom-economical fashion. Thus, we have contributed to the development of a novel synthetic methodology which extends the organic chemistry toolbox for the preparation of complex molecules.

3.5.4. Experimental section

3.5.4.1. Materials and methods

General considerations have been described in *Experimental section* of *Chapter 1*. Additionally, $Ni(cod)_2$ and tricyclohexylphosphine were purchased from Sigma-Aldrich Co. Alkynylboronates have been prepared following the procedures described in the literature. The other commercially available chemicals were purchased and used as received without further purifications. The carboborylative cyclization reactions were carried out under argon atmosphere in anhydrous toluene stored over activated molecular sieves 4 Å (VWR) and Ar-degassed.

3.5.4.2. Synthesis of alkynylboronates

3.5.4.2.1. General procedure for the synthesis of alkynylboronates

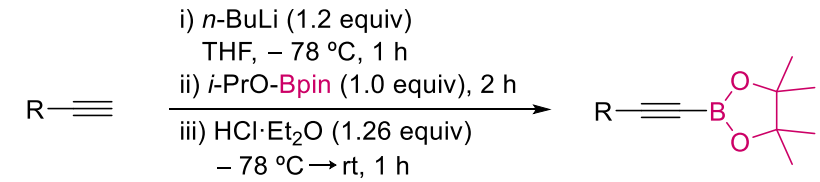

24: R = Ph
25: R =TMS
31: R = *p*-Tol
32: R = *n*-Hex

To a solution of the corresponding acetylene derivative (1.2 equiv, 12 mmol) in THF (0.6 M) at –78 °C under an argon atmosphere, *n*-BuLi was added dropwise (1.2 equiv, 1.6 M or 2.5 M in hexanes, 12 mmol). The reaction was stirred for 1 h. Then, the resulting mixture was added using a double-ended needle to a solution of 2-isopropoxy-4,4,5,5-tetramethyl-1,3,2-dioxaborolane (1 equiv, 10 mmol) in THF (0.5 M) under an argon atmosphere at –78 °C. After being stirred for 2 h, the reaction mixture was quenched with $HCl{\cdot}Et_2O$ (1.26 equiv, 12.6 mmol), and the mixture was warmed at room temperature and stirred for one more hour. The solvent was evaporated under vacuum and DCM was added to the residue (20 mL) to remove the lithium salts by simple filtration. The solvent was evaporated again, affording the pure product. Solid alkynylboronates were crystallized from pentane, whereas oily alkynylboronates were used without further purification.[299]

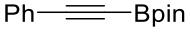

4,4,5,5-Tetramethyl-2-(phenylethynyl)-1,3,2-dioxaborolane (24):[299] The product was obtained as a pale yellow solid in 93% yield (2.1 g). ^{1}H NMR (300 MHz, $CDCl_3$) δ 7.53 (dd, J = 8.0, 1.6 Hz, 2H), 7.38 – 7.30 (m, 3H), 1.32 (s, 12H).

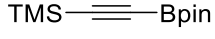

Trimethyl((4,4,5,5-tetramethyl-1,3,2-dioxaborolan-2-yl)ethynyl)silane (25):[300] The product was obtained as a white solid in 88% yield (2.0 g). ^{1}H NMR (300 MHz, $CDCl_3$) δ 1.27 (s, 12H), 0.19 (s, 9H).

[299] Y. Nishihara, M. Miyasaka, M. Okamoto, H. Takahashi, E. Inoue, K. Tanemura, K. Takagi, *J. Am. Chem. Soc.* **2007**, *129*, 12634–12635.
[300] E. A. Romero, R. Jazzara, G. Bertrand, *Chem. Sci.* **2017**, *8*, 165–168.

4,4,5,5-Tetramethyl-2-(*p*-tolylethynyl)-1,3,2-dioxaborolane:[300] The product was obtained as a pale yellow solid in 95% yield (2.3 g). ^{1}H NMR (300 MHz, $CDCl_3$) δ 7.42 (d, J = 8.1 Hz, 2H), 7.11 (d, J = 8.1 Hz, 2H), 2.34 (s, 3H), 1.32 (s, 12H).

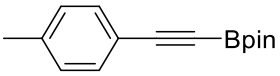

4,4,5,5-Tetramethyl-2-(oct-1-yn-1-yl)-1,3,2-dioxaborolane:[301] The product was obtained as a pale yellow oil in 98% yield (1.9 g). ^{1}H NMR (300 MHz, $CDCl_3$) δ 2.25 (t, J = 7.1 Hz, 2H), 1.61 – 1.48 (m, 3H), 1.44 – 1.32 (m, 5H), 1.27 (s, 12H), 0.88 (t, J = 6.7 Hz, 3H).

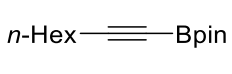

3.5.4.3. Synthesis of enyne d^2-1ea

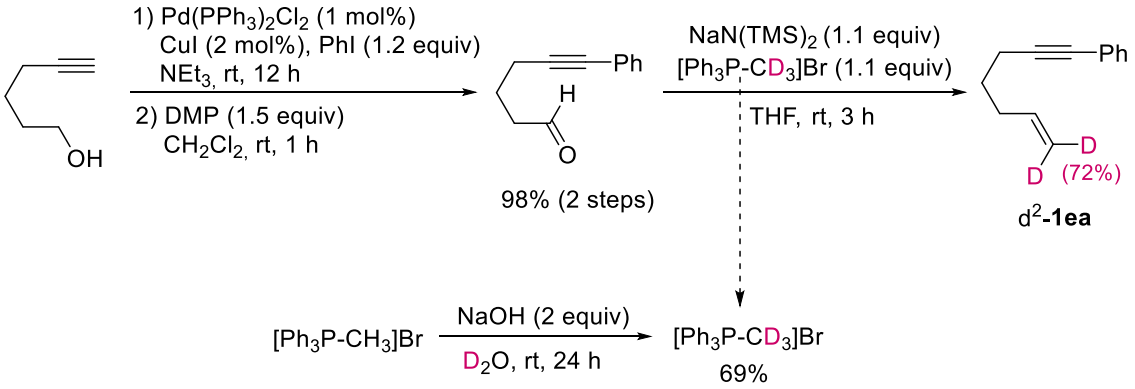

(Hept-6-en-1-yn-1-yl-7,7-*d*^{2})benzene (d^2-**1a)**: The product was obtained following several steps: (1) the *general procedure for a Sonogashira reaction,* (2) oxidation procedure to the corresponding aldehyde with Dess-Martin periodinane and (3) Wittig reaction to obtained de deuterated enyne. Step (1) is described in the *General procedure for the synthesis of propargylic alcohols* (see *Chapter 1, section 3.1.2.2*), and Step (2) is described in *the General procedure for the synthesis of enynones* ***1g*** (see *Chapter 1, section 3.1.2.9*). Here, Step (3) is described:[302] to a suspension of [Ph_3P-CD_3]Br (1.1 equiv, 2.8 mmol, previously synthetized following the literature[302]) in THF (0.15 M) at room temperature, $NaN(SiMe_3)_2$ was added (1.1 equiv, 2.8 mmol), resulting in the formation of a bright yellow solution. After 30 min, the previously isolated aldehyde (1 equiv, 2.5 mmol) was added in solution of THF (0.8 M). The mixture was stirred for 3 h until the complete consumption of the aldehyde. Then, water was added (10 mL) and the reaction mixture was extracted with EtOAc, washed with brine and dried over anhydrous $MgSO_4$. The solvent was removed under vacuum and the enyne was purified by column chromatography (cyclohexane). The product was obtained with 72% deuterium incorporation as a colorless oil in 24% yield (103 mg). ^{1}H NMR (300 MHz, $CDCl_3$) δ 7.36 (dd, J = 6.5, 3.2 Hz, 2H), 7.27 – 7.21 (m, 3H), 5.83 – 5-71 (m, 1H), 5.07 – 4.92 (m, 0.56H, *28% H*), 2.39 (t, J = 7.1 Hz, 2H), 2.19 (dd, J = 14.3, 7.1 Hz, 2H), 1.67 (quin, J = 7.1 Hz, 2H). ^{2}H NMR (77 MHz, $CDCl_3$) δ 5.29 – 4.97 (m, 2D). ^{13}C NMR (75 MHz, $CDCl_3$) δ 137.9 (d, J = 7.2 Hz, CD_2), 131.7 (2 × CH), 128.3 (2 × CH), 127.6 (CH), 124.2 (C), 90.1 (C), 81.0 (C), 32.9 (CH_2), 28.1 (CH_2), 18.9 (CH_2). HRMS (APCI, MeOH) calcd. for $C_{13}H_{12}D_2$ [M + H]$^+$: 173.1221; Found: 173.1228.

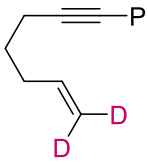

[300] E. A. Romero, R. Jazzara, G. Bertrand, *Chem. Sci.* **2017**, *8*, 165–168.
[301] E. C. Hansen, D. Lee, *J. Am. Chem. Soc.* **2005**, *127*, 3252–3253.
[302] S. Fortier, J. R. Walensky, G. Wu, T. W. Hayton, *J. Am. Chem. Soc.* **2011**, *133*, 6894–6897.

3.5.4.4. General procedure for carboborylative cyclization of enynes

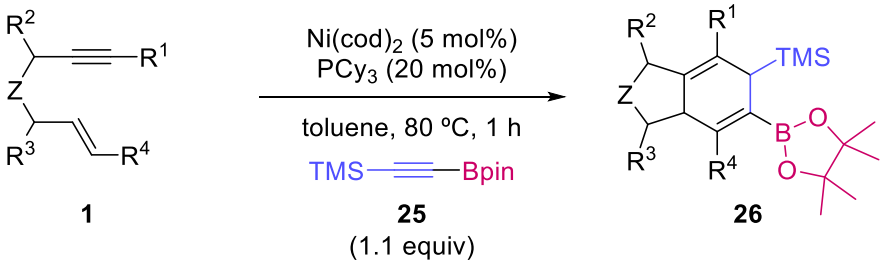

1 **25** (1.1 equiv) **26**

A vial was charged with $Ni(cod)_2$ (5.5 mg, 0.02 mmol), tricyclohexylphosphine (22.4 mg, 0.08 mmol), alkynylboronate **25** (98.6 mg, 0.44 mmol) and a stir bar in air. The vial was sealed by a septum, dried under vacuum and backfilled with Ar (three times). Then, anhydrous and Ar-degassed toluene (0.5 ml) was added, and the mixture was stirred at 80 °C for 5 minutes (the reaction turns dark red). Then, a solution of the corresponding enyne **1** (0.4 mmol) in toluene (1 mL) was added with slow addition by a syringe pump during 1 h. The resulting mixture was stirred for an additional hour at 80 °C. When the complete consumption of the enyne was verified by TLC, the solvent was evaporated under vacuum and the product was purified by column chromatography in silica gel.

Trimethyl(4-phenyl-6-(4,4,5,5-tetramethyl-1,3,2-dioxaborolan-2-yl)-1,3,5,7a-tetrahydroisobenzofuran-5-yl)silane (26aa): The compound was purified by column chromatography (cyclohexane/EtOAc 95:5) and was obtained as a yellow oil in 26% yield (42 mg). ^{1}H NMR (300 MHz, $CDCl_3$) δ 7.40 – 7.16 (m, 5H), 6.44 (s, 1H), 4.73 (d, J = 12.7 Hz, 1H), 4.26 (t, J = 6.0 Hz, 1H), 4.16 (d, J = 12.7 Hz, 1H), 3.41 – 3.22 (m, 3H), 1.30 (s, 12H), -0.17 (s, 9H). ^{13}C NMR (75 MHz, $CDCl_3$) δ 141.6 (C), 135.4 (CH), 132.2 (C), 130.1 (C), 128.2 (2 × CH), 128.0 (2 × CH), 127.1 (CH), 83.7 (2 × C), 71.7 (CH_2), 69.5 (CH_2), 42.9 (CH), 39.5 (CH), 25.1 (2 × CH_3), 25.0 (2 × CH_3), -1.5 (3 × CH_3). HRMS (ESI, MeOH) calcd. for $C_{23}H_{33}BO_3Si$ [M + Na]$^+$: 419.2292; Found: 419.2201.

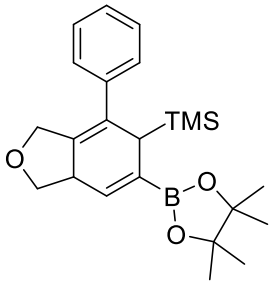

5-(4,4,5,5-Tetramethyl-1,3,2-dioxaborolan-2-yl)-2-tosyl-6-(trimethylsilyl)-2,3,3a,6-tetrahydro-1*H*-isoindole (26ba): The compound was purified by column chromatography (cyclohexane/EtOAc 9:1) and was obtained as a white solid in 57% yield (108 mg). M.p. = 144 – 146 °C. ^{1}H NMR (300 MHz, $CDCl_3$) δ 7.70 (d, J = 8.2 Hz, 2H), 7.31 (d, J = 8.2 Hz, 2H), 6.07 (s, 1H), 6.01 (s, 1H), 4.14 (d, J = 15.4 Hz, 1H), 3.92 – 3.83 (m, 1H), 3.80 (d, J = 15.4 Hz, 1H), 2.71 – 2.50 (m, 3H), 2.42 (s, 3H), 1.25 (d, J = 3.0 Hz, 12H), 0.14 (s, 9H). ^{13}C NMR (75 MHz, $CDCl_3$) δ 143.7 (C), 139.7 (C), 133.1 (C), 129.8 (2 × CH), 127.8 (2 × CH), 121.1 (CH), 120.2 (CH), 83.6 (2 × C), 55.2 (CH_2), 51.1 (CH_2), 36.6 (CH), 30.9 (CH), 25.1 (2 × CH_3), 24.9 (2 × CH_3), 21.6 (CH_3), 0.5 (3 × CH_3). HRMS (ESI, MeOH) calcd. for $C_{24}H_{36}BNO_4SSi$ [M + Na]$^+$: 496.2227; Found: 496.2126.

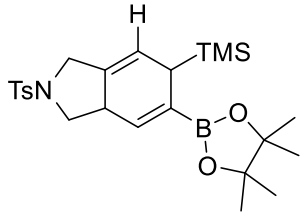

7-(4-Methoxyphenyl)-5-(4,4,5,5-tetramethyl-1,3,2-dioxaborolan-2-yl)-2-tosyl-6-(trimethylsilyl)-2,3,3a,6-tetrahydro-1*H*-isoindole (26bd): The compound was purified by column chromatography (cyclohexane/EtOAc 9:1) and was obtained as a pale yellow solid in 61% yield (140 mg). M.p. = 52 – 54 °C. ^{1}H NMR (300 MHz, $CDCl_3$) *δ* 7.62 (d, *J* = 8.2 Hz, 2H), 7.24 (d, *J* = 8.2 Hz, 2H), 7.13 (d, *J* = 8.7 Hz, 2H), 6.84 (d, *J* = 8.7 Hz, 2H), 6.30 (s, 1H), 4.42 (d, *J* = 13.9 Hz, 1H), 3.95 – 3.85 (m, 1H), 3.82 (s, 3H), 3.53 (d, *J* = 13.9 Hz, 1H), 3.31 – 3.21 (m, 1H), 3.07 (d, *J* = 2.9 Hz, 1H), 2.63 (t, *J* = 9.7 Hz, 1H), 2.38 (s, 3H), 1.26 (s, 12H), -0.24 (s, 9H). ^{13}C NMR (75 MHz, $CDCl_3$) δ 158.7 (C), 143.4 (C), 135.0 (CH), 133.8 (C), 133.6 (C), 133.2 (C), 129.7 (2 × CH), 129.1 (2 × CH), 127.6 (2 × CH), 125.0 (CH), 113.6 (2 × CH), 83.7 (2 × C), 55.2 (CH_3), 52.0 (CH_2), 50.5 (CH_2), 41.5 (CH), 39.7 (CH), 25.0 (2 × CH_3), 24.9 (2 × CH_3), 21.5 (CH_3), -1.6 (3 × CH_3). HRMS (ESI, MeOH) calcd. for $C_{31}H_{42}BNO_5SSi$ [M + Na]$^+$: 602.2646; Found: 602.2546.

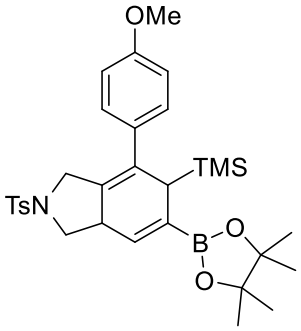

8-Phenyl-6-(4,4,5,5-tetramethyl-1,3,2-dioxaborolan-2-yl)-2-tosyl-7-(trimethylsilyl)-1,2,3,4,4a,7-hexahydroisoquinoline (6bl): The compound was purified by column chromatography (cyclohexane/EtOAc 9:1) and was obtained as a white solid in 40% yield (90 mg). M.p. = 165 – 167 °C. ^{1}H NMR (300 MHz, $CDCl_3$) *δ* 7.42 (d, *J* = 8.3 Hz, 2H), 7.23 (d, *J* = 8.3 Hz, 2H), 7.29 – 7.02 (m, 5H), 5.96 (s, 1H), 3.82 (d, *J* = 11.8 Hz, 1H), 3.43 (d, *J* = 11.8 Hz, 1H), 2.41 (s, 3H), 2.37 – 2.14 (m, 2H), 1.93 – 1.72 (m, 3H), 1.70 – 1.60 (m, 1H), 1.02 (s, 6H), 0.90 (s, 6H), 0.16 (s, 9H). ^{13}C NMR (75 MHz, $CDCl_3$) δ 147.4 (C), 143.3 (C), 140.0 (C), 139.9 (CH), 138.7 (C), 133.6 (C), 129.6 (4 × CH), 127.6 (4 × CH), 127.2 (CH), 83.5 (2 × C), 50.2 (CH_2), 46.4 (CH_2), 40.9 (CH), 38.4 (CH), 30.1 (CH_2), 25.5 (2 × CH_3), 25.3 (2 × CH_3), 21.6 (CH_3), -0.4 (3 × CH_3). HRMS (ESI, MeOH) calcd. for $C_{31}H_{42}BNO_4SSi$ [M + Na]$^+$: 586.2697; Found: 586.2593.

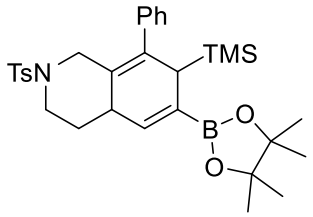

7-Ethyl-5-(4,4,5,5-tetramethyl-1,3,2-dioxaborolan-2-yl)-2-tosyl-6-(trimethylsilyl)-2,3,3a,6-tetrahydro-1*H*-isoindole (26bo): The compound was purified by column chromatography (cyclohexane/EtOAc 9:1) and was obtained as a colorless oil in 99% yield (204 mg). ^{1}H NMR (300 MHz, $CDCl_3$) *δ* 7.70 (d, *J* = 8.3 Hz, 2H), 7.30 (d, *J* = 8.3 Hz, 2H), 6.25 (d, *J* = 1.5 Hz, 1H), 4.11 (d, *J* = 13.6 Hz, 1H), 3.86 (t, *J* = 8.6 Hz, 1H), 3.68 (d, *J* = 13.6 Hz, 1H), 3.07 – 2.91 (m, 1H), 2.60 (d, *J* = 4.4 Hz, 1H), 2.55 (dd, *J* = 11.0, 8.8 Hz, 1H), 2.41 (s, 3H), 2.05 (dq, *J* = 14.7, 7.6 Hz, 1H), 1.94 – 1.79 (m, 1H), 1.23 (s, 12H), 0.87 (t, *J* = 7.6 Hz, 3H), -0.05 (s, 9H). ^{13}C NMR (75 MHz, $CDCl_3$) *δ* 143.5 (C), 135.4 (CH), 134.3 (C), 133.0 (C), 129.6 (2 × CH), 127.7 (2 × CH), 123.4 (C), 83.5 (2 × C), 52.4 (CH_2), 49.1 (CH_2), 40.9 (CH), 37.5 (CH), 26.4 (CH_2), 24.9 (4 × CH_3), 21.5 (CH_3), 11.8 (CH_3), -1.2 (3 × CH_3). HRMS (ESI, MeOH) calcd. for $C_{26}H_{40}BNO_4SSi$ [M + Na]$^+$: 524.2540; Found: 524.2432.

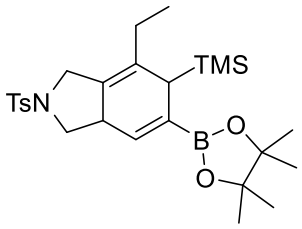

7-Butyl-5-(4,4,5,5-tetramethyl-1,3,2-dioxaborolan-2-yl)-2-tosyl-6-(trimethylsilyl)-2,3,3a,6-tetrahydro-1*H*-isoindole (26bq): The compound was purified by column chromatography (cyclohexane/EtOAc 9:1) and was obtained as a colorless oil in 22% yield with 50% of conversion (21 mg). ^{1}H NMR (300 MHz, $CDCl_3$) δ 7.70 (d, J = 8.2 Hz, 2H), 7.30 (d, J = 8.2 Hz, 2H), 6.25 (d, J = 1.5 Hz, 1H), 4.09 (d, J = 13.6 Hz, 1H), 3.85 (t, J = 8.2 Hz, 1H), 3.69 (d, J = 13.6 Hz, 1H), 3.06 – 2.92 (m, 1H), 2.58 (d, J = 3.6 Hz, 1H), 2.55 (dd, J = 9.3, 7.1 Hz, 1H), 2.41 (s, 3H), 2.08 – 1.59 (m, 4H), 1.23 (d, J = 2.6 Hz, 12H), 0.82 (t, J = 7.0 Hz, 3H), -0.06 (s, 9H). ^{13}C NMR (75 MHz, $CDCl_3$) δ 143.5 (C), 135.6 (CH) , 133.1 (2 × C), 129.6 (2 × CH), 127.7 (2 × CH), 123.9 (C), 83.5 (2 × C), 52.5 (CH_2), 49.3 (CH_2), 40.9 (CH), 37.8 (CH), 33.2 (CH_2), 29.5 (CH_2), 25.0 (2 × CH_3), 24.9 (2 × CH_3), 22.8 (CH_2), 21.5 (CH_3), 14.0 (CH_3), -1.2 (3 × CH_3). HRMS (ESI, MeOH) calcd. for $C_{28}H_{44}BNO_4SSi$ $[M]^+$: 552.2853; Found: 552.2757.

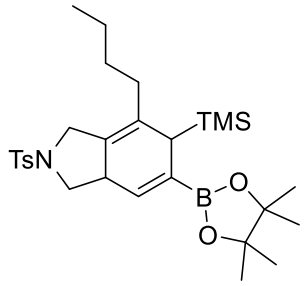

7-Methyl-2-phenyl-5-(4,4,5,5-tetramethyl-1,3,2-dioxaborolan-2-yl)-6-(trimethylsilyl)-2,3,3a,6-tetrahydro-1*H*-isoindole (26bw): The compound was purified by column chromatography (cyclohexane/EtOAc 9:1) and was obtained as a yellow oil in 63% yield (99 mg). ^{1}H NMR (300 MHz, $CDCl_3$) δ 6.89 – 6.59 (m, 5H), 6.54 (s, 1H), 4.19 (d, J = 12.7 Hz, 1H), 4.10 (d, J = 12.7 Hz, 1H), 4.02 – 3.79 (m, 1H), 3.35 – 3.25 (m, 1H), 2.92 – 2.79 (m, 1H), 2.61 (s, 1H), 1.80 (s, 3H), 1.30 (s, 12H), 0.06 (s, 9H). ^{13}C NMR (75 MHz, $CDCl_3$) δ 148.2 (C), 137.4 (CH), 129.2 (2 × CH), 126.9 (C), 126.1 (C), 116.2 (CH), 112.1 (2 × CH), 83.6 (2 × C), 52.5 (CH_2), 50.6 (CH_2), 41.0 (CH), 40.6 (CH), 25.1 (2 × CH_3), 24.9 (2 × CH_3), 20.1 (CH_3), -1.1 (3 × CH_3). HRMS (ESI, MeOH) calcd. for $C_{24}H_{36}BNO_2Si$ $[M + H]^+$: 410.2608; Found: 410.2698.

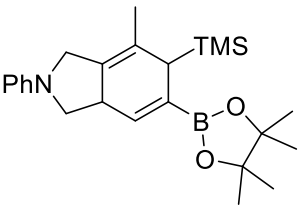

7-Methyl-1-phenyl-5-(4,4,5,5-tetramethyl-1,3,2-dioxaborolan-2-yl)-2-tosyl-6-(trimethylsilyl)-2,3,3a,6-tetrahydro-1*H*-isoindole (26by): The compound was purified by column chromatography (cyclohexane/EtOAc 9:1) and a mixture of two diastereomers (6.7:1) was obtained as a brown oil in 78% yield (49 mg). ^{1}H NMR (300 MHz, $CDCl_3$) δ 7.58 (d, J = 8.3 Hz, 2H), 7.38 – 7.19 (m, 5H), 7.09 (d, J = 8.3 Hz, 2H), 6.32 (d, J = 1.4 Hz, 1H), 5.10 (s, 1H), 3.94 (t, J = 8.5 Hz, 1H), 3.43 – 3.27 (m, 1H), 2.91 (dd, J = 10.3, 8.8 Hz, 1H), 2.40 (s, 3H), 2.34 (t, J = 5.0 Hz, 1H), 1.25 (s, 12H), -0.16 (s, 9H). ^{13}C NMR (75 MHz, $CDCl_3$) δ 143.2 (C), 142.2 (C), 135.2 (CH), 134.4 (C), 129.4 (2 × CH), 129.3 (C), 128.8 (C), 128.2 (2 × CH), 127.8 (2 × CH), 127.2 (2 × CH), 126.9 (CH), 83.6 (2 × C), 64.7 (CH), 53.1 (CH_2), 40.6 (CH), 40.1 (CH), 25.0 (2 × CH_3), 24.8 (2 × CH_3), 21.6 (CH_3), 20.0 (CH_3), -1.4 (3 × CH_3). HRMS (ESI, MeOH) calcd. for $C_{31}H_{42}BNO_4SSi$ $[M + Na]^+$: 586.2697; Found: 586.2583.

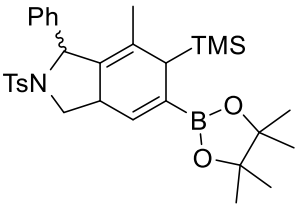

3,7-Dimethyl-5-(4,4,5,5-tetramethyl-1,3,2-dioxaborolan-2-yl)-2-tosyl-6-(trimethylsilyl)-2,3,3a,6-tetrahydro-1*H*-isoindole (26bz): The compound was purified by column chromatography (cyclohexane/EtOAc 9:1) and a mixture of two diastereomers (1.6:1) was obtained as a pale yellow solid in 53% yield (49 mg). M.p. = 146 – 148 °C. ^{1}H NMR ***major diast*** (300 MHz, $CDCl_3$) δ 7.63 (d, J = 8.3 Hz, 2H), 7.23 (d, J = 8.3 Hz, 2H), 6.21 (d, J = 1.2 Hz, 1H), 4.09 (d, J = 13.9 Hz, 1H), 3.95 (s, 1H), 3.75 (d, J = 13.9 Hz, 1H), 2.73 (dd, J = 9.9, 5.7 Hz, 1H), 2.42 (d, J = 5.2 Hz), 2.37 (s, 3H), 1.55 (s, 3H), 1.20 (s, 12H), -0.06 (s, 9H). ^{13}C NMR ***major diast*** (75 MHz, $CDCl_3$) δ 143.4 (C), 134.8 (CH), 133.1 (C), 129.7 (2 × CH),

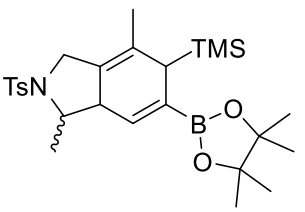

127.8 (2 × CH), 127.4 (CH), 122.0 (C), 83.6 (2 × C), 60.9 (CH), 51.4 (CH_2), 49.3 (CH), 40.7 (CH), 25.0 (2 × CH_3), 24.9 (2 × CH_3), 21.5 (CH_3), 19.5 (CH_3), -1.3 (3 × CH_3). ^{1}H NMR ***minor diast*** (300 MHz, $CDCl_3$) *δ* 7.68 (d, *J* = 8.2 Hz, 2H), 7.28 (d, *J* = 8.2 Hz, 2H), 6.08 (s, 1H), 4.21 – 4.11 (m, 2H), 2.70 – 2.56 (m, 2H), 2.34 (s, 3H), 1.70 – 1.65 (m, 1H), 1.20 (s, 12H), 0.92 (d, *J* = 6.6 Hz, 3H), -0.19 (s, 9H). ^{13}C NMR ***minor diast*** (75 MHz, $CDCl_3$) *δ* 143.2 (C), 136.3 (CH), 134.3 (C), 129.7 (2 × CH), 128.7 (C), 127.0 (2 × CH), 123.7 (C), 83.5 (2 × C), 57.8 (CH_2), 47.6 (CH), 43.8 (CH), 40.2 (CH), 25.0 (2 × CH_3), 24.8 (2 × CH_3), 20.1 (CH_3), 19.7 (CH_3), -1.5 (3 × CH_3). HRMS (ESI, MeOH) calcd. for $C_{26}H_{40}BNO_4SSi$ [M + Na]$^+$: 524.2540; Found: 524.2451.

Dimethyl 7-methyl-5-(4,4,5,5-tetramethyl-1,3,2-dioxaborolan-2-yl)-6-(trimethylsilyl)-1,3,3a,6-tetrahydro-2*H*-indene-2,2-dicarboxylate (26cb): The compound was purified by column chromatography (cyclohexane/EtOAc 9:1) and was obtained as a yellow oil in 58% yield (103 mg). ^{1}H NMR (300 MHz, $CDCl_3$) *δ* 6.41 (s, 1H), 3.73 (s, 3H), 3.69 (s, 3H), 3.01 (d, *J* = 17.0 Hz, 1H), 2.87 (d, *J* = 17.0 Hz, 1H), 2.62 (dd, *J* = 11.7, 7.7 Hz, 1H), 2.50 (s, 1H), 1.90 – 1.78 (m, 2H), 1.69 (s, 3H), 1.24 (s, 12H), -0.04 (s, 9H). ^{13}C NMR (75 MHz, $CDCl_3$) *δ* 172.8 (C), 172.5 (C), 139.3 (CH), 127.2 (C), 127.0 (C), 83.4 (2 × C), 58.4 (C), 52.8 (CH_3), 52.7 (CH_3), 41.7 (CH), 40.7 (CH), 39.5 (CH_2), 36.4 (CH_2), 25.0 (2 × CH_3), 24.8 (2 × CH_3), 19.9 (CH_3), -1.2 (3 × CH_3). HRMS (ESI, MeOH) calcd. for $C_{23}H_{37}BO_6Si$ [M + Na]$^+$: 471.2452; Found: 471.2341.

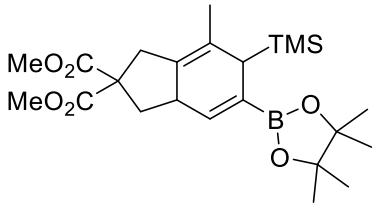

Dimethyl 7-(4-methoxyphenyl)-5-(4,4,5,5-tetramethyl-1,3,2-dioxaborolan-2-yl)-6-(trimethylsilyl)-1,3,3a,6-tetrahydro-2*H*-indene-2,2-dicarboxylate (26ce): The compound was purified by column chromatography (cyclohexane/EtOAc 9:1) and was obtained as a yellow oil in 41% yield (90 mg). ^{1}H NMR (300 MHz, $CDCl_3$) *δ* 7.23 (d, *J* = 8.7 Hz, 2H), 6.84 (d, *J* = 8.7 Hz, 2H), 6.44 (s, 1H), 3.80 (s, 3H), 3.76 (s, 3H), 3.60 (s, 3H), 3.36 (d, *J* = 17.5 Hz, 1H), 3.13 – 3.05 (m, 2H), 2.71 (d, *J* = 17.5 Hz, 1H), 2.63 (dd, *J* = 12.1, 7.5 Hz, 1H), 1.97 (t, *J* = 12.1 Hz, 1H), 1.28 (s, 12H), -0.21 (s, 9H). ^{13}C NMR (75 MHz, $CDCl_3$) *δ* 173.1 (C), 172.3 (C), 158.3 (C), 138.8 (CH), 134.7 (C), 132.6 (C), 129.8 (2 × CH), 128.9 (C), 113.4 (2 × CH), 83.5 (2 × C), 58.3 (C), 55.3 (CH_3), 52.9 (CH_3), 52.6 (CH_3), 42.2 (CH), 40.0 (CH), 39.4 (CH_2), 37.7 (CH_2), 25.1 (2 × CH_3), 25.0 (2 × CH_3), -1.5 (3 × CH_3). HRMS (ESI, MeOH) calcd. for $C_{29}H_{41}BO_7Si$ [M + Na]$^+$: 563.2715; Found: 563.2631.

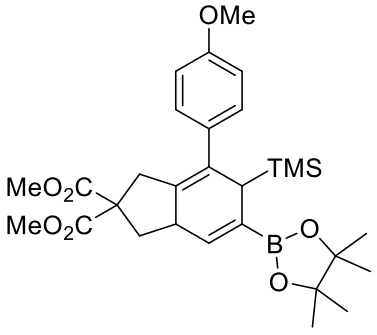

Dimethyl 4-methyl-7-phenyl-5-(4,4,5,5-tetramethyl-1,3,2-dioxaborolan-2-yl)-6-(trimethylsilyl)-1,3,3a,6-tetrahydro-2*H*-indene-2,2-dicarboxylate (26ci): The compound was purified by column chromatography (cyclohexane/EtOAc 9:1) and was obtained as a brown oil in 27% yield (57 mg). ^{1}H NMR (300 MHz, $CDCl_3$) *δ* 7.41 – 7.30 (m, 3H), 7.27 – 7.14 (m, 2H), 3.79 (s, 1H), 3.63 (s, 1H), 3.48 (d, *J* = 17.6 Hz, 1H), 3.22 (d, *J* = 3.8 Hz, 1H), 3.13 – 2.98 (m, 1H), 2.66 (dd, *J* = 17.6, 10.3 Hz, 1H), 2.14 – 1.96 (m, 1H), 1.30 (s, 12H), 1.12 (d, *J* = 11.3 Hz, 3H), -0.22 (s, 9H). ^{13}C NMR (75 MHz, $CDCl_3$) *δ* 173.0 (C), 172.4 (C), 145.3 (C), 142.5 (C), 133.4 (C), 129.5 (C), 128.7 (2 × CH), 128.0 (2 × CH), 126.5 (CH), 83.1 (2 × C), 58.2 (C), 53.0 (CH_3), 52.7

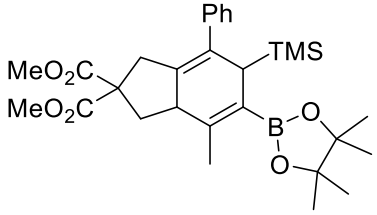

(CH_3), 47.0 (CH), 41.8 (CH), 38.7 (CH_2), 37.3 (CH_2), 25.3 (2 × CH_3), 25.2 (2 × CH_3), 19.3 (CH_3), -1.2 (3 × CH_3). HRMS (ESI, MeOH) calcd. for $C_{29}H_{41}BO_6Si$ [M + Na]$^+$: 547.2765; Found: 547.2673.

Trimethyl(4-phenyl-6-(4,4,5,5-tetramethyl-1,3,2-dioxaborolan-2-yl)-2,3,5,7a-tetrahydro-1*H*-inden-5-yl)silane (26ea): The compound was purified by column chromatography (cyclohexane/EtOAc 95:5) and was obtained as a brown oil in 82% yield (130 mg). ^{1}H NMR (300 MHz, $CDCl_3$) δ 7.36 – 7.28 (m, 4H), 7.24 – 7.14 (m, 1H), 6.54 (s, 1H), 3.16 (d, J = 4.6 Hz, 1H), 3.03 – 2.90 (m, 1H), 2.70 – 2.56 (m, 1H), 2.24 – 2.02 (m, 3H), 1.76 – 1.50 (m, 2H), 1.30 (s, 12H), -0.19 (s, 9H). ^{13}C NMR (75 MHz, $CDCl_3$) δ 143.4 (C), 141.2 (CH), 134.4 (C), 131.1 (C), 128.9 (2 × CH), 127.8 (2 × CH), 126.2 (CH), 83.4 (2 × C), 43.8 (CH), 40.0 (CH), 32.3 (CH_2), 29.7 (CH_2), 25.2 (2 × CH_3), 25.1 (2 × CH_3), 24.0 (CH_2), -1.30 (3 × CH_3). HRMS (ESI, MeOH) calcd. for $C_{24}H_{35}BO_2Si$ [M + Na]$^+$: 417.2499; Found: 417.2393.

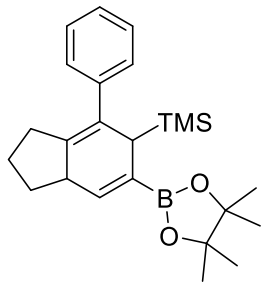

Trimethyl(6-(4,4,5,5-tetramethyl-1,3,2-dioxaborolan-2-yl)-4-(*p*-tolyl)-2,3,5,7a-tetrahydro-1*H*-inden-5-yl)silane (26eb): The compound was purified by column chromatography (cyclohexane/EtOAc 95:5) and was obtained as a brown oil in 99% yield (175 mg). ^{1}H NMR (300 MHz, $CDCl_3$) δ 7.21 (d, J = 8.1 Hz, 2H), 7.09 (d, J = 8.1 Hz, 2H), 6.54 (s, 1H), 3.13 (d, J = 4.7 Hz, 1H), 2.99 – 2.87 (m, 1H), 2.69 – 2.55 (m, 1H), 2.33 (s, 3H), 2.23 – 2.03 (m, 2H), 1.85 – 1.60 (m, 3H), 1.29 (s, 12H), -0.20 (s, 9H). ^{13}C NMR (75 MHz, $CDCl_3$) δ 141.2 (CH), 140.3 (C), 135.5 (C), 133.8 (C), 130.9(C), 128.7 (2 × CH), 128.5 (2 × CH), 83.3 (2 × C), 43.7 (CH), 39.8 (CH), 32.3 (CH_2), 29.7 (CH_2), 25.1 (2 × CH_3), 25.0 (2 × CH_3), 23.9 (CH_2), 21.3 (CH_3), -1.3 (3 × CH_3). HRMS (ESI, MeOH) calcd. for $C_{25}H_{37}BO_2Si$ [M + Na]$^+$: 431.2656; Found: 431.2556.

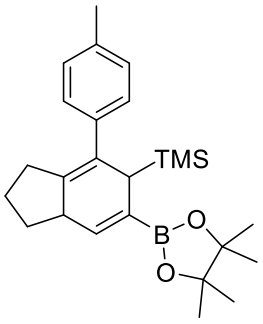

(4-(4-Fluorophenyl)-6-(4,4,5,5-tetramethyl-1,3,2-dioxaborolan-2-yl)-2,3,5,7a-tetrahydro-1*H*-inden-5-yl)trimethylsilane (26ec): The compound was purified by column chromatography (cyclohexane/EtOAc 95:5) and was obtained as a brown oil in 99% yield (164 mg). ^{1}H NMR (300 MHz, $CDCl_3$) δ 7.30 (dd, J = 8.8, 5.6 Hz, 2H), 6.97 (t, J = 8.8 Hz, 2H), 6.53 (s, 1H), 3.09 (d, J = 4.7 Hz, 1H), 2.99 – 2.88 (m, 1H), 2.66 – 2.50 (m, 1H), 2.21 – 1.99 (m, 2H), 1.86 – 1.58 (m, 3H), 1.29 (s, 12H), -0.19 (s, 9H). ^{13}C NMR (75 MHz, $CDCl_3$) δ 161.3 (d, J = 244.7 Hz, C) , 141.1 (CH), 139.2 (d, J = 3.3 Hz, C), 134.5 (C), 130.3 (d, J = 7.7 Hz, 2 × CH), 130.1 (C), 114.6 (d, J = 21.0 Hz, 2 × CH), 83.4 (2 × C), 43.7 (CH), 40.1 (CH), 32.2 (CH_2), 29.6 (CH_2), 25.1 (2 × CH_3), 25.0 (2 × CH_3), 23.9 (CH_2), -1.3 (3 × CH_3). ^{19}F NMR (282 MHz, $CDCl_3$) δ -116.58. HRMS (ESI, MeOH) calcd. for $C_{24}H_{35}BFO_2Si$ [M + Na]$^+$: 435.2405; Found: 435.2313.

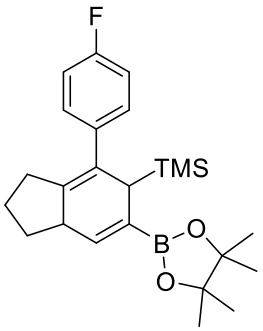

(4-Butyl-6-(4,4,5,5-tetramethyl-1,3,2-dioxaborolan-2-yl)-2,3,5,7a-tetrahydro-1*H*-inden-5-yl)trimethylsilane (26ed): The compound was purified by column chromatography (cyclohexane/EtOAc 95:5) and was obtained as a light brown oil in 69% yield (104 mg). ^{1}H NMR (300 MHz, $CDCl_3$) δ 6.50 (s, 1H), 2.78 – 2.65 (m, 1H), 2.61 (d, J = 4.1 Hz, 1H), 2.46 – 2.35 (m, 1H), 2.33 – 2.15 (m, 4H), 2.12 – 1.96 (m, 2H), 1.88 – 1.51 (m, 5H), 1.26 (s, 12H), 0.95 – 0.84 (m, 3H), -0.02 (s, 9H). ^{13}C NMR (75 MHz, $CDCl_3$) δ 142.0 (CH), 131.3 (C), 129.9 (C), 83.2 (2 × C), 43.9 (CH), 37.9 (CH), 33.7 (CH_2), 32.8 (CH_2), 29.8 (CH_2), 27.8 (CH_2), 25.0 (2 × CH_3), 24.6 (2 × CH_3), 23.1 (CH_2), 14.2 (CH_3), -0.8 (3 × CH_3). HRMS (ESI, MeOH) calcd. for $C_{22}H_{39}BO_2Si$ [M + Na]$^+$: 397.2812; Found: 397.2707.

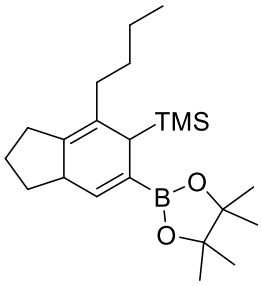

2,7-Diphenyl-5-(4,4,5,5-tetramethyl-1,3,2-dioxaborolan-2-yl)-6-(trimethylsilyl)-2,3,3a,6-tetrahydro-1*H*-isoindol-1-one (26fb): The compound was purified by column chromatography (cyclohexane/EtOAc 4:1) and was obtained as a light brown solid in 26% yield (50 mg). M.p. = 206 – 208 °C. ^{1}H NMR (300 MHz, $CDCl_3$) δ 7.61 (d, J = 7.7 Hz, 2H), 7.48 (dd, J = 8.0, 1.4 Hz, 2H), 7.38 – 7.27 (m, 5H), 7.06 (t, J = 7.3 Hz, 1H), 6.54 (s, 1H), 4.06 (t, J = 7.5 Hz, 1H), 3.65 (d, J = 8.8 Hz, 1H), 3.61 – 3.56 (m, 1H), 3.37 (d, J = 4.5 Hz, 1H), 1.32 (s, 12H), -0.10 (s, 9H). ^{13}C NMR (75 MHz, $CDCl_3$) δ 165.6 (C), 150.4 (C), 140.2 (C), 138.6 (C), 136.1 (CH), 129.7 (2 × CH), 128.6 (2 × CH), 128.1 (CH), 127.3 (2 × CH), 124.0 (CH), 121.5 (C), 119.9 (2 × CH), 83.9 (2 × C), 51.4 (CH_2), 45.6 (CH), 36.5 (CH), 25.1 (4 × CH_3), -1.0 (3 × CH_3). HRMS (ESI, MeOH) calcd. for $C_{29}H_{36}BNO_3SSi$ [M + Na]$^+$: 508.2558; Found: 508.2464.

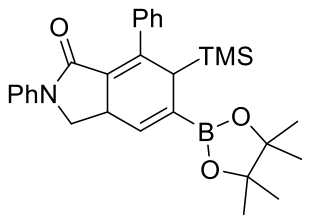

Dimethyl 7-(4-cyanophenyl)-5-(4,4,5,5-tetramethyl-1,3,2-dioxaborolan-2-yl)-6-(trimethylsilyl)-1,3,3a,4-tetrahydro-2*H*-indene-2,2-dicarboxylate (28cf): The compound was purified by column chromatography (cyclohexane/EtOAc 9:1) and was obtained as a yellow oil in 70% yield (150 mg). ^{1}H NMR (300 MHz, $CDCl_3$) δ 7.58 (d, J = 8.5 Hz, 2H), 7.28 (d, J = 8.5 Hz, 2H), 3.75 (s, 3H), 3.65 (s, 3H), 3.38 (d, J = 18.3 Hz, 1H), 2.78 – 2.66 (m, 2H), 2.62 (d, J = 15.2 Hz, 1H), 2.57 – 2.43 (m, 1H), 1.89 (dd, J = 12.9, 8.8 Hz, 1H), 1.64 (t, J = 16.1 Hz, 1H), 1.31 (s, 12H), -0.16 (s, 9H). ^{13}C NMR (75 MHz, $CDCl_3$) δ 172.0 (C), 171.8 (C), 153.2 (C), 146.9 (C), 142.4 (C), 134.4 (C), 131.7 (2 × CH), 129.6 (2 × CH), 119.0 (C), 110.0 (C), 83.7 (2 × C), 59.8 (C), 52.9 (CH_3), 52.7 (CH_3), 39.7 (CH_2), 38.4 (CH_2), 33.7 (CH), 25.3 (2 × CH_3), 24.9 (2 × CH_3), 2.2 (3 × CH_3). HRMS (ESI, MeOH) calcd. for $C_{29}H_{38}BNO_6Si$ [M + Na]$^+$: 558.2561; Found: 558.2442.

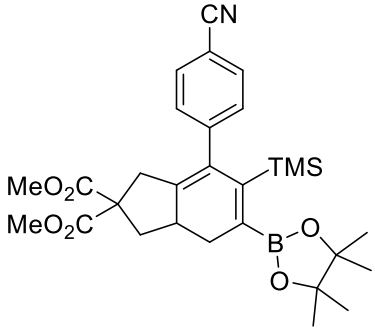

Byproducts (29)

4-(4-Methoxyphenyl)-2-tosyl-6-(trimethylsilyl)isoindoline (29bd): The compound was obtained by the evolution of **3f** with time, and it was purified by crystallization in EtOH. ^{1}H NMR (300 MHz, $CDCl_3$) δ 7.76 (d, J = 8.3 Hz, 2H), 7.33 (d, J = 7.6 Hz, 2H), 7.27 (d, J = 7.6 Hz, 2H), 6.98 (d, J = 8.3 Hz, 2H), 4.67 (d, J = 6.4 Hz, 4H), 3.87 (s, 3H), 2.40 (s, 3H), 0.26 (s, 9H). ^{13}C NMR (75 MHz, $CDCl_3$) δ 159.4 (C), 143.8 (C), 141.3 (C), 136.7 (C), 136.4 (C), 134.9 (C), 133.8 (CH), 133.0 (C), 132.3 (C), 129.9 (2 × CH), 129.3 (2 × CH), 127.8 (2 × CH), 125.9 (CH), 114.3 (2 × CH), 55.5 (CH_3), 54.0 (CH_2), 53.8 (CH_2), 21.6 (CH_3), -1.0 (3 × CH_3). HRMS (TOF EI, MeOH) calcd. for $C_{25}H_{29}NO_3SSi$ $[M]^+$: 451.1637; Found: 451.1648.

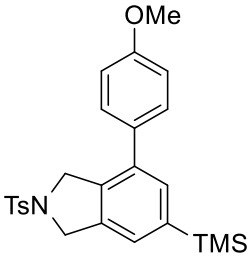

Trimethyl(4-phenyl-2,3-dihydro-1*H*-inden-5-yl)silane (29ea): The compound was obtained by the evolution of **3a** with time, and it was purified by column chromatography (cyclohexane). ^{1}H NMR (300 MHz, $CDCl_3$) δ 7.49 – 7.40 (m, 5H), 7.38 – 7.31 (m, 2H), 2.99 (dd, J = 15.5, 7.3 Hz, 4H), 2.06 (quint, J = 7.3 Hz, 2H), 0.30 (s, 9H). ^{13}C NMR (75 MHz, $CDCl_3$) δ 144.6 (C), 143.1 (C), 141.8 (C), 138.7 (C), 138.0 (C), 131.9 (CH), 128.8 (2 × CH), 128.5 (CH), 128.4 (2 × CH), 127.0 (CH), 33.3 (CH_2), 32.9 (CH_2), 25.7 (CH_2), -0.8 (3 × CH_3). HRMS (TOF EI, MeOH) calcd. for $C_{18}H_{22}Si$ $[M]^+$: 266.1491; Found: 266.1487.

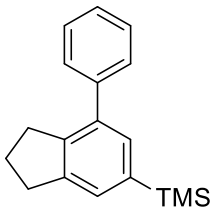

Carbocyclization products (30)

(*E*)-1-(1-Tosyl-4-(4-(trimethylsilyl)but-3-yn-2-ylidene)pyrrolidin-3-yl)propan-2-one (30gb): The compound was purified by column chromatography (cyclohexane/EtOAc 9:1) and was obtained as a yellow oil in 10% yield (16 mg). ^{1}H NMR (300 MHz, $CDCl_3$) δ 7.68 (d, J = 8.1 Hz, 2H), 7.34 (d, J = 8.1 Hz, 2H), 4.04 (d, J = 15.5 Hz, 1H), 3.45 (d, J = 15.5 Hz, 1H), 3.29 (d, J = 9.5 Hz, 2H), 3.01 (dd, J = 9.5, 6.6 Hz, 1H), 2.87 (d, J = 18.0 Hz, 1H), 2.64 (dd, J = 18.0, 11.1 Hz, 1H), 2.43 (s, 3H), 2.12 (s, 3H), 1.67 (s, 3H), 0.11 (s, 9H). ^{13}C NMR (75 MHz, $CDCl_3$) δ 207.1 (C), 147.5 (C), 144.1 (C), 131.6 (C), 129.9 (2 × CH), 128.1 (2 × CH), 112.0 (C), 104.3 (C), 98.5 (C), 53.4 (CH_2), 50.8 (CH_2), 45.9 (CH_2), 38.6 (CH), 29.9 (CH_3), 21.7 (CH_3), 19.1 (CH_3), -0.0 (3 × CH_3). HRMS (ESI, MeOH) calcd. for $C_{21}H_{29}NO_3SSi$ $[M + H]^+$: 404.1637; Found: 404.1719.

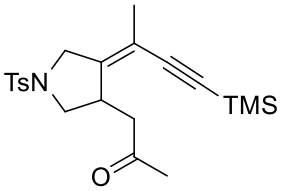

(*E*)-1-Phenyl-2-(1-tosyl-4-(4-(trimethylsilyl)but-3-yn-2-ylidene)pyrrolidin-3-yl)ethan-1-one (30gc): The compound was purified by column chromatography (cyclohexane/EtOAc 9:1) and was obtained as a light brown solid in 43% yield (79 mg). M.p. = 55 – 57 °C. ^{1}H NMR (300 MHz, $CDCl_3$) δ 7.92 (d, J = 8.2 Hz, 2H), 7.69 (d, J = 8.2 Hz, 2H), 7.61 – 7.54 (m, 1H), 7.50 – 7.41 (m, 2H), 7.31 (d, J = 8.1 Hz, 2H), 4.10 (d, J = 15.0 Hz, 1H), 3.55 (d, J = 15.0 Hz, 2H), 3.48 – 3.35 (m, 2H), 3.20 – 3.04 (m, 2H), 2.41 (s, 3H), 1.71 (s, 3H), -0.01 (s, 9H). ^{13}C NMR (75 MHz, $CDCl_3$) δ 198.4 (C), 147.7 (C), 144.0 (C), 136.5 (C), 133.3 (CH), 131.7 (C), 129.8 (2 × CH), 128.6 (2 × CH), 128.0 (2 × CH), 127.9 (2 × CH), 112.1 (C), 104.2 (C), 98.7 (C), 53.5 (CH_2), 50.9 (CH_2), 41.1 (CH_2), 38.9 (CH), 21.6 (CH_3), 19.1 (CH_3), -0.2 (3 × CH_3). HRMS (ESI, MeOH) calcd. for $C_{26}H_{31}NO_3SSi$ $[M + H]^+$: 466.1794; Found: 466.1874.

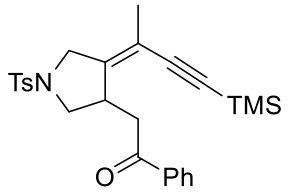

**nOe experiments to confirm the configuration of the double bond:*

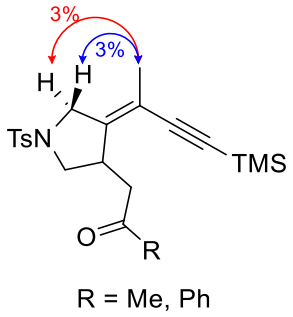

R = Me, Ph

3.5.4.5. Transformations of silyl-boronates

3.5.4.5.1. General procedure for oxidation of boronates

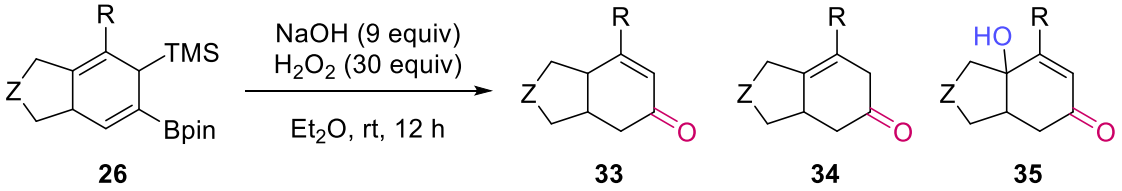

26 **33** **34** **35**

A solution of the corresponding boronate **26** (1 equiv, 0.4 mmol) in diethyl ether (2.5 mL, 0.2 M) was treated with NaOH (3 N, 9 equiv) and H_2O_2 (30%, 30 equiv) at 0 °C. The mixture was stirred overnight at room temperature. The resulting suspension was extracted with diethyl ether (2 × 5 mL). The combined organic layers were washed with brine, dried over anhydrous $MgSO_4$, filtered and concentrated under vacuum. The resulting residue was purified by column chromatography to give the corresponding oxidized product (cyclohexane/EtOAc 7:3 was used as an eluent).[100]

7-(4-Methoxyphenyl)-2-tosyl-1,2,3,3a,4,7a-hexahydro-5*H*-isoindol-5-one (33ea): The

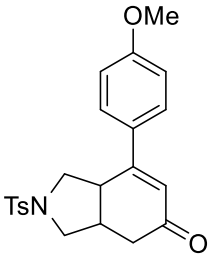

compound was purified by column chromatography (cyclohexane/EtOAc 7:3) and was obtained as a yellow oil in 60% yield (45 mg). ^{1}H NMR (300 MHz, $CDCl_3$) δ 7.67 (d, J = 8.2 Hz, 2H), 7.38 (d, J = 8.9 Hz, 2H), 7.31 (d, J = 8.2 Hz, 2H), 6.91 (d, J = 8.9 Hz, 2H), 6.28 (s, 1H), 3.85 (s, 3H), 3.81 – 3.74 (m, 3H), 3.59 (dd, J = 10.3, 6.1 Hz, 1H), 3.47 (dd, J = 14.8, 8.6 Hz, 1H), 3.22 (dd, J = 10.3, 2.8 Hz, 1H), 3.16 – 3.08 (m, 1H), 2.94 – 2.83 (m, 1H), 2.44 (s, 3H). ^{13}C NMR (75 MHz, $CDCl_3$) δ 197.3 (C), 161.9 (C), 155.8 (C), 144.0 (C), 133.8 (C), 130.0 (2 × CH), 128.2 (2 × CH), 127.5 (2 × CH), 123.5 (CH), 114.6 (2 × CH), 55.6 (CH_3), 52.8 (CH_2), 51.3 (CH_2), 39.7 (CH), 37.6 (CH), 37.5 (CH_2), 21.7 (CH_3). HRMS (ESI, MeOH) calcd. for $C_{22}H_{23}NO_4S$ [M + Na]$^+$: 420.1348; Found: 420.1247.

[100] T. Xi, Z. Lu, *ACS Catal.* **2017**, *7*, 1181–1185.

7-Phenyl-1,2,3,3a,4,6-hexahydro-5*H*-inden-5-one (34ea): The compound was purified by column chromatography (cyclohexane/EtOAc 9:1) and was obtained as a yellow oil in 48% yield (15 mg). ^{1}H NMR (300 MHz, $CDCl_3$) δ 7.39 – 7.31 (m, 2H), 7.30 – 7.20 (m, 3H), 3.30 – 3.10 (m, 2H), 2.88 – 2.69 (m, 1H), 2.61 – 2.41 (m, 2H), 2.29 – 2.11 (m, 2H), 1.95 – 1.80 (m, 2H), 1.78 – 1.57 (m, 1H), 1.75 – 1.57 (m, 1H), 1.48 – 1.29 (m, 1H). ^{13}C NMR (75 MHz, $CDCl_3$) δ 211.8 (C), 143.3 (C), 141.0 (C), 128.4 (2 × CH), 127.4 (2 × CH), 126.8 (CH), 125.3 (C), 44.9 (CH_2), 44.5 (CH_2), 41.8 (CH), 33.9 (CH_2), 30.5 (CH_2), 25.4 (CH_2). HRMS (TOF EI, MeOH) calcd. for $C_{15}H_{16}O$ $[M]^+$: 212.1201; Found: 212.1197.

7a-Hydroxy-7-phenyl-1,2,3,3a,4,7a-hexahydro-5*H*-inden-5-one (35ea): The compound was obtained by oxidation in air of **34ea** with time, and it was purified by column chromatography (cyclohexane/EtOAc 7:3) and was obtained as a yellow oil. ^{1}H NMR (300 MHz, $CDCl_3$) δ 7.70 (br s, 1H), 7.58 (dd, J = 6.6, 3.0 Hz, 2H), 7.46 – 7.37 (m, 3H), 6.28 (s, 1H), 3.28 – 3.14 (m, 1H), 2.77 (dd, J = 16.9, 6.3 Hz, 1H), 2.47 (dd, J = 16.9, 9.7 Hz, 1H), 2.18 – 2.12 (m, 3H), 1.89 (dt, J = 13.7, 6.8 Hz, 2H), 1.50 (dt, J = 18.8, 6.4 Hz, 1H). ^{13}C NMR (75 MHz, $CDCl_3$) δ 198.8 (C), 159.9 (C), 137.1 (C), 129.8 (CH), 129.7 (CH), 128.8 (2 × CH), 128.0 (2 × CH), 92.8 (C), 44.1 (CH), 40.8 (CH_2), 36.1 (CH_2), 30.2 (CH_2), 22.9 (CH_2). HRMS (TOF EI, MeOH) calcd. for $C_{15}H_{16}O$ $[M]^+$: 251.1150; Found: 251.1049.

3.5.4.5.2. General procedure for Fleming-Tamao oxidation

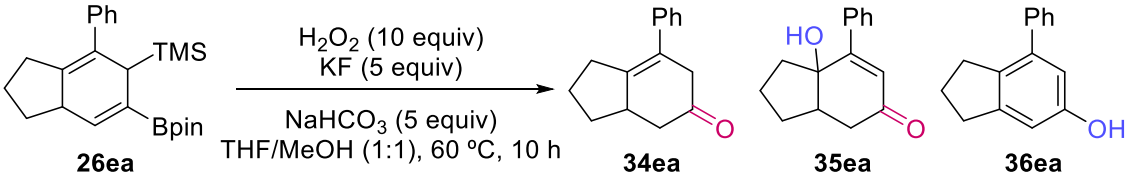

A round-bottom flask equipped with a magnetic stirring bar, was charged with KF (1.5 mmol, 5 equiv), $NaHCO_3$ (1.5 mmol, 5 equiv), **26ea** (0.3 mmol, 1.0 equiv), THF (0.05 M, 6 mL) and MeOH (0.05 M, 6.0 mL). Then, 30% aq. H_2O_2 (3 mmol, 10 equiv) was added. The resulting mixture was stirred at 60 ºC for 10 h before a saturated aqueous solution of $Na_2S_2O_3$ (5 mL) was added. The resulting solution was extracted with EtOAc and washed with brine, dried over anhydrous Na_2SO4. After filtration and evaporation of the solvent under vacuum, the residue was purified by column chromatography.[303]

7-Phenyl-1,2,3,3a,4,6-hexahydro-5*H*-inden-5-one (34ea): The compound was purified by column chromatography (cyclohexane/EtOAc 9:1) and was obtained as a yellow oil in 17% yield (15 mg). Spectroscopy data is described in *General procedure for oxidation of boronates.*

7a-Hydroxy-7-phenyl-1,2,3,3a,4,7a-hexahydro-5*H*-inden-5-one (35ea): The compound was purified by column chromatography (cyclohexane/EtOAc 7:3) and was obtained as a yellow oil in 9% yield. Spectroscopy data is described in *General procedure for oxidation of boronates.*

[303] Z. Zuo, J. Yang, Z. Huang, *Angew. Chem. Int. Ed.* **2016**, *55*, 10839–10843.

7-Phenyl-2,3-dihydro-1*H*-inden-5-ol (36ea): The compound was purified by column chromatography (cyclohexane/EtOAc 7:3) and was obtained as a yellow oil in 24% yield (16 mg). ^{1}H NMR (300 MHz, $CDCl_3$) δ 7.47 – 7.30 (m, 5H), 6.74 (s,1H), 6.70 (s, 1H), 4.92 (br s, 1H), 2.91 (dt, J = 10.8, 7.3 Hz, 4H), 2.05 (p, J = 7.3 Hz, 2H). ^{13}C NMR (75 MHz, $CDCl_3$) δ 154.6 (C), 146.8 (C), 141.1 (C), 139.0 (C), 134.1 (C), 128.4 (2 × CH), 128.2 (2 × CH), 127.0 (CH), 113.4 (CH), 110.6 (CH), 33.3 (CH_2), 32.0 (CH_2), 26.0 (CH_2). HRMS (TOF EI, MeOH) calcd. for $C_{15}H_{14}O$ $[M]^+$: 210.1045; Found: 210.1039.

3.5.4.6. Mechanistic studies

3.5.4.6.1. Reaction with simple alkenes and alkynes

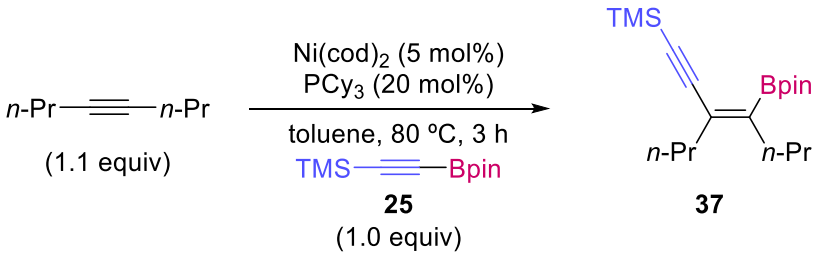

(*E*)-Trimethyl(3-propyl-4-(4,4,5,5-tetramethyl-1,3,2-dioxaborolan-2-yl)hept-3-en-1-yn-1-yl)silane (37):[269] The product was synthetized following *the General procedure for the carboborylative cyclization reaction* and a mixture of isomers cis:trans (94:6) was obtained as yellow oil in 62% yield (120 mg). ^{1}H NMR (300 MHz, $CDCl_3$) δ 2.16 (dd, J = 8.7, 6.8 Hz, 4H), 1.63 – 1.46 (m, 2H), 1.43 – 1.32 (m, 2H), 1.30 (s, 12H), 0.94 (t, J = 7.0 Hz, 3H), 0.89 (t, J = 7.0 Hz, 3H), 0.17 (s, 9H).

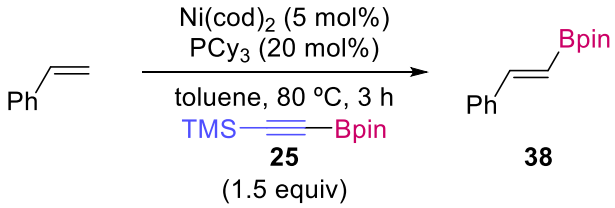

(*E*)-4,4,5,5-Tetramethyl-2-styryl-1,3,2-dioxaborolane (38):[304] The product was synthetized following *the General procedure for the carboborylative cyclization reaction* and was obtained as brown oil in 58% yield (53 mg). ^{1}H NMR (300 MHz, $CDCl_3$) δ 7.49 (dd, J = 7.8, 1.5 Hz, 2H), 7.40 (d, J = 18.4 Hz, 1H), 7.33 (dd, J = 7.7, 1.7 Hz, 3H), 6.17 (d, J = 18.4 Hz, 1H), 1.32 (s, 12H).

[269] M. Suginome, M. Shirakura, A. Yamamoto, *J. Am. Chem. Soc.* **2006**, *128*, 14438–14439.
[304] J. Szyling, A. Franczyk, K. Stefanowska, H. Maciejewski, J. Walkowiak, *ACS Sustain. Chem. Eng.* **2018**, *6*, 10980–10988.

3.5.4.6.2. Deuteration experiments

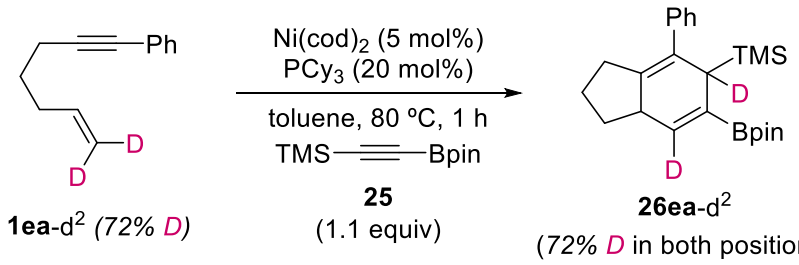

1ea-d^2 *(72% D)* — **25** (1.1 equiv) — **26ea**-d^2 (*72% D* in both positions)

Trimethyl(4-phenyl-6-(4,4,5,5-tetramethyl-1,3,2-dioxaborolan-2-yl)-2,3,5,7a-tetrahydro-1*H*-inden-5-yl-5,7-*d*^{2})silane (26ea-d^2**):** The product was synthetized following *the General procedure for the carboborylative cyclization reaction* and was obtained as a brown oil in 80% yield (127 mg). ^{1}H NMR (300 MHz, $CDCl_3$) δ 7.37 – 7.28 (m, 4H), 7.21 – 7.15 (m, 1H), 6.55 (s, 0.28 H, *28% H*), 3.15 (d, *J* = 5.3 Hz, 0.28 H, *28% H*), 2.96 (t, *J* = 9.3 Hz, 1H), 2.74 – 2.56 (m, 1H), 2.27 – 2.02 (m, 3H), 1.74 – 1.50 (m, 2H), 1.30 (s, 12H), -0.19 (s, 9H). ^{2}H NMR (77 MHz, $CDCl_3$) δ 6.64 (s, 1D), 3.20 (s, 1D). ^{13}C NMR (75 MHz, $CDCl_3$) δ 143.3 (C), 141.2 (d, *J* = 2.6 Hz, CD), 134.4 (C), 131.1 (C), 128.8 (2 × CH), 127.8 (2 × CH), 126.1 (CH), 83.3 (2 × C), 43.6 (CH), 39.9 (d, *J* = 4.0 Hz, CD), 32.2 (CH_2), 29.7 (CH_2), 25.1 (2 × CH_3), 25.0 (2 × CH_3), 23.9 (CH_2), -1.3 (3 × CH_3). HRMS (APCI, MeOH) calcd. for $C_{24}H_{33}D_2BO_2Si$ $[M + H]^+$: 397.2625; Found: 397.2711.

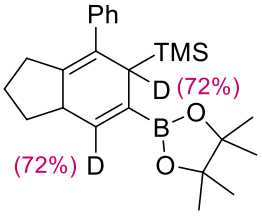

3.5.4.6.3. Stochiometric experiment

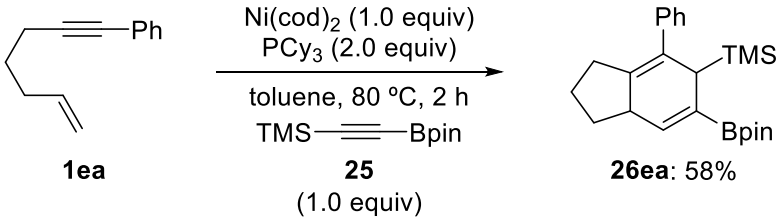

1ea — **25** (1.0 equiv) — **26ea**: 58%

CONCLUSIONES – CONCLUSIONS

4. CONCLUSIONES

Capítulo 2. El sistema $FeBr_2$/biquinolina/MeMgCl cataliza la reacción de ciclación hidroborilativa de eninos con pinacolborano hacia la obtención de alquilboronatos de forma completamente átomo-económica. La reacción tiene lugar en condiciones suaves de reacción y muestra un alcance estructural variado con buena compatibilidad de grupos funcionales. Sin embargo, los alquenos internos son inactivos bajo esas condiciones de reacción. La formación de especies de dialquil-Fe es clave para el transcurso de la reacción, ya que generan un hidruro de Fe intermedio catalíticamente activo a partir de la metátesis σ con HBpin. El mecanismo propuesto parece muy favorable y transcurre con energías de activación muy bajas, por lo que la evolución de la reacción a través del mismo resulta altamente probable. Durante todo el ciclo catalítico, el metal conserva su estado de oxidación Fe(II) sin observarse reducción.

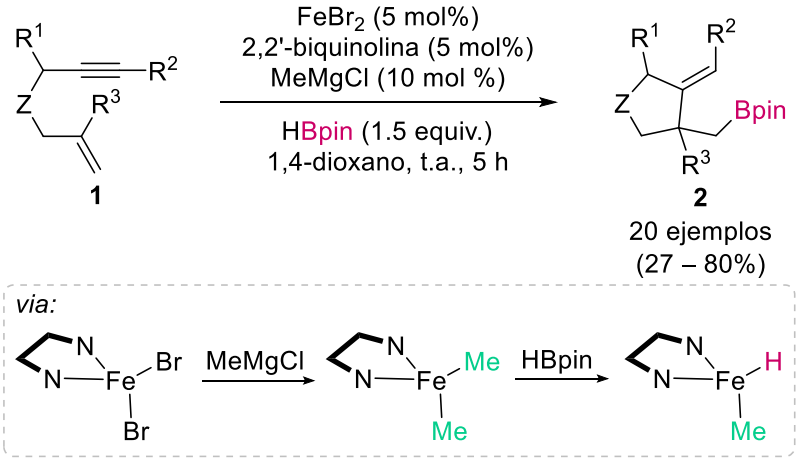

Capítulo 3. La combinación de $Ni(acac)_2$/Xantphos ha permitido llevar a cabo la reacción de ciclación hidroborilativa de eninos de forma catalítica. En función de la sustitución presente en el alquino, se observa una regioselectividad dispar, pudiéndose obtener alquil- y alquenilboronatos con buenos rendimientos. El proceso es compatible con eninos de diversa naturaleza, excepto aquellos que presentan sustitución en el carbono terminal del alqueno. Se propone que la reacción transcurre por un ciclo catalítico Ni(0)–Ni(II) que comienza con una ciclometalación oxidante con el enino, seguida de una metátesis σ con HBpin, siendo clave la formación de hidruros de Ni intermedios que justifican la regioselectividad observada.

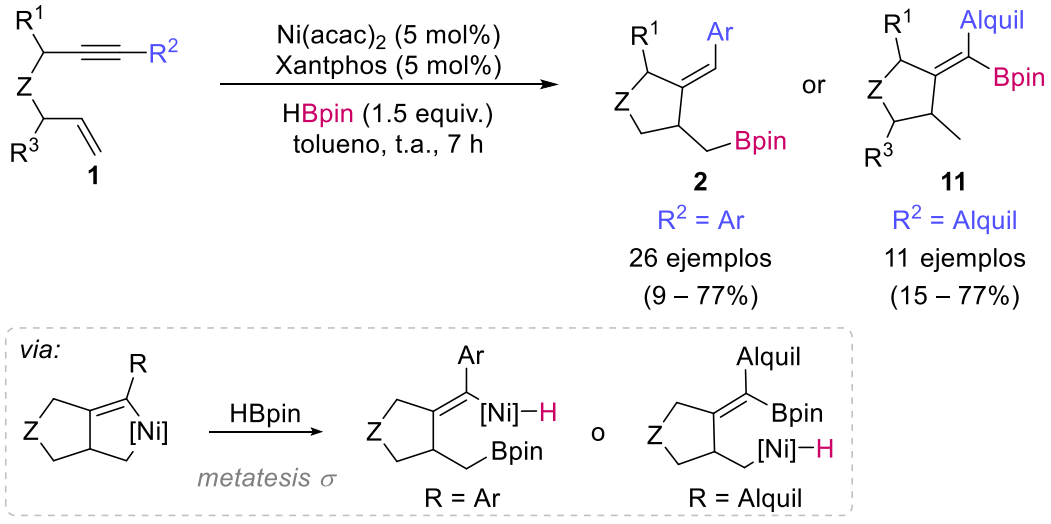

Capítulo 4. Los reactivos de diboro junto con un sistema catalítico de Ni adecuado han dado lugar al desarrollo de la primera ciclación diborilativa de eninos de forma completamente átomo-económica. Los diboronatos obtenidos son útiles e interesantes intermedios sintéticos, ya que es posible funcionalizar selectivamente cada uno de los restos de boro presentes. La activación del enino tiene lugar previamente a la reacción con B_2pin_2, mediante una ciclometalación oxidante con intervención de uno o dos átomos metálicos de Ni.

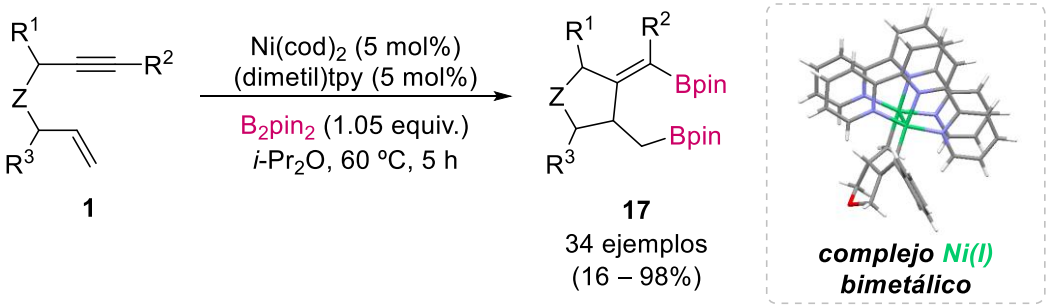

Capítulo 5. El empleo de alquinilboronatos y cantidades catalíticas de $Ni(cod)_2/PCy_3$ ha permitido desarrollar la primera ciclación carboborilativa de eninos, sintetizando 1,4-ciclohexadienos con buenos rendimientos. Los experimentos mecanísticos descartan la adición oxidante del enlace C–B y la ciclometalación oxidante del enino como posibles caminos de reacción. En su lugar, la ciclometalación oxidante de los restos alquino presentes se propone como mecanismo de reacción para explicar los biciclos obtenidos. La isomerización de los dobles enlaces ocurre al final del proceso como resultado de la mayor estabilidad de estos compuestos frente a los 1,3-dienos intermedios.

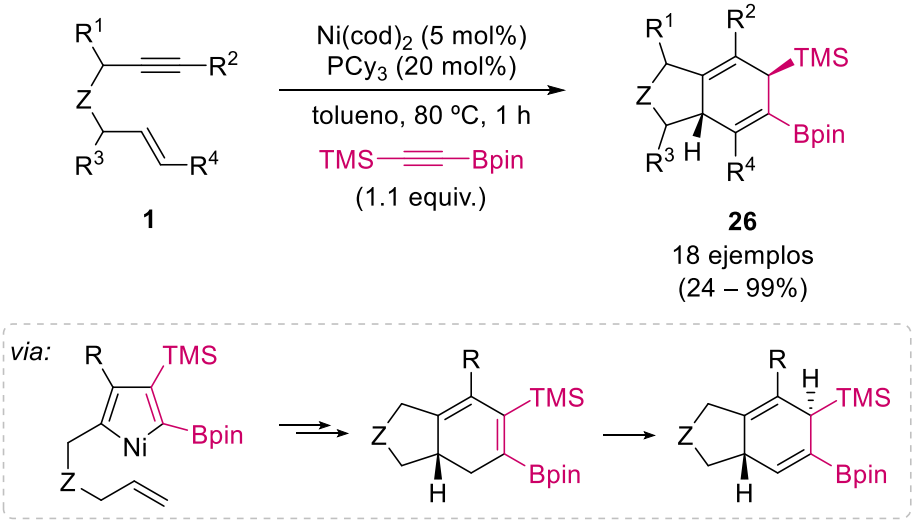

4. CONCLUSIONS

Chapter 2. The $FeBr_2$/biquinoline/MeMgCl system catalyzes the atom-economical hydroborylative cyclization reaction of enynes with pinacolborane, furnishing alkylboronates. The reaction takes places under smooth conditions, and shows a broad scope with high functional group tolerance. However, internal alkenes are ineffective under optimal reaction conditions. The formation of dialkyl-Fe species is the key for the reaction pathway, since they can generate a catalytically active iron hydride intermediate by σ-metathesis with HBpin. The proposed reaction mechanism shows extremely low activation energies for all the steps, what makes it feasible and highly likely. Metal seems to remain at Fe(II) oxidation state during catalytic cycle.

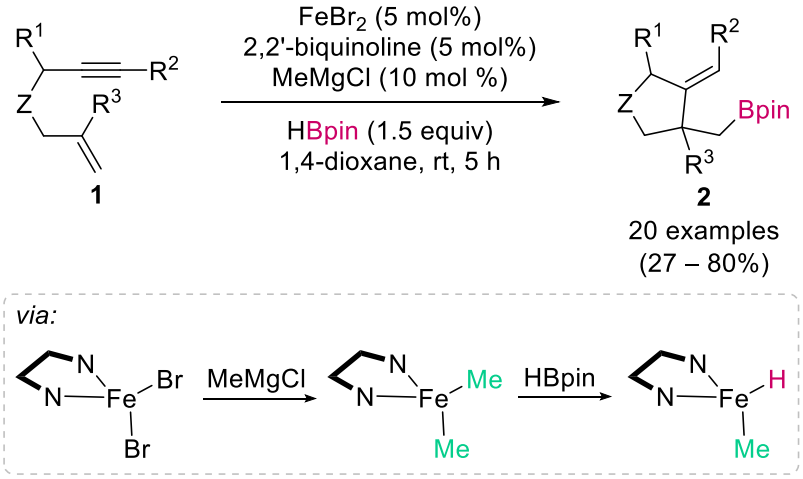

Chapter 3. Combination of $Ni(acac)_2$/Xantphos has led to carry out the hydroborylative cyclization of enynes in a catalytic fashion. Depending on the substitution of the alkyne, different regioselectivity is observed, affording both alkyl- and alkenylboronates in good yields. This methodology is compatible with several enynes, except for those that have substituted the distal carbon of the alkene. The reaction pathway implies a Ni(0)–Ni(II) catalytic cycle which starts with an oxidative cyclometalation of the enyne, followed by σ-metathesis with HBpin. Formation of nickel hydrides intermediates is key for explaining the observed regioselectivity.

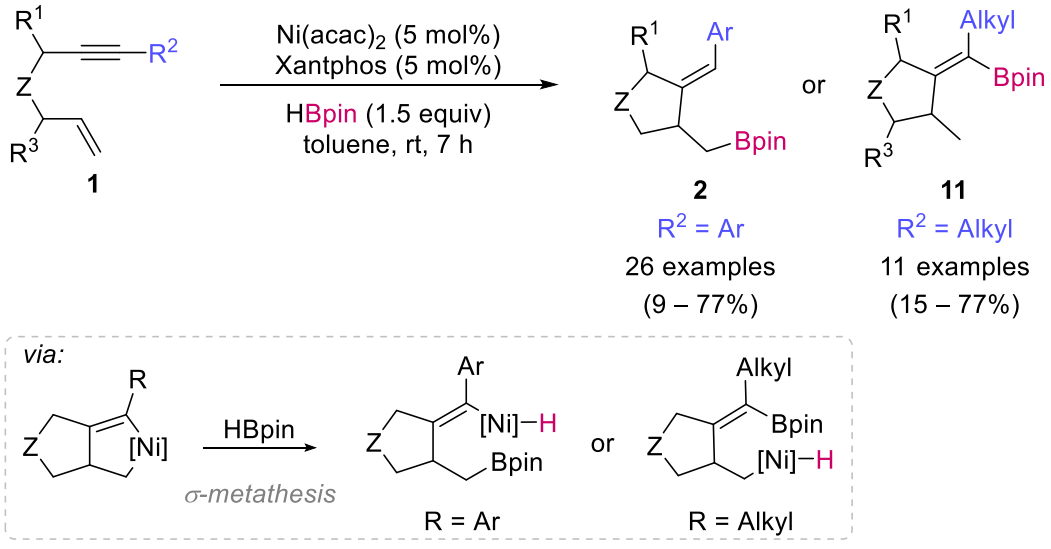

Chapter 4. Diboron reagents, along with a suitable Ni catalytic system allow the development of the first atom-economical diborylative cyclization of enynes. The resulting diboronates, whose both boron units can be selectively functionalized, are useful and attractive synthetic intermediates. Activation of the organic substrate takes place prior to reaction with the borylation reagent, through an oxidative cyclometalation involving one or two nickel atoms.

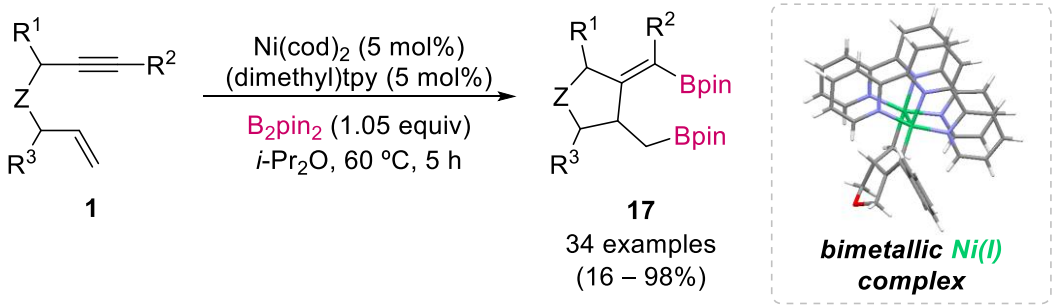

Chapter 5. The use of alkynylboronates and catalytic amounts of $Ni(cod)_2/PCy_3$ has led us to the development of the first carboborylative cyclization reaction of enynes, yielding 1,4-cyclohexadiene in high yields. Mechanistic experiments disregard both the oxidative addition of C–B bond and the oxidative cyclometalation of the enyne. Instead, an initial oxidative cyclometalation involving the present alkyne groups is proposed to explain the bicycles obtained. An off-cycle isomerization of the double bonds is suggested, since these compounds are more stable than the corresponding 1,3-dienes.

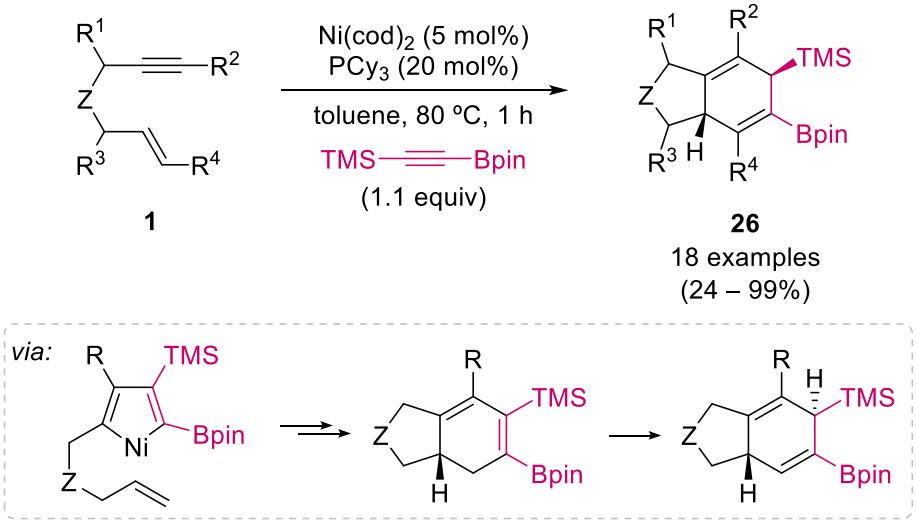

APPENDICES

APPENDIX I: Crystallographic data

❖ Crystal data of complex 6

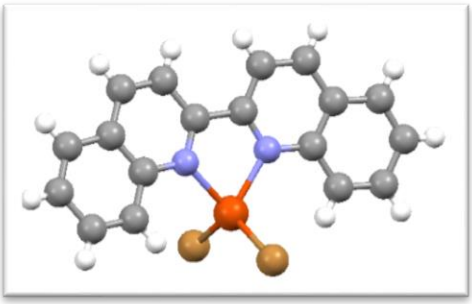

A crystal (0.173 x 0.034 x 0.021 mm^3) was placed onto a thin glass optical fiber or a nylon loop and mounted on a XtaLab Synergy-S Dualflex diffractometer equipped with a HyPix-6000HE HPC area detector for data collection at 100.00(10) K. A preliminary set of cell constants and an orientation matrix were calculated from a small sampling of reflections.[305] A short pre-experiment was run, from which an optimal data collection strategy was determined. The full data collection was carried out using a PhotonJet (Cu) X-ray Source with frame times of 10.29 and 41.16 seconds and a detector distance of 31.2 mm. Series of frames were collected in 0.50° steps in ω at different 2θ, κ, and ϕ settings. After the intensity data were corrected for absorption, the final cell constants were calculated from the xyz centroids of 4322 strong reflections from the actual data collection after integration.[305] See **Table A.1** for additional crystal and refinement information. The structure was solved using ShelXT[306] and refined using ShelXL.[307] The space group $P2_1/c$ was determined based on systematic absences. Most or all non-hydrogen atoms were assigned from the solution. Full-matrix least squares / difference Fourier cycles were performed which located any remaining non-hydrogen atoms. All non-hydrogen atoms were refined with anisotropic displacement parameters. All hydrogen atoms were placed in ideal positions and refined as riding atoms with relative isotropic displacement parameters. The final full matrix least squares refinement converged to $R1 = 0.0437$ (F^2, $I > 2s(I)$) and $wR2 = 0.1205$ (F^2, all data). The structure is the one suggested. The asymmetric unit contains one molecule in a general position. The structure is isomorphous with several late transition metal analogs, including chlorido-ligated Fe, Co, and Zn, bromido-ligated Co, Ni, and Zn, and iodido-ligated Co. Structure manipulation and figure generation were performed using Olex2.[308] Unless noted otherwise all structural diagrams containing thermal displacement ellipsoids are drawn at the 50 % probability level.

Table A.1. Crystal data and structure refinement.

Identification code	**6**	
Empirical formula	C18 H12 Br2 Fe N2	
Formula weight	471.97	
Temperature	100.00(10) K	
Wavelength	1.54184 Å	
Crystal system	monoclinic	
Space group	$P2_1/c$	
Unit cell dimensions	a = 7.8219(3) Å	α = 90°
	b = 12.2458(4) Å	β = 91.3940(10)°
	c = 17.3128(6) Å	γ = 90°
Volume	1620.66(10) $Å^3$	

[305] *CrysAlisPro*, version 171.39.46; Rigaku Corporation: Oxford, UK, **2018**.
[306] G. M. Sheldrick, *SHELXT*, version 2018/2; *Acta. Crystallogr.* **2015**, *A71*, 3–8.
[307] G. M. Sheldrick, *SHELXL*, version 2018/3; *Acta. Crystallogr.* **2015**, *C71*, 3–8.
[308] O. V. Dolomanov, L. J. Bourhis, R. J. Gildea, J. A. K. Howard, H. Puschmann, *Olex2*, version 1.2-ac3; *J. Appl. Cryst.* **2009**, *42*, 339–341.

Z	4
Density (calculated)	1.934 mg/m^3
Absorption coefficient	13.222 mm^{-1}
***F*(000)**	920
Crystal color, morphology	colourless, needle
Crystal size	0.173 x 0.034 x 0.021 mm^3
Theta range for data collection	4.457 to 77.849°
Index ranges	$-9 \leq h \leq 9$, $-14 \leq k \leq 14$, $-13 \leq l \leq 21$
Reflections collected	11638
Independent reflections	3299 [*R*(int) = 0.0553]
Observed reflections	2723
Completeness to theta = 67.684°	99.7%
Absorption correction	Multi-scan
Max. and min. transmission	1.00000 and 0.72117
Refinement method	Full-matrix least-squares on F^2
Data / restraints / parameters	3299 / 0 / 208
Goodness-of-fit on F^2	1.066
Final *R* indices [*I*>2sigma(*I*)]	*R*1 = 0.0437, *wR*2 = 0.1139
***R* indices (all data)**	*R*1 = 0.0548, *wR*2 = 0.1205
Largest diff. peak and hole	1.001 and -0.727 e.Å^{-3}

❖ Crystal data of complex 7

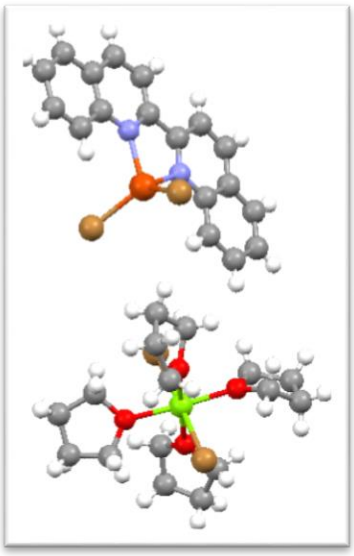

A crystal (0.354 x 0.217 x 0.102 mm^3) was placed onto a thin glass optical fiber or a nylon loop and mounted on a XtaLab Synergy-S Dualflex diffractometer equipped with a HyPix-6000HE HPC area detector for data collection at 100.00(10) K. A preliminary set of cell constants and an orientation matrix were calculated from a small sampling of reflections.[305] A short pre-experiment was run, from which an optimal data collection strategy was determined. The full data collection was carried out using a PhotonJet (Cu) X-ray Source with frame times of 0.71 and 2.83 seconds and a detector distance of 31.2 mm. Series of frames were collected in 0.50° steps in ω at different 2θ, κ, and ϕ settings. After the intensity data were corrected for absorption, the final cell constants were calculated from the xyz centroids of 33577 strong reflections from the actual data collection after integration.[305] See **Table A.2** for additional crystal and refinement information. The structure was solved using ShelXT[306] and refined using ShelXL.[307] The space group *C*2/*c* was determined based on systematic absences and intensity statistics. Most or all non-hydrogen atoms were assigned from the solution. Full-matrix least squares / difference Fourier cycles were performed which located any remaining non-hydrogen atoms. All non-hydrogen atoms were refined with anisotropic displacement parameters. All hydrogen atoms were placed in ideal positions and refined as riding atoms with relative isotropic displacement parameters. The final full matrix least squares refinement converged to *R*1 = 0.0507 (F^2, $I > 2\sigma(I)$) and *wR*2 = 0.1497

(F^2, all data). The structure is the one suggested. The asymmetric unit contains one iron complex and three cocrystallized THF solvent molecules in general positions and one-half of a magnesium complex located along a crystallographic two-fold axis that includes the Mg atom. One -CH_2CH_2- linkage of THF molecule O5/C35-C38 is modeled as disordered over two positions (0.59:0.41). Structure manipulation and figure generation were performed using Olex2.[308] Unless noted otherwise all structural diagrams containing thermal displacement ellipsoids are drawn at the 50 % probability level.

Table A.2. Crystal data and structure refinement.

Identification code	**7**	
Empirical formula	$C_{38}H_{52}$ Br_3 Fe $Mg_{0.50}$ N_2O_5	
Formula weight	924.55	
Temperature	100.00(10) K	
Wavelength	1.54184 Å	
Crystal system	monoclinic	
Space group	*C*2/*c*	
Unit cell dimensions	*a* = 19.8177(2) Å	α = 90°
	b = 14.8785(2) Å	β = 103.1140(10)°
	c = 27.6616(3) Å	γ = 90°
Volume	7943.52(16) $Å^3$	
Z	8	
Density (calculated)	1.546 mg/m^3	
Absorption coefficient	7.002 mm^{-1}	
***F*(000)**	3768	
Crystal color, morphology	light yellow, block	
Crystal size	0.354 x 0.217 x 0.102 mm^3	
Theta range for data collection	3.281 to 77.872°	
Index ranges	$-25 \leq h \leq 19$, $-18 \leq k \leq 18$, $-33 \leq l \leq 35$	
Reflections collected	68174	
Independent reflections	8407 [*R*(int) = 0.0629]	
Observed reflections	7814	
Completeness to theta = 74.504°	99.9%	
Absorption correction	Multi-scan	
Max. and min. transmission	1.00000 and 0.21400	
Refinement method	Full-matrix least-squares on F^2	
Data / restraints / parameters	8407 / 7 / 454	
Goodness-of-fit on F^2	1.065	
Final *R* indices [*I*>2sigma(*I*)]	*R*1 = 0.0507, *wR*2 = 0.1476	
***R* indices (all data)**	*R*1 = 0.0534, *wR*2 = 0.1497	
Largest diff. peak and hole	1.418 and -1.189 e.$Å^{-3}$	

❖ Crystal data of complex 8

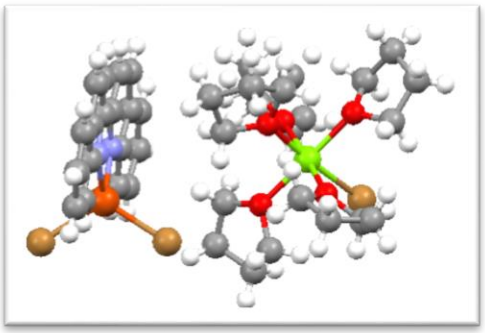

A crystal (0.284 x 0.199 x 0.09 mm^3) was placed onto a thin glass optical fiber or a nylon loop and mounted on a XtaLab Synergy-S Dualflex diffractometer equipped with a HyPix-6000HE HPC area detector for data collection at 100.00(10) K. A preliminary set of cell constants and an orientation matrix were calculated from a small sampling of reflections.[305] A short pre-experiment was run, from which an optimal data collection strategy was determined. The full data collection was carried out using a PhotonJet (Cu) X-ray Source with frame times of 0.10 and 0.38 seconds and a detector distance of 31.2 mm. Series of frames were collected in 0.50 steps in ω at different 2θ, κ, and ϕ settings. After the intensity data were corrected for absorption, the final cell constants were calculated from the xyz centroids of 34637 strong reflections from the actual data collection after integration.[305] See **Table A.3** for additional crystal and refinement information. The structure was solved using ShelXT[306] and refined using ShelXL.[307] The space group $P2_1/n$ was determined based on systematic absences. Most or all non-hydrogen atoms were assigned from the solution. Full-matrix least squares / difference Fourier cycles were performed which located any remaining non-hydrogen atoms. All non-hydrogen atoms were refined with anisotropic displacement parameters. All hydrogen atoms were placed in ideal positions and refined as riding atoms with relative isotropic displacement parameters. The final full matrix least squares refinement converged to $R1 = 0.0368$ ($F2$, $I > 2\sigma(I)$) and $wR2 = 0.1059$ (F^2, all data). The structure is the one suggested. The asymmetric unit contains one cationic magnesium complex and one anionic iron complex, in general positions, and one-half of a cocrystallized THF solvent molecule, located at a crystallographic inversion center. One -CH_2- linkage in THF ligand O3/C27-C30 is modeled as disordered over two positions (0.84:0.16) and the cocrystallized THF solvent molecule is modeled as disordered over a crystallographic inversion center (0.50:0.50). Structure manipulation and figure generation were performed using Olex2.[308] Unless noted otherwise all structural diagrams containing thermal displacement ellipsoids are drawn at the 50 % probability level.

Table A.3. Crystal data and structure refinement.

Identification code	**8**	
Empirical formula	$C_{40}H_{56}Br_3FeMgN_2O_{5.50}$	
Formula weight	972.75	
Temperature	100.00(10) K	
Wavelength	1.54184 Å	
Crystal system	monoclinic	
Space group	$P2_1/n$	
Unit cell dimensions	a = 9.89560(10) Å	$\alpha = 90°$
	b = 25.2496(2) Å	$\beta = 94.4950(10)°$
	c = 16.60500(10) Å	$\gamma = 90°$
Volume	4136.16(6) $Å^3$	
Z	4	
Density (calculated)	1.562 mg/m^3	
Absorption coefficient	6.833 mm^{-1}	
***F*(000)**	1988	

Crystal color, morphology	dark green, block
Crystal size	0.284 x 0.199 x 0.09 mm^3
Theta range for data collection	3.192 to 79.234°
Index ranges	$-12 \leq h \leq 12$, $-31 \leq k \leq 31$, $-16 \leq l \leq 21$
Reflections collected	52456
Independent reflections	8728 [*R*(int) = 0.0493]
Observed reflections	8293
Completeness to theta = 74.504°	99.9%
Absorption correction	Multi-scan
Max. and min. transmission	1.00000 and 0.34972
Refinement method	Full-matrix least-squares on F^2
Data / restraints / parameters	8728 / 43 / 500
Goodness-of-fit on F^2	1.062
Final *R* indices [*I*>2sigma(*I*)]	*R*1 = 0.0368, *wR*2 = 0.1030
***R* indices (all data)**	*R*1 = 0.0388, *wR*2 = 0.1059
Largest diff. peak and hole	1.087 and -0.994 e.$Å^{-3}$

❖ Crystal data of complex 9

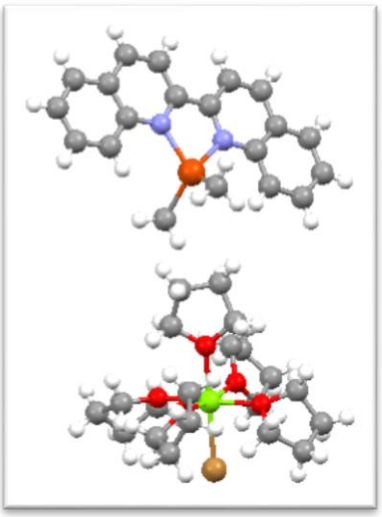

A crystal (0.376 x 0.06 x 0.043 mm^3) was placed onto a thin glass optical fiber or a nylon loop and mounted on a XtaLab Synergy-S Dualflex diffractometer equipped with a HyPix-6000HE HPC area detector for data collection at 173.00(10) K. A preliminary set of cell constants and an orientation matrix were calculated from a small sampling of reflections.[305] A short pre-experiment was run, from which an optimal data collection strategy was determined. The full data collection was carried out using a PhotonJet (Cu) X-ray Source with frame times of 0.58 and 2.32 seconds and a detector distance of 31.2 mm. Series of frames were collected in 0.50° steps in ω at different 2θ, κ, and ϕ settings. After the intensity data were corrected for absorption, the final cell constants were calculated from the xyz centroids of 28014 strong reflections from the actual data collection after integration.[305] See **Table A.4** for additional crystal and refinement information. The structure was solved using[306] and refined using ShelXL.[307] The space group $P2_1/n$ was determined based on systematic absences. Most or all non-hydrogen atoms were assigned from the solution. Full-matrix least squares / difference Fourier cycles were performed which located any remaining non-hydrogen atoms. All non-hydrogen atoms were refined with anisotropic displacement parameters. All hydrogen atoms were placed in ideal positions and refined as riding atoms with relative isotropic displacement parameters. The final full matrix least squares refinement converged to *R*1 = 0.0364 (F^2, $I > 2\sigma(I)$) and *wR*2 = 0.1010 (F^2, all data). The structure is the one suggested. The asymmetric unit contains one cationic magnesium complex, one anionic iron complex, and two cocrystallized THF solvent molecules, all in general positions. Hydrogen atoms on methyl ligands C1 and C2 were located in the difference Fourier map and then given a riding model. Several THF ligand and cocrystallized molecules are modeled as disordered. Over two positions are O1/C21-C24, 0.71:0.29, O3/C29-C32, 0.64:0.36, O4/C33-C36, 0.59:0.41, and O7/C45-C48, 0.78:0.22. Over three positions is

O6/C41-C44, 0.53:0.30:0.17. Structure manipulation and figure generation were performed using Olex2.[308] Unless noted otherwise all structural diagrams containing thermal displacement ellipsoids are drawn at the 50 % probability level.

Table A.4. Crystal data and structure refinement.

Identification code	**9**
Empirical formula	$C_{48}H_{74}BrFeMgN_2O_7$
Formula weight	951.16
Temperature	173.00(10) K
Wavelength	1.54184 Å
Crystal system	monoclinic
Space group	$P2_1/n$
Unit cell dimensions	a = 13.55330(10) Å α = 90°
	b = 23.0409(2) Å β = 105.7020(10)°
	c = 16.09900(10) Å γ = 90°
Volume	4839.79(7) Å^3
Z	4
Density (calculated)	1.305 mg/m^3
Absorption coefficient	3.988 mm^{-1}
***F*(000)**	2020
Crystal color, morphology	brown, needle
Crystal size	0.376 x 0.06 x 0.043 mm^3
Theta range for data collection	3.437 to 77.820°
Index ranges	$-17 \leq h \leq 17$, $-29 \leq k \leq 28$, $-20 \leq l \leq 16$
Reflections collected	50302
Independent reflections	10130 [R(int) = 0.0393]
Observed reflections	8966
Completeness to theta = 74.504°	99.6%
Absorption correction	Multi-scan
Max. and min. transmission	1.00000 and 0.45759
Refinement method	Full-matrix least-squares on F^2
Data / restraints / parameters	10130 / 171 / 640
Goodness-of-fit on F^2	1.064
Final *R* indices [*I*>2sigma(*I*)]	$R1$ = 0.0364, $wR2$ = 0.0978
***R* indices (all data)**	$R1$ = 0.0411, $wR2$ = 0.1010
Largest diff. peak and hole	0.309 and -0.794 e.Å^{-3}

❖ Crystal data of complex 10

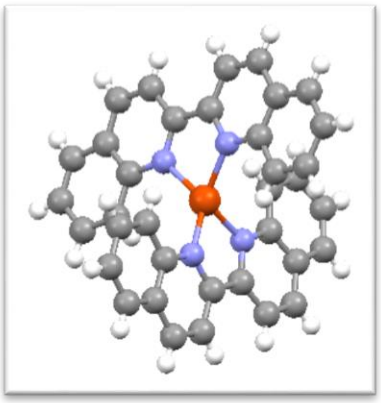

A crystal (0.253 x 0.226 x 0.164 mm^3) was placed onto a thin glass optical fiber or a nylon loop and mounted on a XtaLab Synergy-S Dualflex diffractometer equipped with a HyPix-6000HE HPC area detector for data collection at 100.00(10) K. A preliminary set of cell constants and an orientation matrix were calculated from a small sampling of reflections.[305] A short pre-experiment was run, from which an optimal data collection strategy was determined. The full data collection was carried out using a PhotonJet (Cu) X-ray Source with frame times of 0.47 and 1.89 seconds and a detector distance of 31.2 mm. Series of frames were collected in 0.50° steps in ω at different 2θ, κ, and ϕ settings. After the intensity data were corrected for absorption, the final cell constants were calculated from the xyz centroids of 19254 strong reflections from the actual data collection after integration.[305] See **Table A.5** for additional crystal and refinement information. The structure was solved using ShelXT[306] and refined using ShelXL.[307] The space group $P2_1/c$ was determined based on systematic absences. Most or all non-hydrogen atoms were assigned from the solution. Full-matrix least squares / difference Fourier cycles were performed which located any remaining non-hydrogen atoms. All non-hydrogen atoms were refined with anisotropic displacement parameters. All hydrogen atoms were placed in ideal positions and refined as riding atoms with relative isotropic displacement parameters. The final full matrix least squares refinement converged to $R1 = 0.0401$ (F^2, $I > 2\sigma(I)$) and $wR2 = 0.1189$ (F^2, all data). The structure is similar to the one suggested. The asymmetric unit contains one iron complex and one cocrystallized dioxane solvent molecule in general positions. The angle between the N1-Fe1-N2 and N3-Fe1-N4 planes is 89.17(4) degrees. Structure manipulation and figure generation were performed using Olex2.[308] Unless noted otherwise all structural diagrams containing thermal displacement ellipsoids are drawn at the 50 % probability level.

Table A.5. Crystal data and structure refinement.

Identification code	**10**	
Empirical formula	$C_{40}H_{32}FeN_4O_2$	
Formula weight	656.54	
Temperature	100.00(10) K	
Wavelength	1.54184 Å	
Crystal system	monoclinic	
Space group	$P2_1/c$	
Unit cell dimensions	a = 11.73540(10) Å	α = 90°
	b = 19.1365(2) Å	β = 104.8690(10)°
	c = 14.20940(10) Å	γ = 90°
Volume	3084.22(5) Å^3	
Z	4	
Density (calculated)	1.414 mg/m^3	
Absorption coefficient	4.269 mm^{-1}	
***F*(000)**	1368	
Crystal color, morphology	purple-black, block	
Crystal size	0.253 x 0.226 x 0.164 mm^3	

Theta range for data collection	3.897 to 78.025°
Index ranges	$-14 \leq h \leq 9$, $-24 \leq k \leq 22$, $-18 \leq l \leq 17$
Reflections collected	30612
Independent reflections	6478 [*R*(int) = 0.0360]
Observed reflections	6023
Completeness to theta = 74.504°	99.9%
Absorption correction	Multi-scan
Max. and min. transmission	1.00000 and 0.24382
Refinement method	Full-matrix least-squares on F^2
Data / restraints / parameters	6478 / 0 / 424
Goodness-of-fit on F^2	1.115
Final *R* indices [*I*>2sigma(*I*)]	*R*1 = 0.0401, *wR*2 = 0.1170
***R* indices (all data)**	*R*1 = 0.0424, *wR*2 = 0.1189
Largest diff. peak and hole	0.462 and -0.706 e.Å^{-3}

❖ Crystal data of alkenylboronate 11by

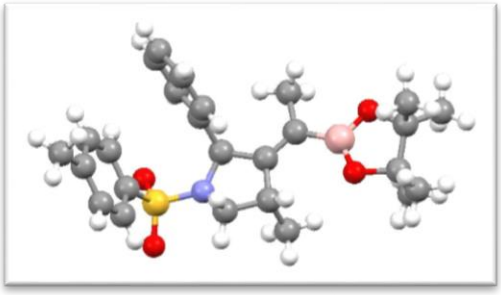

A clear colourless prismatic-like specimen of $C_{26}H_{34}BNO_4S$, approximate dimensions 0.088 mm x 0.096 mm x 0.139 mm, was used for the X-ray crystallographic analysis. The X-ray intensity data were measured. The total exposure time was 13.57 hours. The frames were integrated with the Bruker SAINT software package using a narrow-frame algorithm. The integration of the data using a monoclinic unit cell yielded a total of 35191 reflections to a maximum θ angle of 25.35° (0.83 Å resolution), of which 4535 were independent (average redundancy 7.760, completeness = 100.0%, R_{int} = 13.21%, R_{sig} = 8.47%) and 2886 (63.64%) were greater than $2\sigma(F^2)$. The final cell constants of a = 6.4192(4) Å, b = 32.5924(18) Å, c = 11.9890(6) Å, β = 99.366(4)°, volume = 2474.9(2) Å^3, are based upon the refinement of the XYZ-centroids of 1815 reflections above 20 σ(I) with 4.999° < 2θ < 40.43°. Data were corrected for absorption effects using the multi-scan method (SADABS). The ratio of minimum to maximum apparent transmission was 0.851. The calculated minimum and maximum transmission coefficients (based on crystal size) are 0.9780 and 0.9860. The final anisotropic full-matrix least-squares refinement on F^2 with 305 variables converged at R1 = 5.14%, for the observed data and wR2 = 12.57% for all data. The goodness-of-fit was 1.005. The largest peak in the final difference electron density synthesis was 0.212 e^-/Å^3 and the largest hole was -0.285 e^-/Å^3 with an RMS deviation of 0.056 e^-/Å^3. On the basis of the final model, the calculated density was 1.254 g/cm^3 and F(000), 1000 e^-.

Table A.6. Sample and crystal data

Identification code	**11by** (CCDC number 1819416)
Chemical formula	$C_{26}H_{34}BNO_4S$
Formula weight	467.41 g/mol
Temperature	200(2) K
Wavelength	0.71073 Å
Crystal size	0.088 x 0.096 x 0.139 mm

Crystal habit	clear colourless prismatic	
Crystal system	monoclinic	
Space group	P 1 21/c 1	
Unit cell dimensions	a = 6.4192(4) Å	α = 90°
	b = 32.5924(18) Å	β = 99.366(4)°
	c = 11.9890(6) Å	γ = 90°
Volume	2474.9(2) $Å^3$	
Z	4	
Density (calculated)	1.254 g/cm^3	
Absorption coefficient	0.163 mm^{-1}	
F(000)	1000	

Table A.7. Data collection and structure refinement

Theta range for data collection	1.25 to 25.35°	
Index ranges	-7<=h<=7, -39<=k<=39, -12<=l<=14	
Reflections collected	35191	
Independent reflections	4535 [R(int) = 0.1321]	
Coverage of independent reflections	100.0%	
Absorption correction	multi-scan	
Max. and min. transmission	0.9860 and 0.9780	
Refinement method	Full-matrix least-squares on F^2	
Refinement program	SHELXL-2014/7 (Sheldrick, 2014)	
Function minimized	$\Sigma\, w(F_o^2 - F_c^2)^2$	
Data / restraints / parameters	4535 / 0 / 305	
Goodness-of-fit on F^2	1.005	
Final R indices	2886 data; I>2σ(I)	R1 = 0.0514, wR2 = 0.1000
	all data	R1 = 0.1042, wR2 = 0.1257
Weighting scheme	$w=1/[\sigma^2(F_o^2)+(0.0360P)^2+1.6820P]$ where $P=(F_o^2+2F_c^2)/3$	
Largest diff. peak and hole	0.212 and -0.285 $eÅ^{-3}$	
R.M.S. deviation from mean	0.056 $eÅ^{-3}$	

❖ Crystal data of diboronate 17cb

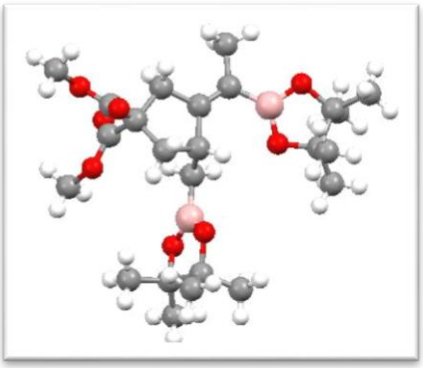

A clear colourless prismatic-like specimen of $C_{26}H_{34}BNO_4S$, approximate dimensions 0.088 mm x 0.096 mm x 0.139 mm, was used for the X-ray crystallographic analysis. The X-ray intensity data were measured. The total exposure time was 13.57 hours. The frames were integrated with the Bruker SAINT software package using a narrow-frame algorithm. The integration of the data using a monoclinic unit cell yielded a total of 35191 reflections to a maximum θ angle of 25.35° (0.83 Å resolution), of which 4535 were independent (average redundancy 7.760, completeness = 100.0%, R_{int} = 13.21%, R_{sig} = 8.47%) and 2886 (63.64%) were greater than $2\sigma(F^2)$. The final cell constants of a = 6.4192(4) Å, b = 32.5924(18) Å, c = 11.9890(6) Å, β = 99.366(4)°, volume = 2474.9(2) $Å^3$, are based upon the refinement of the XYZ-centroids of 1815 reflections above 20 σ(I) with 4.999° <

2θ < 40.43°. Data were corrected for absorption effects using the multi-scan method (SADABS). The ratio of minimum to maximum apparent transmission was 0.851. The calculated minimum and maximum transmission coefficients (based on crystal size) are 0.9780 and 0.9860. The final anisotropic full-matrix least-squares refinement on F^2 with 305 variables converged at R1 = 5.14%, for the observed data and wR2 = 12.57% for all data. The goodness-of-fit was 1.005. The largest peak in the final difference electron density synthesis was 0.212 $e^-/Å^3$ and the largest hole was -0.285 $e^-/Å^3$ with an RMS deviation of 0.056 $e^-/Å^3$. On the basis of the final model, the calculated density was 1.254 g/cm^3 and F(000), 1000 e^-.

Table A.8. Sample and crystal data

Identification code	**17cb** (CCDC number 1834503)	
Chemical formula	$C_{24}H_{40}B_2O_8$	
Formula weight	478.18 g/mol	
Temperature	346(2) K	
Wavelength	0.71073 Å	
Crystal size	0.327 x 0.412 x 0.631 mm	
Crystal habit	clear colourless prismatic	
Crystal system	monoclinic	
Space group	P 1 21/c 1	
Unit cell dimensions	a = 17.5993(7) Å	α = 90°
	b = 12.1222(5) Å	β = 99.767(2)°
	c = 13.0306(4) Å	γ = 90°
Volume	2739.68(18) $Å^3$	
Z	4	
Density (calculated)	1.159 g/cm^3	
Absorption coefficient	0.084 mm^{-1}	
F(000)	1032	

Table A.9. Data collection and structure refinement

Theta range for data collection	2.05 to 25.35°	
Index ranges	-21<=h<=21, -14<=k<=14, -15<=l<=15	
Reflections collected	98852	
Independent reflections	5015 [R(int) = 0.0515]	
Coverage of independent reflections	100.0%	
Absorption correction	multi-scan	
Max. and min. transmission	0.9730 and 0.9490	
Refinement method	Full-matrix least-squares on F^2	
Refinement program	SHELXL-2014/7 (Sheldrick, 2014)	
Function minimized	$\Sigma\, w(F_o^2 - F_c^2)^2$	
Data / restraints / parameters	5015 / 0 / 318	
Goodness-of-fit on F^2	1.044	
Final R indices	3929 data; I>2σ(I)	R1 = 0.0480, wR2 = 0.1188
	all data	R1 = 0.0643, wR2 = 0.1344
Weighting scheme	$w=1/[\sigma^2(F_o^2)+(0.0631P)^2+1.4330P]$ where $P=(F_o^2+2F_c^2)/3$	
Largest diff. peak and hole	0.273 and -0.270 $eÅ^{-3}$	
R.M.S. deviation from mean	0.058 $eÅ^{-3}$	

❖ Crystal data of complex 22

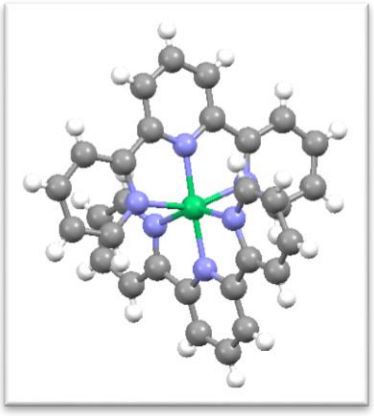

A crystal (0.589 x 0.041 x 0.026 mm^3) was placed onto a thin glass optical fiber or a nylon loop and mounted on a XtaLab Synergy-S Dualflex diffractometer equipped with a HyPix-6000HE HPC area detector for data collection at 172.99(10) K. A preliminary set of cell constants and an orientation matrix were calculated from a small sampling of reflections.[305] A short pre-experiment was run, from which an optimal data collection strategy was determined. The full data collection was carried out using a PhotonJet (Cu) X-ray Source with frame times of 7.09 and 28.37 seconds and a detector distance of 31.2 mm. Series of frames were collected in 0.50° steps in ω at different 2θ, κ, and ϕ settings. After the intensity data were corrected for absorption, the final cell constants were calculated from the xyz centroids of 23899 strong reflections from the actual data collection after integration.[305] See **Table A.10** for additional crystal and refinement information. The structure was solved using ShelXT[306] and refined using ShelXL.[307] The space group *Fdd*2 was determined based on systematic absences and intensity statistics. Most or all non-hydrogen atoms were assigned from the solution. Full-matrix least squares / difference Fourier cycles were performed which located any remaining non-hydrogen atoms. All non-hydrogen atoms were refined with anisotropic displacement parameters. All hydrogen atoms were placed in ideal positions and refined as riding atoms with relative isotropic displacement parameters. The final full matrix least squares refinement converged to $R1$ = 0.0327 (F^2, $I > 2\sigma(I)$) and $wR2$ = 0.0937 (F^2, all data). The structure is similar to the one suggested. The asymmetric unit contains two molecules in general positions. The structure is isomorphous with single crystal X-ray diffraction structures of Ti, Cr, V, Fe, Mo, Ru, and W analogs. Structure manipulation and figure generation were performed using Olex2.[308] Unless noted otherwise all structural diagrams containing thermal displacement ellipsoids are drawn at the 50 % probability level.

Table A.10. Crystal data and structure refinement.

Identification code	**22** (CCDC number 1891622)	
Empirical formula	C30 H22 N6 Ni	
Formula weight	525.24	
Temperature	172.99(10) K	
Wavelength	1.54184 Å	
Crystal system	orthorhombic	
Space group	*Fdd*2	
Unit cell dimensions	*a* = 56.2329(5) Å	α = 90°
	b = 39.4759(4) Å	β = 90°
	c = 8.49770(10) Å	γ = 90°
Volume	18863.6(3) $Å^3$	
Z	32	
Density (calculated)	1.480 mg/m^3	
Absorption coefficient	1.444 mm^{-1}	
***F*(000)**	8704	
Crystal color, morphology	blue-black, needle	
Crystal size	0.589 x 0.041 x 0.026 mm^3	

Theta range for data collection	2.735 to 77.880°
Index ranges	$-70 \leq h \leq 64$, $-50 \leq k \leq 50$, $-10 \leq l \leq 6$
Reflections collected	31051
Independent reflections	6724 [*R*(int) = 0.0306]
Observed reflections	6557
Completeness to theta = 74.504°	99.9%
Absorption correction	Multi-scan
Max. and min. transmission	1.00000 and 0.71074
Refinement method	Full-matrix least-squares on F^2
Data / restraints / parameters	6724 / 1 / 668
Goodness-of-fit on F^2	1.060
Final *R* indices [*I*>2sigma(*I*)]	*R*1 = 0.0327, *wR*2 = 0.0930
***R* indices (all data)**	*R*1 = 0.0334, *wR*2 = 0.0937
Largest diff. peak and hole	0.44(3)

❖ Crystal data of complex 23

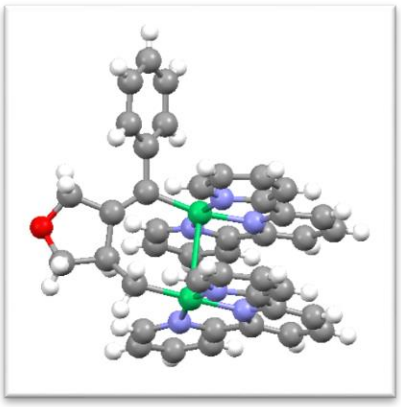

A crystal (0.176 x 0.091 x 0.051 mm^3) was placed onto a thin glass optical fiber or a nylon loop and mounted on a XtaLab Synergy-S Dualflex diffractometer equipped with a HyPix-6000HE HPC area detector for data collection at 100.01(10) K. A preliminary set of cell constants and an orientation matrix were calculated from a small sampling of reflections.[305] A short pre-experiment was run, from which an optimal data collection strategy was determined. The full data collection was carried out using a PhotonJet (Cu) X-ray Source with frame times of 1.18 and 4.71 seconds and a detector distance of 31.2 mm. Series of frames were collected in 0.50° steps in ω at different 2θ, κ, and ϕ settings. After the intensity data were corrected for absorption, the final cell constants were calculated from the xyz centroids of 20456 strong reflections from the actual data collection after integration.[305] See **Table A.11** for additional crystal and refinement information. The structure was solved using ShelXT[306] and refined using ShelXL.[307] The space group $P2_1/n$ was determined based on systematic absences. Most or all non-hydrogen atoms were assigned from the solution. Full-matrix least squares / difference Fourier cycles were performed which located any remaining non-hydrogen atoms. All non-hydrogen atoms were refined with anisotropic displacement parameters. All hydrogen atoms were placed in ideal positions and refined as riding atoms with relative isotropic displacement parameters. Reflection contributions from highly disordered solvent were fixed and added to the calculated structure factors using the SQUEEZE routine of program Platon, which determined there to be 365 electrons in 1379 Å^3 per unit cell treated in this manner. Because the exact identity and amount of solvent were unknown, no solvent was included in the atom list or molecular formula; thus all calculated quantities that derive from the molecular formula (e.g., F(000), density, molecular weight, etc.) are known to be incorrect. The final full matrix least squares refinement converged to *R*1 = 0.0433 (F^2, $I > 2\sigma(I)$) and *wR*2 = 0.1285 (F^2, all data). The structure is the one suggested. The asymmetric unit contains one dinickel molecule in a general position and solvent for which atoms were not assigned (see above). Structure manipulation and figure generation were performed using Olex2.[308] Unless noted otherwise all structural diagrams containing thermal displacement ellipsoids are drawn at the 50 % probability level.

Table A.11. Crystal data and structure refinement.

Identification code	**23** (CCDC number 1891623)
Empirical formula	C42 H34 N6 Ni2 O
Formula weight	756.17
Temperature	100.01(10) K
Wavelength	1.54184 Å
Crystal system	monoclinic
Space group	$P2_1/n$
Unit cell dimensions	a = 17.9470(2) Å α = 90° b = 13.0923(2) Å β = 98.0760(10)° c = 18.6405(2) Å γ = 90°
Volume	4336.47(9) $Å^3$
Z	4
Density (calculated)	1.158 mg/m^3
Absorption coefficient	1.352 mm^{-1}
***F*(000)**	1568
Crystal color, morphology	black, block
Crystal size	0.176 x 0.091 x 0.051 mm^3
Theta range for data collection	3.201 to 78.767°
Index ranges	$-18 \leq h \leq 22$, $-16 \leq k \leq 16$, $-23 \leq l \leq 15$
Reflections collected	44957
Independent reflections	9101 [R(int) = 0.0395]
Observed reflections	7596
Completeness to theta = 74.504°	99.6%
Absorption correction	Multi-scan
Max. and min. transmission	1.00000 and 0.76944
Refinement method	Full-matrix least-squares on F^2
Data / restraints / parameters	9101 / 0 / 460
Goodness-of-fit on F^2	1.048
Final *R* indices [*I*>2sigma(*I*)]	$R1$ = 0.0433, $wR2$ = 0.1221
***R* indices (all data)**	$R1$ = 0.0510, $wR2$ = 0.1285
Largest diff. peak and hole	0.341 and -0.297 $e.Å^{-3}$

❖ Crystal data of compound 26ba

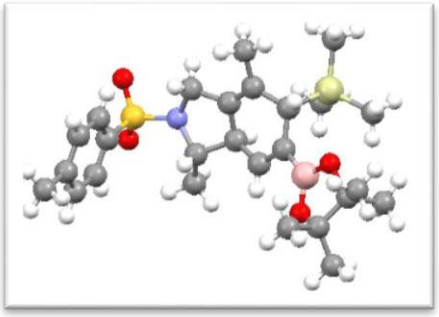

A clear colourless ribbon-like specimen of $C_{26}H_{40}BNO_4SSi$, approximate dimensions 0.042 mm x 0.076 mm x 0.407 mm, was used for the X-ray crystallographic analysis. The X-ray intensity data were measured. The total exposure time was 10.78 hours. The frames were integrated with the Bruker SAINT software package using a narrow-frame algorithm. The integration of the data using a triclinic unit cell yielded a total of 57615 reflections to a maximum θ angle of 25.35° (0.83 Å resolution), of which 5016 were independent (average redundancy 11.486, completeness = 99.8%, R_{int} = 4.63%, R_{sig} = 2.48%) and 4208(83.89%) were greater than $2\sigma(F^2)$. The final cell constants of a = 6.2772(3) Å, b = 14.5507(9) Å, c = 16.3083(9) Å, α = 110.526(2)°, β = 92.393(2)°, γ = 99.506(2)°, volume = 1367.81(13) $Å^3$, are based upon the refinement of the XYZ-centroids of 9867 reflections above 20 σ(I) with 5.119° < 2θ < 51.40°. Data were corrected for absorption effects using the multi-scan method (SADABS). The ratio of minimum to maximum apparent transmission was 0.918. The calculated minimum and maximum transmission coefficients (based on crystal size) are 0.9250 and 0.9920. The final anisotropic full-matrix least-squares refinement on F^2 with 317 variables converged at R1 = 4.88%, for the observed data and wR2 = 15.40% for all data. The goodness-of-fit was 1.077. The largest peak in the final difference electron density synthesis was 1.537 $e^-/Å^3$ and the largest hole was -0.514 $e^-/Å^3$ with an RMS deviation of 0.101 $e^-/Å^3$. On the basis of the final model, the calculated density was 1.218 g/cm^3 and F(000), 540 e^-.

Table A.12. Sample and crystal data.

Identification code	**26ba** (CCDC number 1906093)	
Chemical formula	$C_{26}H_{40}BNO_4SSi$	
Formula weight	501.55 g/mol	
Temperature	150(2) K	
Wavelength	0.71073 Å	
Crystal size	0.042 x 0.076 x 0.407 mm	
Crystal habit	clear colourless ribbon	
Crystal system	triclinic	
Space group	P -1	
Unit cell dimensions	a = 6.2772(3) Å	α = 110.526(2)°
	b = 14.5507(9) Å	β = 92.393(2)°
	c = 16.3083(9) Å	γ = 99.506(2)°
Volume	1367.81(13) $Å^3$	
Z	2	
Density (calculated)	1.218 g/cm^3	
Absorption coefficient	0.193 mm^{-1}	
F(000)	540	

Table A.13. Data collection and structure refinement.

Theta range for data collection	1.34 to 25.35°
Index ranges	-7<=h<=7, -17<=k<=17, -19<=l<=19
Reflections collected	57615
Independent reflections	5016 [R(int) = 0.0463]

Coverage of independent reflections	99.8%	
Absorption correction	multi-scan	
Max. and min. transmission	0.9920 and 0.9250	
Refinement method	Full-matrix least-squares on F^2	
Refinement program	SHELXL-2014/7 (Sheldrick, 2014)	
Function minimized	$\Sigma\ w(F_o^2 - F_c^2)^2$	
Data / restraints / parameters	5016 / 0 / 317	
Goodness-of-fit on F^2	1.077	
Final R indices	4208 data; I>2σ(I)	R1 = 0.0488, wR2 = 0.1340
	all data	R1 = 0.0624, wR2 = 0.1540
Weighting scheme	$w=1/[\sigma^2(F_o^2)+(0.0797P)^2+1.6474P]$ where $P=(F_o^2+2F_c^2)/3$	
Largest diff. peak and hole	1.537 and -0.514 eÅ^{-3}	
R.M.S. deviation from mean	0.101 eÅ^{-3}	

❖ Crystal data of compound 26fb

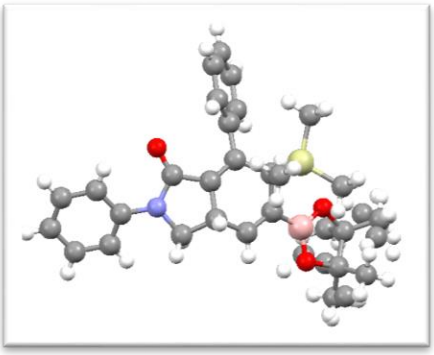

A clear colourless prismatic-like specimen of $C_{29}H_{36}BNO_3Si$, approximate dimensions 0.149 mm x 0.265 mm x 0.364 mm, was used for the X-ray crystallographic analysis. The X-ray intensity data were measured. The total exposure time was 6.85 hours. The frames were integrated with the Bruker SAINT software package using a narrow-frame algorithm. The integration of the data using a monoclinic unit cell yielded a total of 93357 reflections to a maximum θ angle of 25.35° (0.83 Å resolution), of which 5045 were independent (average redundancy 18.505, completeness = 100.0%, R_{int} = 4.60%, R_{sig} = 1.75%) and 4198(83.21%) were greater than $2\sigma(F^2)$. The final cell constants of a = 16.1719(6) Å, b = 7.1438(3) Å, c = 23.8565(7) Å, β = 92.232(2)°, volume = 2754.02(17) Å^3, are based upon the refinement of the XYZ-centroids of 9807 reflections above 20 σ(I) with 5.041° < 2θ < 52.13°. Data were corrected for absorption effects using the multi-scan method (SADABS). The ratio of minimum to maximum apparent transmission was 0.950. The calculated minimum and maximum transmission coefficients (based on crystal size) are 0.9590 and 0.9830. The structure was solved and refined using the Bruker SHELXTL Software Package, using the space group P 1 21/c 1, with Z = 4 for the formula unit, $C_{29}H_{36}BNO_3Si$. The final anisotropic full-matrix least-squares refinement on F^2 with 349 variables converged at R1 = 4.89%, for the observed data and wR2 = 16.41% for all data. The goodness-of-fit was 1.145. The largest peak in the final difference electron density synthesis was 0.659 e$^-$/Å^3 and the largest hole was -0.363 e$^-$/Å^3 with an RMS deviation of 0.097 e$^-$/Å^3. On the basis of the final model, the calculated density was 1.171 g/cm^3 and F(000), 1040 e$^-$.

Table A.14. Sample and crystal data.

Identification code	**26fb** (CCDC number 1906092)
Chemical formula	$C_{29}H_{36}BNO_3Si$
Formula weight	485.49 g/mol
Temperature	150(2) K
Wavelength	0.71073 Å
Crystal size	0.149 x 0.265 x 0.364 mm

Crystal habit	clear colourless prismatic	
Crystal system	monoclinic	
Space group	P 1 21/c 1	
Unit cell dimensions	a = 16.1719(6) Å	α = 90°
	b = 7.1438(3) Å	β = 92.232(2)°
	c = 23.8565(7) Å	γ = 90°
Volume	2754.02(17) $Å^3$	
Z	4	
Density (calculated)	1.171 g/cm^3	
Absorption coefficient	0.115 mm^{-1}	
F(000)	1040	

Table A.15. Data collection and structure refinement.

Theta range for data collection	1.26 to 25.35°	
Index ranges	-19<=h<=19, -8<=k<=8, -28<=l<=28	
Reflections collected	93357	
Independent reflections	5045 [R(int) = 0.0460]	
Coverage of independent reflections	100.0%	
Absorption correction	multi-scan	
Max. and min. transmission	0.9830 and 0.9590	
Structure solution technique	direct methods	
Structure solution program	SHELXS-97 (Sheldrick 2008)	
Refinement method	Full-matrix least-squares on F^2	
Refinement program	SHELXL-2014 (Sheldrick 2014)	
Function minimized	$\Sigma w(F_o^2 - F_c^2)^2$	
Data / restraints / parameters	5045 / 12 / 349	
Goodness-of-fit on F^2	1.145	
Final R indices	4198 data; I>2σ(I)	R1 = 0.0489, wR2 = 0.1380
	all data	R1 = 0.0645, wR2 = 0.1641
Weighting scheme	$w=1/[\sigma^2(F_o^2)+(0.0897P)^2+1.7187P]$ where $P=(F_o^2+2F_c^2)/3$	
Largest diff. peak and hole	0.659 and -0.363 $eÅ^{-3}$	
R.M.S. deviation from mean	0.097 $eÅ^{-3}$	

❖ Crystal data of compound 29bd

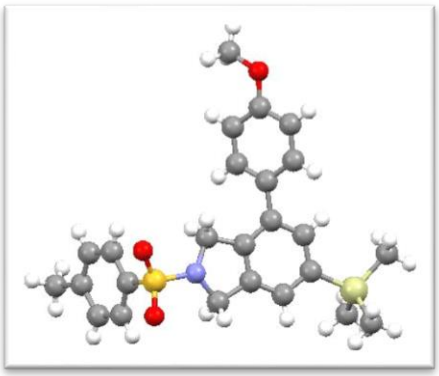

A clear colourless needle-like specimen of $C_{25}H_{29}NO_3SSi$, approximate dimensions 0.038 mm x 0.060 mm x 0.215 mm, was used for the X-ray crystallographic analysis. The X-ray intensity data were measured. The total exposure time was 50.43 hours. The frames were integrated with the Bruker SAINT software package using a narrow-frame algorithm. The integration of the data using a monoclinic unit cell yielded a total of 69872 reflections to a maximum θ angle of 25.35° (0.83 Å resolution), of which 4483 were independent (average redundancy 15.586, completeness = 99.8%, R_{int} = 10.14%, R_{sig} = 5.10%) and 2739(61.10%) were greater than $2\sigma(F^2)$. The final cell constants of a = 12.3068(5) Å, b = 25.0445(13) Å, c = 7.9739(4) Å, β = 92.360(2)°, volume = 2455.6(2) $Å^3$,

are based upon the refinement of the XYZ-centroids of 7966 reflections above 20 σ(I) with 5.365° < 2θ < 40.75°. Data were corrected for absorption effects using the multi-scan method (SADABS). The ratio of minimum to maximum apparent transmission was 0.873. The calculated minimum and maximum transmission coefficients (based on crystal size) are 0.9570 and 0.9920. The final anisotropic full-matrix least-squares refinement on F^2 with 285 variables converged at R1 = 5.70%, for the observed data and wR2 = 20.46% for all data. The goodness-of-fit was 1.097. The largest peak in the final difference electron density synthesis was 0.345 $e^-/Å^3$ and the largest hole was -0.596 $e^-/Å^3$ with an RMS deviation of 0.162 $e^-/Å^3$. On the basis of the final model, the calculated density was 1.222 g/cm^3 and F(000), 960 e^-.

Table A.16. Sample and crystal data.

Identification code	**29bd** (CCDC number 1906094)	
Chemical formula	$C_{25}H_{29}NO_3SSi$	
Formula weight	451.64 g/mol	
Temperature	296(2) K	
Wavelength	0.71073 Å	
Crystal size	0.038 x 0.060 x 0.215 mm	
Crystal habit	clear colourless needle	
Crystal system	monoclinic	
Space group	P 1 21/c 1	
Unit cell dimensions	a = 12.3068(5) Å	α = 90°
	b = 25.0445(13) Å	β = 92.360(2)°
	c = 7.9739(4) Å	γ = 90°
Volume	2455.6(2) $Å^3$	
Z	4	
Density (calculated)	1.222 g/cm^3	
Absorption coefficient	0.206 mm^{-1}	
F(000)	960	

Table A.17. Data collection and structure refinement.

Theta range for data collection	1.63 to 25.35°	
Index ranges	-14<=h<=14, -30<=k<=30, -9<=l<=9	
Reflections collected	69872	
Independent reflections	4483 [R(int) = 0.1014]	
Coverage of independent reflections	99.8%	
Absorption correction	multi-scan	
Max. and min. transmission	0.9920 and 0.9570	
Refinement method	Full-matrix least-squares on F^2	
Refinement program	SHELXL-2014/7 (Sheldrick, 2014)	
Function minimized	$\Sigma w(F_o^2 - F_c^2)^2$	
Data / restraints / parameters	4483 / 0 / 285	
Goodness-of-fit on F^2	1.097	
Δ/σ_{max}	0.001	
Final R indices	2739 data; I>2σ(I)	R1 = 0.0570, wR2 = 0.1591
	all data	R1 = 0.1200, wR2 = 0.2046
Weighting scheme	$w=1/[\sigma^2(F_o^2)+(0.1145P)^2+0.1694P]$ where $P=(F_o^2+2F_c^2)/3$	
Largest diff. peak and hole	0.345 and -0.596 $eÅ^{-3}$	
R.M.S. deviation from mean	0.162 $eÅ^{-3}$	